VISIT…

DRUGS AND THE PHARMACEUTICAL SCIENCES VOLUME 128

Affinity Capillary Electrophoresis in Pharmaceutics and Biopharmaceutics

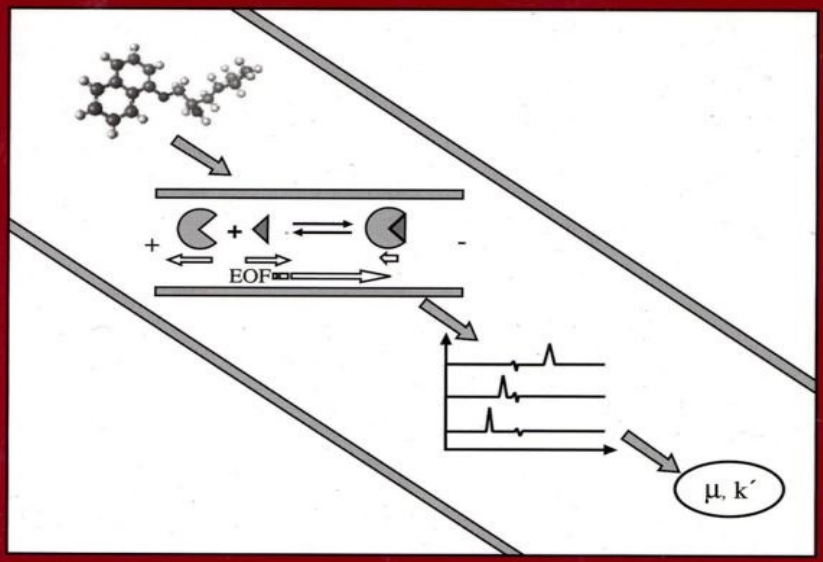

edited by
Reinhard H. H. Neubert
Hans-Hermann Rüttinger

Affinity Capillary Electrophoresis in Pharmaceutics and Biopharmaceutics

edited by

Reinhard H. H. Neubert
Hans-Hermann Rüttinger

Martin-Luther-University Halle-Wittenberg
Halle, Germany

MARCEL DEKKER, INC. NEW YORK • BASEL

Library of Congress Cataloging-in-Publication Data
A catalog record for this book is available from the Library of Congress.

ISBN: 0-8247-0951-9

This book is printed on acid-free paper.

Headquarters
Marcel Dekker, Inc.
270 Madison Avenue, New York, NY 10016
tel: 212-696-9000; fax: 212-685-4540

Eastern Hemisphere Distribution
Marcel Dekker AG
Hutgasse 4, Postfach 812, CH-4001 Basel, Switzerland
tel: 41-61-260-6300; fax: 41-61-260-6333

World Wide Web
http://www.dekker.com

The publisher offers discounts on this book when ordered in bulk quantities. For more information, write to Special Sales/Professional Marketing at the headquarters address above.

Copyright © 2003 by Marcel Dekker, Inc. All Rights Reserved.

Neither this book nor any part may be reproduced or transmitted in any form or by any means, electronic or mechanical, including photocopying, microfilming, and recording, or by any information storage and retrieval system, without permission in writing from the publisher.

Current printing (last digit):
10 9 8 7 6 5 4 3 2 1

PRINTED IN THE UNITED STATES OF AMERICA

DRUGS AND THE PHARMACEUTICAL SCIENCES

Executive Editor

James Swarbrick
PharmaceuTech, Inc
Pinehurst, North Carolina

Advisory Board

Larry L Augsburger
University of Maryland
Baltimore, Maryland

David E Nichols
Purdue University
West Lafayette, Indiana

Douwe D Breimer
Gorlaeus Laboratories
Leiden, The Netherlands

Stephen G Schulman
University of Florida
Gainesville, Florida

Trevor M Jones
The Association of the
British Pharmaceutical Industry
London, United Kingdom

Jerome P Skelly
Alexandria, Virginia

Hans E Junginger
Leiden/Amsterdam Center
for Drug Research
Leiden, The Netherlands

Felix Theeuwes
Alza Corporation
Palo Alto, California

Vincent H L Lee
University of Southern California
Los Angeles, California

Geoffrey T Tucker
University of Sheffield
Royal Hallamshire Hospital
Sheffield, United Kingdom

Peter G Welling
Institut de Recherche Jouvelnal
Fresnes, France

© 2003 by Marcel Dekker, Inc.

DRUGS AND THE PHARMACEUTICAL SCIENCES

A Series of Textbooks and Monographs

1. Pharmacokinetics, *Milo Gibaldi and Donald Perrier*
2. Good Manufacturing Practices for Pharmaceuticals: A Plan for Total Quality Control, *Sidney H. Willig, Murray M. Tuckerman, and William S. Hitchings IV*
3. Microencapsulation, *edited by J. R. Nixon*
4. Drug Metabolism: Chemical and Biochemical Aspects, *Bernard Testa and Peter Jenner*
5. New Drugs: Discovery and Development, *edited by Alan A. Rubin*
6. Sustained and Controlled Release Drug Delivery Systems, *edited by Joseph R. Robinson*
7. Modern Pharmaceutics, *edited by Gilbert S. Banker and Christopher T. Rhodes*
8. Prescription Drugs in Short Supply: Case Histories, *Michael A. Schwartz*
9. Activated Charcoal: Antidotal and Other Medical Uses, *David O. Cooney*
10. Concepts in Drug Metabolism (in two parts), *edited by Peter Jenner and Bernard Testa*
11. Pharmaceutical Analysis: Modern Methods (in two parts), *edited by James W. Munson*
12. Techniques of Solubilization of Drugs, *edited by Samuel H. Yalkowsky*
13. Orphan Drugs, *edited by Fred E. Karch*
14. Novel Drug Delivery Systems: Fundamentals, Developmental Concepts, Biomedical Assessments, *Yie W. Chien*
15. Pharmacokinetics: Second Edition, Revised and Expanded, *Milo Gibaldi and Donald Perrier*
16. Good Manufacturing Practices for Pharmaceuticals: A Plan for Total Quality Control, Second Edition, Revised and Expanded, *Sidney H. Willig, Murray M. Tuckerman, and William S. Hitchings IV*
17. Formulation of Veterinary Dosage Forms, *edited by Jack Blodinger*
18. Dermatological Formulations: Percutaneous Absorption, *Brian W. Barry*
19. The Clinical Research Process in the Pharmaceutical Industry, *edited by Gary M. Matoren*
20. Microencapsulation and Related Drug Processes, *Patrick B. Deasy*
21. Drugs and Nutrients: The Interactive Effects, *edited by Daphne A. Roe and T. Colin Campbell*
22. Biotechnology of Industrial Antibiotics, *Erick J. Vandamme*

© 2003 by Marcel Dekker, Inc.

23 Pharmaceutical Process Validation, *edited by Bernard T Loftus and Robert A Nash*
24 Anticancer and Interferon Agents Synthesis and Properties, *edited by Raphael M Ottenbrite and George B Butler*
25 Pharmaceutical Statistics Practical and Clinical Applications, *Sanford Bolton*
26 Drug Dynamics for Analytical, Clinical, and Biological Chemists, *Benjamin J Gudzinowicz, Burrows T Younkin, Jr., and Michael J Gudzinowicz*
27 Modern Analysis of Antibiotics, *edited by Adjoran Aszalos*
28 Solubility and Related Properties, *Kenneth C James*
29 Controlled Drug Delivery Fundamentals and Applications, Second Edition, Revised and Expanded, *edited by Joseph R Robinson and Vincent H Lee*
30 New Drug Approval Process Clinical and Regulatory Management, *edited by Richard A Guarino*
31 Transdermal Controlled Systemic Medications, *edited by Yie W Chien*
32 Drug Delivery Devices Fundamentals and Applications, *edited by Praveen Tyle*
33 Pharmacokinetics Regulatory • Industrial • Academic Perspectives, *edited by Peter G Welling and Francis L S Tse*
34 Clinical Drug Trials and Tribulations, *edited by Allen E Cato*
35 Transdermal Drug Delivery Developmental Issues and Research Initiatives, *edited by Jonathan Hadgraft and Richard H Guy*
36 Aqueous Polymeric Coatings for Pharmaceutical Dosage Forms, *edited by James W McGinity*
37 Pharmaceutical Pelletization Technology, *edited by Isaac Ghebre-Sellassie*
38 Good Laboratory Practice Regulations, *edited by Allen F Hirsch*
39 Nasal Systemic Drug Delivery, *Yie W Chien, Kenneth S E Su, and Shyi-Feu Chang*
40 Modern Pharmaceutics Second Edition, Revised and Expanded, *edited by Gilbert S Banker and Christopher T Rhodes*
41 Specialized Drug Delivery Systems Manufacturing and Production Technology, *edited by Praveen Tyle*
42 Topical Drug Delivery Formulations, *edited by David W Osborne and Anton H Amann*
43 Drug Stability Principles and Practices, *Jens T Carstensen*
44 Pharmaceutical Statistics Practical and Clinical Applications, Second Edition, Revised and Expanded, *Sanford Bolton*
45 Biodegradable Polymers as Drug Delivery Systems, *edited by Mark Chasin and Robert Langer*
46 Preclinical Drug Disposition A Laboratory Handbook, *Francis L S Tse and James J Jaffe*
47 HPLC in the Pharmaceutical Industry, *edited by Godwin W Fong and Stanley K Lam*
48 Pharmaceutical Bioequivalence, *edited by Peter G Welling, Francis L S Tse, and Shrikant V Dinghe*

© 2003 by Marcel Dekker, Inc.

49. Pharmaceutical Dissolution Testing, *Umesh V. Banakar*
50. Novel Drug Delivery Systems: Second Edition, Revised and Expanded, *Yie W. Chien*
51. Managing the Clinical Drug Development Process, *David M. Cocchetto and Ronald V. Nardi*
52. Good Manufacturing Practices for Pharmaceuticals: A Plan for Total Quality Control, Third Edition, *edited by Sidney H. Willig and James R. Stoker*
53. Prodrugs: Topical and Ocular Drug Delivery, *edited by Kenneth B. Sloan*
54. Pharmaceutical Inhalation Aerosol Technology, *edited by Anthony J. Hickey*
55. Radiopharmaceuticals: Chemistry and Pharmacology, *edited by Adrian D. Nunn*
56. New Drug Approval Process: Second Edition, Revised and Expanded, *edited by Richard A. Guarino*
57. Pharmaceutical Process Validation: Second Edition, Revised and Expanded, *edited by Ira R. Berry and Robert A. Nash*
58. Ophthalmic Drug Delivery Systems, *edited by Ashim K. Mitra*
59. Pharmaceutical Skin Penetration Enhancement, *edited by Kenneth A. Walters and Jonathan Hadgraft*
60. Colonic Drug Absorption and Metabolism, *edited by Peter R. Bieck*
61. Pharmaceutical Particulate Carriers: Therapeutic Applications, *edited by Alain Rolland*
62. Drug Permeation Enhancement: Theory and Applications, *edited by Dean S. Hsieh*
63. Glycopeptide Antibiotics, *edited by Ramakrishnan Nagarajan*
64. Achieving Sterility in Medical and Pharmaceutical Products, *Nigel A. Halls*
65. Multiparticulate Oral Drug Delivery, *edited by Isaac Ghebre-Sellassie*
66. Colloidal Drug Delivery Systems, *edited by Jörg Kreuter*
67. Pharmacokinetics: Regulatory • Industrial • Academic Perspectives, Second Edition, *edited by Peter G. Welling and Francis L. S. Tse*
68. Drug Stability: Principles and Practices, Second Edition, Revised and Expanded, *Jens T. Carstensen*
69. Good Laboratory Practice Regulations: Second Edition, Revised and Expanded, *edited by Sandy Weinberg*
70. Physical Characterization of Pharmaceutical Solids, *edited by Harry G. Brittain*
71. Pharmaceutical Powder Compaction Technology, *edited by Göran Alderborn and Christer Nyström*
72. Modern Pharmaceutics: Third Edition, Revised and Expanded, *edited by Gilbert S. Banker and Christopher T. Rhodes*
73. Microencapsulation: Methods and Industrial Applications, *edited by Simon Benita*
74. Oral Mucosal Drug Delivery, *edited by Michael J. Rathbone*
75. Clinical Research in Pharmaceutical Development, *edited by Barry Bleidt and Michael Montagne*

© 2003 by Marcel Dekker, Inc.

76 The Drug Development Process Increasing Efficiency and Cost Effectiveness, *edited by Peter G Welling, Louis Lasagna, and Umesh V Banakar*
77 Microparticulate Systems for the Delivery of Proteins and Vaccines, *edited by Smadar Cohen and Howard Bernstein*
78 Good Manufacturing Practices for Pharmaceuticals A Plan for Total Quality Control, Fourth Edition, Revised and Expanded, *Sidney H Willig and James R Stoker*
79 Aqueous Polymeric Coatings for Pharmaceutical Dosage Forms Second Edition, Revised and Expanded, *edited by James W McGinity*
80 Pharmaceutical Statistics Practical and Clinical Applications, Third Edition, *Sanford Bolton*
81 Handbook of Pharmaceutical Granulation Technology, *edited by Dilip M Parikh*
82 Biotechnology of Antibiotics Second Edition, Revised and Expanded, *edited by William R Strohl*
83 Mechanisms of Transdermal Drug Delivery, *edited by Russell O Potts and Richard H Guy*
84 Pharmaceutical Enzymes, *edited by Albert Lauwers and Simon Scharpe*
85 Development of Biopharmaceutical Parenteral Dosage Forms, *edited by John A Bontempo*
86 Pharmaceutical Project Management, *edited by Tony Kennedy*
87 Drug Products for Clinical Trials An International Guide to Formulation • Production • Quality Control, *edited by Donald C Monkhouse and Christopher T Rhodes*
88 Development and Formulation of Veterinary Dosage Forms Second Edition, Revised and Expanded, *edited by Gregory E Hardee and J Desmond Baggot*
89 Receptor-Based Drug Design, *edited by Paul Leff*
90 Automation and Validation of Information in Pharmaceutical Processing, *edited by Joseph F deSpautz*
91 Dermal Absorption and Toxicity Assessment, *edited by Michael S Roberts and Kenneth A Walters*
92 Pharmaceutical Experimental Design, *Gareth A Lewis, Didier Mathieu, and Roger Phan-Tan-Luu*
93 Preparing for FDA Pre-Approval Inspections, *edited by Martin D Hynes III*
94 Pharmaceutical Excipients Characterization by IR, Raman, and NMR Spectroscopy, *David E Bugay and W Paul Findlay*
95 Polymorphism in Pharmaceutical Solids, *edited by Harry G Brittain*
96 Freeze-Drying/Lyophilization of Pharmaceutical and Biological Products, *edited by Louis Rey and Joan C May*
97 Percutaneous Absorption Drugs–Cosmetics–Mechanisms–Methodology, Third Edition, Revised and Expanded, *edited by Robert L Bronaugh and Howard I Maibach*

© 2003 by Marcel Dekker, Inc.

98. Bioadhesive Drug Delivery Systems: Fundamentals, Novel Approaches, and Development, *edited by Edith Mathiowitz, Donald E. Chickering III, and Claus-Michael Lehr*
99. Protein Formulation and Delivery, *edited by Eugene J. McNally*
100. New Drug Approval Process: Third Edition, The Global Challenge, *edited by Richard A. Guarino*
101. Peptide and Protein Drug Analysis, *edited by Ronald E. Reid*
102. Transport Processes in Pharmaceutical Systems, *edited by Gordon L. Amidon, Ping I. Lee, and Elizabeth M. Topp*
103. Excipient Toxicity and Safety, *edited by Myra L. Weiner and Lois A. Kotkoskie*
104. The Clinical Audit in Pharmaceutical Development, *edited by Michael R. Hamrell*
105. Pharmaceutical Emulsions and Suspensions, *edited by Francoise Nielloud and Gilberte Marti-Mestres*
106. Oral Drug Absorption: Prediction and Assessment, *edited by Jennifer B. Dressman and Hans Lennernäs*
107. Drug Stability: Principles and Practices, Third Edition, Revised and Expanded, *edited by Jens T. Carstensen and C. T. Rhodes*
108. Containment in the Pharmaceutical Industry, *edited by James P. Wood*
109. Good Manufacturing Practices for Pharmaceuticals: A Plan for Total Quality Control from Manufacturer to Consumer, Fifth Edition, Revised and Expanded, *Sidney H. Willig*
110. Advanced Pharmaceutical Solids, *Jens T. Carstensen*
111. Endotoxins: Pyrogens, LAL Testing, and Depyrogenation, Second Edition, Revised and Expanded, *Kevin L. Williams*
112. Pharmaceutical Process Engineering, *Anthony J. Hickey and David Ganderton*
113. Pharmacogenomics, *edited by Werner Kalow, Urs A. Meyer, and Rachel F. Tyndale*
114. Handbook of Drug Screening, *edited by Ramakrishna Seethala and Prabhavathi B. Fernandes*
115. Drug Targeting Technology: Physical • Chemical • Biological Methods, *edited by Hans Schreier*
116. Drug–Drug Interactions, *edited by A. David Rodrigues*
117. Handbook of Pharmaceutical Analysis, *edited by Lena Ohannesian and Anthony J. Streeter*
118. Pharmaceutical Process Scale-Up, *edited by Michael Levin*
119. Dermatological and Transdermal Formulations, *edited by Kenneth A. Walters*
120. Clinical Drug Trials and Tribulations: Second Edition, Revised and Expanded, *edited by Allen Cato, Lynda Sutton, and Allen Cato III*
121. Modern Pharmaceutics: Fourth Edition, Revised and Expanded, *edited by Gilbert S. Banker and Christopher T. Rhodes*
122. Surfactants and Polymers in Drug Delivery, *Martin Malmsten*
123. Transdermal Drug Delivery: Second Edition, Revised and Expanded, *edited by Richard H. Guy and Jonathan Hadgraft*

© 2003 by Marcel Dekker, Inc.

124 Good Laboratory Practice Regulations Second Edition, Revised and Expanded, *edited by Sandy Weinberg*
125 Parenteral Quality Control Sterility, Pyrogen, Particulate, and Package Integrity Testing Third Edition, Revised and Expanded, *Michael J Akers, Daniel S Larrimore, and Dana Morton Guazzo*
126 Modified-Release Drug Delivery Technology, *edited by Michael J Rathbone, Jonathan Hadgraft, and Michael S Roberts*
127 Simulation for Designing Clinical Trials A Pharmacokinetic-Pharmacodynamic Modeling Perspective, *edited by Hui C Kimko and Stephen B Duffull*
128 Affinity Capillary Electrophoresis in Pharmaceutics and Biopharmaceutics, *edited by Reinhard H H Neubert and Hans-Hermann Rüttinger*

ADDITIONAL VOLUMES IN PREPARATION

Pharmaceutical Process Validation An International Third Edition, Revised and Expanded, *edited by Robert A Nash and Alfred H Wachter*

Ophthalmic Drug Delivery Systems Second Edition, Revised and Expanded, *edited by Ashim K Mitra*

Pharmaceutical Gene Delivery Systems, *edited by Alain Rolland and Sean M Sullivan*

Biomarkers in Clinical Drug Development, *edited by John Bloom*

Pharmaceutical Inhalation Aerosol Technology Second Edition, Revised and Expanded, *edited by Anthony J Hickey*

Pharmaceutical Extrusion Technology, *edited by Isaac Ghebre-Sellassie and Charles Martin*

© 2003 by Marcel Dekker, Inc.

Preface

Since the pioneering accomplishments of Hjertén (1) and particularly of Jorgenson and Lukacs (2), capillary electrophoresis (CE) has undergone a dynamic development, producing a variety of applications. In chemical and pharmaceutical analysis, CE was employed mainly to separate and quantify drugs; this subject has recently been reviewed (3). The implementation of CE in quality control or drug profiling in biological systems has been illustrated in numerous studies. Capillary electrophoresis separations can be performed in different modes, using the same technical equipment. Capillary zone electrophoresis (CZE) and micellar electrokinetic chromatography (MEKC), introduced by Terabe et al. (4), are most frequently employed.

In recent years, much of the research work in the pharmaceutical sciences was focused on the development of effective vehicle systems, such as micelles, microemulsions, and liposomes, for drugs that are critical with respect to bioavailability. Knowledge of this subject is a prerequisite to developing vehicle systems for special administration routes, such as dermal, transdermal, intravenous, and nasal.

In pharmaceutics, therefore, simple and effective methods and procedures are needed to characterize the interactions of drugs with pharmaceutical excipients (polysaccharides, cyclodextrins, etc.) and vehicle systems (micelles, microemulsions, and liposomes) in order to optimize the load of vehicle systems with the drugs.

© 2003 by Marcel Dekker, Inc.

On the other hand, more and more research interest has been focused on the interactions of drugs and vehicle systems with biological target structures such as receptors (cells, proteins, nucleic acids, etc.). In recent years, interactions between proteins and nucleic acids were studied to generate artificial viral systems for gene therapy. Another interesting focus is the study of immunoreactions.

In biopharmaceutics, effective methods are strongly needed, not only to characterize the interactions of drugs and vehicles with biological structures in order to optimize pharmaceutical vehicle systems, but also to study the interactions between biological molecules and to investigate immunoreactions.

All experimental techniques used for measuring the affinity of one molecule for another are based on the measurement of changes in physicochemical properties of the drug, depending on the properties and the concentration of the interacting partner. Changes in size, charge, and other properties of the complex may result in measurable differences in molecular weight (size exclusion methods), sedimentation (ultracentrifugation), diffusion rate (immunodiffusion, equilibrium dialysis), spectroscopic properties (fluorescence quenching, spectral shift), and electrophoretic migration.

In recent years, classic CE has been modified in several ways. This book, therefore, first gives a brief introduction to the principles and techniques of CE (Chapter 1).

Affinity capillary electrophoresis (ACE) relates changes in the electrophoretic mobility of a drug (analyte) after complexation with a substrate (pharmaceutical excipient, vehicle system, and biological structure) present in the background electrolyte to the association constant K_A. The electrophoretic mobility of a molecule (drug) in free solution is proportional to its electrical charge, q, and inversely related to the hydrodynamic radius, r, which depends on the molecular mass, M. If the drug (injected as the sample) shows interaction with a substrate, its mobility should be shifted compared to the one obtained in free solution. A quantification is possible and leads to association constants. The principle of ACE as well as the methods for explaining and quantifying the results are described in Chapter 2.

Interaction equilibria, e.g., between drugs, excipients, vehicle systems, and biological structures, reflect the sum of interactions, which are nonspecific (hydrophobic) and specific (electrostatic dipole–dipole and dipole–induced dipole and hydrogen bonding). The soft method of ACE does not disturb the sensitive equilibria via any chemical modification.

In the past few years, the use of ACE in pharmaceutics and biopharmaceutics has expanded to the following areas:

© 2003 by Marcel Dekker, Inc.

- To measure physicochemical and thermodynamical parameters of drugs
- To characterize the affinity of drugs to pharmaceutical excipients (polysaccharides, other native and synthetic polymers, cyclodextrins, etc.) and vehicle systems (micelles, microemulsions, and liposomes)
- To determine binding constants between drugs and biological structures (e.g., receptors, cells, peptide fragments), proteins (e.g., enzymes), nucleic acids, and plasmids
- To characterize interactions between biologically relevant molecules, e.g., protein–protein and protein–nucleic acid interactions, as well as immunoreactions

The first part of this book presents theoretical basics necessary to understand the principles and techniques of CE as well as ACE. This knowledge opens access to potential applications in pharmaceutics, e.g., the investigation of interaction partners improving the solubility of lipophilic and barely water-soluble drugs and the determination of the effects of amphiphilic ion-pairing or complexation reagents (e.g., pharmaceutical excipients) on the permeation as well as absorption behavior of hydrophilic drugs. ACE enables the calculation of equilibrium constants, which are a measure of the strength of interaction. Although MEKC and ACE are based on the same principle, the recent literature (as well as this book) discusses these methods separately. However, MEKC can be considered a special case of ACE, differing only in the mode of mathematical description. In addition, the general calculation of association constants (K_A) and partition coefficients (K_P) is described.

Part II starts with the possibilities of ACE for characterizing the relevant physicochemical properties of drugs such as lipophilicity/hydrophilicity as well as thermodynamic parameters such as enthalpy of solubilization. This part also characterizes interactions between pharmaceutical excipients such as amphiphilic substances (below CMC) and cyclodextrins, which are of interest for influencing the bioavailability of drugs from pharmaceutical formulations. The same holds for interactions of drugs with pharmaceutical vehicle systems such as micelles, microemulsions, and liposomes.

Part III presents the methods based on ACE for studying interactions of drugs and pharmaceutical vehicle systems with biological structures such as receptors, proteins, polysaccharides, and nucleic acids. This part also describes and discusses methods for characterizing protein–protein interactions and immunoreactions.

Part IV covers the relevance of new combination (i.e., hyphenation) techniques such as CE-ESI- (electrospray ionization) MS (mass spectrometry) and CE-ESI-TOF- (time of flight) MS for ACE.

© 2003 by Marcel Dekker, Inc.

This book outlines the fascinating possibilities of the application of ACE and related technologies in the most interesting emerging fields of pharmaceutics (controlled drug delivery) and biopharmaceutics (drug targeting).

Reinhard H. H. Neubert

REFERENCES

1. S Hjertén. Free Zone Electrophoresis. Almquist and Wiksells, Uppsala, Sweden, 1967.
2. JW Jorgenson, KD Lukacs. Zone electrophoresis in open-tubular glass capillaries. Anal Chem 53:1298–1302, 1981.
3. LA Holland, NP Chetwyn, MD Perkins, SM Lunte. Capillary electrophoresis in pharmaceutical analysis. Pharm Res 14:372–387, 1997.
4. S Terabe, K Otsuka, K Ichikawa, A Tsuchiya, T Ando. Electrokinetic separations with micellar solutions and open-tubular capillaries. Anal Chem 56:111–113, 1984.

© 2003 by Marcel Dekker, Inc.

Contents

Preface
Contributors

Part I: Principles and Theory

1. Principles of Capillary Electrophoresis
   Jörg Schiewe

2. Theory of Affinity Electrophoresis
   Hans-Hermann Rüttinger

Part II: Application of Affinity Capillary Electrophoresis in Pharmaceutics

3. Determination of Physicochemical Parameters
   Yasushi Ishihama

4. Affinity of Drugs to Excipients
   Manuela Plätzer and Reinhard H. H. Neubert

© 2003 by Marcel Dekker, Inc.

5. Affinity of Drugs to Pharmaceutical Vehicle Systems: Micelles
Maria A. Schwarz and Peter C. Hauser

6. Affinity of Drugs to Pharmaceutical Vehicle Systems: Microemulsions
Yahya Mrestani

7. Interaction of Drugs with Liposomes and Proteoliposomes
Caroline Engvall and Per Lundahl

8. Interactions Between Chiral Drugs and Cyclodextrins
Gottfried Blaschke and Bezhan Chankvetadze

Part III: Application of Affinity Capillary Electrophoresis in Biopharmaceutics

9. Affinity of Drugs to Proteins and Protein–Protein Interactions
Steffen Kiessig and Frank Thunecke

10. Affinity Capillary Electrophoresis: DNA Interactions with Peptides, Proteins, and Modified DNA
Michael W. Linscheid

11. Characterization of Polysaccharide Interactions
Charuwan Thanawiroon, Wenjun Mao, and Robert J. Linhardt

12. Characterization of Immunoreactions
Andrea Kühn, Steffen Kiessig, and Frank Thunecke

Part IV: New Combination Techniques and Conclusions

13. Hyphenation of Affinity Capillary Electrophoresis with Mass Spectrometry
Klaus Raith

14. Conclusions
Reinhard H. H. Neubert and Hans-Hermann Rüttinger

© 2003 by Marcel Dekker, Inc.

Contributors

Gottfried Blaschke, Ph.D. Institute of Pharmaceutical and Medicinal Chemistry, University of Münster, Münster, Germany

Bezhan Chankvetadze, Ph.D.* Department of Chemistry, Tbilisi State University, Tbilisi, Georgia

Caroline Engvall, M.Sc.Pharm. Department of Biochemistry, Biomedical Center, Uppsala University, Uppsala, Sweden

Peter C. Hauser, Ph.D. Department of Chemistry, University of Basel, Basel, Switzerland

Yasushi Ishihama, Ph.D.† Analytical Research Laboratories, Eisai Co., Ltd., Tsukuba, Ibaraki, Japan

Steffen Kiessig, Ph.D. Business Unit Separation and Quantification, Solvias AG, Basel, Switzerland

**Current affiliation*: Institute of Pharmaceutical and Medicinal Chemistry, University of Münster, Münster, Germany.

†Current affiliation: Protein Interaction Laboratory, Department of Biochemistry and Molecular Biology, University of Southern Denmark, Odense, Denmark.

© 2003 by Marcel Dekker, Inc.

Andrea Kühn Department of Pharmacy, Martin-Luther-University Halle-Wittenberg, Halle, Germany

Robert J. Linhardt, Ph.D. Departments of Chemistry, Medicinal and Natural Products Chemistry, and Chemical and Biochemical Engineering, University of Iowa, Iowa City, Iowa, U.S.A.

Michael W. Linscheid, Ph.D. Department of Chemistry, Humboldt Universität zu Berlin, Berlin, Germany

Per Lundahl, Ph.D. Department of Biochemistry, Biomedical Center, Uppsala University, Uppsala, Sweden

Wenjun Mao, Ph.D. Departments of Chemistry, Medicinal and Natural Products Chemistry, and Chemical and Biochemical Engineering, University of Iowa, Iowa City, Iowa, U.S.A.

Yahya Mrestani, Ph.D. Department of Pharmacy, Institute of Pharmaceutics and Biopharmaceutics, Martin-Luther-University Halle-Wittenberg, Halle, Germany

Reinhard H. H. Neubert, Ph.D. Department of Pharmacy, Institute of Pharmaceutics and Biopharmaceutics, Martin-Luther-University Halle-Wittenberg, Halle, Germany

Manuela Plätzer, Ph.D. Department of Pharmacy, Institute of Pharmaceutics and Biopharmaceutics, Martin-Luther-University Halle-Wittenberg, Halle, Germany

Klaus Raith, Ph.D. Department of Pharmacy, Institute of Pharmaceutics and Biopharmaceutics, Martin-Luther-University Halle-Wittenberg, Halle, Germany

Hans-Hermann Rüttinger, Ph.D. Department of Pharmacy, Institute of Pharmaceutical Chemistry, Martin-Luther-University Halle-Wittenberg, Halle, Germany

Jörg Schiewe, Ph.D. Boehringer Ingelheim Pharma KG, Ingelheim, Germany

© 2003 by Marcel Dekker, Inc.

Maria A. Schwarz, Ph.D. Department of Chemistry, University of Basel, Basel, Switzerland

Charuwan Thanawiroon, M.S. Departments of Chemistry, Medicinal and Natural Products Chemistry, and Chemical and Biochemical Engineering, University of Iowa, Iowa City, Iowa, U.S.A.

Frank Thunecke, Ph.D. Environmental Biotechnology Centre, UFZ Centre for Environmental Research, Leipzig, Germany

© 2003 by Marcel Dekker, Inc.

1
Principles of Capillary Electrophoresis

Jörg Schiewe
Boehringer Ingelheim Pharma KG, Ingelheim, Germany

I. HISTORICAL REVIEW

Over the last 10 years, capillary electrophoresis has matured into a powerful analysis technique focusing on water-soluble ionic analytes. It therefore complements the long-established method of reversed-phase HPLC, where separation is based on hydrophobic interactions of the mainly nonpolar analytes. Pioneering work using electrophoresis as a separation method was first performed by Tiselius dating back to 1937 (1). He found that proteins in buffer solution migrate in the electric field in one direction and at a rate determined by their charge and size. In the early years electrophoretic separation was performed in anticonvective media such as agarose and polyacrylamide gels to minimize solute-zone broadening caused by thermal diffusion and convection. The introduction of open tubular colums in the early 1970s with column diameters in the submillimeter range was an important milestone in free solution electrophoresis, and led to a significant increase in separation efficiency (2,3). Due to their small diameters (50–100 μm), the currents flowing through the capillary are very small, only in the microampere range, thus allowing a high separation voltage up to 30,000 volts at a concurrently low power consumption in the range of milliwatts. Because of the favorable ratio of surface area to volume of narrow-bore capillaries, the negative effects of Joule heating could be minimized, resulting in considerably enhanced separation efficiencies of typically 250,000 theoretical plates (4). A further advantage of the possibility of utilizing high voltages is the significant reduction in analysis time, which in turn decreases zone broadening, leading to high separation efficiency. During the 1980s many

© 2003 by Marcel Dekker, Inc.

practical aspects of sample introduction and analyte detection were solved, helping to establish capillary zone electrophoresis (CZE) as a high-performance analytical technique. The first capillary zone electrophoresis systems became commercially available in the late 1980s.

II. SEPARATION PRINCIPLE IN CAPILLARY ZONE ELECTROPHORESIS

The electrophoretic separation principle is based on the velocity differences of charged solute species moving in an applied electric field. The direction and velocity of that movement are determined by the sum of two vector components, the migration and the electroosmotic flow (EOF). The solute velocity $\vec{\nu}$ is represented as the product of the electric field strength $\vec{E}$ and the sum of ionic mobility $\vec{u}_{\text{Ion}}$ and EOF coefficient $\vec{\mu}_{EOF}$:

$$\vec{\nu} = \vec{E} \cdot (\vec{u}_{\text{Ion}} + \vec{\mu}_{EOF}) \tag{1}$$

Whereas the ionic mobility is a physical constant specific to individual ionic species, the EOF is dependent on the properties of the interface of capillary wall and solution.

To perform capillary electrophoresis the following basic components are necessary: a high voltage power source, a detector and a buffer filled capillary (see Fig. 1).

A. Migration

The migration of a charged species, e.g., its motion under the force of an electric field, is given by Eq. (2), where the strength of the electric field $\vec{E}$ is simply a function of the applied voltage $\vec{U}$ divided by the capillary length L:

$$\vec{\nu} = \vec{E} \cdot \vec{u}_{\text{Ion}}; \quad \vec{E} = \frac{\vec{U}}{L} \tag{2}$$

The ionic mobility $\vec{u}_{\text{Ion}}$ itself depends on the ratio of the charge and size of a specific ion. The electrical force $\vec{F}_e$ experienced by an ion of charge q can be expressed as

$$\vec{F}_e = q \cdot \vec{E} \tag{3}$$

This force is counterbalanced by the frictional force $\vec{F}_{\text{fr}}$, which in the case of a spherical ionic species is given by Stokes law:

$$\vec{F}_{\text{fr}} = 6\pi \cdot \eta \cdot r \cdot \vec{\nu} \tag{4}$$

© 2003 by Marcel Dekker, Inc.

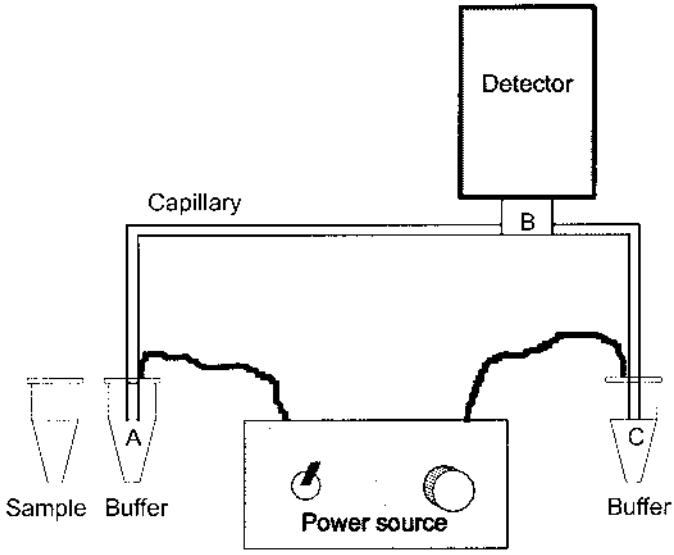

Fig. 1 Schematic drawing of the basic components of a capillary electrophoresis system. The distance $\overline{AB}$ denotes the effective length l and $\overline{AC}$ the total length L of the capillary.

During electrophoresis, a steady state establishes where the vector sum of electrical force and frictional force is zero; therefore, a constant migration velocity $\vec{\nu}$ is attained, given by:

$$q \cdot \vec{E} = 6\pi \cdot \eta \cdot r \cdot \vec{\nu}; \quad \vec{\nu} = \frac{q \cdot \vec{E}}{6\pi \cdot \eta \cdot r} \tag{5}$$

Substitution of $\vec{\nu}$ in Eq. (2) by the expression in Eq. (5) leads to the definition of the ionic mobility $\vec{u}_{\text{Ion}}$:

$$\vec{u}_{\text{Ion}} = \frac{q}{6\pi \cdot \eta \cdot r} \tag{6}$$

From this equation it is evident that the mobility $\vec{u}_{\text{Ion}}$ of an ionic species is directly proportional to the ratio of charge to radius q/r and reciprocal to the viscosity η of the solution. Thus, small, highly charged ions have high mobilities, whereas large, less charged species have low mobilities.

The electrophoretic mobility usually found in standard reference tables is a physical constant determined for complete dissociation extrapolated to infinite dilution. However, the mobility of ionic species measured under practical conditions often depends on protonation/deprotonation equilibria

© 2003 by Marcel Dekker, Inc.

influencing the effective charge of that specific ion and therefore depends on pH (for example, see Fig. 2). In other words, two species of the same ionic mobility but of different pK_a value can be separated in CZE when the pH of the buffer is selected accordingly. Besides the influence of the pH, chemical equilibria leading to a change of the charge (e.g., complexation reactions) also affect the electrophoretic mobility in the same way.

B. Electroosmotic Flow (EOF)

The second parameter influencing the movement of all solutes in free-zone electrophoresis is the electroosmotic flow. It can be described as a bulk hydraulic flow of liquid in the capillary driven by the applied electric field. It is a consequence of the surface charge of the inner capillary wall. In buffer-filled capillaries, an electrical double layer is established on the inner wall due to electrostatic forces. The double layer can be quantitatively described by the zeta-potential $\vec{\zeta}$, and it consists of a rigid Stern layer and a movable diffuse layer. The EOF results from the movement of the diffuse layer of electrolyte ions in the vicinity of the capillary wall under the force of the electric field applied. Because of the solvated state of the layer forming ions, their movement drags the whole bulk of solution.

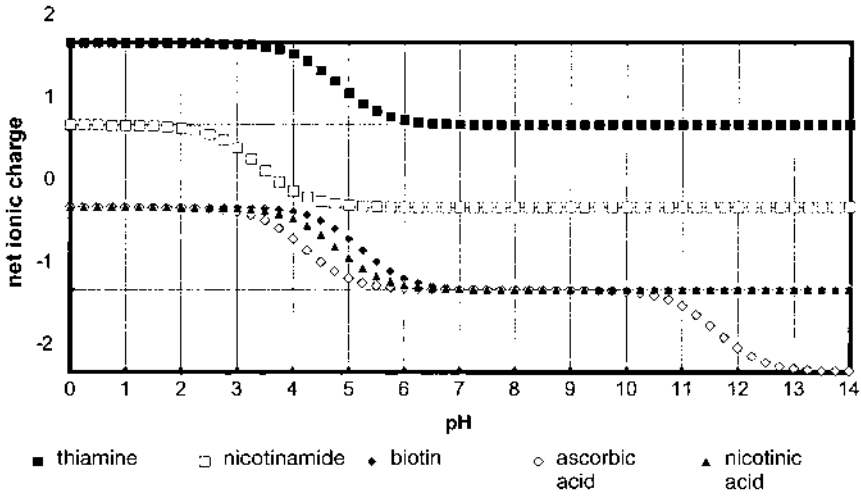

Fig. 2 Net ionic charge of thiamine (pK_a = 4.80), nicotinamide (pK_a = 3.42), biotin (pK_a = 5.20), ascorbic acid (pK_{a1} = 4.17; pK_{a2} = 11.57) and nicotinic acid (pK_a = 4.76).

© 2003 by Marcel Dekker, Inc.

The electroosmotic flow velocity can be given as

$$\vec{\nu}_{EOF} = \vec{\zeta} \cdot \frac{\varepsilon}{4 \cdot \pi \cdot \eta} \cdot \vec{E} \tag{7}$$

ε denotes the dielectric constant of the electrolyte solution. The factor $\vec{\zeta} \cdot (\varepsilon / 4 \cdot \pi \cdot \eta)$ on the right-hand side of Eq. (7) is also referred to as the electroosmotic mobility $\vec{\mu}_{EOF}$.

Since the driving force of the flow is uniformly distributed across the diameter of the capillary, the flow profile is essentially flat. This flat profile contributes to the very high separation efficiency of CZE. Electroosmotic pumping therefore is beneficial, in contrast to laminar flow generated by a HPLC pump, where a parabolic flow profile is established. The electroosmotic flow rate and its flat profile are generally independent of the capillary diameter. However, if the internal diameter of the capillary exceeds 250 μm, the flat profile is increasingly disrupted.

The capillaries most commonly utilized for CZE are made of silicate (glass) material, particularly fused silica. Under aqueous conditions the wall silanol groups can deprotonate and the capillary wall will form a negative charge. Hence, cations from solution are attracted to this negatively charged capillary surface, leading to an electrical double layer having a positively charged diffuse zone that moves toward the cathode. This causes a net flow of all solutes, cations, neutrals, and even anions (as long as their electrophoretic mobility does not exceed the electroosmotic flow coefficient) toward the cathode. Thus, all these species can be detected in a single run (for example, see Fig. 3).

For fused silica the magnitude of the EOF is controlled by the pH value of the electrophoretic buffer used. At high pH where the silanol groups are predominantly deprotonated, the EOF is significantly greater than at low pH (pH < 4) where they become protonated. Depending on the specific conditions, the EOF can vary by more than one order of magnitude between pH 2 and pH 12. In nonionic materials such as Teflon and other polymers, electroosmotic flow is also encountered. The electrical double layer in this case results from adsorption of buffer anions to the polymer surface.

1. Electroosmotic Flow Control

While the electroosmotic flow is a positive attribute of electrophoresis in most cases, there are instances where EOF needs to be carefully controlled. For example, too high an electroosmotic flow may decrease resolution, especially of cations with similar mobility. In a different case, when analyzing anions of very different mobilities (anorganic and organic) in one run, the electroosmotic flow needs to be reversed (5). Furthermore, alternative elec-

© 2003 by Marcel Dekker, Inc.

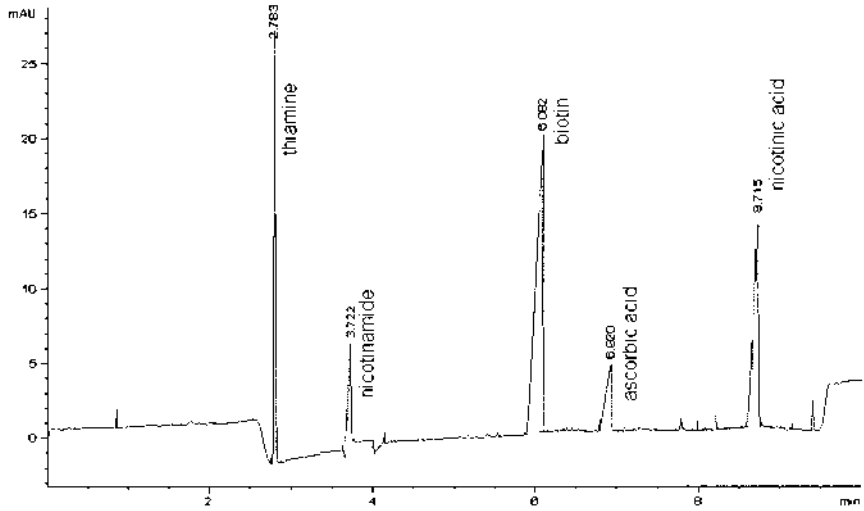

Fig. 3 Electropherogram of five water-soluble vitamines: thiamine (cationic), nicotinamide (nonionic), biotin (anionic), ascorbic acid (anionic), and nicotinic acid (anionic) in 20 *mM* phosphate run buffer at pH 8.0.

trophoretic separation modes, such as capillary isotachophoresis (CITP), capillary isoelectric focusing (CIEF), and capillary gel electrophoresis (CGE), require zero EOF.

The electroosmotic flow can be effected in several ways. Most effectively, the zeta-potential can be influenced by capillary wall coating. This coating can be achieved either by adsorption of cationic surfactants, such as cetyl-tributyl-ammonim bromide (CTAB), dissolved in the electrophoresis buffer or by chemical reaction of the surface silanol groups with organic silanes. Both methods have advantages and disadvantages. While adding organic surfactants can reverse the electroosmotic flow, it may also affect the separation of ions due to formation of ion complexes or changes in the ionic mobility. On the other hand, surface modification by chemical silanization is often unstable, especially when working with basic buffer solutions.

Another preferred method for reducing the electroosmotic flow is based on increasing the buffer viscosity. This is usually achieved by filling the capillary with polymeric gels. Thereby, electroosmotic flow is reduced to zero; the ionic mobility, nevertheless, is also affected [see Eq. (6)]. Additionally, in capillary gel electrophoresis the separation of ionic species is achieved mainly by the sieving effect of the gel, which is advantageous when separating ionic species having the same mobility, such as polynucleotides.

© 2003 by Marcel Dekker, Inc.

To complete the picture there are two, more academic methods to affect the EOF. One, applying an external electrical field across the radius of the capillary (6), and the other, to reduce EOF by applying a back-pressure (7). While the external electrical field approach is a method directly modifying the zeta-potential of the capillary wall, it is not applicable with commercial apparatuses. The back-pressure technique, on the other hand, has the disadvantage that the flat electroosmotic flow profile is disrupted by superposition of a pressure-driven laminar flow profile; hence, the efficiency of separation deteriorates.

C. Factors Affecting Efficiency

The definition of separation efficiency known from chromatography, expressed as height equivalent to a theoretical plate (HETP), can be applied in the same way to CZE:

$$\text{HETP} = \frac{\sigma^2}{l} \tag{8}$$

σ^2 denotes the coefficient of variance of a Gausian peak, and l is the effective length of the capillary (length from site of injection to site of detection). Based on this definition the number of theoretical plates N along the effective length of the capillary l can be expressed as

$$N = \frac{l}{\text{HETP}} = \left(\frac{l}{\sigma}\right)^2 \tag{9}$$

Equations (8) and (9) show, that separation efficiency is determined by the peak width, in these equations expressed as the coefficient of variance σ^2. The smaller is σ^2, the narrower is the peak, and hence the greater is the efficiency to separate two neighboring peaks.

The width of a peak, or, in other words, the length of a solute zone, is affected primarily by diffusion phenomena leading to a broadening of the solute zone. In addition, in capillary zone electrophoresis, zone broadening can be caused by thermal effects, electrodispersion, or adsorptive effects. All these effects can be expressed as coefficients of variance σ_i^2, adding to a total coefficient of variance of the system σ_{total}^2:

$$\sigma_{\text{total}}^2 = \sum \sigma_i^2 = \sigma_{\text{Diff}}^2 + \sigma_{\text{Therm}}^2 + \sigma_{\text{Electrodisp}}^2 + \sigma_{Ads}^2 + \cdots \tag{10}$$

In the following, the major factors affecting separation efficiency are discussed.

Under ideal practical conditions, e.g., no Joule heating and no solute–wall interactions, diffusion is the sole contribution to zone broadening. Since the flow profile in CZE is flat, radial diffusion can be neglected, and only

© 2003 by Marcel Dekker, Inc.

longitudinal diffusion can be considered to be effective, leading to this equation to describe the diffusion term:

$$\sigma^2_{\text{Diff}} = 2 \cdot D \cdot t \tag{11}$$

While the diffusion coefficient D is a physical constant for a particular species, t denotes the migration time, which is proportional to the velocity of migration $\vec{\nu}$ [Eq. (2)] and the effective length of the capillary l. Hence, it follows that

$$\sigma^2_{\text{Diff}} = \frac{2 \cdot D \cdot l}{\vec{u}_{\text{Ion}} \cdot \vec{E}} \tag{12}$$

Substituting Eq. (12) into Eq. (9) yields a fundamental expression for the plate number:

$$N = \frac{\vec{u}_{\text{Ion}} \cdot \vec{E} \cdot l}{2 \cdot D} \tag{13}$$

Since the electric field $\vec{E}$ can be expressed as $\vec{U}/L$, with L being the total length of the capillary, Eq. (13) can be transformed into

$$N = \frac{\vec{u}_{\text{Ion}} \cdot f}{2 \cdot D} \cdot \vec{U} \tag{14}$$

f being the ratio l/L of effective length l to total length L of the capillary ($l/L = \langle 0.5 \ldots 1.0 \rangle$). From Eq. (14) it follows that the separation efficiency N is directly proportional to the voltage $\vec{U}$ applied. Please note that, in contrast, the height equivalent of a theoretical plate (HETP) is inversely related to the field strength $\vec{E}$ [combination of Eqs. (8) and (12)]. The higher the electrical field strength, the smaller the height equivalent of a theoretical plate, or, in other words, the more theoretical plates per unit length.

In conventional slab-gel electrophoresis the feasibility of using high voltages is limited, due to considerable power consumption leading to heating of the gel slab. Heating is problematic, since it can cause nonuniform temperature gradients, local viscosity changes, and, therefore, zone broadening.

When an electric current is passed through a conductive medium, heat is generated (Joule heating). The temperature increase depends on the power, i.e., the product of current and voltage, and is determined by the conductivity of the buffer and the voltage applied. Significantly elevated temperatures will result when power generation exceeds the amount of heat that can be dissipated.

The use of narrow-bore capillaries greatly reduces this heating effect, because heat can be more efficiently dissipated due to a favorable surface-

© 2003 by Marcel Dekker, Inc.

to-volume ratio. This improved heat dissipation means that higher operating voltages on the order of several ten thousand volts can be applied. It is advantageous to use narrow-inner-diameter capillaries with large outer diameters. The smaller the inner dimensions, the higher the surface-to-volume ratio, which helps to dissipate the generated heat through the capillary wall. The large outer diameter is advantageous due to an improvement of heat transfer to the surroundings.

Zone broadening due to Joule heating can be limited by the reduction of the applied voltage, although this also means a decrease in efficiency. Furthermore, it can be reduced by use of low-conductivity buffers, i.e., buffers that contain ions of low mobility, such as TRIS, borate, histidine, and CAPS. The most efficient way to remove heat from the outer capillary wall is by active capillary cooling. This can most efficiently be accomplished with a cooling system that thermostats the capillary using high-velocity air or a liquid coolant.

Another effect contributing to zone broadening is electrodispersion, i.e., conductivity differences of solute and buffer ions leading to nonsymmetrical peaks. Local differences in conductivity are created along the capillary length due to zones of different ionic mobilities of solutes to be separated that contribute differently to the net current flowing. This means that the voltage applied to the ends of the capillary is not linearly dropped over the length of the capillary. This effect is shown in Figure 4: Zones of low ionic mobility have a lower conductivity. Hence, the voltage drop is much greater, resulting in a much greater electric field strength. For high-mobility ions the opposite holds: A higher conductivity of that zone creates less voltage drop, and thus the local electric field in that zone is much less.

Longitudinal diffusion now leads to movement of ions out of the solute zone into the neighboring volume elements governed by the mobility of the buffer ions. For low-mobility ions this means that they experience a lower electric field strength than inside the solute zone. Therefore, ions diffusing into the buffer volume element upstream of the solute zone (left-hand side in Fig. 4) will move with a lower velocity [according to Eq. (2)] and lag behind the solute zone, ultimately leading to pronounced peak tailing. Low-mobility ions diffusing into the downstream buffer volume element also move more slowly than those inside the solute zone and, hence, will fall back into the moving front. So the peak shape is unsymmetrical: a sharp front and a skewed tailing edge for ions with a lower mobility compared to the buffer.

For high-mobility ions, electrodispersion leads to peak fronting. In this case ions diffusing out of the solute zone upstream will experience a higher electric field and are accelerated back into the solute zone (sharp trailing

© 2003 by Marcel Dekker, Inc.

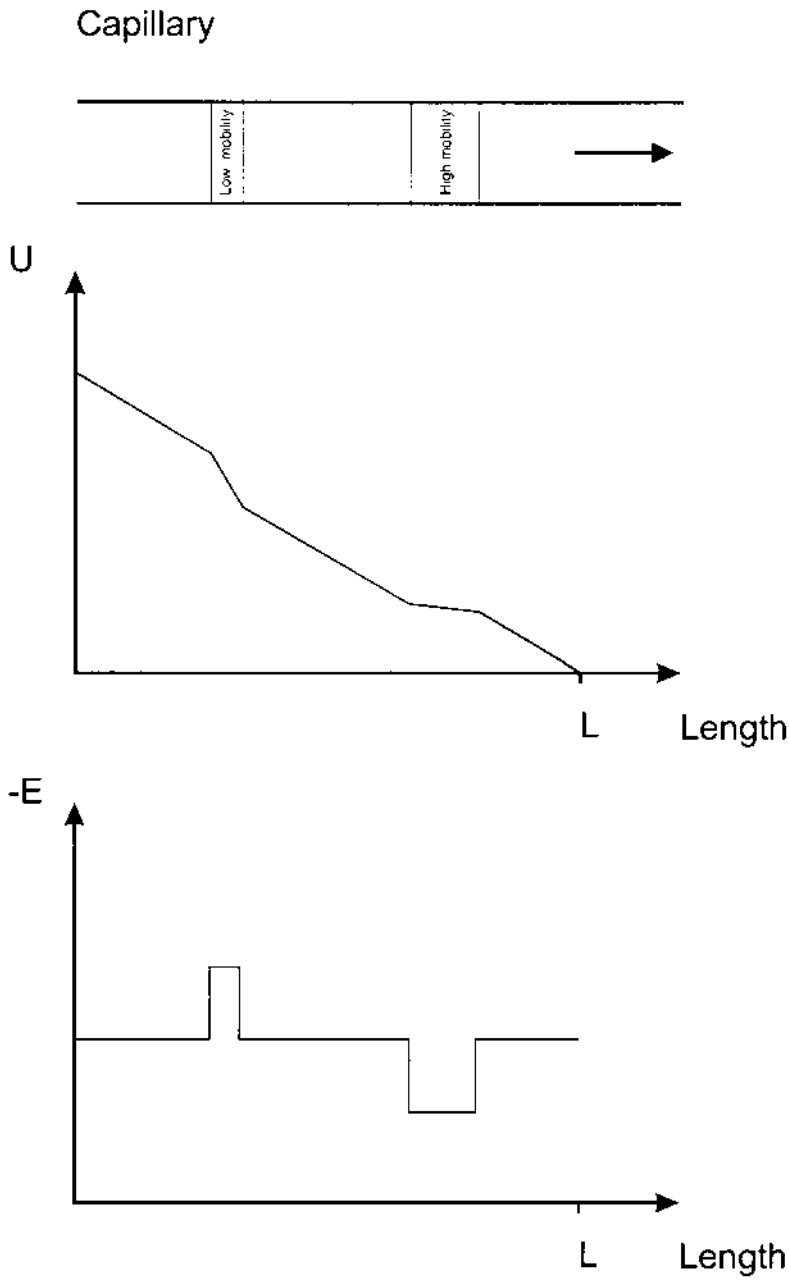

Fig. 4 Illustration of the effect of electrodispersion that is based on local differences of the electric field along the capillary.

© 2003 by Marcel Dekker, Inc.

edge of the peak). Those diffusing into the buffer downstream are accelerated too, but they are drawn away from the solute zone (skewed peak front).

Neutral species remain unaffected by electrodispersion, giving rise to symmetrical peaks. An example electropherogram illustrating peak fronting and peak tailing is shown in Figure 5.

Interactions between the solutes and the capillary wall also have a negative effect on the efficiency in capillary zone electrophoresis. Both hydrophobic interactions and electrostatic interactions of cations with the negatively charged capillary wall can be the cause of solute adsorption. Significant adsorption has been found for high-molecular-weight species, e.g., peptides and proteins. Because of the increased surface-area-to-volume ratio of narrow-bore capillaries, this effect is even more pronounced.

Solute adsorption can be minimized most effectively by capillary wall coating, thereby decreasing the free energy of hydrophobic or ionic interactions. Coating can be achieved either by covalently bonded organic modifiers, e.g., polyacrylamides, sulfonic acids, polyethylene glycols, maltose, and polyvinyl pyrolidinone, or by dynamic deactivation (i.e., addition of

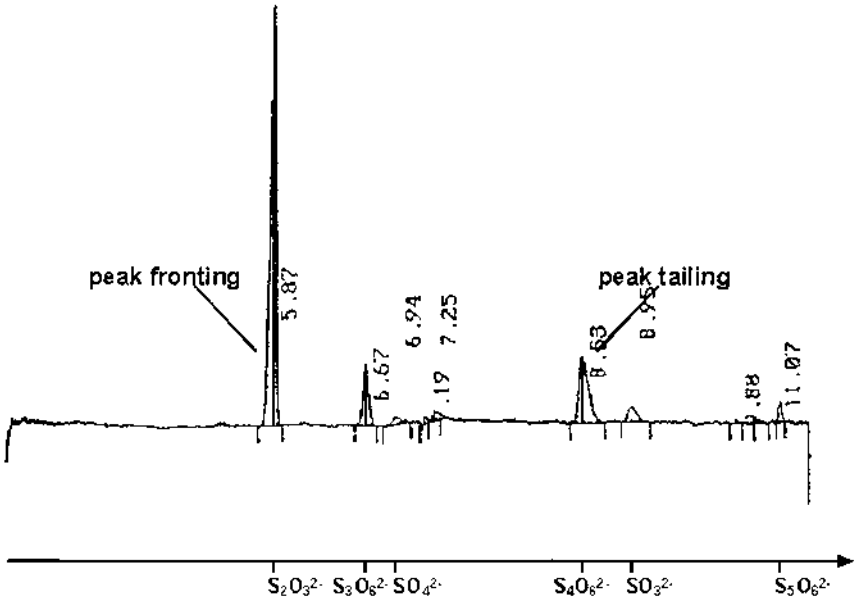

Fig. 5 Electropherogram of six sulfur anions illustrating peak fronting [thiosulfate ($S_2O_3^{2-}$)] and peak tailing [tetrathionate ($S_4O_6^{2-}$)]; for better visibility of peak asymmetry, the perpendicular peak axis is drawn as a solid line. Separation in 20 *mM* chromate run buffer at pH 8.3.

© 2003 by Marcel Dekker, Inc.

modifiers to the buffer solution; see also Sec. II.B.1). Both methods can be used to eliminate or reverse the charge on the capillary wall, alter hydrophobicity, and, hence, limit solute adsorption.

D. Resolution

Capillary zone electrophoresis is a separation technique that benefits from very high efficiency, not selectivity. This is in contrast to chromatography, for which the converse is true. Differences in mobility in the range of 0.01% can be enough for complete resolution of neighboring peaks. The resolution R is defined as

$$R = \frac{t_2 - t_1}{4 \cdot \sigma} \tag{15}$$

t_i denotes the migration time of one species and σ is the standard variation as a measure of the peak width. Substituting t_i and σ in consideration of the efficiency N, Eq. (15) can be written in this form:

$$R = \frac{\Delta \vec{u}_{\text{Ion}}}{4} \cdot \sqrt{\frac{\vec{U}}{2D(\vec{u}_{\text{Av}} + \vec{\mu}_{EOF})}} \tag{16}$$

with $\Delta \vec{u}_{\text{Ion}}$ and $\vec{u}_{\text{Av}}$ denoting the difference and the average ionic mobility of the two ions, respectively.

From Eq. (16) it is evident that, analogous to efficiency, a gain in resolution results from higher voltages $\vec{U}$, although it is only a square root dependency. The voltage must be increased four times to double the resolution.

The effect of the electroosmotic flow on the resolution is also evident from Eq. (16). A high electroosmotic flow in the direction of the moving ions can significantly diminish resolution. Theoretically, infinite resolution of two peaks could be reached when $\vec{\mu}_{EOF}$ is equal but opposite to the average mobility $\vec{u}_{\text{Av}}$. In this case one of the solutes would migrate in the direction of the detector and the other one in the opposite direction. In other words, the separation run would be infinitely long. Thus, for a practical separation the electroosmotic flow should be controlled in a way to achieve baseline resolution ($R = 1$) at minimal separation time.

E. Benefit of Small Capillary Diameters

As just mentioned, the application of high voltages is beneficial because efficiency and resolution increase with increasing voltage. Higher voltages increase the current i through the capillary and this results in higher Joule

© 2003 by Marcel Dekker, Inc.

heating. To avoid band broadening or an interruption of conductivity by formation of gas bubbles, the heat has to be carried away by cooling. The amount of Joule heating that can be dissipated sets an upper limit on the maximum voltage applicable. The heat W generated per unit length of the capillary by the current i flowing through the capillary is equal to the electrical power $U \cdot i$:

$$W = \frac{U \cdot i}{L} = \frac{U^2}{R \cdot L} \tag{17}$$

According to this equation, W is a function of the voltage U squared and the resistance R. The resistance itself depends on the length L, the diameter of the capillary d, and the buffer conductivity κ:

$$R = \frac{4L}{\pi \cdot d^2 \cdot \kappa} \tag{18}$$

Substitution of R in Eq. (17) by Eq. (18) and rearrangement leads to an expression for the maximum voltage applicable:

$$U_{\max} = \sqrt{\frac{4W_{\max}}{\pi \cdot \kappa}} \cdot \frac{L}{d} \tag{19}$$

From this equation it is evident that the maximum voltage depends on the square root of the maximum heat that can be dissipated, the conductivity of the buffer, and the two geometry parameters of the capillary, length L and diameter d. Equation (19) can be rewritten to yield an expression for $E_{\max}$:

$$E_{\max} = \sqrt{\frac{4W_{\max}}{\pi \cdot \kappa}} \cdot \frac{1}{d} \tag{20}$$

Substitution of Eq. (20) into the expression of the efficiency [Eq. (13)] and rearrangement yields an equation for the maximum number of theoretical plates per unit length:

$$\frac{N_{\max}}{l} = \frac{1}{\mathrm{HETP}} = \frac{\vec{u}_{\mathrm{Ion}}}{2D} \sqrt{\frac{4W_{\max}}{\pi \cdot \kappa}} \cdot \frac{1}{d} \tag{21}$$

From this equation it can be seen that the efficiency per unit length is inversely proportional to the capillary diameter. Decreasing the diameter of the capillary will decrease the height equivalent to a theoretical plate. The efficiency per unit length increases. Therefore, smaller-diameter capillaries can be used at shorter lengths, which ultimately decreases the separation time.

Recently, a lot of work in electrophoretic separation has focused on employing chip-based systems, which benefit from the enhancement of ef-

© 2003 by Marcel Dekker, Inc.

ficiency at reduced analysis times due to miniaturization (8). The main arguments for electrophoresis on chips are reduced consumables (sample, reagent, mobile phase), leading to lower costs and waste, and increased sample throughput, based on the increase in efficiency per unit length and time.

III. ALTERNATIVE ELECTROPHORETIC MODES

A. Overview

Capillary zone electrophoresis (CZE) is the most common electrophoretic separation technique due to its simplicity of operation and its flexibility. It is the standard mode for drug analysis, identification of impurities, and pharmacokinetic studies. Other separation modes, such as capillary isotachophoresis (CITP), micellar electrokinetc chromatography (MEKC), capillary electrochromatography (CEC), capillary gel electrophoresis (CGE), capillary isoelectric focusing, and affinity capillary electrophoresis (ACE), have their advantages in solving specific separation problems, since the separation mechanism of each mode is different.

B. Capillary Isotachophoresis

In contrast to CZE, capillary isotachophoresis is a moving-boundary technique. A combination of two buffer systems, a leading buffer and a terminating buffer, is used, and the sample is injected between the two buffer zones prior to the separation run. After a high voltage is applied to both ends of the capillary, a steady state forms, where the solutes form zones according to their different mobilities. The leading buffer is selected to have the highest mobility, whereas the terminating buffer has the lowest mobility. This means that the solute zones move in the order of their mobilities, sandwiched between leading and terminating buffer, until eventually steady state is reached where all zones move at the same velocity. From the condition that the current flowing through the solution is constant in all zones it follows that

$$i = \frac{dq}{dt} = F \cdot A \cdot z_i \cdot c_i \cdot \vec{\nu}_i = F \cdot A \cdot z_i \cdot c_i \cdot \vec{u}_i \cdot \vec{E}_i = \text{const.} \tag{22}$$

In this equation, F denotes the Faraday constant, A is the cross-sectional area of the capillary, z_i is the number of charges, and c_i is the concentration of species i. Having isotachophoretic equilibrium, the term $c_i \cdot \vec{u}_i \cdot \vec{E}_i$ is equal in each of the solute zones.

From Eq. (22) it is evident that if the mobility of the ions (and therefore the conductivity in each zone) is different; constant velocity can be achieved

© 2003 by Marcel Dekker, Inc.

only when the electric field strength also varies from zone to zone, establishing the lowest field across the zone of highest mobility. This phenomenon maintains very sharp boundaries between the zones. When an ion diffuses into a neighboring zone, its velocity changes and it is immediately accelerated or decelerated to reenter its own zone.

Another characteristic feature of CITP is that well-defined concentrations are achieved in each of the solute zones, which are ultimately determined by the concentration of the leading buffer:

$$\frac{c_i}{c_{\text{lead}}} = \frac{\vec{u}_i}{\vec{u}_i + \vec{u}_c} \cdot \frac{\vec{u}_{\text{lead}} + \vec{u}_c}{\vec{u}_{\text{lead}}} \tag{23}$$

According to Kohlrausch, the concentration c_i of a solute i in the adjacent zone can be calculated from the concentration c_{lead} of the leading buffer and the ratio of the ionic mobilities $\vec{u}_i$ and $\vec{u}_{\text{lead}}$, with $\vec{u}_c$ being the ionic mobility of the counterion. That means that zones with lower concentration than the leading buffer are concentrated (sharpened) and that zones of higher concentration are diluted (broadened).

Because zones of constant concentration are moving with constant velocity toward the detector, the detector signal is obtained in the form of steps rather than peaks, as in the case of CZE. Since according to Kohlrausch's relation [Eq. (23)] the information from the sample quantity is no longer related to the concentration of the solute zone, its volume, i.e., the length of that zone, is proportional to the solute quantity in the sample. Therefore, in CITP a characteristic separation plot contains steps of different length.

And CITP is favorably utilized in the analysis of low-molecular-weight ionic species. A difficulty often arises with finding suitable buffer systems that provide leading and terminating ions and also form the appropriate buffer pH. One of the advantages is that the capillary can be loaded with sample up to 30–50% of its length, enabling the analysis of very dilute samples. Furthermore, the principle of predetermined solute concentrations in isotachophoresis is also used as preconcentration step for very dilute samples prior to CZE, MEKC, or CGE.

A subsequent advantage of the zone sharpening effect in CITP is that zone broadening due to diffusion is minimized; in addition, a high ratio of the concentrations of two sample components can be analyzed without loss of analysis performance.

C. Micellar Electrokinetic Chromatography

Micellar electrokinetic chromatography is a hybrid of electrophoresis and chromatography. Introduced by Terabe in 1984 (9), MEKC is one of the most widely used CE modes. Ionic micelles, formed from surfactants added

© 2003 by Marcel Dekker, Inc.

to the run buffer in concentrations above their critical micelle concentration, are used as pseudostationary phase. Due to the chromatographic nature of the separation process, both neutral and ionic compounds can be separated with this mode. Differently from chromatography, MEKC benefits from the flat flow profile of the EOF, leading to the high separation efficiency that is typical of an electrophoretic separation.

The surfactants utilized to form the micelles can be cationic, anionic, zwitterionic, neutral, or mixtures thereof. Often the anionic tensid sodium dodecylsulfate (SDS) is used, forming negatively charged micelles that migrate toward the anode, i.e., in the direction opposite to the EOF. Since under neutral or basic pH conditions the EOF is usually faster than the migration velocity of the micelles, they are drawn toward the cathode, where the detector is placed. During migration of the micelles, the solutes, ionic or nonionic in nature, partition in and out of the micelle, interacting in a chromatographic manner through either hydrophobic or electrostatic interactions. The more hydrophobic the solute is, the longer is the interaction with the micelle. Since the separation mechanism is essentially chromatographic, it can be described as follows:

$$k' = \frac{t_r - t_0}{t_0 \cdot \left(1 - \dfrac{t_r}{t_m}\right)} \tag{24}$$

k' denotes the capacity factor, t_r is the retention time of the solute, t_0 is the retention time of the unretained solute (EOF migration time for neutral species), and t_m is the micelle retention time. Generally, the capacity factor increases with the surfactant concentration. However, the maximum concentration feasible in practical work is limited, since an increase in concentration also increases the current flowing and, hence, Joule heating.

The selectivity can easily be manipulated in MEKC. For instance, selectivity changes significantly when the physicochemical proprties of the micelles are varied by using different surfactants with different structutre or alkyl chain length. Additionally, MEKC can be performed utilizing bile salts or microemulsions. As in chromatography, organic modifiers can be added to change the solute micelle interactions. Organic solvents such as methanol, iso-propanol, and acetonitrile have been used in practical work.

Micellar electrokinetic chromatography is applied for the analysis of a wide variety of organic substances, ionic and nonionic in nature. For instance, for the determination of the content of active pharmaceutical ingredients in tablets, creams, and injectables, the MEKC mode often offers advantages over the CZE mode.

© 2003 by Marcel Dekker, Inc.

D. Capillary Electrochromatography

Capillary electrochromatography is very similar to MEKC. It is a technique where the flow of the mobile phase through a column packed with an HPLC stationary phase is effected by the application of an external voltage. In contrast to high-pressure pumping, no back-pressure arises, allowing the use of smaller particle sizes than in HPLC. This, together with the flat flow profile of the EOF, leads to a very high separation efficiency. The higher sample capacity of CEC versus CZE is an additional advantage. And CEC was combined with pressure pumping to reduce the retention time. This method is referred to as pCEC (10).

E. Capillary Gel Electrophoresis

Separation with capillary gel electrophoresis is based on the mechanism of size exclusion. Therefore, GCE is directly comparable to traditional slab or tube gel electrophoresis, since the separation mechanisms are identical.

In CGE the capillary is filled with a gel containing cross-linked or linear polymers. The gel thereby acts as molecular sieve. Traditionally, cross-linked polyacrylamides and agarose have been utilized in the slab and tube format. Polyacrylamides when cross-linked have smaller pore sizes and are used for protein separations. The larger pore sizes of agarose gels are more suitable for DNA separation. Polyacrylamides yield very viscous gels. Therefore, polymerization is usually done on column, which has a lot of practical problems.

More recently, polymer solutions of entangled linear polymers, such as polyethylene glycol and hydroxymethyl cellulose, have been utilized for CGE. The practical advantage is that prepolymerized material can be dissolved in the run buffer and repeatedly filled into the capillary by pressure loading. In order to avoid having gel pushed out of the capillary during electrophoresis, the EOF has to be eliminated through coating of the capillary wall.

Gel electrophoresis and, more recently, CGE have been employed principally in molecular biology and biochemical science for the separation of macromolecules such as proteins and nucleic acids. And GCE has been successfully used in oligonucleotide purity analysis, antisense gene therapy, DNA sequencing, PCR product analysis, and DNA forensics.

F. Capillary Isoelectric Focusing

Capillary isoelectric focusing is a high-resolution electrophoretic technique used to separate compounds with different isoelectric points and finds wide

© 2003 by Marcel Dekker, Inc.

application in protein analysis. This technique can be used to separate proteins that differ only by 0.002 pI units. Similar to CGE it is a traditional gel electrophoretic technique extensively used in biochemistry.

Capillary isoelectric focusing is based on the migration of zwitterionic analytes in a continuous pH gradient. Therefore, the capillary is filled with the sample and a mixture of ampholytes having pI values that span the desired pH range, for example, pH 3–10. One of the ends of the capillary, at the cathode, is dipped into a basic solution (e.g., sodium hydroxide); the other end, at the anode, is dipped in acidic solution (e.g., phosphoric acid). Upon application of an electric field, the ampholytes move to a region where they become uncharged, thus forming a continuous pH gradient. In this gradient the sample proteins are focused into a volume element in the capillary where the pH equals their pI value. The protein zones are very narrow, since a protein that enters a zone of different pH will become charged and migrate back. During focusing, the EOF needs to be eliminated to prevent the ampholytes and solutes from being drawn out of the capillary.

The status of the isoelectric focusing process can be followed by the current reading. When steady state is reached where no sample migration occurs anymore, the current drops to zero. After focusing, the ampholytes and solutes are mobilized again in order to pass the detector. Mobilization can be accomplished by replacing one of the solutions in the reservoirs at the capillary end with a salt (e.g., sodium chloride), or the volume in the capillary is pushed out by applying pressure.

An advantage of CIEF is that the total length of the capillary is filled with sample and ampholyte mixture; thus, larger quantities of proteins can be separated. It therefore can be advantageously used as a sample preconcentration step prior to capillary gel electrophoresis. Furthermore, CIEF is a suitable and very precise method for measuring the isoelectric point of biomolecules.

G. Affinity Capillary Electrophoresis

Affinity capillary electrophoresis is an electrophoretic mode that takes advantage of the specific interactions of receptors, antibodies, or ligands with the analyte. In contrast to other CE modes, ACE is not dedicated to general analysis, but rather is focused on measuring molecular interactions of the solute with specific receptors.

Affinity capillary electrophoresis is an approach where the migration pattern of interacting molecules are used to identify and quantify specific binding and estimate binding constants. Therefore, the solutes are first separated conventionally by CE. In a second run, the run buffer is doped with a specific complex-forming substance, and the change in the retention time

© 2003 by Marcel Dekker, Inc.

of the solutes is then recorded. Although, formally MEKC can also be considered an ACE method, where hydrophobic or electrostatic interactions between solute and micelle take place, the term ACE generally seems to be more or less confined to stronger and more specific interactions with well-defined stoichiometry.

Three different interacting phases can be distinguished in ACE: the stationary, pseudostationary, and mobile phases. First, the interaction can take place at the surface of a coated capillary wall or at a stationary phase present in the capillary. This approach is analogous to CEC, as discussed previously. Second, the interaction can take place in pseudostationary phases, such as micelles, microemulsions, and liposomes. Third, the interaction can take place when both the solute and the affinity molecule are in free solution. For studying these interactions, two analysis methods have been developed.

For slowly dissociating, strong binding complexes, the complex will not dissociate during separation. Here the sample is preincubated and the affinity interaction takes place in the sample vial. After injection of the sample into the capillary, bound and unbound solute are separated and quantified (frontal analysis), whereas weak binding complexes with rapid on–off kinetics are analyzed under constant-equilibrium conditions, usually by evaluation of mobility changes. Therefore, both components, solute and affinity molecule, are filled into the capillary and a plug of pure run buffer is injected (vacancy electrophoresis). After the voltage is switched on, two negative peaks will appear, corresponding to both components, caused by local deficiencies of solute and affinity molecule.

A detailed description of the theory of ACE will be given in Chapter 2.

IV. CAPILLARY ELECTROPHORETIC SEPARATION IN NONAQUEOUS MEDIA

Nonaqueous capillary electrophoresis is a new technique that matured over the last couple of years to complement the electrophoretic techniques performed under aqueous conditions. Consequently, it extends the applicability of CE to those analytes that are insoluble or only sparsely soluble in water, including several classes of pharmaceutical compounds and long-chain fatty acids, vitamins, and surfactants, to name only a few.

The use of organic solvents in nonaqueous capillary electrophoresis not only increases the solubility of the solutes, but also allows one to control important characteristics of the separation. For instance, the solvent properties affect the acid–base behavior of the analytes on a wider scale than

© 2003 by Marcel Dekker, Inc.

possible in water. The pK_a values can differ up to many orders of magnitude. Hence, electrophoretic mobilities can be controlled efficiently, and separations not possible in aqueous CE can be performed with excellent selectivities (11).

In general terms, the ionic mobility is determined by the properties of the analyte and the solvent. By substitution of the charge in Eq. (6) by the product of the capacity of a sphere ($4\pi \cdot \varepsilon_0 \cdot \varepsilon_r \cdot r$) and its zeta-potential ζ_{Ion}, a universal expression for the ionic mobility can be derived:

$$\vec{u}_{\text{Ion}} = \frac{2 \cdot \varepsilon_0}{3} \cdot \left(\frac{\varepsilon_r}{\eta}\right)_S \cdot \vec{\zeta}_{\text{Ion}} \tag{25}$$

This equation shows that the ionic mobility is directly proportional to the ratio of dielectric constant and viscosity of the solvent $(\varepsilon_r/\eta)_S$. Since the migration time of an ion significantly decreases with increasing ionic mobility, a high dielectric constant–viscosity ratio of the solvent is advantageous. It can also be shown that the separation efficiency per unit length benefits from a high ionic mobility. Solvents with a high $(\varepsilon_r/\eta)_S$ ratio are acetonitrile and *N*-methyl formamide, which have an even higher dielectric contant–viscosity ratio than water, followed by methanol, for which $(\varepsilon_r/\eta)_S$ is two-thirds that of water.

The mixing of solvents in various ratios turned out to be a powerful optimization tool in nonaqueous CE, since a favorable ratio of mixture dielectric constant to its viscosity enhances separation efficiency and analysis speed.

Electroosmotic flow also occurs in nonaqueous media when using fused-silica capillaries. Its magnitude is determined by the solvents $(\varepsilon_r/\eta)_S$ in a similar way to that of the ionic mobility. A remarkably high electroosmotic flow is found in neat acetonitrile. It is believed that due to the lack of autoprotolysis, in this solvent virtually no anions exist at a certain purity level. Acetonitrile can accept protons from dissociating surface silanol functions, and the negative charge of the capillary wall is balanced solely by these solvated protons. Hence, the ionic strength is extremely low, which leads to less effective shielding of the negative surface potential of the capillary wall.

Due to the low conductivity in organic solvents, the currents are found to be orders of magnitude smaller than in aqueous CE. Hence, Joule heating virtually does not occur, even at high background electrolyte concentrations up to 0.1 mol/L. This allows us to work at a very high separation voltage. Nevertheless, the ability of a solvent to dissolve ionic species limits the number of solvents that can be used in CE. For instance, common buffer ions used in aqueous CE, such as phosphate and borate, cannot be employed

© 2003 by Marcel Dekker, Inc.

in acetonitrile and alcohols. Therefore, in acetonitrile–methanol mixtures, acetic acid/ammonium acetate is widely used as background electrolyte.

Also the selectivity of a separation can be increased by the addition of ions. Tjornelund and Hansen added magnesium ions to the buffer in order to separate tetracycline antibiotics in *N*-methyl formamide as metal chelates (12). Another example is the separation of several sulfonamides in acetonitrile by adding silver ions. Compounds such as N-containing heterocyclics were found to build selective charge transfer complexes with Ag^+, which improves the selectivity of the separation. Phenols, carboxylic acids, and alcohols interact with anions such as ClO_4^-, BF_4^-, NO_3^-, $CH_3SO_3^-$, and Cl^- in acetonitrile as solvent. The resulting electrophoretic mobility of the weak Bronsted acids (HA) in the presence of such anions is the result of the formation of complexes of the type $[X^- \ldots HA]$ due to the formation of hydrogen bonds (13).

Besides its application as a separation technique, nonaqueous CE has also been used as a powerful method to measure fundamental physicochemical parameters in organic solvents and, thus, to contribute to a broader understanding of solvation phenomena, protolysis, and electochemistry in nonaqueous media.

REFERENCES

1. A. Tiselius. Trans. Faraday Soc. 33 (1937), 524.
2. S. Hjerten. Chromatogr. Rev. 9 (1967), 122.
3. R. Virtanen. Acta Polytech. Scand. 123 (1974), 1.
4. J. Romano, P. Jandik, W.R. Jones, P.E. Jackson. J. Chromatogr. 546 (1991), 411.
5. P. Jandik, W.R. Jones, A. Weston, P.R. Brown. LC/GC Int. 5 (1991), 20.
6. M.A. Hayes, A.G. Ewing. Anal. Chem. 64 (1992), 512.
7. K. Bächmann, B. Göttlicher, I. Haag, M. Hannina. GIT 6 (1993), 514.
8. C.S. Effenhauser, A. Paulus, A. Manz, H.M. Widmer. Anal. Chem. 66 (1994), 2949.
9. S. Terabe. Trends Anal. Chem. 8 (1989), 129.
10. C. Rentel, P. Gfrörer, E. Bayer. Electrophoresis 20 (1999), 2329.
11. I. Bjornsdottir, J. Tjorelund, S.H. Hansen. Electrophoresis 19 (1998), 2179.
12. J. Tjornelund, S.T. Hansen. J. Pharm. Biomed. Anal. 15 (1997), 1077.
13. T. Okada. J. Chromatogr. A 771 (1997), 275.

© 2003 by Marcel Dekker, Inc.

2
Theory of Affinity Electrophoresis

Hans-Hermann Rüttinger
Martin-Luther-University Halle-Wittenberg, Halle, Germany

I. INTRODUCTION

More or less specific noncovalent molecular interactions are ubiquitous in biological systems. Signal transduction such as hormone–receptor binding, transcription of hereditary information, enzyme substrate binding, and regulation of enzyme activity are only few examples. The effects of drugs in these systems can often be explained in terms of binding to receptors, enzymes, or ion channels. Even the bioavailibility of drugs is modified by complexation to constituents of exipients and food or intestinal fluids.

In most cases these interactions can be regarded as equilibrium reactions governed by the law of mass action. Association constants provide a measure of the affinity of a ligand molecule to a substrate; hence the tendency to form associates can be compared on a thermodynamic level. This provides information on the energetics of binding via the following relationship:

$$\Delta G = -RT \ln K_{eq}$$

The binding enthalpy can be obtained from the temperature dependence of K_{eq}.

For a simple 1:1 association of ligand L to substrate S,

$$S + L \rightleftarrows SL$$

By the mass action law,

$$K_A = \frac{[SL]}{[S] \cdot [L]} \tag{1}$$

© 2003 by Marcel Dekker, Inc.

If the activity coefficients are neglected (set to unity), the association constant is obtained by any analytical procedure that measures the apparent concentrations of S, L, and SL without disturbing the equilibrium.

A variety of spectroscopic methods that produce different signals from bound and free substrate, such as UV-vis spectroscopy, IR spectroscopy and NMR spectroscopy, have been established for this purpose. Electrochemical methods, such as potentiometry and polarography, have been applied as well (1).

All these methods benefit from the different behavior of free vs. bound substrate. Association involves changes of molecular size and/or charge, which controls electrophoretic mobility. Capillary electrophoresis provides mobility data as well as analytical concentrations with a minimal consumption of substances. During the past decade a variety of methods have been developed using mobility data or direct concentration readings from the detector to get information on the association constants (2–4).

II. EVALUATION OF ELECTROPHORETIC MOBILITY

A. Simple 1:1 Association

A low concentration of substrate is injected into a capillary containing the ligand with concentration [L]. On condition that the equilibrium is rapidly established (dynamic equilibrium), the *effective net mobility* of the substrate μ corresponds to the sum of the mobility of free and bound substrate weighted by their molar fractions:

$$\mu = x_S \cdot \mu_s + x_{SL} \cdot \mu_{SL} \tag{2}$$

The molar fractions are defined as

$$x_s = \frac{[\mathrm{S}]}{[\mathrm{S}] + [\mathrm{SL}]} \qquad \text{and} \qquad x_{SL} = \frac{[\mathrm{SL}]}{[\mathrm{S}] + [\mathrm{SL}]} \tag{3}$$

Analogous to chromatography, the ratio of bound to free substrate molecules is defined as capacity factor k':

$$k' = \frac{n_{SL}}{n_S} \tag{4}$$

Since the molecules are dissolved in the same volume, k' can also be written as the concentration ratio:

$$k' = \frac{[\mathrm{SL}]}{[\mathrm{S}]}$$

© 2003 by Marcel Dekker, Inc.

Inserting k' into Eq. (1) gives

$$k' = K_A \cdot [\mathrm{L}] \tag{5}$$

In protein-binding investigations the fractional saturation, defined as the fraction of protein molecules that are saturated with ligand is used as working function.

$$Y = \frac{[\mathrm{SL}]}{[\mathrm{S}] + [\mathrm{SL}]} \tag{6}$$

Combining Eq. (3) and (5) produces

$$x_s = \frac{1}{1 + k'} \tag{7}$$

$$Y = \frac{k'}{1 + k'} \tag{8}$$

If there exists no further species of S and interaction with the capillary wall can be excluded, then Eq. (2) simplifies to

$$\mu = x_s \cdot \mu_s + (1 - x_S) \cdot \mu_{SL} \tag{9}$$

$$\mu = \frac{1}{1 + k'} \cdot \mu_s + \frac{k'}{1 + k'} \cdot \mu_{SL} \tag{10}$$

$$\mu = \frac{\mu_S + k' \cdot \mu_{SL}}{1 + k'} \tag{11}$$

Subtraction of μ_S from Eq. (11) yields

$$\mu - \mu_S = \frac{\mu_S + k' \cdot \mu_{SL} - \mu_S - k' \cdot \mu_s}{1 + k'} \tag{12}$$

$$\frac{\mu - \mu_S}{\mu_{SL} - \mu_S} = \frac{k'}{1 + k'} = Y \tag{13}$$

Replacing k' with Eq. (5) gives

$$\frac{\mu - \mu_S}{\mu_{SL} - \mu_S} = \frac{K_A \cdot [\mathrm{L}]}{1 + K_A \cdot [\mathrm{L}]} \tag{14}$$

or

$$\mu = \frac{\mu_S + K_A \cdot [\mathrm{L}] \cdot \mu_{SL}}{1 + K_A \cdot [\mathrm{L}]} \tag{15}$$

A typical mobility plot calculated with Eq. (15) is given in Fig. 1 for $K_A = 10^5$ L/mol. All mobilities are between μ_S and μ_{SL}.

© 2003 by Marcel Dekker, Inc.

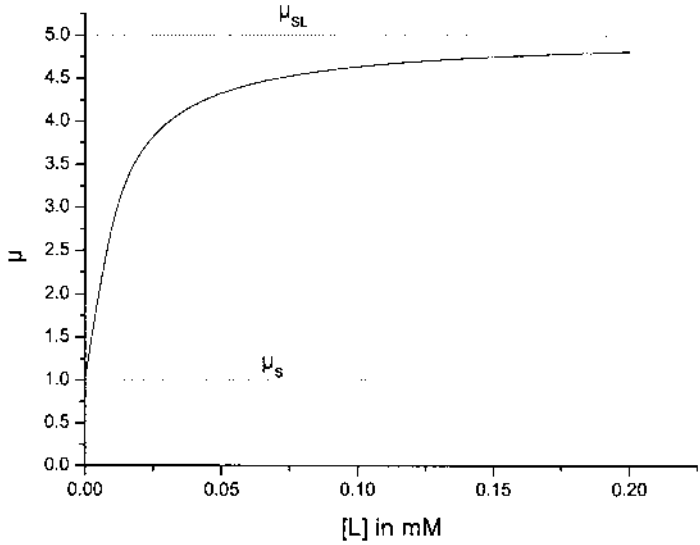

Fig. 1 Typical binding curve using Eq. (15).

Nonlinear regression analysis of a plot of μ or Y against [L] provides the association constant K_A, and the electrophoretic mobility of the pure complex μ_{SL} from the experimental data. μ_S corresponds to the substrate mobility at [L] = 0. [L] can be approximated as the added ligand concentration only when the ligand concentration is much greater than the solute concentration or when the binding constant is small.

Since all electrophoretic mobility values are proportional to the reciprocal viscosity of the buffer, as derived in Chapter 1, the experimental mobility values μ must be normalized to the same buffer viscosity to eliminate all other influences on the experimental data besides the association equilibrium. Some commercial capillary zone electrophoresis (CZE) instruments allow the application of a constant pressure to the capillary. With such an instrument the viscosity of the buffer can be determined by injecting a neutral marker into the buffer and then calculating the viscosity from the time that the marker needs to travel through the capillary at a set pressure. During this experiment the high voltage is switched off.

In this case the traveling time t_d of the marker relates to the hydrodynamic flow velocity v at the applied pressure:

$$v = \frac{l_d}{t_d} \tag{16}$$

© 2003 by Marcel Dekker, Inc.

where l_d is the length of the capillary from the injection point to the detector. Viscosity is then calculated using the Hagen–Poiseuilles law (5):

$$\eta = \frac{\pi \cdot \Delta p \cdot r^4}{8 \cdot v \cdot l} \tag{17}$$

where l is the total length of the capillary. Since only viscosity ratios have to be determined, only the traveling-time ratios have to be considered, provided that all measurements are done with the same capillary at constant pressure.

Evaluation of experimental data is much easier when Eq. (14) is converted to a linear form. There are three linearizations established in practice:

Double reciprocal plot (Benesi–Hildebrand or Lineweaver–Burk):

$$\frac{1}{\mu - \mu_S} = \frac{1}{(\mu_{SL} - \mu_S) \cdot K_A} \cdot \frac{1}{[\mathrm{L}]} + \frac{1}{\mu_{SL} - \mu_S} \tag{18}$$

Y-reciprocal plot:

$$\frac{[\mathrm{L}]}{\mu - \mu_S} = \frac{1}{\mu_{SL} - \mu_S} \cdot [\mathrm{L}] + \frac{1}{(\mu_{SL} - \mu_S) \cdot K_A} \tag{19}$$

X-reciprocal plot (Scatchard or Eadie):

$$\frac{\mu - \mu_S}{[\mathrm{L}]} = -K_A \cdot (\mu - \mu_S) + K_A \cdot (\mu_{SL} - \mu_S) \tag{20}$$

The names of the linearization methods correspond to the established methods in protein affinity research and alternatively in enzymology. All these transformations change the statistical weights of the data points and differ in their susceptibility to experimental uncertainties. The double reciprocal plot places too much emphasis on the data points at the lowest ligand concentrations. Therefore the estimated mobility of the complex (μ_{SL}) resulting from the intersection point shows more uncertainty. Deviations from the model, e.g., the influence of higher-order equilibria, slow equilibration, and partial adsorption at the capillary wall, often cause only slight deviations from linearity but yield incorrect equilibrium constants. A detailed discussion of statistical errors is given in Refs. 6–9.

B. Higher-Order Equilibria

If the substrate is able to bind more than one ligand, then additional complex species are produced that contribute to the measured mean mobility. For

© 2003 by Marcel Dekker, Inc.

illustration, two binding sites are assumed. Binding of a ligand to site 1 leads to SL(1), controlled by the microscopic equilibrium constant k_1, the first occupation of binding site 2 yields SL(2). Both forms of *SL* can bind a second ligand, leading to the same product (SL_2):

$$\begin{array}{ccc} \mathrm{S} & \overset{k_1}{\underset{+L}{\rightleftharpoons}} & \mathrm{SL(1)} \\ k_2 \Downarrow +\mathrm{L} & & +\mathrm{L} \Downarrow k_{12} \\ \mathrm{SL(2)} & \overset{k_{21}}{\underset{+L}{\rightleftharpoons}} & \mathrm{SL_2} \end{array}$$

The resultant different complexes with the same stoichiometry [SL(1) and SL(2)] generally can't be separated by electrophoresis because of the same size and charge. Only the macroscopic equilibrium constants K_1 and K_2 can be derived from electrophoresis data.

The macroscopic equilibrium constants describe not a specific interaction, but the sum of every possible interaction between substrate and ligand at a particular stoichiometry:

$$K_1 = \frac{[\mathrm{SL}]}{[\mathrm{S}]\cdot[\mathrm{L}]} = \frac{[\mathrm{SL(1)}] + [\mathrm{SL(2)}]}{[\mathrm{S}]\cdot[\mathrm{L}]} = k_1 + k_2 \tag{21}$$

and

$$K_2 = \frac{[\mathrm{SL_2}]}{[\mathrm{SL}]\cdot[\mathrm{L}]} = \frac{[\mathrm{SL_2}]}{([\mathrm{SL(1)}] + [\mathrm{SL(2)}])\cdot[\mathrm{L}]} = \frac{k_1 k_{12}}{k_1 + k_2} = \frac{k_1 k_{21}}{k_1 + k_2} \tag{22}$$

Binding of additional ligands to a small substrate is often hindered for steric reasons (anticooperative binding). In most of the protein associations, however, the first association step favors the following binding steps. This behavior, called *cooperative binding*, leads to the formation of more highly coordinated species in the analyte.

If higher complexes are present, for a correct description of the electrophoretic behavior, Eq. (2) must be extended:

$$\mu = x_S \mu_S + \sum_{i=1}^{n} x_i \mu_{SL_i} \tag{23}$$

with

$$x_1 = \frac{[\mathrm{SL}]}{[\mathrm{S}] + [\mathrm{SL}] + [\mathrm{SL_2}] + \cdots + [\mathrm{SL}_n]}$$

© 2003 by Marcel Dekker, Inc.

with n being the highest coordination number. In general,

$$x_i = \frac{[SL_i]}{[S] + \sum_{m=1}^{n} [SL_m]} \tag{24}$$

The x_i are related to the capacity factors as follows:

$$x_i = \frac{k_i'}{1 + \sum_{m=1}^{n} k_m'} \tag{25}$$

with

$$k_i = \prod_{m=1}^{i} K_m \cdot [L]^i \tag{26}$$

$$\mu - \mu_S = \frac{\sum_{i=1}^{n} (\mu_i - \mu_S) \cdot k_i'}{1 + \sum_{i=1}^{n} k_i'} \tag{27}$$

and, as a general formulation of Eq. (14),

$$\mu - \mu_S = \frac{\sum_{i=1}^{n} \left((\mu_i - \mu_S) \cdot [L]^i \cdot \prod_{m=1}^{i} K_m \right)}{1 + \sum_{i=1}^{n} \left([L]^i \cdot \prod_{m=1}^{i} K_m \right)} \tag{28}$$

Bowser and Chen (10) have calculated some theoretical binding isotherms ($\mu - \mu_s = f([L])$ for anticooperative, noncooperative, and cooperative complex formation at two equivalent binding sites with arbitrarily chosen microscopic constants; see Table 1.

A smaller secondary microscopic association constant compared to the first binding constant ($k_1 = k_2 > k_{21} = k_{12}$) results in anticooperative binding behavior in cases A and B. If $k_1 = k_2 < k_{21} = k_{12}$, as in cases D and E, the cooperative binding yields a higher amount of higher-order complexes.

The binding isotherms in Fig. 2 don't seem to be evidence of higher binding orders at first glance. In the Scatchard plot in Fig. 3, plots following the linearization procedures of Eqs. (18) to (20) almost show a clear deviation from linearity for anticooperative binding or cooperative binding, whereas the noncooperative binding simulates a simple 1:1 complexation

© 2003 by Marcel Dekker, Inc.

Table 1 Microscopic and Macroscopic Equilibrium Constants for the Curves in Figs. 2 and 3

	$k_1 = k_2$ [M^{-1}]	$k_{21} = k_{12}$ [M^{-1}]	K_1 [M^{-1}]	K_1K_2 [M^{-2}]
A (anticooperative)	50	10	100	500
B (anticooperative)	50	20	100	1,000
C (noncooperative)	50	50	100	2,500
D (cooperative)	50	100	100	5,000
E (cooperative)	50	200	100	10,000

(curve C). In that case, and if the mobility of the different species are very similar, ACE fails to detect higher-order equilibria. When measurements are made in only a limited range of concentrations, these plots may be misinterpreted as decisive proof of a 1:1 complexation, in as much as statistical errors hide a small curvature in the low-concentration range.

Nonlinear regression analysis, taking into account all the equilibria, seems to be a reasonable way to get a true picture of the processes taking place and finally to get the relevant data. In practice, however, it is not possible to decide whether the mathematical model describes the reality

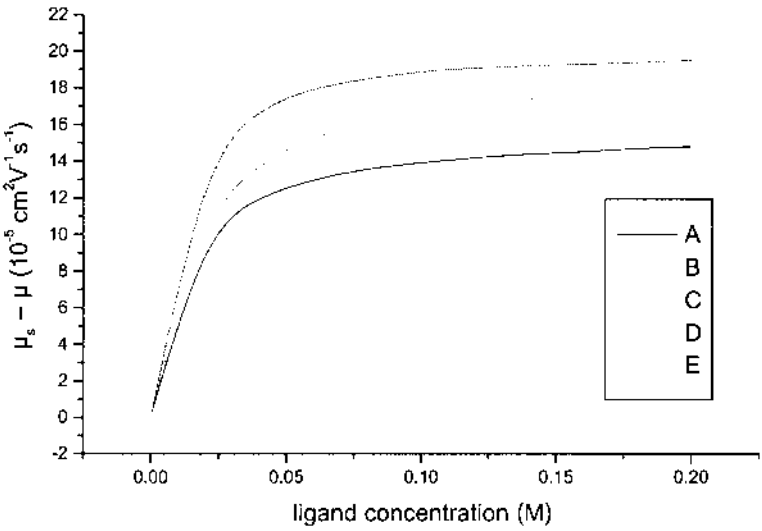

Fig. 2 Binding of a ligand at two binding sites with different cooperativities.

© 2003 by Marcel Dekker, Inc.

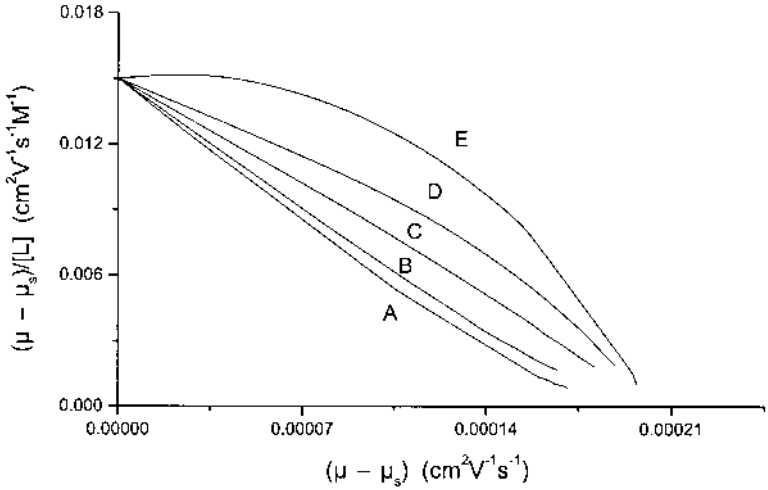

Fig. 3 Scatchard plots of mobility data for second-order binding with different cooperativities.

correctly if too many independent parameters are involved. Due to the statistical errors of the observed mobility data and other imponderabilities, regression analysis fails. In some cases the equations can be simplified. If binding is highly cooperative, then the concentrations of complexes with lower stoichiometry are very small and all bonded substrate is attributed to the complex of the highest stoichiometry:

$$K_A = \frac{[SL_n]}{[S] \cdot [L]^n} \tag{29}$$

In this case only a simple adaptation of Eq. (5) is needed and inserting k' into Eq. (10) immediately provides the formula for the binding function:

$$k' = \frac{[SL_n]}{[S]} = K_A \cdot [L]^n \tag{30}$$

And, analogous to Eq. (15),

$$\mu = \frac{\mu_S + K_A \cdot [L]^n \cdot \mu_{SL_n}}{1 + K_A \cdot [L]^n} \tag{31}$$

Evaluation of Eq. (28) is best done by nonlinear regression analysis, which yields K_A, n, and μ_{SL_n}. If μ_{SL_n} can be estimated from the apparent mobility at high ligand concentrations, then the coordination number is eas-

© 2003 by Marcel Dekker, Inc.

ily gained from the slope of a double logarithmic plot of Eq. (30). From Eq. (13) it follows that

$$k' = \frac{Y}{1 - Y} = K_A \cdot [\mathrm{L}]^n \tag{32}$$

This plot is known as a *Hill plot* in protein-binding chemistry and enzyme kinetics (11). Transformation of Eq. (13) also provides the relation for the mobilities:

$$k' = \frac{\mu - \mu_s}{\mu_{SL_n} - \mu} \tag{33}$$

Another simplification can be made if all binding sites are independent (noncooperative binding) and they can be attributed to classes of identical sites. In protein–drug affinity studies the fraction of drug molecules bound (D_b) per protein molecule (P) is given by

$$r = \frac{\mathrm{D}_b}{\mathrm{P}_{\mathrm{total}}} = \sum_{i=1}^{m} n_i \cdot \frac{K_i[\mathrm{D}_f]}{1 + K_i[\mathrm{D}_f]} \tag{34}$$

where n_i is the number of different binding sites of class i (12,13). If only one class of independent binding sites exists, then

$$r = \frac{\mathrm{D}_b}{\mathrm{P}_{\mathrm{total}}} = n \cdot \frac{K_A[\mathrm{D}_f]}{1 + K_A[\mathrm{D}_f]} \tag{35}$$

When the protein is the substrate, the drug is the ligand, and [SL] is the sum of all complexes, r then corresponds to Y.

Provided the mobilities of the different protein–drug complexes are nearly the same, but different from the free drug, r and n can be calculated from the mobility data, analogously to Eq. (14):

$$\frac{\mu - \mu_S}{\mu_{SL} - \mu_S} = n \cdot \frac{K_A \cdot [\mathrm{L}]}{1 + K_A \cdot [\mathrm{L}]} \tag{36}$$

A scatchard plot yields a straight line, as already shown in Fig. 3, curve C. The reasonable assumption that the mobilities of the protein complexes are nearly the same results from the minor change of the protein's size when a small drug molecule binds to it. A significant alteration of mobility can arise from charged ligand if the protein carries only a low intrinsic charge at the apparent pH value. Binding of phosphate to ovalbumin causes a constant fractional increase in charge for each addition of a phosphate ion. This is taken into account via an additional factor introduced in Eq. (36) (14,15).

© 2003 by Marcel Dekker, Inc.

C. Association Equilibria with More Than One Additive

Buffer electrolytes for CZE separations often contain a mixture of additives that modify the electrophoretic mobility of the analytes to achieve an optimal separation. Most buffer compositions had been empirically found. Theoretical treatment of the interacting equilibria can give more insight into the underlying processes and be helpful in finding good separation conditions. Another area of interest that benefits from ACE theory involves the effects of pharmaceutical exipients on drugs and biological systems containing more than one interacting substance. Since most analytes are weak acids or bases, protonation/deprotonation is involved as a secondary equilibrium in almost all affinity reactions.

Here we exemplify the principles with a substrate interacting competitively with two different ligands (16). This model assumes that there are no interactions between ligands L and I and that the substrate can bind only one additive at a time. The following equilibria hold:

$$S + L \rightleftharpoons SL$$

$$S + I \rightleftharpoons SI$$

The corresponding equilibrium constants are:

$$K_{SL} = \frac{[SL]}{[S] \cdot [L]} \tag{37}$$

$$K_{SL} = \frac{[SI]}{[S] \cdot [I]} \tag{38}$$

This yields the following capacity factors:

$$k'_{SL} = K_{SL} \cdot [L] \tag{39}$$

$$k'_{SI} = K_{SI} \cdot [I] \tag{40}$$

$$\mu = \frac{\mu_s + \mu_{SL} \cdot k'_{SL} + \mu_{SI} \cdot k'_{SI}}{1 + k'_{SL} + k'_{SI}} \tag{41}$$

Analogous to Eq. (15), the mobility depends on the concentrations of the two ligands, L and I:

$$\mu = \frac{\mu_S + \mu_{SL} \cdot K_{SL} \cdot [L] + \mu_{SI} \cdot K_{SI} \cdot [I]}{1 + K_{SL} \cdot [L] + K_{SI} \cdot [I]} \tag{42}$$

Experimental data with the independent variables L and I can be plotted, producing a 3-dimensional binding isotherm, and a multivariate regression analysis gives the association constants K_{SL} and K_{SI} as well as the mobility of the corresponding complexes.

© 2003 by Marcel Dekker, Inc.

Instead of 3-D plots, traces of the binding isotherm surface through a plane parallel to the [L]/[I] plane (contour diagrams) or profile plots (traces through the μ/[L] or μ/[I] plane can be used to explain certain special conditions.

Bowser et al. (17) calculated profile plots of binding isotherms assuming the following conditions: $K_{SL} = 50\ M^{-1}$, $K_{SI} = 50\ M^{-1}$, $\mu_S = 0\ cm^2V^{-1}s^{-1}$, $\mu_S = 0\ cm^2V^{-1}s^{-1}$, $\mu_{SL} = 3 \times 10^{-5}\ cm^2V^{-1}s^{-1}$, $\mu_{SI} = 5 \times 10^{-5}\ cm^2V^{-1}s^{-1}$.

In Fig. 4, mobility is plotted against [L] at constant concentrations of I. Addition of charged ligands accelerates the analytes. The lowest curve, with [L] = 0, begins at zero, because μ_S is zero, and tends toward μ_{SL} at the highest concentration of L. The isotherm corresponding to the highest concentration of I and [L = 0] tends toward μ_{SI}, and mobility diminishes as, with increasing [L], the lower mobility of the associate SL gains more influence. The dashed line indicates a concentration where both influences compensate one another, thus producing the same mobility for all concentrations of L. This concentration of I is called the *dengsu concentration*. *Dengsu* means ''same velocity'' in Chinese. Figure 5 shows a mobility plot of [I] with [L] as parameter. All binding isotherms cross at the same point, where [L] is at dengsu concentration. This concentration is calculated by setting

$$\frac{\partial \mu}{\partial [L]} = 0, \qquad \text{reflecting that } \mu \text{ is independent of [L]}$$

Applied to Eq. (42):

$$\frac{(\mu_{SL} - \mu) \cdot K_{SL} + K_{SL} \cdot K_{SI} \cdot [I] \cdot (\mu_{SL} - \mu_{SI})}{(1 + K_{SL} \cdot [L] + K_{SI} \cdot [I])^2} = 0 \tag{43}$$

$$[I]_D = -\frac{\mu_{SL} - \mu}{K_I \cdot (\mu_{SL} - \mu_{SI})} \tag{44}$$

Equation (44) gives a positive value for dengsu concentration only when both binding additives shift the mobility in the same direction and

$$|\mu_{SI} - \mu| > |\mu_{SL} - \mu|$$

Conversely, if

$$|\mu_{SL} - \mu| > |\mu_{SI} - \mu|$$

there will be a dengsu concentration for I.

The presence of a dengsu concentration is a strong indication that the second additive interacts with the analyte in 1:1 stoichiometry and there is no interaction between the additives. The shapes of the binding isotherms confirm the stoichimetries of the complexes.

© 2003 by Marcel Dekker, Inc.

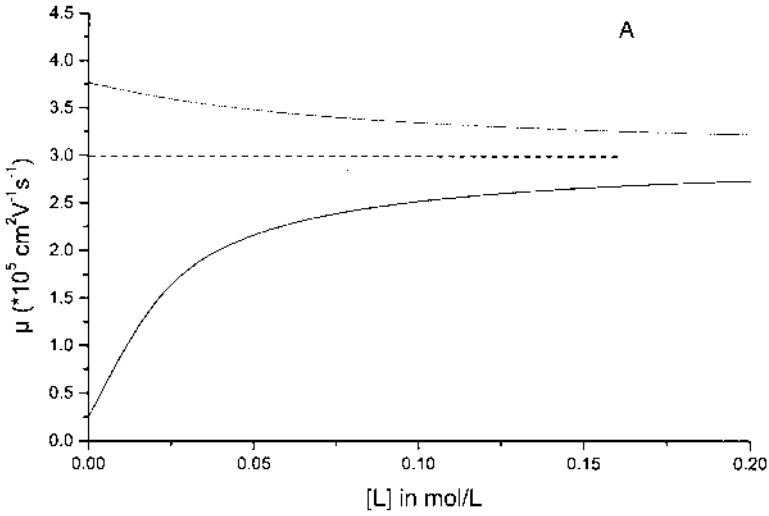

Fig. 4 Calculated mobility with constant [I] at different concentrations of L.

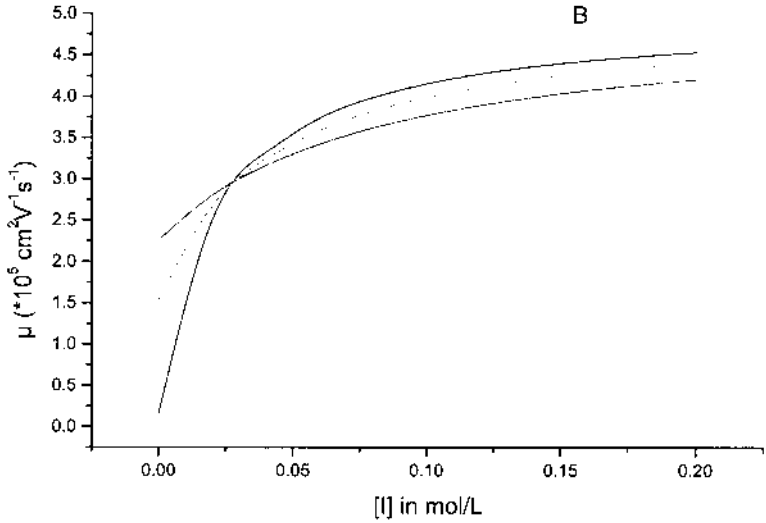

Fig. 5 Calculated mobility with constant [L] at different concentrations of I.

© 2003 by Marcel Dekker, Inc.

D. Micellar Electrochromatography

With micelles, microemulsions, or liposomes, a second phase is introduced into the separating system. As in chromatography, exchange of the analyte between the mobile and the stationary phases controls the separation process. Contrary to classical chromatography, both phases are mobile, moving with different velocities. As in all electrophoresis techniques, the net mobility of an analyte is the mean mobility of its fraction in the aqueous and the micellar phases:

$$\mu = x_{\text{aqu}} \cdot \mu_{\text{aqu}} + x_{\text{mic}} \cdot \mu_{\text{mic}} \tag{45}$$

Introduction of micellar electrochromatography by Terabe and coworkers (18) extended the separation power of capillary electrophoresis to uncharged molecules. But charged molecules with same mobility can also be separated due to their different partitions between aqueous and micellar phases. This partition behavior may be regarded as an affinity to the micellar phase and therefore is treated in this chapter. Instead of the mass action law, the Nernst partition law describes the phase partition equilibrium:

$$K_p = \frac{[\text{S}]_{\text{mic}}}{[\text{S}]_{\text{aqu}}} \tag{46}$$

The capacity factor k' is the same as in Eq. (4), but we must take into consideration that the phases are different in their volumes:

$$k' = \frac{n_{\text{mic}}}{\text{n}_{\text{aqu}}} = \frac{[\text{S}]_{\text{mic}} \cdot V_{\text{mic}}}{[\text{S}]_{\text{aqu}} \cdot V_{\text{aqu}}} \tag{47}$$

$$k' = K_p \cdot \frac{V_{\text{mic}}}{V_{\text{aqu}}} \tag{48}$$

The volume of the micellar phase is crucial for the determination of partition coefficients. In most cases it is regarded as being proportional to the concentration exceeding the critical micellar concentration of the surfactant:

$$V_{\text{mic}} = v \cdot (c_{\text{Surf}} - c_{cmc}) \cdot V_0 \tag{49}$$

Equation (49) and all relations derived therefrom apply only for $(c_{\text{surf}} - c_{cmc}) > 0$; otherwise no micellar phase exists.

The rest of the total volume V_0 is accounted as to the aqueous phase:

$$V_0 = V_{\text{mic}} + V_{\text{aqu}} \tag{50}$$

© 2003 by Marcel Dekker, Inc.

giving

$$k' = K_p \cdot \frac{v \cdot (c_{\text{Surf}} - c_{cmc})}{1 - v(c_{\text{Surf}} - c_{cmc})} \tag{51}$$

Capacity factor k' is introduced into Eq. (13) to give

$$\frac{\mu - \mu_S}{\mu_{\text{mic}} - \mu_S} = \frac{K \cdot v \cdot (c_{\text{Surf}} - c_{cmc})}{1 + K_p \cdot v \cdot (c_{\text{Surf}} - c_{cmc}) - v \cdot (c_{\text{Surf}} - c_{cmc})} \tag{52}$$

Experimental net mobility values are plotted against surfactant concentration to give a binding curve very similar to the binding isotherms of the complex equilibria. It should, however, be taken into consideration that concentrations below the critical micellar concentration don't fulfill the assumptions underlying Eq. (49). If there is any change in mobility due to surfactant concentrations below the critical micellar concentration, then this effect must be attributed to complex formation, as in affinity electrophoresis or absorption of the surfactant at the capillary wall. Other influences, such as the viscosity of the buffer electrolyte and eof drift, are considered carefully to be eliminated. The partition coefficient K_p and the specific micellar volume can be estimated via multivariate regression analysis. For this purpose the mobility of the micelles μ_{mic} and the critical micellar concentration should be known from other experiments. The mobility of the micelles can be determined by a hydrophobic marker that dissolves only in the micellar phase, not in the aqueous buffer phase. It is assumed that the uptake of the analyte does not change the mobility of the micelles itself or change its size.

There are several possibilities for the determination of the critical micellar concentration. If the micelles are formed from charged surfactants, a plot of the electrophoretic current at constant high voltage against the surfactant concentration shows an inflection point at the c_{cmc}. It should be noted that the critical micellar concentration changes with temperature, the kind and concentration of counterions, and other buffer ingredients.

The partition coefficient relates to the hydrophobic character of a substance. Its logarithm is proportional to the free energy of the transfer of a substance from the aqueous phase to the micellar phase. Correlation of these partition coefficients with the partition coefficients of other systems, such as octanol/water, results in a straight line on a logarithmic scale. Some correlations are given in Chapters 5 and 6.

Equations (49) to (52) are derived for the simple case in which only one surfactant forms one type of micelles. Depending on surfactant concentration and other buffer constituents, a more or less complicated mixture of micelles differing in form and/or composition coexist in the buffer. All of these micelles may exhibit different partition behavior in relation to a certain

© 2003 by Marcel Dekker, Inc.

substrate and have at least a different micellar mobility. Theoretical treatment of these circumstances leads to an extended form of Eq. (52), including the partition coefficients of the different micelles, their specific volumes, mobilities, and critical concentrations (19). If the systems contain too many variables, multivariate regression analysis fails and only mean partition coefficients can be extracted.

If micelles are very small, they can't regarded as a separate phase and the aggregates between substrate and surfactants are better described as higher-order complexes.

III. DIRECT EVALUATION OF CONCENTRATIONS FROM ELECTROPHEROGRAMS

As already pointed out, any method that gives the equilibrium concentrations is capable of defining the equilibrium constant. Contrary to most spectrometric methods, normal separation processes disturb the composition of the reaction mixture. Thus methods that treat the equilibrium mixture as a mixture of inert substances are not generally suitable.

A. Complete Separation of the Equilibrium Mixture

In some cases the equilibration rate is very slow compared to the time scale of the analytical separation. The pre-equilibrated reaction mixture behaves indeed as a mixture of inert components and can be separated by capillary electrophoresis. The concentrations are directly derived from the peak areas or peak heights after calibration. This method is suitable if ligand and substrate are separable and the migration time does not exceed 1% of the half-life of complex decomposition.

B. Separation Methods Under Equilibrium Conditions

Several variants of separation methods based on dialysis, ultrafiltration, and size exclusion chromatography have been developed that work under equilibrium conditions. Size exclusion chromatography especially has become the method of choice for binding measurements. The Hummel–Dreyer method, the vacancy peak method, and frontal analysis are variants that also apply to capillary electrophoresis. In comparison to chromatographic methods, capillary electrophoresis is faster, needs only minimal amounts of substances, and contains no stationary phase that may absorb parts of the equilibrium mixture or must be pre-equilibrated.

Capillary electrophoresis exhibits an extremely high separation power,

© 2003 by Marcel Dekker, Inc.

and only little differences of the complexes in size or charge are sufficient for the determination of association constants. A critical comparison of these methods for drug–protein binding studies is given by Busch et al. (20).

1. Frontal Analysis

In frontal analysis, a large plug of the pre-equilibrated mixture, containing the substrate, the ligand, and the complex formed in the buffer, is injected into the capillary. The capillary is filled only with buffer. Figure 6a shows the concentration profiles of the different constituents along the capillary. After the high voltage has been switched on, the ligand exhibits a higher mobility as the substrate in this example moves away from the starting range and leaves the substrate behind at the same concentration as it had in the nonseparated mixture. As shown in Fig. 6b, the complex moves with the same velocity as the ligand; but as the substrate disappears, the complex dissociates and the ligand is liberated and reaches the initial concentration.

If the ligand is not UV active but the substrate and the complex are registered by the UV detector, the electropherogram consists of a plateau

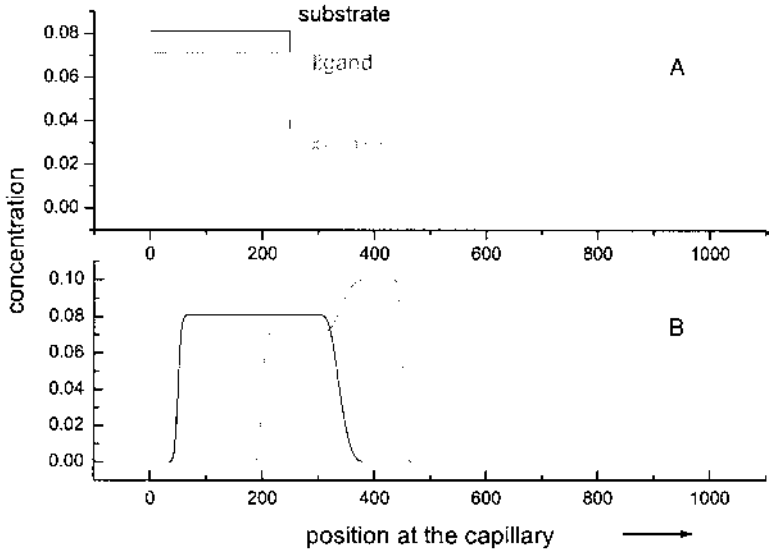

Fig. 6 Simulation of concentration distribution in frontal analysis: capillary lenth 50 cm; injection length 12.5 cm, corresponding 245 nL at 50-μm i.d. of capillary; association constant 5000 M^{-1}; initial concentration substrate 0.11 *mM*, ligand 0.1 *mM*; mobility of substrate 10, of complex 40, of ligand 40 $\times$ 10^{-5} cm^2V^{-1}; B is 50 seconds after application of 25 kV.

© 2003 by Marcel Dekker, Inc.

corresponding to the absorbancy of the complex plus substrate, immediately followed by a plateau corresponding to the concentration of the free substrate. The detector signal is easy to calibrate by injecting a sample plug of known concentration without the ligand.

Knowing the initial concentrations of substrate and ligand and the fraction of unbound substrate in the reaction mixture, the association constant can be calculated. The binding isotherm needs the measurement of five to ten reaction mixtures of different initial concentration ratios, but with commercial instruments this is easily automated, and the higher consumption of sample volume (about 80 nL) doesn't matter.

2. Hummel–Dreyer Method

As the other methods, the Hummel–Dreyer method was first developed for chromatography and then adapted to capillary electrophoresis (21). A small sample of the ligand, dissolved in buffer, is injected into the capillary. The capillary as well as source and destination vial are filled with buffer containing the substrate. In the ligand-containing sample, the initial concentration of the free substrate is depleted to the equilibrium concentration (see Fig. 7a). The depletion peak moves with the velocity of the substrate, and its area corresponds to the bound substrate. As demonstrated in Fig. 7b, the

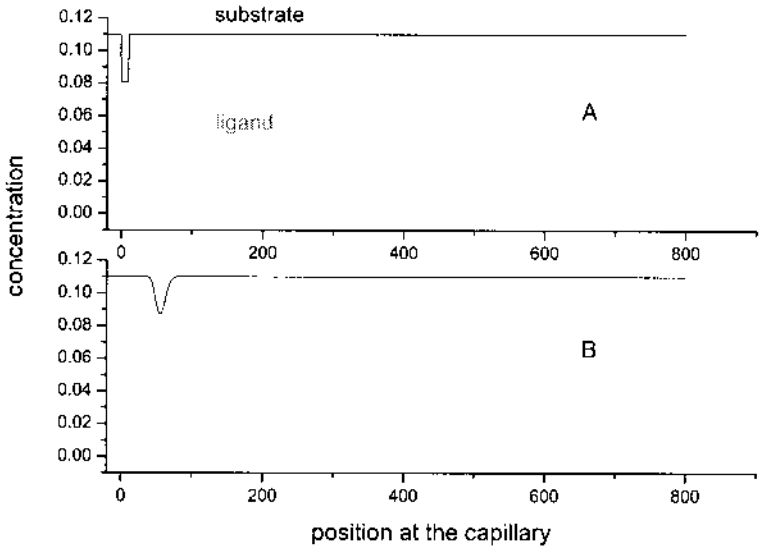

Fig. 7 Same conditions as in Fig. 5, but injection of 0.1 *mM* solution of ligand into the substrate-containing buffer, injection length 1.5 mm.

© 2003 by Marcel Dekker, Inc.

complex and the ligand cause a positive peak. Calculated in concentration units, the positive complex peak embodies the same area as the negative peak of the substrate depletion. To get the concentration of free substrate, the negative peak area must be calibrated against the substrate concentration. This is done by injection of different concentrations of substrate (without ligand) into the capillary.

3. Vacancy Method

In the vacancy method, the separation buffer contains all the complex-forming ingredients; as sample, an empty buffer solution is injected. The concentration gaps in Fig. 8b move in the electric field according to the mobility of the corresponding substances that were depleted in concentration. The substrate vacancy peak area corresponds to the amount of free substrate, whereas the complex vacancy peak area corresponds to the amount of complex that was displaced during injection. For calibration the buffer is mixed with increasing concentrations of substrate and then injected. By plotting the added substrate against the peak area, the free concentration can be determined by interpolating to zero absorbancy, the concentration needed to fill up the vacancy peak.

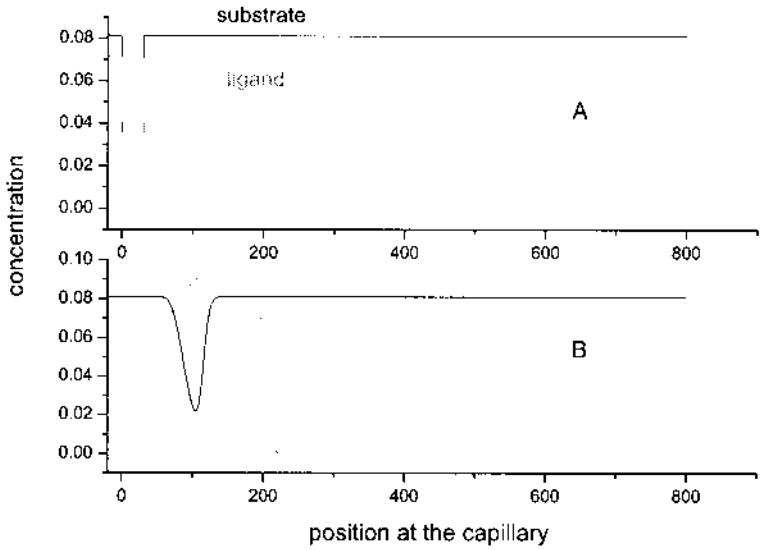

Fig. 8 Same conditions as in Fig. 6, but injection of empty buffer into the substrate and ligand-containing capillary, injection length 1.5 mm.

© 2003 by Marcel Dekker, Inc.

IV. CONCLUSIONS

Affinity capillary electrophoresis is a versatile method for the determination of binding constants. It needs only a very small amount of substance and, as a result of the high-resolution power of capillary zone electrophoresis, the method can even be applied for the determination of the affinity of individual components of an crude mixture against a certain ligand. Hummel–Dreyer and vacancy analysis provide additional data from the peak area, whereas frontal analysis directly reads the concentrations from the detector response. The latter methods need a greater amount of substance to be investigated and a more tedious procedure for calibration. Compared to the classical methods, such as size exclusion chromatography and dialysis, all the capillary electrophoretic methods save a lot of time and substance. Limitations arise from interactions of the analytes with the capillary wall, which produces tailing and shifts in migration time and EOF. The concentration of additional electrolytes in the sample must be kept as low as possible, because it could destroy the constancy of the electrical field and the pH in the capillary. The low sensitivity of the usual UV detector may be a problem, keeping in mind that in ACE sample concentration must be an order of magnitude lower than the ligand concentration in the buffer. Here CZE-MS hyphenation is a very promising technique.

As with other methods, ACE and its relatives provide experimental data corresponding to a mean value of concentrations governed by interrelated equilibria. Determination of association constants requires a suitable mathematical model with only few parameters to be estimated.

REFERENCES

1. KA Connors. Binding Constants. The measurement of molecular complex stability. Wiley, New York, 1987.
2. RHH Neubert, MA Schwarz, Y Mrestani, M Plätzer, K Raith. Affinity capillary electrophoresis in pharmaceutics. Pharm Res 16:1663–1673, 1999.
3. RM Guijt-van Duijn, J Frank, GWK van Dedem, E Baltussen. Recent advances in affinity capillary electrophoresis. Electrophoresis 21:3905–3918, 2000.
4. NHH Heegard, RT Kennedy. Identification, quantitation and characterization of biomolecules by capillary electrophoretic analysis of binding interactions. Electrophoresis 20:3122–3133, 1999.
5. RB Bird, WE Stewart, E Lightfoot. Transport Phenomena. Wiley, New York, 1960.
6. KL Rundlett, DW Armstrong. Examination of the origin, variation, and proper use of expressions for the estimation of association constants by capillary electrophoresis. J Chromatogr A 721:173–186, 1996.

© 2003 by Marcel Dekker, Inc.

7. MT Bowser, DDY Chen. Binding constants from rectangular hyperbolae. I: J Phys Chem 102:8063–8071, 1998; II: J Phys Chem 103:197–202, 1999.
8. KL Rundlett, DW Armstrong. Methods for the determination of binding constants by capillary electrophoresis. Electrophoresis 22:1419–1427, 2001.
9. KL Rundlett, DW Armstrong. Methods for estimation of binding constants by capillary electrophoresis. Electrophoresis 18:2194–2202, 1997.
10. MT Bowser, DDY Chen. Higher-order equilibria and their effect on analyte migration behavior in capillary electrophoresis. Anal Chem 70:3261–3270, 1998.
11. A Schellenberger (ed.). Enzymkatalyse. 1st ed. VEB Gustav Fischer Verlag, Jena, Germany, 1989, p. 113.
12. IM Klotz, DL Hunston. Biochemistry 16:3065–3069, 1971.
13. HA Feldmann. Anal Biochem 48:317–338, 1972.
14. RH Drewe, DJ Winzor. An electrophoretic study of the reversible binding of phosphate to ovalbumin. Biochem J 159:737–741, 1976.
15. DJ Winzor. Measurement of binding constants by capillary electrophoresis. J Chromatogr A 696:1630–1637, 1995.
16. X Peng, MT Browser, P Britz-McKibbin, GM Bebault, JR Morris, DDY Chen. Quantitative description of analyte migration behavior based on dynamic complexation in capillary electrophoresis with one or more additives. Electrophoresis 18:706–716, 1997.
17. MT Bowser, AR Kranack, DDY Chen. Properties of multivariate binding isotherms in capillary electrophoresis. Anal Chem 70:1076–1084, 1998.
18. S Terabe, K Otsuka, K Ichikawa, A Tsuchiya, T Ando. Electrokinetic separations with micellar solutions and open-tubular capillaries. Anal Chem 56:111–113, 1984.
19. KL Rundlett, DW Armstrong. Effects of micelles and mixed micelles on efficiency and selectivity of antibiotic-based capillary electrphoretic enantioseparations. Anal Chem 67:2088–2095, 1995.
20. MHA Busch, LB Carels, HFM Boelens, JC Kraak, H Poppe. Comparison of five methods for the study of drug–protein binding in affinity capillary electrophoresis. J Chromatogr A 777:311–328, 1997.
21. JP Hummel, WJ Dreyer. Measurement of protein-binding phenomena by gel filtration. Biochem Biophys Acta 63:530–532, 1962.

© 2003 by Marcel Dekker, Inc.

3
Determination of Physicochemical Parameters

Yasushi Ishihama*
Eisai Co., Ltd., Tsukuba, Ibaraki, Japan

I. ACID DISSOCIATION CONSTANT (pK_a)

A. Introduction

Ionization of drugs is important because it affects not only the physicochemical properties of the drugs, such as lipophilicity (1,2) and solubility (3–6), but also several parameters related to cell–drug interactions, such as membrane permeability, plasma protein binding, metabolism, tissue penetration, and target protein binding (7–9). The acid dissociation constant (pK_a) is an index of the extent of ionization of a drug at different pH values and is therefore an important parameter that reflects optimization of the drug structure (Fig. 1).

Traditionally, potentiometric titration, spectrophotometry, solubility, and liquid–liquid partitioning have been used for determination of pK_a. Among these, the solubility and partitioning methods are time-consuming for measurement of pK_a in the high-throughput mode. While the automated titration method is also slow, titration with organic solvents is effective for sparing soluble drugs (10). The most promising method is spectrophotometry, because it is rapid and sensitive to sparing soluble drugs (11). However, its major disadvantage is that it cannot be applied to compounds lacking chromophores close to ionophores. In addition, all the foregoing methods are affected by the purity/stability of the samples. Other chromatographic approaches, such as HPLC, are suitable for samples with low purity/stability (12). However, it is difficult to apply the single HPLC condition to a wide range of compounds with varied hydrophobicity.

Current affiliation: University of Southern Denmark, Odense, Denmark.

© 2003 by Marcel Dekker, Inc.

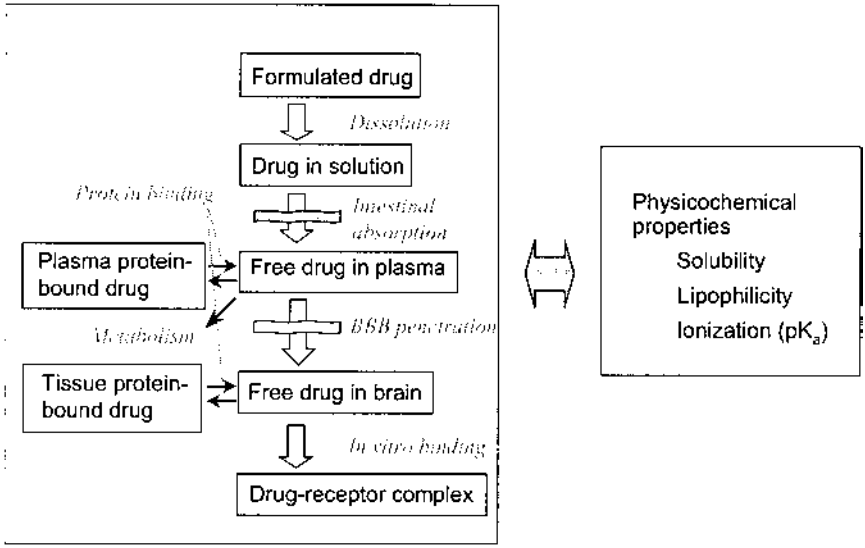

Fig. 1 Pathway of orally dosed CNS drugs.

On the other hand, computation of pK_a by using appropriate software is quite useful if the accuracy is well validated for a wide range of compounds. Unfortunately, however, the computed values of pK_a are often inaccurate at present (13,14).

The first work on pK_a determination by zone electrophoresis using paper strips was described by Waldron-Edward in 1965 (15). Also, Kiso et al. in 1968 showed the relationship between pH, mobility, and pK_a using a hyperbolic tangent function (16). Unfortunately, these methods had not been widely accepted because of the manual operation and lower reproducibility of the paper electrophoresis format. The automated capillary electrophoresis (CE) instrument allows rapid and accurate pK_a determination. Beckers et al. showed that thermodynamic pK_a (pK_a^{th}) and absolute ionic mobility values of several monovalent weak acids were determined accurately using effective mobility and activity at two pH points (17). Cai et al. reported pK_a values of two monovalent weak bases and *p*-aminobenzoic acid (18). Cleveland et al. established the thermodynamic pK_a determination method using nonlinear regression analysis for monovalent compounds (19). We derived the general equation and applied it to multivalent compounds (20). Until then, there were many reports on pK_a determination by CE for cephalosporins (21), sulfonated azo-dyes (22), ropinirole and its impurities (23), cytokinins (24), and so on.

© 2003 by Marcel Dekker, Inc.

The most attractive feature of this technique is its universal applicability to a wide range of compounds; i.e., the mobility always shifts when the extent of ionization of the analyte is modified, because mobility is proportional to net charge. Therefore, unlike the spectrophotometric method, the applicability of CE method is independent of the structural diversity of the analytes. In addition, the detection limit of pK_a by capillary electrophoresis with an ultraviolet (UV) detector is approximately 10^{-6} M (19,20). However, the CE method has one disadvantage: Measurements under acidic conditions are quite time-consuming and less reproducible because of the suppression of the electroosmotic flow (EOF) inside the fused-silica capillary (25). The use of an anionic polymer-coated capillary was effective in overcoming this shortfall (26), but the analysis time remained unsatisfactory for meeting the requirement of drug discovery processes. Recently, three different groups reported the faster CE methods for pK_a determination using the assistance of pressure (14,27–29). Among them, we accomplished the highest throughput (more than 96 compounds per day) using the combination of pressure with photodiode array (PDA) detection, which implies that the analysis of a compounds library based on microplate was possible (14,27).

In this section, the conventional CE method for pK_a determination as well as the rapid method with pressure and a PDA is described. In addition, the theoretical consideration for different models employed so far is discussed.

B. Theory and Method

1. Theory

For a monobasic weak acid, HA, the thermodymanic dissociation constant (K_a^{th}) is defined as follows:

$$K_a^{\text{th}} = \frac{\gamma_{A^-}}{\gamma_{HA}} \times \frac{\{H^+\}[A^-]}{[HA]} = \frac{\gamma_{A^-}}{\gamma_{HA}} K_a' \tag{1}$$

where γ is an activity coefficient and $\{H^+\}$ is the activity of a proton. Assuming that γ_{HA} is equal to 1, Eq. (1) becomes

$$pK_a^{\text{th}} = pK_a' - \log \gamma_{A^-} \tag{2}$$

where K_a' is an acidity constant defined as

$$K_a' = \frac{\{H^+\}[A^-]}{[HA]} \tag{3}$$

The activity coefficient of the anion A^- in dilute solutions can be calculated from Debye–Hückel theory as follows:

© 2003 by Marcel Dekker, Inc.

$$-\log\ \gamma_{A^-} = \frac{0.5085z^2\sqrt{I}}{1\ +\ 0.3281a\sqrt{I}} \tag{4}$$

where z is the valence of the ion, I is the ionic strength of the background electrolyte, and a, which is ion size, in angstroms, is generally unknown and which is assumed to be 5 Å through this study. This equation is valid when the ionic strength is less than 0.1 and the temperature is 25°C. Substitution of Eq. (4) into Eq. (2) gives

$$\mathrm{p}K_a^{\mathrm{th}} = \mathrm{p}K_a' + \frac{0.5085z^2\sqrt{I}}{1\ +\ 0.3281a\sqrt{I}} \tag{5}$$

The effective mobility can be expressed in another form:

$$\mu_{\mathrm{eff}} = Z \times \mu_{A^-} \tag{6}$$

where μ_{A^-} (>0) is a constant equal to the mobility of the perfectly dissociated ion at an ionic strength and Z is the charge number, given by

$$Z = \frac{(0)[\mathrm{HA}] + (-1)[\mathrm{A}^-]}{[\mathrm{HA}] + [\mathrm{A}^-]} \tag{7}$$

The effective mobility, calculated from Eqs. (3), (6), and (7), is given by

$$\mu_{\mathrm{eff}} = \frac{-K_a'}{K_a' + \{\mathrm{H}^+\}} \times \mu_{A^-} \tag{8}$$

The negative sign indicates mobilization toward the anode. Hence, the thermodynamic dissociation constant for the weak acid is obtained from Eqs. (5) and (8) as follows:

$$\mathrm{p}K_a^{\mathrm{th}} = \mathrm{pH} - \log\left(\frac{-\mu_{\mathrm{eff}}}{\mu_{A^-} + \mu_{\mathrm{eff}}}\right) + \frac{0.5085z^2\sqrt{I}}{1\ +\ 0.3281a\sqrt{I}} \tag{9}$$

For a weak base, analogous equations are derived as

$$\mu_{\mathrm{eff}} = \frac{\{\mathrm{H}^+\}}{K_a' + \{\mathrm{H}^+\}} \times \mu_{A^-} \tag{10}$$

$$\mathrm{p}K_b^{\mathrm{th}} = \mathrm{pH} + \log\left(\frac{\mu_{\mathrm{eff}}}{\mu_{A^-} - \mu_{\mathrm{eff}}}\right) - \frac{0.5085z^2\sqrt{I}}{1\ +\ 0.3281a\sqrt{I}} \tag{11}$$

For multivalent ions, an equation representing the solute mobility must be derived that considers all the existing ionic species. For instance, the following equilibrium was established for an ampholyte, $\mathrm{BH}_n\mathrm{A}$:

© 2003 by Marcel Dekker, Inc.

$$\mathrm{BA}^{n-} \overset{+H^+}{\rightleftharpoons} \cdots \mathrm{BH}_{n-i}A^{i-} \cdots \mathrm{BH}_{n-1}\mathrm{A}^- \overset{+H^+}{\rightleftharpoons} \mathrm{BH}_n\mathrm{A} \overset{+H^+}{\rightleftharpoons}$$
$$\mathrm{BH}_{n+1}\mathrm{A}^+ \cdots \mathrm{BH}_{n+j}\mathrm{A}^{j+} \cdots \overset{+H^+}{\rightleftharpoons} \mathrm{BH}_{n+m}\mathrm{A}^{m+} \tag{12}$$

Thus, we obtain the charge number

$$\begin{aligned} Z &= \frac{-\sum_{i=1}^{n} i[\mathrm{BH}_{n-i}\mathrm{A}^{i-}] + \sum_{j=1}^{m} j[\mathrm{BH}_{n+j}\mathrm{A}^{j+}]}{\sum_{i=1}^{n} [\mathrm{BH}_{n-i}\mathrm{A}^{i-}] + [\mathrm{BH}_n A] + \sum_{j=1}^{m} [\mathrm{BH}_{n+j}\mathrm{A}^{j+}]} \\ &= \frac{-f(n)\sum_{i=1}^{n}\left(\dfrac{i}{\{\mathrm{H}^+\}^i}\prod_{k=1}^{i} K'_{ak}\right) + f(m)\sum_{j=1}^{m}\dfrac{j\{\mathrm{H}^+\}^j}{\prod_{l=1}^{j} K'_{bl}}}{f(n)\sum_{i=1}^{n}\left(\dfrac{\prod_{k=1}^{i} K'_{ak}}{\{\mathrm{H}^+\}^i}\right) + 1 + f(m)\sum_{j=1}^{m}\left(\dfrac{\{\mathrm{H}^+\}^j}{\prod_{l=1}^{j} K'_{bl}}\right)} \end{aligned} \tag{13}$$

where $f(x)$, K'_{ai}, and K'_{bj} are given by

$$f(x) = 0 \quad (x = 0), \qquad f(x) = 1 \quad (x \neq 0) \tag{14}$$

$$K'_{ai} = \frac{\{\mathrm{H}^+\}[\mathrm{BH}_{n-i}\mathrm{A}^{i-}]}{[\mathrm{BH}_{n-i+1}\mathrm{A}^{(i-1)-}]} \quad (i = 1, 2, \ldots, n) \tag{15}$$

$$K'_{bj} = \frac{\{\mathrm{H}^+\}\lfloor \mathrm{BH}_{n+j-1}\mathrm{A}^{(j-1)-}\rfloor}{[\mathrm{BH}_{n+j}\mathrm{A}^{j+}]} \quad (j = 1, 2, \ldots, m) \tag{16}$$

with α_i (>0) and β_j defined as the mobility of $\mathrm{BH}_{n-i}\mathrm{A}^{i-}$ and $\mathrm{BH}_{n+j}\mathrm{A}^{j+}$, respectively, at an ionic strength. Then, given that α_i is not equal to $i\alpha_1$, the effective mobility is given by

$$\mu_{\mathrm{eff}} = \frac{-f(n)\sum_{i=1}^{n}\left(\dfrac{\alpha_i}{\{\mathrm{H}^+\}^i}\prod_{k=1}^{i} K'_{ak}\right) + f(m)\sum_{j=1}^{m}\dfrac{\beta_j\{\mathrm{H}^+\}^j}{\prod_{l=1}^{j} K'_{bl}}}{f(n)\sum_{i=1}^{n}\left(\dfrac{\prod_{k=1}^{i} K'_{ak}}{\{\mathrm{H}^+\}^i}\right) + 1 + f(m)\sum_{j=1}^{m}\left(\dfrac{\{\mathrm{H}^+\}^j}{\prod_{l=1}^{j} K'_{bl}}\right)} \tag{17}$$

© 2003 by Marcel Dekker, Inc.

2. Method

The method for pK_a determination consists of three steps:

1. Preparation of buffers with the same ionic strength
2. Measurement of effective mobilities at pHs
3. Regression analysis of the pH-metric mobility data to obtain pK_a.

Table 1 shows an example of buffers with $I = 0.05$.

In step 2, the migration times of the solute and the marker of the electroosmosis, such as mesityl oxide, were measured at each pH and converted to the effective mobility. When the CE instrument is equipped with a photodiode array detector, the spectrophotometric method is available simultaneously. The buffers should be exchanged every five runs, because the pH of the buffer was changed by electrolysis during CE analyses. The details of the experimental conditions are described in Ref. 20.

In step 3, a multiline-fitting program was run to optimize the pK_a' values to minimize the sum of residual squares between calculated and observed mobilities from Eq. (17). Figure 2 shows an example of the MS Excel spreadsheet for pK_a' calculation. The solver function of MS Excel could be used to perform the multiline-fitting analysis.

For the rapid pK_a measurement with daily throughput of 96 compounds using a pressure-assisted mode with a photodiode array detector, the following modifications were required.

Sample preparation: 10 *mM* stock solutions in dimethylsulfoxide (DMSO) were used.

Pressure application: 1.5 psi was applied during each CE run.

Peak separation by wavelength: The migration times of the solute and DMSO were measured at different wavelengths.

Bundling the methods at different pHs: The methods at measured pHs

Table 1 Preparation of CE Buffers

pH range	Constituent	Stock solution	Ionic strength
2.7–3.3	Phosphate	1 *M* H_3PO_4/1 *M* NaH_2PO_4	0.05
3.4–5.4	Acetate	1 *M* CH_3COOH/1 *M* CH_3COONa	0.05
5.7–8.0	Phosphate	0.1 *M* NaH_2PO_4/0.1 *M* Na_2HPO_4	0.05
7.5–9.2	Borate	0.1 *M* $Na_2B_4O_7$/0.4 *M* H_3BO_3	0.05
9.2–12.1	Borate	0.1 *M* $Na_2B_4O_7$/0.1 *N* NaOH	0.05

© 2003 by Marcel Dekker, Inc.

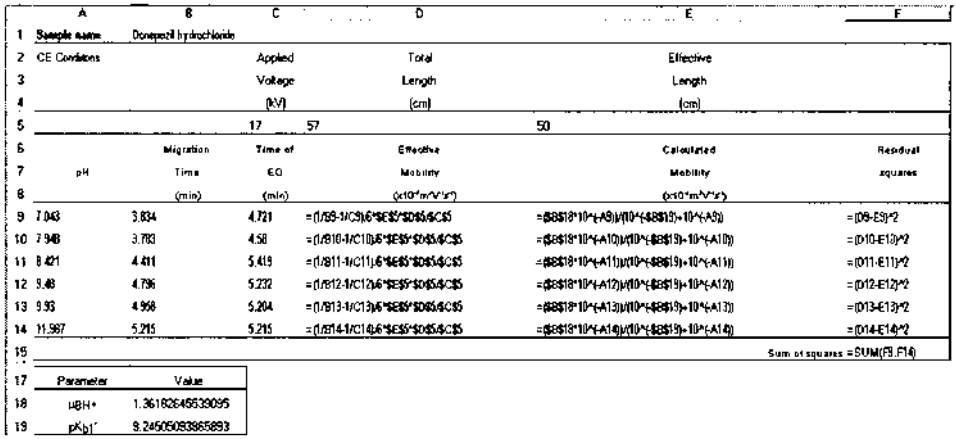

	A	B	C	D	E	F
1	Sample name	Donepezil hydrochloride				
2	CE Conditions		Applied	Total	Effective	
3			Voltage	Length	Length	
4			(kV)	(cm)	(cm)	
5			17	57	50	
6		Migration	Time of	Effective	Calculated	Residual
7	pH	Time	EO	Mobility	Mobility	squares
8		(min)	(min)	(x10^-9 m^2/V*s)	(x10^-9 m^2/V*s)	
9	7.043	3.834	4.721	=(1/59-1/C9)/6*$E$5/$D$5/$C$5	=($B$18*10^(-A9))/(10^(-$B$19)+10^(-A9))	=(D9-E9)^2
10	7.948	3.783	4.58	=(1/610-1/C10)/6*$E$5/$D$5/$C$5	=($B$18*10^(-A10))/(10^(-$B$19)+10^(-A10))	=(D10-E10)^2
11	8.421	4.411	5.419	=(1/611-1/C11)/6*$E$5/$D$5/$C$5	=($B$18*10^(-A11))/(10^(-$B$19)+10^(-A11))	=(D11-E11)^2
12	9.48	4.796	5.232	=(1/612-1/C12)/6*$E$5/$D$5/$C$5	=($B$18*10^(-A12))/(10^(-$B$19)+10^(-A12))	=(D12-E12)^2
13	9.93	4.958	5.204	=(1/613-1/C13)/6*$E$5/$D$5/$C$5	=($B$18*10^(-A13))/(10^(-$B$19)+10^(-A13))	=(D13-E13)^2
14	11.987	5.215	5.215	=(1/614-1/C14)/6*$E$5/$D$5/$C$5	=($B$18*10^(-A14))/(10^(-$B$19)+10^(-A14))	=(D14-E14)^2
15						Sum of squares =SUM(F9:F14)

17	Parameter	Value
18	μ_{BH^+}	1.361826456539095
19	pK_{b1}'	9.245050933865893

Fig. 2 MS Excel® spreadsheet for multiline-fitting analysis.

were bundled into one method to shorten the run time as well as the data analysis time.

In detail, 50 μL each of the sample stock solutions of the maximum 96 compounds in DMSO (10–30 *mM*) were prepared in a 96-well microplate. Then, 10 μL of each solution was transferred to each well of a 96-well sample tray of the CE instrument, diluted 20-fold with water. The transfer and dilution steps were done automatically, using an autodropper, in less than 1 minute. The separation buffers employed were the same as those for the nonpressure mode (nine buffers with pH 3–11). An untreated fused-silica capillary with 50-μm ID and 31-cm length was employed. Applied voltage was 10 kV. Pressure at 1.5 psi was applied at the anode vial. The time program of the method consisted of nine cycles of three steps, such as a buffer-rinsing step (100 psi, 15 s), an injection step (0.5 psi, 10 s), and a separation step (0.9 or 1.5 min). The obtained migration times for the DMSO and the drugs at appropriate wavelength were converted to effective mobilities as follows:

$$\mu_{eff} = \left\{ \frac{1}{(t_m - a(n-1))} - \frac{1}{(t_0 - a(n-1))} \right\} \times \frac{Ll}{V} \tag{18}$$

where μ_{eff} is the effective mobility, t_m is the migration time of the drug, t_0 is the migration time of DMSO, L is the total length of the capillary, l is the length to the detector, V is the applied voltage, a is the time for one cycle, and n is the number of cycles. Then the same procedure as for

© 2003 by Marcel Dekker, Inc.

the normal CE mode was applied to obtain pK_a' from the effective mobilities at pHs.

Here, the rinsing and other preparation steps are included in the time scale. The type of data registration may be different in other commercial instruments.

C. Evaluation of a Typical pH–Mobility Curve

Figure 3 shows a typical example of the pH–mobility curve for a monobasic drug, donepezil hydrochloride. The observed mobilities at different pHs were well in agreement with the regressed values from Eq. (17). The obtained pK_a value is 9.2, which is consistent with the result via the UV method (9.1). Similar results were reported for weak acids, amphoteric compounds, as well as peptides with seven ionic groups (20).

1. Calculation Procedure

So far, two different approaches have been reported for calculating the thermodynamic pK_a value from the mobility at different pHs. Gluck et al. developed the corrected-pH approach (30). They used buffers with different ionic strengths and performed the regression analysis using the following equation for weak acid:

$$\mu_{\text{eff}} = \frac{[\text{H}_c]}{K_a^{\text{th}} + [\text{H}_c]} \cdot \mu_A \tag{19}$$

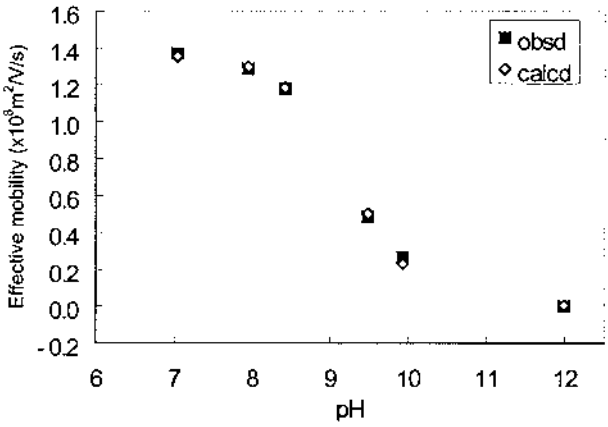

Fig. 3 Dependence of effective mobility on pH for donepezil hydrochloride.

© 2003 by Marcel Dekker, Inc.

where

$$pH_c = pH - \log \gamma \tag{20}$$

In contrast, we developed another approach using buffers with the same ionic strength, where the regression analysis was performed using Eq. (17) to determine not pK_a^{th} but pK_a'. Then, pK_a^{th} was calculated from log γ using Eq. (2).

Although these approaches seem to be similar, the former method has several limitations; it should be recognized that intrinsic mobility (μ_{A^-}) depends on the ionic strength of the buffer, as shown in Ref. 17. Also, the activity coefficients of the zwitterions could not be calculated via the Debye–Hückel equation, and other methods, such as melting point depression, should be used to obtain the activity coefficients of the zwitterions (31). On the other hand, the latter method is directly applicable to the zwitterions to obtain their acidity constants.

The other point of employing these methods is the pH range for measurement. It is well known that at a low pH less than 3 or a high pH over 11, the interaction between solutes and proton or hydroxide ion should be considered, and the measurement values at this pH range include error (31).

Another cause of error is the intrinsic mobility of multiply charged species. The mobility of doubly charged species is not always double the mobility of a single-charged species, as is the case with betahistine (14). Although some groups used this invalid assumption (18,28), this is one cause error.

2. Buffer

The buffer constituents are also important for measuring the proper electrophoretic mobility. So far, phosphate, acetate, borate, citrate, formate, HEPES, CHES, MES, CAPS, AMPSO, TAPS, Tricine, MOPS, and ACES have been used. We reported that the influence of these ingredients on the mobility of some drugs was negligible (20). Also, Gluck & Cleveland (32) corrected the mobility of solutes using the mobility of toluenesulfonic acid, whose charge, i.e., mobility, should be constant in the measured pH range. Consequently, the obtained pK_a was independent of the mobility correction. They also reported that the pH correction using a reference solute with the known pK_a value did not improve the accuracy of the measurement. They concluded that pH measurement of the buffers employed should be performed using a pH meter prior to analysis. The change of pH during CE analysis should also be considered, because the electrolysis reaction occurs in the electrode vial. This change depends on the volume and the concentration of the buffer

© 2003 by Marcel Dekker, Inc.

as well as on the analysis time for one run. Jia et al. reported the stability of buffer pH (28). Under their conditions, the pH stability was adequate for a 20-compound run, although CO_2 absorption should be considered, especially for pH 10 and 11 buffers.

3. Effect of Temperature

In CE, temperature control is quite important (see Chapter 1), because the viscosity of the buffer employed depends on the temperature. In addition, in the case of pK_a measurement, the pK_a of the solute as well as the pH of the buffer is changed when the temperature is changed. In our method described earlier, the value of the applied voltage was set according to the deviation from Ohm's law, which results from the temperature rise of the solution inside the capillary (20). Gluck et al. measured the buffer temperature using Co(II), which has temperature-dependent absorbance at 495 nm (30). Under their conditions, the temperature rise was less than 1 degree.

4. Pressure-Assisted System for Rapid Measurement (14)

Figure 4 presents an example of rapid pK_a measurement using a pressure-assisted system in combination with a photodiode array (PDA) detector. The migration time of DMSO (EOF marker) was measured at 220 nm, whereas the migration time of the analyte, naphazoline, was measured at 270 nm. The CE run time as well as data analysis time was drastically reduced. Consequently, this system allows the analysis of more than 96 compounds in one day. The limitation of this method is the application to drugs without UV chromophore at more than 250 nm. In some cases, it was effective to remove DMSO by evaporation under vacuum followed by the addition of methanol or acetonitrile as a neutral marker.

5. Limitation of the CE Method for pK_a Measurement

One of the limitations is the application of solutes with solubility lower than 0.1 μg/mL. In general, they could not be analyzed by this method at present. In such cases, the addition of some organic solvents to the separation buffers followed by extrapolation to 100% aqueous solutions was effective, although the throughput was decreased. Also, one should be careful when applying this method to solutes with close pK_a values, as pointed out Ref. 30.

D. Conclusion

Capillary electrophoresis is one of the powerful tools for pK_a measurement, especially when the pressure-assisted CE system with PDA detector is employed. It allows one to measure pK_a values of more than 96 candidate drugs

© 2003 by Marcel Dekker, Inc.

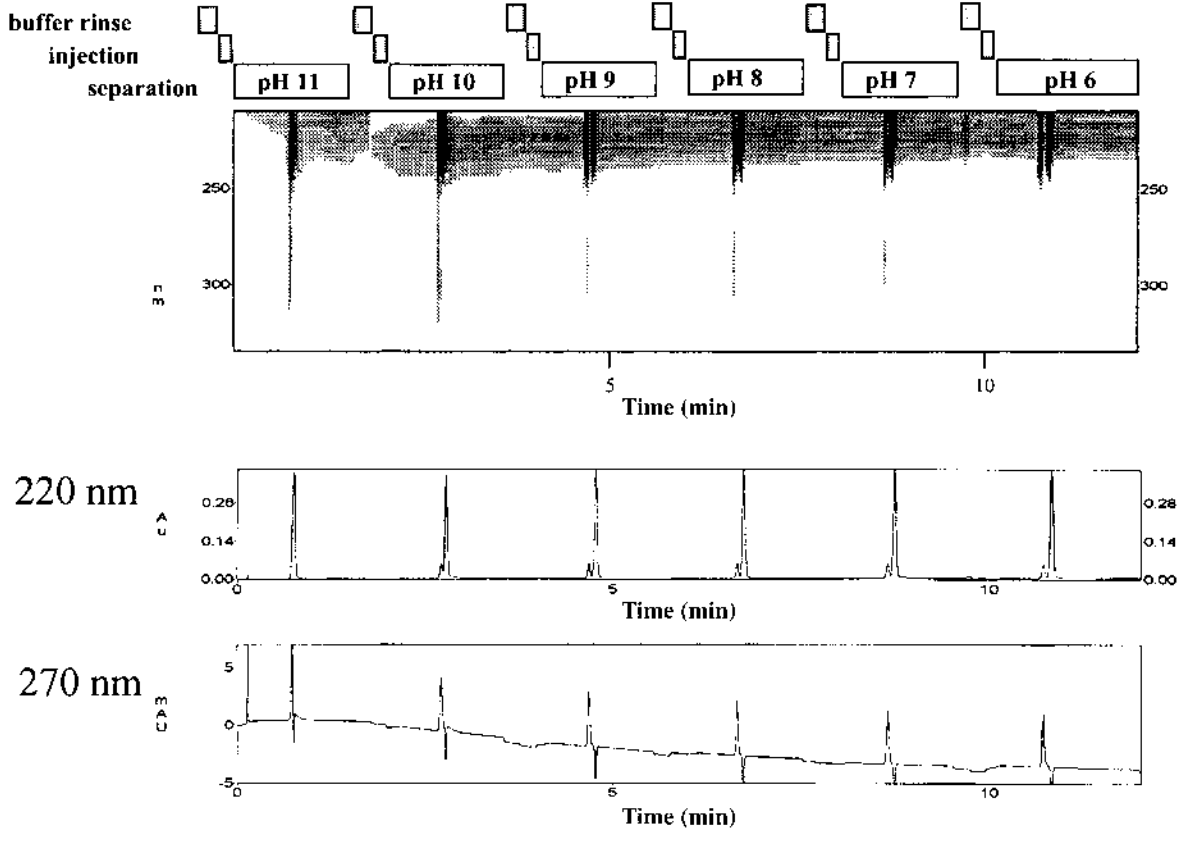

Fig. 4 Electropherograms of naphazoline for rapid pK_a determination.

© 2003 by Marcel Dekker, Inc.

in one day, and the information obtained should facilitate the selection of an appropriate drug or the design of an optimal structure in the stage of lead optimization. In addition, this method would be useful for characterizing the compound libraries, although more throughput should be required.

II. LIPOPHILICITY

A. Introduction

Lipophilicity is an essential property of molecules whose roles in biological systems are numerous and essential, because it is highly related to solubility, membrane permeability, as well as protein binding, and so on. So far, the logarithm of partition coefficient between 1-octanol and water, log P_{ow}, has been used for a lipophilicity scale (33). However, the measurement of log P_{ow} by conventional shake-flask technique has several limitations, such as reproducibility, speed, and sample amount required. Alternative approaches using reversed-phase HPLC and EKC are promising because of the lower consumption of samples and easy automation. In RP-HPLC, when C8 or C18 bonded phase was used, some correction for hydrogen-bond ability would be required (34). Another approach in RP-HPLC is to use octanol (1,35) or phospholipid (36) to coat the stationary phase dynamically. However, there are some limitations, such as the low stability of the dynamic-coated stationary phase and inapplicability to the ionic species (35). Recently, phospholipid-bonded columns were commercialized as ''IAM chromatography'' columns (2). Unfortunately, several groups reported that the stability of the stationary phase was not satisfactory (37). On the other hand, in EKC, the pseudostationary phases, such as micelles (38–46) and microemulsion (47–49), have been examined as a tool to estimate log P_{ow} indirectly. Among them, sodium cholate (SC) micelle (42) and SDS-heptane-1-butanol-buffer microemulsion (47) showed the best correlation to log P_{ow}. This conclusion was also supported by linear free-energy relationship (LFER) analysis [50] as well as solvation-energy descriptor (SED) vector analysis (51), as described later. Recently, two groups reported the application of microemulsion electrokinetic chromatography (MEEKC) (see also Chapter 6) to pesticides and druglike compound libraries (52,53). The limitation of this indirect approach is its application to ionic compounds, because the interaction between ionic solutes and ionic surfactants should be considered in both aqueous and pseudostationary phases (49). Gluck et al. reported the measurement at pH 1.19 and 12 to neutralize the ionic solutes (54). However, the analysis time at pH 1.19 was quite long, because of the EOF suppression. We reported a pH dependence of lipophilicity from MEEKC. In this case, SMIL-coated capillary (sulfated polymer coating) fa-

© 2003 by Marcel Dekker, Inc.

cilitated the CE run time (55). Also, Kibbey et al. used sulfonic acid–coated capillary and measured log Pow indirectly at pH 3 and 10, depending on the pH where the solute was neutralized (53).

Regarding other pseudostationary phases for measurement of lipophilicity or lipophilicity-related properties (e.g., intestinal absorption, brain penetration), there are several reports on the use of vesicles such as phospholipid bilayer liposome (56–58), lysophospholipid micelle (59), DTAB/SDS vesicle (60), and double-chain synthetic surfactant vesicle (61), which are described in other chapters.

In this section, MEEKC with SDS-heptane-1-butanol buffer is described as a tool for determination of lipophilicity of drugs. In addition, the comparison between the scale from MEEKC and other scales will be presented.

B. Theory and Method

1. Theory

In EKC, the retention factor, k, of a neutral solute can be calculated as follows:

$$k = \frac{t_s - t_0}{t_0(1 - t_s/t_m)} \tag{21}$$

where t_0, t_s, and t_m are the migration times of the electro-osmotic flow, the solute, and the microemulsion, respectively. When the volume of the microemulsion phase, V_m, is constant, k is proportional to the partition coefficient between the two phases, P_{mw}, as follows:

$$k = P_{mw}\left(\frac{V_m}{V_{aq}}\right) \tag{22}$$

where V_{aq} is the volume of the aqueous phase. Therefore, when the partitioning behavior in both the microemulsion system and the other system is subject to the same properties of the solutes, the logarithm of k can be represented by

$$\log k = a \log P + b \tag{23}$$

This linear relationship is based on the change in the free energy in the partitioning process between the two phases.

For MEEKC, the migration index (MI) scale is quite effective in improving the reproducibility. This was introduced by Muijselaar et al. in MEKC (44) and then modified to extend the range of the migration window of the reference compounds as follows (47):

© 2003 by Marcel Dekker, Inc.

$$\text{MI} = c \log k + d \tag{24}$$

where c and d are the slope and the intercept, respectively, of a calibration line between log k values of reference solutes such as alkylbenzenes and their carbon number. In addition, a solute, with its MI value determined previously using alkylbenzenes, could be added to a set of the reference standards. The MI is applied for all neutral solutes migrating from t_0 to t_m, and this is independent of the volume of the microemulsion as well as the micelles in MEKC. Therefore, the influence of the variation in the microemulsion preparation is minimized.

2. Method

a. Preparation of Microemulsion. SDS (1.44 wt%), 1-butanol (6.49 wt%), and heptane (0.82 wt%) were added to the buffer solution of 50 *mM* phosphate/100 *mM* borate at pH 7.0 and mixed by ultrasonication in a water bath for 30 min. The transparent solution was then left to stand for 1 hour at room temperature. The solution was filtered through a 0.45-μm filter prior to use.

b. MEEKC Conditions. An uncoated fused-silica capillary of 50-μm ID and 27-cm length was employed under neutral conditions. For the measurement under acidic conditions, the use of dextran sulfate–coated capillary (26,55) was effective to reduce the run time. The wavelength of the UV detection was set at 214 nm. The applied voltage was 7.5 kV, and the temperature of the capillary coolant was 25°C. The tracers for the aqueous and microemulsion phases were methanol and dodecylbenzene, respectively. The reference compounds were benzaldehyde, benzene, toluene, ethylbenzene, propylbenzene, and butylbenzene. All samples were dissolved in the microemulsion solution.

C. Results and Discussion

It is well known that partitioning behavior is greatly affected by the hydrogen bond abilities of both the solvents and the solutes (34). To investigate the influence of the hydrogen bond effect on the microemulsion system, some heteroaromatic compounds, which contain a ring heteroatom such as nitrogen, oxygen, or sulfur, and their alkyl derivatives were examined, and the obtained MI values were compared with log P_{ow}. Consequently, the obtained MI values were highly correlated with log P_{ow} without any correction as follows:

$$\log P_{ow} = 0.518\text{MI} - 0.854 \tag{25}$$

$$N = 53, \qquad r = 0.996, \qquad s = 0.094, \qquad F = 6083$$

© 2003 by Marcel Dekker, Inc.

where r is the correlation coefficient, s is the standard deviation from regression, and F is the value of the F-ratio between regression and residual variances. In Fig. 5, the relationship between log P_{ow} from Eq. (25) and observed log P_{ow} is shown. The deviation was within 0.2 log P units for 53 solutes. Recently Klotz et al. also reported a similar observation for a wider range of the compounds, such as pesticides (52).

1. Reproducibility

For the measurement of log P_{ow}, a highly reproducible method is required, because log P_{ow} should be a single and universal scale. We reported that batch-to-batch reproducibility of k for nitrobenzene was over 20%, compared to less than 1% when MI was used instead of k. The RSD values for nine solutes with log P_{ow} of 1.10–3.37 are less than 0.7% for MI (47). This is because MI is independent of the concentration of the components when the structure of the aggregate is not changed (44).

2. Thermodynamic Parameters

We reported the thermodynamic parameters for the partitioning process for 14 phenol derivatives (47). Values of enthalpy and entropy changes ranged

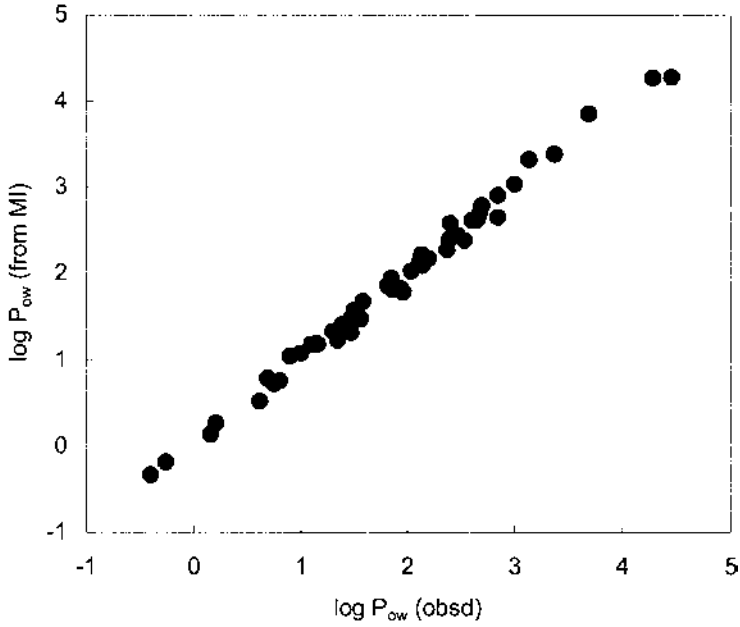

Fig. 5 Relationship between observed log P_{ow} values and those calculated from MI.

© 2003 by Marcel Dekker, Inc.

from −16.5 to −3.1 kJ/mol and from −9.5 to 22.3 J/mol/K, respectively. These values in the microemulsion system were slightly larger than those in the SDS micellar system. Regarding the free-energy changes, the microemulsion was correlated with the micellar system (correlation coefficient, r, is 0.93). However, surprisingly, not only enthalpy changes but also entropy changes in both systems showed little correlation (r = 0.44 for enthalpy change, 0.33 for entropy change). Interestingly, the microemulsion system was similar to gel-phase liposome (r = 0.71 for enthalpy change, 0.75 for entropy change), which was a more reasonable model of biomembrane, although the reason for the correlation was not clear.

3. Linear Free-Energy Relationship (LFER)

The LFER, which is also known as the *linear solvation-energy relationship* (LSER), was developed by Taft et al. (62) and established by Abraham and coworkers (63). The LFER has been used for characterization of two-phase partitioning processes of solutes such as octanol–water and chromatographic processes such as HPLC, GLC, and TLC. The general equation is expressed as follows:

$$\log \text{SP} = c + r\text{R}_2 + s\pi_2^{\text{H}} + a \sum \alpha_2^{\text{H}} + b \sum \beta_2 + vV_{\text{x}} \tag{26}$$

where SP is some property of a series of solutes in a given solvent system, R_2 is the excess molar refraction, π_2^{H} is the solute dipolarity/polarizability, $\Sigma\, \alpha_2^{\text{H}}$ and $\Sigma\, \beta_2$ are the solute hydrogen-bond acidity and basicity, respectively, and V_x is the McGowan characteristic volume. The obtained coefficients indicate the contribution of each descriptor to the whole process, and the set of these coefficients characterizes the system by comparing it with sets from other, different systems. We applied this approach to MEEKC and indicated that the correlation between MEEKC and octanol–water systems is not due to some fortuitous cancellation of effects, but arises because the solute factors that influence the two processes are exactly the same (50).

In addition, to quantify the analogy between different log SP values, we developed an approach where the obtained coefficients are used as a five-dimensional vector and the analogy is expressed as an angle between two target vectors (51).

The SED coefficient vector of lipophilicity scale i (LS_i), $\vec{\omega}_i$, is defined as follows:

$$\vec{\omega}_i = (r_i,\ s_i,\ a_i,\ b_i,\ v_i) \tag{27}$$

© 2003 by Marcel Dekker, Inc.

The analogy between LS_i and LS_j is expressed as cos θ_{ij} between $\vec{\omega}_i$ and $\vec{\omega}_j$ as follows:

$$\cos\ \theta_{ij} = \frac{\vec{\omega}_i \cdot \vec{\omega}_j}{|\vec{\omega}_i||\vec{\omega}_j|}$$

$$= \frac{r_i r_j + s_i s_j + a_i a_j + b_i b_j + v_i v_j}{\sqrt{r_i^2 + s_i^2 + a_i^2 + b_i^2 + v_i^2}\sqrt{r_j^2 + s_j^2 + a_j^2 + b_j^2 + v_j^2}} \qquad (28)$$

Thus, as the correlation gets higher, the value of cos θ_{ij} gets closer to 1. When the analogy of LS_j (j = 1, 2, . . .) to LS_i is examined, the analogy ranking of LS_j (j = 1, 2, . . .) to LS_i is established according to cos θ_{ij}.

Using this vector approach, the analogy between log P_{ow} and other reported systems was quantified. The results are indicated in Table 2.

Consequently, the SDS microemulsion system is the best model for indirect measurement of log P_{ow}. However, this is valid only for neutral solutes. We reported that the relationship between MI and log P_{ow} for ionic solutes is different from that for neutral solutes (49). This would be caused by the ionic interaction between ionic solutes and the ionic microemulsion as well as ionic surfactant monomer in the aqueous phase. Kibbey et al. used pH 10 buffer for neutral and weak basic compounds and pH 3 buffer for weak acidic compounds (53). Although their purpose was to avoid measuring electrophoretic mobility in the aqueous phase, this approach is also helpful for measuring log P_{ow} indirectly.

Table 2 Analogy Between Octanol–Water and Other Systems

Analogy ranking	System	Analogy (cos θ)
1	SDS microemulsion	0.999
2	SC micelle	0.998
3	RP-TLC	0.986
4	ODS-HPLC	0.983
5	IAM-HPLC	0.983
6	SDS micelle	0.974
7	DTAC micelle	0.972
8	Alkane–water	0.877

© 2003 by Marcel Dekker, Inc.

D. Conclusion

Electrokinetic chromatography (EKC) using microemulsion is one of the most powerful tools for the rapid measurement of log P_{ow} with high reproducibility. Because it is relatively easy to manipulate the pseudostationary phases of EKC, a lot of phases have been reported for the measurement not only of physicochemical properties but also of the separation selectivity, such as polymer micelles (64) and double-chain surfactant vesicles (56–58,60,61). These phases are also interesting in terms of the correlation to bioactivity.

III. OTHER PARAMETERS

Solubility is one of the most important physicochemical properties for orally administrated drugs, and log P_{ow} and melting point (mp) are used as predictors, because log P_{ow} and mp are correlated with the solvation energy and the crystal lattice energy, respectively. Recently, rapid solubility measurement methods using a DMSO dissolution process were reported (3,4,65,66). The values obtained reflect only the solvation process, not the breakage process of the crystal packing. Therefore, these solubility values were well correlated with lipophilicity such as log P_{ow}. Thus, some approaches to lipophilicity measurement, such as MEEKC, should be helpful in predicting solvation-solubility. However, for thermodynamic solubility, in my knowledge there is no method with satisfactory throughput for a drug discovery stage.

Membrane permeability is another important parameter for drugs, because it is related to intestinal absorption and brain penetration. Lipophilicity is also useful in predicting these phenomena. In addition, liposome with phospholipid would be more reliable for measuring biomembrane permeability. Recently, some groups reported an EKC approach with phospholipid vesicles (56–58).

Plasma protein binding is also an important parameter in the pharmacokinetic field. Frontal analysis combined with capillary zone electrophoresis (CZE-FA) (67–69) is a powerful technique for high-throughput assay, because it is relatively rapid and easy to automate, in comparison with conventional methods such as dialysis, ultrafiltration, and ultracentrifugation. Recently, we introduced the EKC approach with ionic CDs to frontal analysis for anionic drugs that cannot be analyzed by conventional CZE-FA (70). In this approach, ionic CDs work as an EKC pseudostationary not for proteins but for small solutes.

Capillary electrophoresis is also effective for monitoring the confor-

© 2003 by Marcel Dekker, Inc.

mational stability of proteins. Hilser et al. reported the analysis of thermally induced unfolding of lysozyme using CZE (71). We also reported nanoscale monitoring of the unfolding of recombinant dehydrofolate reductases as well as five other proteins using an in-column incubation method (72). Figure 6 compares the transition temperatures obtained by CE with those obtained by circular dichroism (CD).

Similar approaches were also reported for chemically induced unfolding and a pH-induced one (73,74). Recently, Righetti reviewed the protein unfolding processes measured by CE and other techniques (75).

IV. CONCLUSION

Although CE has been developed as a separation tool, it has quite useful characteristics for measuring the physicochemical properties of drugs with higher throughput and lower sample consumption in comparison with conventional methods. With the recent advances in combinatorial chemistry and in vitro pharmacological assay, rapid and reliable analytical methods for physicochemical parameter measurement are required to accelerate the drug

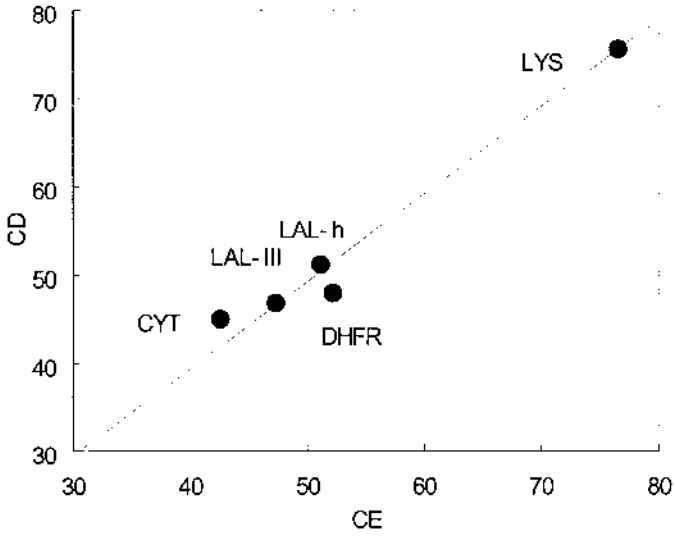

Fig. 6 Transition temperature of protein unfolding measured by CE and CD. Proteins: lysozyme from chicken egg (LYS), α-lactalbumin from human milk (LAL-h), α-lactalbumin type III from bovine milk (LAL-III), cytochrome c from bovine heart (CYT), recombinant dihydrofolate reductase (DHFR).

© 2003 by Marcel Dekker, Inc.

discovery process. To meet this demand, CE has already been used for pK_a and lipophilicity by several pharmaceutical companies for the drug discovery stage (14,28,29,65), and it could be employed for membrane permeability when a suitable pseudostationary phase is established. On the other hand, proteins are also suitable for applying CE to measure their properties. As a tool for physicochemical measurement, CE would be explored more in the pharmaceutical or medicinal field.

ABBREVIATIONS

HEPES	4-(2-hydroxyethyl)piperazine-1-ethanesulfonic acid
CHES	2-(cyclohexylamino)ethanesulfonic acid
MES	2-morpholinoethanesulfonic acid monohydrate
CAPS	3-(cyclohexylamino)-1-propanesulfonic acid
CAPSO	3-(cyclohexylamino)-2-hydroxy-1-propanesulfonic acid
AMPSO	3-([1,1-dimethyl-2-hydroxyethyl]amino)-2-hydroxypropanesulfonic acid
TAPS	[(2-hydroxy-1,1-bis[hydroxymethyl]ethyl)amino]-1-propanesulfonic acid
Tricine	*N*-tris(hydroxymethyl)methylglycine
MOPS	3-morpholinopropanesulfonic acid
ACES	*N*-(carbamoylmethyl)-2-aminoethanesulfonic acid
LFER	linear free-energy relationship
SED	solvation-energy descriptor
SMIL	successive multi-ionic polymer layers
MEEKC	microemulsion electrokinetic chromatography

REFERENCES

1. F Lombardo, MY Shalaeva, KA Tupper, F Gao, MH Abraham. *E* log P_{oct}: A tool for lipophilicity determination in drug discovery. J. Med. Chem. 43:2922–2928 (2000).
2. C Pidgeon, S Ong, H Liu, X Qiu, M Pidgeon, AH Dantzig, J Munroe, WJ Hornback, JS Kasher, L Glunz, T Szczerba. IAM chromatography: an in vitro screening for predicting drug membrane permeability. J. Med. Chem. 38:590–594 (1995).
3. CA Lipinski, F Lombardo, BW Dominy, PJ Feeney. Experimental and computational approaches to estimate solubility and permeability in drug discovery and development settings. Adv. Drug Del. Rev. 16:243–266 (1996).
4. CD Bevan, RS Lloyd. A high-throughput screening method for the determination of aqueous drug solubility using laser nephelometry in microtiter plates. Anal. Chem. 72:1781–1787 (2000).

© 2003 by Marcel Dekker, Inc.

5. A Avdeef, CM Berger, C Brownell. pH-Metric solubility: correlation between the acid–base titration and the saturation shake-flask solubility-pH methods. Pharm. Res. 17:85–89 (2000).
6. T Tokumura. A screening system of solubility for drug design and discovery. Pharm. Tech. Japan 16:1839–1847 (2000).
7. K Balon, BU Riebesehl, BW Muller. Drug liposome partitioning as a tool for prediction of human passive intestinal absorption. Pharm. Res. 16:882–888 (1999).
8. M Kancy, F Senner, K Gubernator. Physicochemical high-throughput screening: parallel artificial membrane permeation assay in the description of passive absorption processes. J. Med. Chem. 41:1007–1010 (1998).
9. Danelian E, Larlen A, Karlsson R, Winiwarter S, Hansson A, Lofas S, Lennernas H, Hamalainen MD. SPR biosensor studies of the direct interaction between 27 drugs and a liposome surface: correlation with fraction absorbed in humans. J. Med. Chem. 43:2083–2086 (2000).
10. A Avdeef. Assessment of distribution-pH profiles. In: Pliska, V., Testa B., van de Waterbeemd, H., eds. Lipophilicity in Drug Action and Toxicology. VCH: Weinheim, Germany, 1996, pp 109–139.
11. RI Allen, KJ Box, JEA Comer, KY Tam KY. Multiwavelength spectrophotometric determination of acid dissociation constants of ionizable drugs. J. Pharm. Biomed. Anal. 17:699–712 (1998).
12. JA Lewis, DC Lommen, WD Raddatz, JW Dolan, R Snyder, I Modinar. Computer simulation for prediction of separation as a function of pH for reversed-phase HPLC. I. Accuracy of a theory-based model. J. Chromatogr. 592:183–195 (1992).
13. DD Perrin, B Dempsey, EP Serjeant. pK_a prediction for organic acids and bases. Chapman and Hall: New York, 1981.
14. Y Ishihama, M Nakamura, T Miwa, T Kajima, N Asakawa. A rapid method for pK_a determination of drugs using pressure-assisted capillary electrophoresis with photodiode array detection in drug discovery. J. Pharm. Sci. 91:933–942 (2002).
15. D Waldron-Edward. The microdetermination of acid and base dissociation constants by paper electrophoresis. J. Chromatogr. 20:556–562 (1965).
16. Y Kiso, M Kobayashi, Y Kitaoka, K Kawamoto, J Takada. A theoretical study on the zone mobility–pH curve in paper electrophoresis of low-molecular-weight compounds with a dissociable proton and its application to phosphorus compounds. J. Chromatogr. 36:215–228 (1968).
17. JL Beckers, FM Everaerts, MT Ackermans. Determination of absolute mobilities, pK values, and separation numbers by capillary electrophoresis. Effective mobility as a parameter for screening. J. Chromatogr. 537:407–428 (1991).
18. J Cai, JT Smith, Z El Rassi. Determination of the ionization constants of weak electrolytes by capillary zone electrophoresis. J. High Resolut. Chromaogr. 15: 30–32 (1992).
19. JA Cleveland, MH Benko, SJ Gluck, YM Walbroehl. Automated pK_a determination at low solute concentrations by capillary electrophoresis. J. Chromatogr. A 652:301–308 (1993).

© 2003 by Marcel Dekker, Inc.

20. Y Ishihama, Y Oda, N Asakawa. Microscale determination of dissociation constants of multivalent pharmaceuticals by capillary electrophoresis. J. Pharm. Sci. 83:1500–1507 (1994).
21. Y Mrestani, R Neubert, A Munk, M Wiese. Determination of dissociation constants of cephalosporins by capillary electrophoresis. J. Chromatogr. A 803: 273–278 (1998).
22. M Perez-Urquiza, JL Beltran. Determination of the dissociation constants of sulfonated azo dyes by capillary zone electrophoresis and spectrophotometry methods. J. Chromatogr. A 917:331–336 (2001).
23. P Coufal, K Stulik, HA Claessens, MJ Hardy, M Webb. Determination of the dissociation constants of ropinirole and some impurities and their quantification using capillary zone electrophoresis. J. Chromatogr. B 720:197–204 (1998).
24. P Bartak, P Bednar, Z Stransky, P Bocek, R Vespalec. Determination of dissociation constants of cytokinins by capillary zone electrophoresis. J. Chromatogr. A 878:249–259 (2000).
25. H Katayama, Y Ishihama, N Asakawa. Development of novel capillary coating based on physical adsorption for capillary electrophoresis. Anal. Sci. 14:407–408 (1998).
26. H Katayama, Y Ishihama, N Asakawa. Stable capillary coating with successive multiple ionic polymer layers. Anal. Chem. 70:2254–2260 (1998).
27. Y Ishihama, T Miwa, N. Asakawa. A high-throughput pK_a screening method in drug discovery using capillary electrophoresis. Proceedings of the 20th symposium on capillary electrophoresis, Hyogo, Japan, 2000, pp 104–105.
28. ZJ Jia, T Ramstad, M Zhong. Medium-throughput pK_a screening of pharmaceuticals by pressure-assisted capillary electrophoresis. Electrophoresis 22: 1112–1118 (2001).
29. CE Kibby, SK Poole, B Robinson, JD Jackson, D Durham. An integrated process for measuring the physicochemical properties of drug candidates in a preclinical discovery environment. J. Pharm. Sci. 90:1164–1175 (2001).
30. SJ Gluck, KP Steele, MH Benko. Determination of acidity constants of monoprotic and diprotic acids by capillary electrophoresis. J. Chromatogr. A 745:117–125, 1996.
31. DD Perrin, B Dempsey. Buffers for pH and Metal Ion Control. Chapman and Hall: London, 1974.
32. SJ Gluck, JA Cleveland Jr. Investigation of experimental approaches to the determination of pK_a values by capillary electrophoresis. J. Chromatogr. A 680: 49–56 (1994).
33. C Hansch, D Hoekman, H Gao. Comparative QSAR: toward a deeper understanding of cheicobiological interactions. Chem. Rev. 96:1045–1075 (1996).
34. C Yamagami, M Yokota, N Takao. Hydrogen bond effects of ester and amide groups in heteroaromatic compounds on the relationship between the capacity factor and the octanol–water partition coefficients. J. Chromatogr. A 662:49–60 (1994).
35. M Cichna, P Markl, JFK Huber, Determination of true octanol–water partition coefficients by means of solvent generated liquid–liquid chromatography. J. Pharm. Biomed. Anal. 13:339–351 (1995).

© 2003 by Marcel Dekker, Inc.

36. K Miyake, F Kitaura, N Mizuno, H Terada. Phosphatidylcholine-coated silica as a useful stationary phase for high-performance liquid chromatographic determination of partition coefficients between octanol–water. J. Chromatogr. 389:47–56 (1989).
37. S Demare, D Roy, JY Legendre. J. Liquid Chromatogr. 22:2675 (1999).
38. Y Ishihama, Y Oda, K Uchikawa, N Asakawa. Correlation of octanol–water partition coefficients with capacity factors measured by micellar electrokinetic chromatography. Chem. Pharm. Bull. 42:1525–1527 (1994).
39. N Chen, Y Zhang, S Terabe, T Nakagawa. Effect of physicochemical properties and molecular structure on the micelle–water partition coefficient in micellar electrokinetic chromatography. J. Chromatogr. A 678:327–332 (1994).
40. BJ Herbert, JG Dorsey. *N*-Octanol–water partition coefficient estimation by micellar electrokinetic capillary chromatography. Anal. Chem. 67:744–749 (1995).
41. JT Smith, DV Vinjamoori. Rapid determination of logarithmic partition coefficients between *N*-octanol and water using micellar electrokinetic capillary chromatography. J. Chromatogr. B 669:59–66 (1995).
42. S Yang, JG Bumgarner, LFR Kruk, MG Khaledi. Quantitative structure–activity relationships studies with micellar electrokinetic chromatography. Influence of surfactant type and mixed micelles on estimation of hydrophobicity and bioavailability. J. Chromatogr. A 721:323–335 (1996).
43. MA Garcia, JC Diez-Masa, ML Marina. Correlation between the logarithm of capacity factors for aromatic compounds in micellar electrokinetic chromatography and their octanol–water partition coefficients. J. Chromatogr. A 742:251–256 (1996).
44. PG Muijselaar, HA Claessens, CA Cramers. Characterization of pseudostationary phases in micellar electrokinetic chromatography by applying linear solvation-energy relationships and retention indexes. Anal. Chem. 69:1184–1191 (1997).
45. YS Wu, HK Lee, SFY Li. Rapid estimation of octanol–water partition coefficients of pesticides by micellar electrokinetic chromatography. Electrophoresis 19:1719–1727 (1998).
46. M Hanna, V de Biasi, B Bond, C Salter, AJ Hutt, P Camilleri. Estimation of the partitioning characteristics of drugs: a comparison of a large and diverse drug series utilizing chromatographic and electrophoretic methodology. Anal. Chem. 70:2092–2099 (1998).
47. Y Ishihama, Y Oda, K Uchikawa, N Asakawa. Evaluation of solute hydrophobicity by microemulsion electrokinetic chromatography. Anal. Chem. 67:1588–1595 (1995).
48. Y Ishihama, Y Oda, N Asakawa. A hydrophobicity scale based on the migration index from microemulsion electrokinetic chromatography of anionic solutes. Anal. Chem. 68:1028–1032 (1996).
49. Y Ishihama, Y Oda, N Asakawa. Hydrophobicity of cationic solutes measured by electrokinetic chromatography with cationic microemulsions. Anal. Chem. 68:4281–4284 (1996).
50. MH Abraham, C Treiner, M Roses, C Rafols, Y Ishihama. Linear free-energy

© 2003 by Marcel Dekker, Inc.

relationship analysis of microemulsion electrokinetic chromatographic determination of lipophilicity. J. Chromatogr. A 752:243–249 (1996).
51. Y Ishihama, N Asakawa. Characterization of lipophilicity scales using vectors from solvation-energy descriptors. J. Pharm. Sci. 88:1305–1312 (1999).
52. WL Klotz, MR Schure, JP Foley. Determination of octanol–water partition coefficients of pesticides by microemulsion electrokinetic chromatography. J. Chromatogr. A 930:145–154 (2001).
53. CE Kibbey, SK Poole, B Robinson, JD Jackson, D Durhum. An integrated process for measuring the physicochemical properties of drug candidates in a preclinical discovery environment. J. Pharm. Sci. 90:1164–1175 (2001).
54. SJ Gluck, MH Benko, RK Hallberg, KP Steele. Indirect determination of octanol–water partition coefficients by microemulsion electrokinetic chromatography. J. Chromatogr. A 744:141–146 (1996).
55. Y Ishihama, H Katayama, N Asakawa. Novel sulfated polymer-coated capillary for the determination of hydrophobicity and the dissociation constants of solutes in acidic regions. Proceedings of 10th International Symposium on HPCE and Related Microscale Techniques, Kyoto, 1997, p 112.
56. Y Zhang, R Zhang, S Hjerten, P Lundahl. Liposome capillary electrophoresis for analysis of interactions between lipid bilayers and solutes. Electrophoresis 16:1519–1523 (1995).
57. H Nakamura, I Sugiyama, A Sano. Liposome electrokinetic chromatography as a novel tool for the separation of hydrophobic compounds. Anal. Sci. 12: 973–975 (1996).
58. SK Wiedmer, J Hautala, JM Holopainen, PKJ Kinnunen, M-L Riekkola. Study on liposomes by capillary electrophoresis. Electrophoresis 22:1305–1313 (2001).
59. JA Masucci, GW Caldwell, JP Foley. Comparison of the retention behavior of beta-blockers using immobilized artificial membrane chromatography and lysophospholipid micellar electrokinetic chromatography. J. Chromatogr. A 810: 95–103 (1998).
60. M Hong, BS Weekley, SJ Grieb, JP Foley. Electrokinetic chromatography using thermodynamically stable vesicles and mixed micelles formed from oppositely charged surfactants. Anal. Chem. 70:1394–1403 (1998).
61. AA Agbodjan, H Bui, MG Khaledi. Study of solute partitioning in biomembrane-mimetic pseudophases by electrokinetic chromatography: dihexadecyl phosphate small unilamellar vesicles. Langmuir 17:2893–2899 (2001).
62. RW Taft, MH Abraham, GR Famini, RM Doherty, JL Abboud, MJ Kamlet. Solubility properties in polymers and biological media 5: an analysis of the physicochemical properties which influence octanol–water partition coefficients of aliphatic and aromatic solutes. J. Pharm. Sci. 74:807–814 (1985).
63. MH Abraham. Scales of solute hydrogen-bonding: their construction and application to physicochemical and biological processes. Chem. Soc. Rev. 22: 73–83 (1993).
64. C Fujimoto. Application of linear solvation energy relationships to polymeric pseudostationary phases in micellar electrokinetic chromatography. Electrophoresis 22:1322–1329 (2001).

© 2003 by Marcel Dekker, Inc.

65. EH Kerns. High-throughput physicochemical profiling for drug discovery. J. Pharm. Sci. 90:1838–1858 (2001).
66. Y Sugaya, T Yoshiba, T Kajima, Y Ishihama. Development of solubility screening methods in drug discovery. Yakugakuzasshi 122:237–246 (2002).
67. MHA Busch, JC Kraak, H Poppe. Principles and limitations of methods available for the determination of binding constants with affinity capillary electrophoresis. J. Chromatogr. A 777:329–353 (1997).
68. A Shibukawa, Y Kuroda, T Nakagawa. High-performance frontal analysis for drug–protein binding study. J. Pharm. Biomed. Anal. 18(6):1047–1055 (1999).
69. PA McDonnell, GW Caldwell, JA Masucci. Using capillary electrophoresis/frontal analysis to screen drugs interacting with human serum proteins. Electrophoresis 19:448–454 (1998).
70. Y Ishihama, T Miwa, N Asakawa. Drug–plasma protein binding assay by electrokinetic chromatography–frontal analysis. Electrophoresis 23:951–955 (2002).
71. VJ Hilser, GD Worosila, E Freire. Analysis of thermal-induced proteins folding/unfolding transitions using free-solution capillary electrophoresis. Anal. Biochem. 208:125–131 (1993).
72. Y Ishihama, Y Oda, N Asakawa, M Iwakura. Nanoscale monitoring of the thermally induced unfolding of proteins using capillary electrophoresis with in-column incubation. Anal. Sci. 13:931–938 (1997).
73. F Kilar, S Hjerten. Unfolding of human serum transferrin in urea studied by high-performance capillary electrophoresis. J. Chromatogr. 638:269–276 (1993).
74. M Kats, PC Richberg, DE Hughes. Conformational diversity and conformational transitions of a monoclonal antibody monitored by circular dichroism and capillary electrophoresis. Anal. Chem. 67:2943–2948 (1995).
75. PG Righetti, B Verzola. Folding/unfolding/refolding of proteins: present methodologies in comparison with capillary zone electrophoresis. Electrophoresis 22:2359–2374 (2001).

© 2003 by Marcel Dekker, Inc.

4
Affinity of Drugs to Excipients

Manuela Plätzer and Reinhard H. H. Neubert
Martin-Luther-University Halle-Wittenberg, Halle, Germany

I. INTRODUCTION

Many techniques have been developed to measure the affinity of one molecule for another, to determine apparent equilibrium constants for molecular association. All experimental techniques used for measuring equilibrium constants base on titrating changes in physicochemical properties of molecules depending on the concentration of the substrate. The system response has to be different for free versus complexed molecules. Changes in size, charge, and other properties might result in measurable differences in diffusion rate (immunodiffusion, equilibrium dialysis), molecular weight (size exclusion methods), sedimentation (ultracentrifugation), solubility, spectroscopic properties (fluorescence quenching, spectral shift), and electrophoretic migration. They can be measured using spectroscopic methods, calorimetry, potentiometry, nuclear magnetic resonance (1), ultrafiltration, or phase solubility experiments (2). Conventional methods involve the separation of bound and free molecules through the use of filtration or equilibrium dialysis and subsequent detection by spectroscopic methods as well as fluorescence measurement or scintillation counting. The components of interest are radioactively or fluorescently labeled (3).

Affinity capillary electrophoresis (ACE) (4), the most common method used in CE to determine interactions between molecules, involves measuring changes in electrophoretic mobility of the analyte through buffer solutions containing dissolved complexation agents. Analysis of the magnitude of the change in mobility of the analyte, injected as sample, as a function of the concentration of receptor yields binding constants. Some different experimental setups using the analytes in background electrolyte and the receptor

© 2003 by Marcel Dekker, Inc.

as sample are also reported. Binding constants can be calculated under the following conditions.

The analyte must undergo a change in electrophoretic mobility upon complexation. That's why one of the binding partners must have a sufficient charge.
At least one of the binding partners must be detectable by the method.
There must be a fast adjustment of equilibrium between the free and the complexed form of analyte, compared with the separation time.
There are no interactions of binding partners with the capillary wall.
The electric field does not influence the formation.
A coelectrophoresed reference for converting detection times into mobilities must not be influenced by the presence of the binding partners.

In contrast to classical gel electrophoresis, ACE is performed in homogenous media without stabilizing agents, and almost physiological conditions are possible. Mostly, modifications of the binding partners are not required. Binding studies have been applied to proteins, antibiotics, and carbohydrates in aqueous as well as nonaqueous systems. The determination of binding constants is helpful for understanding pharmacological events and for predicting the actions of drugs and drug candidates against various compounds. Studies with ACE have been used for rapid screening as well as for determination of binding constants of particular ligands and receptors.

ACE (5–7) is suitable for investigating even slight interactions, using simple experimental conditions. This method needs only small quantities of binding partners. An analysis of mixed analytes is made possible by interpreting migration times instead of peak areas.

A. Excipients

This section reviews the binding studies performed to characterize interactions between possible excipients and drugs. The main focus is on cyclodextrin–drug interactions, because in the literature there are a lot of papers dealing with the determination of their binding constants. Furthermore a lot of basic research work concerning the mathematical descriptions and the effect of changing conditions was performed on these systems. Therefore, cyclodextrins and the mathematical description of their interactions with drugs are extensively discussed here. Other excipients of interest are shown in the following overview (Table 1) and will be discussed shortly in the text. Food components are also able to modify the bioavailability of drugs. These important effects are not well explored and there are only a few papers dealing with their prediction using affinity capillary electrophoresis. The

© 2003 by Marcel Dekker, Inc.

Table 1 Excipients and Food Components of Interest for Affinity Capillary Electrophoresis

Carbohydrates	Cyclodextrins	
	Biopolymers	Hyaluronic acid
		Heparin
		Pectins
		Carrageenan
		Cellulose, starch
Proteins	Albumin	
	α_1 Acid glycoprotein	
	Specific target proteins	
Food components	Fatty acids	
	Proteins	
	Carbohydrates	

majority of these investigations was performed using different carbohydrates as binding partners.

The interactions between drugs and proteins such as albumin, acidic glycoprotein, and other possible target proteins are discussed in specific chapters. Some important applications of ACE concerning drug carrier systems (simple and mixed micelles, microemulsions, liposomes) are covered in subsequent chapters of this book.

II. CYCLODEXTRINS

Cyclodextrins (CDs) are cyclic, nonreducing oligosaccharides obtained from enzymatic degradation of starch. The most common forms are the α-, β-, and γ-species, composed of 6, 7, and 8 α-(1 $\rightarrow$ 4)-linked glucopyranose units, respectively (8). See Fig. 1. Cyclodextrins are water soluble, since all of the free hydroxyl groups are oriented to the outer surface of the ring. As a result the internal cavity is relatively hydrophobic. And CDs are capable of accommodating guest molecules that fit into their characteristic cavities (4.5–8 Å) and thus to form inclusion complexes. This inclusion phenomenon may be stereoselective because of the chiral properties of the constituent glucose molecules (9).

The inclusion into the hydrophobic cavity causes modifications of solubility, bioavailability, and delivery properties of many bioactive molecules. Furthermore the stability of many guest molecules is improved, e.g., against

© 2003 by Marcel Dekker, Inc.

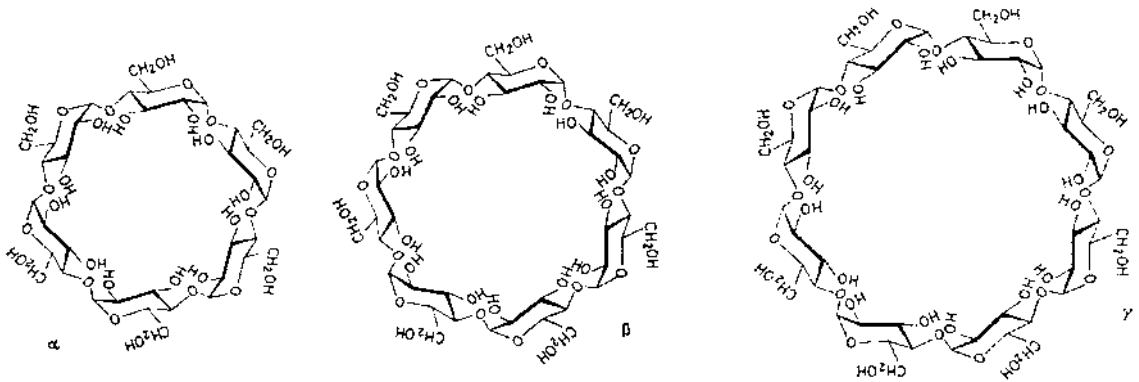

Fig. 1 Structure of common cyclodextrins.

© 2003 by Marcel Dekker, Inc.

heat, oxidation, hydrolysis, or evaporation. For that reason, they are used in pharmaceutical formulations to modify the bioavailability of drugs by enhancing solubility, controlling drug delivery, or improving stability (10). In general, only the free form of drugs administered as CD complexes is absorbed through biomembranes, and the rate of absorption may therefore depend on the binding strength of the inclusion complex. Thus a strong complexation may counteract the bioavailability. Cyclodextrins are also used in the food, cosmetics, and textile industries. In the chemical industry they are used as catalysts. On the other hand, CDs have been used extensively as chiral selectors for analytical methods such as HPLC, GC, SPE, and CE. Gas chromatography (GC) at chiral columns is effective for the direct enantiomer separation of small vaporized compounds. A high number of separations of pharmaceutical compounds at chiral stationary phases in HPLC have been described (11). The merits of the CE enantiomeric separation are its high separation efficiency, low operating costs, high versatility, and extremely small volumes of sample and media. The easy change of separation media enables rapid method development and optimization. Furthermore, CDs do not interfere with UV-photometric detection. Therefore, the electrophoretic separation is largely studied as an alternative or complementary technique to conventional chromatographic methods. The optimum conditions of enantiomeric separations can be well predicted on the basis of the binding constants. The more the binding constant varies between the (+) and the (−) form of the analyte, the higher is the selectivity of the separation. The optimum concentration is inversely proportional to the average of the binding constants, while the difference in electrophoretic mobilities of the enantiomer pair correlates well with the relative difference of their binding constants. An extensive review of enantiomeric separations using CDs in CE was given by Chu and Cheng (12). Furthermore, there is a growing field of enantiomer separations by electrochromatography utilizing CDs as stationary phases (13). For details see Chapter 8 by Blaschke and Chankvetadze.

The formation of inclusion complexes is influenced mainly by steric parameters of ligands (geometry and size) and by the possibility of creating hydrophobic interactions and hydrogen bonds (physicochemical properties). Hydrophobic interactions predominate in the cavity, and they can act in concert with polar interactions that occur with hydroxyl groups located at the outer lip of the CDs. There are no covalent bonds (14).

Cyclodextrins are commonly available in three different sizes (i.e., α, β, γ), and further CD derivatives are now commercially obtainable. Native CDs are often used in CE, since they are not very expensive and numerous compounds are baseline-resolved in chiral separation using CD as buffer additives. β-Cyclodextrin interacts with a wide variety of compounds, but

© 2003 by Marcel Dekker, Inc.

a serious limitation to its broader employment is its unusually low solubility in water. Therefore, derivatization, especially of β-CD, is applied to overcome this problem and to increase the complex stability by enabling more specific interactions between the analytes and the CDs. The hydroxyl groups on the exterior of CDs are accessible as starting points for structural modification; therefore, various functional groups have been incorporated in CD molecules to change both the polarity and the shape of the cavity. As a result, a variety of drugs may be incorporated into one of these derivatives and a better stereoselectivity through stricter sterical requirements for complexation is reached. Another advantage is the reduced nephrotoxicity in comparison with β-CD, which is explained by the improved solubility (15). Table 2 gives a survey of different chemically modified CDs. The abbreviations printed in parentheses are used in the following text. In addition to the substituent type, the mean number of derivatized hydroxyl groups in the CD molecule is important for the capability of the derivative to separate chiral compounds (16). Therefore, the degree of substitution (DS) has to be declared for commercial products. Unfortunately, there are often complex mixtures of homologues and isomers, differing in their degree of substitution, resulting from each reaction, and the DS is only an approximate value characterizing the composition. Note that the DS, included in Tables 2 and 5, is defined as the number of functionalized groups per CD, not per glucose unit.

The introduction of charged CDs has merits for enantioseparation, because their addition to the running buffer allows the separation of electrically neutral analytes. Furthermore, they enable better resolution of analytes bearing the opposite charge, owing to an enlarged separation window and ion-pair interactions (17). The countercurrent migration principle of negatively charged CDs allows coupling CE to mass spectrometry (MS) without contaminating the ion source and losing signal intensity (18). Using highly alkaline pH values the native CDs (pK_A approximately 12) can also act as negative buffer additives (19).

A further modification is the creation of polymers out of CDs, which are also used for enantioseparations (20–22). They are obtained by radical copolymerization and often exhibit enormous solubility (23).

Cyclodextrins are difficult to analyze because they show no appreciable UV absorbance and are often uncharged. Furthermore, they are not easy to label with visualizing agents because of their low reactivity. Therefore, cyclodextrins are often detected as inclusion complexes (45,46). A review dealing with the detection and separation of cyclodextrins as well as the determination of binding constants is given by Larsen and Zimmermann (47).

© 2003 by Marcel Dekker, Inc.

Table 2 Different Types of Cyclodextrins with Their Functional Groups

Neutral CDs	
Native α-, β-, γ-CD	—
Methyl-CD (Me):	—CH_3
DS 14: dimethyl-β-CD (DM), DS 21: trimethyl-β (TM)	
Ethyl-CD (Et) (24)	—CH_2—CH_3
Octyl-CD	—$(CH_2)_7$—CH_3
Hydroxyethyl-CD (HE)	—CH_2—CH_2—OH
Hydroxypropyl-CD (HP) (15,25)	—CH_2—CH_2—CH_2—OH or —CH_2—CHOH—CH_3
Glucosyl-CD (Glu)	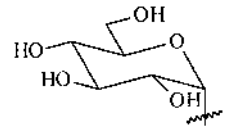
Maltosyl-CD (Malt) (17) and other branched CDs	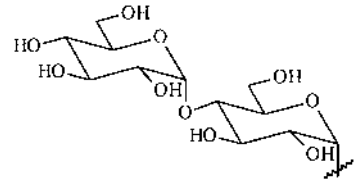
Acetyl-CD (Ac) (26)	—CO—CH_3
2,6-Di-*O*-methyl-3-*O*-acetyl (DMA) (27)	Me and Ac
Anionic CDs	
Sulfoethylether-CD (SEE) (28,29)	—$(CH_2)_2$—$SO_3^-Na^+$
Sulfopropylether-CD (SPE) (30)	—$(CH_2)_3$—$SO_3^-Na^+$
Sulfobutylether-CD (SBE) (28,31)	—$(CH_2)_4$—$SO_3^-Na^+$
Carboxymethyl-CD (CM) (32)	—CH_2—COOH
Carboxyethyl-CD (CE) (32)	—CH_2—CH_2—COOH
Phosphate-CD (Ph) (33,34)	—$PO_3^-Na^+$
Sulfated CD (Sul) (35)	—$SO_3^-Na^+$
Succinyl-CD (Suc) (32)	—CO—CH_2—CH_2—COOH
Cationic CDs (quaternary ammonium-CD)	
O-(2-Hydroxy-3-trimethyl-ammonio-n-propyl)-β-CD (HTMAP) (30,36)	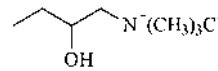
Mono-(6-amino-6-deoxy)-CD (NH_2) (37,38)	—NH_2

© 2003 by Marcel Dekker, Inc.

Table 2 Continued

6-Methylamino-CD (MeNH)	—NH—CH_3
6^A,6^D-dimethylamino-β-CD	(—NH—CH_3)$_2$
Heptamethylamino-β-CD (39)	(—NH—CH_3)$_7$
6-Trimethylammonio-deoxy-CD (TMA)	—N(CH_3)$_3$
6[(3-Aminoethyl)amino]-6-deoxy-CD (AEA)	—NH—CH_2—CH_2—NH_2
Histamine-modified CD (40,41): 6-Deoxy-6-*N*-histamino (hm) 6-Deoxy-6-[4-(2-amino-ethyl)imidazoyl] (mh)	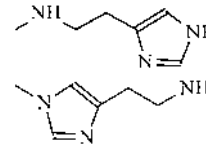
1-(1-Naphthyl)ethylcarbamoyl-CD (NEC) (42)	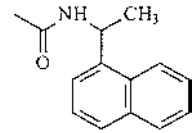
Zwitterionic CDs Mono-(6-δ-glutamylamino-6-deoxy)-β-CD (GluNH) (43)	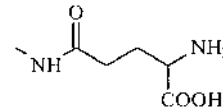
6^A-(Carboxymethyl)thio-6^B-amino-6^A,6^B-dideoxy-β-CD (44)	—NH_3^+, —S—CH_2—COO^-
6^A-Pyrrolidinyl-6^B-(O-carboxy-phenyl)thio-6^A,6^B-dideoxy-β-CD (44)	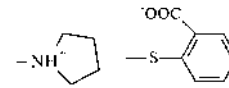
Amphoteric CD: CM-/QA-CD (36)	HTMAP and CM

A. Determination of Binding Constants

The principle of ACE is shown in Fig. 2. The receptor is usually dissolved at a certain concentration in the buffer electrolyte, which is in both electrode vessels and in the capillary. Maintaining all other conditions constant, only the concentration of the receptor in the buffer system is varied in a defined concentration range. The drugs (center molecules/ligands) are injected as a narrow sample zone. While migrating through the tube, the drugs interact with the receptor molecules. As a consequence the magnitude of electro-

© 2003 by Marcel Dekker, Inc.

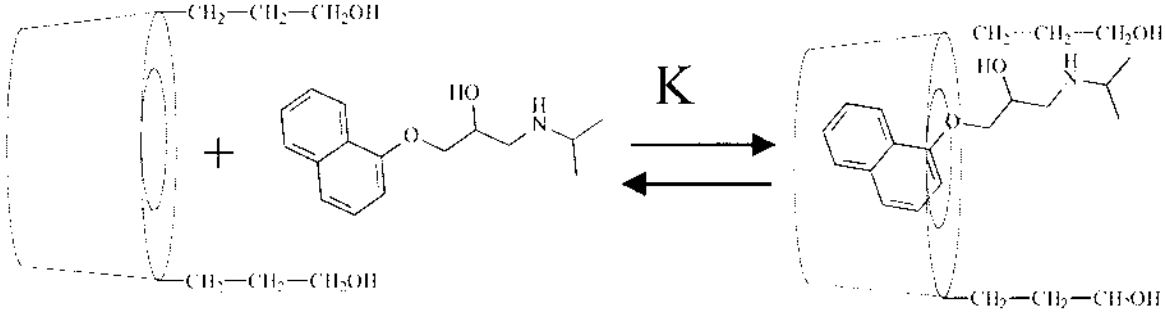

Receptor (CD)	Center molecule (Drug)	Complex
M_{CD}	M_D	M_{DCD}
q_{CD}	q_D	q_{DCD}
$\mu_{CD} \sim q_{CD}/M_{CD}^{2/3}$	$\mu_D \sim q_D/M_D^{2/3}$	$\mu_{DCD} \sim (q_{CD}+q_D)/(M_{CD}+M_D)^{2/3}$

Fig. 2 Schematic principle of ACE: interaction between a hydroxypropylated CD and propranolol.

© 2003 by Marcel Dekker, Inc.

phoretic mobility changes, depending on the magnitude of binding constant as well as the concentration, size, and charge of the binding partners. The electrophoretic mobility μ of a molecule in free solution is proportional to its electrical charge, q, and inversely related to the hydrodynamic radius, r, which depends on the molecular mass, M. One of the most widely used mathematical descriptions of this relationship was found by Offord (48) and is shown in Fig. 2. If the drug binds to a cyclodextrin, the change in μ occurs due to the change in the mass M_{D+CD}. There is no change in net charge using neutral CDs because they have no electrical charge in aqueous solution below pH 12 ($\mu_{ep} = 0$ cm^2 V^{-1} s^{-1}). Using ionic CDs, electrostatic interactions also play a role, and stronger interactions are often observed.

By increasing the amount of neutral CDs in the running buffer, the peaks of drug shift toward the position of neutral molecules [electroosmotic flow (EOF)], the mobilities decrease. This phenomenon is based on the increase in mass of inclusion complexes, compared with free drug. With increasing concentration of CD in the buffer, the degree of complexation increases to an equilibrium. The greater the change of the electrophoretic mobility of the drug affected by the CD, the more accurate is the measurement of the binding constant.

The electrophoretic mobility of the drugs is determined from the electropherogram by the known equation, taking into account the electro-osmotic flow. Often, small and highly hydrophilic compounds, which are not retained by the CDs, are preferred to measure the EOF. Methanol, acetone, benzyl alcohol, mesityl oxide, and dimethylsulfoxide (DMSO) are frequently used marker substances. As shown by Berglund et al. using ^{1}H-NMR spectroscopy, the presence of DMSO did not lead to a shift of H-3 and H-5 protons of CD located in the hydrophobic cavity, and thus there is no evidence for an interaction between DMSO and CDs (49). Note that migration times are inversely proportional to electrophoretic mobilities and should not be directly substituted for mobilities (50). The electrophoretic mobility of the drug in free solution, μ_D, can be determined from an experiment without CD in the running buffer. Because of using only the migration time of the drug, not its peak area, exact concentration does not have to be adjusted as long as the peak is still detectable in the electropherogram. Another advantage of ACE is that there is no need of absolute purity of the drug, due to the electrophoretic separation from other compounds. A marker that binds completely to the charged cyclodextrins could be used to measure μ_{DCD}. To date, however, accurate markers have been available only for micellar systems. Therefore, the complex mobility has to be calculated or estimated via a multipoint graph.

Figure 3 shows typical electropherograms of propranolol using different concentrations of cyclodextrin [CD] in the running buffer. There is a

© 2003 by Marcel Dekker, Inc.

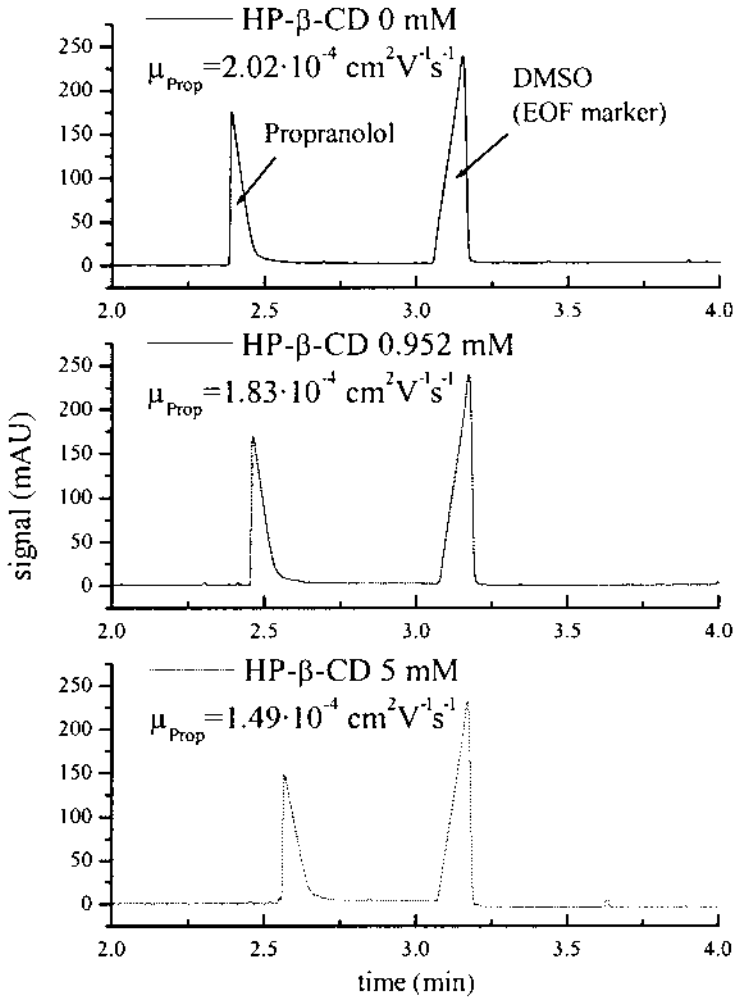

Fig. 3 Electropherogram of propranolol HCl for three different concentrations of HP-β-CD (0, 0.952, and 5 mM), phosphate buffer 10 mM, pH 7.4 (separation conditions: fused-silica capillary 560(645) $\times$ 0.05 mm; pressure injection 250 mbar s; 30 kV).

© 2003 by Marcel Dekker, Inc.

change in mobility of propranolol. With increasing amounts of neutral CD, the peaks of drug shift toward the EOF and the mobilities become smaller. With increasing concentration of CD in the buffer, the degree of complexation increases.

There are several ways to estimate binding constants. For *graphical determination*, the electrophoretic mobilities are plotted against the logarithm of the complexing agent's concentration. At the inflection point, half-complexation occurs and the constant is equal to the reciprocal of the concentration of the complexing agent (51). From the plateaus of the graph, the mobilities of free and complexed forms of the drug are determinable.

A mathematical description based on the mass action law was derived in Chapter 2. In this ideal system, the change in drug mobility observed when the CD is introduced into the capillary is caused solely by the complexation of the drug with the CD:

$$K_B = \frac{[\mathrm{DCD}_n]}{[\mathrm{D}][\mathrm{CD}]^n} = \frac{k_B}{[\mathrm{CD}]^n} \tag{1}$$

[D] represents the concentration of free drug, [CD] is the concentration of cyclodextrin in running buffer, and [DCD_n] is the concentration of the cyclodextrin–drug complex. The capacity factor k_B represents the ratio of bound to dissolved drug. The value of unknown stoichiometric coefficient, n, describes the sum of all equilibria and can be a rational number equal to or greater than zero. The effective mobility μ_{eff} of drug in a solution containing CDs is the weighted average of the mobilities of the drug in free and complexed states, where μ_{DCD_n} is the mobility of the CD–drug complex, which is derived from the maximum peak shift. Because of the size relations between drugs and CD, the stoichiometric coefficient n should not exceed a value of 2. Provided that there is a slight difference between the migration times of aggregates ($\mu_{DCD} \approx \mu_{DCD_n}$) but a significant difference between the mobilities of free and bound drug ($\mu_D \neq \mu_{DCD}$), the effective electrophoretic mobility is given by

$$\mu_{\mathrm{eff}} = \frac{1}{1 + K_B[\mathrm{CD}]}\,\mu_D + \frac{K_B[\mathrm{CD}]}{1 + K_B[\mathrm{CD}]}\,\mu_{DCD} \tag{2}$$

The formation constants and complex mobilities were calculated by several groups, assuming a 1:1 interaction (stoichiometric coefficient $n = 1$) based on this derivation but by different mathematical approaches.

After rearranging Eq. (2), the values of μ_{DCD} and K_B can be estimated by *nonlinear* least squares curve-fitting *methods* (similar to the Michaelis–Menten equation) or the expression can be rearranged under different linear forms ($y = mx + n$), where $y = (\mu_{\mathrm{eff}} - \mu_D)$ and $x = [\mathrm{CD}]$. Well known are

© 2003 by Marcel Dekker, Inc.

the *double reciprocal plot* (a plot of $1/y$ versus $1/x$, where $K_B = n/m$), the *y-reciprocal plot* (plotting x/y versus x, where the binding constant is $K_B = m/n$), and the *x-reciprocal plot* (or Scatchard plot), where a plot of y/x versus y yields the binding constant K_B from the negative slope ($-m$).

While the linear transformations appear to be identical, since one equation can be algebraically rearranged to produce the others, these plotting methods are not necessarily equivalent, due to the difference in the relative uncertainties in the x and y variables before and after transformation for plotting (50). These problems have been thoroughly documented and explained by Rundlett and Armstrong (52–54). Linear plotting methods can give binding constants and other parameters that are comparable to those obtained from nonlinear curve fitting provided that the data are properly weighted for linear regression. When the data are not weighted, the double reciprocal plot places too much emphasis on the data points taken at low CD concentration. Therefore, the estimated mobility of complexes resulting from the point of intersection with the ordinate is more uncertain. In addition, compared to other plotting methods, the double reciprocal plot can mask deviations from linearity. The *x*-reciprocal plot has been criticized for using the dependent variable on both the x and y axes, thus complicating statistical analysis.

The influence of increasing buffer viscosity by adding CDs is often corrected by using the EOF in calculating mobilities. Chen and coworkers have found a viscosity correction factor ($f = \eta_{[CD]}/\eta_0$) to improve the calculation of partition coefficients (55). All mobilities must be converted to an ideal state where the drug mobility is affected only by the binding with the receptor ($\mu_{corr} = f \cdot \mu_{eff}$). The factor exceeds 1.1 above a CD concentration of 20 mM. Therefore, it is useful to apply this factor to calculations using higher CD concentrations. The same group also investigated the complexation when more than one additive species is present in the BGE. There are some other papers that describe the viscosity correction via the use of relative current values. Increasing the receptor concentration may also change the conductivity and ionic strength of the BGE, thus changing electrophoretic mobilities.

As an example for calculating binding constants by the different equations, the interactions between three β-blockers and HP-β-CD are examined. The plots are shown in Fig. 4. The effective mobilities are corrected by the use of the viscosity correction factor introduced by Chen et al. (55).

The calculated binding constants assuming a 1:1 interaction are listed in Table 3. There is a clear difference between the plotting methods. Only by using the *x*-reciprocal plot does it become clear that there seem to be higher order equilibria between the compounds. The nonlinear regression leads to similar results as with the *y*-reciprocal fit. The double reciprocal

© 2003 by Marcel Dekker, Inc.

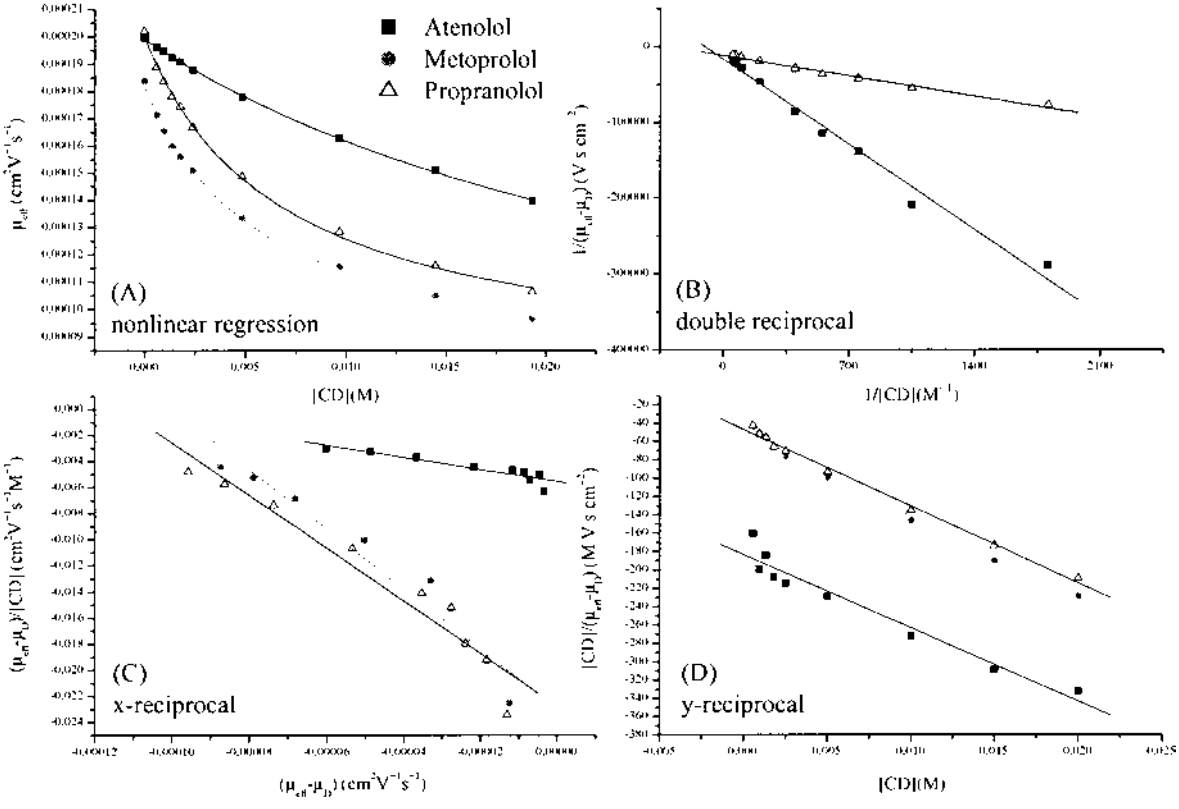

Fig. 4 Interaction of HP-β-CD with three β-blockers: (A) nonlinear curve fitting, (B) double reciprocal fit, (C) *x*-reciprocal fit, (D) *y*-reciprocal fit. Experimental conditions same as in Fig. 3.

© 2003 by Marcel Dekker, Inc.

Table 3 Binding Constants Calculated by Using Equations Assuming a 1:1 Complexation Stoichiometry

	Nonlinear fit	Double reciprocal, weighted	*x*-reciprocal	*y*-reciprocal
Atenolol	32.31 ± 3.28	101.52 ± 40.26 43.47 ± 13.98	46.45 ± 6.99	43.62 ± 5.21
Metoprolol	170.09 ± 12.13	307.42 ± 37.26 253.35 ± 22.32	217.83 ± 15.72	196.81 ± 14.30
Propranolol	157.46 ± 13.10	290.83 ± 46.46 213.60 ± 23.88	201.93 ± 19.87	179.11 ± 14.23

plot shows similar results to the *x*-reciprocal plot only when the data are weighted (low-CD-concentration data show a smaller influence). The calculated values of binding constants increase in the order of nonlinear fit, *y*-reciprocal fit, *x*-reciprocal fit, and double reciprocal fit. There is also a sight increase in relative deviation. It becomes clear that weak interactions (atenolol) are better described by nonlinear-fitting methods. Nevertheless, binding constants show the same tendency when calculated by all of the plotting methods. But the data presented clearly show that the constants determined by the different methods are not directly comparable.

It is interesting that not just the lipophilic character of the drugs (increasing from atenolol to propranolol) determines the strength of interaction, but also the molecule size. The aromatic ring system of propranolol is bigger than that of metoprolol. The hydrophilic side chain is exactly the same for all compounds. Therefore, the data presented give evidence for the assumption that only the aromatic rings are included in the cavity of the CD. There is a second side chain at metoprolol and atenolol, which has a rather hydrophilic one. Note also that by using derivatized CDs, the constants may vary with the degree of substitution of the batch used. Using HP-β-CD with a higher degree of substitution (7.3 instead of 4.7), the binding constants of metoprolol and propranolol decrease, whereas the constant of atenolol increases (data not shown). A possible explanation is that by the increase in hydroxypropylic groups, the accessibility of the hydrophobic cavity decreases (steric hindrance) but the ability to form hydrogen bonds increases.

Average values of complex mobilities obtained using nonlinear curve fitting assuming a 1:1 interaction were used to calculate the stoichiometric coefficients and stability constants through another nonlinear curve fitting [Eq. (3)]. The μ_{DCD} values were applied because they show a good approach

© 2003 by Marcel Dekker, Inc.

to real values, which can be estimated by extrapolation of the diagrams of mobilities (56):

$$K_B[\mathrm{CD}]^n = \frac{\mu_D - \mu_{\mathrm{eff}}}{\mu_{\mathrm{eff}} - \mu_{DCD_n}} \tag{3}$$

This equation is also known as the *mobility ratio method* for determination of K_B assuming a 1:1 interaction. Under the simplification that all complex mobilities are equal, the stoichiometric coefficient can be calculated. The calculated values for the three β-blockers are summarized in Table 4. The values for the binding constants are in good accordance with the data resulting from nonlinear and y-reciprocal fitting. Although the x-reciprocal plots of Metoprolol and Propranolol showed nonlinear behaviour only for Propranolol a stoichiometric coefficient under 1 was calculated. This indicates that beside 1:1 complexes between drug and cyclodextrin also 2:1 complexes are possible. Another explanation of the nonlinear behaviour is that at low CD concentrations are to many drug molecules present in comparison with CD molecules and there is no proper adjustment of the equilibrium.

The results for K_B using the different methods are not directly comparable. K_B values resulting from assumption of a 1:1 interaction are consecutive constants, whereas values calculated in the second case represent the product of all equilibria. Nevertheless the strength of interactions tends to be the same for each drug investigated.

A number of ACE assays dealing with the characterization of interactions between cyclodextrines as auxiliary substances and drugs have been presented. Other authors put more emphasis on the description of separation phenomenona by determination of binding constants. Model substances such as phenols are often used to examine the influence of ligand size and substitution as well as to evaluate the mathematical approaches for the calculation of binding constants.

A complex overview of the current literature is given in Table 5. There the method used for the determination of binding constants is listed in ad-

Table 4 Binding Constants and Stoichiometric Coefficients According to Eq. (3)

	K_B [M^{-1}]	n
Atenolol	35.4 ± 3.1	0.976 ± 0.034
Metoprolol	146.7 ± 15.9	0.988 ± 0.055
Propranolol	138.5 ± 6.72	0.885 ± 0.019

© 2003 by Marcel Dekker, Inc.

dition to the binding partners used. The rightmost column gives the reference number and lists some additional information from the publication.

The addition of organic solvents to the background electrolyte often yields reduced binding constants. It is known that methanol is able to form complexes with CDs. That leads to a competition of the background modifier with the analyte. Another reasonable explanation for the reduced binding constants is given by Penn et al. (91), who found no influence of the modifier on the selectivity of enantioseparation. This is explained by the enhanced affinity of the analytes to the bulk buffer, which was quantified by the increased solubility of the analyte in organic solutions. The binding constants in ^2H_2O are 10–30% greater than those in H_2O as background electrolyte (95), which was explained by the stronger hydrogen bonding of ^2H_2O. By comparing the influences of different CDs on drug mobility it was seen that β-CDs show greater effects on mobility than α- and γ-CDs. One of the most important reasons is the volume of the cavity of the CDs: α-CD has a small one, γ-CD a rather big one. Therefore, α-CDs showed interactions with compounds with a single aromatic ring and a limited number of substituents. The *p*-phenolates exhibit higher binding constants to α-CD compared with their *o*- and *m*-homologes. γ-CD is suitable to bind bigger molecules, such as polycyclic aromaytic hydrocarbons. The cavity of β-CD seems to be the most suitable for most drugs to fit in. The affinity favored by one of the derivatized β-CDs depends on the structural properties of each drug.

Generally, lipophilic substances show strong interactions with all CDs, but steric effects have greater influence on complexation than dissociation degree. There are only a few papers examining stoichiometric coefficients. Our own calculations confirm that the stoichiometric coefficients are almost 1 for all examined drugs. But there are some exceptions, like ibuprofen and ketoprofen. These substances show maximum formation constants with β-CDs, and stoichiometric coefficients from 0.7 to 1.3 were calculated. Examining different profenic acids it was shown that nearly all molecules are incorporated into the cavity because the saturation equilibrium is reached at a concentration of β-CD higher than 6 mM. Hydrophilic substances show fewer interactions than lipophilic ones.

III. SACCHARIDES AND PECTINS

Drugs interact not only with proteins but also with other compounds present in the body. There are different saccharides arising from food components or peroral formulations. It is widely known that food components can lead

© 2003 by Marcel Dekker, Inc.

Table 5 Papers Describing the Determination of Binding Constants Between CDs and Small Compounds

Substance	Cyclodextrin used	Analysis	Reference; comments
Amino acids			
Acetyl-phenylalanine (D, L)	6-TMA-6-deoxy-β (DS 1)	Nonlinear regression	57
Alanylphenylalanine, leucylphenylalanine	β	Double reciprocal	58; addition of urea, η-correction, pH-independent K_B
Dansyl-amino acids	HP-β (DS 6.3)	Nonlinear regression	59; pH dependence, pK_a shift during complexation
Dansyl-amino acids	β	Double reciprocal	60; nonaqueous CE (*N*-methylformamide), η-correction
Dansyl-amino acids	β	Nonlinear regression	61; estimation of Stokes radii and diffusion coefficents
Dansyl-amino acids	β	Mobility ratio	62
Dimethylamino-naphthalene Sulfonyl-amino acids	(β, HP-β), γ	Nonlinear regression	63
Dinitrobenzoyl-amino acids	β-CD NEC-β-CD	Linear mobility ratio method	42 K_B not determined for NEC-β-CD
Dipeptides (Ala-Phe, Phe-Phe)	CM-β (DS 3.5), succinyl-β (DS 2.8)	Nonlinear regression	64; η-correction
Tryptophan	α	Nonlinear regression	65; η-correction
Possible drugs			
Adamantane carboxylic acids	β, CM-β, Me-β	*x*-reciprocal	66; indirect detection (sodium chromate)
Amphetamine	Me-β	Graphical methods Double reciprocal *x*-reciprocal *y*-reciprocal Nonlinear regression	67; correlation between log *P* and K_B

© 2003 by Marcel Dekker, Inc.

Benzoate	β	Nonlinear regression	61
Benzylamine; salicylic, sorbic, and 1-naphthylacetic acid	α, β, γ, Me-β, HP-β	Nonlinear regression	46; indirect detection
Carprofen, flurbiprofen, ketoprofen, naproxen, suprofen, benzoin, methylether benzoin	CD-NH_2, TM-β	Graphical method	38; K_B in dual systems
Carprofen, flurbiprofen, ketoprofen, naproxen, suprofen, pranoprofen, indoprofen	β, HP-β, HP-γ, DM-β, TM-β	Mobility ratio	68; log K values
Chlorprenaline, primaquine, sulpiride	Ph-β	Double reciprocal	34
Chlortalidone	CD-NH_2	Graphical method	37
Homatropine	β	Nonlinear regression	69; considered dissociation constants [pH]
Ibuprofen	β	Nonlinear regression	70; effect of temperature, K_B for charged and uncharged drug
Ibuprofen, fenoprofen	β	Nonlinear regression	71; considered dissociation constants [pH]
Ibuprofen, salicylate, benzoates, adamantane carboxylate	α, β, γ, δ, ε, ξ, η, θ	y-reciprocal	72; drug in BGE, CD as sample according to IAD method of Ref. 46
Imidazoles (bifonazole, sulconazole, econazole, oxiconazole, miconazole, clotrimazole,)	β	Nonlinear regression	73; η-correction, determination of stoichiometric coefficients
Leucovorin, 5-methyltetrahydrofolate	γ	Nonlinear regression	74; addition of urea, η-correction of velocities
Mandelic acid	γ	Nonlinear regression	75
Methylbenzoates	β	Nonlinear regression	76; influence of counterions, comparison with retention factors in HPLC
Naproxen	HP-β	Nonlinear regression	77; pH dependence
Nicotine	β	x-reciprocal	49; pH and T dependence of K_B

© 2003 by Marcel Dekker, Inc.

Table 5 Continued

Substance	Cyclodextrin used	Analysis	Reference; comments
Nucleotides	β	y-reciprocal	78; η-correction, model for predicting migration times
Orciprenalin	Me-β (DS 10.5–14.7)	Linear plot including plug length	79; partial filling technique
p-Aminosalicylic acid (PAS), dimethylamino benzoic acid (DMAB)	α, β, Me-β (DS 12.6), DM-β, TM-β, HP-β	Nonlinear regression	80; indirect detection, separation of amino acids with PAS/DMAB in BGE
Phenylalkylamine derivatives	DM-β	Nonlinear regression	81; MeOH influence, η-correction using current
Propranolol	β Me-β	Nonlinear regression	62 82–84; η correction using current, no K_B
Quinine, propranolol, tetracycline, ibuprofen, ketoprofen, salicylic acid	α, β, γ, HP-β, Me-β	Double reciprocal x-reciprocal Nonlinear regression	56; modified analysis, determination of stoichiometric coefficients
Retinoic acid	Me-β	Graphical method	51
Rutin	Me-β	Graphical method	85
Salbutamol	β Et-β (DS 13.9, 14.8)	Nonlinear regression	86; η-correction, pH and T dependence of K_B
Salbutamol and impurities	DM-β	Nonlinear regression	87
Sulfonamides	β	Nonlinear regression	88
Ticonazole	HP-β β β, Me-β, DM-β, HP-β (DS 4.9–7)	Nonlinear regression	89; MeOH as additive reduced K_B 90; ACN influence (reduced K_B) 91; MeOH and cyclohexanol as additive (reduced K_B)
Uniconazole, diniconazole	CM-β	Double reciprocal x-reciprocal y-reciprocal	92; influence of T

© 2003 by Marcel Dekker, Inc.

Model substances			
Benzopyrenes	β, γ, HP-γ	Capacity factors calculated	93; capacity factor in presence of SDS, 2-propanol, and acetonitrile; bile salt micelles were not compatible with CD
Biphenol, phenylphenol, phenol	HP-β	Double reciprocal *x*-reciprocal *y*-reciprocal	94; higher-order equilibria
2-Naphthalenesulfonate	β	Double reciprocal	95; substituion of H_2O in buffer by ^2H_2O leads to an increase in K_B
p- and *m*-Nitrophenol	α	Double reciprocal *x*-reciprocal	52
2-Phenoxypropionic acid, 2-(4-chlorophenoxy)propionic acid	HP-β	*y*-reciprocal Mobility ratio	52
o-, *m*-, *p*-Nitrophenolates	α, β	Double reciprocal	96
o-, *m*-, *p*-Nitrophenolates	α, β, HP-α, HP-β, Me-β	Nonlinear regression	97; η-correction
Phenol, *p*-nitrophenol, benzoic acid	β, HP-β	Double reciprocal	55,98; capacity factor, η-correction, mixture of CDs in BGE
Phenol, naphthol	HP-β, SBE-β	Nonlinear regression	99; η-correction, mixtures of CDs in BGE
Tetraphenylborate, tetraphennylphosphonium ions	β, DM-β, γ	Nonlinear regression	100; calculation of absolute mobilities and hydrodynamic radii, η-correction

© 2003 by Marcel Dekker, Inc.

to a modification of the bioavailability of drugs. Predicting these effects is difficult.

Polysaccharides in general show a wide enantioselectivity, which can be partly ascribed to their helical structure. *Malto-oligosaccharides* are formed by acidic or enzymatic degradation of starch. Helices, composed of six glucose units each, of linear α-1.4-glucosides with different chain lengths, can form inclusion complexes with some low-molecular-weight substances. Malto-oligosaccharides are widely used as chiral selectors for the separation of pharmaceuticals by capillary electrophoresis. One of the first papers is from D'Hulst and Verbecke (101), and several groups also performed such separations (102). The separation efficiency often increases with the number of hexoses in the chain. Furthermore it was shown that maltodextrins are highly efficient in separating acidic (103,104) as well as basic drugs (105). Interactions between different starch degradation products and the β-blocker propranolol were studied using permeation experiments as well as ACE (106). In the presence of malto-oligosaccharides, the transport of propranolol across artificial lipid membranes was retarded. Affinity capillary electrophoresis of the drug with starch in the background electrolyte showed only slight interactions. Such interaction was too small for the reliable determination of binding constants, but it could be responsible for the retarded transport across the membranes.

Dextrins, polysaccharides derived from starch, are mixtures of linear α-(1,4)-linked D-glucose units, whereas *dextrans*, which are storage polysaccharides produced by yeast and bacteria from sugar, are polymers in which the glucose units are joined almost exclusively by α-(1,6)-linkages. Several dextrans and dextrins were used by Nishi et al. for enantioseparation of drugs (107). Additionally, they determined the capacity factor using an equation derived from the mobility ratio method. There was an increase in capacity factor with increasing polysaccharide concentration.

The complexation of polyiodides and dextrinoligomers was studied by Hong et al. (108). The effects of the degree of polymerization, the I_2/I^- ratio as well as buffer pH and ionic strength were investigated. The same group used fluorescently labled amylodextrin oligomers to study certain carbohydrate–drug interactions (109). The drugs were used as buffer additives, and the separation pattern of the oligomers injected as sample was investigated. The pH, the ionic strength, and the organic additives to the buffer, as well as the nature of the drugs, played an important role in complexation. The results of electrophoresis were in close agreement with a previous ^{13}C NMR study.

The same group investigated the separation of fluorescently labled sugars by different CDs as well as linear polysaccharides (dextrin 10, dextran, laminarin, and alginic acid) and oligosaccharides in the presence of borate

© 2003 by Marcel Dekker, Inc.

(110). None of the saccharides, except for dextrin 10 and malto-oligomers, displayed enantioselectivity for the sugars as the CDs.

The dependence of the mobilities of *amylopectin* and *amylose* on iodine concentration in the background electrolyte and applied temperature was studied by Brewster et al. (111). The method was used for the separation and identification of different plant starches, but no binding constants were calculated.

Interactions between acetylated and amidated *pectins* (1.4-α-glycosidic bond galacturonic acid) and different drugs were studied using ACE. It was shown that ACE is a suitable method for characterizing these interactions at the molecular level. Calculating the equilibrium binding constants, it was found that the structure and size of the drugs used have a stronger influence on the binding of drugs to pectins than charge and hydrophilic character (112).

The highly charged mucopolysaccharide *heparin*, extracted from bovine lung tissue and intestinal mucosa of pigs and cattle, has a large number of sulfate groups, which are responsible for its strong anionic character, good aqueous solubility, and electrophoretic mobility. It is composed of alternating α-1,4-linked glucouronic acid (partially sulfated at C2) and N-sulfated glucosamine. Stalcup and Agyei reported chiral discriminating abilities of heparin for drugs containing at least two nitrogens, with one of them incorporated in an heterocyclic aromatic ring (113). The authors concluded that the chiral mechanism is a combination of ionic, hydrogen-bonding, and hydrophobic interactions, by which the superstructure of heparin may play a role. Heparin and chondroitin sulfate, also an acidic mucopolysaccharide, were used as chiral selectors for neutral and basic drugs (114).

Hyaluronan (HA) is an acidic linear mucopolysaccharide, consisting of regularly alternating units of *N*-acetylglucosamine and glucuronic acid linked by 1,4- or 1,3-β-glycosidic bonds. Hyaluronan, as well as its salt hyaluronate, is a component of skin, the vitreous humor of the eye, the synovial fluid, and other tissues. It plays an important role in stabilization of the vitreous gel structure. Like the other substances, HA is able to interact with a wide variety of drugs. Because of the high increase in viscosity with increasing concentrations of HA in the BGE, effective correction modes have to be applied for determination of binding constants. Furthermore, the variation in chain length may influence the separations.

Carrageenans, composed of repeated sulfated and nonsulfated galactose and 3,6-anhydrogalactose units joined by alternating α-(1,3)- and β-(1,4)-glucosidic linkages, as well as *chitosan*, are applied in tablet formation. Because of the sulfatation, interactions with cationic drugs are likely. Beck and Neau used a λ-carageenan for enantiomeric separations of propranolol, pindolol, laudanosine and other drugs (115,116).

© 2003 by Marcel Dekker, Inc.

Nishi has found that *chondroitin sulfate A* and *C* are more effective in the resolution of basic drugs than dextran or dextrin and even dextran sulfate because of additional ionic interactions with sulfate or carboxylic groups. The small ionic character of chondroitin sulfate C leads to large enantioselectivity under acidic conditions, whereas heparin was not so effective. Using neutral polysaccharides, only hydrophobic interactions and hydrogen bonding may occur (117).

The effect of an additive (*Brij 35*) on the mobilities of different porphyrins (photodynamic anticancer drugs) was studied in a nonaqueous capillary electrophoresis system based on a 1:1 complexation model (118).

The interactions of drugs with various amphiphilic substances, which could be used as excipients, are discussed in the next chapter.

REFERENCES

1. B Chankvetadze, G Endresz, G Schulte, D Bergenthal, G Blaschke. Capillary electrophoresis and ^{1}H NMR studies on chiral recognition of atropisomeric binaphthyl derivatives by cyclodextrin hosts. J Chromatogr A 732:143–150, 1996.
2. G Dollo, P Le Corre, F Chevanne, R Le Verge. Inclusion complexation of amide-typed local anaestetics with β-cyclodextrin and its derivatives. II. Evaluation of affinity constants and in vitro transfer rate constants. Int J Pharm 136:165–174, 1996.
3. J Oravcová, B Böhs, W Lindner. Drug–protein binding studies. New trends in analytical and experimental methodology. J Chromatogr B 677:1–28, 1996.
4. Y-H Chu, LZ Avila, HA Biebuyck, GM Whitesides. Use of affinity capillary electrophoresis to measure binding constants of ligands to proteins. J Med Chem 35:2915–2917, 1992.
5. Y-H Chu, LZ Avila, J Gao, GM Whitesides. Affinity capillary electrophoresis. Acc Chem Res 28:461–468 1995.
6. LZ Avila, Y-H Chu, EC Blossey, GM Whitesides. Use of affinity capillary electrophoresis to determine kinetic and equilibrium constants for binding of arylsulfonamides to bovine carbonic anhydrase. J Med Chem 36:126–133, 1993.
7. FA Gomez, LZ Avila, Y-H Chu, GM Whitesides. Determination of binding constants of ligands to proteins by affinity capillary electrophoresis compensation for electroosmotic flow. Anal Chem 66:1785–1791, 1994.
8. J Szejtli. Cyclodextrins and their inclusion complexes. Akadémiai Kiadó, Budapest, 1982.
9. D Duchene (ed.). New Trends in Cyclodextrins and derivatives. Editions de Santé, Paris, 1991.
10. J Szejtli. Cyclodextrin Technology. Kluwer, Dordrecht, 1988.
11. F Bresolle, M Audran, T-N Pham, JJ Vallon. Cyclodextrins and enantiomeric

© 2003 by Marcel Dekker, Inc.

separations of drugs by liquid chromatography and capillary electrophoresis: basic principles and new developments. J Chromatogr B 687:303–336, 1996.
12. Y-H Chu, CC Cheng. Affinity capillary electrophoresis in biomolecular recognition. Cell Mol Life Sci 54:663–683, 1998.
13. V Schurig, D Wistuba. Recent innovations in enantiomer separation by electrochromatography utilizing modified cyclodextrins as stationary phases. Electrophoresis 20:2313–2328, 1999.
14. F Cramer. Cyclodextrine—Alte Bekannte in neuem Gewande. Starch 35:203–206, 1983.
15. J Pitha, J Pitha. Amorphous water-soluble derivatives of cyclodextrins. Nontoxic dissolution-enhancing excipients. J Pharm Sci 74:987–990, 1985.
16. K Otsuka, S Honda, J Kato, S Terabe, K Kimata, N Tanaka. Effects of compositions of dimethyl-β-cyclodextrins on enantiomer separations by cyclodextrin-modified capillary zone electrophoresis. J Pharm Biomed Anal 17: 1177–1190, 1998.
17. S Izumoto, H Nishi. Enatiomer separation of drugs by capillary electrophoresis using mixtures of β-cyclodextrin sulfate and neutral cyclodextrins. Electrophoresis 20:189–197, 1999.
18. G Schulte, S Heitmeier, B Chankvetadze, G Blaschke. Chiral capillary electrophoresis–electrospray mass spectrometry coupling with charged cyclodextrin derivatives as chiral selectors. J Chromatogr A 800:77–82, 1998.
19. K Bächmann, A Bazzanella, I Haag, K-Y Han. Charged native β-cyclodextrin as a pseudostationary phase in electrokinetic chromatography. Fresenius J Anal Chem 357:32–36, 1997.
20. L Ma, J Han, H Wang, J Gu, R Fu. Capillary electrophoresis enantioseparation of drugs using β-cyclodextrin polymer Intramolecular synergistic effect. Electrophoresis 20:1900–1903, 1999.
21. M Chiari, V Desperati, M Cretich, G Crini, L Janus, M Morcellet. Vinylpyrrolidine-β-cyclodextrin copolymer. A novel chiral selector for capillary electrophoresis. Electrophoresis 20:2614–2618, 1999.
22. A Harada. Design and construction of supramolecular architectures consisting of cyclodextrins and polymers. Adv Polymer Sci 133:141–191, 1997.
23. M Chiari, M Cretich, G Crini, L Janus, M Morcellet. Allylamine-β-cyclodextrin copolymer. A novel chiral selector for capillary electrophoresis. J Chromatogr A 894:95–103, 2000.
24. V Lemesle-Lamache, D Wouessidjewe, M Taverna, D Ferrier, B Perly, D Duchene. Physicochemical characterization of different batches of ethylated β-cyclodextrins. J Pharm Sci 86:1051–1056, 1997.
25. K Harata, CT Rao, J Pitha, K Fukunaga, K Uekama. Crystal structure of 2-*O*-[(*S*)-2-hydroxypropyl]cyclomaltoheptaose. Carbohydr Res 222:37–45, 1991.
26. JB Vincent, G Vigh. Nonaqueous capillary electrophoretic separation of enantiomers using the single isomer heptakis(2,3-diacetyl-6-sulfato)-cyclodextrin as chiral-resolving agent. J Chromatogr A 816:233–241, 1998.
27. F Hirayama, S Mieda, Y Miyamoto, H Arima, K Uekama. Heptakis(2,6-di-

© 2003 by Marcel Dekker, Inc.

O-methyl-3-*O*-acetyl)-β-cyclodextrin: a water-soluble cyclodextrin derivative with low hemolytic activity. J Pharm Sci 88:970–975, 1999.
28. B Chankvetadze, G Endresz, G Blaschke. Charged cyclodextrin derivatives as chiral selectors in capillary electrophoresis. Chem Soc Rev 25:141–146, 1996.
29. RJ Tait, DJ Skanchy, DO Thompson, NC Chetwyn, DA Dunshee, RA Rajewski, VJ Stella, JF Strobaugh. Characterization of sulphoalkyl ether derivatives of β-cyclodextrin by capillary electrophoresis with indirect UV detection. J Pharm Biomed Anal 10:615–622, 1992.
30. H Jakubetz, M Juza, V Schurig. Electrokinetic chromatography employing an anionic and a cationic β-cyclodextrin derivative. Electrophoresis 18:897–904, 1997.
31. RJ Tait, DO Thompson, VJ Stella, JF Stobaugh. Sulfobutyl ether β-cyclodextrin as a chiral discriminator for use with capillary electrophoresis. Anal Chem 66:4013–4018, 1994.
32. T Schmitt, H Engelhardt. Charged and uncharged cyclodextrins as chiral selectors in capillary electrophoresis. Chromatographia 37:475–481, 1993.
33. H Nishi. Separation of binaphtyl enantiomers by capillary zone electrophoresis and electrokinetic chromatography. J High Res Chromatogr 18:659–664, 1995.
34. Y Tanaka, M Yanagawa, S Terabe. Separation of neutral and basic enantiomers by cyclodextrin electrokinetic chromatography using anionic cyclodextrin derivatives as chiral pseudo-stationary phases. J High Res Chromatogr 19:421–433, 1996.
35. AM Stalcup, KH Gahm. Application of sulfated cyclodextrin to chiral separations by capillary zone electrophoresis. Anal Chem 68:1360–1368, 1996.
36. Y Tanaka, S Terabe. Enantiomer separation of acidic racemates by capillary electrophoresis using cationic and amphoteric β-cyclodextrins as chiral selectors. J Chromatogr A 781:151–160, 1997.
37. F Lelièvre, P Gareil, A Jardy. Selectivity in capillary electrophoresis application to chiral separations with cyclodextrins. Anal Chem 69:385–392, 1997.
38. F Lelièvre, P Gareil, Y Bahaddi, H Galons. Intrinsic selectivity in capillary electrophoresis for chiral separations with dual cyclodextrin systems. Anal Chem 69:393–401, 1997.
39. S Fanali, E Camera. Use of methylamino-β-cyclodextrin in capillary electrophoresis. Resolution of acidic and basic enantiomers. Chromatographia 43: 247–253, 1996.
40. G Galaverna, R Corradini, A Dossena, R Marchelli, G Vecchio. Histamine-modified β-cyclodextrins for the enantiomeric separation of dansyl-amino acids in capillary electrophoresis. Electrophoresis 18:905–911, 1997.
41. G Galaverna, R Corradini, A Dossena, R Marchelli. Histamine-modified cationic β-cyclodextrins as chiral selectors for the enantiomeric separation of hydroxy acids and carboxylic acids by capillary electrophoresis. Electrophoresis 20:2619–2629, 1999.
42. K-H Gahm, AM Stalcup. Capillary zone electrophoresis study of naphthylethylcarbamoylated β-cyclodextrins. Anal Chem 67:19–25, 1995.

© 2003 by Marcel Dekker, Inc.

43. F Lelièvre, C Gueit, P Gareil, Y Bahaddi, H Galons. Use of zwitterionic cyclodextrin as a chiral agent for the separation of enantiomers by capillary electrophoresis. Electrophoresis 18:891–896, 1997.
44. I Tabushi, Y Kuroda, T Mizutani. Artificial receptors for amino acids in water. Local environmental effect on polar recognition by 6A-amino-6B-carboxy- and 6B-amino-6A-carboxy-β-cyclodextrins. J Am Chem Soc 108:4514–4518, 1986.
45. SG Penn, RW Chiu, CA Monnig. Separation and analysis of cyclodextrins by capillary electrophoresis with dynamic fluorescence labeling and detection. J Chromatogr A 680:233–241, 1994.
46. Y-H Lee, T-I Lin. Capillary electrophoretic analysis of cyclodextrins and determination of formation constants for inclusion complexes. Electrophoresis 17:333–340, 1996.
47. KL Larsen, W Zimmermann. Analysis and characterization of cyclodextrins and their inclusion complexes by affinity capillary electrophoresis. J Chromatogr A 836:3–14, 1999.
48. RE Offord. Electrophoretic mobilities of peptides on paper and their use in the determination of amide groups. Nature 211:591–593, 1966.
49. J Berglund, L Cedergren, SB Andersson. Determination of the stability constant for the inclusion complex between β-cyclodextrin and nicotine using capillary electrophoresis. Int J Pharm 156:195–200, 1997.
50. KL Rundlett, DW Armstrong. Methods for estimation of binding constants by capillary electrophoresis. Electrophoresis 18:2194–2202, 1997.
51. P Gareil, D Pernin, J-P Gramond, F Guyon. Free solution capillary electrophoresis as a new method for determining inclusion constants for the complexes between cyclodextrins and drugs. J High Res Chromatogr 16:195–197, 1993.
52. KL Rundlett, DW Armstrong. Examination of the origin, variation, and proper use of expressions for the estimation of association constants by capillary electrophoresis. J Chromatogr A 721:173–186, 1996.
53. KL Rundlett, DW Armstrong. Methods for the determination of binding constants by capillary electrophoresis. Electrophoresis 22:1419–1427, 2001.
54. KL Rundlett, DW Armstrong. Effect of micelles and mixed micelles on efficiency and selectivity of antibiotic-based capillary electrophoresis enantioseparations. Anal Chem 67:2088–2095, 1995.
55. X Peng, MT Bowser, P Britz-McKibbin, GM Bebault, JR Morris, DDY Chen. Quantitative description of analyte migration behavior based on dynamic complexation in capillary electrophoresis with one or more additives. Electrophoresis 18:706–716, 1997.
56. M Plätzer, MA Schwarz, RHH Neubert. Determination of formation constants of cyclodextrin-inclusion complexes using affinity capillary electrophoresis. J Microcolumn Sep 11:215–222, 1999.
57. H Yamamura, A Akasaki, Y Yamada, K Kano, T Katsuhara, S Araki, M Kawai, T Tsuda. Capillary zone electrophoretic chiral discrimination using cationic cyclodextrin derivative: determination of velocity and association

© 2003 by Marcel Dekker, Inc.

constants of each enantiomer of the amino acid derivative with 6-trimethylammonio-deoxy-β-cyclodextrin. Electrophoresis 22:478–483, 2001.
58. J Li, KC Waldron. Estimation of the pH-independent binding constants of alanylphenylalanine and leucylphenylalanine stereoisomers with β-cyclodextrin in the presence of urea. Electrophoresis 20:171–179, 1999.
59. AM Rizzi, L Kremser. pK_a shift-associated effects in enantioseparations by cyclodextrin-mediated capillary zone electrophoresis. Electrophoresis 20: 2715–2722, 1999.
60. IE Valkó, H Sirén, M-L Riekkola. Determination of association constants of dansyl-amino acids and β-cyclodextrin in *N*-methylformamide by capillary electrophoresis. Electrophoresis 18:919–923, 1997.
61. TH Seals, C Sheng, JM Davis. Influence of neutral cyclodextrin concentration on plate numbers in capillary electrophoresis. Electrophoresis 22:1957–1973, 2001.
62. SG Penn, G Liu, ET Bergström, DM Goodall, JS Loran. Systematic approach to treatment of enantiomeric separations in capillary electrophoresis and liquid chromatography. I. Initial evaluation using propranolol and dansylated amino acids. J Chromatogr A 680:147–155, 1994.
63. CL Copper, JB Davis, RO Cole, MJ Sepaniak. Separations of derivatized amino acid enantiomers by cyclodextrin-modified capillary electrophoresis Mechanistic and molecular modeling studies. Electrophoresis 15:785–792, 1994.
64. S Sabbah, GKE Scriba. Separation of dipeptide and tripeptide enantiomers in capillary electrophoresis using carboxymethyl-beta-cyclodextrin and succinyl-beta-cyclodextrin. Influence of the amino acid sequence, nature of the cyclodextrin and pH. Electrophoresis 22:1385–1393, 2001.
65. S Fanali, P Boček. A practical procedure for the determination of association constants of the analyte–chiral selector equilibria by capillary zone electrophoresis. Electrophoresis 17:1912–1924, 1996.
66. E-S Kwak, FA Gomez. Determination of the binding of β-cyclodextrin derivatives to adamantane carboxylic acids using capillary electrophoresis. Chromatographia 43:659–662, 1996.
67. A Salvador, E Varesio, M Dreux, J-L Veuthey. Binding constant dependency of amphetamines with various commercial methylated β-cyclodextrins. Electrophoresis 20:2670–2679, 1999.
68. F Lelièvre, P Gareil. Chiral separations of underivatized arylpropionic acids by capillary zone electrophoresis with various cyclodextrins: acidity and inclusion constant determinations. J Chromatogr A 735:311–320, 1996.
69. YY Rawjee, RL Williams, G Vigh. Capillary electrophoretic chiral separations using β-cyclodextrin as resolving agent. II. Bases: chiral selectivity as a function of pH and the concentration of β-cyclodextrin. J Chromatogr A 652: 233–245, 1993.
70. JC Reijenga, BA Ingelse, FM Everaerts. Thermodydnamics of chiral selectivity in capillary electrophoresis separation of ibuprofen enantiomers with β-cyclodextrin. J Chromatogr A 792:371–378, 1997.
71. YY Rawjee, DU Staerk, G Vigh. Capillary electrophoretic chiral separations

© 2003 by Marcel Dekker, Inc.

with cyclodextrin additives I. Acids: Chiral selectivity as a function of pH and the concentration of β-cyclodextrin for fenoprofen and ibuprofen. J Chromatogr A 635:291–306, 1993.
72. KL Larsen, T Endo, H Ueda, W Zimmermann. Inclusion complex formation constants of α-, β-, γ-, δ-, ε-, ξ-, η- and θ-cyclodextrins determined with capillary zone electrophoresis. Carbohydr Res 309:153–159, 1998.
73. YC Guillaume, E Peyrin. Symmetry breaking during the formation of beta-cyclodextrin-imidazole inclusion compounds. Capillary electrophoresis study. Anal Chem 71:2046–2052, 1999.
74. A Shibukawa, DK Lloyd, IW Wainer. Simultaneous chiral separation of leucovorin and its major metabolite 5-methyltetrahydrofolate by capillary electrophoresis using cyclodextrins as chiral selectors. Estimation of the formation constant and mobility of the solute–cyclodextrin complex. Chromatographia 35:419–429, 1993.
75. IE Valkó, HAH Billiet, J Frank, KChAM Luyben. Factors affecting the separation of mandelic acid enantiomers by capillary electrophoresis. Chromatographia 38:730–736, 1994.
76. PD Ferguson, DM Goodall, JS Loran. Systematic approach to links between separations in capillary electrophoresis and liquid chromatography. IV. Application of binding constant-retention factor relationship to the separation of 2-, 3-, and 4-methylbenzoate anions using beta-cyclodextrin as selector. J Chromatogr A 768:29–38, 1997.
77. YY Rawjee, G Vigh. A peak resolution model for the capillary electrophoretic separation of the enantiomers of weak acids with hydroxypropyl-beta-cyclodextrin-containing background electrolytes. Anal Chem 66:619–627, 1994.
78. P Britz–McKibbin, DDY Chen. Prediction of the migration behavior of analytes in capillary electrophoresis based on three fundamental parameters. J Chromatogr A 781:23–34, 1997.
79. A Amini, N Merclin, S Bastami, D Westerlund. Determination of association constants between enantiomers of orciprenaline and methyl-β-cyclodextrin as chiral selector by capillary zone electrophoresis using a partial filling technique. Electrophoresis 20:180–188, 1999.
80. Y-H Lee, T-I Lin. Capillary electrophoretic determination of amino acids. Improvement by cyclodextrin additives. J Chromatogr A 716:335–346, 1995.
81. É Szökó, J Gyimesi, L Barcza, K Magyar. Determination of binding constants and the influence of methanol on the separation of drug enantiomers in cyclodextrin-modified capillary electrophoresis. J Chromatogr A 745:181–187, 1996.
82. SAC Wren, RC Rowe. Theoretical aspects of chiral separation in capillary electrophoresis. I. Initial evaluation of a model. J Chromatogr 603:235–241, 1992.
83. SAC Wren, RC Rowe. Theoretical aspects of chiral separation in capillary electrophoresis. II. The role of organic solvent. J Chromatogr 609:363–367, 1992.
84. SAC Wren, RC Rowe. Theoretical aspects of chiral separation in capillary

© 2003 by Marcel Dekker, Inc.

electrophoresis III. Application to β-blockers. J Chromatogr 635:113–118, 1993.
85. S Letellier, B Maupas, JP Gramond, F Guyon, P Gareil. Determination of the formation constant for the inclusion complex between rutin and methyl-β-cyclodextrin. Anal Chim Acta 315:357–363, 1995.
86. V Lemesle-Lamache, M Taverna, D Wouessidjewe, D Duchêne, D Ferrier. Determination of the binding constant of salbutamol to unmodified and ethylated cyclodextrins by affinity capillary electrophoresis. J Chromatogr A 735: 321–332, 1996.
87. MM Rogan, KD Altria, DM Goodall. Enantiomeric separation of salbutamol and related impurities using capillary electrophoresis. Electrophoresis 15: 808–817, 1994.
88. CE Lin, WC Lin, WC Chiou, EC Lin, CC Chang. Migration behavior and separation of sulfonamides in capillary zone electrophoresis. I. Influence of buffer pH and electrolyte modifier. J Chromatogr A 755:261–269, 1996.
89. SG Penn, DM Goodall, JS Loran. Differential binding of tioconazole enantiomers to hydroxypropyl-beta-cyclodextrin studied by capillary electrophoresis. J Chromatogr 636:149–152, 1993.
90. PD Ferguson, DM Goodall, JS Loran. Systematic approach to the treatment of enantiomeric separations in capillary electrophoresis and liquid chromatography. III. A binding constant-retention factor relationship and effects of acetonitrile on the chiral separation of ticonazole. J Chromatogr A 745:25–35, 1996.
91. SG Penn, ET Bergström, DM Goodall, JS Loran. Capillary electrophoresis with chiral selectors. Optimization of separation and determination of thermodynamic parameters for binding of ticonazole enantiomers to cyclodextrins. Anal Chem 66:2866–2873, 1994.
92. Y Martin-Biosca, C Garcia-Ruiz, ML Marina. Fast enantiomeric separation of uniconazole and diconazole by electrokinetic chromatography using an anionic cyclodextrin. Application to the determination of analyte-selector apparent binding constants for enantiomers. Electrophoresis 21:3240–3248, 2000.
93. CL Copper, MJ Sepaniak. Cyclodextrin-modified micellar electrokinetic capillary chromatography separations of benzopyrene isomers. Correlation with computationally derived host–guest energies. Anal Chem 66:147–154, 1994.
94. MT Bowser, DDY Chen. Higher-order equilibria and their effect on analyte migration behavior in capillary electrophoresis. Anal Chem 70:3261–3270, 1998.
95. S Hamai, H Sakurai. ^2H_2O effects on the inclusional complexation of cyclodextrin with sodium 2-naphthalenesulfonate in capillary electrophoresis and UV spectrometry. J Chromatogr A 800:327–332, 1998.
96. S Bose, J Yang, DS Hage. Guidelines in selecting ligand concentrations for the determination of binding constants by affinity capillary electrophoresis. J Chromatogr B 697:77–88, 1997.
97. SG Penn, ET Bergström, I Knights, G Liu, A Ruddick, DM Goodall. Capillary electrophoresis as a method for determining binding constants: application to

© 2003 by Marcel Dekker, Inc.

the binding of cyclodextrins and nitrophenolates. J Phys Chem 99:3875–3880, 1995.
98. MT Bowser, DDY Chen. Dynamic complexation of solutes in capillary electrophoresis. Electrophoresis 19:383–387, 1998.
99. AR Kranack, MT Bowser, DDY Chen. The effects of a mixture of charged and neutral additives on analyte migration behavior in capillary electrophoresis. Electrophoresis 19:388–396, 1998.
100. T Nhujak, DM Goodall. Comparison of binding of tetraphenylborate and tetraphenylphosphonium ions to cyclodextrins studied by capillary electrophoresis. Electrophoresis 22:117–122, 2001.
101. A D'Hulst, N Verbecke. Chiral separation by capillary electrophoresis with oligosaccharides. J Chromatogr 608:275–287, 1992.
102. H Soini, M Stefansson, M-L Riekkola, MV Novotny. Malto-oligosaccharides as chiral selectors for the separation of pharmaceuticals by capillary electrophoresis. Anal Chem 66:3477–3484, 1994.
103. A D'Hulst, N Verbeke. Quantitation in chiral capillary electrophoresis: theoretical and practical considerations. Electrophoresis 15:854–863, 1994.
104. A D'Hulst, N Verbecke. Separation of enantiomers of coumarinic anticoagulant drugs by capillary electrophoresis using maltodextrins as chiral modifiers. Chirality 6:225–229, 1994.
105. A D'Hulst, N Verbeke. Chiral analysis of basic drugs by oligosaccharide-mediated capillary electrophoresis. J Chromatogr A 735:283–293, 1996.
106. G Dongowski, RHH Neubert, M Plätzer, M Schwarz, B Schnorrenberger, H Anger. Interactions between food components and drugs. Part 6. Influence of starch degradation products on propranolol transport. Pharmazie 53:871–875, 1998.
107. H Nishi, S Izumoto, K Nakamura, H Nakai, T Sato. Dextran and dextrin as chiral selectors in capillary zone electrophoresis. Chromatographia 42:617–630, 1996.
108. M Hong, H Soini, MV Novotny. Affinity capillary electrophoretic studies of complexation between dextrin oligomers and polyiodides. Electrophoresis 21: 1513–1520, 2000.
109. M Hong, H Soini, A Baker, MV Novotny. Complexation between amylodextrin oligomers and selected pharmaceuticals measured through capillary electrophoresis. Anal Chem 70:3590–3597, 1998.
110. M Stefansson, M Novotny. Electrophoretic resolution of monosaccharide enantiomers in borate–oligosaccharide complexation media. J Am Chem Soc 115:11573–11580, 1993.
111. JD Brewster, ML Fishman. Capillary electrophoresis of plant starches as the iodine complexes. J Chromatogr A 693:382–387, 1995.
112. G Dongowski, B Schnorrenberger, M Plätzer, M Schwarz, R Neubert. Interactions between food components and drugs. Part 5. Effect of acetylation and amidation of pectins on the interaction with drugs. Int J Pharm 158:99–107, 1997.
113. AM Stalcup, NM Agyei. Heparin: a chiral mobile-phase additive for capillary zone electrophoresis. Anal Chem 66:3054–3059, 1994.

© 2003 by Marcel Dekker, Inc.

114. H Nishi, K Nakamura, H Nakai, T Sato. Enantiomeric separation of drugs by mucopolysaccharide-mediated electrokinetic chromatography. Anal Chem 67: 2334–2341, 1995.
115. GM Beck, SH Neau. λ-carrageenan: A novel chiral selector for capillary electrophoresis. Chirality 8:503–510, 1996.
116. GM Beck, SH Neau. Optimization of λ-carrageenan as chiral selector in capillary electrophoretic separations. Chirality 12:614–620, 2000.
117. H Nishi. Enantiomer separation of basic drugs by capillary electrophoresis using ionic and neutral polysaccharides as chiral selectors. J Chromatogr A 735:345–351, 1996.
118. MT Bowser, ED Sternberg, DDY Chen. Quantitative description of migration behavior of porphyrins based on the dynamic complexation model in a nonaqueous capillary electrophoresis system. Electrophoresis 18:82–91, 1997.

© 2003 by Marcel Dekker, Inc.

5

Affinity of Drugs to Pharmaceutical Vehicle Systems: Micelles

Maria A. Schwarz and Peter C. Hauser
University of Basel, Basel, Switzerland

I. INTRODUCTION

Micellar electrokinetic chromatography (MEKC) is a separation technique in which the basic properties of micellar liquid chromatography and capillary electrophoresis are combined. It was first described by Terabe et al. (1) in 1984 for the separation of nonionic aromatic compounds and is a powerful separation technique for lipophilic and nonionic species. By addition of surfactants to the background electrolyte, new options for solving electrophoretic separation problems are opened, but it is also possible to apply this technique to the study of affinities of drugs and other molecules of interest to surface-active compounds. The term *micellar affinity capillary electrophoresis* (MACE) is used to describe the study of such interactions employing the same phenomena as present in MEKC. Of main interest is not the achievement of good separation or high detection sensitivity but the study of the effect of the type of micelle-forming compounds and its concentration [above the critical micelle concentration (CMC)] on the mobility of the solutes/drug. This is affected by the affinity of the solute to the micelle. Although MACE and ACE (affinity to nonmicellar buffer additives) are based upon the same principle, in the recent literature both methods are discussed separately.

In drug studies, of main interest is the application of colloidal systems, which show specific and unspecific interaction with mainly lipophilic substances. An obvious application is the study of highly lipophilic and poorly absorbable drugs that are administered orally or transdermally (2). Such interactions with surface-active agents may either cause a diminution of the

© 2003 by Marcel Dekker, Inc.

bioavailability by trapping the drug in the micelle or, on the other hand, lead to an improved solubility (solubilizing effect) and facilitated transfer of the drug solute across biological barriers (e.g., the wall of the gastrointestinal tract and the skin) and therefore to an improved bioavailability (3,4). To estimate the change of the bioavailability of drugs, mainly following oral administration, the characterization of these interactions is necessary.

The interactions between lipophilic or hydrophilic drug and micellar phases are caused by weak physicochemical forces such as hydrophobic (unspecific) and electrostatic effects (specifically: dipole–dipole, dipole–induced dipole) and steric effects, whereas the hydrophobic binding to the micellar systems is dominant.

An indirect indication of the presence of interactions between micellar phase and drugs is given by molecular and dynamic parameters of the drug and the micelles (ionic mobility, diffusion coefficient, hydrodynamic radius, apparent molecular mass), which are altered by the solubilization of lipophilic substances in a significant manner.

A variety of very different methods may be employed for the characterization of solubilization and distribution equilibria between surface-active compounds [e.g., sodium dodecylsulfate (SDS), dodecyldimethylammonium, palmitoylcholine (4)] and drugs. C-13 and H-1 NMR studies may be used to gain structural information on the alteration of the micellar phase during a solubilization process (5–7). By following the Brownian motion of molecules, diffusion coefficients can be obtained and also the hydrodynamic radii as well as the charge of the micellar complexes. The molecular weight of colloidal particles can be obtained by exploiting scattering effects such as extended light scattering (8) and small-angle neutron scattering (9). In one of the few publications dealing with equilibrium constants and distribution coefficients it is demonstrated that with electronic absorption spectroscopy and fluorescence measurements the binding constants of drugs to anionic micellar phases can be determined (10–12).

With micellar affinity electrophoresis the distribution behavior of drugs can be studied easily simply by observing the effect of the micellar composition and concentration on the ionic mobility. By examining the alteration of the electrophoretic properties of the solubilized drugs, a more precise characterization is possible than by studying the micellar phase itself or the complete system (13,14). This is of particular interest in the early stages of bioavailability studies for the acquisition of important parameters characterizing the interaction between drugs and different micellar partners.

For such drug studies by ACE, so far exclusively bile salts or mixtures thereof have been used because of their physiological acceptance. This is in contrast to MEKC, where other, more common amphophilic substances are employed. Bile salts are natively present in the duodenum and jejunum,

© 2003 by Marcel Dekker, Inc.

mainly in the form of glycine and taurine derivatives. Their physiological importance lies in the ability to lower the surface tension of water, to emulsify fats, and thus to promote the enzymatic attack. These properties make these compounds suitable for the improvement of the solubility of lipophilic drugs. The MACE technique has so far been used to study the effect of the lipophilicity, polarity, and charge of pure and mixed (incorporating phospholipids and fatty acids) bile salt micelles on a range of lipophilic but also hydrophilic drugs.

II. METHODS AND THEORY

Surfactants are amphophilic molecules, which consist of a hydrophobic carbohydrate part and a hydrophilic head group. In capillary zone electrophoresis (CZE), different types, i.e., anionic, cationic, but also neutral, tensides are employed. The ability of such molecules to interact with ionic and nonionic species has been used in ion chromatography and, in particular, in SDS-poly-(acrylamide) gel electrophoresis (PAGE) (15).

In MEKC, mainly anionic surface-active compounds, in particular SDS, are used. SDS and all other anionic surfactants have a net negative charge over a wide range of pH values, and therefore the micelles have a corresponding electrophoretic mobility toward the anode (opposite the direction of electro-osmotic flow). Anionic species do not interact with the negatively charged surface of the capillary, which is favorable in common CZE but especially in ACE. Therefore, SDS is the best-studied tenside in MEKC. Long-chain cationic ammonium species have also been employed for mainly anionic and neutral solutes (16). Bile salts as representatives of anionic surfactants have been used for the analysis of ionic and nonionic compounds and also for the separation of optical isomers (17–19).

In MACE, the alteration of the ionic mobility as a factor of the tenside concentration in the background electrolyte solution is a measure of the strength of interaction, which may be evaluated graphically. In Fig. 1, a schematic representation of MEKC is given for the separation of micelle and EOF markers as well as drug solutes of different lipophilicity. If the substances are neutral, their position between the EOF marker and the micelle marker is given only by their lipophilicity, which controls their affinity to the micellar phase. This means that S3 in Fig. 1 has the lowest hydrophilicity.

A more detailed characterization of the interactions is obtained by calculating the equilibrium constants according to Eq. (2). By fitting (parameters: K_P and $\bar{\nu}$, CMC = const.) Eq. (2) to the experimentally obtained values (measured ionic mobility of drug $\rightarrow k_P$ (capacity factor)/concentration gra-

© 2003 by Marcel Dekker, Inc.

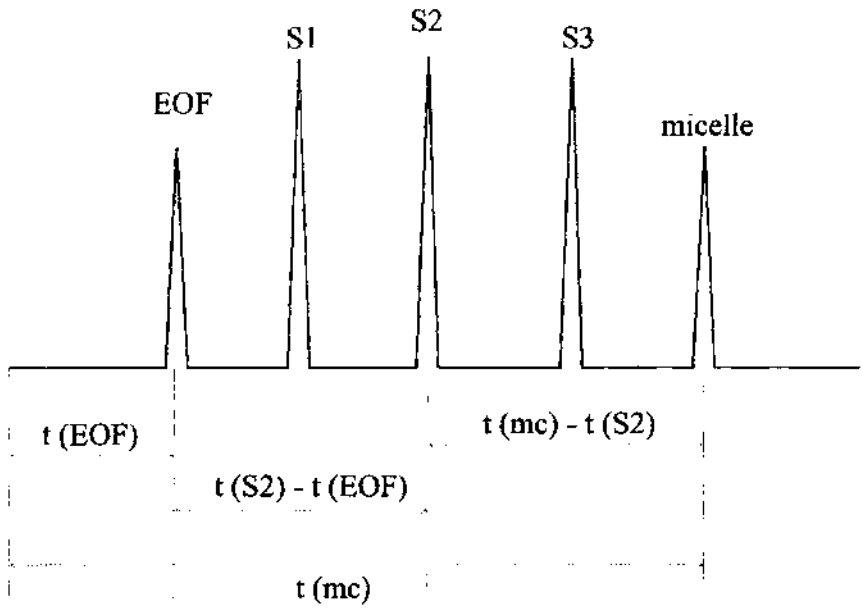

Fig. 1 Schematic representation of the separation principle of MEKC. An EOF/micelle marker and three solutes differing in lipophilicity in the presence of anionic micelles in the background buffer are present. The lipophilicity increases in the sequence $S_1 < S_2 < S_3$: *t*—migration time of EOF (nonionic solutes); S (solute); mc —micelle.

dient $[s_0]$) the distribution coefficient K_P can be calculated. The mobilities of the drugs μ_D (in the absence of the micellar phase) have to be known as well as the resulting ionic mobility in the presence of the micellar phase and the mobility of the vehicle (micelle, mixed micelles) alone. The parameter $\mu = f([s_0])$ represents the real electrophoretic mobility of the ions without any contribution from the electroosmotic flow ($\mu = \mu_{\text{measured}} - \mu_{EOF}$). The determination of the mobility of the vehicles μ_{mc} will be discussed shortly.

Analogously to chromatography, the capacity factor k_P can be defined as the ratio of the residence times of the analyte molecule in the mobile (aqueous) and ''stationary'' (micellar) phases (Nernstian distribution). The mathematical description is based on the assumption that attainment of the distribution equilibrium takes much less time than the duration of the migration of the solute. The components involved should not show any interaction with the capillary wall. As in almost all cases where UV detection is

© 2003 by Marcel Dekker, Inc.

employed, all the micellar solutions should be UV transparent. To calculate k_P and K_P (partition coefficient), a pronounced difference between the ionic mobility of the micellar phase and the mobility of the drug in the buffer is necessary. K_P and k_P are given as follows ($[D]_{mc/aq}$—concentration of drug in micellar or aqueous phase, [s]—concentration of surfactant, $V_{mc/aq}$—volume of micellar or aqueous phase, $\bar{\nu}$—partial molar volume of micelle):

$$K_P = \frac{[D]_{mc}}{[D]_{aq}} = k_P \frac{V_{aq}}{V_{mc}} \tag{1}$$

$$k_P = \frac{\mu_D - \mu}{\mu - \mu_{mc}} = K_P \frac{\bar{\nu}([s_0] - CMC)}{1 - \bar{\nu}([s_0] - CMC)} \tag{2}$$

For Eq. (2) it is assumed that the volume of the micellar phase is proportional to the tenside concentration and that the partial molar volume $\bar{\nu}$ remains constant. (See Chapter 2.) A further prerequisite for the application of Eq. (2) is a constant ionic mobility of the micellar phase independent of the uptake of a solute (μ_{mc} = const.). In contrast to HPLC, substances that have an infinitely high k_P value, i.e., that are completely dissolved in the micellar phase, can be detected. In this case the sample molecule migrates with the mobility of the micelle. In the presence of several different micellar phases (coexistence of simple and mixed micelles), the calculation of k_P is possible only when partial capacity factors are known (20). The determination of k_P is then considerably more complicated.

A second possible mathematical approach is to consider the equilibria via complexation or aggregation (21,22). Assuming that a drug compound can bind several tenside molecules in steps (concentration gradient), the brutto equilibria constants or stability constants K_A can be given as follows. Normally the aggregation constant is calculated for 1:1 reactions or other known stoichiometric ratios (z):

$$K_A = \frac{[Ds_z]}{[D][s]^z} = \frac{k_A}{[s]^z} \tag{3}$$

Simplifications in the calculation of k_A that can be made in the case of micellar phases (20) lead to following equation:

$$k_A = \frac{\mu_D - \mu}{\mu - \mu_{Db_z}} = K_A[s]^z \tag{4}$$

By fitting parameters to the experimentally obtained data, the equilibrium constant K_A and z can also be determined.

Szoekoe et al. (23) assume several parallel complex formation equilibria with different aggregates [the number of degrees of association is dependent on the bile salts (BS) concentration]. Each micelle with an iden-

© 2003 by Marcel Dekker, Inc.

tical aggregation number is taken as one type of ligand. The basis of this assumption is the knowledge of the number and type of the micelle-like aggregates.

III. APPLICATION OF METHODS

For the assessment of the bioavailability of lipophilic drugs, the adaptation of in vivo conditions is of high interest. This means, for example, the use of naturally occurring mixed BS micelles, which are formed mainly from fats ingested with the food as the drug vehicle system. In order to obtain information on the ratio of hydrophobic forces to polar/ionic interactions, it is also useful to investigate at pH values and lipid concentrations that are outside the biologically relevant range. For this reason, numerous investigations with simple, binary, and ternary micellar bile salt systems have been described alongside studies involving the classical ionic tensides.

A. Vehicle Systems: Bile Salts and Mixed Bile Salts

The bile salts and their ability to form mixed micelles is discussed in some detail in order to foster a better understanding of their applications. It is highly important for the electrophoretic characterization of the micellar phase, and therefore for the calculation of the distribution coefficients, to have a thorough understanding of the mode of micelle formation and structural changes achieved by alteration of the surfactant concentration and micelle composition as well as to develop strategies for micelle optimization.

Bile salts are amphiphilic molecules. Micelles are formed between concentrations of 0.6 and 10 mM, depending on temperature, the pH value, and the ionic strength. Bile salts are distinguished from classical surface-active compounds by their unusual structure, which shows a convex hydrophobic upper side and a concave hydrophilic lower side as well as a hydrophilic side chain. Striking are smaller aggregation numbers and relatively higher critical micelle concentrations, in particular for taurine-conjugated bile salts. For low detergent concentrations, above the CMC, and low ionic strength, bile salts form spherical-shaped micelles. The maximal size of these aggregates is on the order of R_h = 10–16 Å, with average aggregation numbers of m = 10–12. Taurine-conjugated bile salts are more hydrophilic than glycine-conjugated ones; most lipophilic are the nonconjugated bile salts. The growth of the micelles to secondary micelles is described as polymerization between the hydrophilic surface of the single primary micelles. The aggregates are stabilized by intermicellar hydrogen bonds. If a micelle is formed from several lipidlike chemical species, of which at least one species forms

© 2003 by Marcel Dekker, Inc.

micelles in aqueous phase, then this is termed a *mixed* micelle. The ability of bile salts to dissolve lipids (in particular, phospholipids) is related to the structure and radius of the mixed micelle and therefore its electrophoretic properties. Both are dependent on the absolute concentration of bile salt and lipid as well as their mixing ratio (24–29). According to one model for mixed micelle formation (24) proposed in the literature, the increase of the PC concentration (phosphatidylcholine) up to 30 mol % leads to only a marginal increase in the radius of the bile salt micelle, but the size diversity becomes higher. At concentrations higher than 35 mol % the spherical-shaped micelles assume a more ellipsoidal form (''mixed-disk model'') and the maximum packing density is reached. When the lipid concentration is increased further, a drastic increase in the micellar radii is observed, and a transformation to multilamellar vesicles takes place. The interpretation of ionic mobilities of drugs in MACE has to account for these structural changes of the micellar phase. This includes ternary mixed micelles with fatty acids.

B. Simple Micelles: Bile Salts

Different di- and trihydroxy bile salts and drugs that differ in lipophilicity, basicity, and structure (HBA and HBD) have been compared in order to examine solvatochromic equilibria (30,31).

The principle exploited in the determination of thermodynamic equilibrium constants is the indirect measurement of the capacity factor, depending on the tenside concentration. In Fig. 2a, a typical electropherogram of cationic drugs with cholate in the background electrolyte is shown. A pronounced shift in the migration times of the drugs is observed because of their strong affinity to the bile salt phase. The peak broadening is caused by the polydispersity of the micellar phase (micelles with different aggregation numbers).

The mobility of the drugs, μ, is a function of the mobility of the solute on its own, the strength of the interaction with the buffer components, as well as their mobility in the electric field [see Eq. (2)]. The maximum shift of μ is limited by the mobility of the reagent in the background, in this case by the mobility of the bile salt micelle. An overview of the displacement of drug mobility is given in Fig. 2b. Strongly lipophilic drugs such as propranolol and quinine are shifted from the cationic to the anionic side. Atenolol and etilefrine, representative of hydrophilic drugs, display only a relatively small change in mobility. A comparison of the effects of DHBS (glycodeoxycholic acid, glycochenodeoxycholic acid) and THBS (glycocholic acid) on the example of propranolol is given in Fig. 3.

It has been shown that beside the type of bile salt (lipophilicity, ag-

© 2003 by Marcel Dekker, Inc.

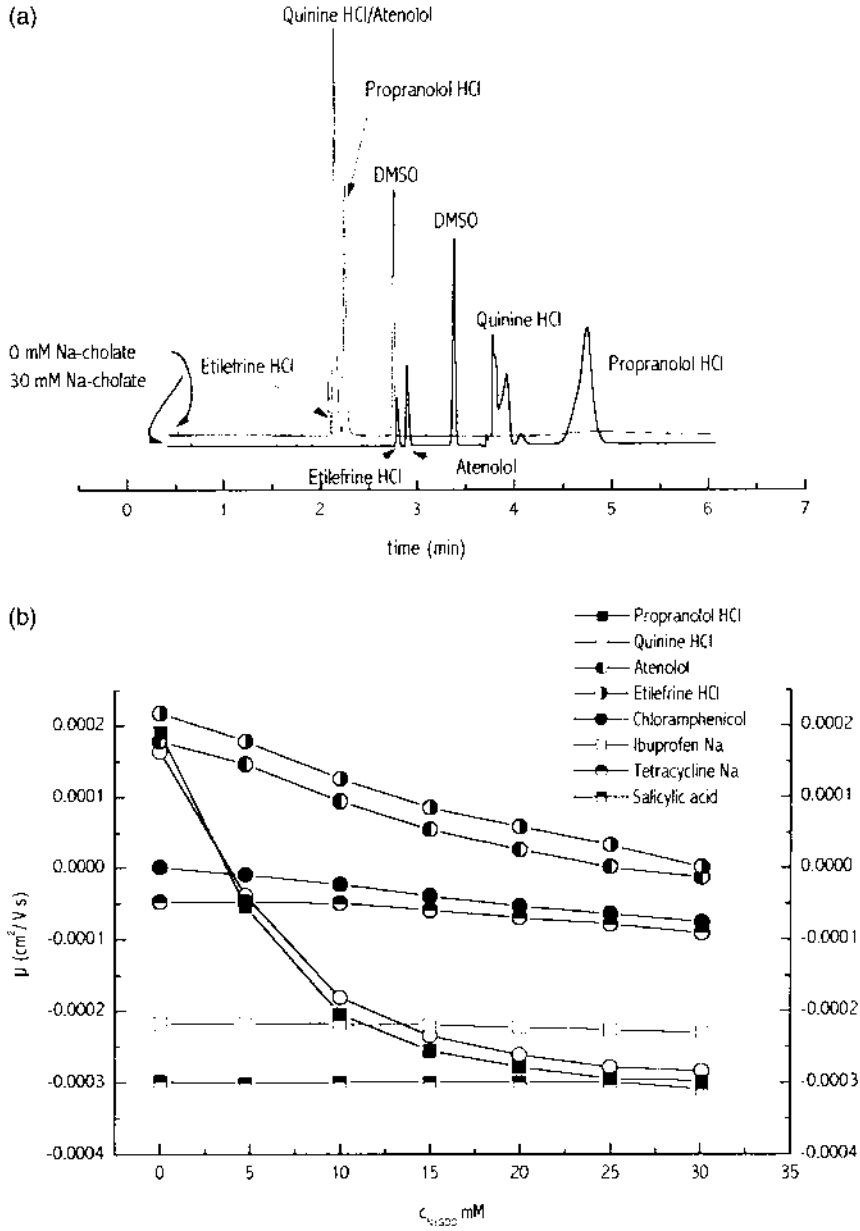

Fig. 2 (a) Electropherogram of cationic drugs with and without BS in the background electrolyte; (b) electrophoretic ionic mobilities μ of different drugs as influenced by BS concentration (buffer: x mM BS, 20 mM phosphate, pH = 7.4, detection 220 nm), NaGDC—glycodeoxycholic acid, Na.

© 2003 by Marcel Dekker, Inc.

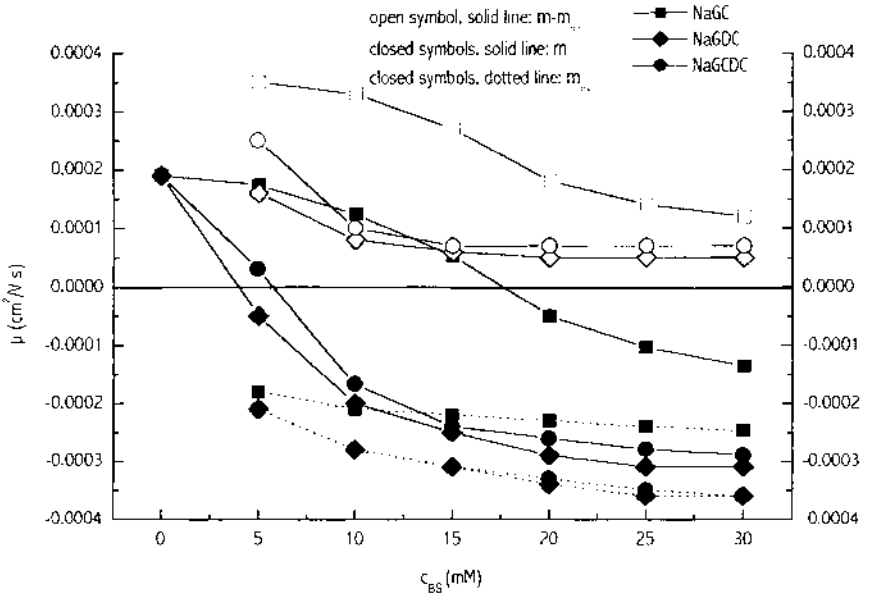

Fig. 3 Electrophoretic ionic mobilities μ of propranolol as influenced by BS concentration; buffer: x mM BS, 20 mM phosphate, pH = 7.4, detection 220 nm; m—electrophoretic ionic mobility μ, GC—glycocholic acid, GDC—glycodeoxycholic acid, GCDC—glycochenodeoxycholic acid.

gregation number of micelles), the pH value and the addition of metal ions may also have a strong effect on the equilibria. The reason for the increase of interaction with smaller pH values is the increasing aggregation of the bile salt micelles (formation of secondary micelles with helixlike structure) and the increased potential difference between the micelle and the cationic drugs (electrostatic interactions are influenced).

C. Binary Micelles: Bile Salt/Phosphatidylcholine

Because of their similarity to the composition of human bile, which consists mainly of bile salts, phospholipids, and cholesterol, of interest for pharmaceutical studies are mainly binary bile salt micelles (BS/PL) (32,33). The function of the bile is to emulsify lipids in food and to dissolve the fission products of lipids as well as fat-soluble vitamins. The spontaneous formation of micelles is a necessary prerequisite to a contact of the lipophilic fission products with the intestinal wall. For affinity measurements, micellar sys-

© 2003 by Marcel Dekker, Inc.

tems have therefore been used whose content of phospholipids ensures the formation of mixed micelles and not of multilamellar vesicles (34).

When mixed micelles are used, in contrast to simple micelles, a much stronger alteration of the ionic mobility of these micellar vehicles is caused by the higher increase in volume/radius and the reduction of the charge. This means that an estimation of $\Delta\mu$ directly from the electropherogram without marking the mixed micelle is no longer possible.

Typical electropherograms of cationic drugs are shown in Fig. 4a. If for a constant absolute concentration of bile salt the phospholipid concentration (DPPC) is increased in the mixed micelle, lipophilic drugs such as propranolol are shifted strongly to the right, which is caused partly by the reduction of the EOF. The effect of the phospholipid concentration on the ionic mobility of solutes is given in a more comprehensive form in Fig. 4b. The graph shows, among other data, the mobility of the micelle for different compositions. Simple as well as mixed micelles may coexist within the range plotted (a and b); above about 15 mM DPPC the formation of vesicles cannot be excluded. The three marked ranges, a, b, and c, are a result of the characteristic behavior of propanolol. For the concentration interval b, the mobilities of propanolol and the micelle are almost completely identical, which means that the drug is almost completely dissolved in the micellar phase. A further shift of the ionic mobility above this concentration (10 mM DPPC) is not determined by the distribution equilibrium, but only by the composition of the micelle and the resulting mobility thereof. Propanolol could be used as marker above app. 10 mM, which corresponds to a mole fraction of 30%.

The fact that for c, no alteration of the electrophoretic properties of the drug was observed leads to the conclusion that the micelle constitution is constant. Any phospholipids or lipids, which form stable and consistent mixed micelles, may be used.

D. Ternary Micelles: Bile Salt/Phosphatidylcholine/ Fatty Acids

Studies of the nature of the interaction between bile salts and fatty acids have, to date, yielded only limited and contradictory information and are therefore only of limited use for affinity studies. Fatty acid molecules are clearly dissolved in the micellar phase and form a ternary mixed micelle with modified properties related to binary mixed micelles.

In Fig. 5 a comparison of two electropherograms is given that were obtained with CE buffers containing a binary and a ternary mixed micellar phase. In presence of ternary mixed micelles in the background buffer, propanolol and quinine migrate with the same velocity, which indicates that

© 2003 by Marcel Dekker, Inc.

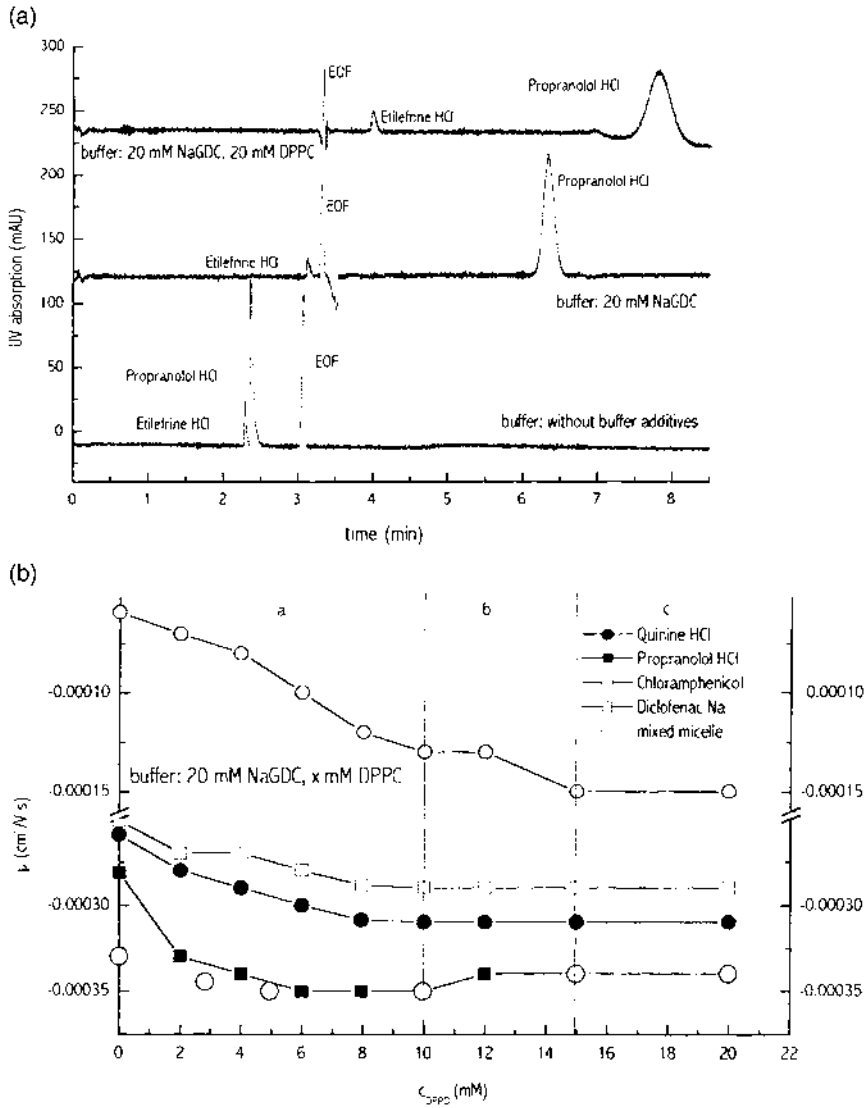

Fig. 4 (a) Electropherogram of cationic drugs with and without BS/DPPC in the background electrolyte; (b) electrophoretic ionic mobilities μ of different drugs as influenced by DPPC concentration; buffer: x mM DPPC, 20 mM BS, 20 mM phosphate, pH = 7.4, detection 220 nm, NaGDC—glycodeoxycholic acid, Na. (From Ref. 31. With permission.)

© 2003 by Marcel Dekker, Inc.

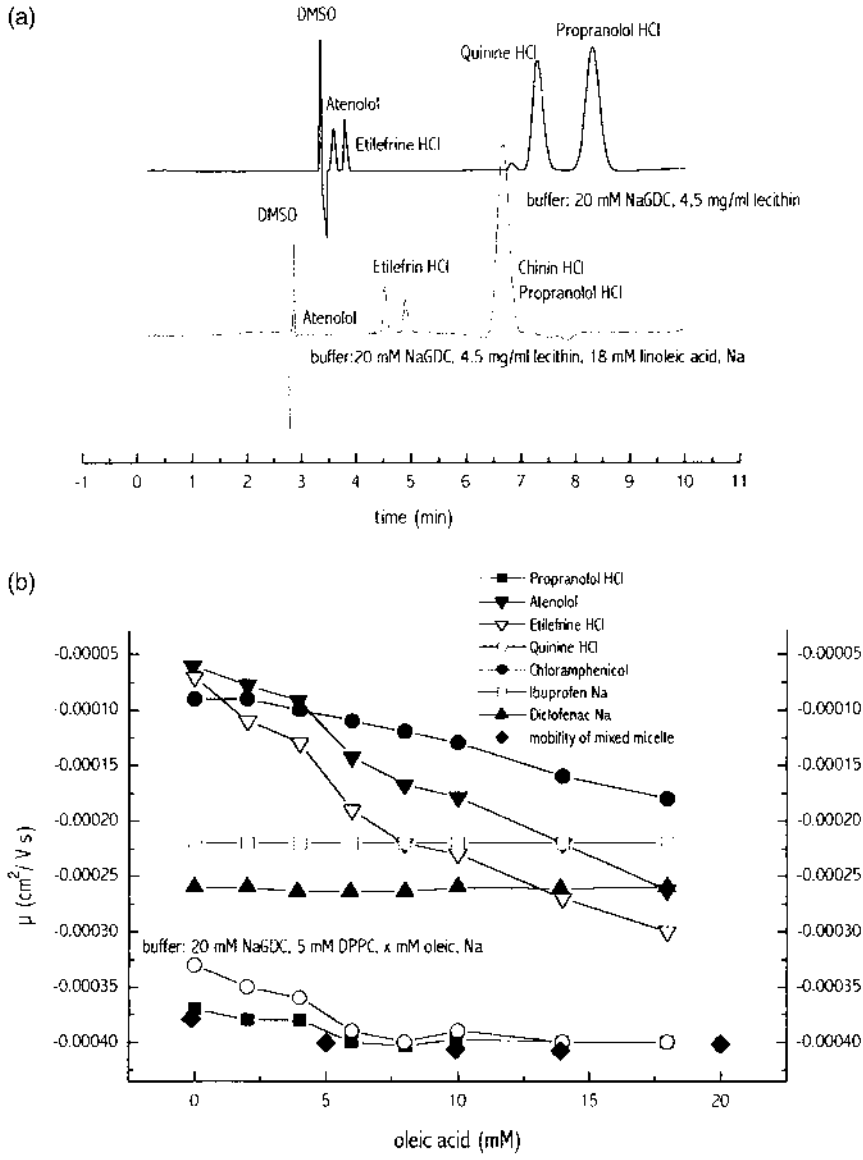

Fig. 5 (a) Electropherogram of cationic drugs with and without FA (fatty acids) in the background electrolyte; (b) electrophoretic ionic mobilities μ of different drugs as influenced by FA concentration; buffer: x mM FA, PL, 20 mM BS, 20 mM phosphate, pH = 7.4, detection 220 nm. (From Ref. 35. With permission.)

© 2003 by Marcel Dekker, Inc.

both are present exclusively in the micellar phase ($k_P = \infty$). Not expected is the fairly large influence of the ternary micelles containing FS on the distribution of hydrophilic, cationic drugs (Fig. 5b). In comparison to saturated fatty acids, the unsaturated FA show a higher capacity. It is interesting to note that the type of bile salt (DHBS or THBS) has only a limited effect on the formation of ternary systems (35).

E. Characterization of Micellar Phase

Methods. In order to be able to calculate the capacity factor and the distribution coefficient, it is necessary to know the ionic mobility of the micellar phase. This in turn means that the physicochemical properties of the surface-active substances have to be known, particularly when mixed micelles are formed (mixing behavior, aggregation constant, mixing ratio, and structure of vehicle). Also useful may be knowledge of the dependence of micellar aggregation properties on changes in pH value and ionic strength of the electrolyte. Various methods relying on electrophoretic measurements are discussed.

If micellar phases are injected into a buffer-filled capillary for the purpose of determining their ionic mobility, a dilution is taking place, which leads to a measured migration time that corresponds to a lower, unknown, concentration. One possibility is the use of chemical substances that are completely dissolved in the micellar phase (micelles are present in background electrolyte and solute) for marking the latter. The velocity of the micelle can then be calculated directly from the migration of the marker (for $k_P = \infty$). Compounds, which are almost insoluble in water and have sufficient lipophilicity to become enriched in the micelle, are ideal. Only a few markers have been found suitable for bile salt micelles. Flavonoids (31) and NBDPE (36) have been suggested in the literature for determining the mobility of the micelles. Because of their influence on the overall mobility of the micelles and its solubilization mechanism, differing results were obtained for low bile salt concentrations. For higher concentrations, with pure micelles and micelles of higher aggregation numbers, these error are negligible.

For systems, which cannot be marked easily, the displacement method is an alternative, in particular for low concentration ranges (36). This is a modification of isotachophoresis, because current flow is not constant with time and field strength is a function of the position along the capillary. Instead of analyte peaks, profiles are obtained (Fig. 6a) as injection and separation are carried out in one step. Although this method is not suitable for all micellar systems, one outstanding advantage is the higher UV sensitivity (which is important for most surface-active compounds). Because of the reliance of the method on displacement, the micellar phase is not diluted.

© 2003 by Marcel Dekker, Inc.

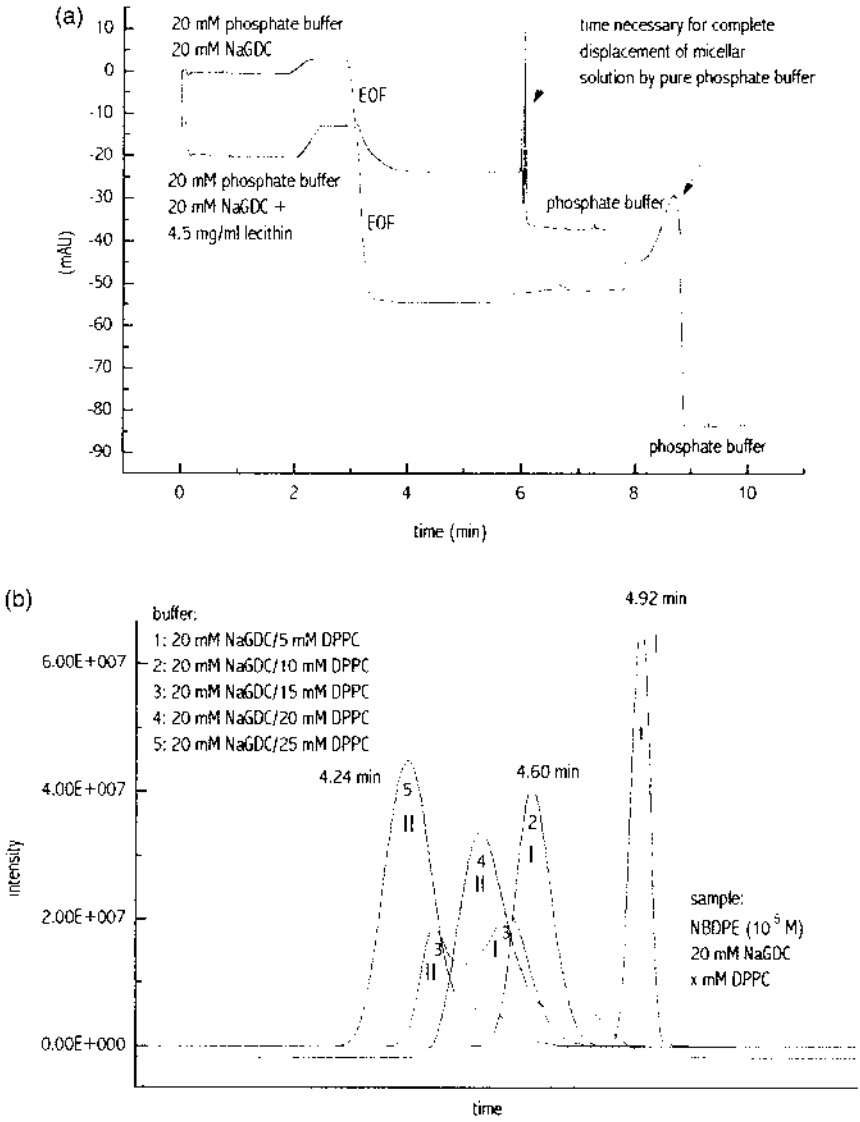

Fig. 6 (a) Displacement profile of micellar solutions, pH = 7.4, UV detection at 200 nm; (b) overlaid electropherograms of binary mixed micelles marked with NBDPE. The DPPC concentration in each sample is equivalent to that in buffer. Detection: LIF. (Modified from Ref. 36. With permission.)

© 2003 by Marcel Dekker, Inc.

The marking method is more easily carried out for the more lipophilic mixed micelles, such as binary micelles (BS/PL). Fluorescence-active phospholipids are suitable for the sensitive LIF detection. Unlike in UV detection, the marker substance can be used down to concentrations of 10^{-6} M, which means that only a very small fraction of the micelles contain the marker. The exchange of the marked lipid molecules between micelles is considerably faster than their migration times, which means that the ionic mobility of the mixed micelles is only negligibly influenced by dissolution of such low concentrations of markers. In the case of a slow exchange rate of the marker molecule for lipidlike vesicles different species may be observed (Fig. 6b). When a combination of UV and LIF detection (Fig. 7) is applied to situations where the system is in equilibrium (mixed micellar systems are present in the background electrolyte solution) and normal CE conditions are employed (the background electrolyte solution contains only buffer without micellar components), interesting conclusions with regard to the micellar compositions are possible (20,36).

Further information regarding the composition of mixed micelles can be obtained by coupling to mass spectrometry. However, the use of surfactants in electrospray ionization will always be fraught with difficulties because contamination of the interface with nonvolatile tensides causes undesirable effects. Stable mixed micelles can be measured only by employing nonequilibrium conditions (only buffers without micellar components). Two further variants of MEKC-MS have been developed and successfully used in recent years, but these are not readily employed for the electrophoretic characterization of micelles, since either a partial filling technique or surfactants of high molecular mass have to be used (37).

IV. DISCUSSION

In principle any ionic or neutral tenside could be used instead of the bile salts. For neutral tensides, the micelle would not have to be marked when the EOF is known. The distribution coefficients can be obtained from Eq. (2) by adjustment of the parameters ($\bar{\nu}$, CMC; see Sec. II). The differing behaviors of the solutes can be demonstrated more clearly in this procedure then when plotting μ vs. surfactant concentration ([s]) (Fig. 8a). It is also interesting to note that in contrast to studies with SDS, the function (k_P vs. surfactant concentration) is not linear (38). Decisive, when determining k_p, is the measurement of the mobility of the micelle as a function of the increase of surfactant concentration. This is also dependent on the type of marker. Because most micelle markers (Dodecanphenon (39,40), Sudan III (41,42)) show an extremely low water solubility, these are not useful for

© 2003 by Marcel Dekker, Inc.

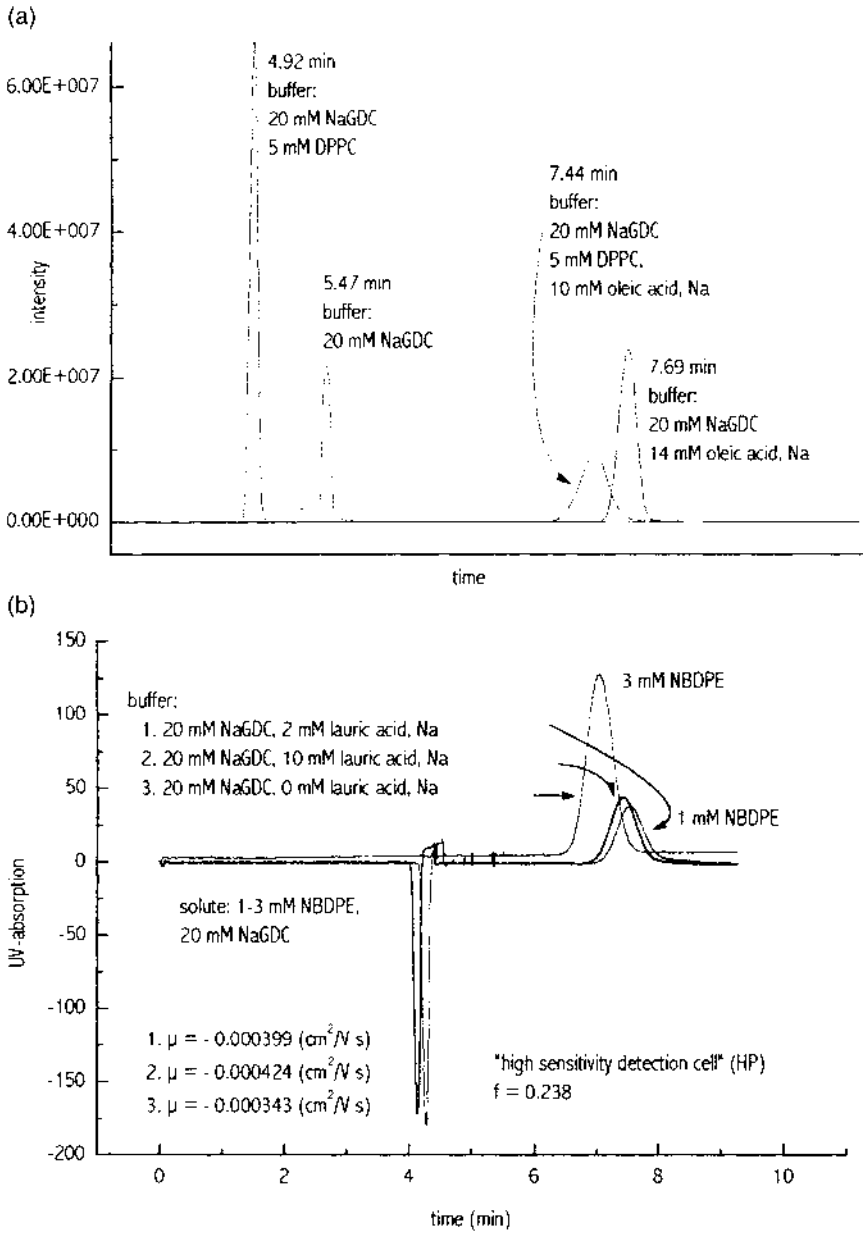

Fig. 7 Electropherograms illustrating the marking with NBDPE for binary and ternary micellar systems (BS/PC/FA). (a) Detection by LIF, a comparison between simple and binary micelles; (b) detection by UV using a high-sensitivity detection cell; buffers contained x mM DPPC, y mM FA and 20 mM phosphate, pH = 7.4. (Modified from Ref. 36. With permission.)

© 2003 by Marcel Dekker, Inc.

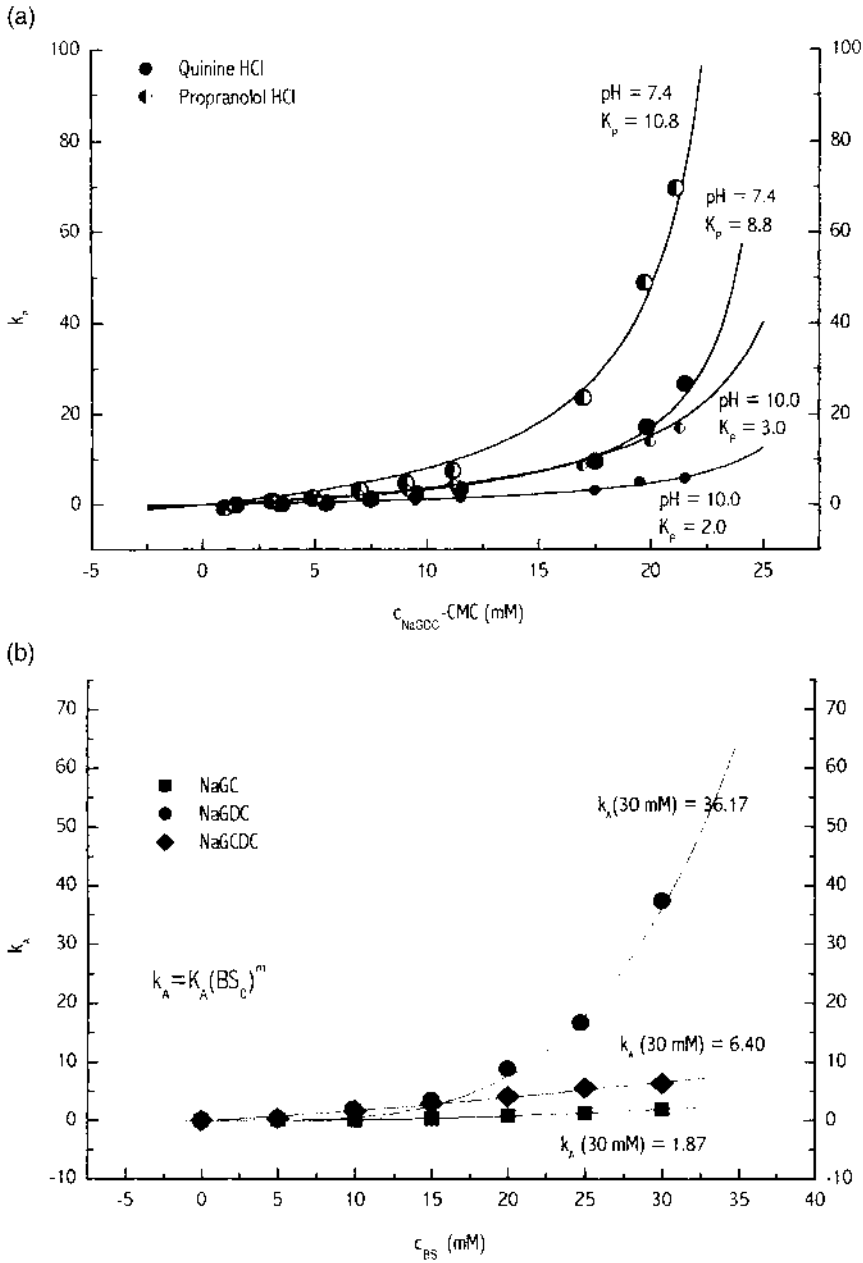

Fig. 8 (a) Dependence of k_P on C_{GDCA} at different pH (20 mM buffer, pH = 7.4: phosphate, pH = 10.0: boric acid/NaOH), fitted function of Eq. (2); (b) dependence of k_A on $C_{GDCA,GCDCA,GCA}$ (20 mM phosphate buffer, pH = 7.4), fitted function of Eq. (4). (From Ref. 31. With permission.)

© 2003 by Marcel Dekker, Inc.

marking bile salt micelles, which are relatively hydrophilic compared to SDS. Also, their large molecular size leads to a wrong (slow) micellar mobility in the case of the rather small, anionic bile salt micelles and therefore to imprecise capacity factors.

K_P and $\bar{\nu}$ can, in contrast to k_p, not be determined via the concentration gradient for binary and ternary mixed micelles, because for the calculation of the Nernstian distribution a constant CMC and an almost constant partial molar volume must be assumed. The calculation of aggregation constants of simple bile salt systems based on Eq. (4) yields similar results (Fig. 8b). Assuming the formation of several concurrent complexes, a brutto stability constant can be calculated. For each application of any tenside, suitable markers have to be found. The completeness of dissolution in the micellar phase is, among other parameters, dependent on the pH value and the ionic strength of the counterions. Therefore, the displacement method should be used, which is not dependent on the chemical solubilization properties of markers. For electrophoretic MACE studies, it is advantageous for the micellar constitution (structure of micelle, type of phase: micellar or lamellar) to be known for the relevant range of concentrations (surfactant, lipids).

Because ionic interactions other than hydrophobic ones are taking place, the contribution of electrostatic interactions can be estimated through studies outside the physiological pH ranges. The charge on the drug substance has an important role, along with the altered solubilization properties of the micelles (e.g., formation of secondary micelles at acidic pH; see Sec. III.A). Also important are the molecular dimensions of the drug (steric effects) and the presence of HBA and HBD.

V. CONCLUSION AND OUTLOOK

In the pharmaceutical sciences, improved and supplemental methods for quantifying binding phenomena between drugs and drug delivery systems are needed. Besides quantification of binding interactions, effects taking place in biological lipid membranes when applying lipophilic drugs can be studied through MACE.

Using a nonequilibrium approach, strong binding can be studied (ligand–receptor complex) (43). However, of particular interest in ACE and MACE is the characterization of weak interactions, since the rate of complex formation and the exchange of solute between aqueous and micellar phase could be too fast to be studied with conventional structure determination methods (MS, NMR). The alternative to those methods, namely, to measure in an equilibrium state, makes MACE highly attractive. Thus, weak bond strengths (acid–base and complex/partition equilibria) are measurable.

© 2003 by Marcel Dekker, Inc.

MACE is a fast, manageable, and reliable method for affinity studies with weak binding ligands because of its simple experimental conditions. It is useful for in vitro investigations to gain valuable information before conducting in vivo tests. In order to calculate the equilibrium parameters by employment of simple micellar systems, two different mathematical models can be applied, the distribution model (K_P) and the complex formation model (K_A). However, comparative studies by using K_P and K_A are meaningful only within similar systems.

A wide spectrum of drugs and drug delivery systems can be investigated with direct and indirect methods by optical (UV/vis, fluorescence), electrochemical (conductivity, amperometry), or other detection techniques (MS). With specific variations of complexing agent systems but also variations in the measurement conditions, the interacting strength can be controlled. Therefore, fast and selective developments of drug delivery systems are conceivable. Such investigations had previously been carried out by permeability studies, almost exclusively on artificial lipid membranes in vitro and in vivo with animals.

So far only bile salt systems have been employed, but other pharmaceutically relevant surfactants may also be characterized by means of electrophoretical binding studies described in this chapter.

ABBREVIATIONS

ACE	affinity capillary electrophoresis
BS	bile salt
CMC	critical micelle concentration
DHBS	dihydroxy bile salt
DPPC	dipalmitoylphosphatidylcholine
FA	fatty acid
HBA	hydrogen bonding acceptor
HBD	hydrogen bonding donator
LIF	laser-induced fluorescence
MACE	micellar affinity capillary electrophoresis
MEKC	micellar electrokinetic chromatography
NBDPE	1,2-dipalmitoyl-sn-glycero-3-(*N*-(7-nitro-2-1,3-benzooxadiazol-4-yl))-phosphoethanolamin
PC	phosphatidylcholine
PL	phospholipid
THBS	trihydroxy bile salt

© 2003 by Marcel Dekker, Inc.

REFERENCES

1. S Terabe, K Otsuka, K Ichikawa, A Tsuchiya, T Ando. Electrokinetic separations in micellar solutions and open-tubular capillaries. Anal Chem 56:111–113, 1984.
2. AJ Hoogstraate, PW Wertz, CA Squiere, A Bos-van Geest, W Abraham, MD Garrison, JC Verhoef, HE Junginger, HE Bodde. Effects of the penetration enhancer glycodeoxycholate on the lipid integrity in porcine buccal epithelium in vitro. Eur J Pharm Sci 5:189–198, 1997.
3. MA Hammad, BW Mueller. Increasing drug solubility by means of bile salt-phosphatidylcholine-based mixed micelles. Eur J Pharm Biopharm 46:361–367, 1998.
4. D Khossravi. Drug–surfactant interactions: effect on transport properties. J Int Pharm 155:179–190, 1997.
5. MG Casarotto, DJ Craik. C-13 and H-1-NMR studies of the interaction of tricyclic antidepressant drugs with dodecyldimethylammonium chloride micelles. J Phys Chem 96:3146–3151, 1992.
6. CPF Borges, S Honda, H Imasato, P Berci, M Tabak. Synthesis, characterization and interactions with ionic micelles of tetraacetylated dipyridamole. Spectrochim Acta A 51:2575–2584, 1995.
7. VE Yushmanov, JR Perussi, H Imasato, M Tabak. Interaction of papaverine with micelles of surfactants with different charge study by H-1-NMR. Biochim Biophys Acta–Biomembrans 1189:74–80, 1994.
8. M Janich, J Graener, J Lange, R Neubert. Extended light-scattering investigations on dihydroxy bile salt micelles in low-salt aqueous solutions. J Phys Chem B 102:5957–5962, 1998.
9. M Janich, J Graener, R Neubert. Extended light-scattering investigations on dihydroxy bile salt micelles in low-salt aqueous solutions. J Phys Chem B 102: 5957–5962, 1998.
10. W Caetano, M Tabak. Interaction of chlorpromazine and trifluoperazine with anionic sodium dodecyl sulfate (SDS) micelles: electronic absorption and fluorescence studies. J Coll Inter Sci 225:69–81, 2000.
11. PM Nassar, LE Almeida, M Tabak. Binding of dipyridamole to phospholipid vesicles: a fluorescence study. Biochim Biophys acta Biomemranes 1328:140–150, 1997.
12. CPF Borges, IE Borissevitch, M Tabak. Charge-dependent and ph-dependent binding sites of dipyridamole in ionic micelles—A fluorescence study. J Lumin 65:105–112, 1995.
13. A Fuertoes-Matei, J Li, KC Waldron. Micellar electrokinetic chromatographic study of interaction between enkephalin peptide analogs and charged micelles. J Chromatogr B 695:39–47, 1997.
14. PG Muijselaar, HA Claessens, CA Cramers. Migration behavior of monovalent weak acids in micellar electrokinetic chromatography: mobility model versus retention model. J Chromatogr A 765:295–306, 1997.
15. M Pagano. Application of electrophoresis and related methods, such as western

© 2003 by Marcel Dekker, Inc.

blotting and zymography, to the study of some proteins and enzymes. Anal Chim Acta 383:119–125, 1999.
16. J Vindevogel, P Sandra. Introduction to micellar electrokinetic chromatography. Heidelberg: Huethig, 1992, pp 171–203.
17. S Terabe, M Shibata, Y Miyashita. Chiral separation by electrokinetic chromatography with bile-salt micelles. J Chromatogr A 480:403–411, 1989.
18. H Nishi, T Fukuyama, M Matsuo. Chiral separation of optical isomeric drugs using micellar electrokinetic chromatography and bile salt. J Microcolumn (Sep 1):234–242, 1989.
19. A Aumatell, RJ Wells. Enantiomeric differentiation of a wide range of pharmacologically active substances by cyclodextrin-modified micellar electrokinetic capillary chromatography using a bile salt. J Chromatogr A 688:329–337, 1994.
20. MA Schwarz. Charakterisierung von Wechselwirkungen zwischen Wirkstoffen und Gallensalzen mittels mizellarer elektrokinetischer Affinitaetschromatographie (MEAC). PhD dissertation, Martin Luther University, Halle, Germany, 1998.
21. RHH Neubert, MA Schwarz, Y Mrestani, M Plaetzer, K Raith. Review, affinity capillary electrophoresis in pharmazeutics. Pharm Res 16:1663–1673, 1999.
22. E Szoekoe, J Gyimesi, Z Szakacs, M Tarnai. Equilibrium binding model of bile salt–mediated chiral micellar electrokinetic capillary chromatography. Electrophoresis 20:2754–2760, 1999.
23. E Szoekoe. Equilibrium-binding model of bile salt–mediated chiral micellar electrokinetic capillary chromatography. Electrophoresis 20:2751–2760, 1999.
24. P Schurtenberger, NA Mazer, W Kanzig. Dynamic laser-light-scattering studies of the micelle to vesicle transition in a model and native bile. Hepatology 4: 143–147, 1984.
25. NA Mazer, GB Benedeck, MC Carey. Quasielastic light-scattering studies of aqueous biliary lipid systems. Mixed micelles formation in bile salt–lecithin solutions. Biochemistry 19:601–615, 1980.
26. K Müller. Structural aspects of bile salt–lecithin mixed micelles. Hepatology 4:134S–137S, 1984.
27. RP Hjelm, P Thiyagarajan, H Alkan-Onyuksel. Organization of phosphatidylcholine and bile salt in rodlike mixed micelles. J Phys Chem 96:8653–8661, 1992.
28. P Schurtenberger, NA Mazer, W Kanzig. Micelle-to-vesicle transition in aqueous solution of bile salt and lecithin. J Phys Chem 89:1042–1049, 1985.
29. MA Long, EW Kaler, SP Lee, GD Wignall. Characterization of lecithin–taurodeoxycholate mixed micelles using small-angle neutron scattering and static and dynamic light scattering. J Phys Chem 98:4402–4410, 1994.
30. MA Schwarz, RH Neubert, G Dongowski. Characterization of interactions between bile salts and drugs by micellar electrokinetic capillary chromatography. Part I. Pharm Res 13:1174–1180, 1996.
31. MA Schwarz, RH Neubert, HH Ruettinger. Application of capillary electrophoresis for characterizing interactions between drugs and bile salt. J Chromatogr A 781:377–389, 1997.

© 2003 by Marcel Dekker, Inc.

32. JR Oreilly, OI Corrigan, CM Odriscoll. The effect of mixed micellar systems, bile salt fatty acid, on the solubility and intestinal absorption of clofazimine (B663) in the anesthetized rat. Int J Pharm 109:147–154, 1994.
33. B Fritzsch, RHH Neubert, G Dongowski, L Heinevetter. Interactions between food components and drugs—part 8: effect of pectins and bile acid preparations forming stable mixed micelles on transport of quinine in vitro. Pharmazie 55: 59–61, 2000.
34. MA Schwarz, K Raith, HH Ruettinger, G Dongowski, RHH Neubert. Investigations of interactions between drugs and mixed bile salt/lecithin micelles—a characterization by micellar affinity capillary electrophoresis. Part III. J Chromatogr A 781:377–389, 1997.
35. MA Schwarz, K Raith, G Dongowski, R Neubert. Effect on the partition equilibrium of various drugs by the formation of mixed bile salt/phosphatidylcholine/fatty acid micelles. A characterization by micellar affinity capillary electrophoresis. Part IV. J Chromatogr A 809:219–229, 1998.
36. MA Schwarz, K Raith, RHH Neubert. Characterization of micelles by capillary electrophoresis. Electrophoresis 19:2145–2150, 1998.
37. H Ozaki, S Terabe. On-line micellar electrokinetic chromatography mass spectrometry with high-molecular-mass surfactant. J Chromatogr A 794:317–325, 1998.
38. S Terabe, K Otsuka, T Ando. Electrokinetic chromatography with micellar solution and open-tubular capillary. Anal Chem 57:834–841, 1985.
39. SY Yang, MG Khaledi. Linear solvation energy relationships in micellar liquid chromatography and micellar electrokinetic capillary chromatography. J Chromatogr 692:301–310, 1995.
40. AD Harman, RG Kibbey, MA Sablik, Y Fintschenko, WE Kurtin, MM Bushey. Micellar electrokinetic capillary chromatography analysis of the behavior of bilirubin in micellar solutions. J Chromatogr A 652:525–533, 1993.
41. PGHM Muijselaar, HA Claessens, CA Cramers. Application of the retention index concept in micellar electrokinetic capillary chromatography. Anal Chem 66:635–644, 1994.
42. S Terabe, K Otsuka, T Ando. Band broadening in electrokinetic chromatography with micellar solutions and open-tubular capillaries. Anal Chem 61:251–260, 1989.
43. YH Chu, WJ Lees, A Stassinopoulos, CT Walsh. Using affinity capillary electrophoresis to determine binding stoichiometries of protein–ligand interactions. Biochem 33:10616, 1994.

© 2003 by Marcel Dekker, Inc.

6

Affinity of Drugs to Pharmaceutical Vehicle Systems: Microemulsions

Yahya Mrestani
Martin-Luther-University Halle-Wittenberg, Halle, Germany

I. INTRODUCTION

Microemulsion electrokinetic chromatography (MEEKC) is a mode of micellar electrokinetic chromatography (MEKC) and capillary electrophoresis (CE) that is capable of separating charged and uncharged drugs. The separation mechanism of MEEKC is similar to that of MEKC. Microemulsions (ME) are colloidal systems and are defined as macroscopically homogeneous, optically transparent fluids having more than one liquid phase. They are formed using water, oil, and a suitable surfactant/cosurfactant. Microemulsions have been known since 1943, and the high solubilizing ability of these emulsions has been extensively used in industry (1). Microemulsions have interesting physicochemical properties. They are thermodynamically stable and can solubilize substances up to a saturation concentration. Since the oily, amphiphilic, and aqueous components can be considered to coexist in one homogeneous phase, microemulsions have a rather unique solubilization capacity for ionic, hydrophilic, as well as lipophilic substances. Therefore, they represent interesting media for pharmaceutical formulations (2–4). Recently, microemulsions have also been used in high-performance liquid chromatography (HPLC) (5), and in a number of papers the use of microemulsion electrokinetic chromatography for the separation of a wide range of compounds (among these pharmaceuticals and excipients) has been described (6). The MEEKC technique has even been used for the separation of proteins. In pharmaceutics, it is important to know the partition of drugs between aqueous and oily phases of a microemulsion. In the literature, a direct method for the investigation of the partition of a drug between these

© 2003 by Marcel Dekker, Inc.

two phases is not known. Using the MEEKC technique it is possible to characterize affinity to ME as well as drug partition in microemulsions. The migration of the colloidal phase of the ME can be determined by compounds that are completely solubilized by the microemulsion phase, such as dodecylbenzene, dodecylbenzoyl propionic acid, and sudan. For the determination of the electroosmotic flow (EOF), acetone, methanol, and dimethyl sulfoxide were used as marker substances. However, in most of these studies identical or very similar MEEKC systems have been used. The microemulsions most often consist of oil, sodium dodecylsulfate, *n*-butanol, and aqueous buffer. Figure 1 presents a scheme of the microemulsion droplet showing the short-chain alcohol, dodecylsulfate, the *n*-octane droplet, and the sodium ions surrounding the droplet of the colloidal phase of the ME.

The reason for this is that if a stable, optically transparent emulsion is to be obtained, the relationship between the amount of the oil phase and the surfactants has to be within a relatively narrow range. Microemulsion electrokinetic chromatography has been shown to be a highly applicable technique for the analysis of complex mixtures such as multicomponent formulations and drug-related impurities. This technique opens a new way to determine water-insoluble neutral species such as steroids, which are difficult to analyze by CE. It is therefore likely that the MEEKC method will be increasingly applied for pharmaceutical and biopharmaceutical analyses in coming years.

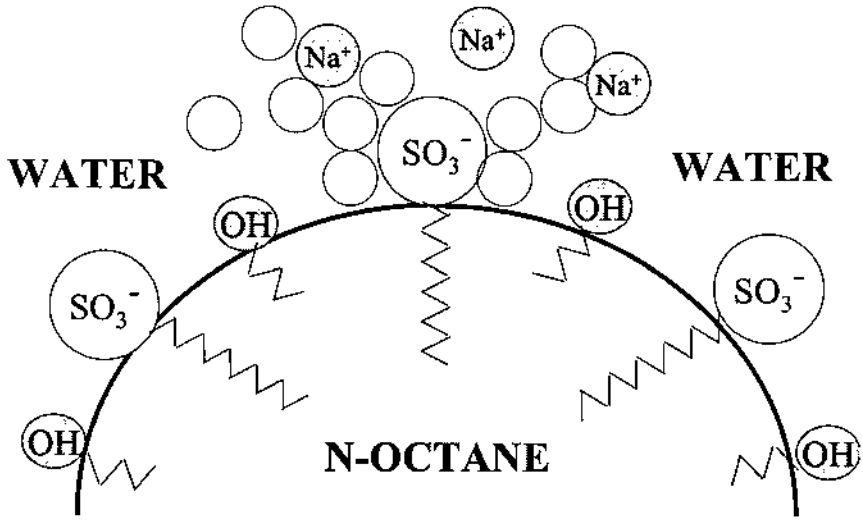

Fig. 1 Scheme of the surfactant-coated oil droplet.

© 2003 by Marcel Dekker, Inc.

Figure 2 shows a scheme of the MEEKC separation principle. When a neutral analyte is injected into the capillary, it will be chromatographically distributed between the microemulsion droplet and the aqueous buffer phase. Water-insoluble drugs will favor inclusion in the oil droplet rather than the buffer phase. Hydrophobic drugs will reside more frequently in the oil droplet than do water-soluble drugs. The separation basis is similar (7,8) to that involved in micellar electrokinetic chromatography. When the solute is dissolved in the negatively charged droplet, it will attempt to migrate against the EOF. Therefore, solutes that are strongly hydrophobic will have long retention times, for they reside predominantly in the microemulsion droplet. Therefore, the analyte will migrate at a velocity between the two extremes, i.e., the electroosmotic velocity v_{eo} and the velocity of the microemulsion v_{mc}. The migration time of the analyte, t_r, will be between the migration time of the microemulsion droplet and the migration time of the EOF solvent front. The velocity of the microemulsion droplet can be determined experimentally from the migration time of the extremely hydrophobic analyte.

II. MICROEMULSION ELECTROKINETIC CHROMATOGRAPHY

A. Principles

As in chromatography, the retention factor (k') in MEEKC is defined as the ratio of the number of moles of the solute in the micellar pseudostationary

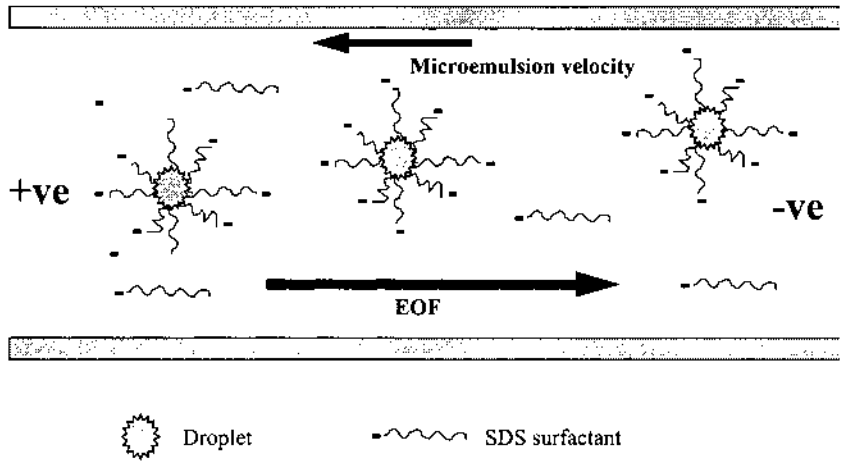

Fig. 2 Scheme of the MEEKC principle.

© 2003 by Marcel Dekker, Inc.

phase, n_{mc}, and that in the bulk aqueous phase, n_{aq}. The retention factor is directly proportional to the microemulsion (ME)–water partition coefficient, P_{mw}, and the phase ratio, Φ:

$$k' = \frac{n_{mc}}{n_{aq}} = P_{mw}\Phi \tag{1}$$

The retention factor in MEEKC for uncharged solutes can be determined from migration time data using Eq. (2). The equation is relevant to MEKC (9):

$$k' = \frac{t_r - t_{eo}}{t_{eo}\left(1 - \dfrac{t_r}{t_{me}}\right)} \tag{2}$$

where t_{eo} is the migration time of the electro-osmotic flow marker, t_{me} is the migration time of the ME marker, and t_r is the solute migration time.

The retention factor k′ of charged solutes can be determined from migration time data using Eq. (3) (10,11):

$$k' = \frac{t_r - t_0}{t_o\left(1 - \dfrac{t_r}{t_{me}}\right)} = \frac{\mu_0 - \mu_r}{\mu_r - \mu_{me}} \tag{3}$$

where t_r is the migration time of a drug measured from the electropherogram, t_0 is the migration time of the drug in the absence of ME, t_{me} is the migration time of the ME, μ_0 are the electrophoretic mobilities of the drug in the absence of ME, μ_r are the electrophoretic mobilities of the drug in the ME, and μ_{me} are the electrophoretic mobilities of the ME.

B. Microemulsion Preparation Procedure

There are a number of procedures that can be adopted when preparing the microemulsions. The most common approach is to weigh the ingredients together, which produces a cloudy suspension. This suspension is then sonicated for 30 minutes to generate an optically clear solution. An alternative approach (10,11) is to vortex-mix the aqueous buffer/surfactant solution and oil together. The butan-1-ol is then added dropwise until an optically clear solution is spontaneously generated when the surface tension in the solution sufficiently approaches zero. It has been shown that evaporation losses of heptane were reduced if it was added to the microemulsion ingredients after the butan-1-ol. An alternative means of producing the microemulsion is to mix the surfactant, cosurfactant, and oil together and then to add the buffer containing additional surfactant to the stirred mixture until a clear solution

© 2003 by Marcel Dekker, Inc.

is obtained. It has also been reported that it is necessary to sonicate the microemulsion buffer for an extensive period (12) to prevent the microemulsion from becoming turbid upon standing at room temperature. But this procedure would depend on the microemulsion composition.

III. VALIDATION ASPECTS

A. Tracers for Microemulsion Phases

To obtain a true k' in MEEKC, it is important to trace the migration of the pseudostationary phase accurately. Sudan III, timepidium bromide, and quine, which have generally been used as tracers for micelles in MEKC, could not be employed as tracers for microemulsions consisting of sodium dodecylsulfate salt (SDS) or cetyltrimethylammonium bromide (CTAB), n-butanol and heptane (12). An iteration method based on a linear relationship between log k' and the carbon number for alkylbenzenes (13) seems to provide a reasonable value of the migration time of the microemulsions. Dodecylbenzene shows a migration time larger than the value calculated by the iteration method and those of other hydrophobic compounds, such as phenanthrene, fluoranthrene, and sudan III (Table 1). Methanol and ethanol were used as tracers for the aqueous phase.

B. Surfactant Type

The choice of the surfactant has a marked effect on the EOF, on the separation, and on the oil droplet charge and size. Sodium dodecylsulfate represents an anionic surfactant (10) penetrating into the oil droplet. Anionic bile salt surfactants such as sodium cholate have also been used (14,15) to generate negatively charged droplets. Mrestani et al. (14) described the effect of surfactants on the k' of cephalosporins in various vehicle systems (microemulsions, mixed micelles, and micelles) consisting of cationic and anionic surfactants (SDS, bile salts, DTAB, and Tween) (see upcoming Table

Table 1 Migration Velocity of Tracers

Tracer	v_{mc} (tracer)/v_{mc} (calcd)
Sudan III	0.995
Dodecylbenzene	1.003

v_{mc} (tracer): velocity of sudan III or dodecylbenzene; v_{mc} (calcd): velocity calculated by iteration.
Source: Ref. 13.

© 2003 by Marcel Dekker, Inc.

2). It is also possible to form microemulsions using cationic surfactants (DTAB) (11,14,16). Dodecyltrimethylammonium bromide (DTAB) is a positively charged surfactant containing a C12 alkyl chain that penetrates into the oil droplet. The cationic surfactant molecules form an adsorbed bilayer on the capillary wall, which reverses the direction of the EOF. Microemulsions consisting of neutral surfactants such as Triton X-100 (17), isopropylmyristate, and Tween or Tagat, respectively, have been studied with regard to their solubilization capacity for lipophilic drugs (18). It has been shown that in contrast to single and mixed micellar phases, drugs like propranolol and diclofenac can easily be solubilized. Microemulsions consisting of neutral surfactants are not useful for the separation of neutral solutes because the neutral droplets migrate at the same velocity as the EOF and the neutral solutes. Increasing the surfactant concentration leads to increasing the ionic strength of the buffer, which reduces the EOF level and increases the analysis time. Increased chain length of the surfactant stabilizes the microemulsion (19) because it reduces the polydispersity of the emulsion droplet size. Higher concentration of the surfactant increases the migration factor of neutral drugs because it increases the charge density (20) on the droplet size of the colloidal phase.

C. Alcohol Type

Butanol and methanol were used in most applications of microemulsions. Ishihama et al. investigated the effect of alcohol on the migration factor of the solute in different systems and on the migration of SDS micelles with or without alcohol. Sudan III migrated as tracer for micelles of SDS faster than dodecylbenzene in the SDS/butanol system (10–12). Due to the addition of butanol to the ME solution, the CMC values decrease very sharply.

D. Oil Type

Generally, heptane or octanol has been used as the colloidal oil phase in the microemulsion systems (21–23). Octanol, heptane, and hexane show similar selectivity and migration time for the separation of a number of neutral solutes (24). A number of other oils were used in the microemulsion systems, for instance, ethyl acetate (25), hexanol (26), butyl chloride (27), and a chiral oil for chiral separation (28).

E. Buffer Type

Phosphate–borate buffer is the most frequently used solution for the preparation of microemulsion systems. An increase in the buffer concentration

© 2003 by Marcel Dekker, Inc.

leads to the suppression of the EOF and generates high currents in the capillary. Generally, MEEKC has been performed using low ionic strength (5–10 mM) (29).

F. Organic Solvents

In MEEKC, organic solvents such as acetonitrile and methanol are added to the buffer solution to reduce the migration time or to improve the resolution. For example, the addition of 8% (v/v) methanol to the MEEKC buffer leads to shorter migration times but exhibiting the same selectivity (12). The addition of 15% (v/v) acetonitrile to the MEEKC buffer also leads to an improvement of the resolution of the neutral solute (25). Furthermore, the addition of organic solvents to the microemulsion solution influences the aggregation, the radius, and the CMC of the micelles. The level of solvent that can be added to MEKC buffers is generally limited to a maximum such as 30% v/v. At levels greater than this, the micelles are disrupted and selectivity is lost. It was found that there were also limits to the maximum solvent contents that could be used in MEEKC. When these limits were exceeded, the microemulsion buffers disintegrated into a cloudy two-phase system, which could not be used for separation.

G. Effect of pH

Typically, buffers in the region of pH 7–9 have been used in MEEKC. At these pH values the buffers generate a high electroosmotic flow (EOF). Extreme values of pH have been used in MEECK specifically to suppress solute ionization. For example, a pH of 1.2 of the buffer has been used to prevent the ionization of acids (30,31). To eliminate the ionization of basic compounds, a buffer at pH 12 has been used. These pH values were used in MEEKC to measure the solubility of ionic compounds (30). High-pH carbonate buffers (31) were applied in place of the standard borate or phosphate buffers.

IV. APPLICATIONS

A. Affinity of Drugs to Microemulsion Systems

1. Determination of the Enthalpy $\Delta H°$ and Entropy $\Delta S°$ of Solubilization in Microemulsion Systems

In pharmaceutics it is important to know the affinity of drugs to microemulsion. In only a few works were the affinity and the partition behavior of drugs in microemulsions using MEEKC studied (14,32). The partition

© 2003 by Marcel Dekker, Inc.

coefficients and the thermodynamics were calculated similar to MEKC. For the calculation of the partition coefficients [Eq. (4)] in microemulsion systems, knowledge of the partial specific volumes of the ME and of the CMC is necessary. Calculation of the partial specific volumes of the ME and of the CMC in the microemulsion system is very difficult. Since the ME systems are very sensible, one cannot change here the concentration of the surfactants, the viscosity of the ME solution, and the surface tension. In all corresponding studies it was assumed that the partial specific volumes of the ME and the CMC in the microemulsion system were the same as those in the case of an SDS micellar system containing alcohol (10,11). Therefore, P_{mw} can be calculated from the capacity factor according to Eq. (4):

$$k' = \frac{P_{mw}\upsilon(C_t - \text{CMC})}{[1 - \upsilon(C_t - \text{CMC})]} \tag{4}$$

where υ is the partial molar volume of the surfactant, C_t is the surfactant concentration, CMC is the critical micelle concentration, and P_{mw} is the partition coefficient of the solute between the micellar phase and the aqueous phase.

Partition coefficients at different temperatures should follow the van't Hoff equation:

$$\ln P_{mw} = \frac{\Delta H^\circ}{RT} - \frac{\Delta S^\circ}{R} \tag{5}$$

where ΔH° is the enthalpy associated with the micellar solubilization or the transition of the solute from the aqueous phase to the micelle, ΔS° is the corresponding entropy, R is the gas constant, and T is the absolute temperature.

The Gibbs free-energy ΔG° for the solubilization in ME can be calculated as follows:

$$\Delta G^\circ = \Delta H^\circ - T\Delta S^\circ \tag{6}$$

The more negative ΔG° is, the more the equilibrium is moved to the micelle side.

2. Affinity of Cephalosporins to Microemulsions

Microemulsion electrokinetic chromatography was introduced to study the affinity of various cephalosporins [cefpim, cefpirom, cefaloridin, cefaclor, cephalexin, cefuroxim, cefotaxim] in microemulsions and micellar (MC) systems. The affinity of various cephalosporins in microemulsions was characterized calculating the capacity factor. The capacity factor values of the cephalosporins in micellar systems and in microemulsions are given in Table

© 2003 by Marcel Dekker, Inc.

2. As can be seen in the table, ME shows higher k' values than MC, except for ceforuxim and cefotaxim. The higher k' values of cephalosporins in ME indicated that the microemulsion has a stronger affinity than the micellar system. The addition of Tween 20 to the glycodeoxycholate (GDC) micellar and microemulsion systems (MC3, ME2) generated higher k' values for cephalosporins than for other systems. This could be expected because the anionic charges located at the surface of the GDC are shielded on the addition of Tween 20, which has a long polyoxyethylene chain (Table 2).

The plots of log k' vs. log P_{ow} and the plots of log $k'(y)$ vs. log $k'(z)$ were studied for seven cephalosporins. A linear relationship was obtained in micellar solution and in microemulsion solution (Tables 3 and 4). The results obtained indicate that the capacity factor determined by EKC could be used both as parameter to characterize the partition behavior of drugs in ME and MC and as hydrophobic parameter instead of log P_{ow}. k' appears to be an evident parameter, and it shows a better diversification than P_{ow}. In the 1-octanol/water system, we did not found high values of the partition coefficients. In contrast, the ME systems used provide a better characterization of the drugs according to their hydrophilic/lipophilic properties.

B. Separation of Drugs using Microemulsions

1. Proteins

The MEEKC technique is effective for the separation of complex mixtures. A typical example is the separation of proteins (33). This separation was carried out using a microemulsion system consisting of SDS-heptane-butane-1-ol in 2.5 *mM* borate buffer, pH 8.5–9.5. The optimal conditions for the separation of proteins depend on the SDS concentration. The maximum resolution was obtained at 120 *mM* SDS. The resolution obtained by MEEKC for ribonuclease A, carbonic anhydrase II, β-lactoglobulin A, and myoglobulin was better than those obtained by CE or by MEKC. The highest number of theoretical was found for myoglobin. The results were compared with those obtained in micellar electrokinetic chromatography and capillary zone electrophoresis. In the investigation MEEKC exhibited a better resolution than CE or MEKC. The MEEKC technique opens a new way to analyze various protein mixtures in different injection formulations.

2. Vitamins

Capillary zone electrophoresis is a powerful tool for the separation of water-soluble vitamins, such as nicotinic acid and vitamin C, with high-pH borate or phosphate buffers. Most simultaneous separations have been performed for fat-soluble vitamins, such as vitamins A and E, by MEKC. Here, organic

© 2003 by Marcel Dekker, Inc.

Table 2 Migration Factors and Partition Coefficient Values of Cephalosporins in Various Systems

	MC1 SDS	MC2 GDC	MC3 GDC Tween	ME1 SDS	ME2 GDC Tween	P_{ow}
1—Cefpim	0.166	0.156	0.350	0.179	0.300	0.01
2—Cefpirom	0.272	0.198	0.385	0.371	0.376	0.02
3—Cephaloridin	0.279	0.198	0.509	0.382	0.503	0.03
4—Cephalexin	0.239	0.305	0.549	0.161	0.764	0.01
5—Cefaclor	0.202	0.350	0.268	0.292	0.867	0.02
6—Cefuroxim	0.562	1.129	16.98	0.730	18.19	0.68
7—Cefotaxim	0.510	1.279	—	0.522	—	0.74

MC, micellar systems: MC1: 1.44% SDS (wt %)/buffer; MC2: 1.44% GDC (wt %)/buffer; MC3: 4% GDC, 5.685% Tween (wt %)/buffer.
ME, microemulsions: ME1: 6.49% 1-butanol/0.82% *n*-heptane, 1.44% SDS (wt %)/buffer; ME2: 6.49% 1-butanol/0.82% *n*-heptane, 1.44% GDC, 5.685% Tween (wt %)/buffer.
Source: Ref. 14.

solvents should be added to the micelle solution. And MEECK has been used to determine water- and fat-soluble vitamins (22) (Fig. 3). Altria analyzed a complex multivitamin pharmaceutical formulation using an SDS-octanol-butane-1-ol microemulsion (22). The MEEKC technique was also used for the separation of vitamin test mixtures using various oil and surfactant types (16). For the preparation of the microemulsion, this study used sodium dodecylsulfate (SDS) or trimethyltetradecylammonium bromide

Table 3 Linear Relationships Between log P_{ow} in Octanol–Water System and log k' in Microemulsion System at pH 7.0

	$\log k'(x) = a \log P_{ow} + b$				
x	a	B	R^a	SD[b]	P^c
ME1	−0.284	0.518	0.901	0.602	0.00075
ME2	1.315	0.886	0.931	0.265	0.00686
ME3	0.753	0.941	0.932	0.327	0.00223

[a] R, correlation cefficient.
[b] SD, standard deviation of the fit.
[c] P, probability.
ME3: 6.49% 1-butanol/0.82% *n*-heptane, 1.44% DTAB/(wt %)/buffer.
Source: Ref. 14.

© 2003 by Marcel Dekker, Inc.

Table 4 Linear Relationships Between log $k'(z)$ and log $k'(y)$ in Various Systems at pH 7.0

	log $k'(x) = a \log P_{ow} + b$				
(y)–(z)	a	b	R	SD	P
MC1–ME1	0.029	0.833	0.956	0.602	0.00075
MC2–ME1	1.054	2.070	0.983	0.132	0.00041
MC2–ME2	−0.464	1.164	0.911	0.213	0.00431
MC3–ME2	0.095	0.920	0.949	0.329	0.00376
MC4–ME3	1.188	1.731	0.990	0.122	0.00002
ME2–ME3	−0.599	1.203	0.984	0.159	0.00038

MC4: 1.44% DTAB/0.566 Tween (wt %)/buffer.
Source: Ref. 14.

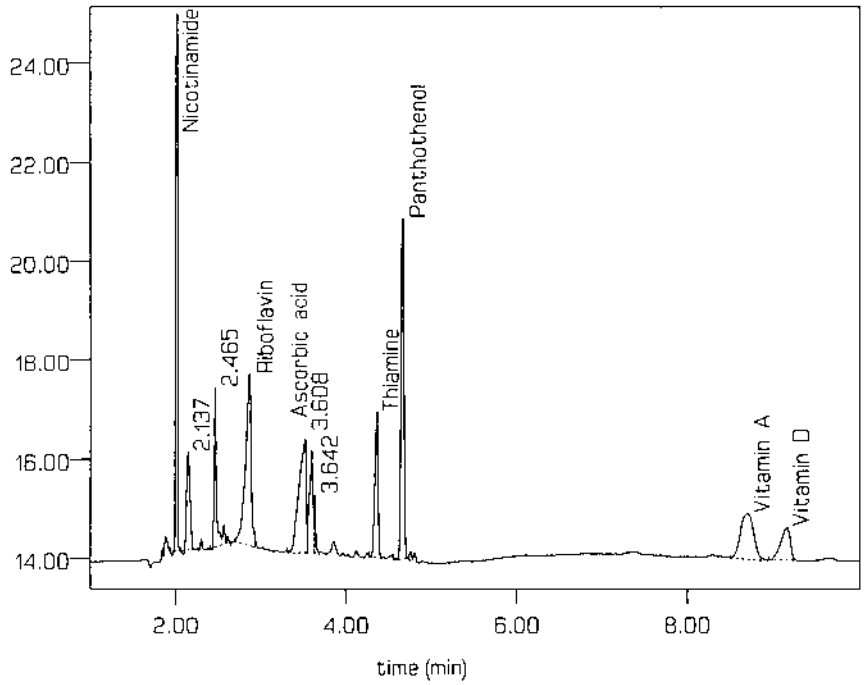

Fig. 3 Separation of vitamins and excipient compounds.

© 2003 by Marcel Dekker, Inc.

(TTAB) as surfactant and diethylether, *n*-heptane, cyclohexane, chloroform, or octanol as oil phase. Table 5 summarizes the values of *N* for the test mixtures in microemulsions containing different organic solvents with cationic surfactants.

3. Antibiotics and Cephalosporins

Separation of antibiotics and cephalosporins can be achieved successfully by CZE because most of them are ionic species. As an alternative to CZE, antibiotics and cephalosporins have been separated by MEEKC. The separation of cephalosporins in different systems (micelles, mixed micelles, and microemulsions) was investigated. The best separation was achieved in microemulsions (Fig. 4). Figure 4 shows that cephalosporins have better affinity to ME in the ME systems than in the MC systems. The affinity of cephalosporins in the ME systems decreases with decrease in the migration time. The MEEKC was also particularly suitable for neutral cephalosporins that could not be separated by CZE or MEKC (14) (see Fig. 5). The method provided good reproducibility and rapid separation with high efficiency.

4. Steroids

The determination of steroids using CZE is very difficult, because steroids are electrically neutral and highly water insoluble. However, these compounds are also too hydrophobic to be separated by conventional MEKC with a surfactant alone. Additives to the micellar solutions, such as urea and organic solvents, turned out to be effective for the separation of the steroids. And MEEKC as a new technique was also used for the separation and determination of steroids (26). The steroids were separated by MEEKC using

Table 5 Number of Theoretical Plates (*N*) for the Test Mixture Component in Microemulsions Containing Different Organic Solvents with TTAB

Vitamin	Nonorganic solvent	Diethyl ether	2-Methyl-2-propanol	*n*-Amyl alcohol
Thiamine	17,685	24,869	31,595	32,167
Nicotinic acid	55,824	54,078	131,386	178,873
Pyridoxol	102,166	298,184	383,196	98,883
Nicotinamide	104,435	116	399,787	120,365
Vitamin E	57,689	75,190	179,738	128,694
Vitamin A	21,640	22,691	289,364	114,164

Source: Ref. 16.

© 2003 by Marcel Dekker, Inc.

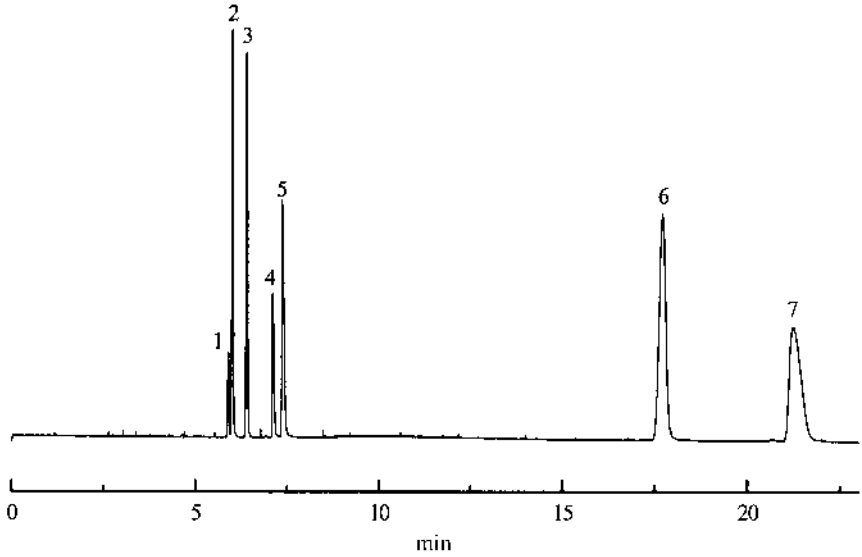

Fig. 4 Electropherogram of cephalosorins (1—cefpim, 2—cefpirom, 3—cephaloridin, 4—cephlexin, 5—cefaclor, 6—cefuroxim, 7—cefotaxin) in a microemulsion system. Buffer, pH 7.0, 10 *mM* phosphate containing 6.49% 1-butanol/0.82% *n*-heptane, 1.44% glycodeoxycholic acid (GDC), and 5.685% Tween. Capillary, 48.5- (40 cm to detector) × 50-μm ID; 30 kV; detection, 265 nm. (From Ref. 14.)

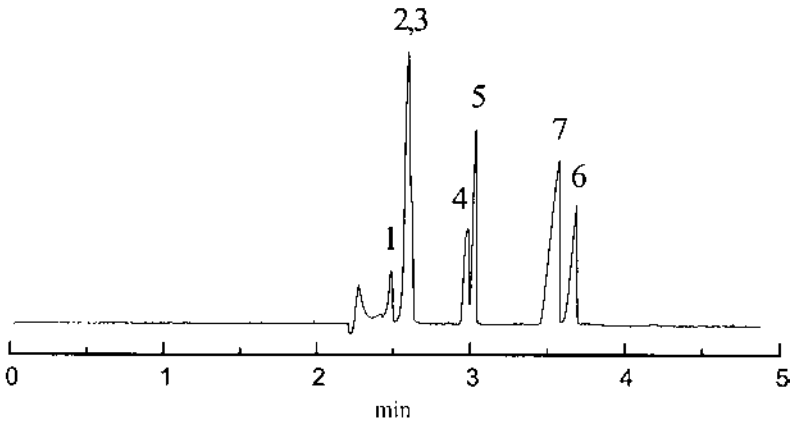

Fig. 5 Electropherogram of cephalosorins in a micellar system. Buffer, pH 7.0, 10 *mM* phosphate containing 1.44% GDC, 48.5- (40 cm to detector) × 50-μm ID; 30 kV; detection, 265 nm. Conditions: See Fig. 4. (From Ref. 14.)

© 2003 by Marcel Dekker, Inc.

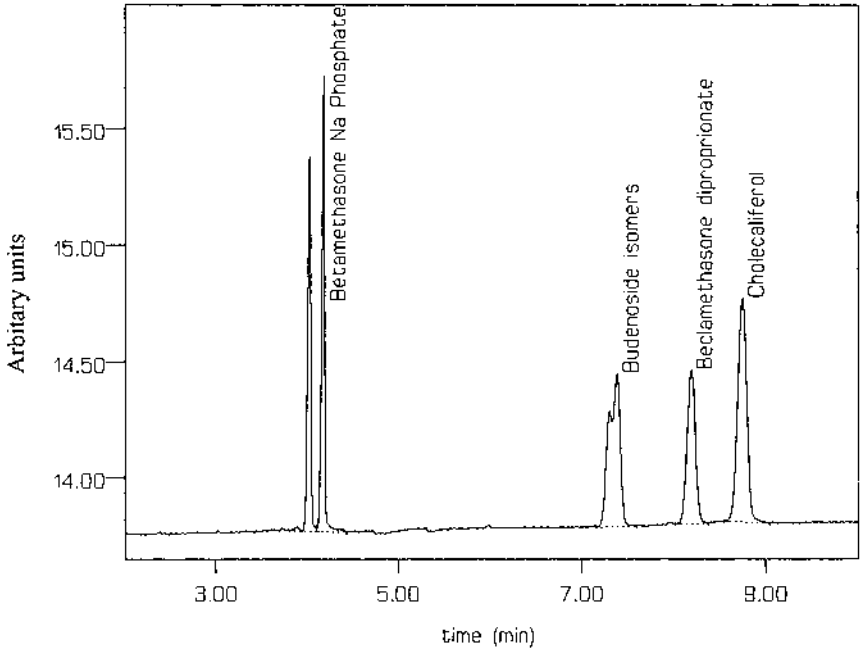

Fig. 6 Separation of water-soluble and insoluble steroids.

n-hexanol, SDS, and *n*-butanol in 20 *mM* phosphate buffer at pH 10 (Fig. 6).

11-β-Hydroxysteroid dehydrogenase activity in rat intestine was measured using MEEKC, and the results were compared with those obtained by MEKC and HPLC (Table 6).

Table 6 Comparison of the Determination of 11-β-Hydroxysteroid Dehydrogenase Activity by HPLC, MEKC, and MEEKC

Sample	HPLC	MEKC	MEEKC
1	0.00	0.00	0.00
2	0.42	0.45	0.44
3	0.96	0.92	0.94

Source: Ref. 26.

© 2003 by Marcel Dekker, Inc.

5. Carbohydrates

The importance of carbohydrates in biochemistry, medicine, the food industry, etc. is steadily increasing. In general, for the determination and separation of carbohydrates it is necessary to derivative them. The combination of HPCE and LIF offers unique possibilities in this long-neglected area. Miksik et al. studied the separation of highly insoluble diphenyl hydrazines of dicarbonyl sugars using MEEKC and MEKC (24) (see Table 7). The separations were carried out using an untreated fused-silica capillary at 20 kV; detection was 220 nm. The microemulsion system was composed of 5 *mM* borate buffer, pH 8.0, SDS (3.31% w/w), *n*-butanol (6.61%, w/w), and *n*-octanol (0.8%, w/w). The separation by MEEKC turned out to be significantly better than the separation obtained by MEKC. The hydrophobic derivatization resulted in better selectivity and rather high plate numbers.

6. Fatty Acids

The separation and determination of long-chain fatty acids using conventional CE are very difficult, because these compounds have poor aqueous solubility and low UV activity. It is possible to separate them in aqueous organic solutions, nonaqueous solutions, or micellar systems. All these sep-

Table 7 Electrophoretic Characteristics of Separated Compounds

Compound	t (min)	N ($\times 10^{-3}$)	R
D-Galactosone, monodiphenylhydrazone	28.8	162	51.33
5-Keto-D-fructose, bisdiphenylhydrazone	29.7	100	1.80
D-Glucosone, monodiphanylhydrazone	30.7	127	2.60
D-Galactosone, monodiphenylhydrazone, acetyl derivative	40.0	254	25.95
D-Xylosone, monodiphenylhydrazone, acetyl derivative	40.5	187	1.25
6-Deoxy-D-glucosone, monodiphenylhydrazone, acetyl derivative	42.1	201	3.65
2-Furylglyoxyoxal, bisdiphenylhydrazone	43.5	252	3.00
D-Glucosone, bisdiphenylhydrazone	43.8	188	0.88
5-Hydroxy-2,3-dioxopentanal, trisdiphenylhydrazone	44.5	170	1.48
2-Furylglyoxal, bisdiphenylhydrazone	46.0, 46.6	113, 105	2.50, 1.03

Migration time (t), number of theoretical plates N ($\times 10^{-3}$), and resolution (R) (to the preceding peak).
[a]Refers to the peak of endoosmotic flow.
Source: Ref. 24.

© 2003 by Marcel Dekker, Inc.

arations were investigated in indirect UV detection mode. Derivatives of fatty acids, such as phenacyl esters, are often prepared to give enhanced UV detection. A mixture of saturated fatty acids containing an even number of carbon atoms (C2–C20) was successfully separated as phenacyl esters by MEEKC with a cholate-heptane-butane-1-ol-borate microemulsion and detection at 243 nm (15). And MEEKC exhibited better separation of ion-chain fatty acids than MEKC under the same conditions using SDS as micellar phase.

7. Cardiac Glycosides

Cardiac glycosides, such as dioxin, acetyldigoxin, acetyldigitoxin, and deslanoside, are pharmaceutically important drugs used for the treatment of congestive heart failure and atrial fibrillation. These drugs were administrated in very low doses. Therefore, it is very important to develop new and sensitive methods or techniques for the determination of these drugs in water and in biological media. Debusschere et al. demonstrated the use of MEEKC and MECK for the separation of neutral and poorly water-soluble cardiac glycosides (34). The results obtained by MEKC were compared with those obtained in MEEKC using different microemulsion compositions. Table 8 summarizes this comparison.

8. Basic Drugs

The MEEKC technique has previously been reported to be useful for the determination and separation of a range of water-soluble and insoluble basic drugs (22). Generally, basic drugs are resolved in CE using low-pH buffers, and separation occurs due to differences in charge-to-mass ratios. Figure 7 presents the separation for a range of basic drugs using MEEKC (22). The separation order obtained is based on both electrophoretic mobility and partitioning. The borate buffer used in this method gives a pH of 9.5, which will limit the ionization of basic drugs, depending on their pK_a values. How-

Table 8 Composition of Microemulsions (ME) A to D. Borate buffer: $Na_2B_4O_7$, 0.05 mol^{-1}, pH 9.2

	ME (A)	ME (B)	ME (C)	ME (D)
SDS (%)	1.66	0.83	1.20	0.83
Heptane (%)	0.81	0.42	0.60	0.20
1-Butanol (%)	6.61	6.61	6.61	6.61
Borate buffer (%)	90.92	92.14	91.59	92.36

Source: Ref. 34.

© 2003 by Marcel Dekker, Inc.

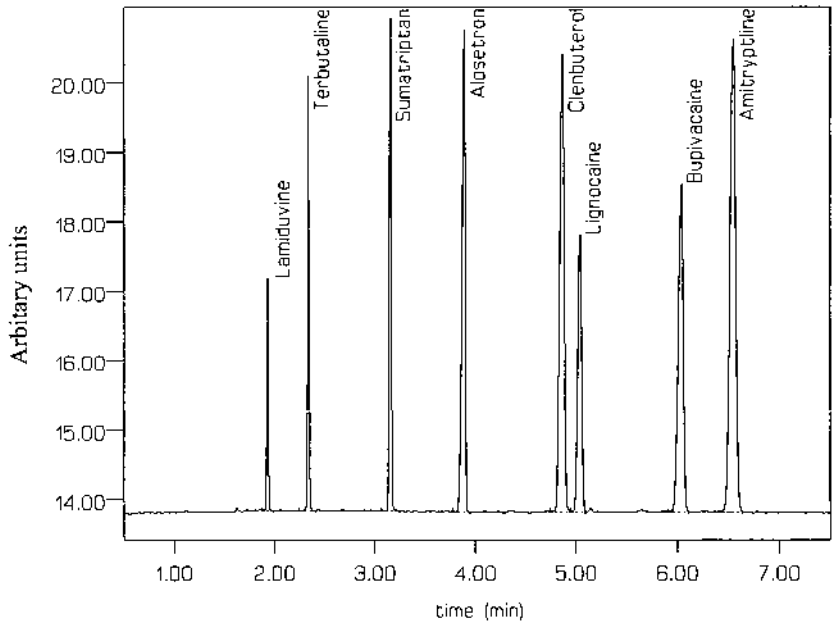

Fig. 7 Separation of a range of water-soluble and insoluble basic drugs. (From Ref. 22.)

ever, some basic drugs remain ionized at this high pH, and they interact with the droplet through both partitioning and ion pair interactions. It is possible to use microemulsions of a pH of 13 (21) where basic drugs will be unionized and the separations based purely on partitioning effects.

9. Acidic Drugs

Electrokinetic chromatography was introduced to determine the separation and the partitioning behavior of various acidic drugs in microemulsions (14,18). The partitioning behavior of acidic drugs in microemulsion was characterized by the capacity factor. The required parameters for the determination of the capacity factor were measured by EKC using cationic and anionic microemulsion systems consisting of the surfactants/*n*-heptane/1-butanol/10 *mM* phosphate buffer solution, pH 7.0. Although these drugs are polar solutes and have acidic characteristics, they show different partition behavior. Hydrophobic interaction, electrostatic interaction, and hydrogen bonding interaction play a significant role in the partition behavior between the acidic drugs and the microemulsion systems. Figure 8 shows the separation for a range of both water-soluble and insoluble acidic drugs (22).

© 2003 by Marcel Dekker, Inc.

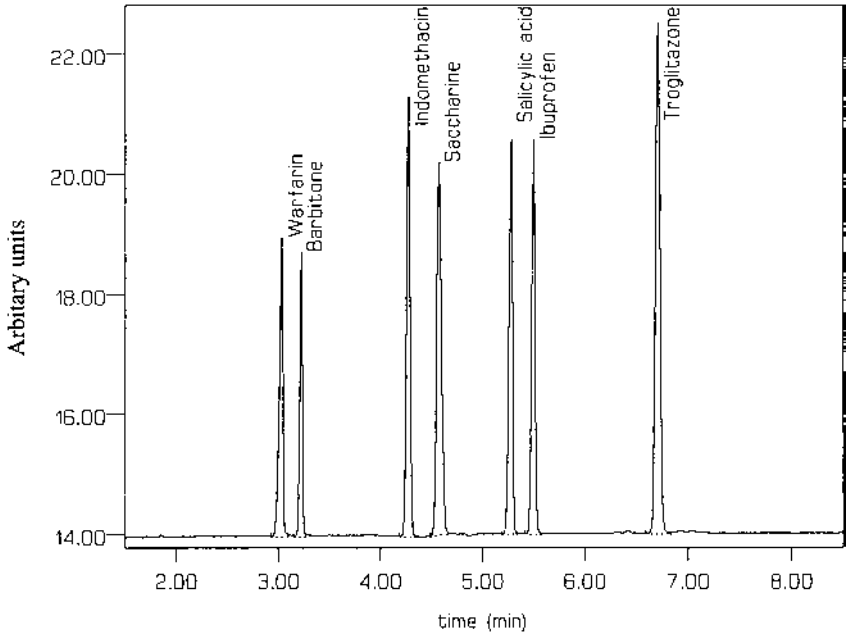

Fig. 8 Separation of acidic drugs. (From Ref. 22.)

These drugs are ionized at this high pH, and therefore the separation is obtained due to a combination of both partitioning and electrophoresis. It is also possible to use a microemulsion buffer at a low pH where the acids will be unionized and separated by partitioning only. Microemulsion at pH 12 was used to determine the log *P* value of acidic solutes in their unionized form (30).

10. Analgesics/Cold Medicine Ingredients

A test mixture of seven cold medicines were separated (9) using a heptane-SDS-butane-1-ol microemulsion. Separation efficiencies obtained in MEEKC (9) were higher than those obtained in MEKC for the same test mixture. Antipyrene analgesics were separated (27) using either octane, heptane, or 1-butyl chloride as the core oil. Octane was shown to give the best migration time precision in a short precision study. Figure 9 shows the efficient separation of a range of analgesics and cold medicine ingredients using the MEEKC method. These analgesics include basic drugs such as chlorpheniramine, neutral solutes such as paracetamol, and acidic analytes such as salicyclic acid. The method was also used to analyze cold medicine

© 2003 by Marcel Dekker, Inc.

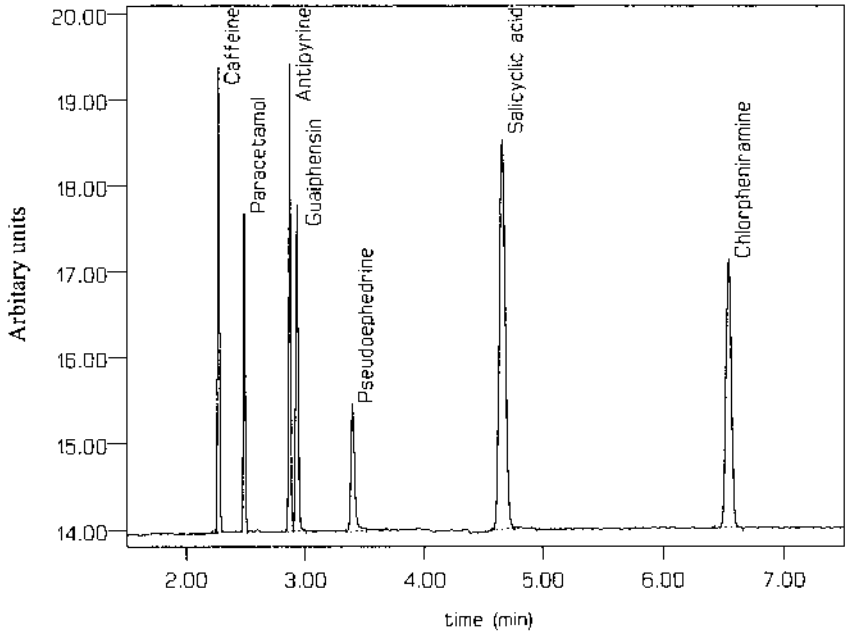

Fig. 9 Separation of a range of cold medicine ingredients. For the microemulsion compositions, see Table 10. (From Ref. 27.)

ingredients in a liquid formulation. The components of this formulation include both charged and neutral components. Table 9 gives some quantitative data (22) from this analysis.

11. Dyes

The MEEKC technique has also been used (29) to analyze the dye components in fountain pen ink. The sample was diluted with MEEKC buffer and was resolved into a broad range of efficient, well-separated water-soluble and insoluble components.

12. Analysis of Natural Products

The MEEKC technique has been applied to the separation and identification of the active components in Rheum plant extracts. The highly insoluble components were extracted into chloroform or ethanol. A microemulsion comprising ethylacetate-SDS and butane-1-ol was used for the separation. Resolution was further increased by the addition of acetonetrile. This method was used to quantify components in plant extracts. Recovery data in the

© 2003 by Marcel Dekker, Inc.

Table 9 Quantitative Application and Repeatability of the MEEKC Method

	Label claim	MEEKC assay results
Sudafed™ Expectorant assay results		
Guaiphenisin	20 mg/mL	20.95 mg/mL
Pseudoephedrine	6 mg/mL	5.86 mg/mL
Ethylhydroxybenzoate	0.1% w/v	0.096% w/v
Propylhydroxybenzoate	0.01% w/v	0.01% w/v
Trogliazatone tablets	200 mg/tablet	199.4 mg/tablet

Injection precision measurements

	Internal standard	No. injections	PAR (% RSD)
Methylparaben	Ethylparaben	10	0.31%
Propylparaben	Ethylparaben	10	0.63%

PAR is the peak area ratio of the solute peak area compared to the area of the internal standard peak.
Source: Ref. 22.

range of 95–104% were reported. Figure 10 shows the complex separation obtained for a methanolic plant extract using a SDS-octane-butane-1-ol microemulsion system with detection at 200 nm.

13. Other Applications

Recent representative applications of MEEKC are given in Table 10.

V. CONCLUSION

The MEEKC technique is used for the separation of every kind of drug, including cationic, neutral, and anionic drugs, because of its high resolution. Other than separation, physicochemical properties can also be determined by MEEKC. Direct enantiomer separation can be successful using chiral selectors such as chiral surfactants or chiral additives. The retention factor and the thermodynamic properties determined by MEEKC provide fundamental information on various interactions between drugs and pharmaceutical vehicle systems with a minimum of substance consumption and time spent. In addition, the relationship between log k' and log P_{ow} provides quantitative data on the hydrophobicity/hydrophilicity properties and the partitioning behavior of drugs in several vehicle systems playing an important

© 2003 by Marcel Dekker, Inc.

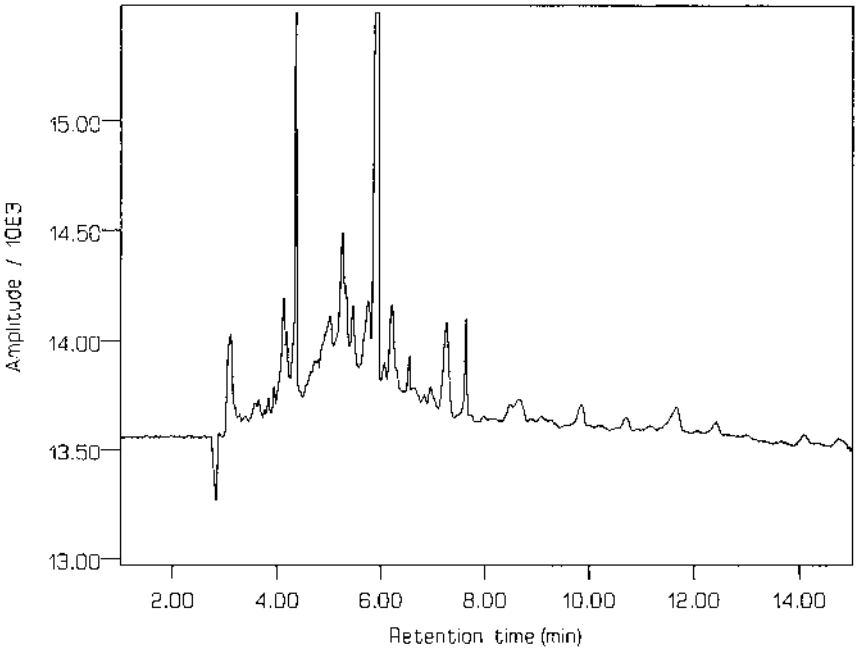

Fig. 10 Analysis of methanolic plant extract using MEEKC, SDS-octanol-butane-1-ol microemulsion, detection at 200 nm. (From Ref. 6.)

role in pharmaceutical technology. Therefore, the method described is a very effective tool not only for characterizing the interaction between drugs and vehicle systems but also for optimizing the vehicle systems.

ABBREVIATIONS

CEC	capillary electrophoresis
CMC	critical micelle concentration
CZE	capillary zone electrophoresis
CTAB	cetyltrimethylammonium bromide
DTAB	dodecyltrimethylammonium bromide
EKC	electrokinetic chromatography
EOF	electroosmotic flow
GC	gas chromatography
GDC	glycodeoxycholate
HPLC	high-performance liquid chromatography

© 2003 by Marcel Dekker, Inc.

Table 10 Recent Representative Applications of MEEKC

Compounds/applications	Microemulsion systems	Refs.
Polycyclic aromatic hydrocarbons	3.31% (w/w) SDS, 0.8% (w/w) octanol, 6.6% (w/w) butane-1-ol, 89.27/10 *mM* borate buffer, 10% (v/v) ethanol	35
Ketones and β-diketones	SDS, heptane, butane-1-ol, high-pH carbonate buffer	36
Pharmaceutical excipients	3.31 g SDS, 0.81 g octane, 6.61 g butane-1-ol, 10 *mM* borate buffer	22
Agrochemical	SDS, octane, butane-1-ol	20
Chiral separation	0.6% (w/w) SDS, 12.2% (w/w) butane-1-ol, 0.5 (w/w) (2R,3R)-di-*n*-butyl tartrate, 15 mm tris-hydroxyamino-methane buffer, pH 8.1	28
Bioanalysis	3.31% (w/w) SDS, 0.81% (w/w) octane, 6.61% (w/w) 1-butanol, 10 *mM* borate buffer, pH 9.5	29
Cold medicine ingredients	1.66 SDS, 0.81% heptane, 6.61% butane-1-ol, borate-phosphate buffer, pH 7	9, 27
Natural-product analysis	75 *mM* SDS, 1000 *mM* *n*-butanol, 90 *mM* *n*-octanol, phosphate-borate buffer, pH 7	29, 37
Drug characterization	(1) 1.44% GDC, 5.68% Tween, 6.49% butane-1-ol, 0.82% heptane (2) 1.44% DTAB, 6.49% butane-1-ol, 0.82% heptane	14

IPM	isopropylmyristate
MEEKC	microemulsion electrokinetic chromatography
MEKC	micellar electrokinetic chromatography
ME	microemulsions
MC	micellar
SDS	sodium dodecylsulfate salt
TTAB	trimethyltetradecylammonium bromide
UV	ultraviolet

ACKNOWLEDGMENTS

The author wishes to thank Dr. Kevin D. Altria, Pharmaceutical Development, GlaxoWellcome R&D, Park Road, Ware, Herts., SG12 ODP, UK, for help in the preparation of the figures.

© 2003 by Marcel Dekker, Inc.

REFERENCES

1. Shah, D.O., Schecter, R.S. (1977). Improved oil recovery by surfactant and polymer flooding. Academic Presss, New York.
2. Kleipert, S., Seibenbrodt, I., Lüders, F., Bornschein, M. (1989). Mikroemulsionen und ihre potentielle pharmazeutische Nutzung. Pharmazie 44:433–444.
3. Gallarat, M., Gasco, M.R., Trotta, M., Chetoni, P., Saettone, M. (1993). Preparation and evaluation in vitro of solutions and O/W microemulsions containing levobunolol as ion pair. Int. J. Pharm. 100:219–225.
4. Kleipert, S., Seibenbrodt, I. (1993). Poloxamer systems as potential ophthalmics. II. Microemulsions. Eur. J. Pharm. Biopharm. 39:25–30.
5. Berthod, A., De Carvalho, M. (1992). Oil in water microemulsion as mobile phase in liquid chromatography. Anal. Chem. 64:2267–2272.
6. Altria, K.D. (2000). Background theory and applications of microemulsion electrokinetic chromatography. J. Chromatogr. A 892:171–186.
7. Terabe, S., Otsuka, K., Ichikawa, K., Tsuchiya, A., Ando T. (1984). Electrokinetic separation with micellar solution and open-tubular capillaries. Anal. Chem. 56:111–113.
8. Terabe, S., Otsuka, K., Ichikawa, K., Ando T. (1985). Electrokinetic chromatography with micellar solution and open-tubular capillary. Anal. Chem. 57: 834–841.
9. Terabe, S., Matsubara, N., Ishihama, Y., Okada, Y. (1992). Microemulsion electrokinetic chromatography: comparison with micellar electrokinetic chromatography. J. Chromatogr. 608:23–29.
10. Ishihama, Y., Oda, Y., Asakawa, N. (1996). A hydrophobicity scale based on the migration index from microemulsion electrokinetic chromatography of anionic solutes. Anal. Chem. 68:1028–1032.
11. Ishihama, Y., Oda, Y., Asakawa, N. (1996). Hydrophobicity of cationic solutes measured by electrokinetic chromatography with cationic microemulsions. Anal. Chem. 68:4281–4284.
12. Ishihama, Y., Oda, Y., Asakawa, N. (1995). Evaluation of solute hydrophobicity by microemulsion electrokinetic chromatography. Anal. Chem. 67:1588–1595.
13. Bushey, M.M., Jorgenson, J.W. (1989). Separation of dansylated methyl-d3-amine by micellar electrokinetic capillary chromatography with methanol modified mobile phase. Anal. Chem. 61:491–493.
14. Mrestani, Y., El-Mokdad, N., Rüttinger, H., Neubert, R. (1998). Characterization of partitioning behavior of cephalosporins using microemulsion and micellar electrokinetic chromatography. Electrophoresis 19:2895–2899.
15. Miksik, I., Deyl, Z. (1998). Microemulsion electrokinetic chromatography of fatty acids as phenacyl esters. J. Chromatogr. 807:111–119.
16. Boso, R.L., Bellini, M.S., Miksik, I., Deyl, Z. (1995). Microemulsion electrokinetic chromatography with different organic modifiers: separation of water- and lipid-soluble vitamins. J. Chromatogr. 709:11–19.
17. Watarai, H., Takahashi, I. (1998). Comparison of three different microemulsion systems as the run buffer for the capillary electrophoretic separation. Anal. Commun. 35:289–292.

© 2003 by Marcel Dekker, Inc.

18. Mrestani, Y., Neubert, R., Krause, A. (1998). Partition behavior of drugs in microemulsions measured by electrokinetic chromatography. Pharm. Res. 15: 799–801.
19. Sicoli, F., Langevin, D. (1995). J. Phys. Chem. 99:14819–1423.
20. Song, L., Qu, Q., Yu, W., Li, G. (1995). Separation of six phenylureas and chlorsulfuron standards by micellar, mixed micellar and microemulsion electrokinetic chromatography. J. Chromatogr. A 699:371–382.
21. Watarai, H. (1997). Microemulsions in separation sciences. J. Chromatogr. A 780:93–102.
22. Altria, K.D. (1999). Application of microemulsion electrokinetic chromatography to the analysis of a wide range of pharmaceuticals and excipients. J. Chromatogr. A 844:371–386.
23. Szcs, R., Van Hove, E., Sandra, P. (1996). Micellar and microemulsion electrokinetic chromatography of hop bitter acids. J. High Resolut. Chromatogr. 19:189–192.
24. Miksik, I., Gabriel, J., Deyl, Z. (1997). Microemulsion electrokinetic chromatography of diphenylhydrazones of dicarbonyl sugars. J. Chromatogr. A 772: 297–303.
25. Li, G., Hu, Z. (1998). Separation and identification of active components in the extract of natural products by microemulsion electrokinetic chromatography. Analyst 123:1501–1505.
26. Vomastova, L., Miksik, I., Deyl, Z. (1996). Microemulsion and micellar electrokinetic chromatography of steroids. J. Chromatogr. B 681:107–113.
27. Fu, X., Lu, J., Zhu, A. (1996). Microemulsion electrokinetic chromatographic separation of antipyretic analgesic ingredients. J. Chromatogr. A 735:353–356.
28. Aiken, J.H., Huie, C.W. (1993). Use of microemulsion system to incorporate a lipophilic chiral selector in electrokinetic capillary chromatography. Chromatographia 35:448–450.
29. Altria, K.D. (1999). Highly efficient and selective separations of a wide range of analytes obtained by an optimized microemulsion electrokinetic chromatography method. Chromatographia 49:457–464.
30. Gluck, S.J., Benko, M.H., Hallberg, R.K., Steele, K.P. (1996). Indirect determination of octanol–water partition coefficients by microemulsion electrokinetic chromatography. J. Chromatogr. A 744:141–146.
31. Watarai, H. (1991). Microemulsion capillary electrophoresis. Chem. Lett. 391–394.
32. Mrestani, Y., Neubert, R. (2000). Characterization of cephalosporin transfer between aqueous and colloidal phases by micellar electrokinetic chromatography. J. Chromatogr. A 871:439–448.
33. Zhou, G.-H., Luo, G.-A., Zhang, X.-D. (1999). Microemulsion electrokinetic chromatography of proteins. J. Chromatogr. 853:277–284.
34. Debusschere, L., Demesmay, C., Rocca, J.L., Lachatre, G., Lotfi, H. (1997). Separation of cardiac glycoside by micellar electrokinetic chromatography and microemulsion electrokinetic chromatography. J. Chromatogr. A 779:227–233.
35. Ishihama, Y., Oda, Y., Uchikawa, K., Asakawa, N. (1995). Paper presented at

© 2003 by Marcel Dekker, Inc.

the 7th International Symposium on High-Performance Capillary Electrophoresis, Würzburg, Germany.
36. Boso, R.L., Bellini, M.S., Miksik, I., Deyl, Z. (1995). Microemulsion electrokinetic chromatography with different organic modifiers: separation of water- and lipid-soluble vitamins. J. Chromatogr. A 709:11–20.
37. Song, L., Zhang, S., Ou, Q., Yu, W. (1995). Electrokinetic chromatograpy of diterpenoid alkaloids from aconitum sinomontanum nakai. J. Microcol. Sep. 7: 123–126.

© 2003 by Marcel Dekker, Inc.

7

Interaction of Drugs with Liposomes and Proteoliposomes

Caroline Engvall and Per Lundahl
Uppsala University, Uppsala, Sweden

I. INTRODUCTION

Liposomes (1,2) are flexible membrane shells enclosing aqueous compartments. The membranes are spontaneously formed in water by self-assembly of phospholipid molecules into bimolecular layers. Each liposome may have a single membrane (*unilamellar vesicle*) (Fig. 1) or contain a number of concentric bilayer shells separated by aqueous layers (*multilamellar vesicle*). The sizes of liposomes range from tenths of nanometers to micrometers. Small liposomes are thermodynamically unstable due to the curvature of the bilayer, whereas larger liposomes show higher stability, although they tend to fuse or aggregate at high liposome concentration.

Liposomes are widely used as models for biological membranes in several scientific disciplines. Another currently very active research area is the use of liposomes as vehicles to deliver drugs to target organs in the body (1–5). Large or hydrophilic drug molecules diffuse only slowly across the bilayer (Fig. 1). For example, oligonucleotides can be encapsulated in liposomes. The stability of such a system has been analyzed by capillary electrophoresis in linear polyacrylamide solution (6). Strongly hydrophobic drugs are adsorbed in the bilayer and will be released gradually (3) (not illustrated).

Orally administered drugs partition into the lipid bilayer in the process of diffusing across the apical and basolateral membranes of the intestinal brush border cells into the blood, as illustrated in Figure 2. About 1800 such drugs are commercially available. A small surface area of the polar parts of the drug molecule generally favors entry into the hydrophobic interior of

© 2003 by Marcel Dekker, Inc.

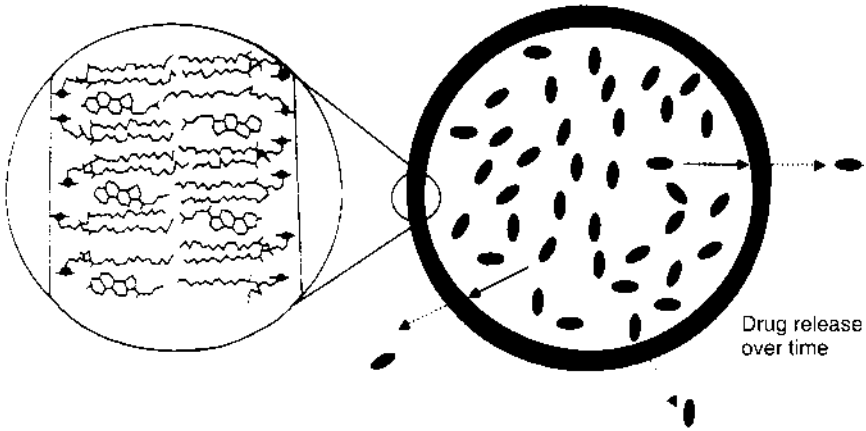

Fig. 1 Schematic illustration of a liposome encapsulating a hydrophilic drug. The membrane contains phospholipid and cholesterol molecules. (Reprinted with permission from Ref. 3 with slight modification. Copyright 1998 Adis International.)

the membrane (8). However, the solubility of the drug in water must be reasonably high to achieve a sufficient concentration gradient across the membrane in relation to the potency of the drug (9). Several structural features of biological membranes affect drug partitioning and diffusion in ways that are poorly understood. Detailed modeling of solute transport through biological membranes will require better knowledge of their structures (10).

Some solutes show specific affinity for particular binding sites of membrane proteins. Nonspecific partitioning into the lipid bilayer will occur in parallel with the specific binding if the concentration of free solute is sufficient. Biospecific binding sites on transmembrane proteins are in several known cases exposed on a hydrophilic face of the protein. For the P-glycoprotein that is responsible for the efflux of xenobiotics, e.g., drugs, from cells (11,12), the site may be situated in the hydrophobic transmembrane region of the membrane protein. Specific solute–membrane protein interactions can be analyzed in several ways (13), e.g., by frontal chromatography or Hummel and Dreyer size-exclusion chromatography for determination of the number of sites and the affinity expressed as an equilibrium constant, as reviewed in Refs. 14–16, where the binding of cytochalasin B to the glucose transporter GLUT1 is the main example. The P-glycoprotein is another membrane protein that has been studied by the frontal analysis technique (17). Related methods have been used to measure the binding of drugs to plasma proteins (18–20).

Nonspecific drug partitioning into biological membranes can be mod-

© 2003 by Marcel Dekker, Inc.

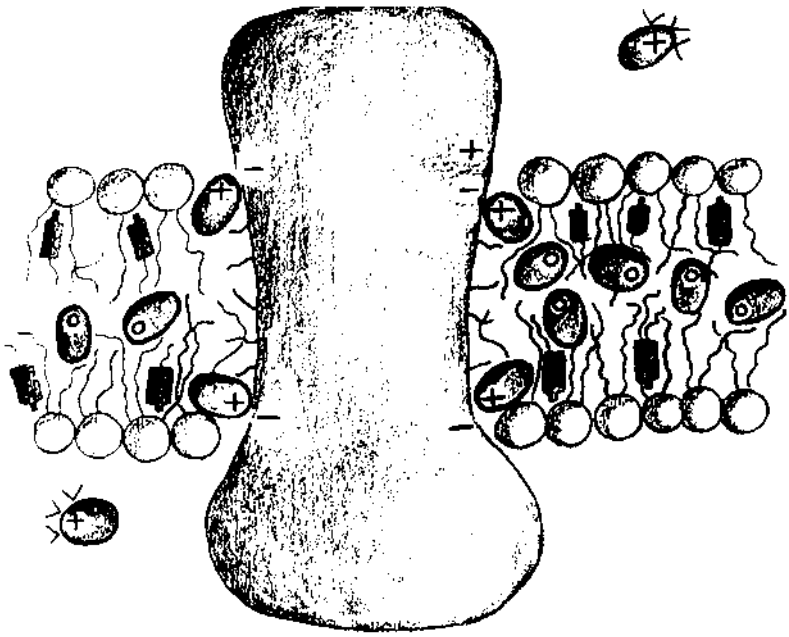

Fig. 2 Schematic illustration of a phospholipid bilayer containing cholesterol (tailed black bodies) and a transmembrane protein (dumbbell) into which charged drug molecules (egg-shaped) partition, thereby interacting electrostatically with the protein molecule. In the bilayer the drug is depicted as being noncharged except when it interacts with a charge on the protein. (Reprinted from Ref. 7. Copyright 2001 by the authors of Ref. 7.)

eled by use of red blood cells or ghosts, red blood cell membrane vesicles, proteoliposomal membranes, phospholipid bilayers, artificial lipid monolayers, surfactant vesicles, or micelles. For example, the partitioning of solutes into lipid bilayers or red blood cell membranes has been analyzed by the use of centrifugation or ultrafiltration, immobilized-liposome chromatography (ILC) (7,21–28), pH-titration (29–31), capillary electrophoresis (CE) (32–34) (see Chapter 1), surface optical methods (35,36), or spectrophotometry (37). The ILC technique has also been applied to the analysis of interactions between certain water-soluble octapeptides and lipid bilayers (38) and for membrane partition studies of oligopeptides (39). Chromatographic and electrophoretic methods for analyses of drug–protein interactions are reviewed in Refs. 14–16, 18–20, and 40–44.

Capillary separation methods have been applied to the analysis of drugs (45–49) and of liposomes, microsomes, and viruses (34,50–53). De-

© 2003 by Marcel Dekker, Inc.

tection methods and ways to increase the sensitivity of detection have been reviewed (54,55). By use of laser-induced fluorescence detection, even individual liposomes can be monitored (56). The use of CE for interaction studies has been presented in several reviews (41–44,57,58). The CE methods for studies of specific as well as nonspecific (partitioning) interactions are often collectively called *affinity CE*. To our knowledge only two reports deal with CE studies of interactions between solutes and phospholipid bilayers in a pseudostationary liposome phase in coated fused-silica capillaries (32,50). Uncoated fused-silica capillaries have similarly been applied to electrokinetic chromatography (EKC) analysis of solute interactions with both liposomes (33,34) and surfactant vesicles (59,60).

The basic principle is shared by several methods: In chromatographic or electrophoretic systems where the liposomes (vesicles) are immobilized, pseudostationary, or carried by an electroendosmotic flow, migrating amphiphilic drug molecules partition between the water outside the liposomes, the lipid bilayer of the liposome, and the aqueous compartment within the liposome (Fig. 3). In all cases the migration rate basically reflects the par-

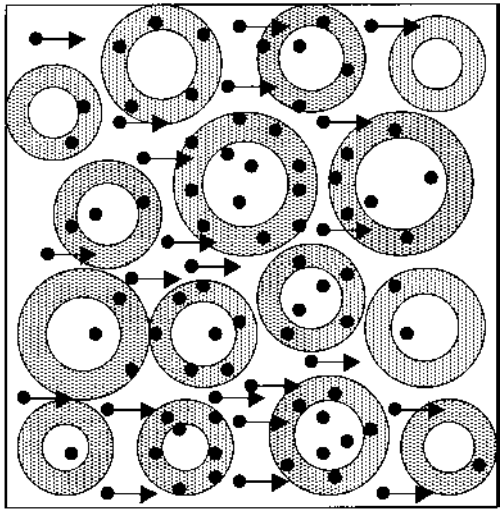

Fig. 3 A migrating zone of solute molecules (spots) interacting with lipid bilayers (rings) in a chromatographic or electrophoretic separation system. The free solute molecules move (arrows) relative to the liposomes or vesicles in a flow of eluent or in an electric field. The solute molecules may either partition into the membranes and diffuse between the external and internal aqueous compartments of the structures as depicted, or interact with the external surface of the membranes and stay outside.

© 2003 by Marcel Dekker, Inc.

titioning and the affinity of the solute to the (proteo)liposomal systems used. In this chapter, therefore, chromatographic, electrophoretic, and electrokinetic analyses are described.

II. METHODS

A. Preparation of Liposomes and Proteoliposomes

Large multilamellar liposomes are prepared by hydration of a lipid film obtained by evaporation of organic solvent(s) in which the lipids were dissolved (1,61). Sonication only decreases the average size of liposomes, whereas unilamellar liposomes of homogeneous size can be obtained by extrusion of multilamellar liposomes, i.e., by forcing a suspension of the material through filter pores of a suitable uniform size (62). An increase in the sizes of liposomes, and thereby their internal volume per lipid amount (63), can be accomplished by freezing and thawing (64). Emulsions containing lipid, water, and organic solvents allow the preparation of liposomes by reversed-phase methods (50,65).

Small unilamellar liposomes can, furthermore, be prepared from detergent-solubilized phospholipid by dilution to obtain a detergent concentration below the critical micelle concentration, by detergent removal via dialysis or size-exclusion chromatography (61), or by adsorption of the detergent to hydrophobic beads (66). If a membrane protein solubilized by complex formation with a detergent is included in the detergent–lipid mixture, the protein molecules will become inserted in the lipid bilayers as the detergent concentration is lowered (67–70). This process is often called *reconstitution* of the membrane protein. The structures formed are proteoliposomes or, when certain conditions prevail, 2D crystals of the protein (71,72).

B. Characterization of Liposomes

The phospholipid concentration in a (proteo)liposome suspension can be determined by phosphorus analysis (73) and the protein concentration by automated amino acid analysis or by a calibrated colorimetric protein assay (74). Thin-layer chromatography (75) and sodium dodecylsulfate-(poly)acrylamide gel electrophoresis (SDS-PAGE) are helpful for analyses of the lipid and protein composition, respectively. Size-exclusion chromatography allows estimation of the size distribution of the (proteo)liposomes and crude fractionation of the material as reviewed in Ref. 76. Accurate determinations of size distributions require analyses by static or dynamic

© 2003 by Marcel Dekker, Inc.

(quasi-elastic) light scattering techniques or by electron microscopy (77). The CE analyses of liposomes have been reported (34,50).

C. Immobilization of Liposomes

Liposomes or proteoliposomes have been immobilized in various ways for chromatographic interaction studies. The early development of such methods has been reviewed in Refs. 76, 78, and 79. For example, (proteo)liposomes have been entrapped in gel beads by dialysis procedures (24,80–84) or freeze-thawing (84–87), adsorbed in gels by use of alkyl ligands (23,84,88–90) or avidin–biotin binding (28,83,91–93), or covalently coupled to a gel (94). All of these immobilization methods have been applied for the purpose of solute–bilayer interaction analyses by ILC: dialysis (24), freeze-thawing (7,21,22,25–27), adsorption to alkyl ligands (23), avidin–biotin binding (28,92,93), and covalent coupling (94).

The CE and EKC analyses by use of suspended liposomes share several features with ILC analyses on liposomes that are entrapped and suspended in the aqueous compartments of microcavities of the gel in which they reside. This is achieved by dialysis or by freezing and thawing. Dialysis entrapment is accomplished by removal of a detergent from a mixture of gel beads and detergent-solubilized phospholipids. Liposomes are thereby formed in the gel matrix, and a fraction of them become too large to escape from the microcavities in which they were assembled. Freeze-thawing entrapment results from rehydration of dry gel beads with a liposome suspension, followed by liposome fusion induced by freeze-thawing (−75/+25°C). After removal of nonimmobilized material by centrifugal washings, ILC gel beds have been packed in glass columns of 5-mm I.D.

D. Chromatography of Drugs with Liposomes or Proteoliposomes as Interacting Phase

Upon chromatography of drugs on a liposomal stationary phase, the drugs spend more time in the lipid bilayers and are thereby eluted later the more strongly they partition into the hydrophobic region of the bilayer. In order to obtain suitable retention volumes, the amount of phospholipid in the column should be adapted to the range of partition coefficients for the set of drugs to be analyzed. If the range is wide, a column containing a small amount of lipids may be used for the most hydrophobic drugs, whereas columns with more lipids are better suited for drugs of medium or low hydrophobicity (26). The partitioning of drugs and other solutes into the bilayer and their affinity to the membrane will be modified by the presence of nonphospholipid components such as cholesterol and membrane proteins

© 2003 by Marcel Dekker, Inc.

in the bilayers (7). The chromatographic retention volume is normalized with regard to the phospholipid amount to provide a capacity factor, K_s (M^{-1}), that reflects the drug partitioning into the lipid bilayer. K_s is defined by (25)

$$K_s = \frac{V_R - V_0}{A}$$

where V_R is the retention volume of the drug, V_0 is the elution volume of an analyte that does not interact with the bilayers, and A is the amount of phospholipids. The nonspecific binding to the gel can be taken into account (7) but changes the log K_s values only marginally. For example, sulfasalazine is retarded fairly strongly on the gel matrix, which lowers the log K_s value by approximately 0.1 unit compared to the value given in Ref. 27. By calculation of the bilayer volume, the log K_s values can be transformed into partition coefficients (28,93).

Analysis of the hitherto largest set of drugs by ILC is described in Ref. 27. Interactions with bilayers containing proteins and cholesterol were reported in Refs. 7 and 25.

E. Affinity Capillary Electrophoresis or Electrokinetic Chromatography of Drugs with Liposomes or Surfactant Vesicles as Interacting Phase

General points of view on electrophoretic interaction analyses are given in Chapter 1. This research field has been reviewed by Heegaard (Ref. 41) and by Heegaard and Kennedy (Ref. 42). Several CE or capillary EKC analyses of interactions between drugs, peptides, or other solutes and lipid or surfactant bilayers have been reported. To our knowledge no effects have been observed of the electric field on the binding or partitioning of solutes. Polyacrylamide-coated (32) or polyimide-coated (50) capillaries have been used for CE analysis of solute interactions, with small unilamellar liposomes filling most of the capillary (32) or with larger unilamellar liposomes (355 $\pm$ 210 nm) applied as a zone (50). Uncoated fused-silica capillaries were used for analogous EKC analyses with vesicles formed by oppositely charged surfactants, approximately 110–140 nm (59) or about 50 nm in size (growing with time) (60), or with unilamellar phospholipid liposomes produced by extrusion through 0.1-μm pores to attain a size of approximately 120 nm (33,34). The effects of the curvature of the bilayer on the partitioning of solutes may be marginal. The CE and the capillary EKC analyses are closely related, since in both cases the analytes migrate relative to the liposomes or vesicles in an electric field. In the electrokinetic approach the electroendosmosis drives a flow of buffer with the dissolved or suspended components through the capillary, whereas in the electrophoretic approach

© 2003 by Marcel Dekker, Inc.

the wall of the capillary is coated to largely suppress the electroendosmosis. However, the differences between the two methods are marginal, and the same experimental setup can be used for zonal ACE of liposomes for determination of their mobilities, surface charge, and stability (34,50) and for analyses of solute–bilayer interactions (32,34,50) and for EKC analyses of the latter type (33,34).

III. APPLICATIONS

A. Chromatography of Drugs with Liposomes or Other Membrane Structures as Interacting Phase

The elution profiles of drugs from an ILC gel bed of 5-mm diameter are broad (Fig. 4A). The drugs have therefore usually been analyzed one by one. A capillary continuous bed containing liposomes immobilized on alkyl ligands gave similarly broad peaks (Fig. 4B). Unexpectedly, the log K_s values for 15 drugs determined on liposomes prepared from synthetic phosphatidylcholine (1-palmitoyl-2-oleoyl-*sn*-glycero-3-phosphocholine) in a 5-mm ILC bed (27) correlated poorly with the log K_s values obtained from egg L-α-phosphatidylcholine liposomes in the capillary continuous beds (23) (not illustrated). In contrast, liposomes of different phospholipid compositions entrapped in dextran-grafted agarose gel beads (Superdex 200 prep grade) provided similar sets of log K_s values upon ILC in ordinary 5-mm columns (25,27). In fact there is a fair correlation between log K_s values on, e.g., egg yolk phospholipid (EPL) liposomes and log octanol/water partition coefficients (log P_{oct}) (Fig. 5). Log K_s and log P_{oct} are linearly related for neutral and positively and negatively charged drugs. The slopes of the three correlation lines are similar to one another, whereas the intercepts differ significantly. However, the points are widely scattered around the straight lines. Individual drugs are thus subject to effects in addition to hydrophobic partitioning upon interaction with the phospholipid bilayers. For example, at log P_{oct} = 3, the range of the corresponding log K_s values in Fig. 5 is 1–4. A similar plot of log K_s values determined on the egg phosphatidylcholine liposomes in capillary continuous beds (23) versus the log P_{oct} values resembled Fig. 5, with seemingly different regression lines for the positively charged, neutral, and negatively charged drugs, although the number of points was only 15.

Several ILC studies covering drug interaction with liposomes and, correspondingly, proteoliposomes, cytoskeleton-depleted red blood cell membrane vesicles, red blood cell membranes, or red cells and ghosts have been reported (7,8,21–28,40,76,91,92,94). The log K_s values for interaction of

© 2003 by Marcel Dekker, Inc.

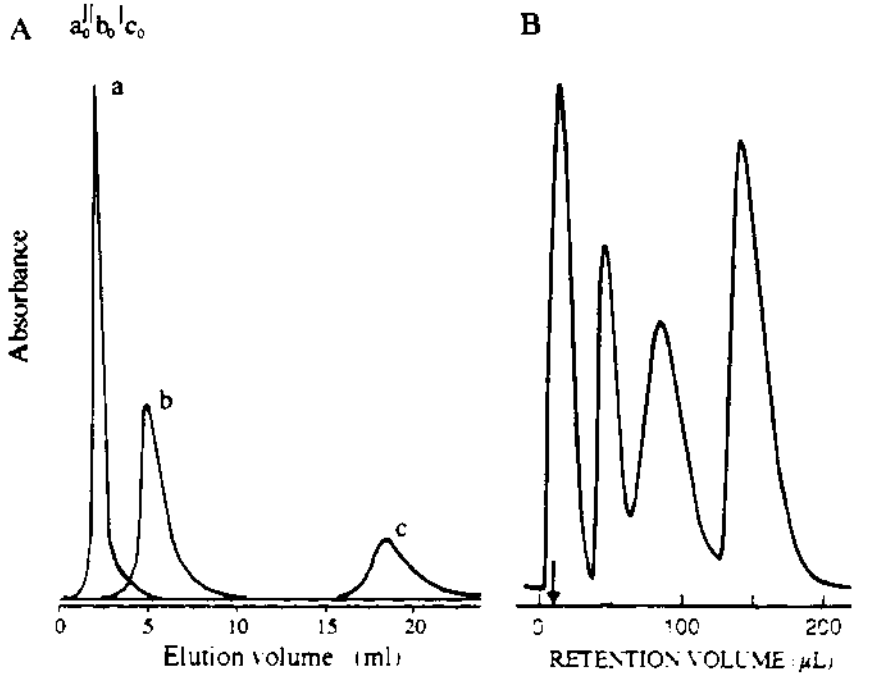

Fig. 4 Elution profiles for (A) propranolol (a), promethazine (b), and chlorpromazine (c) applied separately on a 5-mm ILC column containing cytoskeleton-depleted red blood cell membrane vesicles entrapped in dextran-grafted agarose gel beads (1.4 μmol phospholipid, 0.5 mL/min) and (B), from left to right, acetylsalicylic acid, salicylic acid, warfarin, and pindolol on a capillary continuous bed containing liposomes immobilized by use of C_4 ligands (1.0 μmol phospholipid, 10 μL/min). The elution volumes in the absence of lipid are shown (a_0, b_0, and c_0, and the arrow, respectively). (Part A is reprinted with permission, with slight modification, from Ref. 26. Copyright 1999 Elsevier Science. Part B is reprinted with permission from Ref. 23. Copyright 1996 Elsevier Science.)

drugs with liposomes differed in certain respects from the log K_s values obtained by chromatography on immobilized human red cells/red cell ghosts (25). For a set of drugs eluted from an egg yolk phospholipid liposome column, the log K_s values covered the range 0.2–4.0, whereas the immobilized cells and ghosts, with asymmetric phospholipid bilayers containing cholesterol and glycosylated membrane proteins connected to a cytoskeleton, showed a range of log K_s values of only 1.6–3.2 for the same drugs (25).

© 2003 by Marcel Dekker, Inc.

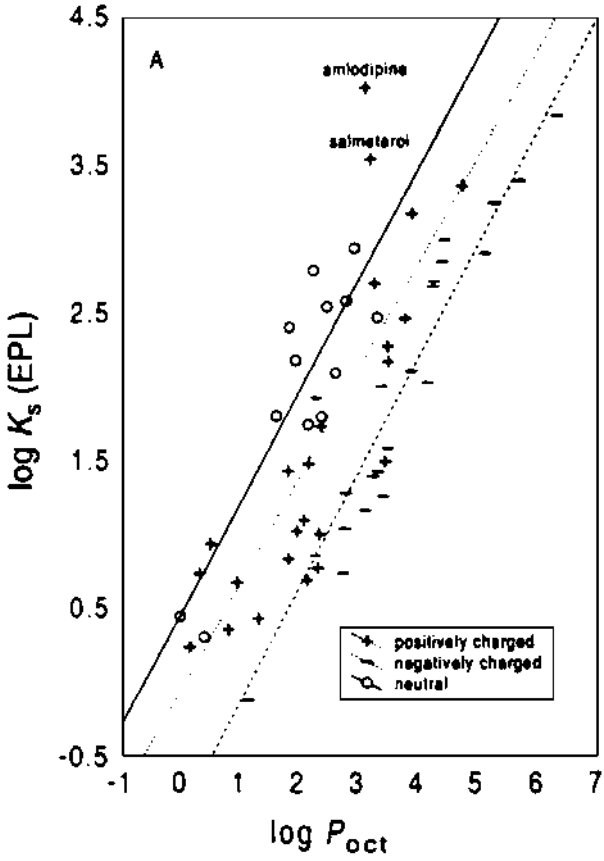

Fig. 5 Relationship between the log K_s values obtained by chromatography on entrapped egg yolk phospholipid (EPL) liposomes and the log P_{oct} values from octanol/water partitioning analyses, for neutral drugs (upper line) and for positively (center line) and negatively (lower line) charged drugs. (Reprinted with permission from Ref. 27. Copyright 2001 Elsevier Science.)

The interactions obviously differed between the lipid bilayers and the natural membranes. Furthermore, cholesterol slightly hinders the drug partitioning into the liquid-crystalline bilayers, in agreement with several previous reports, and the drug molecules interact electrostatically with membrane proteins at the hydrophilic interface adjacent to the polar headgroups of the phospholipid molecules (7).

© 2003 by Marcel Dekker, Inc.

B. Affinity Capillary Electrophoresis of Drugs with Liposomes as Interacting Pseudostationary Phase

The ACE analysis of interactions between drugs and phospholipid bilayers of liposomes present as a pseudostationary phase was performed by Zhang et al. (32). The capillaries were treated to eliminate electroendosmosis. Freshly prepared and essentially neutral small unilamellar liposomes composed of egg phosphatidylcholine were sucked into the capillary. These liposomes increased both the retention of four negatively charged drugs and the separation between the substances (Fig. 6). The chromatographic retentions of these drugs on immobilized phosphatidylcholine liposomes, ex-

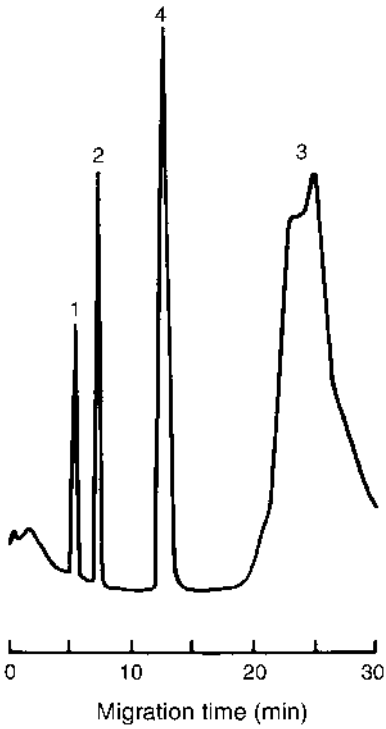

Fig. 6 Separation of (1) salicylic acid, (2) acetylsalicylic acid, (3) sulfasalazine, and (4) warfarin by use of capillary electrophoresis with pseudostationary egg L-α-phosphatidylcholine liposomes (29 mM phospholipid) in a polyacrylamide-coated capillary (100-μm I.D., 25 cm) at pH 7.4. Peak heights 0.02–0.04 absorbance units at 225 nm. (Reprinted with permission, with slight modification, from Ref. 32. Copyright 1995 VCH Verlagsgesellschaft.)

© 2003 by Marcel Dekker, Inc.

pressed as log $K_{s,\mathrm{ILC}}$ (27) and plotted against the electrophoretic partitioning results in Fig. 4 of Ref. 32, log $K_{s,\mathrm{CE}}$, fall nicely on a line defined by a second-order equation (Fig. 7). The liposome ACE method also gave retentions for two octapeptides (32) that confirm the retarding effect of C-terminal CysCys observed by ILC (38).

The interactions between the drugs and the essentially neutral phosphatidylcholine liposomes described by Zhang et al. (32) are little affected by electrostatic interactions, although the ionic strength of the 25 mM sodium phosphate buffer, pH 7.4, is fairly low. Partition analyses with charged drugs and charged liposomes may show effects of electrostatic interactions (25) at the low ionic strengths commonly used for ACE.

Another example of ACE analyses of solute–bilayer interactions was described by Roberts et al. (50), who observed retardation of riboflavin by liposomes. Analyses technically similar to liposomal ACE have been performed with mixed bile salt/phosphatidylcholine/fatty acid micelles (95). The partitioning of basic and acidic drugs depended on the acid–base properties of the drug and on the shape and charge of the mixed micelles.

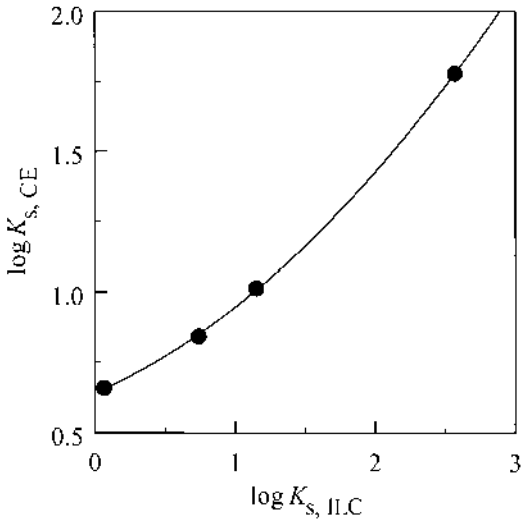

Fig. 7 Log $K_{s,\mathrm{CE}}$ values determined by CE in the presence of egg L-α-phosphatidylcholine liposome (32) versus log $K_{s,\mathrm{ILC}}$ values obtained by ILC on 1-palmitoyl-2-oleoyl-*sn*-phosphocholine liposomes, with a second-degree correlation line (R^2 = 1.00). (The log $K_{s,\mathrm{ILC}}$ values were taken from Ref. 27 and were here corrected for the slight effect of the drug interaction with the dextran-grafted agarose gel [unpublished data].)

© 2003 by Marcel Dekker, Inc.

C. Electrokinetic Chromatography of Drugs with Liposomes or Surfactant Vesicles as Interacting Phase

Liposomes or vesicles have been used as an interacting phase also in EKC analyses. Wiedmer et al. (33) characterized the effects of unilamellar liposomes composed of 1-palmitoyl-2-oleoyl-*sn*-glycero-3-phosphocholine or 1,2-dipalmitoyl-*sn*-glycero-3-phosphocholine (80%) and a negatively charged phospholipid (phosphatidylserine, phosphatidylglycerol, phosphatidic acid, or cardiolipin). The relative migration times of solutes increased with the lipid concentration, as expected, and the separation improved with increasing content of cardiolipin up to 30%. The resolution of the neutral corticosteroids was better at 25°C than at 43°C with 1-palmitoyl-2-oleoyl-*sn*-glycero-3-phosphocholine supplemented with 20% phosphatidylserine (Fig. 8B) or 20% cardiolipin (Fig. 8C). The separations were reported to be highly repeatable. A separation of another set of steroids is illustrated in Fig. 4 of Ref. 34.

Hong et al. applied capillary EKC with dodecyltrimethylammoniumbromide/sodium dodecylsulfate (12.7/21.1 mM) vesicles to the separation of alkylphenones (Fig. 8A) and obtained better resolution than with sodium dodecylsulfate micelles (59). The logarithms of the retention factors for 20 neutral compounds of similar structures showed an excellent linear correlation with log P_{oct} ($R^2 = 0.98$). Similarly, Razak et al. (60) showed that the log capacity factors for interaction between neutral and positively charged analytes and cetyltrimethylammoniumbromide/sodium octylsulfate vesicles correlated linearly with the log P_{oct} values.

D. Electrokinetic Chromatography of Drugs with Micelles or Oil Droplets as Interacting Phase

The foregoing capillary EKC analyses of drugs with surfactant vesicles or liposomes as an interacting phase are closely related to micellar capillary EKC analyses developed by Terabe et al. (96), see Chapter 5. The correlation between partitioning of drug analytes from water into detergent micelles and into octanol has been studied by the latter technique (97–99). Micellar capillary EKC with lysophospholipid micelles gave a retention order of beta-blockers that differed from the order obtained upon immobilized artificial membrane chromatography (100). Micellar liquid chromatography with polyoxyethylene dodecylether micelles has been shown to provide drug-partitioning data similar to those obtained by ILC on egg phospholipid liposomes (101).

Partitioning into oil droplets can be analyzed similarly as partitioning into micelles. Mrestani et al. (102) used microemulsions prepared from non-

© 2003 by Marcel Dekker, Inc.

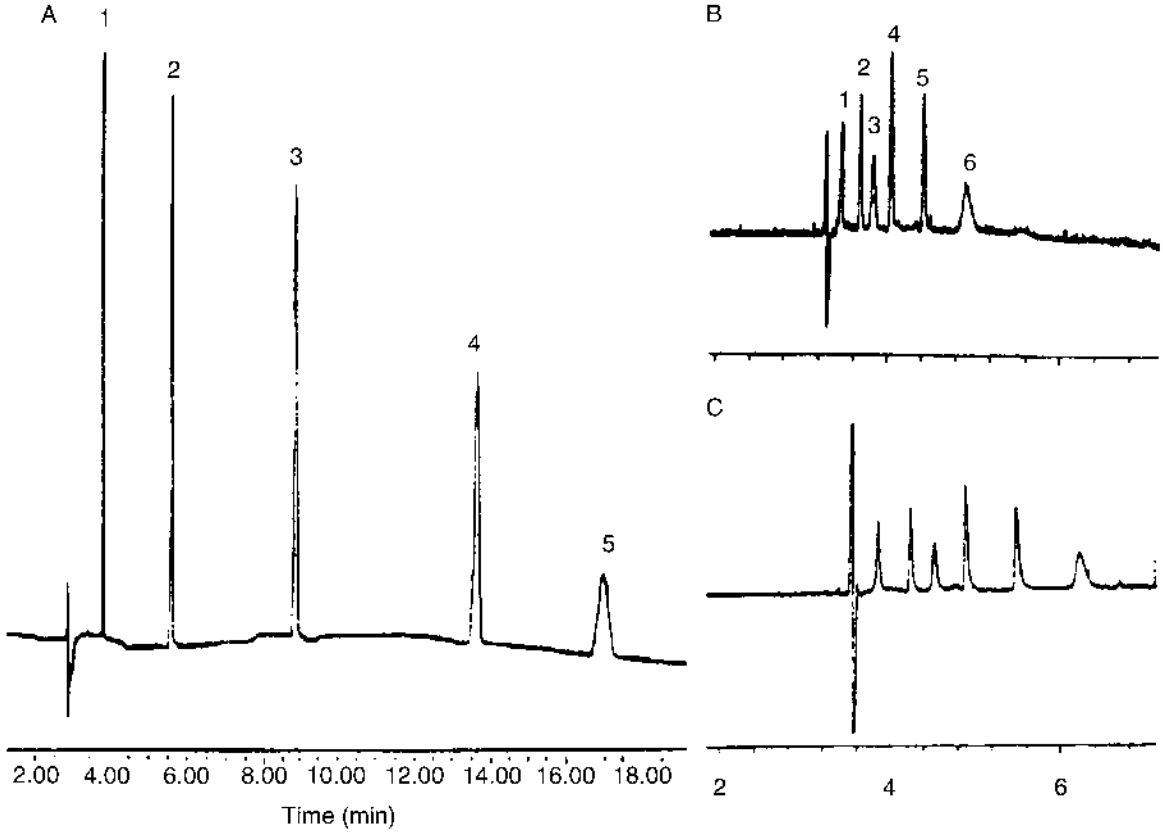

© 2003 by Marcel Dekker, Inc.

ionic detergent and isopropylmyristate in an aqueous phase supplemented with an alcohol. The electrophoretic mobilities of drugs in the aqueous phase alone and in the microemulsion were determined in fused-silica capillaries. Poole et al. (103) showed that EKC in a microemulsion containing sodium dodecylsulfate, butanol, and heptane afforded good estimates of the octanol/water partition coefficients present in the literature for a number of neutral and positively charged (weakly basic) compounds over a wide range of log P_{oct} values.

IV. DISCUSSION

Few studies of drug–liposome interaction analysis by the use of CE or capillary EKC techniques have been reported. Technical problems may be responsible. For example, the liposomes must be essentially free from organic solvents or detergents and the (in)stability (1) of the prepared liposomes suspensions must be considered. Furthermore, the application of rather large amounts of drugs in relation to the liposome content of the capillary for absorbance detection may affect the properties of the bilayer structure. More sensitive detection methods (55) are perhaps required in some cases. These problems do not arise when liposomes entrapped in gel beads are used for chromatographic analyses. Impurities in the bilayers can be washed away, and the drug amounts required for absorbance detection are small in relation to the lipid amounts in such ILC columns, except perhaps for the most hydrophobic drugs. Furthermore, the ILC method has been well characterized and validated, which is not yet the case for the ACE method. Liposomes entrapped in gel bead microcavities have shown only slowly decreasing drug retention over several months (27), whereas the liposomes may have to be freshly prepared for each series of electrophoretic analysis due to the instability of liposomes in suspension. The ILC technique

Fig. 8 Capillary EKC separations of (A) acetophenone (1), propiophenone (2), butyrophenone (3), valerophenone (4), and hexanophenone (5) on vesicles composed of sodium dodecylsulfate and *n*-dodecyltrimethylammoniumbromide at pH 7.2, (B,C) of 1-dehydroaldosterone (1), cortisone (2), cortisol (3), 21-deoxycortisol (4), 11-deoxycortisol (5), and dexamethasone (6) on liposomes composed of 1-palmitoyl-2-oleoyl-*sn*-glycero-3-phosphocholine (80%) and (B) phosphatidylserine or (C) cardiolipin at pH 9, lipid concentrations (B) 2.4 mM and 0.6 mM, (C) 3.6 and 0.9 mM. (Part A is reprinted with permission from Ref. 59, copyright 1998 American Chemical Society; Parts B and C are reprinted with permission from Ref. 33, copyright 2000 Wiley-VCH Verlag, all with slight modifications.)

© 2003 by Marcel Dekker, Inc.

is independent of the electric charge of the drug, whereas the electrophoretic procedure requires the drug to migrate in the electric field at a higher rate than do the liposomes. However, the ACE and EKC methods offer the great advantages that very small amounts of lipids and drugs are required and that the high resolution allows analysis of several substances in each run.

Because most experimental procedures are time-consuming and require drug molecules to be available, computational prediction of the permeability, partitioning, and solubility of a drug enjoys increasing use, e.g., as a screen in synthetic endeavors (104,105). The drug behavior is estimated on the basis of drug descriptors such as hydrogen bonding, lipophilicity, and molecular weight (106,107). This allows statistical comparison between structural features of drug molecules and drug behavior in the body. Exact physicochemical calculations of the rate of drug diffusion across membranes are not yet possible. For some years to come, empirical data will still be required, both in drug design practice and to refine or develop the computer programs used. Partitioning into liposomes provides more detailed information on the potential interaction between individual drug candidates and biological membranes than do calculated or determined P_{oct} values. For accurate prediction of drug behavior, the structural features of the biological membrane must be considered, which exceeds the capability of the currently used computer programs. Other available screening methods, e.g., surface plasmon resonance analysis, can be fast but have the disadvantage that natural membrane structures are difficult to mimic. In contrast, the slower chromatographic and electrophoretic procedures offer the possibility to use realistic membrane compositions or even natural membranes. The different analysis methods should therefore be used in combination to obtain complementary data.

V. CONCLUSIONS AND OUTLOOK

The types of drug solutes studied and the numbers of solutes of each type are limited in the available ACE and capillary EKC studies of solute–phospholipid bilayer interactions (32–34,50). Obviously, more such data are required for safe comparisons, e.g., with ILC or octanol/water partitioning data or surface plasmon resonance results. Pure and well-characterized liposome suspensions may help to allow collection of such data in the near future. The ACE and capillary EKC methods seem adequate for analyses of drug partitioning into biological membranes or membrane models, studies of specific membrane protein–drug interactions, and determinations of the modulation of drug partitioning into membranes by membrane proteins or various lipid phases. The fact that only small amounts of membrane proteins and lipids would be required seems particularly advantageous.

© 2003 by Marcel Dekker, Inc.

ABBREVIATIONS

ACE	affinity capillary electrophoresis
EKC	electrokinetic chromatography
ILC	immobilized-liposome chromatography

REFERENCES

1. DD Lasic. Liposomes: From Physics to Applications. Amsterdam: Elsevier Science, 1993.
2. DD Lasic. Novel applications of liposomes. Trends Biotechnol 16:307–321, 1998.
3. TM Allen. Liposomal drug formulations: rationale for development and what we can expect for the future. Drugs 56:747–756, 1998.
4. E Forssen, M Willis. Ligand-targeted liposomes. Adv Drug Deliv Rev 29: 249–271, 1998.
5. VP Torchilin. Drug targeting. Eur J Pharm Sci 11:S81–S91, 2000.
6. D Chen, DL Cole, GS Srivatsa. Determination of free and encapsulated oligonucleotides in liposome formulated drug product. J Pharm Biomed Anal 22:791–801, 2000.
7. C Lagerquist, F Beigi, A Karlén, H Lennernäs, P Lundahl. Effects of cholesterol and model transmembrane proteins on drug partitioning into lipid bilayers as analyzed by immobilized-liposome chromatography. J Pharm Pharmacol 53:1477–1487, 2001.
8. K Palm, K Luthman, A-L Ungell, G Strandlund, F Beigi, P Lundahl, P Artursson. Evaluation of dynamic polar molecular surface area as predictor of drug absorption: comparison with other computational and experimental predictors. J Med Chem 41:5382–5392, 1998.
9. CA Lipinski. Drug-like properties and the causes of poor solubility and poor permeability. J Pharmacol Toxicol Methods 44:235–249, 2000.
10. OG Mouritsen, K Jørgensen. A new look at lipid-membrane structure in relation to drug research. Pharm Res 15:1507–1519, 1998.
11. G Lehne. P-glycoprotein as a drug target in the treatment of multidrug resistant cancer. Curr Drug Targets 1:85–99, 2000.
12. O van Tellingen. The importance of drug-transporting P-glycoproteins in toxicology. Toxicol Lett 120:31–41, 2001.
13. P Lundahl, A Lundqvist, E Greijer, eds. Quantitative Analysis of Biospecific Interactions. Amsterdam: Harwood Academic, 1998.
14. A Lundqvist, E Brekkan, L Haneskog, Q Yang, J Miyake, P Lundahl. Determination of transmembrane protein affinities for solutes by frontal chromatography. In: P Lundahl, A Lundqvist, E Greijer, eds. Quantitative Analysis of Biospecific Interactions. Amsterdam: Harwood Academic, 1998, pp 79–93.
15. A Lundqvist, P Lundahl. Advantages of quantitative affinity chromatography

© 2003 by Marcel Dekker, Inc.

for the analysis of solute interaction with membrane proteins. J Biochem Biophys Methods 49:507–521, 2001.
16. I Gottschalk, C Lagerquist, S-S Zuo, A Lundqvist, P Lundahl. Immobilized-biomembrane affinity chromatography for binding studies of membrane proteins. J Chromatogr B 768:31–40, 2002.
17. Y Zhang, F Leonessa, R Clarke, IW Wainer. Development of an immobilized P-glycoprotein stationary phase for on-line liquid chromatographic determination of drug-binding affinities. J Chromatogr B 739:33–37, 2000.
18. DS Hage, SA Tweed. Recent advances in chromatographic and electrophoretic methods for the study of drug–protein interactions. J Chromatogr B 699:499–525, 1997.
19. A Shibukawa. Development of high-performance frontal analysis and application to drug–plasma protein binding study. Yakugaku Zasshi 118:554–565, 1998 (in Japanese).
20. A Shibukawa, Y Kuroda, T Nakagawa. High-performance frontal analysis for drug–protein binding study. J Pharm Biomed Anal 18:1047–1055, 1999.
21. F Beigi, Q Yang, P Lundahl. Immobilized-liposome chromatographic analysis of drug partitioning into lipid bilayers. J Chromatogr A 704:315–321, 1995.
22. E Brekkan, L Lu, P Lundahl. Properties of immobilized-liposome–chromatographic supports for interaction analysis. J Chromatogr A 711:33–42, 1995.
23. Y Zhang, C-M Zeng, Y-M Li, S Hjertén, P Lundahl. Immobilized liposome chromatography of drugs on capillary continuous beds for model analysis of drug–membrane interactions. J Chromatogr A 749:13–18, 1996.
24. F Pattarino, M Trotta, S Morel, MR Gasco. Liposomes sterically immobilized in agarose gel beads as stationary phase for column chromatography of drugs. S.T.P. Pharma Sciences 7:199–204, 1997.
25. F Beigi, I Gottschalk, C Lagerquist Hägglund, L Haneskog, E Brekkan, Y Zhang, T Österberg, P Lundahl. Immobilized liposome and biomembrane partitioning chromatography of drugs for prediction of drug transport. Int J Pharm 164:129–137, 1998.
26. F Beigi, P Lundahl. Immobilized biomembrane chromatography of highly lipophilic drugs. J Chromatogr A 852:313–317, 1999.
27. T Österberg, M Svensson, P Lundahl. Chromatographic retention of drug molecules on immobilised liposomes prepared from egg phospholipids and from chemically pure phospholipids. Eur J Pharm Sci 12:427–439, 2001.
28. X-Y Liu, Q Yang, N Kamo, J Miyake. Effect of liposome type and membrane fluidity on drug–membrane partitioning analyzed by immobilized liposome chromatography. J Chromatogr A 913:123–131, 2001.
29. A Avdeef, KJ Box, JEA Comer, C Hibbert, KY Tam. pH-Metric log P 10. Determination of liposomal membrane–water partition coefficients of ionizable drugs. Pharm Res 15:209–215, 1998.
30. K Balon, BU Riebesehl, BW Müller. Drug liposome partitioning as a tool for the prediction of human passive intestinal absorption. Pharm Res 16:882–888, 1999.
31. K Balon, BU Riebesehl, BW Müller. Determination of liposome partitioning of ionizable drugs by titration. J Pharm Sci 88:802–806, 1999.

© 2003 by Marcel Dekker, Inc.

32. Y Zhang, R Zhang, S Hjertén, P Lundahl. Liposome capillary electrophoresis for analysis of interactions between lipid bilayers and solutes. Electrophoresis 16:1519–1523, 1995.
33. SK Wiedmer, JM Holopainen, P Mustakangas, PKJ Kinnunen, M-L Riekkola. Liposomes as carriers in electrokinetic capillary chromatography. Electrophoresis 21:3191–3198, 2000.
34. SK Wiedmer, J Hautala, JM Holopainen, PKJ Kinnunen, M-L Riekkola. Study on liposomes by capillary electrophoresis. Electrophoresis 22:1305–1313, 2001.
35. JJ Ramsden. Partition coefficients of drugs in bilayer lipid membranes. Experientia 49:688–692, 1993.
36. E Danelian, A Karlén, R Karlsson, S Winiwarter, A Hansson, S Löfås, H Lennernäs, MD Hämäläinen. SPR biosensor studies of the direct interaction between 27 drugs and a liposome surface: correlation with fraction absorbed in humans. J Med Chem 43:2083–2086, 2000.
37. AA Omran, K Kitamura, S Takegami, A-AY El-Sayed, M Abdel-Mottaleb. Determination of partition coefficients of diazepam and flurazepam between phosphatidylcholine bilayer vesicles and water by second derivative spectrophotometric method. J Pharm Biomed Anal 25:319–324, 2001.
38. Y Zhang, S Aimoto, L Lu, Q Yang, P Lundahl. Immobilized liposome chromatography for analysis of interactions between lipid bilayers and peptides. Anal Biochem 229:291–298, 1995.
39. L Hjorth Alifrangis, IT Christensen, A Berglund, M Sandberg, L Hovgaard, S Frokjaer. Structure–property model for membrane partitioning of oligopeptides. J Med Chem 43:103–113, 2000.
40. P Lundahl, F Beigi. Immobilized liposome chromatography of drugs for model analysis of drug–membrane interactions. Adv Drug Deliv Rev 23:221–227, 1997.
41. NHH Heegaard. Electrophoretic analysis of reversible interactions. In: P Lundahl, A Lundqvist, E Greijer, eds. Quantitative Analysis of Biospecific Interactions. Amsterdam: Harwood Academic, 1998, pp 1–13.
42. NHH Heegaard, RT Kennedy. Identification, quantitation, and characterization of biomolecules by capillary electrophoretic analysis of binding interactions. Electrophoresis 20:3122–3133, 1999.
43. RHH Neubert, MA Schwarz, Y Mrestani, M Plätzer, K Raith. Affinity capillary electrophoresis in pharmaceutics. Pharm Res 16:1663–1673, 1999.
44. RM Guijt-van Duijn, J Frank, GWK van Dedem, E Baltussen. Recent advances in affinity capillary electrophoresis. Electrophoresis 21:3905–3918, 2000.
45. RHH Neubert, Y Mrestani, M Schwarz, B Colin. Application of micellar electrokinetic chromatography for analyzing antiviral drugs in pharmaceutical semisolid formulations. J Pharm Biomed Anal 16:893–897, 1998.
46. CM Boone, JCM Waterval, H Lingeman, K Ensing, WJM Underberg. Capillary electrophoresis as a versatile tool for the bioanalysis of drugs—a review. J Pharm Biomed Anal 20:831–863, 1999.

© 2003 by Marcel Dekker, Inc.

47. H Nishi. Capillary electrophoresis of drugs: current status in the analysis of pharmaceuticals. Electrophoresis 20:3237–3258, 1999.
48. A Wang, Y Fang. Applications of capillary electrophoresis with electrochemical detection in pharmaceutical and biomedical analyses. Electrophoresis 21: 1281–1290, 2000.
49. Y Mrestani, RHH Neubert. Non-ionic micellar affinity capillary electrophoresis for analysis of interactions between micelles and drugs. J Pharm Biomed Anal 24:637–643, 2001.
50. MA Roberts, L Locascio-Brown, WA MacCrehan, RA Durst. Liposome behavior in capillary electrophoresis. Anal Chem 68:3434–3440, 1996.
51. K Kawakami, Y Nishihara, K Hirano. Compositional homogeneity of liposomal membranes investigated by capillary electrophoresis. J Coll Interface Sci 206:177–180, 1998.
52. SP Radko, A Chrambach. Capillary electrophoresis of subcellular-sized particles. J Chromatogr B 722:1–10, 1999.
53. SP Radko, M Stastna, A Chrambach. Size-dependent electrophoretic migration and separation of liposomes by capillary zone electrophoresis in electrolyte solutions of various ionic strengths. Anal Chem 72:5955–5960, 2000.
54. G Hempel. Strategies to improve the sensitivity in capillary electrophoresis for the analysis of drugs in biological fluids. Electrophoresis 21:691–698, 2000.
55. K Swinney, DJ Bornhop. Detection in capillary electrophoresis. Electrophoresis 21:1239–1250, 2000.
56. CF Duffy, S Gafoor, DP Richards, H Admadzadeh, R O'Kennedy, EA Arriaga. Determination of properties of individual liposomes by capillary electrophoresis with postcolumn laser-induced fluorescence detection. Anal Chem 73: 1855–1861, 2001.
57. G Rippel, H Corstjens, HAH Billiet, J Frank. Affinity capillary electrophoresis. Electrophoresis 18:2175–2183, 1997.
58. Y-H Chu, CC Cheng. Affinity capillary electrophoresis in biomolecular recognition. Cell Mol Life Sci 54:663–683, 1998.
59. M Hong, BS Weekley, SJ Grieb, JP Foley. Electrokinetic chromatography using thermodynamically stable vesicles and mixed micelles formed from oppositely charged surfactants. Anal Chem 70:1394–1403, 1998.
60. JL Razak, BJ Cutak, CK Larive, CE Lunte. Correlation of the capacity factor in vesicular electrokinetic chromatography with the octanol:water partition coefficient for charged and neutral analytes. Pharm Res 18:104–111, 2001.
61. D Lichtenberg, Y Barenholz. Liposomes: preparation, characterization, and preservation. Methods Biochem Anal 33:337–462, 1988.
62. MJ Hope, R Nayar, LD Mayer, PR Cullis. Reduction of liposome size and preparation of unilamellar vesicles by extrusion techniques. In: G Gregoriadis, ed. Liposome Technology. 2nd ed. Vol. I. Liposome Preparation and Related Techniques. Boca Raton, FL: CRC Press, 1993, pp 123–139.
63. HG Enoch, P Strittmatter. Formation and properties of 1000-Å-diameter, single-bilayer phospholipid vesicles. Proc Natl Acad Sci USA 76:145–149, 1979.
64. U Pick. Liposomes with a large trapping capacity prepared by freezing and

© 2003 by Marcel Dekker, Inc.

thawing of sonicated phospholipid mixtures. Arch Biochem Biophys 212: 186–194, 1981.
65. C Pidgeon. Preparation of MLV by the REV method: vesicle structure and optimum solute entrapment. In: G Gregoriadis, ed. Liposome Technology. 2nd ed. Vol. I. Liposome Preparation and Related Techniques. Boca Raton, FL: CRC Press, 1993, pp 99–110.
66. J-L Rigaud, D Levy, G Mosser, O Lambert. Detergent removal by non-polar polystyrene beads. Applications to membrane protein reconstitution and two-dimensional crystallization. Eur Biophys J 27:305–319, 1998.
67. E Racker. Reconstitution of membrane processes. Methods Enzymol 55:699–711, 1979.
68. RD Klausner, J van Renswoude, B Rivnay. Reconstitution of membrane proteins. Methods Enzymol 104:340–347, 1984.
69. J-L Rigaud, B Pitard, D Levy. Reconstitution of membrane proteins into liposomes: application to energy-transducing membrane proteins. Biochim Biophys Acta 1231:223–246, 1995.
70. J Knol, K Sjollema, B Poolman. Detergent-mediated reconstitution of membrane proteins. Biochemistry 37:16410–16415, 1998.
71. W Kühlbrandt. Two-dimensional crystallization of membrane proteins. Q Rev Biophys 25:1–49, 1992.
72. J-L Rigaud, M Chami, O Lambert, D Levy, J-L Ranck. Use of detergents in two-dimensional crystallization of membrane proteins. Biochim Biophys Acta 1508:112–128, 2000.
73. GR Bartlett. Phosphorus assay in column chromatography. J Biol Chem 234: 466–468, 1959.
74. S-S Zuo, P Lundahl. A micro-Bradford membrane protein assay. Anal Biochem 284:162–164, 2000.
75. IJ Cartwright. Separation and analysis of phospholipids by thin layer chromatography. In: JM Graham, JA Higgins, eds. Methods in Molecular Biology. Vol. 19: Biomembrane Protocols: I. Isolation and Analysis. Totowa, NJ: Humana Press, 1993, pp 153–167.
76. P Lundahl, C-M Zeng, C Lagerquist Hägglund, I Gottschalk, E Greijer. Chromatographic approaches to liposomes, proteoliposomes and biomembrane vesicles. J Chromatogr B 722:103–120, 1999.
77. M Almgren, K Edwards, J Gustafsson. Cryotransmission electron microscopy of thin vitrified samples. Curr Opin Colloid Interface Sci 1:270–278, 1996.
78. P Lundahl, Q Yang. Liposome chromatography: a new mode of separation using lipid bilayer. Protein Nucleic acid Enzyme (Tokyo) 35: 1983–1998, 1990 (in Japanese).
79. P Lundahl, Q Yang. Liposome chromatography: liposomes immobilized in gel beads as a stationary phase for aqueous column chromatography. J Chromatogr 544:283–304, 1991.
80. M Wallstén, Q Yang, P Lundahl. Entrapment of lipid vesicles and membrane protein-lipid vesicles in gel bead pores. Biochim Biophys Acta 982:47–52, 1989.

© 2003 by Marcel Dekker, Inc.

81. Q Yang, M Wallstén, P Lundahl. Lipid-vesicle-surface chromatography. J Chromatogr 506:379–389, 1990.
82. Q Yang, P Lundahl. Binding of lysozyme on the surface of entrapped phosphatidylserine–phosphatidylcholine vesicles and an example of high-performance lipid vesicle surface chromatography. J Chromatogr 512:377–386, 1990.
83. Q Yang, X-Y Liu, M Hara, P Lundahl, J Miyake. Quantitative affinity chromatographic studies of mitochondrial cytochrome *c* binding to bacterial photosynthetic reaction center, reconstituted in liposome membranes and immobilized by detergent dialysis and avidin–biotin binding. Anal Chem 280:94–102, 2000.
84. P Lundahl, Q Yang, E Greijer, M Sandberg. Immobilization of liposomes in gel beads. In: Gregoriadis, G. ed. Liposome Technology. 2nd ed. Vol. I. Liposome Preparation and Related Techniques. Boca Raton, FL: CRC Press, 1993, pp 343–361.
85. Q Yang, P Lundahl. Steric immobilization of liposomes in chromatographic gel beads and incorporation of integral membrane proteins into their lipid bilayers. Anal Biochem 218:210–221, 1994.
86. E Brekkan, Q Yang, G Viel, P Lundahl. Immobilization of liposomes and proteoliposomes in gel beads. In: GF Bickerstaff, ed. Methods in Biotechnology. Vol. 1: Immobilization of Enzymes and Cells, Totowa, NJ: Humana Press Inc, 1997, pp. 193–206.
87. A Lundqvist, G Ocklind, L Haneskog, P Lundahl. Freeze–thaw immobilization of liposomes in chromatographic gel beads: evaluation by confocal microscopy and effects of freezing rate. J Mol Recogn 11:52–57, 1998.
88. M Sandberg, P Lundahl, E Greijer, M Belew. Immobilization of phospholipid vesicles on alkyl derivatives of agarose gel beads. Biochim Biophys Acta 924:185–192, 1987.
89. Q Yang, M Wallstén, P Lundahl. Immobilization of phospholipid vesicles and protein-lipid vesicles containing red cell membrane proteins on octyl derivatives of large-pore gels. Biochim Biophys Acta 938:243–256, 1988.
90. L Lu, E Brekkan, L Haneskog, Q Yang, P Lundahl. Effects of pH on the activity of the human red cell glucose transporter Glut1: transport retention chromatography of D-glucose and L-glucose on immobilized Glut1 liposomes. Biochim Biophys Acta 1150:135–146, 1993.
91. Q Yang, X-Y Liu, S-i Ajiki, M Hara, P Lundahl, J Miyake. Avidin–biotin immobilization of unilamellar liposomes in gel beads for chromatographic analysis of drug–membrane partitioning. J Chromatogr B 707:131–141, 1998.
92. X-Y Liu, Q Yang, C Nakamura, J Miyake. Avidin–biotin-immobilized liposome column for chromatographic fluorescence on-line analysis of solute–membrane interactions. J Chromatogr B 750:51–60, 2001.
93. Q Yang, X-Y Liu, K Umetani, N Kamo, J Miyake. Partitioning of triphenylalkylphosphonium homologues in gel bead-immobilized liposomes: chromatographic measurement of their membrane partition coefficients. Biochim Biophys Acta 1417:122–130, 1999.
94. Q Yang, X-Y Liu, M Yoshimoto, R Kuboi, J Miyake. Covalent immobilization

© 2003 by Marcel Dekker, Inc.

of unilamellar liposomes in gel beads for chromatography. Anal Biochem 268: 354–362, 1999.
95. MA Schwarz, K Raith, G Dongowski, RHH Neubert. Effect on the partition equilibrium of various drugs by the formation of mixed bile salt/phosphatidylcholine/fatty acid micelles. A characterization by micellar affinity capillary electrophoresis. Part IV. J Chromatogr A 809:219–229, 1998.
96. S Terabe, K Otsuka, K Ichikawa, A Tsuchiya, T Ando. Electrokinetic separations with micellar solutions and open-tubular capillaries. Anal Chem 56: 111–113, 1984.
97. Y Ishihama, Y Oda, K Uchikawa, N Asakawa. Correlation of octanol–water partition coefficients with capacity factors measured by micellar electrokinetic chromatography. Chem Pharm Bull 42:1525–1527, 1994.
98. JT Smith, DV Vinjamoori. Rapid determination of logarithmic partition coefficients between *n*-octanol and water using micellar electrokinetic capillary chromatography. J Chromatogr B 669:59–66, 1995.
99. MD Trone, MS Leonard, MG Khaledi. Congeneric behavior in estimations of octanol–water partition coefficients by micellar electrokinetic chromatography. Anal Chem 72:1228–1235, 2000.
100. JA Masucci, GW Caldwell, JP Foley. Comparison of the retention behavior of β-blockers using immobilized artificial membrane chromatography and lysophospholipid micellar electrokinetic chromatography. J Chromatogr A 810: 95–103, 1998.
101. M Molero-Monfort, Y Martín-Biosca, S Sagrado, RM Villanueva-Camañas, MJ Medina-Hernández. Micellar liquid chromatography for prediction of drug transport. J Chromatogr A 870:1–11, 2000.
102. Y Mrestani, RHH Neubert, A Krause. Partition behaviour of drugs in microemulsions measured by electrokinetic chromatography. Pharm Res 15:799–801, 1998.
103. SK Poole, D Durham, C Kibbey. Rapid method for estimating the octanol–water partition coefficient (log P_{ow}) by microemulsion electrokinetic chromatography. J Chromatogr B 745:117–126, 2000.
104. S Winiwarter, NM Bonham, F Ax, A Hallberg, H Lennernäs, A Karlén. Correlation of human jejunal permeability (in vivo) of drugs with experimentally and theoretically derived parameters. A multivariate data analysis approach. J Med Chem 41:4939–4949, 1998.
105. JF Blake. Chemoinformatics—predicting the physicochemical properties of ''drug-like'' molecules. Curr Opin Biotechnol 11:104–107, 2000.
106. CA Lipinski, F Lombardo, BW Dominy, PJ Feeney. Experimental and computational approaches to estimate solubility and permeability in drug discovery and development settings. Adv Drug Deliv Rev 46:3–26, 2001.
107. U Norinder, T Österberg. Theoretical calculation and prediction of drug transport processes using simple parameters and partial least squares projections to latent structures (PLS) statistics. The use of electrotopological state indices. J Pharm Sci 90:1076–1085, 2001.

© 2003 by Marcel Dekker, Inc.

8

Interactions Between Chiral Drugs and Cyclodextrins

Gottfried Blaschke
University of Münster, Münster, Germany

Bezhan Chankvetadze*
Tbilisi State University, Tbilisi, Georgia

I. INTRODUCTION

The first example of enantioselective interaction between a chiral guest molecule and cyclodextrin (CD) was described 50 years ago (1). Today it is hard to imagine separation science without the methods based on the enantioselective affinity interactions between chiral analytes and cyclodextrins. Enantioseparations by gas chromatography (GC), high-performance liquid chromatography (HPLC), supercritical fluid chromatography (SFC), capillary electrophoresis (CE), and capillary electrochromatography (CEC) are based largely on these interactions. In addition, enantioselective drug–cyclodextrin interactions are used in various spectrometric (UV, NMR, MS, etc.) and electrochemical techniques, and they may also be applied in pharmaceutical formulations for achieving an enantioselective transport, release, etc. of chiral drugs.

Cyclodextrins have significantly contributed to the development of enantioseparations in CE, where they represent the most widely used chiral selectors. On the other hand, due to its inherently high separation efficiency and diverse technical advantages, CE has contributed enormously to the better understanding of affinity interactions between CDs and chiral analytes. The following text summarizes the recent developments in this field (3–60).

**Current affiliation*: University of Münster, Münster, Germany

© 2003 by Marcel Dekker, Inc.

II. METHODS AND THEORY

A. Advantages of Capillary Electrophoresis for Investigation of Interactions Between Chiral Drugs and Cyclodextrins

1. High Separation Efficiency

Capillary electrophoresis offers a set of important advantages that make it a premier technique for the investigation of enantioselective effects in the affinity interactions between chiral drugs and cyclodextrins. The most important advantage of CE is the inherently high separation efficiency offered by this technique. As already known, the most important contributors to peak resolution (R) are a separation selectivity (α) and an efficiency (N). A relationship between these parameters in CE is described by the following equation (2):

$$R_S = \frac{\sqrt{N}}{4} \frac{\Delta\mu}{\mu_{av}} \tag{1}$$

where R_S is the resolution, N is the peak efficiency, and $\Delta\mu/\mu_{av}$ is the mobility difference between two components ($\Delta\mu$) divided by the arithmetic mean of their mobilities (μ_{av}). This parameter ($\Delta\mu/\mu_{av}$) in CE adequately describes the selectivity of separation (α). In chromatographic techniques, a selectivity of separation is defined by the ratio of the capacity factors $\bar{\bar{k}}_2'/\bar{\bar{k}}_1'$. The capacity factors are determined by the affinity constants of the analytes toward the chiral selector and the so-called phase ratio. At a constant phase ratio, the capacity factors are determined by the binding constants between the selector and the selectand and therefore closely relate to the thermodynamic characteristics of selector and selectand. Thermodynamic quantities do not easily undergo external influence. Therefore, with most separation techniques, except CE, it is difficult to improve separation selectivity and the main issue is to improve the resolution for a given thermodynamic selectivity of recognition. Due to its unique separation principle, CE offers inherently higher peak efficiency in the range of 200,000–1,000,000 per meter, which is difficult to achieve by other separation techniques, such as gas chromatography and simply unimaginable in high-performance liquid chromatography. Thus, in order to observe a baseline enantioseparation in HPLC with a well-packed (chiral) column, a separation selectivity α in the range of 1.15–1.20 is required. This number must be in the range 1.05–1.10 in GC, whereas 1.01–1.02 is sufficient in CE. Thus, due to its inherently high peak efficiency, CE may allow one to observe those enantioselective effects in chiral drug–CD interactions that are impossible to observe by other separation techniques, such as GC and HPLC (3).

© 2003 by Marcel Dekker, Inc.

2. High Separation Selectivity

Equation (1) shows another important advantage of CE. As already mentioned, the separation selectivity in chromatographic techniques very closely relates to the thermodynamic selectivity of recognition (α_r), in that the thermodynamic selectivity of recognition, which is the ratio of the binding constants, is the upper limit of separation selectivity. In contrast, the separation selectivity (α_s) in CE may be expressed by the equation

$$\alpha_s = \frac{\Delta\mu}{\mu_{\text{av}}} \tag{2}$$

The most important point to be noted is that α_s is not limited by the ratio K_2/K_1 and can reach infinitily high values in CE (3,4). Although Eq. (2) does not explicitly contain the binding constants of enantiomers with chiral selector, $\Delta\mu$ and μ_{av} are dependent on these thermodynamic quantities. Capillary electrophoresis offers several possibilities for almost unlimited enhancement of separation selectivity without any significant change of thermodynamic selectivity or recognition (3–5).

3. Chiral Analyte and Selector in Free Solution

One additional advantage of chiral CE over chromatographic techniques is that both the chiral selector and the analyte reside in a free solution in this technique. This makes the investigation of chiral drug–cyclodextrin interactions technically much easier, cheaper, and faster, because unlike chromatographic techniques there is no need to immobilize the receptor (selectors). However, an even more important advantage is that there is no effect of immobilization on the degree of freedom of the selector and the effects of a solid matrix are absent.

4. Miscellaneous Technical Advantages of Capillary Electrophoresis

Capillary electrophoresis is a microseparation technique and requires minute amounts of the chiral drugs and selectors under investigation. This makes the technique cost effective and allows one to investigate exotic chiral selectors and drugs. In the case of chromatographic techniques, the chemistry of immobilization determines the amount of a chiral selector fixed on the solid support (some preliminary functionalization of both support and selector might become necessary in order to facilitate this process). The variation in the amount of free chiral selector is much less in CE than that of immobilized selector in chromatographic techniques. Chiral selectors may also be used in large excess if required in CE.

One major advantage of CE in studies of intermolecular interactions,

© 2003 by Marcel Dekker, Inc.

compared to other, nonseparation techniques, is that this technique allows one to investigate the interaction between multiple guests and a single host, a single guest and multiple host, or even a combination of both. It must be noted that a deconvolution of these arrays of interactions is not an easy task, but it still seems possible and very promising, especially with the recent impressive developments in the fields of combinatorial chemistry, high-throughput screening, and proteomic research.

Capillary electrophoresis saves time not only because of the absence of receptor immobilization, but also because changing and equilibrating a new column is undesirable and time consuming in HPLC. A change of the chiral selector is very fast and easy in CE.

B. Capillary Electrophoresis Methods for Determination of Enantioselective Binding Constants Between Chiral Drugs and Cyclodextrins

1. Affinity Capillary Electrophoresis (ACE)

The equation for the description of equilibrium in zone electrophoresis was first introduced by Tiselius (6). For interactions that produce 1:1 stoichiometry:

$$A + L \leftrightarrow A \cdot L \tag{3}$$

the binding constants can be determined as follows:

$$K[L] = \frac{\mu_f - \mu_i}{\mu_i - \mu_c} \tag{4}$$

where K is the binding constant, [L] is the equilibrium concentration of uncomplexed ligand, μ_f and μ_c are the electrophoretic mobilities of the free and complexed solutes, respectively, and μ_i is the solute mobility at the ligand concentration [L]. The procedure for determining the enantioselective binding constants according Eq. (3) requires the determination of solute mobilities at varying ligand (cyclodextrin) concentrations (μ_i), measuring the limiting mobility of the solute at saturating ligand concentration (μ_c), and plotting $\mu_i - \mu_c$ as a function of free ligand concentration [L]. The method for calculating binding constants based on Eq. (4) was named the mobility ratio method (7).

This technique is not always very convenient for investigation of enantioselective binding constants between chiral drugs and cyclodextrins. Thus, for example, the electrophoretic mobility of the drug–ligand complex (i.e., the mobility at saturating concentration of cyclodextrin, μ_c) needs to be determined. This can be approached at a very high concentration of cyclodextrin (especially when the binding constants are low), which may be

© 2003 by Marcel Dekker, Inc.

higher than the solubility limit of CD. An increase in (chiral) ligand concentration leads to some changes in electrophoretic mobility (due to changes in buffer viscosity, electroosmotic flow (EOF), etc.) that are not related to the drug–ligand binding. This can be a source of systematic error in this technique. Additionally, the graph should be forced through the origin. Thus, the concentration range that should be covered includes the approximation from zero to infinity, which can introduce a substantial error in graphical calculations. In addition, some cyclodextrins cannot easily be dissolved in high concentrations approaching a saturation of binding. This will be significant problem when the binding constants are low.

Various forms of binding isotherms are summarized in Refs. 7–10 and 17 and in Part I of this book.

Equation (4) can be rewritten in the form

$$\mu_i = \frac{\mu_f + \mu_c K[\mathrm{L}]}{1 + \mu_c K[\mathrm{L}]} \tag{5}$$

The equilibrium constants for the interactions described by Eq. (3) can be calculated as follows:

$$K = \frac{[\mathrm{A}\cdot\mathrm{L}]_e}{[\mathrm{A}]_e[\mathrm{L}]_e} \tag{6}$$

or for R- and S-enantiomers, respectively:

$$K_R = \frac{[\mathrm{R}\cdot\mathrm{L}]_e}{[\mathrm{R}]_e[\mathrm{L}]_e}$$

$$K_S = \frac{[\mathrm{S}\cdot\mathrm{L}]_e}{[\mathrm{S}]_e[\mathrm{L}]_e} \tag{7}$$

If one assumes that the initial concentration of a solute and ligand are $[\mathrm{A}]_i$ and $[\mathrm{L}]_i$, respectively, and the degree of complexation is χ, then the equilibrium concentration of the solute ($[\mathrm{A}]_e$), ligand ($[\mathrm{L}]_e$), and solute/ligand complex ($[\mathrm{A}\cdot\mathrm{L}]_e$) can be calculated as follows:

$$[\mathrm{A}]_e = [\mathrm{A}]_i(1 - \chi) \tag{8}$$

$$[\mathrm{L}]_e = [\mathrm{L}]_i - \chi[\mathrm{A}]_i \tag{9}$$

$$[\mathrm{A}\cdot\mathrm{L}]_e = \chi[\mathrm{A}]_i \tag{10}$$

The combination of Eqs. (7) and (8)–(10) yields

$$K_e = \frac{\chi[\mathrm{A}]}{(1 - \chi)[\mathrm{A}]_i([\mathrm{L}]_i - \chi[\mathrm{A}]_i)} \tag{11}$$

Taking into account that in real CE separations the initial concentration of

© 2003 by Marcel Dekker, Inc.

the chiral selector is much higher than that of the analyte, i.e., $[L]_i \gg [A]_i$, Eq. (11) can be rewritten as follows:

$$K_e = \frac{\chi}{(1 - \chi)[L]_i} \tag{12}$$

which can be further rewritten as

$$\chi = \frac{K_R[L]_i}{1 + K_R[L]_i} \tag{13}$$

The combination of Eqs. (18) and (10) gives

$$\mu_e^{\text{eff}} = \frac{(\mu_e^{\text{free}} + \mu_e^{\text{complex}} K_e[L])}{1 + K_e[L]} \tag{14}$$

Similar equations can be written for both enantiomers of chiral analyte. Based on Eq. (14), nonlinear regression techniques allow one to determine the enantioselective binding constants (K_R and K_S) and the mobilities of related transient diastereomeric complexes (μ_R^{complex} and μ_S^{complex}).

It must be noted that the aforementioned calculation techniques as well as those summarized in Part I are not always ideally suited for the determination of the binding constants, and these techniques need to be used with some care. At first, the experimental data must be refined so that only the effect of a binding with a chiral selector on the mobility of analyte enantiomers is included in the final plot. Thus, the effects of an increasing viscosity of the background electrolyte (BGE) with increasing concentrations of a chiral selector, a possible selector adsorption on the capillary wall, an increasing ionic strength of the BGE, a variation of conductivity, etc., must be eliminated from the observed overall mobility. In addition, the equilibrium time scale must be faster than the CE separation time scale, and the concentration of the chiral selector must be varied in a wide range in order to adequately cover binding isotherm (7,8). So far, as with most other techniques, concentrations are used instead of activities in CE; the binding constants are not true thermodynamic equilibrium constants but apparent constants. In addition, most of the linear equations used for equilibrium constant determinations in CE assume 1:1 stoichiometry, while in fact complexes with other stoichiometry are also common.

Bowser and Chen developed a mathematical treatment that takes into account both 1:1 and 1:2 binding stoichiometry between the selector and the selectand (42). The deviations from 1:1 binding stoichiometry were more easily seen with the *x*-reciprocal plot. The diagnostic power of the *y*-reciprocal plot was the weakest among all linear plots. The same authors compared linear and nonlinear regression methods for binding constant calcu-

© 2003 by Marcel Dekker, Inc.

lations and concluded that nonlinear regression gave the most accurate results when the maximum response range was small and when data are collected outside the optimum ligand concentration range (43,44).

2. Alternative Capillary Electrophoresis Methods for Determination of Binding Constants

There are several alternative techniques to ACE that allow one to calculate binding constants in the interactions between two molecular counterparts. It must be noted that all of these techniques in fact are also based on affinity interactions. However, due to some technical and historical reasons, they are named differently.

In the frontal analysis technique (45–51), solute and ligand are premixed and injected as a large sample plug onto the capillary column either by hydrodynamic or electrokinetic injection (45). Equilibrium between the free solute, free ligand, and solute–ligand complex having different mobilities is maintained where the zones temporarily overlap. This produces a broadened plateau of free solute that migrates away from the ligand and ligand–solute complex. The free-solute concentration that is used for the determination of the binding constants based on a Scatchard-type plot is calculated from the height of the resulting plateau.

The frontal analysis technique has been used for the determination of enantioselective binding constants of chiral drugs such as warfarin, verapamil, nilvadipine, and semotidil with proteins such as bovine serum albumin (BSA), human serum albumin (HSA), and plasma lipoproteins (45–51).

Another technique that has been used in CE format for chiral drug–protein interactions is the Hummel–Dreyer method (52). In this technique, the solute is dissolved in the run buffer at varying concentrations, creating a high detector background response. After equilibration of the system, mixtures of the ligand and protein in various ratios are injected into this system as a sample.

In the case of α-AGT, the best fit for (RS)-carvedilol and also for the individual enantiomers was obtained via nonlinear least-squares curve fitting to the following equation (52):

$$B = \sum_{i=1}^{z} \frac{n_i K_{ai} F}{1 + K_{ai} F} + n_i' K_{ai}' F \tag{15}$$

where B is the concentration of drug bound per mole of protein, F is the free-drug concentration, z is the number of classes of specific binding sites, and $n_i' K_{ai}' F$ is the nonspecific binding component (describing the binding to secondary low-affinity binding sites). The interaction of (RS)-, (R)-, and (S)-

© 2003 by Marcel Dekker, Inc.

carvedilol with HSA was characterized by a significantly lower affinity than with AGT, and it was described using the nonspecific binding component ($B = n_i K_{ai} F$).

The binding parameters of (RS)-, (R)-, and (S)-carvedilol to human AGT determined by this technique were in good agreement with the parameters obtained by HPLC, which indicates the reliability of the Hummel–Dreyer method in the CE mode for the evaluation of protein–drug interactions.

Busch et al. used the Hummel–Dreyer method to investigate the interactions between BSA and warfarin (53). For the binding constant calculations these authors used a nonlinear regression of the following equation:

$$r = n \frac{K[\mathrm{D}_f]}{1 + K[\mathrm{D}_f]} \tag{16}$$

where r is the fraction of bound drug molecules, n is the number of binding sites, D_f is the free-drug concentration, and K is the binding constant. Equation (16) allows us also to count the number of binding sites, and it can be expanded to include multiple binding sites (54).

The low selectivity and adsorption effect of proteins on capillary wall have been noted as disadvantages of the Hummel–Dreyer method in CE (54).

In the vacancy peak method, the ligand and solute are dissolved in the run buffer. Buffer without ligand or solute is injected, producing two negative peaks. One peak arises from the free solute and the other peak arises from the solute–ligand complex. The free-solute concentration is calculated from the peak areas. The binding constants are calculated from the free-solute concentration as a function of ligand concentration. The disadvantage of the vacancy peak method is that it requires more sample than the ACE method. In addition, the concentration of the absorbing species in the run buffer should be optimized to obtain good sensitivity and not to saturate the detector.

The binding constants can be also calculated by direct separation of free and complexed analyte. In this method, the solute and ligand are preequilibrated before injecting onto the CE column, where the free solute is separated from both the complexed solute and the ligand. The binding constant is then calculated from a Scatchard plot (55). This unpopular method is applicable only to very stable intermolecular complexes where the dissociation kinetics are slow compared to the separation time scale.

The partial-filling technique is a modification of ACE that has been shown to be very suitable for measuring binding constants. The methodology and interesting examples of application of this technique are summarized in

© 2003 by Marcel Dekker, Inc.

the review paper by Amini et al. (56). The partial-filling technique involves partially filling the capillary with ligand solution and injecting the solute into the capillary. Both the ligand and the solute migrate through the column when a voltage is applied. Equilibrium between the sample and the ligand occurs as the sample zone flows through the ligand zone. In this technique it is possible to keep the ligand concentration constant and to vary the injection plug size (56–59). This technique seems especially useful with those selectors that possess a strong detector response, although one example of application to chiral drug–CD interactions has also been published (59).

III. APPLICATION OF CAPILLARY ELECTROPHORESIS FOR DETERMINATION OF ENANTIOSELECTIVE BINDING CONSTANTS OF CHIRAL DRUG/CYCLODEXTRIN COMPLEXES

Capillary electrophoresis has been applied for the enantioselective determination of the binding constants of chiral drugs with cyclodextrins for basically the following two reasons: (1) optimization of chiral selector concentration and (2) understanding the fine mechanisms of enantioseparations in CE. The first group of studies have been published mainly on the early stage of chiral CE development, whereas the second goal is followed in the most recent studies, mainly by Rizzi and Kremser (10,13) and Scriba et al. (14,15).

The mobility difference ($\Delta\mu_{R,S}$) between the enantiomers in CE can be expressed by the following equation (60):

$$\Delta\mu_{R,S} = \mu_R - \mu_S = \frac{[\mathrm{C}](\mu_f - \mu_c)(K_R - K_S)}{1 + [\mathrm{C}](K_R + K_S) + K_R K_S[\mathrm{C}]^2} \tag{17}$$

where [C] is the concentration of a chiral selector, μ_f is the mobility of a free analyte, μ_c is the mobility of analyte–selector complex and is assumed to be the same for both the complexes of R- and S-enantiomer with a chiral selector, and K_R and K_S are the binding constants.

In order to find the concentration at which the mobility difference between two enantiomers reaches a maximum, one must differentiate Eq. (17) according to the concentration, i.e., to find a partial differential $\partial\,\Delta\mu_{R,S}/\partial[\mathrm{C}]$. After differentiating Eq. (17) and simplification of the obtained result, one may obtain the equation that relates the maximal mobility difference between the enantiomers to the concentration of a chiral selector as follows:

$$[\mathrm{C}]_{\mathrm{opt}} = \frac{1}{\sqrt{K_R K_S}} \tag{18}$$

© 2003 by Marcel Dekker, Inc.

Thus, based on Eq. (18) it becomes possible to determine the concentration of the chiral selector resulting in a maximal mobility difference between the enantiomers, assuming that the binding constants of both enantiomers with chiral selector are known. This method for determination of the optimal CD concentration has been used by several groups.

Kuhn et al. (18) reported the use of the mobility ratio method for the calculation of the binding constants of racemic quinagolide enantiomers to β-CD. Binding constants of 25.5 M^{-1} for (+)-quinagolide and 27.0 M^{-1} (−)-quinagolide were determined. The linearity of the dependence between ligand concentration and the mobility ratio $(\mu_f - \mu_i)/(\mu_i - \mu_c)$ demonstrated the suitability of the model and supported the idea that the quinagolide–β-CD complex has 1:1 stoichiometry. The mobility ratio technique was also used for the determination of binding constants of enantiomers (diastereomers) of (6R,S)-leucovorin (LV) and its biologically active metabolite (6R,S)-methyltetrahydrofolate (ME) to γ-CD (19). A difference greater than the standard deviation was not found between the values of the binding constants of stereoisomers of leucovorin with γ-CD. Nonetheless, acceptable enantioseparation was observed in CE. This result, together with relatively large difference between the mobilities of the complexes of leucovorin stereoisomers with γ-CD, suggested that chiral separation occurs at least in part due to a difference in the electrophoretic velocities of the complexed species.

Goodall and co-workers (20,21) used CE for the determination of the binding constants of tioconazole enantiomers with CD-type chiral selectors and for the optimization of the enantioseparation of this compound. The required corrections to the net mobilities of the solute due to the increased viscosity of the background electrolyte with increasing CD concentration were made in these studies. The effective mobilities of both enantiomers of tioconazole were measured as depending on the concentration of hydroxypropyl-β-CD (HP-β-CD). The treatment of experimental points using the nonlinear least-squares fitting technique gave the binding constants of (−)- and (+)-tioconazole as 201 ± 10 and 231 ± 12 M^{-1}, respectively (20). Using calculated values of binding constants, the optimum concentrations for obtaining the maximum mobility difference between enantiomers and maximum peak resolution were determined. These concentrations were 4.63 and 6.65 *mM*, which were in good agreement with experimental observations. Later, these authors determined the binding constants of tioconazole enantiomers with β-CD and dimethyl-β-CD and established some invariance between the binding strength and enantioselectivity. Excellent agreement was obtained between the calculated and experimentally observed concentration dependence of the mobility difference between the tioconazole enantiomers (Fig. 1). The determination of the binding enthalpy ($\Delta H°$) and binding entropy ($\Delta S°$) of tioconazole enantiomers with β-CD in the same

© 2003 by Marcel Dekker, Inc.

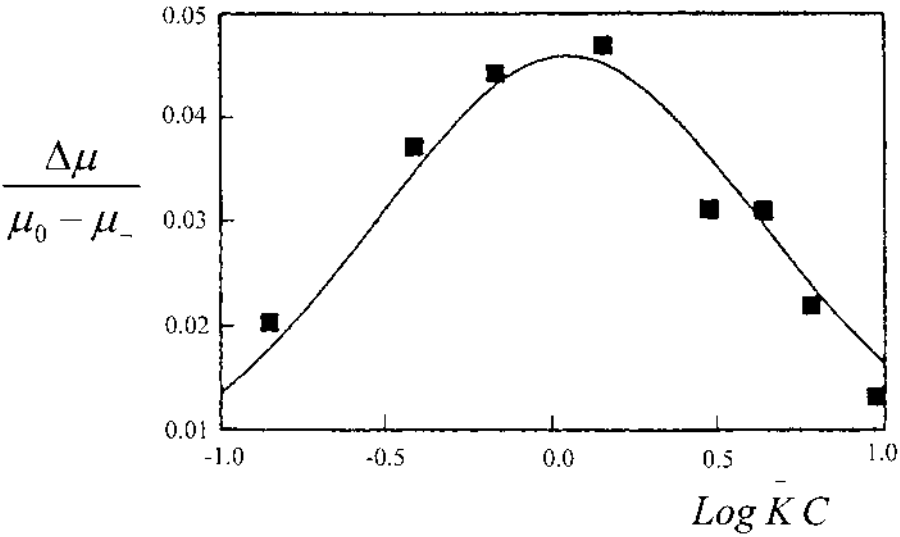

Fig. 1 Measured and predicted enantiomeric mobility difference of tioconazole as a function of free-β-CD concentration. (Reproduced with permission from Ref. 11.)

study indicated that $\Delta H°$ provides the dominant contribution for binding. However, the $\Delta\Delta H°$ and $T\Delta\Delta S°$ terms gave comparable contributions to the enantioselectivity of binding (11). In another study by the same group the binding constants were determined for racemic propranolol and dansylated amino acid derivatives and CE and HPLC were compared. Good correlations were found between these two techniques, not only when performing enantioseparations but also when they were used for calculation of binding constants (21).

Valko et al. (22) studied the separation of mandelic acid enantiomers with γ-CD and calculated very low binding constants 2.8 and 2.4 M^{-1} for the D- and L-enantiomers, respectively. The weak binding of mandelic acid to γ-CD was explained by the large size of the γ-CD torus for such a small molecule as mandelic acid. Unlike the enantiomers of leucovorin and its active metabolite, for which weak binding was associated with low enantioselective (19), fairly high enantioselectivity was found for weakly bonded enantiomers of mandelic acid with γ-CD (K_D/K_L = 1.17).

The binding constants of salbutamol enantiomers and also of several chiral and achiral impurities of this compound with CDs were determined by Rogan et al. (23). The results of these calculations, together with some mobility characteristics of the transient diastereomeric complexes, were used

© 2003 by Marcel Dekker, Inc.

in the discussion of the concentration effect of the chiral selector on the enantioseparation.

Wren et al. (24) determined the binding constants of the enantiomers of propranolol and atenolol with DM-β-CD. The results explained well the experimental observations on the separation of the enantiomers of these compounds in CE. In particular, the enantiomers of propranolol, for which the binding constants and the binding selectivities (K_R/K_S) were higher, were resolved better and at lower DM-β-CD concentration than were the enantiomers of atenolol.

Cooper et al. (25) studied the dependence of the mobility difference of the enantiomers of several dansyl-D,L amino acids on the γ-CD concentration and calculated the binding constants of enantiomers as well as the mobilities of the transient diastereomeric complexes of D- and L-enantiomers. These calculations indicated that the mobilities of transient complexes of γ-CD with both enantiomers of singly charged D,L-dansyl amino acids were the same, whereas the mobilities of the transient diastereomeric complexes between double-charged dansyl-D,L amino acids (glutamine, asparagine) and γ-CD were markedly different. This is an important finding, because the same mobility of transient diastereomeric complexes of the enantiomers of a given compound with the same chiral selector is assumed in some theoretical models of chiral CE separations.

The existence of the aforementioned difference between the mobilities of transient diastereomeric complexes of the enantiomers with the chiral selector may have some important consequences in chiral CE. For instance, the enantioseparation can, in principle, be possible even in those cases when the binding constants of both enantiomers to a given chiral selector are the same. On the other hand, this may allow, in certain cases, observation of the reversal of the enantiomer migration order, depending on the concentration of the chiral selector (17).

The discussion clearly shows the limitations of Eq. (18) for calculating the optimal chiral selector concentration. As already mentioned, Eq. (18) was derived based on the assumption of equal mobility of both diastereomeric complexes, which indeed is not always the case. This means that Eq. (18) is not absolutely reliable for calculation of the optimal chiral selector concentration in CE.

Cooper et al. (26) determined the binding constants and the mobility characteristics for three binaphthyl derivatives with α-, β-, and γ-CDs. As shown, the transient diastereomeric complexes of the enantiomers of these compounds differ from each other in their mobilities. This effect is most pronounced in the case of 1,1′-binaphthalene-2,2′-diyl hydrogen phosphate. The change in enantioseparation depending on the γ-CD concentration could be explained well for each solute–γ-CD pair based on the binding studies.

© 2003 by Marcel Dekker, Inc.

The possible reversal of the migration order of the 1,1′-binaphthalene-2,2′-diyl hydrogen phosphate enantiomers could also be predicted based on these studies, but it has been not verified experimentally.

Baumy et al. (27) determined the binding constants for two 3,4-dihydro-2*H*-1-benzopyran derivatives of β-CD. These binding constants were then used to calculate the optimal concentration of chiral selector for the enantioseparation of the two compounds. The calculation of the optimal concentration of the chiral selector was performed according to Eq. (18). Good agreement was found between the calculated and experimentally observed optimum concentrations for the two compounds.

Gahm and Stalcup (28) determined the binding constants of selected *N*-(3,5-dinitrobenzoyl)-D,L-amino acids (DNB-D,L-AA) with β-CD and then used these data to describe the relative stability of complexes of different CD derivatives with DNB-D,L-phenylalanine (DNB-D,L-PA). The CD derivatives in this study were selectively naphthylethylcarbamoylated β-CDs. The original technique used in this study to characterize the relative complex stability of these CDs with DNB-D,L-PA includes the addition of the latter to the background electrolyte and the injection of the aforementioned CD mixture as an analyte. Independent of the configuration of the pendant group, stronger binding of the amino acids and CD was found with the primary rather than the secondary substituted isomer. This result indirectly indicates that the amino acids form complexes by inclusion in the CD cavity from the secondary side. This study showed that stronger binding at the early stage of chiral CE development does not necessarily improve chiral recognition and that a more important factor is the difference between the binding strengths of the enantiomers.

Sänger-van de Griend et al. (29) determined the binding constants of several local anaesthetics with DM-β-CD. These data showed that the achiral separation of analogues is a result of their mobility difference, whereas the resolution of enantiomers results from the difference in their binding constants with CDs.

Especially high binding constants were calculated for (R)- and (S)-doluxetine enantiomers with the anionic CD derivative SBE-β-CD, i.e., 4840 $\pm$ 120 and 7480 $\pm$ 300 M^{-1}, respectively (30). Although these data seem somewhat overestimated, they are in good agreement with CE separation results, where the enantioresolution of duloxetine was observed using an extremely low concentration (<0.1 mM) of this chiral selector.

Lelievre and Gareil (31) studied chiral separations of nonsteroidal anti-inflammatory drugs (carprofen, flurbiprofen, indoprofen, ketoprofen, naproxen, propafenone, and suprofen) and determined the acidity and inclusion complex formation constants of these chiral compounds with different neutral CDs (β-CD, HP-β-CD, DM-β-CD, TM-β-CD, and HP-γ-CD). In

© 2003 by Marcel Dekker, Inc.

confirmation of several other studies, this study showed again that strong binding between the CD and the enantiomers is not mandatory for the enantioseparation. In particular, TM-β-CD could resolve the enantiomers of all the arylpropionic acid derivatives studied while showing lower complexing ability than the other CDs tested.

Vigh and co-workers intensively used CE for the determination of the binding constants of enantiomers with CDs in their studies on the modeling and optimization of chiral CE separations (32–36).

Together with Eqs. (4) and (5)–(7), Vespalec et al. (37) recommended the use of an equation for the determination of the mean of the host–guest interaction constants. This equation seem to be useful for the determination of the binding constants in some cases, whereas in other cases its use seems impracticable. In particular, the use of this equation for the calculation of the average binding constants of enantiomers does not give marked savings in the time required to perform the experiment. Additionally, this technique provides only the binding constants averaged for the two enantiomers. In chiral separations this constant is of minor intersect, whereas the binding constants of the individual enantiomers to the chiral selector are more informative. On the other hand, reaching the concentration optimum, which is necessary in this technique, is not always possible (for weak complexes), owing to the limited solubility of the CD. Finally, the observed optimum on the mobility difference–concentration curve can be shifted significantly from its intrinsic thermodynamic value because in addition to the selector–selectand binding, other factors may affect the effective mobility of analytes in CE. This can lead to significant errors in the calculation of the mean value of the binding constants.

As mentioned earlier, the basic goal of the aforementioned studies on the determination of enantioselective binding constants between chiral drugs and cyclodextrins has been the determination of the optimal cyclodextrin concentration required for the CE enantioseparation. However, in some of these studies, the authors already paid attention to the fact that the mobility of transient diastereomeric complexes of the two enantiomers with a chiral selector are not always the same (19,26), as this has been assumed in some theoretical models for simplicity reasons. Thus, the mobility difference between the transient diastereomeric complexes can contribute to enantioseparations observed in CE. The more significant consequence of the effect mentioned earlier can be that in some cases the enantiomer migration pattern observed in CE separation can be the result of either the difference in the binding constants or the mobility of diastereomeric complexes (17). This phenomenon has been intuitively correctly supposed to be the reason for the reversal of the enantiomer migration order of dansyl-D,L-phenylalanine depending on the concentration of HP-β-CD in an early study by Schmitt and

© 2003 by Marcel Dekker, Inc.

Engelhardt (61). Even more interesting can be the enantioseparation with equal binding constants of both enantiomers with the chiral selector but different mobility of the transient diastereomeric complexes. This is conceptually possible in chiral CE, in contrast to chromatographic techniques with immobilized chiral selectors (3,4).

In the most recent works by Li and Waldron (38), Rizzi and Kremser (13), and Scriba and coworkers (14,15), binding studies are used to follow the mechanisms underlying enantioseparations in CE. The enantiomer migration order of amphoteric compounds such as amino acids and peptides can be reverted in CE by analyzing the components either in the cathionic or in anionic form (17). In addition, Li and Waldron reported the opposite migration order of the LL/DD enantiomeric pairs of Ala-Phe and Leu-Phe at pH 2.5 and 3.5 using β-CD as chiral selector (38). The origin of this phenomenon is different from that mentioned earlier because the sign of the charge of the dipeptide does not revert in the pH range 2.5–3.5. The reverse migration order was also found for the tripeptide enantiomers Gly-β-L-Asp-D-PheNH_2 and Gly-β-D-Asp-L-PheNH_2 between pH 3.6 and 5.3 in the presence of carboxymethyl-β-cyclodextrin (39). A similar effect was also described for several di- and tripeptides when resolved with various neutral and charged CDs in the studies by Sabbah and Scriba (14,41). In 1999 Rizzi and Kremser reported a detailed study on the influence of the complexation-induced pK_a shift on the mobility of the complexes between dansylated amino acids and hydroxypropyl-β-CD (13). This study provided a key for the explanation of the pH-dependent reversal of the enantiomer migration order mentioned earlier as well as for the concentration-dependent enantiomer migration order reversal described in Ref. 61. It was shown that in the pH range p$K_a \pm 2$ units, complex mobility was the dominant factor, compared to the complexation constants, in determining the migration order of the amino acid enantiomers in several cases and even led to a reversal of the enantiomer migration order with increasing concentration of the cyclodextrin (13). In particular, at pH 2.5, D-DNS-Phe is the preferentially bound enantiomer to HP-β-CD (K_L = 117 and K_D = 147 m^{-1}), and the complex D-DNS-Phe/HP-β-CD also possesses higher mobility at this pH ($\mu_L^{complex}$ = 3.40 $\times$ 10^{-5} and $\mu_D^{complex}$ = 4.28 $\times$ 10^{-5} cm^2 V^{-1} s^{-1}, respectively) (13). This means that at lower CD concentration when the enantiomers migrate favorably in free form, the affinity toward the chiral selector will determine the enantiomer migration order. At high concentrations of CD when the enantiomers favorably migrate in the complexed form, the mobility of transient diastereomeric complex will determine the enantiomer migration order. This would be a sound explanation of the experimental data reported in Ref. 61. However, as mentioned by the authors (13), the aforementioned pattern of the binding constants and the mobilities of the diastereomeric complexes

© 2003 by Marcel Dekker, Inc.

holds at pH 2.5 and not at pH 6.0, at which the experiment was performed in Ref. 61. Based on the detailed investigation of the complexation constants and the mobilities of the complexes between the enantiomers of Ala-Phe and Phe-Phe and carboxymethyl-β-CD, it was found that both the complexation constant and the complex mobility influence the enantiomer migration order (14). At pH 2.5, when the peptides are protonated, complex mobilities of the LL- and DD-dipeptide enantiomers with the cyclodextrin were similar and the migration order was determined by the complexation constants. At pH 3.5–3.8, the pH range slightly above the pK_a values of the carboxylic acid group of dipeptides (which range between 2.8 and 3.6), the influence of the complex mobilities becomes more significant. Thus, the complex mobility apparently determined the enantiomer migration order in the case of Ala-Phe, leading to the migration order DD before LL, while the influence of the complexation constants dominated in the case of Phe-Phe, resulting in the migration order of the LL-peptide before the DD-epimer (14).

Thus, as shown earlier, CE represents a suitable technique for the determination of enantioselective binding constants between chiral drugs and cyclodextrins. The results obtained under appropriate conditions are reasonable and can be applied for optimization purposes as well as for a better understanding of the fine nuances of chiral CE separations. On the other hand, some care must be taken for the proper application of CE methods for the determination of the binding constants as well as when applying these data. A critical review of the calculation of stability constants for the chiral selector–enantiomer interactions from electrophoretic mobilities has been published by Vespalec and Bocek (40).

The main disadvantage of CE for the investigation of interactions between chiral drugs and cyclodextrins is that CE does not provide any direct information on the structure of selector–selectand complexes. In the next section, some complementary techniques for the investigation of chiral drug–cyclodextrin interactions are discussed and parallels are drawn between these techniques and CE.

IV. COMPLEMENTARY TECHNIQUES FOR INVESTIGATION OF CHIRAL DRUG/CYCLODEXTRIN INTERACTIONS

A. Nuclear Magnetic Resonance Spectroscopy

1. Chiral Recognition Pattern

Nuclear magnetic resonance spectroscopy is an established technique for studies of stereoselective intermolecular interactions. The application of this technique in combination with CE has been discussed in several review papers (3,4,62,63). In this overview, the potential of NMR spectroscopy is illustrated using just a few examples from the authors' own studies. The

© 2003 by Marcel Dekker, Inc.

space limitations of this chapter do not allow a thorough discussion of all published results on the subject.

Although the chiral recognition potential of CE seems to be in general higher than that of NMR spectroscopy, sometimes the latter may allow one to observe the enantioselective effects unseen in nonoptimized CE experiments. Several examples of this kind have been described in the literature (see, for example, Ref. 64). Nuclear magnetic resonance spectroscopy provides considerable information on the environment of individual atoms and their involvement in intermolecular and intramolecular interactions, in contrast to most other techniques, which provide characteristics that are averaged over all atoms in the molecule and over all possible complexes in a given selector–selectand system. Thus, complexation-induced chemical shifts (CICS) observed on the individual atoms and functional groups as well as the pattern of the spectrum may provide some preliminary information regarding the structure of selector–selectand complex. Thus, for example, ^{1}H-NMR spectra of chiral drug clenbuterol (CL) complexes with β-CD and heptakis-(2,3-diacetyl-6-sulfo)-β-CD (HDAS-β-CD) shown in Fig. 2 indicate that the aromatic moiety of CL is involved in the complex formation with β-CD and that the *n*-alkyl part is involved in the complex

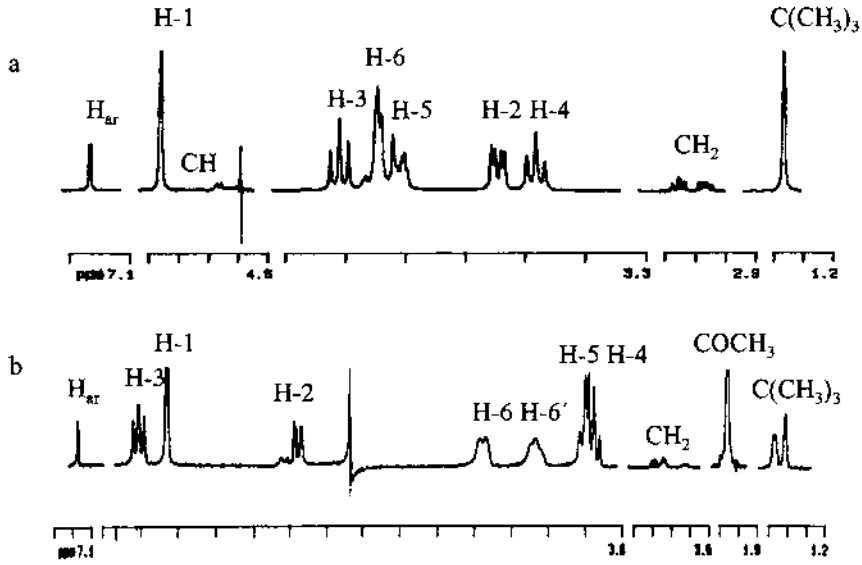

Fig. 2 600 MHz ^{1}H-NMR spectra of (a) (±)-CL/β-CD and (b) (±)-CL/HDAS-β-CD complexes. The external standard was tetramethylsilane and the solvent was D_2O. (Reproduced with permission from Ref. 65.)

© 2003 by Marcel Dekker, Inc.

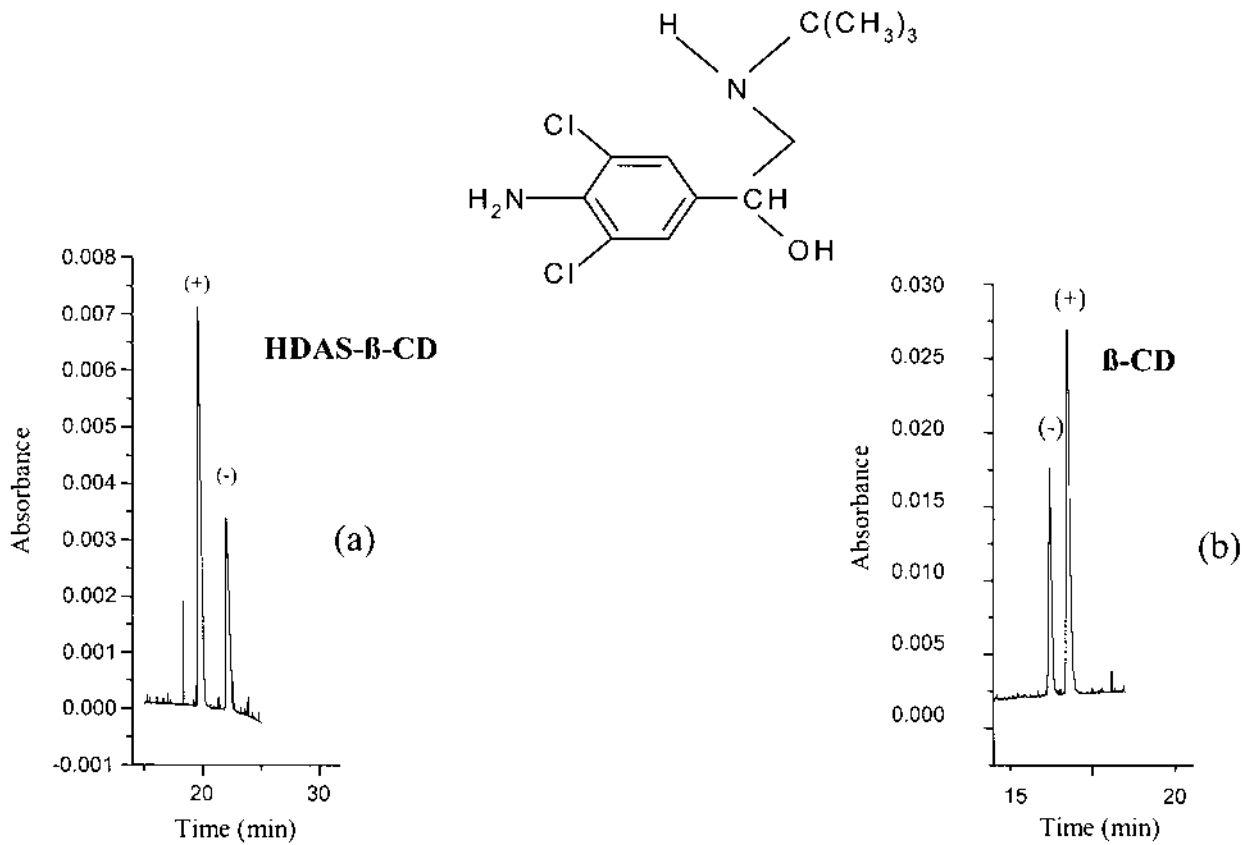

© 2003 by Marcel Dekker, Inc.

formation with HDAS-β-CD. This can be the potential reason for the opposite affinity of CL enantiomers to these two cyclodextrins (Fig. 3) (65).

2. Stoichiometry of Chiral Drug/Cyclodextrin Complexes

Information about the stoichiometry of selector–selectand complex is difficult to gain from CE. However, this knowledge is useful in order to characterize the structure of intermolecular complexes as well as for the calculation of the binding constants. Previous research and review papers (3, 4,62,65) summarize the application of this technique to the problems related to chiral CE. As shown in Fig. 4, despite the involvement of different parts of the CL molecule in complex formation, the stoichiometry of CL complexes most likely is the same (1:1) with β-CD and HDAS-β-CD (65).

3. Binding Constants of Intermolecular Complexes

As mentioned earlier, CE is a useful and flexible microanalytical technique for obtaining reliable binding constants of intermolecular selector–selectand complexes. At first glance, NMR spectrometry offers no marked advantage for the determination of binding constants. It requires a set of samples and may appear more expensive and time consuming than CE. However, NMR spectroscopy is free from some of the aforementioned disadvantages of CE, and in addition it provides multiple sets of data points. Thus, the binding constants determined using NMR experiments may be statistically more reliable. To date, in only a single study were the binding constants determined using both. CE and NMR spectroscopy (Table 1) (16). As these studies indicated, the enantioselective binding constants in β-CD/promethazine complex determined using CE allowed more precise prediction of the optimal β-CD concentration for the enantioseparation of this chiral drug. References 3, 4, 17, 62, and 63, as well as the research papers cited therein, provide more comprehensive information on the enantioselective binding constant determinations by NMR spectroscopy that are related to chiral CE.

4. Structure of Intermolecular Complexes

Nuclear magnetic resonance spectroscopy is the most powerful technique for the determination of the structure of intermolecular complexes in solution

Fig. 3 Enantioseparation of (±)-CL with (a) 1 mg/mL HDAS-β-CD, and (b) 18 mg/mL β-CD. The separation capillary was fused silica with 40/47 cm effective/total length and 50 μm I.D. Detection was performed at the cationic side of the capillary. Applied voltage 20 kV; 100 mM phosphate-TEA buffer, pH 3.0. UV detection (214 nm). (Reproduced with permission from Ref. 65.)

© 2003 by Marcel Dekker, Inc.

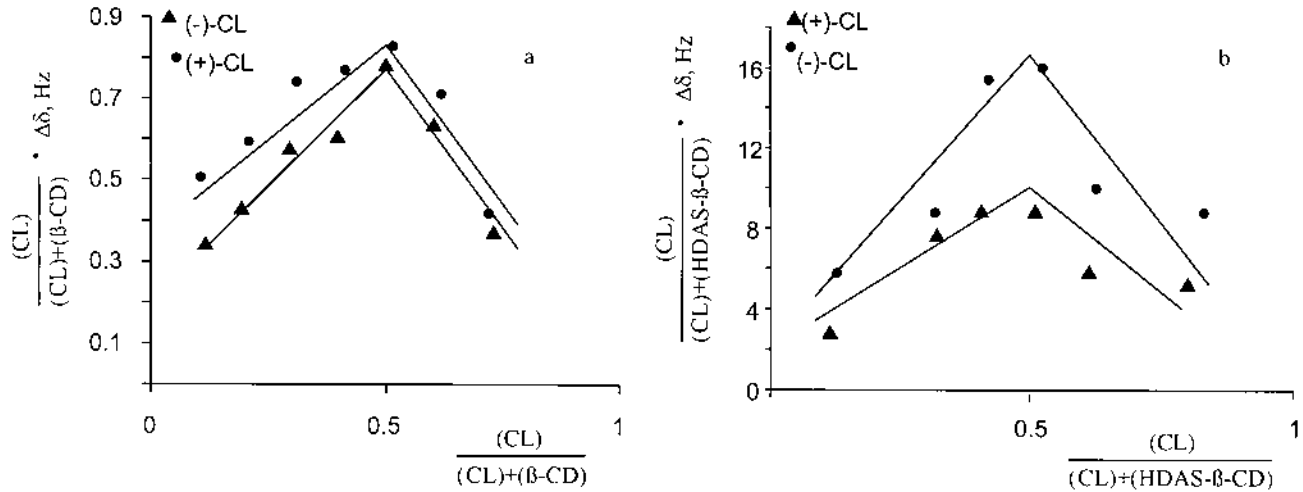

Fig. 4 Continuous variation plots for (a) (±)-CL/β-CD and (b) (±)-CL/HDAS-β-CD complexes. The complexation-induced chemical shifts of aromatic protons were used for the construction of Job's plots in the case of (±)-CL/β-CD complex and the protons of *tert*-butyl moiety in the case of (±)-CL/HDAS-β-CD complex. (Reproduced with permission from Ref. 65.)

© 2003 by Marcel Dekker, Inc.

Table 1 Binding Constants Between β-CD and the Enantiomers of Promethazine Determined Using CE and NMR Spectroscopy

Experimental technique	Curve-fitting method	$K_{(+)}$, M^{-1}	$K_{(-)}$, M^{-1}	$K_{(+)}/K_{(-)}$
CE	*x*-reciprocal	1129	967	1.17
	y-reciprocal	1330	1140	1.17
	Double reciprocal	1029	863	1.19
	Nonlinear curve-fitting	1262	1112	1.10
NMR spectroscopy	Linear regression	2927	1790	1.64

(66). In this short subsection, only structural studies related to chiral CE are mentioned.

The chemical shift pattern, line-shape analysis, and nuclear Overhauser effect (NOE) may be used to obtain information on the structure and dynamics of the complexes. The data obtained using NOE are easier to interpret and seem to be more direct. Several studies illustrate the feasibility of this technique for structure elucidation of complexes relevant to chiral CE (3,63–72). It does not seem reasonable to perform an NOE experiment in a routine way for any selector–selectand complex, because such an experiment requires measurements with rather strong magnets and may be expensive and time consuming. However, in certain cases NOE studies provide unique information that is impossible to obtain using any alternative technique. One example of NOE studies related to chiral CE is shown in Fig. 5 (64). The possible structural reasons for opposite affinity of the enantiomers of chiral drug aminoglutethimide (AGT) toward native β- and γ-CD was investigated in this study. The NOE data depicted in Fig. 5 allow one to deduce the structure of the complexes shown in Fig. 6. Thus, by selective saturation of the aromatic protons in the ortho position of (±)-AGT, equally strong intermolecular NOE effects were observed for both H-3 and H-5 protons of β-CD (Fig. 5a). However, by irradiation of the aromatic protons in the meta position, only a minor effect was observed for the H-3 protons of β-CD and the NOE effect appeared instead on the H-6 protons. These data support a deep inclusion of the *p*-aminophenyl moiety of the AGT molecule in the cavity of β-CD, entering it from the wider secondary side (Fig. 6a). The deep inclusion of the aromatic moiety of the AGT molecule in the cavity of β-CD on the secondary side is also supported by a significant NOE effect observed between the H-3 protons of CD and the ethyl moiety of AGT. Rather strong ''NOE-like'' effects observed on the external CD protons in this experiment make it questionable whether the structure rep-

© 2003 by Marcel Dekker, Inc.

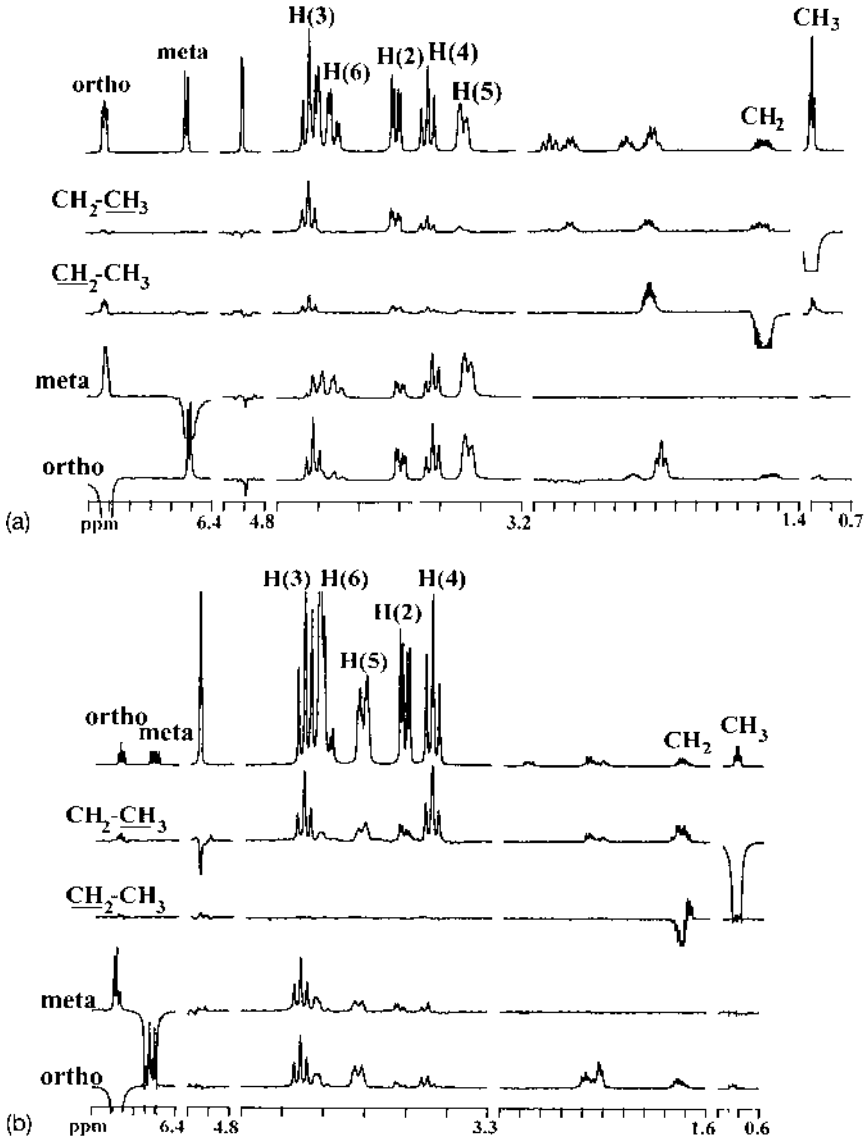

Fig. 5 1D-ROESY spectra of (±)-AGT and two equivalents of (a) β-CD and (b) γ-CD. (Reproduced with permission from Ref. 64.)

© 2003 by Marcel Dekker, Inc.

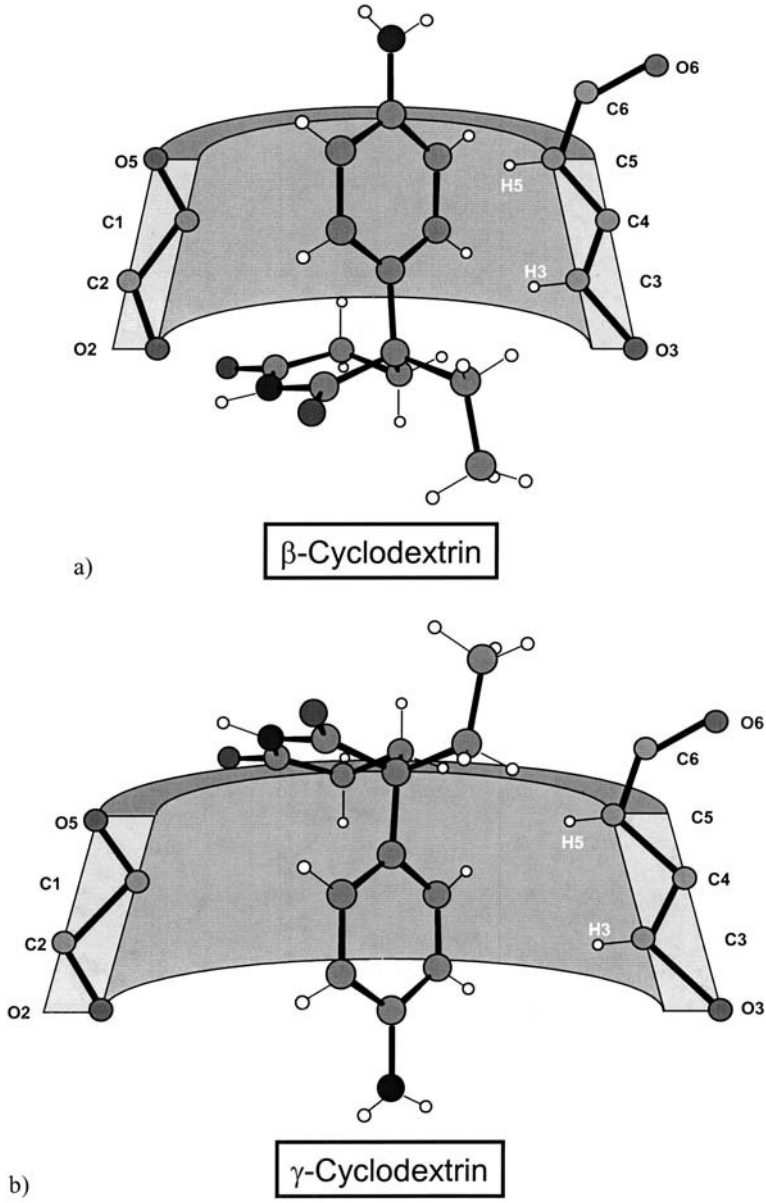

Fig. 6 Structure of AGT complexes with (a) β-CD and (b) γ-CD derived based on the 1D ROESY spectra depicted in Fig. 5. (Reproduced with permission from Ref. 64.)

© 2003 by Marcel Dekker, Inc.

resented in Fig. 6a is the only possible structural element of this complex or whether the alternative structures are also present.

In contrast to the AGT/β-CD complex, the NOE effect decreased for the H-5 protons and remained almost unchanged for H-3 protons when irradiating the protons in the meta position instead of the protons in the ortho position of the aromatic ring of AGT in the (±)-AGT/γ-CD complex (Fig. 5b). These data support a complex formation from the narrower primary side of γ-CD, with the amino group ahead (Fig. 6b). The glutarimide ring is apparently less involved in complex formation in this case. However, the involvement of the methyl group in complex formation by a still-unknown mechanism cannot be completely excluded. The structure of the (±)-AGT/γ-CD complex depicted on Fig. 6b was derived by saturation of the aromatic protons of AGT. The structure was also supported by the data that were obtained when the γ-CD protons were saturated and the response was observed for the aromatic protons of AGT. Thus, when saturating the H-5 protons of γ-CD, the response for the protons in the ortho position of the aromatic ring was more pronounced than the protons in the meta position. However, a similar response was observed for both ortho and meta protons of the aromatic ring when γ-CD protons in position 3 were saturated.

Thus, as illustrated earlier, rotating-frame nuclear Overhauser and exchange spectroscopy (ROESY) experiments may provide a reasonable explanation for the significant qualitative and quantitative differences observed in selector–selectand interactions related to chiral CE. This information becomes even more important when the alternative techniques for structure elucidation fail. This was the case with the AGT/CD complexes that formed monocrystals, but of a twin-type that were not suitable for X-ray crystallographic studies. Although ROESY seems to be a powerful technique for structural investigation of noncovalent complexes in a liquid phase, the experimental data need to be interpreted very carefully. Thus, a detailed analysis of the earlier-described ID-ROESY spectra of the AGT/CD complexes may indicate that the structures shown in Fig. 6 are just fragments of rather complex supramolecular aggregates. This seems even more likely when considering a certain tendency of AGT to form dimers in aqueous solution, which has been also confirmed by the X-ray crystallographic data in the solid state.

B. Mass Spectrometric Techniques

As already mentioned, it is difficult to obtain information on the stoichiometry of cyclodextrin–analyte complexes based on CE separations. Nuclear magnetic resonance and other spectrometric techniques (UV, circular

© 2003 by Marcel Dekker, Inc.

dichroism, etc.) are useful for obtaining this complementary information. For determination of the stoichiometry of a complex using these techniques, the construction of Job's plot is required, which requires a certain amount of sample and, in addition, is rather expensive and time consuming. The advantage of mass spectrometric (MS) techniques that provide m/z ratio is that the stoichiometry can be determined from a single experiment. Another interesting advantage of MS is that this technique may provide information on the individual complexes that may coexist in the solution between a given analyte and a selector, between one selector and multiple analytes, vice versa, or both multiple selectors and multiple analytes. Most other techniques mentioned in this chapter do not allow one to obtain information of this kind. Only CE may allow this for a single selector and multiple analytes or vice versa, but not for multiple analytes and multiple selectors as well as when a given analyte and a given selector from the complexes with a different stoichiometry.

In the electrospray ionization MS (ESI MS) experiment shown in Fig. 7, the relative complex formation ability of AGT was investigated for different sugar derivatives (D-glucose, α-CD, β-CD, and γ-CD). This single experiment indicates that from the sugars studied AGT exhibits the highest affinity toward β-CD, and the complex with 1:1 stoichiometry is formed in this case. Various examples of applications of ESI MS for investigation of chiral drug–CD complexes are summarized in the reviews in Refs. 62 and 63 and the research papers cited therein.

In the ESI MS studies some care must be taken due to the possible formation of ''false peaks'' (73). The time-of-flight (TOF) ESI MS equipment of a new generation with an orthogonal interface design allows one to avoid somewhat experimental artifacts of this kind.

Together with ESI MS, other soft ionization MS techniques, such as matrix-assisted laser desorption/ionization time of flight (MALDI TOF) and fast atom bombardment (FAB) MS, may be used for the determination of the stoichiometry of selector–selectand complexes.

C. X-Ray Crystallography

X-ray crystallography has a long history as a powerful technique for investigating the structure of CDs and their complexes in the solid state. The first experimental evidence of the inclusion complex formation ability of CDs in the solid state was obtained by Hyble et al. in 1965 using this technique (74). X-ray studies of CD complexes have been summarized in several recent reviews (75,76). However, few studies relevant to chiral CE have been published (69,70). This may be for the following reasons: (1) X-ray crys-

© 2003 by Marcel Dekker, Inc.

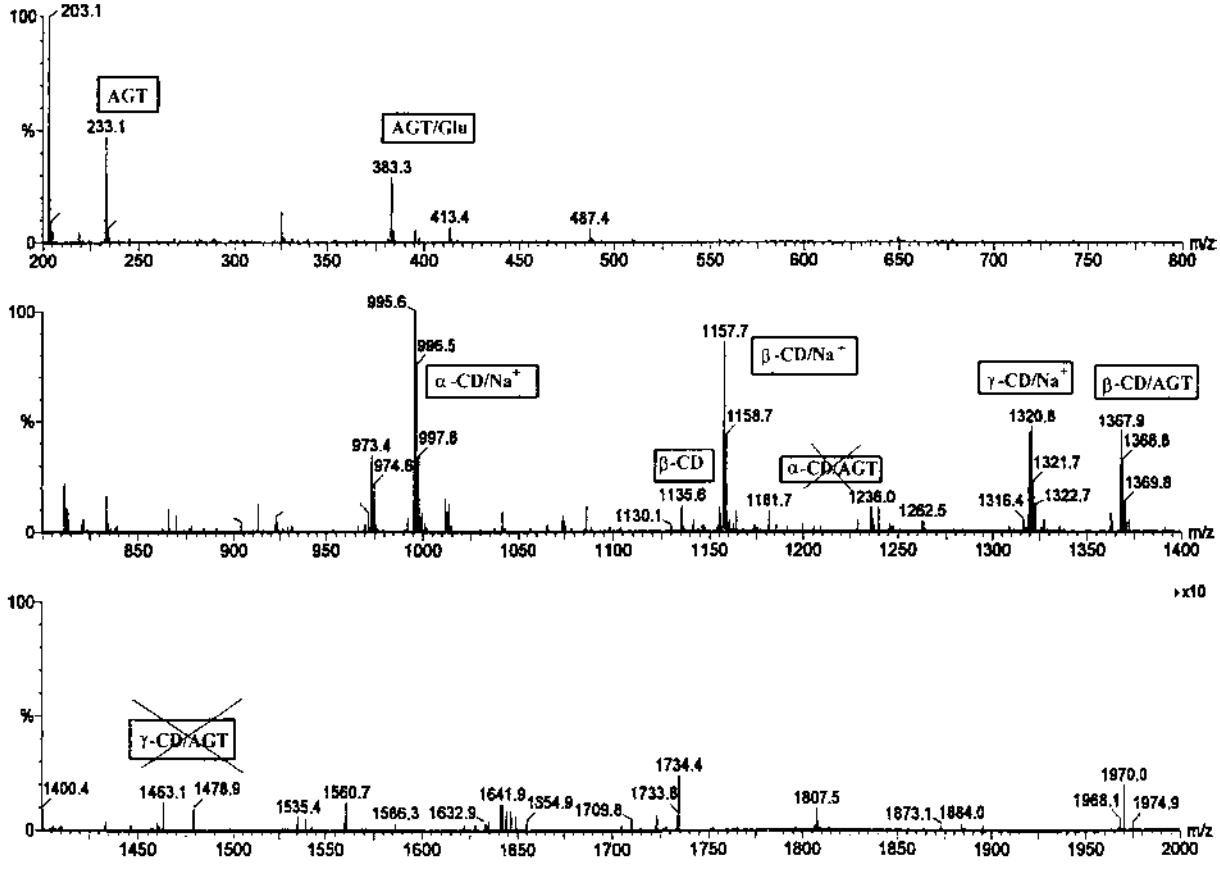

Fig. 7 ESI MS spectrum of 0.1 mg/mL (±)-AGT and equimolar amounts of glucose, α-, β-, and γ-CDs. (Reproduced with permission from Ref. 64.)

© 2003 by Marcel Dekker, Inc.

tallography is a solid-state technique and CE operates in a liquid phase, so these two techniques may not ideally correlate with each other. (2) Growing monocrystals of suitable size containing both counterparts (a selector and a selectand) requires experience. (3) High-quality X-ray crystallographic experiments on monocrystals is time consuming and rather expensive. (4) The structure generation from the experimental data requires powerful computer software and is not always trivial. Despite the aforementioned, X-ray crystallography may sometimes appear very useful for structural studies related to enantioseparations in CE.

ID-ROESY studies performed on the complex between (+)-BrPh and β-CD in solution did not allow one to explain the NOE effect observed on the protons of the maleate counteranion (70). X-ray crystallographic studies performed on the monocrystals obtained from a 1:1 aqueous solution of (+)-BrPh maleate and β-CD (Fig. 8) provide a plausible explanation for the contradiction maintained in Ref. 70. In particular, as shown in Fig. 8, (+)-BrPh forms with β-CD, at least in the solid state, not a 1:1 complex but a complex with 1:2 stoichiometry. In this complex the (+)-BrPh molecule is sandwiched between two molecules of β-CD. The 4-bromophenyl moiety of (+)-BrPh enters the cavity of one of the β-CD molecules, whereas the cavity of another β-CD molecule is occupied by the maleate counteranion. Thus, X-ray crystallography may provide useful information on the supramolecular structure of the selector–selectand complexes and in this way complement well 1D-ROESY data. However, the aforementioned possible differences between the structure of the complexes in solution and in the solid phase must be considered.

D. Molecular Modeling Techniques

Molecular modeling calculations may allow one, in the ideal case, to compute in a reasonable time and rather precisely the energy and structure of intermolecular complexes of biomedical, pharmaceutical, and chemical relevance.

In the early 1990s, several studies were published on the computation of selector–selectand interactions in chiral CE. This relates basically to the interactions between CDs and their chiral guests, which seem to be caused by the fact that CDs are rather rigid molecules of medium size and therefore calculations for these molecules are easier and faster and may be rather precise. In addition, many CDs are well studied by alternative techniques for structure elucidation. Among these, X-ray crystallographic data are of the highest interest.

A separation factor observed in any instrumental technique is defined by the difference between the free energy of formation of transient diaste-

© 2003 by Marcel Dekker, Inc.

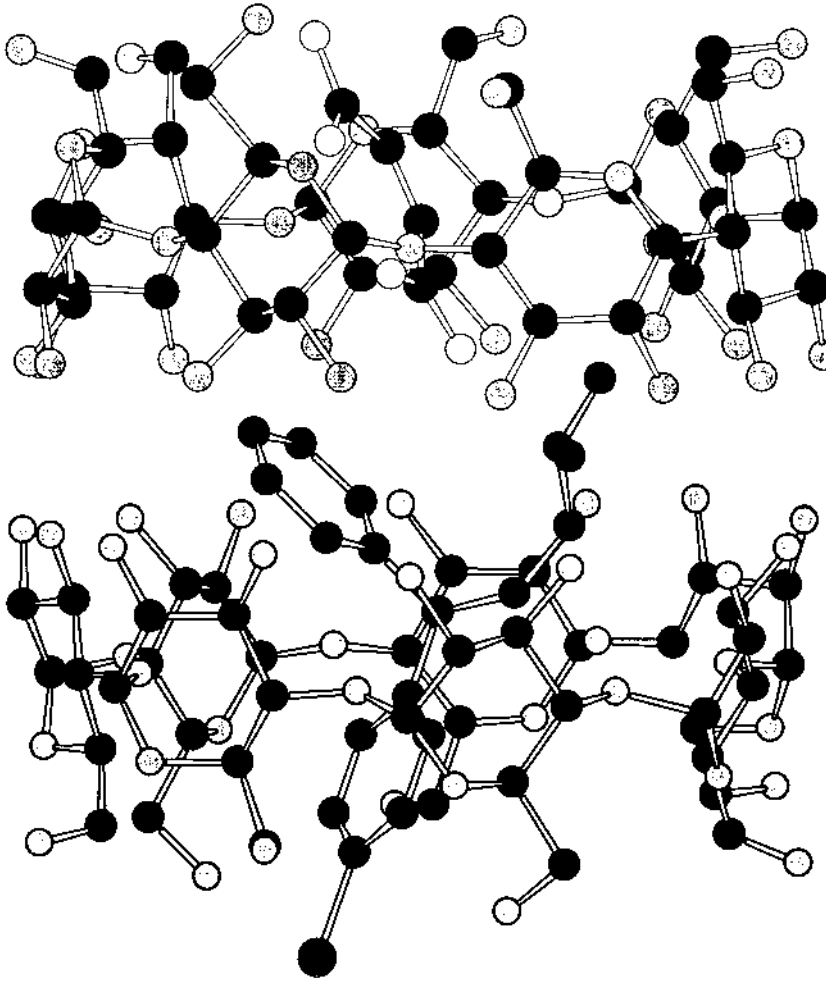

Fig. 8 Structure of (+)-BrPh maleate β-CD complex in the solid state determined by X-ray crystallography. (Reproduced with permission from Ref. 70.)

reomeric complexes between enantiomers and a chiral selector. Therefore, the exact calculation of the absolute energy values is not required in molecular modeling studies related to enantioseparations. This simplifies the calculations. On the other hand, due to the extremely high efficiency of CE, this technique allows one to observe the enantioseparation even in those

© 2003 by Marcel Dekker, Inc.

selector–selectand pairs where the previously mentioned difference between the free energy of formation of diastereomeric complexes is extremely small. The precise calculation of very small energy differences remains a challenging task even for very sophisticated state-of-the-art energy minimization software. Additional care must be taken in order to maximally approach a model to the real separation conditions. Thus, for instance, the molecular modeling calculations are often performed in vacuum without taking into account the effect of the medium. However, the aqueous medium commonly used in CE dramatically affects the hydrophobic and hydrogen-bonding interactions. Moreover, the ionic strength of the buffer plays a decisive role for electrostatic intermolecular interactions. Another important point is the correct selection of the starting and boundary conditions for energy minimization. Incorrectly defined conditions may totally confuse the calculations. For instance, when performing the molecular modeling calculations for the complex between TM-β-CD and (+)-BrPh in a neutral form, energy values were obtained that indicated that the complex formed with the alkylamino moiety included in the cavity of TM-β-CD would be energetically favorable. The structure with the alkylamino moiety included in the cavity was also observed in X-ray experiments performed on the monocrystals obtained from the mixture of aqueous suspension of deprotonated (+)-BrPh as a free base and TM-β-CD. These results are contradictory to the structure derived for brompheniramine hydrochloride/TM-β-CD complex from the 1D-ROESY experiment in solution. The intermolecular NOE effects observed in this experiment clearly indicated the inclusion of the 4-bromophenyl moiety in the cavity of TM-β-CD (70). Taking into consideration that the protonated form of (+)-BrPh was applied for the 1D-ROESY studies in solution, the force-field calculations were performed again for interactions of a single positively charged (+)-BrPh with TM-β-CD. The energy values obtained in this case clearly indicate that the complex formation with the 4-bromophenyl moiety of the (+)-BrPh molecule included in the cavity of TM-β-CD is energetically favorable, which is in agreement with the structure observed using 1D-ROESY studies in solution (70).

A general overview of the molecular modeling techniques applied to chiral hosts can be found in papers by Lipkowitz (77,78). Some special aspects of molecular modeling techniques related to chiral CE and earlier studies on the subject are summarized in Refs. 3, 17, 79, and 80.

In summary, molecular modeling when used in combination with instrumental techniques, especially 1D-ROESY and X-ray crystallography, may significantly contribute to understanding the nature of the intermolecular forces responsible for chiral drug–cyclodextrin interactions and chiral recognition.

© 2003 by Marcel Dekker, Inc.

REFERENCES

1. F Cramer. Einschlussverbindungen der Cyclodextrine. Angew Chem 64:136, 1952.
2. JC Giddings. Generation of variance theoretical plates, resolution and peak capacity in electrophoresis and sedimentations. Separ Sci 4:181–189, 1969.
3. B Chankvetadze, G Blaschke. Enantioseparations in capillary electromigration techniques: recent developments and future trends. J Chromatogr A 906:309–363, 2001.
4. B Chankvetadze. Separation selectivity in chiral capillary electrophoresis with charged selectors. J Chromatogr A 792:269–295, 1997.
5. B Chankvetadze, N Burjanadze, D Bergenthal, G Blaschke. Potential of flow-counterbalanced capillary electrophoresis for analytical and micropreparative separations. Electrophoresis 20:2680–2685, 1999.
6. A Tiselius. Moving boundary method of studying the electrophoresis of proteins. Nova Acta Reg Soc Uppsal Ser IV 7:1–107, 1930.
7. KL Rundlett, DW Armstrong. Examination of the origin, variation, and proper use of expressions for the estimation of association constants by capillary electrophoresis. J Chromatogr A 721:173–186, 1996.
8. KL Rundlett, DW Armstrong. Methods for the estimation of binding constants by capillary electrophoresis. Electrophoresis 18:2194–2202, 1997.
9. KL Rundlett, DW Armstrong. Methods for the determination of binding constants by capillary electrophoresis. Electrophoresis 22:1419–1427, 2001.
10. A Rizzi. Fundamental aspects of chiral separations by capillary electrophoresis. Electrophoresis 22:3079–3106, 2001.
11. SG Penn, ET Bergstrom, DM Goodall, JS Loran. Capillary electrophoresis with chiral selectors: optimization of separation and determination of thermodynamic parameters for binding of tioconazole enantiomers to cyclodextrins. Anal Chem 66:2866–2873, 1994.
12. S Cladrowa-Runge, A Rizzi. Enantioseparations of 6-aminoquinolyl-*N*-hydroxysuccinimidyl carbamate derivatized amino acids by capillary zone electrophoresis using native and substituted β-cyclodextrins as chiral additives II. Evaluation of complexation constants. J Chromatogr A 759:167–175, 1997.
13. A Rizzi, L Kremser. pK_a shift-associated effects in enantioseparations by cyclodextrin-mediated capillary zone electrophoresis. Electrophoresis 20:2715–2722, 1999.
14. S Sabbah, GKE Scriba. Separation of dipeptide and tripeptide enantiomers in capillary electrophoresis using carboxymethyl-β-cyclodextrin and succinyl-β-cyclodextrin: influence of the amino acid sequence, nature of the cyclodextrin and pH. Electrophoresis 22:1385–1393, 2001.
15. S Sabbah, F Süss, GKE Scriba. pH-Dependence of complexation constants and complex mobility in capillary electrophoresis separation of dipeptide enantiomers. Electrophoresis 22:3163–3170, 2001.
16. B Chankvetadze, I Kartozia, N Burjanadze, D Bergenthal, H Luftmann, G Blaschke. Enantioseparation of chiral phenothiazine derivatives in capillary

© 2003 by Marcel Dekker, Inc.

electrophoresis using cyclodextrin-type chiral selectors. Chromatographia 53: S290–S296, 2001.
17. B Chankvetadze. Capillary Electrophoresis in Chiral Analysis. Wiley, Chichester, UK, 1997.
18. R Kuhn, F Stoeklin, F Erni. Chiral separations by host–guest complexation with cyclodextrin and crown ether in capillary zone electrophoresis. Chromatographia 33:32–36, 1992.
19. A Shibukawa, DK Lloyd, IW Wainer. Simultaneous chiral separation of leucovorin and its major metabolite 5-methyl-tetrahydrofolate by capillary electrophoresis using cyclodextrins as chiral selector. Estimation of the formation constants and mobility of the solute–cyclodextrin complexes. Chromatographia 35:419–429, 1993.
20. SG Penn, DM Goodall, JS Loran. Differential binding of tioconazole enantiomers to hydroxypropyl-β-cyclodextrin studied by capillary electrophoresis. J Chromatogr 636:149–152, 1993.
21. SG Penn, GY Liu, ET Bergstrom, DM Goodall, JS Loran. Systematic approach to treatment of enantiomeric separations in capillary electrophoresis and liquid chromatography. 1. Initial evaluation using propranolol and dansylated amino acids. J Chromatogr A 680:147–155, 1994.
22. IE Valko, HA Billiet, J Frank KCHAM Luyben. Factors affecting the separation of mandelic acid enantiomers by capillary electrophoresis. Chromatographia 38:730–736, 1994.
23. MM Rogan, KD Altria, DM Goodall. Enantiomeric separation of salbutamol and related impurities using capillary electrophoresis. Electrophoresis 15:808–817, 1994.
24. SAC Wren, RC Rowe, RS Payne. A theoretical approach to chiral capillary electrophoresis with some practical implications. Electrophoresis 15:774–778, 1994.
25. CL Cooper, JB Davis, RO Cole, M Sepaniak. Separations of derivatized amino acid enantiomers by cyclodextrin-modified cypillary electrophoresis. Mechanistic and molecular modeling studies. Electrophoresis 15:785–792, 1994.
26. CL Cooper, JB Davis, MJ Sepaniak. Mechanisms of enantiomeric resolution in cyclodextrin-modified capillary electrophoretic separations of binaphthyl compounds. Chirality 7:401–408, 1995.
27. P Baumy, P Morin, M Dreux, MC Viaud, S Boye, G Guillaumet. Determination of β-cyclodextrin inclusion complex constants for 3,4-dihydro-2-*H*-1-benzopyran enantiomers by capillary electrophoresis. J Chromatogr A 707:311–326, 1995.
28. KH Gahm, AM Stalcup. Capillary zone electrophoresis study of napthylethylcarbamoylated β-cyclodextrins. Anal Chem 67:19–35, 1995.
29. CE Sänger-van de Griend, K Gröningsson, D Westerlund. Chiral separation of local anaesthetics with capillary electrophoresis. Evaluation of the inclusion complex of the enantiomers with heptakis(2,6-di-*O*-methyl)-β-cyclodextrin. Chromatographia 42:263–268, 1996.
30. EC Rickard, R Bopp, DJ Skanchy, KL Chetwin, B Pahlen, JF Stobaugh. Role

© 2003 by Marcel Dekker, Inc.

of capillary electrophoresis methods in the drug development process. Chirality 8:108–121, 1996.
31. F Lelievre, P Gareil. Chiral separations of underivatized arylpropionic acids by capillary electrophoresis with various cyclodextrins. Acidity and inclusion constants determinations. J Chromatogr A 735:311–320, 1996.
32. YY Rawjee, DU Staerk, G Vigh. Capillary electrophoretic chiral separations with cyclodextrin additives. 1. Acids—chiral selectivity as a function of pH and the concentration of β-cyclodextrin for fenoprofen and ibuprofen. J Chromatogr 635:291–306, 1993.
33. YY Rawjee, RL Williams, G Vigh. Capillary electrophoretic chiral separations using β-cyclodextrin as resolving agent. 2. Bases—chiral selectivity as a function of pH and the concentration of β-cyclodextrin. J Chromatogr A 652:233–244, 1993.
34. YY Rawjee, RL Williams, G Vigh. Capillary electrophoretic chiral separations using cyclodextrin additives. 3. Peak resolution surfaces for ibuprofen and homatropine as a function of the pH and the concentration of β-cyclodextrin. J Chromatogr A 680:599–607, 1994.
35. YY Rawjee, RL Williams, LA Buckingham, G Vigh. Effect of pH and hydroxylpropyl β-cyclodextrin concentration on peak resolution in the capillary electrophoretic separation of the enantiomers of weak bases. J Chromatogr A 688:273–282, 1994.
36. YY Rawjee, G Vigh. A peak resolution model for the capillary electrophoretic separation of the enantiomers of weak acids with hydroxypropyl β-cyclodextrin-containing background electrolytes. Anal Chem 66:619–627, 1994.
37. R Vespalec, S Fanali, P Bocek. Consequences of a maximum existing in the dependence of separation selectivity on concentration of cyclodextrin added as chiral selector in capillary zone electrophoresis. Electrophoresis 15:1523–1525, 1994.
38. JJ Li, K Waldron. Estimation of the pH-independent binding constants of alanylphenylalanine and leucylphenylalanine stereoisomers with β-cyclodextrin in the presence of urea. Electrophoresis 20:171–179, 1999.
39. S Sabah, GKE Scriba. pH-Dependent reversal of the chiral recognition of tripeptide enantiomers by carboxymethyl-β-cyclodextrin. J Chromatogr A 833: 261–266, 1999.
40. R Vespalec, P Bocek. Calculation of constants for the chiral selector–enantiomer interactions from electrophoretic mobilities. J Chromatogr A 875:431–445, 2000.
41. S Sabah, GKE Scriba. Influence of the structure of cyclodextrins and amino acid sequence of dipeptides and tripeptides on the pH-dependent reversal of the migration order in capillary electrophoresis. J Chromatogr A 894:267–272, 2000.
42. MT Bowser, DDY Chen. Higher-order equilibria and their effect on analyte migration behavior in capillary electrophoresis. Anal Chem 70:3261–3270, 1998.
43. MT Bowser, DDY Chen. Monte Carlo simulation of error propagation in the

© 2003 by Marcel Dekker, Inc.

determination of binding constants from rectangular hyperbolae. 1. Ligand concentration range and binding constants. J. Phys Chem 102:8063–8071, 1998.
44. MT Bowser, DDY Chen. Monte Carlo simulation of error propagation in the determination of binding constants from rectangular hyperbolae. 2. Effect of the maximum response range. J Phys Chem 103:197–202, 1999.
45. T Ohara, A Shibukawa, T Nakagawa. Capillary electrophoresis frontal analysis for microanalysis of enantioselective protein binding of a basic drug. Anal Chem 67:3520–3525, 1995.
46. A Shibukawa, Y Kuroda, T Nakagawa. High-performance frontal analysis for drug–protein binding study. J Pharm Biomed Anal 18:1047–1055, 1999.
47. NAL Mohamed, Y Kuroda, A Shibukawa, T Nakagawa, ST Elo Gizawy, HF Askal, ME El Kommos. Binding analysis of nilvadipine to plama lipoproteins by capillary electrophoresis-frontal analysis. J Pharm Biomed Anal 21:1037–1043, 1999.
48. Y Kuroda, A Shibukawa, T Nakagawa. The role of branching glycan of human α_1-acid glycoproten in enantioselective binding to basic drugs as studied by capillary electrophoresis. Anal Biochem 268:9–14, 1999.
49. NAL Mohamed, Y Kuroda, A Shibukawa, T Nakagawa, ST Elo Gizawy, HF Askal, ME El Kommos. Enantioselective binding analysis of verapamil to plasma lipoproteins by capillary electrophoresis-frontal analysis. J Chromatogr A 875:447–453, 2000.
50. MER Rosas, A Shibukawa, Y Yoshikawa, Y Kuroda, T Nakagawa. Binding study of semotiadil and bevosemotiadyl with α_1-acid glycoprotein using high-performance frontal analysis. Anal Biochem 274:27–33, 1999.
51. Y Kuroda, Y Kita, A Shibukawa, T Nakagawa. Role of biantennary glycans and genetic variants of human α_1-acid glycoprotein in enantioselective binding of basic drugs as studied by high-performance frontal analysis/capillary electrophoresis. Pharm Res 18:389–393, 2001.
52. J Oravcova, D Sojkova, W Lindner. Comparison of the Humel–Dreyer method in high-performance liquid chromatography and capillary electrophoresis conditions for study of the interactions of (RS)- (R)- and (S)-carvedilol with isolated plasma proteins. J Chromatogr B 682:349–357, 1996.
53. MHA Busch, LB Carels, HFM Boelens, JC Kraak, H Poppe. Comparison of five methods for the study of drug–protein binding in affinity capillary electrophoresis. J Chromatogr A 777:311–328, 1997.
54. J Oravcova, B Bohs, W Lindner. Drug–protein binding studies—New trends in analytical and experimental methodology. J Chromatogr B 677:1–28, 1996.
55. NHH Heegaard. A heparin-binding peptide from human serum amiloid P component characterized by affinity capillary electrophoresis. Electrophoresis 19: 442–447, 1998.
56. A Amini, U Paulsen-Sorman, D Westerlund. Principle and applications of the partial filling techniques in capillary electrophoresis. Chromatographia 50:497–506, 1999.
57. A Amini, U Paulsen-Sorman, D Westerlund. Dependence of chiral separations on the amount of cyclodextrins as selectors, employing the partial-filling technique in capillary zone electrophoresis. Chromatographia 51:226–230, 2000.

© 2003 by Marcel Dekker, Inc.

58. A Amini, D Westerlund. Evaluation of association constants between drug enantiomers and human α_1-acid glycopotein by applying a partial-filling technique in affinity capillary electrophoresis. Anal Chem 70:1425–1430, 1998.
59. A Amini, N Merclin, S Bastami, D Westerlund. Determination of association constants between enantiomers of orciprenaline and methyl-β-cyclodextrin as chiral selector by capillary zone electrophoresis using a partial filling technique. Electrophoresis 20:180–188, 1999.
60. SAC Wren, RC Rowe. Theoretical aspects of chiral separation in capillary electrophoresis. I. Initial evaluation of a model. J Chromatogr 603:235–241, 1992.
61. T Schmitt, H Engelhardt. Derivatized cyclodextrins for the separation of enantiomers in capillary electrophoresis. HRC—J High Resol Chromatogr 16: 525–529, 1993.
62. B Chankvetadze, G Endresz, G Blaschke. Charged cyclodextrin derivatives as chiral selecots in capillary electrophoresis. Chem Soc Rev 25:141–153, 1996.
63. B Chankvetadze, G Blaschke. Selector–selectand interactions in chiral capillary electrophoresis. Electrophoresis 20:2592–2604, 1999.
64. B Chankvetadze, M Fillet, N Burjanadze, D Bergenthal, C Bergander, H Luftmann, J Crommen, G Blaschke. Enantioseparation of aminoglutethimide with cyclodextrins in capillary electrophoresis and studies of selector–selectand interactions using NMR spectroscopy and electrospray ionization mass spectrometry. Enantiomer 5:313–322, 2000.
65. B Chankvetadze, K Lomsadze, D Bergenthal, J Breitkreutz, K Bergander, G Blaschke. Mechanistic study on the opposite migration order of clenbuterol enantiomers in capillary electrophoresis with β-cyclodextrin and single-isomer heptakis(2,3-diacetyl-6-sulfo-)-β-cyclodextrin. Electrophoresis 22:3178–3184.
66. HJ Schneider, F Hacket, V Rüdiger. NMR studies of cyclodextrins and cyclodextrin complexes. Chem Rev 98:1755–1785, 1998.
67. G Galaverna, R Corradini, A Dossena, R Marcelli. Histamane-modified cationic β-cyclodextrin as chiral selector for the enantiomeric separation of hydroxy acids and carboxylic acids by capillary electrophoresis. Electrophoresis 20: 2619–2629, 1999.
68. U Holzgrabe, H Mallwitz, SK Branch, TM Jefferies, M Wiese. Chiral discrimination by NMR spectroscopy of ephedrine and *N*-methylephedrine induced by β-cyclodextrin, heptakis(2,3-di-*O*-acetyl)-β-cyclodextrin and heptakis-(6-*O*-acetyl)-β-cyclodextrin. Chirality 9:211–219, 1997.
69. B Chankvetadze, G Pintore, N Burjanadze, D Bergenthal, K Bergander, J Breitkreutz, C Mühlenbrock, G Blaschke. Mechanistic study of opposite migration order of dimethindene enantiomers in capillary electrophoresis in the presence of native β-CD and heptakis-(2,3,6-tri-*O*-methyl)-β-CD. J Chromatogr A 875: 455–469, 2000.
70. B Chankvetadze, N Burjanadze, G Pintore, D Bergenthal, K Bergander, J Breitkreutz, C Mühlenbrock, G Blaschke. Separation of brompheniramine enantiomers by capillary electrophoresis and study of chiral recognition mechanisms of cyclodextrins using NMR-spectroscopy, UV-spectrometry, ESI-MS and X-ray crystallography. J Chromatogr A 875:471–484, 2000.

© 2003 by Marcel Dekker, Inc.

71. PK Owens, AF Fell, MW Coleman, M Kinns, JC Berridge. Use of H^1-NMR spectroscopy to determine the enantioselective mechanism of neutral and anionic cyclodextrins in capillary electrophoresis. J Pharm Biomed Anal 15: 1603–1619, 1997.
72. G Galaverna, MC Paganuzzi, R Corradini, A Dossena, R Marcelli. Enantiomeric separation of hydroxy acids and carboxylic acids by diamino-β-cyclodextrin (AB, AC, AD) in capillary electrophoresis. Electrophoresis 22:3171–3177, 2001.
73. P Cescutti, D Carozzo, R Rizzo. Study of the inclusion complexes of aromatic molecules with cyclodextrins using ionspray mass spectrometry. Carbohydr Res 290:105–115, 1996.
74. A Hyble, RE Rundle, DE Williams. The crystal and molecular structure of the cyclohexaamylose–potassium acetate complex. J Am Chem Soc 87:2779–2788, 1965.
75. W Saenger, J Jacob, K Gessler, T Steiner, D Hoffmenn, H Sanabe, K Koizumi, SM Smith, T Takaha. Structure of the common cyclodextrins and their larged analogues—beyond the doughnut. Chem Rev 98:1787–1802, 1998.
76. K Harata. Structural aspects of stereodifferentiation in the solid state. Chem Rev 98:1803–1827, 1998.
77. KB Lipkowitz. Atomistic modeling of enantioselection in chromatography. J Chromatogr A 906:417–442, 2001.
78. KB Lipkowitz. Atomistic modeling of enantioselective binding. Acc Chem Res 33:555–562, 2000.
79. K Kano, Y Tamiya, C Otsuki, T Shimomura, T Ohno, O Hayashida, Y Murakami. Chiral recognition by cyclic oligosaccharides. Enantioselective complexation of binaphthyl derivatives with cyclodextrins. Supramol Chem 2:137, 1993.
80. K Kano, K Minami, K Horiguchi, T Ishihana, M Kodera. Ability of noncyclic oligosccharides to form molecular complexes and its use for chiral separation by capillary zone electrophoresis. J Chromatogr A 694:307–313, 1995.

© 2003 by Marcel Dekker, Inc.

9

Affinity of Drugs to Proteins and Protein–Protein Interactions

Steffen Kiessig
Solvias AG, Basel, Switzerland

Frank Thunecke
UFZ Centre for Environmental Research, Leipzig, Germany

I. SCOPE

This chapter will give an overview of ACE applications for the investigation of drug–protein and protein–protein interactions. It starts with a short introduction on the available experimental setups and methods used for the determination of binding constants. The discussion of drug–protein interactions begins with drug binding to receptor proteins, which function as drug targets to exhibit a pharmacological effect. This is followed by a discussion of the binding of drugs to plasma proteins, which usually function as transport proteins. The possibility of studying the stereoselectivity and especially the enantioselectivity of drug–protein interactions by ACE is also examined. This includes an overview of applications where proteins are used as chiral selectors for the separation of drug enantiomers by capillary electrophoresis. These are not ACE investigations with the aim of calculating binding constants. However, enantiomeric separations are increasingly important in the pharmaceutical industry and one of the applications where the advantages of capillary electrophoresis count most. On the other hand, applications dealing with interactions to antibodies are not included in this chapter. Readers interested in this field are referred to Chapter 12 of this book, ''Characterization of Immunoreactions.'' Applications dealing with immobilized species on the capillary, such as polymer networks and imprinted polymers, and very recent developments in capillary gel electrophoresis

© 2003 by Marcel Dekker, Inc.

(CGE) and capillary electrochromatography (CEC) are also not covered. The authors took care to include all relevant references. Nevertheless, some noteworthy investigations may have been overlooked. Readers more interested in this specific field of ACE are therefore referred to recent reviews (1–7) that deal especially with different aspects of drug–protein binding interactions.

II. INTRODUCTION

The interactions of proteins with various ligands are key processes in the regulation pathways in living organisms. Drugs as extraneous substances to fight pathological symptoms interfere with proteins in different ways. In some cases a specific protein is the target of a drug. Then the molecular structure of the drug should fit properly the binding site of the receptor protein to exhibit a specific pharmacological effect. There should be a high affinity of the drug to the target protein, leading to rather irreversible drug–protein complexes. The drug–protein binding constant gives a quantitative measure and is important during the drug development and design process as well as in preclinical studies to check possible side effects or displacement by other drugs. The affinity of drugs to plasma transport proteins such as albumins, α_1-acid glycoprotein (AGP), and lipoproteins is somewhat different. In most cases the binding is weak and reversible and has two major aspects. On the one hand, the proteins may act as transport vehicles and also prevent drug metabolism, thereby prolonging the duration of drug activity. On the other hand, the drug portion that binds to the plasma proteins is considered unable to diffuse from blood to the extravascular action site. Therefore analytical methods are necessary to determine the extent of binding and to monitor the unbound portion of drug as the species executing the pharmacological effect. Conventional methods used for this determination are equilibrium dialysis, ultrafiltration, and ultracentrifugation. Spectroscopic methods such as UV, fluorescence, and NMR spectroscopy are especially suitable for giving insights into changes in protein conformation during the process of drug binding. Among the separation techniques, chromatographic procedures have been established for many years to explore drug–protein binding. The more recently developed ACE methods gain their attractiveness especially because they work in free solution without the need to immobilize one of the binding partners and because the usual separation solution contains only plain buffer and therefore better mimics native conditions. This is especially important for proteins, which easily tend to denature or at least to change the three-dimensional structure.

A further aspect is the fact that most drugs are small molecules with

© 2003 by Marcel Dekker, Inc.

chiral centers. Proteins as binding partners are built up by L-amino acids and are therefore also chiral species. Drug–protein interaction leads to different diastereomeric complexes, which means that drug enantiomers may have different binding affinities to the receptor protein as well as to serum transport proteins. Nevertheless, a lot of drugs are still administered as racemic mixtures. In recent years, however, regulation agencies such as the FDA force pharmaceutical companies to produce enantiomeric pure drugs in cases where the activity of the enantiomers are very different and to make sure that the less or not acting enantiomer has no pharmacological side effect. This boosted the development of enantioselective syntheses and of methods that are able to distinguish enantiomers and to measure enantiomeric purity. Among those methods, separation techniques are especially important, because they can give a direct measure of the enantiomeric ratio; capillary electrophoretic procedures seem especially suited.

III. DRUG–PROTEIN BINDING

The binding of a drug to a protein can be monitored by capillary electrophoresis, if the at least temporarily established drug–protein complex exhibits mobility changes as compared to the free drug and/or protein, e.g., if the ratio of charge to hydrodynamic radius is different. Whereas a mobility difference between the drug and the drug–protein complex can be most often assumed, the difference between the free protein and the drug–protein complex may frequently be rather insignificant. In recent years, several capillary electrophoretic procedures have been developed to explore binding interactions. They were exhaustively reviewed in recent years (8–10). We will therefore give only a short overview of the most common procedures. The Hummel–Dreyer method and the mobility-shift approach use identical setups, as illustrated in Figure 1A. They differ, however, in the parameter chosen to obtain the binding constant. In both cases one binding partner is added in varying concentrations to the background buffer and the other is injected. When studying drug–protein interactions, the partner of choice to inject and monitor will most often be the protein. First the protein usually contains many more chromophoric groups and will therefore have the better UV detectability. Furthermore adding higher protein concentrations to the background buffer may result in problems because of protein interactions with the inner capillary wall and lower detector sensitivity due to the protein absorption. The mobility-shift approach uses the change in the mobility of the injected species due to the interaction with the component added to the buffer during the survey through the capillary. This requires, however, a mobility difference between the protein and the drug–protein complex if the

© 2003 by Marcel Dekker, Inc.

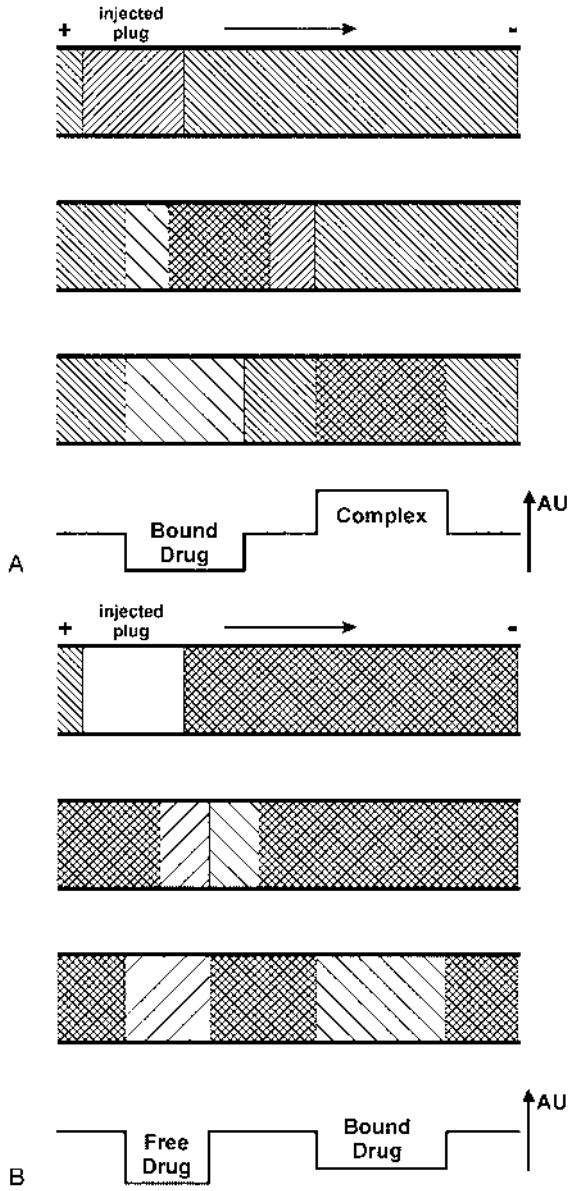

Fig. 1 Schematic representation of the experimental setups of the mobility-shift method and the Hummel–Dreyer method (A); the vacancy peak method and the vacancy affinity capillary electrophoresis method (B); the equilibrium-mixture method and the frontal analysis method (C) for drug–protein binding analysis. drug; protein; drug–protein complex; buffer. (Reprinted with permission from Ref. 38. Copyright 1992 Elsevier Science.)

© 2003 by Marcel Dekker, Inc.

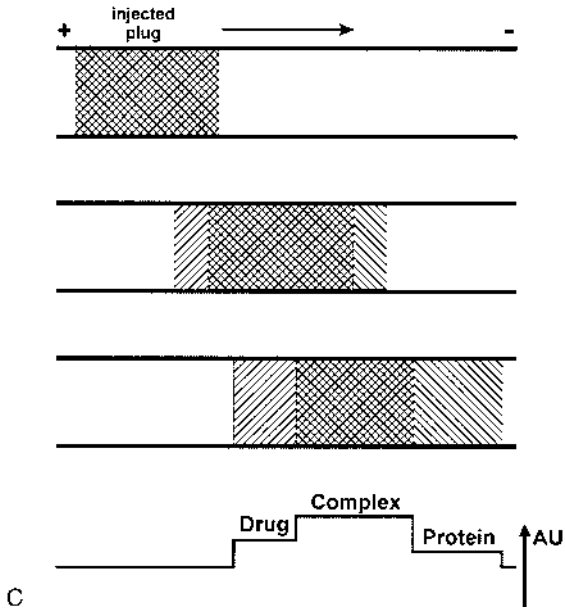

Fig. 1 Continued

protein is injected. The Hummel–Dreyer method uses the peak area of the negative or vacancy peak of the component added to the buffer. A mobility difference between the protein and the drug–protein complex is therefore not required and would rather falsify the calculation of binding data. Both methods are frequently used to investigate the interaction of drugs or other ligands with receptor proteins. The setup of the vacancy peak and the recently developed vacancy affinity capillary electrophoretis (VACE) method (11) is exemplified in Figure 1B. Both interacting species are added to the running buffer, one of them in varying concentrations, and plain buffer is injected. While the VACE method uses the change in the mobilities due to the complex formation to calculate the binding constant, the vacancy peak method uses the peak area of the vacancy peak for that purpose. Up to now there have been only a very few examples in the literature using these approaches. Figure 1C shows the experimental setup of the equilibrium-mixture method and the frontal anlysis method. In both cases the capillary is filled with running buffer and a pre-equilibrated mixture of the interacting binding partners is injected. Whereas in the equilibrium-mixture approach the usual small sample amount for capillary electrophoresis is injected, the frontal analysis method utilizes a large sample plug. The latter one was adapted from chromatograpic procedures and assumes that there is no mo-

© 2003 by Marcel Dekker, Inc.

bility difference between the protein and the drug–protein complex. Most of the published applications dealing with drug interactions with plasma proteins use the frontal analysis method, perhaps because of the simple calculation of the unbound drug concentration from the plateau peak height. The equilibrium-mixture method, in contrast, requires not only a mobility difference between the protein and the drug–protein complex but also separated peaks, because it uses the peak area for the binding constant calculation. This means that the lifetime of the drug–protein complex has to be considerably longer than the time needed for the separation. This is also in contrast to the other methods, which assume that the complexation process is much faster than the migration process, and the measured migration time is therefore averaged by a lot of association–dissociation processes that happened during the course through the capillary.

The choice of the ACE method most suited for a given drug–protein interaction will therefore depend on several factors. Among them are inherent properties of the complexation, such as the estimated dissociation constant, the on/off-rates or multiple binding sites, as well as properties related to the behavior under ACE conditions, such as solubility, detectability, adsorption to the inner capillary wall, and mobility of all species under investigation.

A. Binding to Protein Receptors

The binding of a drug to a target receptor protein is of prime interest to a lot of researchers. First one searches for the native ligand of a target protein. Then one tries to learn more about the binding site of the protein via epitope mapping and searches in combinatorial libraries for known drug leads or in peptide or other libraries for new ones. After this the lead compound has to be modified to fulfill pharmacological criteria. The whole process of drug discovery and development is accompanied by analytical methods necessary to monitor and quantify the binding interactions. Among these methods, capillary electrophoresis is increasingly recognized as a method of choice. The speed of analysis, the minimum volume consumption, and the feasibility of automation are special advantages over conventional methods that also make it attractive for screening procedures. There are, however, not as many examples published as for the interaction with plasma proteins, which are discussed later. One reason may be that the affinity of drugs to target receptor proteins is usually strong, which means in the lower nanomolar range. In this case the calculation of reliable binding constants by ACE requires a nanomolar concentration detection limit, which, on commercial instruments, is possible only through laser-induced fluorescence (LIF), therefore making necessary the fluorescence labeling of one of the binding partners.

The use of ACE methods to investigate protein–ligand interactions was

© 2003 by Marcel Dekker, Inc.

inspired mainly by publications of the Whitesides group in the early 1990s (12–17) and by Heegaard (18,19) and Walsh (20) as well. The Whitesides group used the binding of vancomycin to dipeptides and of bovine carbonic anhydrase to arylsulfonamides as model interactions. They studied the influence of changed electrophoretic conditions on the binding constant calculation and showed how to use ACE for the screening of libraries. The same model systems were later employed by other groups to further investigate methodological aspects (21–24).

Thomas et al. investigated the binding of procainamide metabolites to hemoglobins and histone proteins (25). Nitrosoprocainamide was found to bind to ferrohemoglobin with a dissociation constant in the lower micromolar range. The results were in good agreement with binding studies using flow-injection analysis with electrochemical detection.

Kiessig et al. studied the interaction of the immunosuppressant drug cyclosporin A and some derivatives to its cellular receptor protein cyclophilin (26). The cyclophilin–cyclosporin A complex mediates the immunosuppressive action of cyclosporin A by inhibition of the phosphatase calcineurin. Using ACE in the equilirium-mixture mode, a separation of the cyclophilin–cyclosporin A complex and the unbound cyclophilin was achieved. The approach allowed a qualitative estimation of the binding affinity of cyclosporin A derivatives compared to cyclosporin A. For the calculation of binding constants, electrophoretically mediated microanalysis was applied.

Other immunosuppressive drugs under investigation were FK506 and rapamycin and its affinity to human FKBP12 (27). The hFKBP12-drug complexes were separated from unbound protein and detected by hyphenation to mass spectrometry.

Furthermore, the interaction of the immunosuppressant deoxyspergualin and analogues to members of the heat shock protein family, which are molecular chaperones that are involved in protein folding, especially under cell stress conditions, was published by two research groups (28,29). Both groups used the mobility-shift approach, and the calculated affinities were in the lower micromolar range. Whereas Nadeau et al. (28) investigated the binding of deoxyspergualin, two active analogues, and two inactive metabolites to Hsc70 and Hsp90, Liu et al. (29) focused on the binding of deoxyspergualin to the Hsc70 protein and to peptides from the protein digest to gain more detailed information regarding the protein binding domain.

In another paper, Liu et al. (30) described the interaction of fibronectin with heparin as a model system. The two distinct binding constants in the nanomolar range were derived from Scatchard plots and found in good agreement with published data. The established ACE binding assay was then applied to the molecular interaction of a kedarcidin chromophore with apoprotein. Dissociation constants in the lower micromolar range were calcu-

© 2003 by Marcel Dekker, Inc.

lated and the effect of organic solvents as buffer additives was investigated. Increasing the organic solvent content in the aqueous phase resulted in a reduced binding affinity. This again points to the aspect mentioned in the introduction, that one should avoid deviations from native conditions in ACE whenever possible.

De Lorenzi et al. (31) investigated the interaction of the amyloidogenic protein transthyretin with a pool of drugs chosen for their structural motifs. Amyloidoses are diseases caused by protein misfolding and subunit misassembly. The binding of a drug may stabilize the nativelike state, thereby preventing the pathway that leads to a polymeric toxic fibrillar structure. The mobility-shift approach was utilized for a preliminary screening, followed by frontal analysis to evaluate the number of binding sites; ultrafiltration served as the conventional method to support the results. For 2 in 13 investigated drugs flurbiprofen and flufenamic acid binding constants in the lower micromolar range were established. Whereas the results of the mobility-shift approach and ultrafiltration are in good agreement, the data gained from frontal analysis differed considerably. Frontal analysis was finally applied to investigate the interaction of transthyretin fibrils with the natural ligand thyroxine.

The examples discussed up to now utilized UV detection almost exclusively. This is the standard detection method in commercial instruments, but it is limited to concentrations no lower than micromolar.

Zhou et al. (32) developed a competitive binding assay to investigate the interaction of the viral envelope glycoprotein HIV-1 gp120 with potential oligodeoxynucleotide-based drugs by ACE-LIF using the equilibrium-mixture mode and Scatchard analysis. To establish the assay, a fluorescently tagged 25-mer phosphorothioate oligodeoxynucleotide (GEM) served as probe. The binding of increasing amounts of GEM to gp120 is illustrated in Figure 2A–D. The samples were preincubated for 30 minutes; the electro-

Fig. 2 Representative electropherograms used for the binding studies of phosphorothioate oligodeoxynucleotides and HIV-1 glycoprotein gp120 by ACE-LIF. In the left panel, the dissociation constant between GEM (labeled phosphorothioate oligodeoxynucleotide) and gp120 was measured. The samples contained 40 nM gp120 and 25 nM (A), 31.25 nM (B), 37.5 nM (C), or 43.75 nM (D) of GEM. In the right panel, the competition constant of $Sd(T_2G_4T_2)$ (unlabeled phosphorothioate oligodeoxynucleotide) for the system GEM/gp120 was determined. Samples of 40 nM gp120 and 37.5 nM GEM with concentrations of $Sd(T_2G_4T_2)$ of 0 μM (E), 0.156 μM (F), 0.313 μM (G), 0.625 μM (H), 1.25 μM (I), or 2.5 μM (K) were used. Additionally, all samples contained 6.25 nM fluorescein-labeled proline as internal marker. (Reprinted with permission from Ref. 32. Copyright 2000, Academic Press.)

© 2003 by Marcel Dekker, Inc.

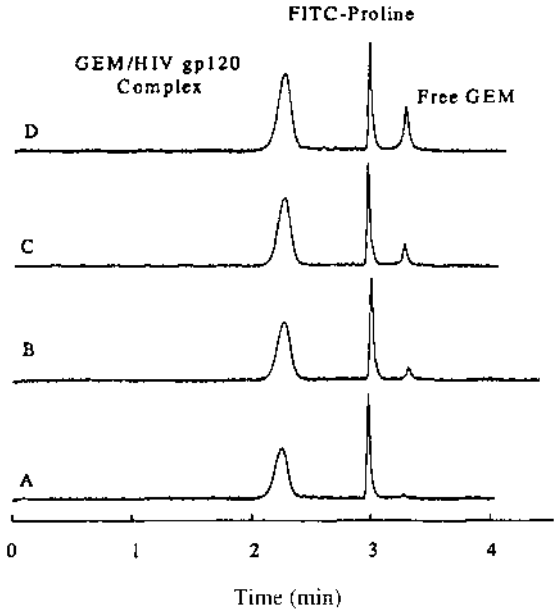

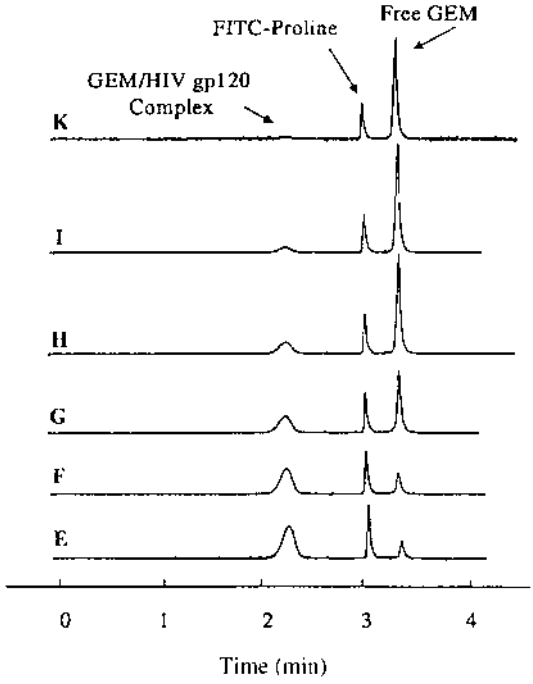

© 2003 by Marcel Dekker, Inc.

pherograms show peaks for the internal marker FITC-proline, the GEM-gp120 complex, and the unbound GEM. A dissociation constant of 0.98 nM was determined. Then the competition of unlabeled drug candidates with the GEM-gp120 binding was examined. The electropherograms utilizing the phosphorothioate oligodeoxynucleotide Sd ($T_2G_4T_2$) are shown in Figure 2E–K. The increasing amount of Sd displaces the GEM from gp120. Therefore the peak representing the unbound GEM increases and the GEM-gp120 complex peak decreases. The simultaneously built Sd-gp120 complex is not labeled and hence is not detected in ACE-LIF.

An example using ACE-LIF for the trace analysis of a drug in biological fluids was presented by the Karger group (33). The interaction of human carbonic anhydrase II with the glaucoma drug dorzolamide was utilized. The carbonic anhydrase was fluorescently labeled at its single cysteine residue and the equilibrium-mixture mode was employed. However, the complex could not be separated from the unbound protein. Therefore a known but weak-binding ligand of carbonic anhydrase, para-carboxybenzenesulfonamide, was added to the background buffer. The labeled protein was preequilibrated with the tight-binding drug dorzolamide and subjected to ACE-LIF. Aside from the peak for the drug–protein complex, a peak for the excess protein emerges that is shifted because of the interaction with the weak-binding ligand in the background buffer. Using this approach, detection limits for dorzolamide of 16.5 pM in aqueous solution and of 62.5 pM in both urine and plasma were achieved.

Affinity capillary electrophoresis is, as already mentioned, also suitable for screening procedures. The aim in this case is not to gain a binding constant for a special protein–ligand interaction but to identify potential binding partners throughout a pool or even a combinatorial library of drugs or other ligands, such as peptides and oligonucleotides (34–36). The hyphenation to mass spectrometry seems an especially promising approach; this is discussed in more detail in Chapter 13.

B. Binding to Plasma Proteins

It is well known that a lot of drugs more or less show affinity to plasma proteins, especially albumins, AGP, and lipoproteins. This binding is somewhat conflicting. Actually, the affinity is unintentional, because the plasma proteins are in general not the targets where drugs should exhibit their pharmacological effect. However, it is now accepted that the binding acts as transport mechanism and has the advantage of preventing the drugs from metabolizing, which could prolong drug efficacy. On the other hand, the binding impedes drug activity, because only the unbound drug fraction can diffuse from blood to the extravascular action site. The situation is further

© 2003 by Marcel Dekker, Inc.

complicated by a few other problems. Some drugs are administered in doses at or above plasma protein binding capacity. In this case the dose-response curve is nonlinear. The binding capacity may be reached even earlier in cases where several drugs are administered simultaneously. Because plasma proteins possess more than one binding site, drug–drug displacement is likely to occur but is hard to predict and may result in side effects. Furthermore, the plasma protein content and ratio vary in individuals, depending, for example, on age, gender, and diseases. Finally, most drugs are chiral compounds, and the enantiomers may exhibit a different activity. However, some of these drugs are administered as racemic mixtures, and the binding to the plasma proteins may also be enantioselective, thereby changing the original enantiomeric ratio. The careful investigation of the interaction of drugs with plasma proteins is therefore imperative to gain straight information about the pharmacokinetics and pharmacodynamics of a drug. Affinity capillary electrophoresis is increasingly recognized as a useful method for delivering data of interest. It is especially attractive because of the opportunity to get information about enantioselective properties without the need to have the purified enantiomers.

Serum albumin has two primary hydrophobic binding sites, known as site I and site II, which are located in domains IIA and IIIA, respectively. Bulky heterocyclic anions with a centered charge are characteristic site I ligands, whereas site II ligands are in general aromatic compounds with a peripherally located charge if any (37).

Kraak et al. (38) reported the first ACE application to study drug binding to a plasma protein. They used the model system warfarin–human serum albumin (HSA) to compare the suitability of the Hummel–Dreyer, frontal analysis, and vacancy peak methods. A more methodologically intended paper from Erim and Kraak (39) used VACE to study the displacement of warfarin from bovine serum albumin (BSA) by furosemide and phenylbutazone. They concluded that VACE is especially suited to examining competitive properties of simultaneously administered compounds toward a given protein–drug system.

Shibukawa et al. (40) discussed the frontal analysis method, also called high-performance frontal analysis (HPFA) or high-performance capillary electrophoresis/frontal analysis (HPCE/FA), compared it to conventional methods, and focused on the application to stereoselective protein binding. The affinity of the drugs warfarin, verapamil, and carbamazepine and the drug candidate BOF-4272 to HSA was investigated.

Ding et al. (41) determined the binding constants and the number of binding sites on one protein molecule of propranolol and verapamil to HSA using frontal analysis. The obtained binding constant was in good agreement with reported results using equilibrium dialysis. In a subsequent paper (42),

© 2003 by Marcel Dekker, Inc.

the study was extended to examine the binding of verapamil and propranolol enantiomers to HSA by frontal analysis. It was found that R-verapamil has a 1.7 times higher affinity to HSA than the S-enantiomer, whereas no stereoselectivity for propranolol was observed. Furthermore, the verapamil-HSA binding system was subjected to displacement interactions by ibuprofen, bupivacaine, and warfarin to gain information about the occupied binding sites of the verapamil enantiomers on HSA based on the knowledge that warfarin binds to site I and ibuprofen binds to site II of HSA. Moreover (43), HSA and BSA were used as chiral selectors to separate ofloxazin, propranolol, and verapamil enantiomers. With ketoprofen and warfarin as displacers, preferred binding sites at both proteins were discussed.

Fung et al. (44) studied the interaction of bilirubin, a product of heme degradation, with HSA by frontal analysis. They examined especially the displacement of bilirubin by aspirin. It was found that the free-bilirubin concentration increased to a clinically significant level when increasing amounts of aspirin were added.

The interaction of the herbicides atrazine and 2,4-D with HSA was investigated by Purcell et al. (45) using the equilibrium-mixture mode. The study was based on the suggestion that HSA serves as carrier protein to transport the herbicides to target organs to exhibit toxicological effects in vivo. The results were combined with data gained from spectroscopic methods.

Moody et al. (46) investigated the interaction of indocyanine green, a tricarbocyanine dye used for medical imaging, with HSA. The dye is only weakly fluorescent in the near-infrared region; but when it binds noncovalently to the protein, its fluorescence is greatly enhanced. The separation of the free and complexed dye is described, and the advantages of noncovalent labeling and diode-LIF are discussed. The same approach was used by Sowell et al. (47) to develop a competitive assay for the determination of binding constants of drugs to HSA by a dye-displacement technique. A heptamethine cyanine dye was employed as noncovalent label for serum albumin, and the displacement of the dye by drugs known to bind to site II of serum albumins (ketoprofen, ibuprofen, quinidine, naproxen, imipramine, clofibrate) was investigated. Figure 3 illustrates the separation of the dye and the dye–HSA complex (Fig. 3A) as well as the competitive binding of quinidine (Fig. 3B) and ketoprofen (Fig. 3C). The applicability of the approach to enantioselective binding is also demonstrated.

In one of the earlier papers, Sun et al. (48) estimated the binding constants of ibuprofen, flurbiprofen, and ketoprofen to HSA and BSA using the mobility-shift mode of ACE. In this case the drugs were actually used as additives to the background buffer to improve the separation of albumin proteins. This is the opposite approach to what is presented in the next

© 2003 by Marcel Dekker, Inc.

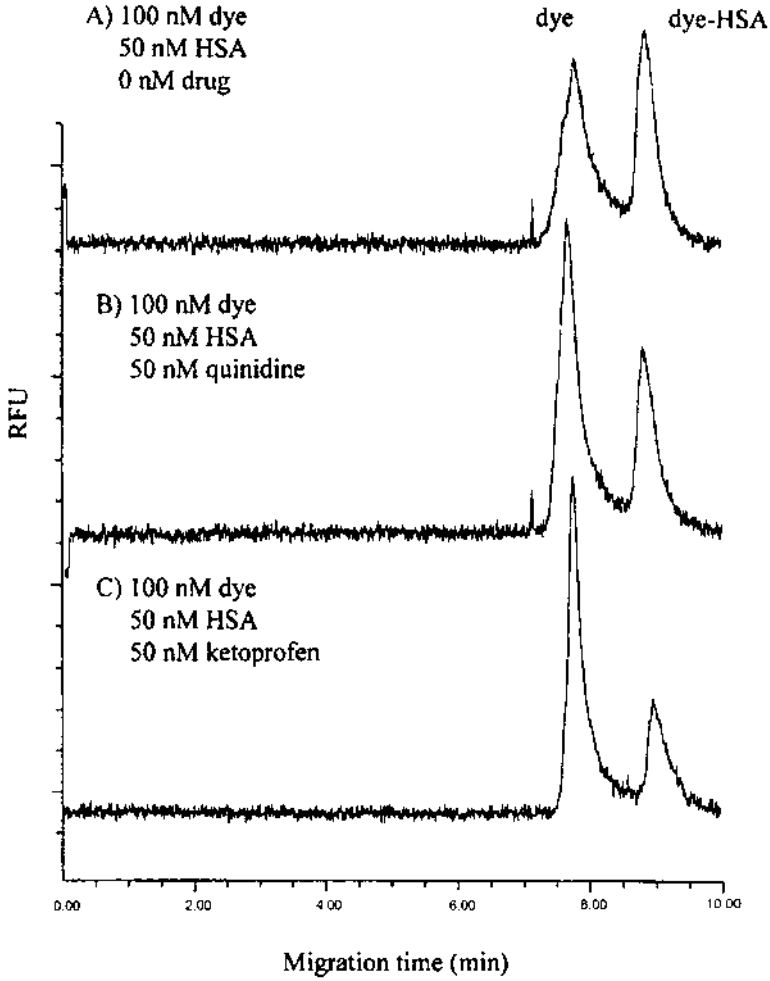

Fig. 3 Electropherograms illustrating the competitive binding of ketoprofen and quinidine to noncovalently dye-labeled human serum albumin. 100 nM heptamethine cyanine dye and (A) 50 nM human serum albumin, (B) 50 nM human serum albumin, 50 nM quinidine, (C) 50 nM human serum albumin, 50 nM ketoprofen. (Reprinted with permission from Ref. 47. Copyright 2001 Wiley-VCH.)

© 2003 by Marcel Dekker, Inc.

section of this chapter, where the proteins are utilized as buffer additives to reach the separation of drug enantiomers.

Another plasma protein that is especially known to bind basic drugs is AGP. It consists of a single polypeptide chain containing 181 amino acids. The five-carbohydrate chains, which are attached to asparagine residues, make it highly glycosylated up to about 45% of its molecular weight. AGP is negatively charged mainly because of the endterminal sialyl residues. Reasons for the observed microheterogeneity of AGP (49) include different branching types of glycans, the distribution on the five glycosilation sites, the possible extension of branches by a lactosamine, and linkages between sialyl and galactose residues. In one of the earlier papers, Shibukawa et al. (50) investigated the binding of verapamil to HSA and AGP using frontal analysis. They compared the estimated binding parameters to those derived from conventional methods and discussed the methodological differences applying the frontal analysis mode in HPLC and HPCE.

Oravcova et al. (51) compared the Hummel–Dreyer approach in HPLC and HPCE using the interaction of racemic carvedilol and its individual enantiomers with HSA and AGP. They found only a nonspecific binding of the drug to HSA, with no stereoselectivity. For the binding to AGP, a high-affinity (lower micromolar range) and nonspecific component was identified. Furthermore, the data suggested that the S-enantiomer of carvedilol binds more strongly to the high-affinity binding site of AGP than the R-enantiomer.

In a similar study, the Hummel–Dreyer method was used for the investigation of the affinity of frusemide, ceftriaxone, and ICI 118551 to HSA and AGP, and a focus was also set on a comparison with HPLC results (52).

Amini and Westerlund (53) evaluated the association constants between the drug enantiomers of disopyramide and remoxipride to AGP by applying a partial-filling technique, which is discussed in the following section. An interesting finding was the strong temperature dependence of the affinity. The association between the enantiomers and AGP reached a maximum at 25°C and decreased at both lower and higher temperatures. It was argued that the effect was due to conformational changes of AGP with varying temperature.

In a couple of subsequent papers, the Shibukawa group investigated how far the carbohydrate chains of AGP are involved in the enantioselective binding of drugs, using frontal analysis (54–56). One paper dealt with the function of the end-terminal sialic acid groups (54) and employed verapamil and propranolol as model drugs and AGP and desialylated AGP as interacting proteins. Representative frontal analysis electropherograms of verapamil are shown in Figure 4. The binding of AGP (Fig. 4B) and asialo AGP (Fig. 4C) to the verapamil enantiomers is visualized by the decrease of the peaks representing the unbound drug concentration, compared to the electrophe-

© 2003 by Marcel Dekker, Inc.

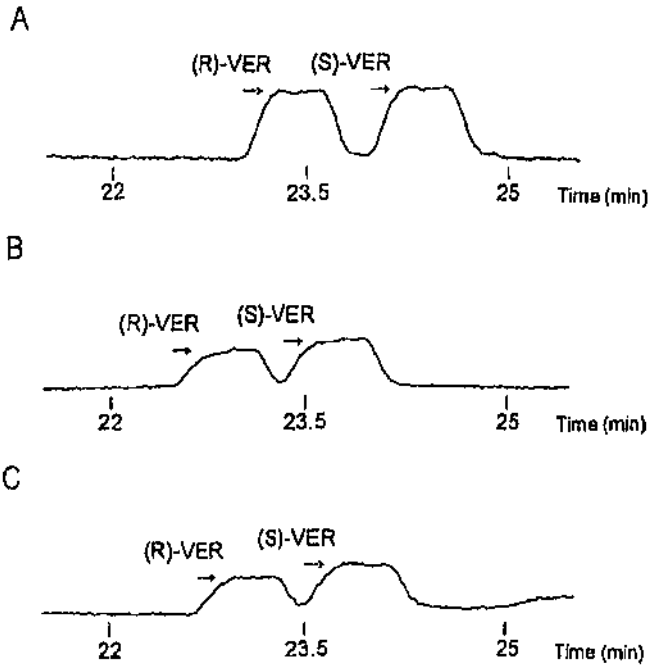

Fig. 4 Stereoselective binding study of verapamil to AGP and desialylated AGP using frontal analysis. Electropherograms of 50 μM racemic verapamil solution (A), 50 μM verapamil solution in 50 μM human α1-acidic glycoprotein solution (B), and 50 μM verapamil solution in 50 μM asiaolo α1-acidic glycoprotein solution (C). (Reprinted with permission from Ref. 54. Copyright 2001 Elsevier Science.)

rogram without AGP (Fig. 4A). Both proteins exhibit a higher affinity for the R-enantiomer, but the affinity is not affected by the desialylation. A β-cyclodextrin derivative served as chiral selector in these experiments. It was found, however, that the sialic acid groups are involved in the enantioselectivity toward the propranolol isomers. Another study employed the same drugs and investigated the role of branching glycan of AGP in the enantioselective binding (55). AGP was separated by lectin affinity chromatography in two subfractions, one containing AGP with biantennary oligosaccharide chains and the other containing AGP void of glycan chains. The results suggested that the branching type of glycan chains does not play a significant role in the chiral recognition of verapamil and propranolol. AGP consists of different isoenzymes coded by different genes and also varying in amino acids near the drug binding site. Two of these genetic variants were investigated regarding their enantioselective binding of disopyramide and ve-

© 2003 by Marcel Dekker, Inc.

rapamil (56). It was found that the isoenzymes differ significantly in their affinity to the disopyramide enantiomers but not to the verapamil isomers.

Furthermore, lipoproteins are plasma proteins known to bind drugs. Lipoproteins consist of a lipophilic core surrounded by a surface layer comprising polar lipids and apolipoproteins. Plasma lipoproteins bind mainly lipophilic neutral drugs and basic drugs. Among the several subclasses, the most important are high-density lipoprotein (HDL) and low-density lipoprotein (LDL) because of their high plasma concentration. Furthermore, LDL is known to suffer from in vivo oxidation, and oxidized LDL has been reported to play an important role in atherogenesis. Binding studies of drugs to lipoproteins are of special interest because of the known significant individual and disease-related differences in plasma lipoprotein concentration.

Mohamed et al. investigated the binding of nilvadipine (57) and verapamil (58) to plasma lipoproteins by frontal analysis. It was found that the total binding affinity of both drugs to LDL was about seven times stronger than to HDL. The oxidation of LDL further enhanced the binding affinity by about an order of magnitude. No stereoselectivity of the binding was observed. The study was then extended to different states of oxidation (59). The binding affinity of both drugs increased with increasing oxidation levels of LDL, but the extent was significantly higher for verapamil.

McDonnell et al. (60) focused on the fact that the unbound drug concentration depends on the sum of binding to all involved plasma proteins. Therefore they determined the binding capacity of a series of beta-adrenoceptor blocking drugs to individual plasma proteins HSA and AGP, to a mixture of HSA, AGP, HDL, and LDL, as well as to whole serum, by frontal analysis. The approach allowed them to subdivide the drugs into high and low binding categories.

C. Proteins as Chiral Selectors

Enantiomers are stereoisomers that do not differ in chemical properties. A separation is therefore possible only by using the interaction with another chiral reagent. The diastereomeric complexes built thereby can possess different chemical properties. In HPLC, the part of the chiral reagent is played most often by a chiral stationary phase. In HPCE, the chiral reagent is usually not immobilized, but mixed to the background buffer and therefore considered a pseudostationary phase. The use of proteins as chiral selectors to separate drug enantiomers in capillary electrophoresis is not an ACE experiment with the aim of gaining binding information, but it takes advantage of the affinity of proteins to drugs and is discussed shortly here. Chiral separations by capillary electrophoretic methods compete in general with well-established HPLC procedures. HPCE is advantageous with respect to

© 2003 by Marcel Dekker, Inc.

cost efficiency and environmental aspects. It is less expensive, because there are no chiral columns necessary and it uses very small volumes of buffer solutions instead of considerable amounts of organic solvents. A disadvantage, compared to HPLC, is the higher concentration detection limit, which is, however, redeemed in part by the opportunity to detect at lower wavelength, where the absorption of drugs is usually higher. Using HPCE for chiral separations, proteins compete with other chiral selectors, especially cyclodextrins, but also carbohydrates, peptides, or amino acids. Here, proteins may not be the first choice, because of the known disadvantages arising from adsorption on the inner capillary wall and inherent high UV absorbance, which further increases the detection limit. Most researchers try to overcome the adsorption difficulties by utilizing coated capillaries. To solve the problem of high background absorbance, the partial-filling (partial-separation-zone) technique was developed (61,62). As the name suggests, the capillary is not completely filled with the buffer solution containing the protein. Hence the detection window is not blocked by a high-absorbance protein solution. An advantage of proteins as chiral selectors might be the broader application range, because of the more and different binding opportunities. Among proteins, the one known to interact with different drugs, such as plasma proteins, are preferable. Separations of drug enantiomers using proteins as chiral selectors are visualized in Figures 5 and 6. Figure 5 illustrates the separation of epinastine using BSA as chiral selector and

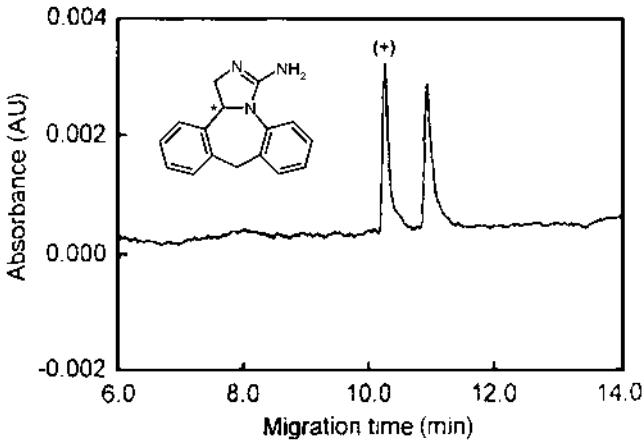

Fig. 5 Separation of (±)-epinastine by capillary electrophoresis using the partial-separation-zone technique and bovine serum albumin as chiral selector. (Reprinted with permission from Ref. 62. Copyright 1995 Elsevier Science.)

© 2003 by Marcel Dekker, Inc.

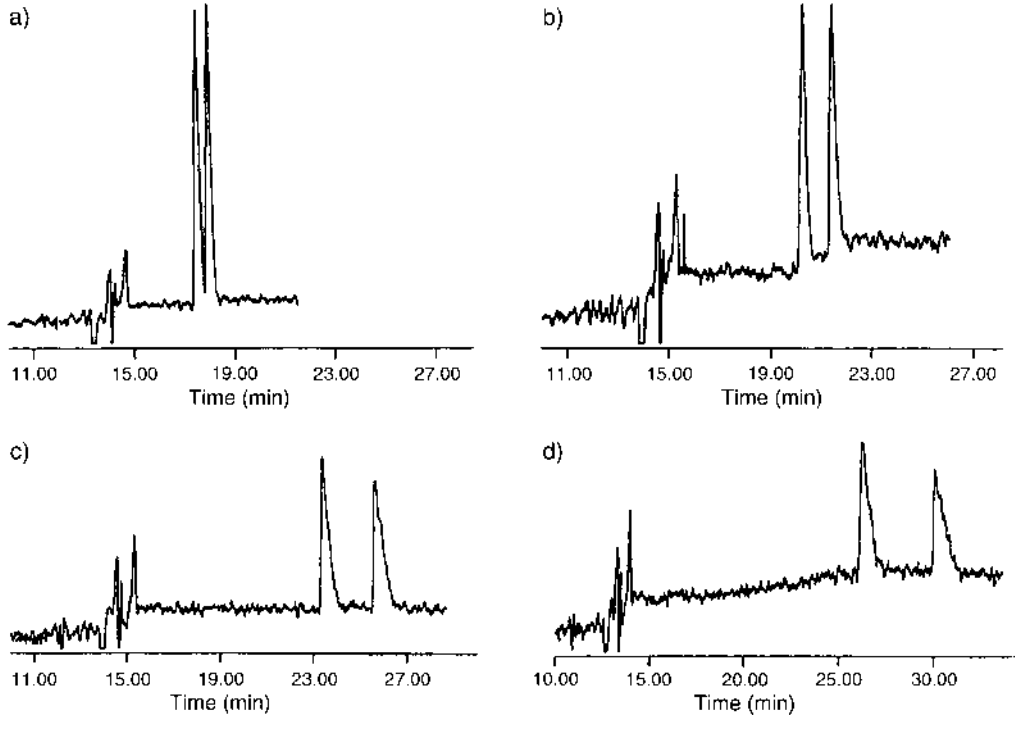

Fig. 6 Effect of slight pH changes on the separation of (±)-pantoprazole. A phosphate buffer (10 mM) containing 55 μM bovine serum albumin and 5% 1-propanol was used. The buffer was adjusted to (a) pH 7.3, (b) pH 7.4, (c) pH 7.6, (d) pH 7.9. (Reprinted with permission from Ref. 63. Copyright 1997 Elsevier Science.)

© 2003 by Marcel Dekker, Inc.

employing the partial-separation-zone technique (62). The separation of pantoprazole enantiomers is shown in Figure 6 (63). It is noteworthy here that even quite small deviations of background buffer pH can lead to considerable changes in separation efficiency. Table 1 summarizes the application of proteins as chiral selectors for the separation of drug enantiomers. Readers more interested in this field are referred to recent reviews by Tanaka and Terabe (64) and Haginaka (65). A further review by De Lorenzi and Massolini (66) deals only with riboflavin-binding proteins but contains an illustrative comparison to HPLC results.

IV. PROTEIN–PROTEIN INTERACTIONS

Protein–protein interactions are key processes in signaling pathways and therefore are a preferred subject of biochemical research. Examples for tight-binding interactions are those of protein antigens to the corresponding antibodies. Other interactions are, however, frequently rather weak to moderate, leading to slight conformational changes or introducing or cleaving small functional groups, which is nevertheless enough to activate or inhibit the target protein. Such interactions are much harder to catch by an analytical method, because they are more likely to be disturbed or aborted by the examining method itself. In that respect, ACE offers the advantage of maintaining nearly native conditions. But the analysis of protein–protein interactions by ACE is hampered mainly by the difficulties arising from high protein content in the running buffer, as discussed earlier. Several examples of antigen–antibody interactions using ACE were reported. These investigations focus more on the measurement of analyte concentrations than on the estimation of binding constants. HSA (96), BSA (97), GFP (98), human growth hormone (99,100), and insulin (101) served as antigens. These examinations are discussed in more detail in Chapter 12, ''Characterization of Immunoreactions.''

There are only a very few reports dealing with ACE investigations of weak to moderate protein–protein interactions, which are interestingly related to HIV research. The ACE technique was used to detect interactions of HIV proteins with possible target proteins of cells. Cellular proteins of T cells were identified as being involved in the incorporation of HIV. The proteins mediated the virus incorporation by binding viral proteins. In combination with surface plasmon resonance ACE, equilibrium-mixture analysis was able to detect the protein–protein interaction by changes in the mobility (102,103). Subsequent studies revealed that some viral proteins share the same binding motif with interferon type I, which was used to explain the regulatory effect on the proliferation of lymphocytes. And ACE was em-

© 2003 by Marcel Dekker, Inc.

Table 1 Separation of Drug Enantiomers by CE Using Proteins as Chiral Selectors

Chiral selector protein	Drugs investigated	Refs.
Bovine serum albumin	Epinastine, homochlorcyclizine, oxyphencyclimine, propranolol, trimebutine	62
	Promethazine	67
	DR-3862, ofloxazin, warfarin	68
	Warfarin	69
	Lamsoprazole, omeprazole, pantoprazole	63
	Ibuprofen, leucovorine	70
	Leucovorine	71
Human serum albumin	Kynurenine	72
	Promethazine, propranolol, propiomazine, thioridazine, verapamil	43, 67, 73–78
Other serum albumins	Ofloxazin	79
α_1-Acid glycoprotein	Promethazine	69
	Disopyramide	80
	Disopyramide, remoxipride	53
	Clorprenaline	62
	Acebutorol, arotinolol, atropine, bupivacaine, clorprenaline, denopamine, eperisone, epinastine, etirefline, fenoterol, homatropine, ketamine, metanephrine, metoprolol, mexiletine, nicardipine, oxyphencyclimine, phenylephrine, pindolol, primaquine, promethazine, sulpiride, terbutaline, tolperizone, trihexyphenidyl, trimebutine, trimetoquinol, trimipramine, verapamil	81
Avidin	Flurbiprofen, ibuprofen, ketoprofen, warfarin	82–84
Succinyl avidin	Bupivacaine, primaquine, trimipramine	83
Streptavidin	Chlorpheniramine, flurbiprofen, ibuprofen, primaquine, trimipramine, warfarin	83

© 2003 by Marcel Dekker, Inc.

Table 1 Continued

Chiral selector protein	Drugs investigated	Refs.
Ovomucoid	Chlorpheniramine, eperisone, tolperisone	85
	Arotinolol, bunitrolol, chlorpheniramine, oxyphencyclimine, pindolol, primaquine, tolperisone, trimebutine, verapamil	62, 86
Ovoglycoprotein	Chlorpheniramine, eperisone, primaquine, tolperisone, verapamil	87
	Alimemazine, chlorpheniramine, eperisone, pindolol, prenylamine, promethazine, thioridazine, tolperisone, trimipramine	88
Conalbumin	Trimetoquinol	62
Cellobiohydrolase I	Alprenolol, labetolol, metoprolol, oxprenolol, pindolol, propranolol, warfarin	61, 89
Fungal cellulase	Pindolol	69
Human serum transferrin	Acebutorol, bupivacaine, labetolol, promethazine, propranolol	90
	Buphenine, clofedanol, chlorpheniramine	91
Pepsin	Cloperastine, oxprenolol, promethazine, propranolol, trimipramine, verapamil	92
Riboflavin-binding protein	Amlodipine, bepridil, lorazepam, nicardipine, nimodipine, oxazepam, practolol, verapamil	93
	Aminogluthethimide, fenoprofen, flurbiprofen, ibuprofen, ketoprofen, oxprenolol, pranoprofen, proglumide	94
	Amlodipine, bepridil, bupivacaine, oxprenolol, prilocaine	95

© 2003 by Marcel Dekker, Inc.

ployed to demonstrate the binding of interferon type I to the cellular receptor protein of the viral protein (104).

The HIV capsid protein p24 plays an important role in virus infectivity. Its interaction with cyclophilins from host cells is a crucial event in viral replication. For the determination of binding data of p24 to cyclophilins, several methods, such as enzymatic assays, surface plasmon resonance, and isothermal titration calorimetry, were used. Furthermore, Kiessig et al. (105) used ACE to explore this protein–protein interaction. It is noteworthy that in this case the equilibrium-mixture approach was successfully applied to determine binding data on the interaction of p24 with a cyclophilin fusion protein, although the dissociation constant was in the range of 10^{-5} M. Representative electropherograms are illustrated in Figure 7. They clearly show a shift of the peak of the fusion protein with increasing amounts of p24 in the pre-equilibrated sample. This shift was used to determine a dissociation constant of $(20 \pm 1.5) \times 10^{-6}$ M. The fluorescent properties of the fusion partner GFP were utilized to screen for putative cyclophilin interaction partners in crude cellular extracts using ACE-LIF.

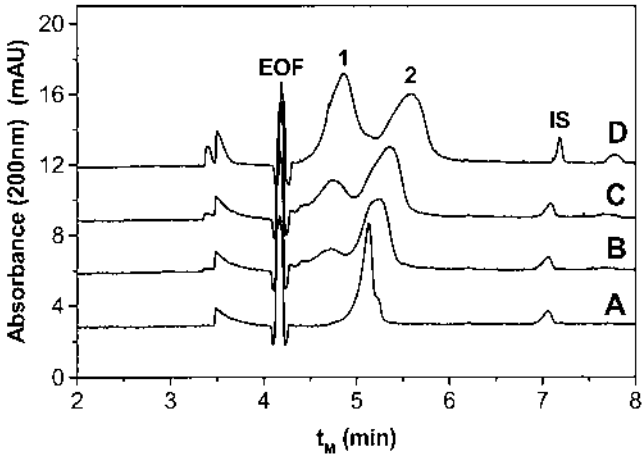

Fig. 7 Monitoring the protein–protein interaction of p24 (1) and rDmCyp20-GFP (2) using ACE. Samples of rDmCyp20-GFP (6 μM) were incubated with increasing concentrations of p24: 0 μM p24 (A), 6 μM p24 (B), 12.5 μM p24 (C), 22 μM p24 (D). EOF indicates the position of the electroosmotic flow marker DMSO. The position of the internal standard Ac-Ala-Ala is marked *IS*. (Reprinted with permission from Ref. 105. Copyright 2001 Wiley-VCH.)

© 2003 by Marcel Dekker, Inc.

V. CONCLUSIONS

It is not hard to predict that with the output of genomics and proteomics, the number of proteins that can be related to specific diseases will increase tremendously in the next few years. Therefore methods that are able to screen combinatorial libraries in the search for interacting drugs are desperately required. Furthermore, efforts to re-examine known drugs for potential interactions with newly identified target proteins will increase, because it lowers costs considerably if a drug that has already passed the regulatory procedures can also be applied to cure a further disease.

The ACE technique has been established as a valuable tool for investigating drug–protein interactions. In comparison to traditional methods it is advantageous with respect to the speed of analysis, the minimum volume consumption, and the ability to separate drug enantiomers. And ACE may therefore be the method of choice in cases where proteins are scarce and difficult to obtain or the stereoselectivity of drug interactions is of special interest. The feasibility of automation makes it additionally attractive for screening procedures. However, up to now the lack of parallel operation in commercial instruments has hampered the opportunity of high-throughput analysis.

ABBREVIATIONS

ACE	affinity capillary electrophoresis
AGP	α_1-acid glycoprotein
BSA	bovine serum albumin
CEC	capillary electrochromatography
CGE	capillary gel electrophoresis
CZE	capillary zone electrophoresis
FDA	Food and Drug Administration
FITC	fluorescein isothiocyanate
GFP	green fluorescent protein
HDL	high-density lipoprotein
HIV	human immunodeficiency virus
hGH	human growth hormone
HPCE	high-performance capillary electrophoresis
HPLC	high-performance liquid chromatography
HSA	human serum albumin
LDL	low-density lipoprotein
LIF	laser-induced fluorescence
MS	mass spectrometry

© 2003 by Marcel Dekker, Inc.

NMR	nuclear magnetic resonance
UV	ultraviolet
VACE	vacancy affinity capillary electrophoresis

REFERENCES

1. IJ Colton, JD Carbeck, J Rao, GM Whitesides. Affinity capillary electrophoresis: a physical-organic tool for studying interactions in biomolecular recognition. Electrophoresis 19:367–382, 1998.
2. NHH Heegaard, S Nilsson, NA Guzman. Affinity capillary electrophoresis: important application areas and some recent developments. J Chromatogr B 715:29–54, 1998.
3. YH Chu, CC Cheng. Affinity capillary electrophoresis in biomolecular recognition. Cell Mol Life Sci 54:663–683, 1998.
4. DS Hage, SA Tweed. Recent advances in chromatographic and electrophoretic methods for the study of drugprotein interactions. J Chromatogr B 699:499–525, 1997.
5. J Oravcova, B Böhs, W Lindner. Drug–protein binding studies. New trends in analytical and experimental methodology. J Chromatogr B 677:1–28, 1996.
6. RHH Neubert, MA Schwarz, Y Mrestani, M Plätzer, K Raith. Affinity capillary electrophoresis in pharmaceutics. Pharm Res 16:1663–1673, 1999.
7. R Kaliszan. Chromatography and capillary electrophoresis in modeling the basic processes of drug action. Trends Anal Chem 18:400–410, 1999.
8. KL Rundlett, DW Armstrong. Methods for the determination of binding constants by capillary electrophoresis. Electrophoresis 22:1419–1427, 2001.
9. MHA Busch, LB Carels, HFM Boelens, JC Kraak, H Poppe. Comparison of five methods for the study of drug–protein binding in affinity capillary electrophoresis. J Chromatogr A 777:311–328, 1997.
10. MHA Busch, JC Kraak, H Poppe. Principles and limitations of methods available for the determination of binding constants with affinity capillary electrophoresis. J Chromatogr A 777:329–353, 1997.
11. MHA Busch, HFM Boelens, JC Kraak, H Poppe. Vacancy affinity capillary electrophoresis, a new method for measuring binding constants. J Chromatogr A 775:313–326, 1997.
12. YH Chu, GM Whitesides. Affinity capillary electrophoresis can simultaneously measure binding constants of multiple peptides to vancomycin. J Org Chem 57:3524–3525, 1992.
13. YH Chu, LZ Avila, HA Biebuyck, GM Whitesides. Using affinity capillary electrophoresis to identify the peptide in a peptide library that binds most tightly to vancomycin. J Org Chem 58:648–652, 1993.
14. FA Gomez, JK Chen, A Tanaka, SL Schreiber, GM Whitesides. Affinity capillary electrophoresis: insights into the binding of SH3 domains by peptides derived from an SH3-binding protein. J Org Chem 59:2885–2886, 1994.
15. FA Gomez, LZ Avila, YH Chu, GM Whitesides. Determination of binding

© 2003 by Marcel Dekker, Inc.

constants of ligands to proteins by affinity capillary electrophoresis: compensation for electroosmotic flow. Anal Chem 66:1785–1791, 1994.
16. YH Chu, LZ Avila, HA Biebuyck, GM Whitesides. Use of affinity capillary electrophoresis to measure binding constants of ligands to proteins. J Med Chem 35:2915–2917, 1992.
17. LZ Avila, YH Chu, EC Blossey, GM Whitesides. Use of affinity capillary electrophoresis to determine kinetic and equilibrium constants for binding of arylsulfonamides to bovine carbonic anhydrase. J Med Chem 36:126–133, 1993.
18. NHH Heegaard, FA Robey. Use of capillary zone electrophoresis to evaluate the binding of anionic carbohydrates to synthetic peptides derived from human serum amyloid P component. Anal Chem 64:2479–2482, 1992.
19. NHH Heegaard, HD Mortensen, P Roepstorff. Demonstration of a heparin-binding site in serum amyloid P component using affinity capillary electrophoresis as an adjunct technique. J Chromatogr A 717:83–90, 1995.
20. YH Chu, WJ Lees, A Stassinopoulos, CT Walsh. Using affinity capillary electrophoresis to determine binding stoichiometries of protein–ligand interaction. Biochemistry 33:10616–10621, 1994.
21. J Liu, KJ Volk, MS Lee, M Pucci, S Handwerger. Binding studies of vancomycin to the cytoplasmic peptidoglycan precursors by affinity capillary electrophoresis. Anal Chem 66:2412–2416, 1994.
22. J Kawaoka, FA Gomez. Use of mobility ratios to estimate binding constants of ligands to proteins in affinity capillary electrophoresis. J Chromatogr B 715:203–210, 1998.
23. E Mito, FA Gomez. Flow-through partial-filling affinity capillary electrophoresis for the estimation of binding constants of ligands to receptors. Chromatographia 50:689–697, 1999.
24. E Mito, Y Zhang, S Esquivel, FA Gomez. Estimation of receptor–ligand interactions by the use of a two-marker system in affinity capillary electrophoresis. Anal Biochem 280:209–215, 2000.
25. CV Thomas, AC Cater, JJ Wheeler. HPCE as an analytical probe for assessing irreversible ligand/macromolecule binding interactions. J Liq Chromatogr 16: 1903–1921, 1993.
26. S Kiessig, H Bang, F Thunecke. Interaction of cyclophilin and cyclosporins monitored by affinity capillary electrophoresis. J Chromatogr A 853:469–477, 1999.
27. YL Hsieh, J Cai, YT Li, JD Henion, B Ganem. Detection of noncovalent FKBP-FK506 and FKBP-Rapamycin complexes by capillary electrophoresis–mass spectrometry and capillary electrophoresis–tandem mass spectrometry. J Am Soc Mass Spectrom 6:85–90, 1995.
28. K Nadeau, SG Nadler, M Saulnier, MA Tepper, CT Walsh. Quantitation of the interaction of the immunosuppressant deoxyspergualin and analogs with Hsc70 and Hsp90. Biochemistry 33:2561–2567, 1994.
29. J Liu, KJ Volk, MS Lee, EH Kerns, IE Rosenberg. Affinity capillary electrophoresis applied to the studies of interactions of a member of heat shock

© 2003 by Marcel Dekker, Inc.

protein family with an immunosuppressant. J Chromatogr A 680:395–403, 1994.
30. J Liu, S Abid, ME Hail, MS Lee, J Hangeland, N Zein. Use of affinity capillary electrophoresis for the study of protein and drug interactions. Analyst 123:1455–1459, 1998.
31. E De Lorenzi, C Galbusera, V Bellotti, P Mangione, G Massolini, E Tabolotti, A Andreola, G Caccialanza. Affinity capillary electrophoresis is a powerful tool to identify transthyretin-binding drugs for potential therapeutic use in amyloidosis. Electrophoresis 21:3280–3289, 2000.
32. W Zhou, KB Tomer, MG Khaledi. Evaluation of the binding between potential anti-HIV DNA-based drugs and viral envelope glycoprotein gp120 by capillary electrophoresis with laser-induced fluorescence detection. Anal Biochem 284:334–341, 2000.
33. RC Tim, RA Kautz, BL Karger. Ultratrace analysis of drugs in biological fluids using affinity probe capillary electrophoresis: analysis of dorzolamide with fluorescently labeled carbonic anhydrase. Electrophoresis 21:220–226, 2000.
34. YH Chu, YM Dunayevskiy, DB Kirby, P Vouros, BL Karger. Affinity capillary electrophoresis–mass spectrometry for screening combinatorial libraries. J Am Chem Soc 118:7827–7835, 1996.
35. S Sun, J Headrick, T Staller, M Sepaniak. Evaluation of a capillary electrophoretic method for rapid screening of single-component combinatory libraries. J Microcolumn Sep 10:653–660, 1998.
36. DI Papac, Z Shahrokh. Mass spectrometry innovations in drug discovery and development. Pharm Res 18:131–145, 2001.
37. T Peters. All about albumin: biochemistry, genetics, and medical applications. Academic Press, San Diego, CA, 1996, pp 76–131.
38. JC Kraak, S Busch, H Poppe. Study of protein–drug binding using capillary zone electrophoresis. J Chromatogr 608:257–264, 1992.
39. FB Erim, JC Kraak. Vacancy affinity capillary electrophoresis to study competitive protein-drug binding. J Chromatogr A 710:205–210, 1998.
40. A Shibukawa, Y Kuroda, T Nakagawa. High-performance frontal analysis for drug–protein binding study. J Pharm Biomed Anal 18:1047–1055, 1999.
41. Y Ding, X Zhu, B Lin. Capillary electrophoresis study of human serum albumin binding to basic drugs. Chromatographia 49:343–346, 1999.
42. Y Ding, X Zhu, B Lin. Study of interaction between drug enantiomers and serum albumin by capillary electrophoresis. Electrophoresis 20:1890–1894, 1999.
43. X Zhu, Y Ding, B Lin, A Jakob, B Koppenhoefer. Study of enantioselective interactions between chiral drugs and serum albumin by capillary electrophoresis. Electrophoresis 20:1869–1877, 1999.
44. YS Fung, DX Sun, CY Yeung. Capillary electrophoresis for determination of free and albumin-bound bilirubin and the investigation of drug interaction with bilirubin-bound albumin. Electrophoresis 21:403–410, 2000.
45. M Purcell, JF Neault, H Malonga, H Arakawa, R Carpentier, HA Tajmir-Riahi. Interactions of atrazine and 2,4-D with human serum albumin studied

© 2003 by Marcel Dekker, Inc.

by gel and capillary electrophoresis, and FTIR spectroscopy. Biochim Biophys Acta 1548:129–138, 2001.
46. ED Moody, PJ Viskari, CL Colyer. Noncovalent labeling of human serum albumin with indocyanine green: a study by capillary electrophoresis with diode laser-induced fluorescence detection. J Chromatogr B 729:55–64, 1999.
47. J Sowell, JC Mason, L Strekowski, G Patonay. Binding constant determination of drugs toward subdomain IIIA of human serum albumin by near-infrared dye-displacement capillary electrophoresis. Electrophoresis 22:2512–2517, 2001.
48. P Sun, A Hoops, RA Hartwick. Enhanced albumin protein separations and protein–drug binding constant measurements using anti-inflammatory drugs as run buffer additives in affinity capillary elctrophoresis. J Chromatogr B 661:335–340, 1994.
49. K Schmid. Human plasma α_1-acid glycoprotein—biochemical properties, the amino acid sequence and the structure of carbohydrate moiety, variants and polymorphism. In: P Baumann, CB Eap, WE Müller, JP Tillement, eds. Alpha$_1$-acid glycoprotein genetics, biochemistry, physiological function, and pharmacology. Alan R. Liss, New York, 1989, pp 7–22.
50. A Shibukawa, Y Yoshimoto, T Ohara, T Nakagawa. High-performance capillary electrophoresis/frontal analysis for the study of protein binding of a basic drug. J Pharm Sci 83:616–619, 1994.
51. J Oravcova, D Sojkova, W Lindner. Comparison of the Hummel–Dreyer method in high-performance liquid chromatography and capillary electrophoresis conditions for study of the interaction of (RS)-, (R)- and (S)-carvedilol with isolated plasma proteins. J Chromatogr B 682:349–357, 1996.
52. MG Quaglia, E Bossu, C DellAquila, M Guidotti. Determination of the binding of a β_2-blocker drug, frusemide and ceftriaxone to serum proteins by capillary zone electrophoresis. J Pharm Biomed Anal 15:1033–1039, 1997.
53. A Amini, D Westerlund. Evaluation of association constants between drug enantiomers and human α_1-acid glycoprotein by applying a partial-filling technique in affinity capillary electrophoresis. Anal Chem 70:1425–1430, 1998.
54. H Shiono, A Shibukawa, Y Kuroda, T Nakagawa. Effect of sialic acid residues of human α_1-acid glycoprotein on stereoselectivity in basic drug–protein binding. Chirality 9:291–296, 1997.
55. Y Kuroda, A Shibukawa, T Nakagawa. The role of branching glycan of human α_1-acid glycoprotein in enantioselective binding to basic drugs as studied by capillary electrophoresis. Anal Biochem 268:9–14, 1999.
56. Y Kuroda, Y Kita, A Shibukawa, T Nakagawa. Role of biantennary glycans and genetic variants of human α_1-acid glycoprotein in enantioselective binding of basic drugs as studied by high-performance frontal analysis/capillary electrophoresis. Pharm Res 18:389–393, 2001.
57. NAL Mohamed, Y Kuiroda, A Shibukawa, T Nakagawa, S ElGizawy, HF Askal, ME ElKommos. Binding analysis of nilvadipine to plasma lipoproteins by capillary electrophoresis–frontal analysis. J Pharm Biomed Anal 21:1037–1043, 1999.
58. NAL Mohamed, Y Kuroda, A Shibukawa, T Nakagawa, S ElGizawy, HF

© 2003 by Marcel Dekker, Inc.

Askal, ME ElKommos. Enantioselective binding analysis of verapamil to plasma lipoproteins by capillary electrophoresis–frontal analysis. J Chromatogr A 875:447–453, 2000.
59. Y Kuroda, B Cao, A Shibukawa, T Nakagawa. Effect of oxidation of low-density lipoprotein on drug binding affinity studied by high-performance frontal analysis–capillary electrophoresis. Electrophoresis 22:3401–3407, 2001.
60. PA McDonnell, GW Caldwell, JA Masucci. Using capillary electrophoresis/frontal analysis to screen drugs interacting with human serum proteins. Electrophoresis 19:448–454, 1998.
61. L Valtecha, J Mohammad, G Pettersson, S Hjerten. Chiral separations of β-blockers by high-performance capillary electrophoresis based on nonimmobilized cellulase as enantioselective protein. J Chromatogr 638:263–267, 1993.
62. Y Tanaka, S Terabe. Partial separation zone technique for the separation of enantiomers by affinity electrokinetic chromatography with proteins as chiral pseudo-stationary phases. J Chromatogr A 694:277–284, 1995.
63. D Eberle, RP Hummel, R Kuhn. Chiral resolution of pantoprazole sodium and related sulfoxides by complex formation with bovine serum albumin in capillary electrophoresis. J Chromatogr A 759:185–192, 1997.
64. Y Tanaka, S Terabe. Recent advances in enantiomer separations by affinity capillary electrophoresis using proteins and peptides. J Biochem Biophys Methods 48:103–116, 2001.
65. J Haginaka. Enantiomer separation of drugs by capillary electrophoresis using proteins as chiral selectors. J Chromatogr A 875:235–254, 2000.
66. E DeLorenzi, G Massolini. Riboflavin-binding proteins as chiral selectors in HPLC and CE. Pharm Sci Technol Today 2:352–364, 1999.
67. XX Zhang, F Hong, WB Chang, YX Ci, YH Ye. Enantiomeric separation of promethazine and D,L-α-amino-β-[4-(1,2-dihydro-2-oxo-quinoline)] propionic acid drugs by capillary zone electrophoresis using albumins as chiral selectors. Anal Chim Acta 392:175–181, 1999.
68. T Arai, M Ichinose, H Kuroda, N Nimura, T Kinoshita. Chiral separation by capillary affinity zone electrophoresis using an albumin-containing support electrolyte. Anal Biochem 217:7–11, 1994.
69. S Busch, JC Kraak, H Poppe. Chiral separations by complexation with proteins in capillary zone electrophoresis. J Chromatogr 635:119–126, 1993.
70. P Sun, N Wu, GE Barker, RA Hartwick. Chiral separations using dextran and bovine serum albumin as run buffer additives in affinity capillary electrophoresis. J Chromatogr 648:475–480, 1993.
71. GE Barker, P Russo, RA Hartwick. Chiral separation of leucovorin with bovine serum albumin using affinity capillary electrophoresis. Anal Chem 64: 3024–3028, 1992.
72. R Vespalec, V Sustacek, P Bocek. Prospects of dissolved albumin as a chiral selector in capillary zone electrophoresis. J Chromatogr 638:255–261, 1993.
73. DK Lloyd, S Li, P Ryan. Investigation of enantioselective ligand–protein binding and displacement interactions using capillary electrophoresis. Chirality 6:230–238, 1994.

© 2003 by Marcel Dekker, Inc.

74. J Yang, DS Hage. Chiral separations in capillary electrophoresis using human serum albumin as a buffer additive. Anal Chem 66:2719–2725, 1994.
75. A Ahmed, H Ibrahim, F Pastore, DK Lloyd. Relationship between retention and effective selector concentration in affinity capillary electrophoresis and high-performance liquid chromatography. Anal Chem 68:3270–3273, 1996.
76. DK Lloyd, A Ahmed, F Pastore. A quantitative relationship between capacity factor and selector concentration in capillary electrophoresis and high-performance liquid chromatography: evidence from the enantioselective resolution of benzoin using human serum albumin as chiral selector. Electrophoresis 18: 958–964, 1997.
77. DK Lloyd, S Li, P Ryan. Protein chiral selectors in free-solution capillary electrophoresis and packed-capillary electrochromatography. J Chromatogr A 694:285–296, 1995.
78. A Ahmed, DK Lloyd. Effect of organic modifiers on retention and enantiomeric separations by capillary electrophoresis with human serum albumin as a chiral selector in solution. J Chromatogr A 766:237–244, 1997.
79. T Arai, N Nimura, T Kinoshita. Investigation of enantioselective ofloxacin–albumin binding and displacement interactions using capillary affinity zone electrophoresis. Biomed Chromatogr 9:68–74, 1995.
80. A Amini, C Pettersson, D Westerlund. Enantioresolution of disopyramide by capillary electrokinetic chromatography with human α_1-acid glycoprotein (AGP) as chiral selector applying a partial-filling technique. Electrophoresis 18:950–957, 1997.
81. Y Tanaka, S Terabe. Separation of the enantiomers of basic drugs by affinity capillary electrophoresis using a partial-filling technique and α_1-acid glycoprotein as chiral selector. Chromatographia 44:119–128, 1997.
82. Y Tanaka, N Matsubara, S Terabe. Separation of enantiomers by affinity electrokinetic chromatography using avidin. Electrophoresis 15:848–853, 1994.
83. Y Tanaka, S Terabe. Studies of enantioselectivities of avidin, avidin–biotin complex and streptavidin by affinity capillary electrophoresis. Chromatographia 49:489–495, 1999.
84. Y Tanaka, Y Kishimoto, S Terabe. Separation of acidic enantiomers by capillary electrophoresis–mass spectrometry employing a partial filling technique. J Chromatogr A 802:83–88, 1998.
85. Y Ishihama, Y Oda, N Asakawa, Y Yoshida, T Sato. Optical resolution by electrokinetic chromatography using ovomucoid as a pseudo-stationary phase. J Chromatogr A 666:193–201, 1994.
86. S Terabe, H Ozaki, Y Tanaka. New pseudostationary phases for electrokinetic chromatography: A high-molecular surfactant and proteins. J Chin Chem Soc 41:251–257, 1994.
87. J Haginaka, N Kanasugi. Separation of drug enantiomers by capillary zone electrophoresis using ovoglycoprotein as a chiral selector. J Chromatogr A 782:281–288, 1997.
88. H Matsunaga, J Haginaka. Separation of basic drug enantiomers by capillary electrophoresis using ovoglycoprotein as a chiral selector: comparison of chi-

© 2003 by Marcel Dekker, Inc.

ral resolution ability of ovoglycoprotein and completely deglycosylated ovoglycoprotein. Electrophoresis 22:3251–3256, 2001.
89. M Hedeland, R Isaksson, C Pettersson. Cellobiohydrolase I as a chiral additive in capillary electrophoresis and liquid chromatography. J Chromatogr A 807:297–305, 1998.
90. F Kilar. Stereoselective interaction of drug enantiomers with human serum transferrin in capillary zone electrophoresis. Electrophoresis 17:1950–1953, 1996.
91. MG Schmid, G Gübitz, F Kilar. Stereoselective interaction of drug enantiomers with human serum transferrin in capillary zone electrophoresis (II). Electrophoresis 19:282–287, 1998.
92. S Fanali, G Caponecchi, Z Aturki. Enantiomeric resolution by capillary zone electrophoresis: use of pepsin for separation of chiral compounds of pharmaceutical interest. J Microcolumn Sep 9:9–14, 1997.
93. E DeLorenzi, G Massolini, DK Lloyd, HL Monaco, C Galbusera, G Caccialanza. Evaluation of quail egg white riboflavin–binding protein as a chiral selector in high-performance liquid chromatography and capillary electrophoresis. J Chromatogr A 790:47–64, 1997.
94. N Mano, Y Oda, Y Ishihama, H Katayama, N Asakawa. Investigation of interactions between drug enantiomers and flavoprotein as a chiral selector by affinity capillary electrophoresis. J Liq Chromatogr 21:1311–1332, 1998.
95. E DeLorenzi, G Massolini, M Quaglia, C Galbusera, G Caccialanza. Evaluation of quail egg white riboflavin–binding protein as a chiral selector in capillary electrophoresis by applying a modified partial-filling technique. Electrophoresis 20:2739–2748, 1999.
96. YH Chu, WJ Lees, A Stassinopoulos, CT Walsh. Using affinity capillary electrophoresis to determine binding stoichiometries of protein–ligand interactions. Biochemistry 33:10616–10621, 1994.
97. NH Chiem, DJ Harrison. Monoclonal antibody binding affinity determined by microchip-based capillary electrophoresis. Electrophoresis 19:3040–3044, 1998.
98. GM Korf, JP Landers, DJ O'Kane. Capillary electrophoresis with laser-induced fluorescence detection for the analysis of free and immune-complexed green fluorescent protein. Anal Biochem 251:210–218, 1997.
99. K Shimura, BL Karger. Affinity probe capillary electrophoresis: Analysis of recombinant human growth hormone with a fluorescent-labeled antibody fragment. Anal Chem 66:9–15, 1994.
100. RG Nielsen, EC Rickard, PF Santa, DA Shakarnas, GS Sittampalam. Separation of antibody–antigen complexes by capillary zone electrophoresis, isoelectric focusing and high-performance size-exclusion chromatography. J Chromatogr 539:177–185, 1991.
101. L Tao, RT Kennedy. Measurement of antibody–antigen dissociation constants using fast capillary electrophoresis with laser-induced fluorescence detection. Electrophoresis 18:112–117, 1997.
102. Y Xiao, W Wu, MP Dierich, YH Chen. HIV-1 gp41 by N-domain binds the potential receptor protein P45. Int Arch Allergy Immunol 121:253–257, 2000.

© 2003 by Marcel Dekker, Inc.

103. YH Chen, Y Xiao, W Wu, Q Wang, G Luon, MP Dierich. HIV-2 transmembrane protein gp36 binds to the putative cellular receptor proteins P45 and P62. Immunobiology 201:317–322, 2000.
104. T Yu, Y Xiao, Y Bai, Q Ru, G Luo, MP Dierich, YH Chen. Human interferon-beta inhibits binding of HIV-1 gp41 to lymphocyte and monocyte cells and binds the potential receptor protein P50 for HIV-1 gp41. Immunol Lett 73: 19–22, 2000.
105. S Kiessig, J Reissmann, C Rascher, G Küllertz, A Fischer, F Thunecke. Application of a green fluorescent fusion protein to study protein–protein interactions by electrophoretic methods. Electrophoresis 22:1428–1435, 2001.

© 2003 by Marcel Dekker, Inc.

10

Affinity Capillary Electrophoresis: DNA Interactions with Peptides, Proteins, and Modified DNA

Michael W. Linscheid
Humboldt-Universität zu Berlin, Berlin, Germany

I. INTRODUCTION

Electrophoresis has been used for a long time as one of the most important separation principles in analytical biochemistry. In particular, it has been applied to the separation of DNA and DNA components. Electrophoretical techniques have predominated in this field for decades and will continue to do so in the future. The advent of capillary electrophoresis (CE) has boosted the development of electrophoretic techniques, because it opened access to higher sensitivity, better resolution, and greater speed of separation (1–3).

In liquid chromatography, affinity purification protocols (4–8) have been known for a long time. Naturally, electrophoresis can be used just as well to observe molecular or noncovalent interactions of DNA oligomers, provided the complex has distinct electrophoretic properties different from those of the free molecules. Therefore, affinity capillary electrophoresis (ACE) can be a powerful tool for studying DNA–drug or DNA–biopolymer interactions. Several reviews discussing these aspects of ACE have been published in recent years (9–19). The crucial aspects of DNA in this field are covered comprehensively in a recent overview article (20).

The techniques called *mobility shift* or *gel shift assay* can be considered a first step in this direction. These are widely used in molecular biology to detect interactions between regulatory proteins for gene expression and specific sequences of polynucleotides (21–23).

Two general approaches are used in affinity CE of DNA complexes,

© 2003 by Marcel Dekker, Inc.

depending on the stability of the complex under investigation. For a system with slow complexation kinetics, such as most high-affinity systems, equilibrium mixture analysis is preferable. In contrast, in the case of relatively rapid on-and-off kinetics, which is a characteristic feature of low-affinity complexes, mobility-change analysis should be applied.

II. PRINCIPLES: DETECTION OF COMPLEX FORMATION

The direct detection of a complex from an equilibrium mixture is certainly the most obvious evidence of specific molecular interactions between components. Electrophoresis of an equilibrium mixture is an easily performed experiment, enabling the determination of complex formation parameters. When the dissociation kinetics of the complex is slow, the complex gives rise to a new peak in the electropherogram, in addition to the peaks of the free component molecules. Since the separation of the free components prevents the reformation of the complex inside the capillary, the complex peak should decrease in size during electrophoresis. The extent of this decrease depends on dissociation kinetics and separation time. In view of that fact, short analysis times, as obtained in CE, are required to detect less stable complexes, which would hardly be detected using previous formats of electrophoresis with longer separation times.

If the interacting molecules show large differences in their mobility, it may be difficult to detect all free and complexed species in the same electrophoretic run. This can be the case when the interacting molecules have opposite charges, a situation not uncommon for proteins and oligonucleotides. On the other hand, in some cases the change of mobilty due to complex formation may be not be sufficient to allow the separation of the complex from one of the interacting components. However, even in such cases, complex formation can be detected using a phenomenon of high-affinity systems. The peak of one of the free components disappears when it is mixed with the other, and it rises again when the binding site of the other is saturated.

III. DETERMINATION OF EQUILIBRIUM CONSTANTS

The ongoing dissociation of the complex during migration typically results in peak deformation of both complex and free species. Although the peaks are well separated, they may be connected by some sort of pedestal. The peak size of the complex diminishes during the analysis, whereas the peak representing the free species remains stable and corresponds to the original sample mixture under equilibrium. Since the peak areas are proportional to

© 2003 by Marcel Dekker, Inc.

concentration, peak integration enables quantitative determinations of each free species in the mixture, which is the basis for the calculation of equilibrium constants. Complexes with relatively slow off-rate constants are usually characterized by small dissociation constants, so one must analyze the equilibrium at a rather low concentration range, corresponding to the dissociation constants. This implies the need for high sensitivity detection, which can be achieved using fluorescence labeling, laser-induced fluorescence (LIF), or ACE coupled with mass spectrometry (MS), even though this last is still not as common as for simple capillary zone electrophoresis.

In the following, some examples will be discussed to highlight the scope and the limitations of ACE for the detection of complex formation between DNA samples and interaction partners such as proteins, peptides, DNA or analogs, and smaller molecules.

IV. PURIFICATION OF TRANSCRIPTION FACTORS

In all living cells the affinity binding of DNA to proteins controls key processes such as DNA replication, DNA repair, and recombination, which eventually allow and regulate the development of any organism. Transcription factors control gene expression by binding to specific DNA elements in the promoter region. It has been found that improper function of such transcription factors in humans contributes to diseases such as cancer and immunodeficiencies. Therefore purification of transcription factors from tissue extracts is essential to understand the processes involved. This task is challenging, because they are normally present at very low concentrations. This problem is further complicated by the fact that several purification steps are needed for the complete purification of a particular transcription factor. Sequence-specific DNA affinity chromatography can be used as a means for classification, assay, and purification of transcription factors. For a recent review see Gadgil et al. (19).

One of the most impressive examples for the detection of a transcription factor was published in 1996, when a mobility-shift assay in a linear-polyacrylamide-filled capillary using fluorescein-labeled DNA showed 100 times higher sensitivity than the conventional slab-gel technique with ^{32}P. Furthermore, the detection of a transcription factor in a single sea urchin egg was demonstrated (24).

V. SYNTHETIC LABELING WITH FLUOROPHORIC GROUPS

Labeling of a component with a fluorophore enables selective detection of the complex even when the separation of the complex from other nonlabeled

© 2003 by Marcel Dekker, Inc.

components is incomplete. The feasibility of prehybridization of a fluorescence-labeled polynucleotide sample and subsequent analysis using CE with LIF detection to identify a specific DNA fragment in a sample was investigated (25,26) (Fig. 1). Here, German et al. used DNA aptamers labeled with a fluoresceine tag to study the DNA–IgE complex.

The complex was determined using carboxyfluorescein as internal stan-

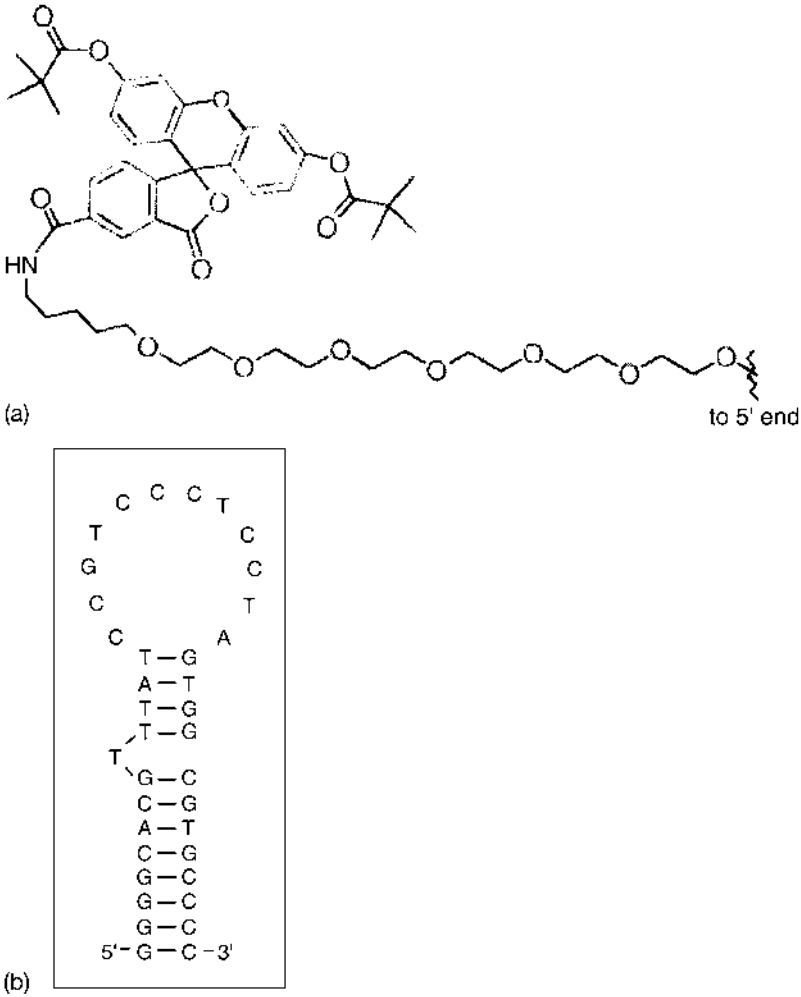

Fig. 1 (a) Structure of the fluorescein–ethylene glycol linker to label the aptamer. (b) Structure of the aptamer without fluorescence label attached. (From Ref. 26.)

© 2003 by Marcel Dekker, Inc.

dard (see Fig. 2). It is evident from the three traces that the complex can easily be separated from the monomers and quantitative determination is achieved. To demonstrate that the signal observed results only from the complex, a competition experiment with unlabeled aptamer, as shown in Fig. 3, was performed. The increase in unbound A* shows clearly that both A and A* bind to the same site of IgE.

VI. CHEMICAL MODIFICATION OF DNA: AFFINITY PRECONCENTRATION

An experiment including several different steps was devised by Watson et al. to determine modifications in DNA (8). 1,N6-Etheno-2′-deoxyadenosine and 3,N4-etheno-2′-deoxycytidine are formed exogenously by a number of genotoxic chemicals as well as endogenously. In addition to an HPLC method, an immunochemical procedure combined with CE was developed. A monoclonal antibody raised to protein conjugates of epsilon dC showed high selectivity in recognition of this DNA adduct. The antibody was immobilized on a solid support and was used in the immunoaffinity enrichment procedure to purify epsilon dC from a large excess of normal nucleotides. The result was that one single epsilon dC adduct could be resolved from about 10^8 normal nucleotides. The coupling of the immunoaffinity enrichment procedure with capillary zone electrophoresis permitted the detection of approximately one epsilon dC adduct in 3×10^6 nucleotides. Similar experiments have been carried out with benzo[a]pyrene metabolite adducts and in conjuction with CE techniques (20,25,27). Carnelley et al. used a fluorescent 90mer oligonucleotide sample labeled with benzo[a]pyrene-7,8-diol 9,10-epoxide (BPDE) in a competitive experiment to detect DNA damage in human lung carcinoma cells. In Fig. 4 the design of the probe is shown, using tetramethylrhodamine as the fluorophore. Figure 5 illustrates the competitive capillary electrophoresis experiment.

VII. USE OF PEPTIDE NUCLEIC ACIDS

The synthesis of DNA analogues with a backbone of poly(*N*-(2-aminoethyl)glycine) (peptide nucleic acids = PNA) instead of phosphate-ribose, which were introduced into affinity labeling by Egholm et al. (28), opened up several new applications for affinity separations (23,28–42). Since this backbone is by far less polar, the behavior of the monomer as well as that of DNA/PNA hybrids is largely different, allowing the complete separation of affinity complexes. In addition, it seems that the stability of duplexes is

© 2003 by Marcel Dekker, Inc.

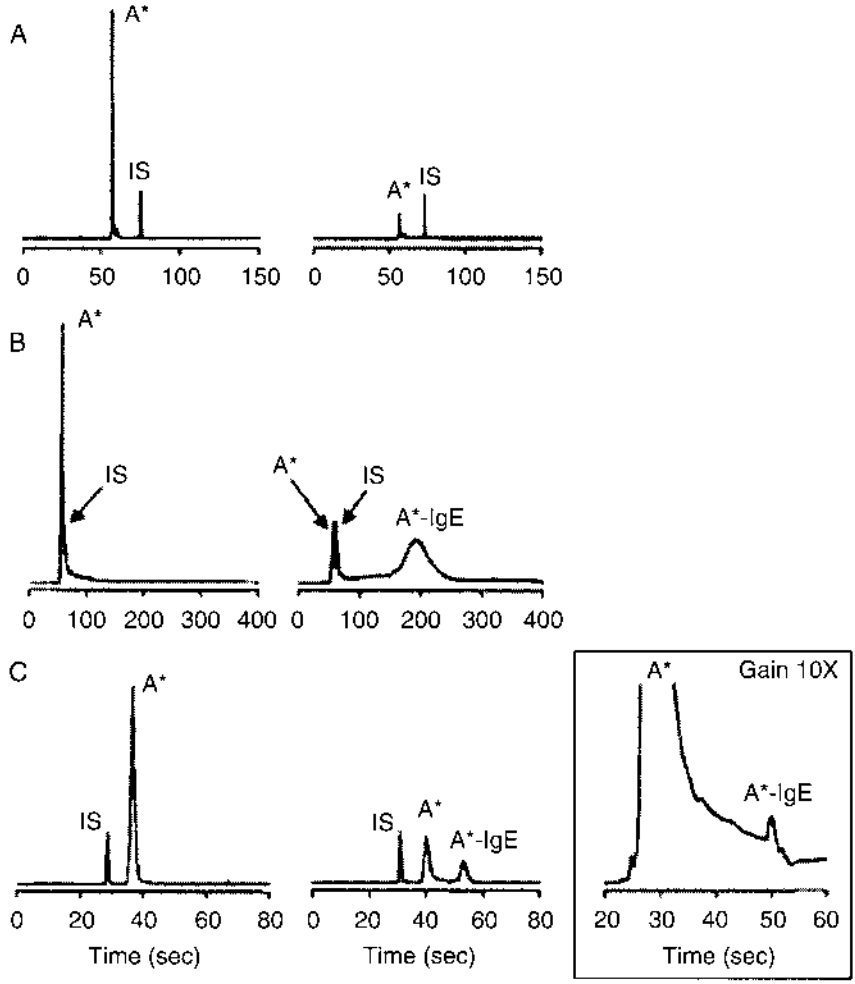

Fig. 2 Determination of IgE using aptamer-based APCE. (A) Electropherograms obtained for 500 nM of A* with 0 (left) and 500 nM (right) IgE. Migration buffer was 10 mM phosphate at pH 7.4, and 10 nM fluorescein was used as internal standard (IS). Injector-to-detector length was 20 cm. (B) Separation of same solutions in 10 mM phosphate at pH 8.2 and gravity-induced flow of 0.02 cm/s. (C) Solutions of 300 nM of A* with no IgE (left), 300 nM IgE (middle), and 1 nM IgE (right) were separated with injector-to-detector length of 7 cm. After 48 s of separation, a vacuum was applied to the outlet to rapidly pull the complex to the detector. 4(5)-Carboxyfluorescein (5 nM) was used as internal standard. Fluorescent signal scale for the 1 nM IgE sample is expanded by 10-fold relative to the other electropherograms. (From Ref. 26.)

© 2003 by Marcel Dekker, Inc.

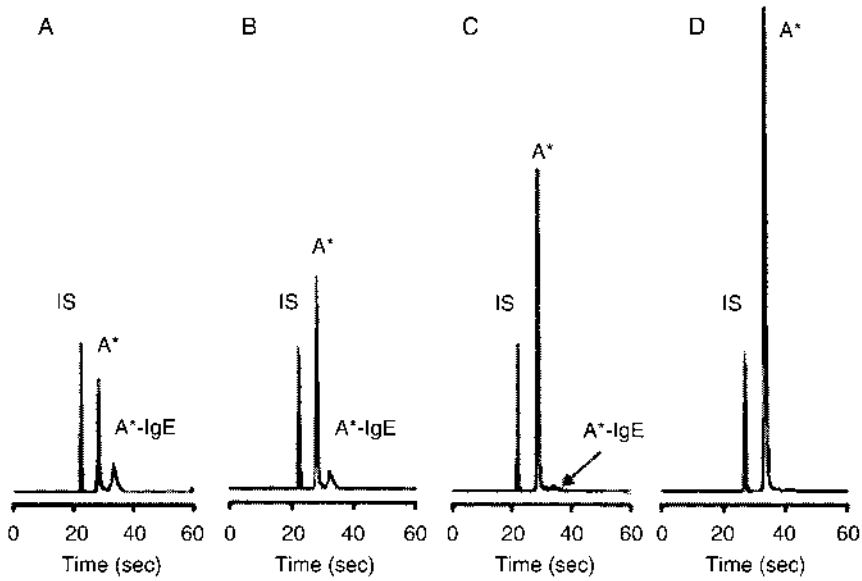

Fig. 3 Competition experiment. All samples contained 200 nM A*, and 5 nM 4(5)-carboxyfluorescein was used as internal standard (IS). Samples A–C contained 200 nM IgE and 0, 200, and 400 nM, respectively, unlabeled aptamer. Sample D is a blank containing just 200 nM A* shown for comparison. Increase of the A* peak with the increase in the concentration of A demonstrates that both A and A* are binding to the same site on the IgE. (From Ref. 26.)

superior to DNA/DNA hybrids, which enhances the possibilities in low-ionic-strength solvents used for electrophoresis (37). Thus the use of such hybrids to detect single base mutations is possible, as shown by several researchers. Nielsen et al. modified a plasmid containing a 10mer PNA flanked by restriction sites to show that only the correct complementary-sequence PNA was able to block the restriction enzymes completely; one mismatch was sufficient to reduce that effect, and two mismatches made the inhibiting effect disappear (29). Perry-O'Keefe et al. (37) demonstrate quite convincingly that certain labeled peptide nucleic acid (PNA)-oligomers as probes in pregel hybridization experiments can work as an alternative to Southern hybridization (Fig. 6). The authors of this study hybridized the PNA probe to a denatured DNA sample at low ionic strength. Then the mixture was loaded directly onto an electrophoresis system for separation. The neutral backbone of PNA allows a hybridization at low ionic strength. Another benefit of that technique can be seen in the low mobility of PNAs. Therefore, the assay is not disturbed by signals of unbound PNA.

© 2003 by Marcel Dekker, Inc.

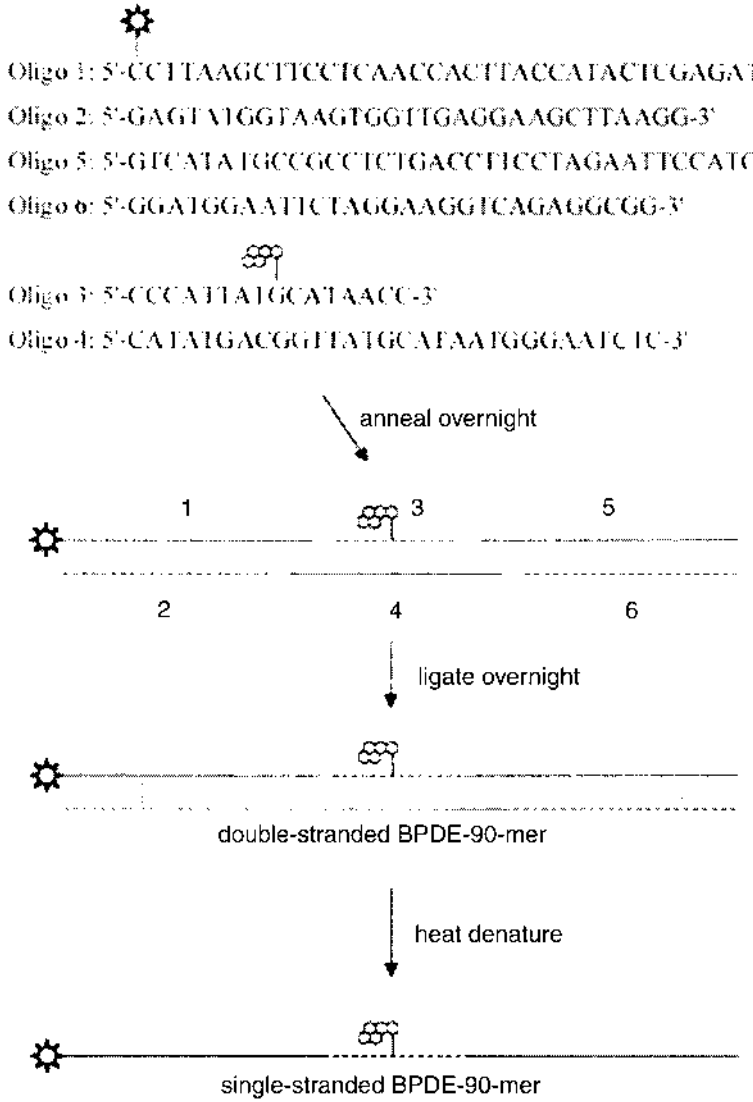

Fig. 4 Schematic representation of the design of the DNA damage probe. A total of six overlapping, complementary oligonucleotides of varying lengths were annealed and ligated to form a 90-base-pair double-stranded DNA molecule. Oligo 1 was labeled at the 5′-end with the fluorescent dye tetramethylrhodamine (TMR). Oligo 3 contained a damaged base, BPDE-N^2-deoxyguanosine, which was introduced by reacting oligo 3 with (±)-anti-BPDE. The dye label and damaged base were on the same strand, to allow for either single- or double-stranded experiments. (From Ref. 25.)

© 2003 by Marcel Dekker, Inc.

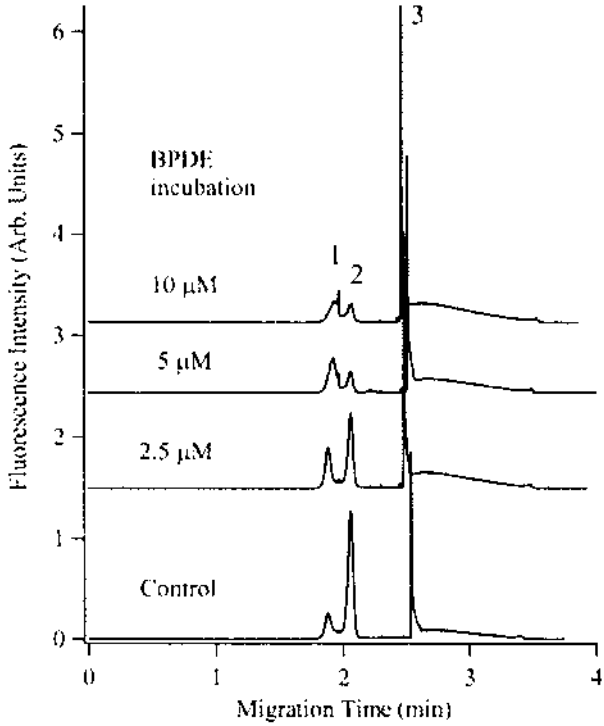

Fig. 5 Representative electropherograms showing competitive assay for BPDE-DNA adducts from human lung carcinoma cells. The cells were incubated with 0, 2.5, 5, and 10 μM BPDE for 2 h and DNA extracted for analysis. Mixtures containing 80 μg/mL of the cellular DNA, 60 nM of the oligonucleotide probe, and 0.4 μg/mL of mouse monoclonal antibody 8E11 were incubated in 20 μL of Tris-glycine buffer (25 mM Tris and 200 mM glycine, pH 8.3) at room temperature for 30 min. A CE/LIF analysis of these mixtures were carried out using a fused-silica capillary 30 cm in length, with 20-μm i.d. and 150-μm o.d.) for separation. The separation buffer contained 25 mM Tris and 200 mM glycine (pH 8.5). The running voltage was 30 kV, and electrokinetic injection was carried out at 10 kV for 10 s. Peaks 1 and 2 correspond to the binary (1:1) and tertiary (1:2) complexes between antibody and the sample. Peak 3 represents the unbound sample. (From Ref. 25.)

Detection of the bound PNA is possible via on-column fluorescence detection. Efficient single base-pair discrimination was achieved routinely using that technique, as shown in Fig. 7. The system was optimized to observed a difference of 25°C between the perfect match and single-mismatched PNA probe. The assay should be applicable for clinical research and diagnostics and may be automated as well.

© 2003 by Marcel Dekker, Inc.

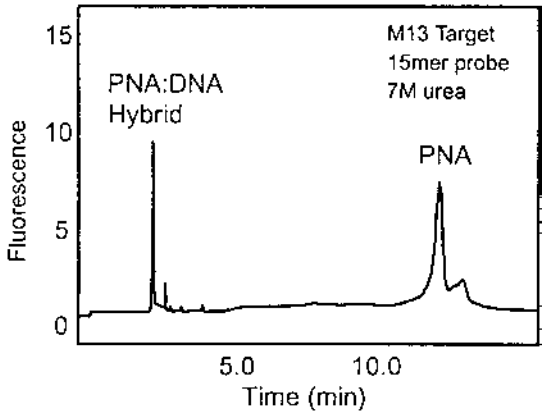

Fig. 6 Free-solution CE separation of PNA/DNA hybrid from excess PNA probe. M13 mp18 ssDNA 4.2×10^{-8} M, and PNA probe 1.3×10^{-7} M. Detection: LIF 488/520 nm. Buffer: TBE, 7 M urea (pH 8.0). CE conditions: 50-mm-i.d. polyacrylamide-coated capillary (27 cm in length and 20 cm to detector), 10 s gravity injection, separation voltage -10 kV. Laser-induced fluorescence detection with excitation at 488 nm and emission at 520 nm. The buffer contained Triszborate (pH 8.0) with 7 M urea buffer. (From Ref. 37.)

VIII. DETECTION OF MUTATIONS

Another approach in the application of affinity protocols is the addition of ethidium bromide to the size-separation medium for double-stranded DNA. This improves the separation capacity of the method at a high field strength to such an extent that even mutations can be detected (43). Theoretical plates up to 10^7 have been obtained, which is vastly superior to what can be achieved in general with DNA oligomers.

The opposite approach is to modify the stationary phase as a macroligand; such a procedure was described by Baba et al. in 1992 (44). Poly(9-vinyladenine) was synthesized and fixed inside the gel matrix. Base-specific separation of oligodeoxynucleotides was achieved with high resolution and high speed. It is no surprise that oligothymidylic acids were selectively separated from the mixture of oligothymidylic and oligodeoxyadenylic acids with efficiencies as high as several 10^6 plates/m.

A similar experiment but with thymidine and adenine exchanging roles was devised by Ozaki and co-workers to analyze mixtures of shorter oligonucleotides with high resolution, supporting the notion that hydrogen bonding can be considered the key factor for separation (45). The pivotal role of Mg^+ ions supports that view. As an example, single mutants in poly-

© 2003 by Marcel Dekker, Inc.

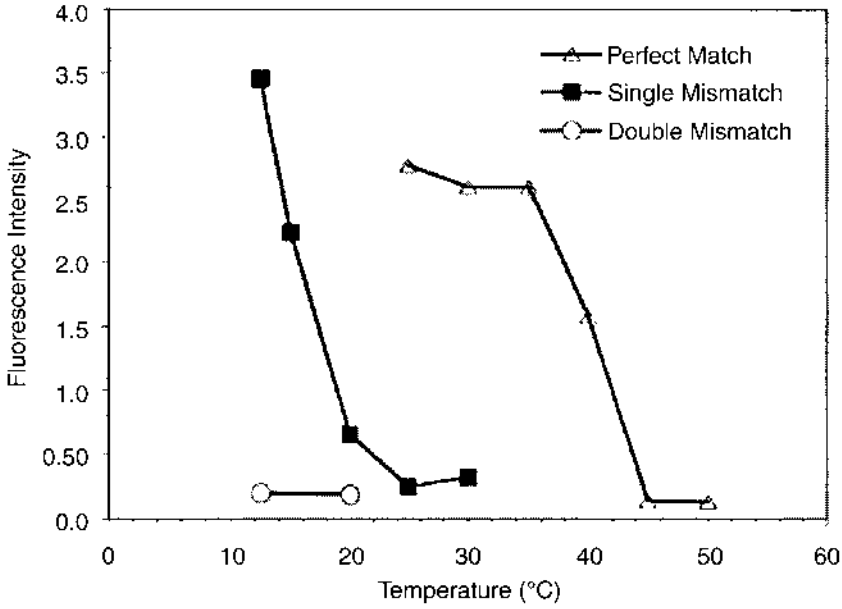

Fig. 7 Fluorescence intensity of the PNA/DNA hybrid vs. separation temperature. Fluorescein-labeled PNA probes with complementary 3′ sequence. Voltage: 20 kV. Detection: LIF 488/520 nm. Buffer: 1× TBE/30% formamide (pH 8.3). The following M13 probes were used: 5′-fluorescein-OO-TTT TCC CAG TCA CGA (perfect match), 5′-fluorescein-OO-TTT TCC CAG GCA CGA (single mismatch), 5′-fluorescein-OO-TTT TCA CAG GCA CGA (double mismatch). (From Ref. 37.)

adenylic acid (dA_{12}) were detected when $(dT)_{12}$ was immobilized at the capillary wall. Thus the assay may be useful for the detection of gene mutations.

Monoclonal antibodies against specific DNA lesions have been developed for several applications (8,9,25,27,46,47), generally to detect chemical modifications, as already discussed. A new technical development, addressing the issue of online monitoring of complex formation, was introduced by Wan and Le (48). Due to the fact that fluorescence polarization is sensitive to changes in rotational diffusion arising from molecular association or dissociation, it is capable of providing information on the formation of affinity complexes prior to or during CE separation. The technique was successfully applied to the system ''trypsin operator and trypsin repressor binding.'' In Figure 8, the experimental setup is shown; the result of a proof-of-concept measurement is given in Figure 9. The binding curves obtained from the correlation of electrophoretic mobility and fluorescence anisotropy are given in Figure 10.

© 2003 by Marcel Dekker, Inc.

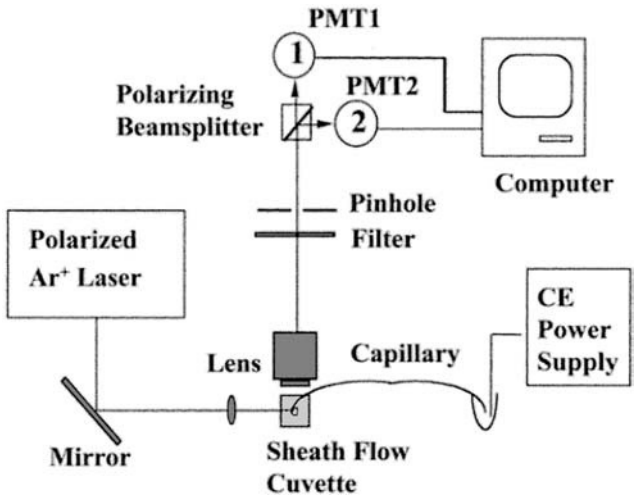

Fig. 8 Schematic diagram showing capillary electrophoresis separation with laser-induced fluorescence polarization detection. (From Ref. 48.)

Overall, the affinity complexes were readily distinguished from the unbound molecules, although the relative increase in fluorescence polarization upon complex formation varied with the molecular size of the binding pairs.

IX. SCREENING OF PEPTIDES

The screening for smaller peptides as published by Li and Martin in 1998 was based on ACE with online UV detection. The binding constants between purified calf thymus DNA and a library of specifically designed tetrapeptides were determined. This peptide library contained unnatural amino acids with thiazole side chains (49). The ACE technique was utilized to separate unbound tetrapeptides from the DNA–peptide complex. The UV signal of the peak representing unbound tetrapeptide decreased incrementally as a result of increasing the concentration of DNA in the equilibrium mixture. The intensity of the peak corresponding to the unbound tetrapeptide was obtained directly from the electropherogram and could be used in the calculation of the DNA–peptide binding constants. The binding constant for the tetrapeptides to calf thymus DNA was obtained from the negative slope of a Scatchard plot. A comparison of the binding constants for different peptides

© 2003 by Marcel Dekker, Inc.

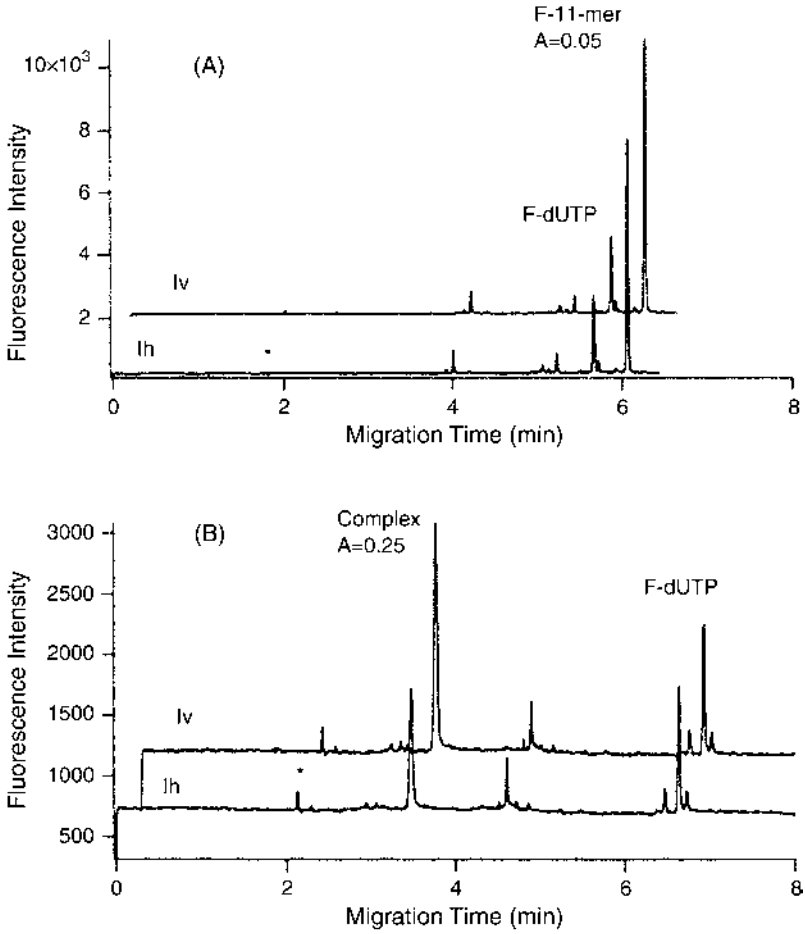

Fig. 9 Electropherograms showing 3 nM fluorescently labeled 11-mer in the absence (A) and in the presence (B) of 0.7 μM SSB protein in the running buffer. The conditions used were as follows: separation capillary, 35 cm, 20-μm i.d.; running buffer, 25 mM disodium tetraborate (pH 9.1); separation voltage, 25 kV; excitation wavelength, 488 nm; emission wavelength, 515 nm; and temperature, 25 (1°C. Approximately 1 nL of sample solution was injected electrokinetically. The asterisk indicates the migration time of the solvent, t_{EOF}. The traces Iv and Ih, corresponding to vertically and horizontally polarized fluorescence intensities, respectively, are shown separated for clarity. (From Ref. 48.)

© 2003 by Marcel Dekker, Inc.

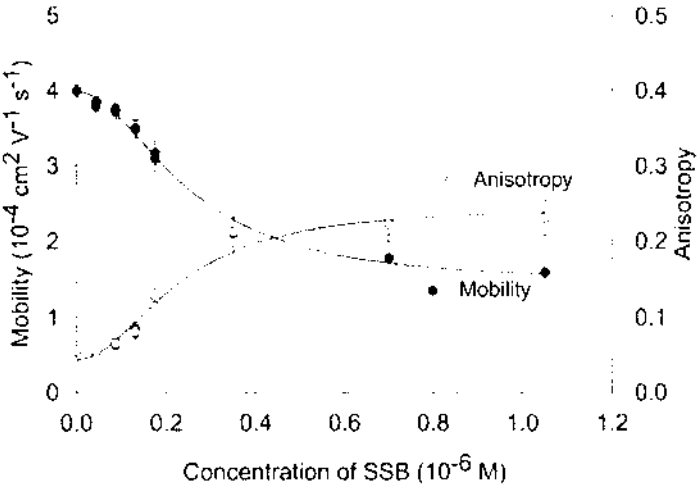

Fig. 10 Binding curves obtained by measuring the electrophoretic mobility (●) and fluorescence anisotropy (○) of F-11-mer at varying concentrations of SSB protein in the running buffer. Conditions were the same as for Figure 9. (From Ref. 48.)

revealed that the tetrapeptides in the library have DNA-binding affinities ranging from 10^2 to 10^6 M^{-1}.

X. DNA–DNA INTERACTIONS

DNA mutations of certain genes are the origin of heritable diseases and cancer. In order to discover and, hopefully, prevent these disorders, gene mutation assays are of increasing importance in diagnostics and clinical assays. Capillary affinity gel electrophoresis was applied to separate oligodeoxynucleotide mixtures using sequence-specific and base-composition-specific recognition. The affinity interaction is based on the formation of a complex between the solved oligodeoxynucleotide sample and a DNA analogue immobilized on the capillary gel. These complexes are named *heteroduplexes*. It has been shown that a selective separation of hexathymidiylic acid from a mixture of four homopolymers and five heteropolymers of hexadeoxynucleotides is possible (50). A combination of size- and sequence-dependent oligonucleotide separation methods using capillary affinity gel electrophoresis has been reviewed by Baba (14,51).

A different approach has been proposed by Muscate et al. (52), who developed a two-step technique. In the first step, all nonspecific solutes are

© 2003 by Marcel Dekker, Inc.

removed from the sample. At low temperatures, oligonucleotides with complementary sequences will bind best to the recognition sequence of the immobilized recognition sequences. Then the bound oligomers can be released by gradually increasing the temperature, until the specific release temperature for each nucleotide is reached. The synthetic strategy for the affinity polymer is shown in Fig. 11. Figure 12 gives an instructive comparison for the separation capabilities of conventional capillary gel eletrophoresis (CGE) and affinity gel elctrophoresis (CAGE). This approach has been used by Katayama et al. (53) to develop an ACE assay for gene mutation analysis using an oligonucleotide polycrylamide conjugate as ligand. The Mg^{2+} concentration was crucial for an efficient separation of oligomers of the same length.

XI. DNA TRIPLE STRAND INTERACTIONS

The PyPuPu and PyPuPy intermolecular triple-stranded DNA (tsDNA) was determined by capillary electrophoresis (CE) (54). The authors report the determination of tsDNA formed by poly(dT20)(dT20) with poly(dA20)-(dA20), and 16-bp dsDNA with 16-nt triplex formation oligonucleotide

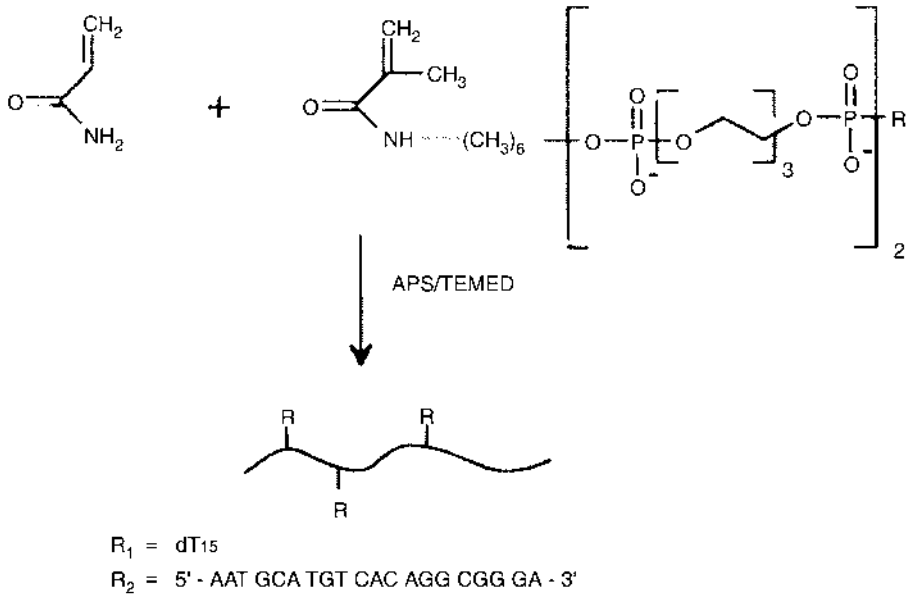

Fig. 11 Synthetic strategy for an affinity polymer. (From Ref. 52.)

© 2003 by Marcel Dekker, Inc.

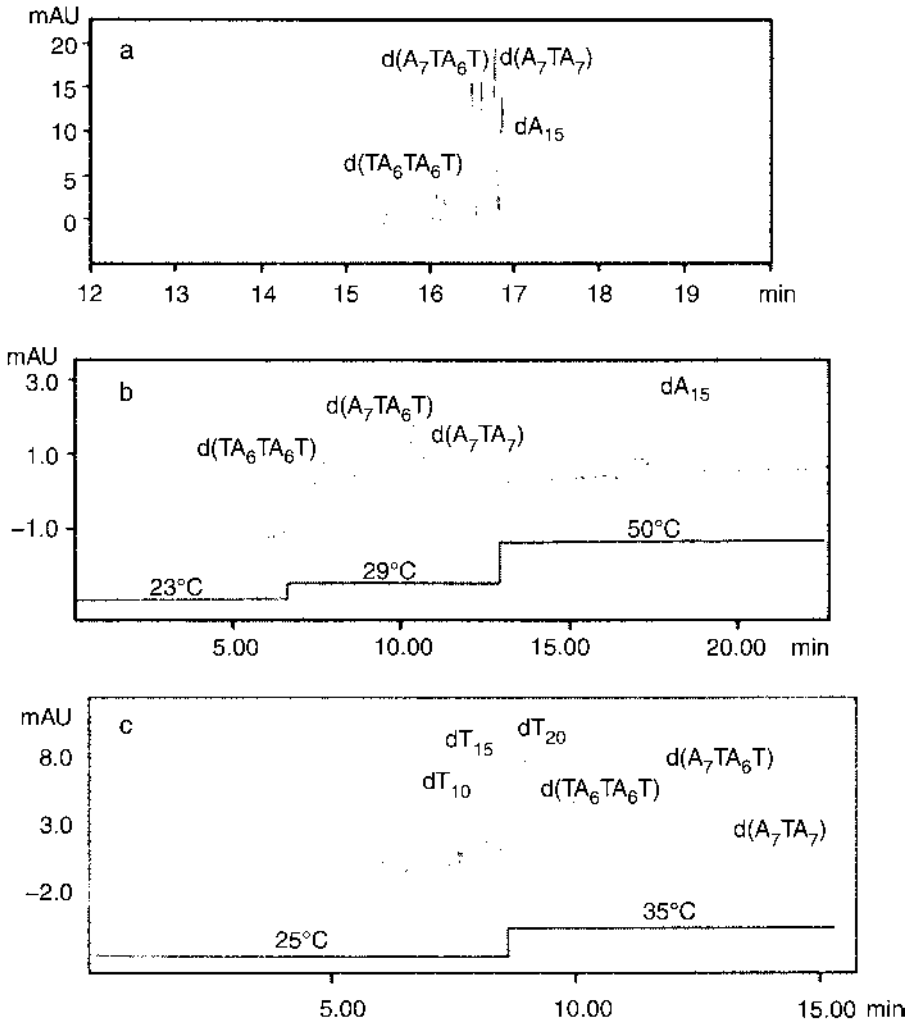

Fig. 12 Electropherograms showing the separation of dA_{15} from oligonucleotides with 1, 2, or 3 mismatches, using conventional CGE (a) and the CAGE approach (b, c). CAGE conditions: (a) 3% T of a dT_{15} affinity polymer, dissolved in 100 mM TB; concentration of each oligonucleotide, 5×10^{-4} OD/μL; capillary, CElect N; (b) coinjection of dA_{15} for 6 s at -6 kV and a mixture of $d(TA_6TA_6T)$, $d(A_7TA_6T)$, and $d(A_7TA_7)$ for 9 s at -8 kV; (c) coinjection of dT_{10}, dT_{15}, and dT_{20} for 4 s at -2 kV and a mixture of $d(TA_6TA_6T)$, $d(A_7TA_6T)$, and $d(A_7TA_7)$ for 9 s at -8 kV; applied voltage, 5 kV; temperature program 6.5 min at 23°C, 6.5 min at 29°C, 50°C. (From Ref. 52.)

© 2003 by Marcel Dekker, Inc.

(TFO) by capillary electrophoresis using a sieving matrix of 1.0% hydroxypropylmethylcellulose (HPMC) containing magnesium ions (2.5 mM). In the presence of magnesium, the tsDNA can be determined by capillary electrophoresis with UV detection. The crucial parameters were investigated in great detail. It was found that the triplex cannot be formed when the buffer pH is lower than 4.0. Online detection, peak area quantification, and automated data analysis by capillary electrophoresis can provide direct analysis of tsDNA.

A typical series of electropherograms is shown in Figure 13. In this context it should be noted that triplex DNA/PNA structures were also found

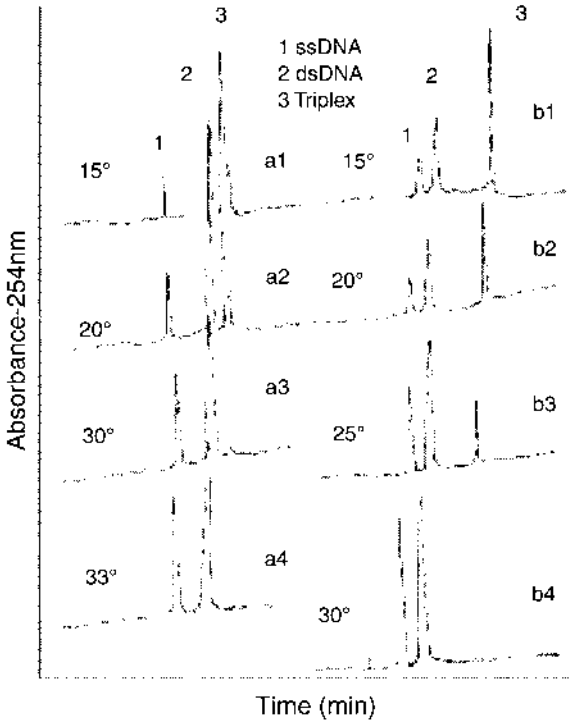

Fig. 13 Electropherograms of triplex-containing samples of dA20 with dT20 (a1–a4) and DS-1 with TFO (b1–b4) at different column temperatures. Conditions: UV detector at 254 nm, 1.0% HPMC sieving matrix, 0.253 TBM running buffer (pH 8.5), electrokinetic injection (10 kV, 5 s), 15-kV running voltage applied for a1 and b1, 13-kV running voltage applied for a2 and b2, 11.5-kV running voltage applied for b3, 10-kV running voltage applied for a3 and b4, and 9-kV running voltage applied for a4. (From Ref. 54.)

© 2003 by Marcel Dekker, Inc.

in a recent study by Nielsen and Egholm, which are the first reported for PNAs (30). This indicates an important potential for future affinity CE applications.

Recently, triplex formation was employed to purify plasmids (55).

Pharmaceutically applicable plasmid DNA is an important issue in gene therapy. A method for affinity purification of plasmids by triple-helix interaction is given as an example. This method is based on sequence-specific binding of an oligonucleotide, immobilized on a large-pore chromatography support, to a target sequence on the plasmid. A 15-mer target sequence was developed that binds strongly to the affinity support under mildly acidic conditions. Plasmid DNA was purified from clarified *Escherichia coli* lysate by incubation with the affinity beads at pH 5.0 and high NaCl concentration. After extensive washing of the beads, purified plasmid DNA was eluted with alkaline buffer. The purified plasmid showed no RNA or cell DNA contamination in HPLC analysis, and total protein concentration was reduced considerably. Due to its mechanical stability and porosity, this support can be used in a continuous affinity purification process, which has a high potential for scale-up.

DNA assays will certainly play an essential role in future medical research, along with proteomics. This makes high-throughput screening methods necessary. Parallel DNA separation chips coupled with high-sensitivity detection such as LIF or mass spectrometry (56) should be able to provide the required structural information in less time than with techniques currently employed (12).

XII. SCREENING FOR PROTEINS TO DETECT GENETIC DISORDERS

A. HIV Protein Detection

The detection of HIV-related proteins is one of the most challenging tasks. This is especially true because AIDS should be diagnosed as early as possible to enable an early and effective therapy of this infection. Pavski and Le (57) used the aptamer strategy to detect reverse transcriptase (RT) of the type 1 human immunodeficiency virus (HIV-1). A direct and specific ACE method was proposed using laser-induced fluorescence (ACE/LIF) as detection principle. Single-stranded DNA aptamers as probes fluorescently labeled were synthesized. The resulting aptamer is specific for HIV-1 RT, and it exhibited no cross-reactivity with RTs of the enhanced avian myeloblastosis virus (AMV), the Moloney murine leukemia virus (MMLV), or denatured HIV-1 RT. An affinity complex of RT 26-HIV-1 RT was stable, with calibration curves linear up to 50 nM (6 μg/mL) HIV-1 RT concentration. Both

© 2003 by Marcel Dekker, Inc.

signals, the free probe and the complex peak, were accessible for analytical quantitation. To prevent unspecific binding, the authors proposed 100-fold dilution of the raw sample.

The work of Zhou and coworkers (58) aimed at a different strategy for the detection of the HIV virus. They studied the binding between HIV-1 gp120 and a phosphorothionate oligodeoxynucleotide, which is considered a potential anti-HIV drug based on antisense action. The detection was based on laser-induced fluorescence detection (ACE-LIF). They used the advantages discussed previously—very different electrophoretic mobilities and the very strong binding between oligodeoxynucleotides and proteins—to obtain sufficient separation and resolution of the signals. Laser-induced fluorescence allowed them to determine the ligands at the necessary low level of concentration. In this study the dissociation constant (K_d) between HIV-1 gp120 and a 25-mer fluorescently tagged phosphorothioate oligodeoxynucleotide (GEM, FITC-CTC TCG CAC CCA TCT CTC TCC TTC T) using Scatchard analysis was reported. Since they determined the the values of competition constants to the unlabeled oligonucleotide as well, these results may prove useful for future drug design.

A different antisense oligonucleotide, a morpholino oligonucleotide analogue, was used for the quantitative monitoring of cellular concentration of complexes. This is difficult based on conventional methods such as radiolabeling of the oligonucleotide and fluorescence confocal microscopy. The authors of the study used capillary electrophoresis coupled with laser-induced fluorescence detection (CE-LIF) (59). HeLa cells, which produce luciferase as the antisense oligomer enters the cell, were scrape-loaded with varying concentrations of the morpholino antisense. Intracellular concentrations of the antisense were found to be in the range of 6–29 nmol/g of total cell protein. Thus for the first time a quantitative correlation between delivered antisense concentration in a cell extract and the subsequent antisense up-regulation of gene expression has been shown.

XIII. OTHER ASPECTS

The detection of small molecules identified by DNA binding is based generally on the affinity purification and subsequent collection of fractions. The identification can be performed by means of the usual techniques employed for structure elucidation or quantitative determination of organic molecules (20).

Endotoxins can be contaminants in many preparations of biopolymers, such as in DNA preparations. They are a major problem in toxicology because they can cause a vehement, sometimes life-threatening response of the

© 2003 by Marcel Dekker, Inc.

immunological system. Endotoxins are lipopolysaccharides (LPS) of the outer membrane of gram-negative bacteria such as *E. coli*. The detection in the underivatized state can be difficult due to the lack of optically active moieties. An indirect UV detection method based on affinity interaction was used to quantify the residual LPS content of a DNA preparation from *E. coli* (60).

XIV. CONCLUSION

Affinity capillary electrophoresis can be considered a powerful tool for the analysis of interactions between DNA, RNA, and synthetic analogues on the one hand and proteins, peptides, and nucleic acid components on the other hand. However, the technique seems not yet widely accepted. This is probably due to the rather high cost of the instrument—the high sensitivity required can be achieved mostly only with laser fluorescence—and the technically demanding use of the setup. The examples discussed here clearly demonstrate general advantages: speed, sensitivity, and the possibility of quantifying the results. It can be expected that the technique will gain in importance, since capillary electrophoresis instruments are readily available with LIF detectors, and the development of microfluidic devices based on chip technologies will have another impact in the coming years. In the future, ACE will replace or accompany the classical separation principles, e.g., gel electrophoresis and HPLC, as well as the less sensitive NMR (61) or the problematic radioactive labeling.

REFERENCES

1. JW Jorgenson and KD Lukacs, Anal. Chem., 1981, 53, 1298.
2. PD Grossman, JC Colburn, HH Lauer, RG Nielsen, RM Riggin, GS Sittampalam, and EC Rickard, Anal. Chem., 1989, 61, 1186.
3. FEP Mikkers, FM Everaerts, and PEMV Th, J. Chrom., 1979, 169, 11.
4. H Bunemann and W Muller, Nucleic Acids Research, 1978, 5, 1059.
5. G Herrick, Nucl. Acids. Res, 1980, 8, 3721.
6. PL Courchesne, MD Jones, JH Robinson, CS Spahr, S McCracken, DL Bentley, R Luethy, and SD Patterson, Electrophoresis, 1998, 19, 956.
7. JE Battersby, VR Mukku, RG Clark, and WS Hancock, Anal Chem, 1995, 67, 447.
8. WP Watson, JP Aston, T Barlow, AE Crane, D Potter, and T Brown, IARC Sci Publ, 1999, 150, 63.
9. Y Baba, Mol Biotechnol, 1996, 6, 143.
10. J Oravcova, B Bohs, and W Lindner, J Chromatogr B Biomed Appl, 1996, 677, 1.

© 2003 by Marcel Dekker, Inc.

11. G Rippel, H Corstjens, HA Billiet, and J Frank, Electrophoresis, 1997, 18, 2175.
12. LA Holland, NP Chetwyn, MD Perkins, and SM Lunte, Pharm Res, 1997, 14, 372.
13. DS Hage, Clin Chem, 1999, 45, 593.
14. Y Baba, J Biochem Biophys Methods, 1999, 41, 91.
15. NH Heegaard and RT Kennedy, Electrophoresis, 1999, 20, 3122.
16. J Haginaka, J Chromatogr A, 2000, 875, 235.
17. B Koppenhoefer, X Zhu, A Jakob, S Wuerthner, and B Lin, J Chromatogr A, 2000, 875, 135.
18. A von Brocke, G Nicholson, and E Bayer, Electrophoresis, 2001, 22, 1251.
19. H Gadgil, LA Jurado, and HW Jarrett, Analytical Biochemistry, 2001, 290, 147–178.
20. KR Mitchelson, Methods Mol Biol, 2001, 162, 3.
21. M Fried and DM Crothers, Nucleic Acids Res, 1981, 9, 6505.
22. MFaD Crothers, Nucleic Acids Research, 1981, 9, 6505.
23. GW Shipps, Jr., KE Pryor, J Xian, DA Skyler, EH Davidson, and J Rebek, Jr, Proc Natl Acad Sci USA, 1997, 94, 11833.
24. J Xian, MG Harrington, and EH Davidson, Proc Natl Acad Sci USA, 1996, 93, 86.
25. TJ Carnelley, S Barker, H Wang, WG Tan, M Weinfeld, and XC Le, Chem Res Toxicol, 2001, 14, 1513.
26. I German, DD Buchanan, and RT Kennedy, Anal Chem, 1998, 70, 4540.
27. WG Tan, TJ Carnelley, P Murphy, H Wang, J Lee, S Barker, M Weinfeld, and XC Le, J Chromatogr A, 2001, 924, 377.
28. M Egholm, O Buchardt, L Christensen, C Behrens, SM Freier, DA Driver, RH Berg, SK Kim, B Norden, and PE Nielsen, Nature, 1993, 365, 566.
29. PE Nielsen, M Egholm, RH Berg, and O Buchardt, Nucleic Acids Res, 1993, 21, 197.
30. PE Nielsen and M Egholm, Bioorg Med Chem, 2001, 9, 2429.
31. BP Zhang, M Egholm, N Paul, M Pingle, and DE Bergstrom, Methods, 2001, 23, 132.
32. C Chen, B Wu, T Wei, M Egholm, and WM Strauss, Mamm Genome, 2000, 11, 384.
33. DP Chandler, JR Stults, S Cebula, BL Schuck, DW Weaver, KK Anderson, M Egholm, and FJ Brockman, Appl Environ Microbiol, 2000, 66, 3438.
34. PE Nielsen and M Egholm, Curr Issues Mol Biol, 1999, 1, 89.
35. C Chen, YK Hong, SD Ontiveros, M Egholm, and WM Strauss, Mamm Genome, 1999, 10, 13.
36. AF Faruqi, M Egholm, and PM Glazer, Proc Natl Acad Sci USA, 1998, 95, 1398.
37. H Perry-O'Keefe, XW Yao, JM Coull, M Fuchs, and M Egholm, Proc Natl Acad Sci USA, 1996, 93, 14670.
38. M Egholm, L Christensen, KL Dueholm, O Buchardt, J Coull, and PE Nielsen, Nucleic Acids Res, 1995, 23, 217.
39. PE Nielsen, M Egholm, and O Buchardt, Bioconjug Chem, 1994, 5, 3.

© 2003 by Marcel Dekker, Inc.

40. PE Nielsen, M Egholm, and O Buchardt, Gene, 1994, 149, 139.
41. P Wittung, PE Nielsen, O Buchardt, M Egholm, and B Norden, Nature, 1994, 368, 561.
42. V Demidov, MD Frank-Kamenetskii, M Egholm, O Buchardt, and PE Nielsen, Nucleic Acids Res, 1993, 21, 2103.
43. A Guttman and N Cooke, Anal Chem, 1991, 63, 2038.
44. Y Baba, M Tsuhako, T Sawa, M Akashi, and E Yashima, Anal Chem, 1992, 64, 1920.
45. Y Ozaki, T Ihara, Y Katayama, and M Maeda, Nucleic Acids Symp Ser, 1997, 37, 235.
46. P Bjork, U Jonsson, H Svedberg, K Larsson, P Lind, J Dillner, G Hedlund, M Dohlsten, and T Kalland, J Biol Chem, 1993, 268, 24232.
47. M Butler, RM Crooke, MJ Graham, KM Lemonidis, M Lougheed, SF Murray, D Witchell, U Steinbrecher, and CF Bennett, J Pharmacol Exp Ther, 2000, 292, 489.
48. QH Wan and XC Le, Anal Chem, 1999, 71, 4183.
49. C Li and LM Martin, Anal Biochem., 1998, 263, 72–78.
50. Y Baba, T Sawa, A Kishida, and M Akashi, Electrophoresis, 1998, 19, 433.
51. Y Baba, Methods Mol Biol, 2001, 163, 347.
52. A Muscate, F Natt, A Paulus, and M Ehrat, Anal Chem., 1998, 70, 1419.
53. Y Katayama, T Arisawa, Y Ozaki, and M Maeda, Chem Lett, 2000, 2000, 106.
54. X Fan, J Liu, H Tang, Y Jin, and TP Wang, Analytical Biochemistry, 2000, 287, 95–101.
55. T Schluep and C Cooney, Nucleic Acids Research, 1998, 26, 4524.
56. NH Heegaard, S Nilsson, and NA Guzman, J Chromatogr B Biomed Sci Appl, 1998, 715, 29.
57. V Pavski and XC Le, Anal Chem, 2001, 73, 6070.
58. W Zhou, KB Tomer, and MG Khaledi, Anal Biochem., 2000, 284, 334–341.
59. J McKeon, M-J Cho, and MG Khaledi, Anal Biochem., 2001, 293, 1–7.
60. R Freitag, M Fix, and O Bruggemann, Electrophoresis, 1997, 18, 1899.
61. RD Jenison, SC Gill, A Pardi, and B Polisky, Science, 1994, 263, 1425.

© 2003 by Marcel Dekker, Inc.

11
Characterization of Polysaccharide Interactions

Charuwan Thanawiroon, Wenjun Mao, and Robert J. Linhardt
University of Iowa, Iowa City, Iowa, U.S.A.

I. INTRODUCTION

In recent years, much attention has been paid to the chemistry and biochemistry of carbohydrates due to their many functions both inside and outside living cells. The glycosaminoglycans (GAGs) are related linear, polydisperse, microheterogeneous polyanionic polysaccharides. The most common GAGs are heparin, heparan sulfate, hyaluronic acid, chondroitin sulfate, dermatan sulfate, and keratan sulfate. The GAGs are generally believed to exert their biological activities through the localization, stabilization, activation, or inactivation of interacting proteins (1). These interactions play important roles in the normal physiology of animals (2) and are also involved in certain pathological processes (3). Heparin, the most studied GAG, is unique in its intracellular location in mast cell and basophil granules. Exogenous heparin is regularly used as an anticoagulant/antithrombotic agent to maintain blood flow in the vasculature through the binding and activation of antithrombin III (ATIII, a coagulation serine protease inhibitor, SERPIN) (1). Heparin has been found to bind a wide range of proteins (1,4), and it regulates a number of important biological activities. Heparan sulfate, structurally similar to heparin, is localized on the external surface of cell membranes and in the extracellular matrix and plays a major role in cell–cell and cell–protein interaction (1). Heparan sulfate (not heparin) is also believed to be an endogenous receptor for circulating growth factors and chemokines that reg-

© 2003 by Marcel Dekker, Inc.

ulate cell growth and migration (1). Other GAGs also bind proteins, but the interactions are generally less well studied than those of heparin and heparan sulfate. In addition to GAGs there are a number of synthetic, semisynthetic, and natural GAG analogues that are of medicinal interest (1). An understanding of how these GAGs and GAG analogues interact with proteins is needed to develop either carbohydrate-based, peptide-based, or synthetic therapeutics for the prevention and treatment of disease processes, including control of coagulation (1) and the control of tumor cell replication, migration, invasion, and vascularization (2,3). In this chapter, the structures and therapeutic potential of these important GAGs, GAG-binding proteins, and the quantitative methods for characterization of polysaccharide–protein binding interactions will be provided as a background. Recent advances in the application of affinity capillary electrophoresis (ACE) to study these specific interactions will be discussed.

II. DEFINITION OF OLIGOSACCHARIDES, POLYSACCHARIDES, GLYCOSAMINOGLYCANS, AND PROTEOGLYCANS

Carbohydrates are classified as monosaccharides, oligosaccharides, or polysaccharides based on their number of monomer units.

Glycosaminoglycans (GAGs) are a family of complex linear anionic polysaccharides found in most animal tissues. The polysaccharides are characterized by a repeating core disaccharide structure typically composed of uronic acid and hexosamine residues. In GAGs, the amino group of the hexosamine residue is either N-acetylated or N-sulfonated; the uronic acid may be either D-glucuronic acid or L-iduronic acid. Moreover, the repeating disaccharide units (i.e., uronic acid–hexosamine) are O-sulfonated to varying degrees at the 6- and/or 4-position of the various hexosamine residues and at the 2-position of the uronic acid residues. Heparin, heparan sulfate, hyaluronic acid, chondroitin sulfate, dermatan sulfate, and keratan sulfate are the most common GAGs.

Proteoglycans (PGs) are a diverse group of proteins unified by their possession of one or more covalently attached GAG chains. With the exception of hyaluronic acid, GAGs are biosynthesized as proteoglycans (1). Some PGs, such as heparin, are biochemically processed into GAGs through the action of proteinases and β-endoglucuronidases (1) (Fig. 1). Thus, both PGs and GAGs are natural components of most animal tissues.

© 2003 by Marcel Dekker, Inc.

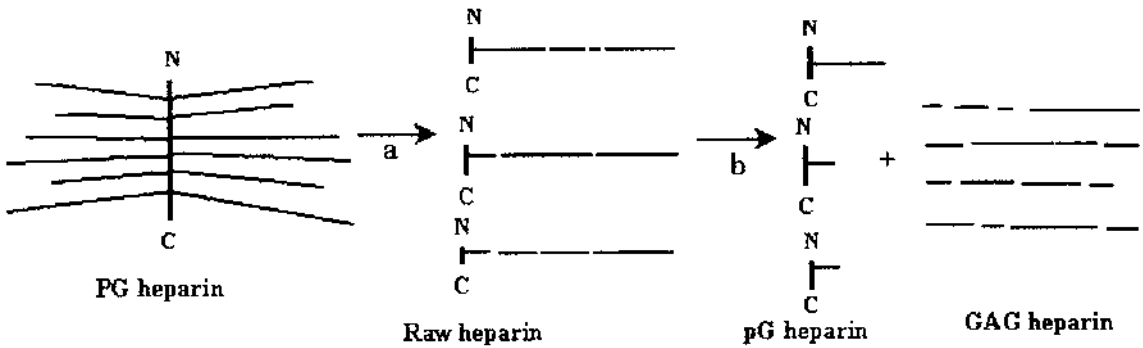

Fig. 1 Structure of heparin proteoglycan. The heparin proteoglycan is released from mast cells on degranulation as raw heparin formed through the action of β-endoglucuronidase and proteinase. (a) Raw heparin can be separated (b) into peptidoglycan heparin and glycosaminoglycan (GAG) heparin. Pharmaceutical heparin is prepared by bleaching raw heparin to remove peptide. (Adapted from Ref. 1.)

© 2003 by Marcel Dekker, Inc.

III. IMPORTANT POLYSACCHARIDES

A. Heparin

Heparin is biosynthesized in mast cells as a PG with approximately 10 GAG side chains (5). When mast cells degranulate, PG heparin is enzymatically degraded to GAG heparin (Fig. 1). Exogenous heparin is used primarily as an anticoagulant/antithrombotic agent. Heparin is produced from mast-cell-rich tissues, such as lung and intestinal mucosa, in metric ton quantities yearly for use as a pharmaceutical agent.

Heparin is a repeating linear copolymer of 1 $\rightarrow$ 4 linked uronic acid and glucosamine residues (6). The uronic acid residue typically consists of 90% iduronic acid and 10% glucuronic acid. Iduronate is a more flexible residue than glucuronate, promoting polysaccharide interaction with proteins. Heparin has a high negative charge density, the result of sulfo and carboxyl groups that are present in its structure. Indeed, the average disaccharide in heparin contains 2.7 sulfo groups. Whereas the most common structure in heparin is the disaccharide containing 3 sulfo groups (7) (Fig. 2), a number of structural variants exist, making it microheterogenous (8). The 2-position of uronic acid residue frequently contains an *O*-sulfo group. The 6-position of the glucosamine residue often contains an *O*-sulfo group while the 3-position infrequently contains an *O*-sulfo group, and the amino functionality at the 2-position of the glucosamine residue may contain an *N*-sulfo group or *N*-acetyl group or be unsubstituted. The presence or absence of these functional groups, as well as the presence of two different uronic acid residues (iduronate and glucuronate), define the sequence of the GAG chain. The length of heparin GAG chains can also vary. Heparin is polydisperse; the average chain in a commercial heparin has a molecular weight of 13,000, with chains ranging in size from 5,000 to 40,000.

Because of its high content of sulfo groups and its sequence microheterogeneity, heparin is able to bind a wide range of proteins and regulate a number of important biological activities (1). These interactions are currently under intensive investigation, and they regulate heparin's effect on lipoprotein lipase, on smooth muscle proliferation, its inhibition of complement activation, anti-inflammatory activity, angiogenic and antiangiogenic activities, anticancer activity, antiviral activity, and its potential use in treating Alzheimer's disease (1).

As a result of heparin's multiplicity of biological activities and its importance as a major pharmaceutical, other polysaccharides and modified polysaccharides have been examined as potential heparin analogues in drug development (1). These heparin analogues include other GAGs, other non-GAGs, sulfated polysaccharides from plant and animal origins such as lam-

© 2003 by Marcel Dekker, Inc.

inarin and acharan sulfate, and synthetic analogues of heparin such as suramin (Fig. 3).

B. Low-Molecular-Weight Heparins

Low-molecular-weight (LMW) heparins are generally prepared through the controlled, partial, chemical or enzymatic depolymerization of commercial GAG heparin (1). Therefore, they are primarily composed of the same small number of major oligosaccharide sequences that make up standard commercial heparins. The LMW heparins are polydisperse mixtures (average molecular weight 4,000–8,000) that have proven to be effective antithrombotic agents (9) for use in a wide variety of disease states, ranging from deep vein thrombosis (10) to nonhemorrhagic stroke (11). The LMW heparins offer several advantages over the anticoagulant heparin (1). They are as safe as heparin, resulting in somewhat less hemorrhagic complications, and they have greater bioavailability and longer half-lives, resulting in better dose control (11). These potential advantages have led to the development of several commercial LMW heparin preparations.

C. Heparin Analogues

There are a number of structural analogues of heparin that have been and are being evaluated as therapeutic agents (Table 1). These analogues include polysaccharide natural products, chemically modified polysaccharides, and synthetic molecules containing anionic groups, including *N*-sulfo groups, *O*-sulfo groups, sulfonyl groups, carboxyl groups, and phosphoryl groups. As with heparin, these analogues exert their activities by interacting with various heparin-binding proteins.

IV. THERAPEUTIC POTENTIAL OF POLYSACCHARIDES

Heparin and heparin analogues are used primarily as anticoagulant and antithrombotic agents to augment the activity of ATIII, resulting in the inactivation of coagulation proteases and blood anticoagulation. Heparin and LMW heparins are the most commonly used clinical anticoagulants. However, there are additional therapeutic areas that are under extensive investigation (Table 2). Some of these are described next in detail.

© 2003 by Marcel Dekker, Inc.

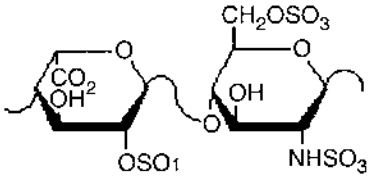

major disaccharide sequence

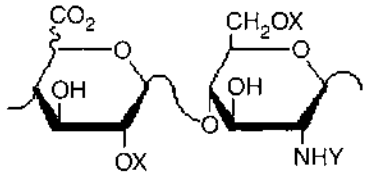

$X = H$ or SO_3, $Y = H$, CH_1CO or SO_3

minor disaccharide sequence

Heparin

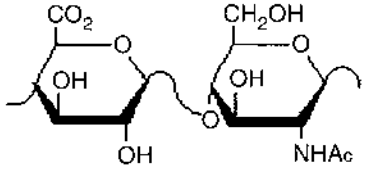

major disaccharide sequence

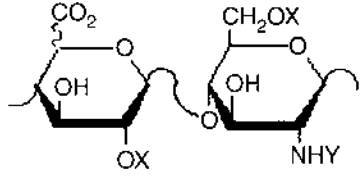

$X = H$ or SO_3, $Y = H$, CH_3CO or SO_3

minor disaccharide sequence

Heparan sulfate

© 2003 by Marcel Dekker, Inc.

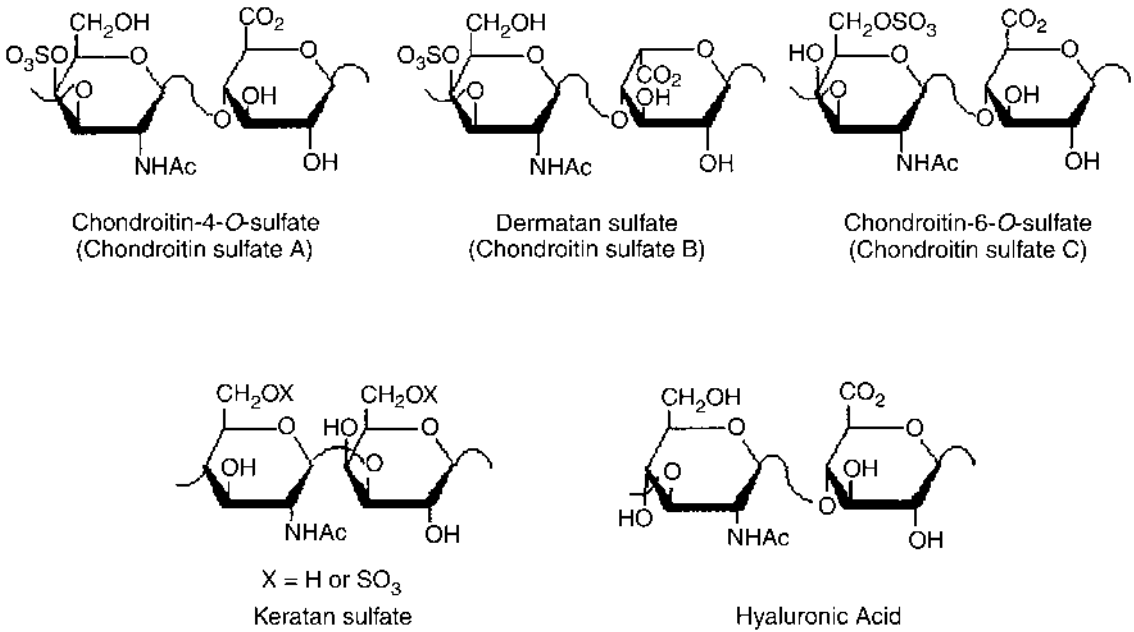

Fig. 2 Structures of the major and minor disaccharide sequences of heparin and heparan sulfate as well as the major disaccharide units of chondroitin sulfate, dermatan sulfate, keratan sulfate, and hyaluronic acid, where Ac is acetyl.

© 2003 by Marcel Dekker, Inc.

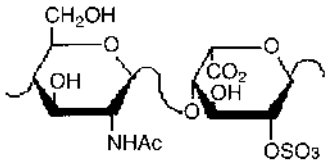

Acharan sulfate

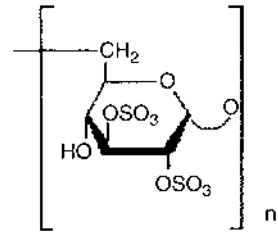

Dextran sulfate

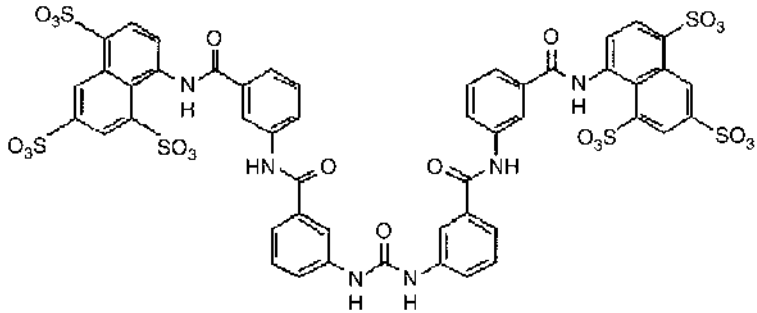

Suramin

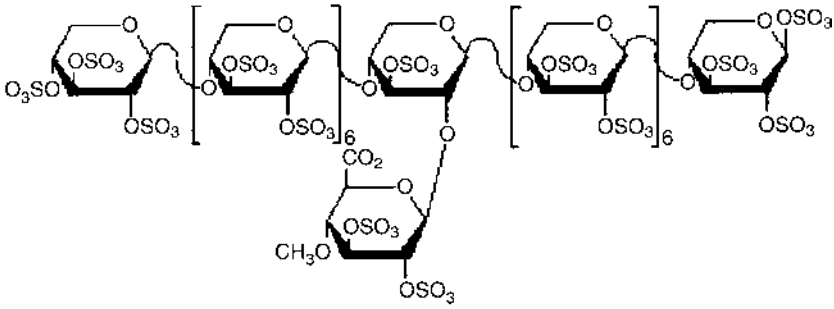

Pentosan polysulfate

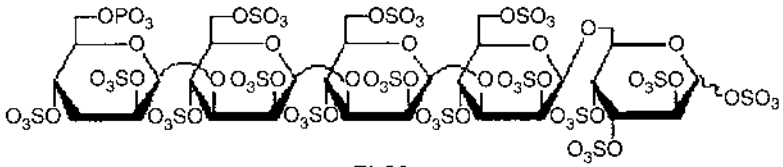

PI-88

© 2003 by Marcel Dekker, Inc.

A. Regulation of Enzymatic Processes

Since this is the major current application for heparin as an anticoagulant/antithrombotic, it is not surprising that much of the research has targeted this type of activity. The extensive evaluation of heparin analogues as anticoagulant/antithrombotic agents has met with some success, including the clinical introduction of LMW heparins and pentosan polysulfate (1,32,33). Recently, heparin analogues have been evaluated as regulators of the complement cascade and proteases, such as elastase, for the treatment of lung disorders, such as hereditary angioedema (48) and asthma (49).

B. Anti-Infection

It is clear that pathogens use endogenous GAGs to localize on the surface of cells and even to gain entrance into cells, resulting in infection (50). The increasing number of reports of antibiotic-resistant microorganisms suggest that new anti-infective mechanisms, such as ones disrupting cellular localization of pathogens, might be valuable. The dengue virus causing hemorrhagic fever in many tropical countries is an example of an infectious disease for which there is no vaccine available and no known specific treatment. An oversulfonated heparan sulfate was shown to be a receptor required for infectivity by this virus (47). In addition, heparin and a heparin decasaccharide (47) were demonstrated to inhibit virus infectivity through their blocking effects at both virus attachment and penetration (51). Interestingly, a heparin analogue, suramin, can also block such infection in vitro (47). Recently, GAGs and their derivatives have been examined as potential inhibitors of dengue virus envelope protein binding to its receptors (52). The molecular size and level of sulfation of GAGs were reported to affect its inhibitory activity.

C. Anticancer

Cancer is a complicated process consisting of well-coordinated multiple steps. Randomized trials to study the effectiveness of LMW heparins as compared with unfractionated heparin in treating venous thromboembolism in cancer patients led to a surprising observation that treatment with heparin

---

Fig. 3 Structures of acharan sulfate, dextran sulfate, suramin, pentosan polysulfate, and phosphomannopentaose sulfate (PI-88). Representative saccharide units comprising each of these polymers are shown, where *n* is the degree of polymerization.

© 2003 by Marcel Dekker, Inc.

Table 1 Heparin Analogues

Analogue	Structure	Current applications	Remarks	Refs.
Heparan sulfate	→4) glucuronic acid (1 → 4) *N*-acetyl glucosamine (1 → <1 sulfo group/ disaccharide	Component of antithrombotic agents	High price and limited availability	6, 8
Chondroitin sulfate and dermatan sulfates	→3) *N*-acetyl galactosamine (1 → 4) glucuronic/iduronic acid (1→, with ~1 sulfo group	Antithrombotic primarily through interaction with heparin cofactor II (HCII)	Binds annexin and other proteins on persulfatation	1, 12–21
Hyaluronic acid	→3) *N*-acetyl glucose amine (1 → 4) glucuronic acid (1→ unsulfated, high MW	Vitreous humor and synovial fluid replacement	Binds link protein and CD44; on persulfation, affords hyaluronidase inhibitors	18–23
Keratan sulfate	galactose and *N*-acetyl glucosamine 6-*O*-sulfo groups	None known		24
Acharan sulfate	→4) 2-sulfo iduronic acid (1 → 4) *N*-acetyl glucosamine (1→	May serve as an antidesiccant, metal chelator, anti-infective, or locomotive (slime) agent in snail	Inhibits heparin's FGF-2 mitogenic activity in vitro; N-sulfation affords unique structural analogs of heparin	19, 21, 25, 26
Carrageenans ι, κ, and λ	sulfo ester of D-galactose and 3,6-anhydro-D-galactose units, linked α-1 → 3 and β-1 → 4 in the polymer	Gelling and thickening agents, pharmaceutical excipients for controlled release	Under in vivo evaluation as inhibitors of tumor growth	27–29

© 2003 by Marcel Dekker, Inc.

Dextran sulfate	A chemically sulfated (1 → 4)-β-D-, (1 → 3)-α-D-branched glucan polymer	Treatment of acute respiratory distress syndrome (ARDS), lipoprotein-releasing activity, in biomaterials as nonthrombogenic surfaces	Inhibitor of human immunodeficiency virus (HIV) binding to T-lymphocytes	1, 30–31
Pentosan polysulfate	(1 → 4)-β-linked xylan oligosaccharide that is branched in the center with a single β-(1 → 2)-4-*O*-methyl-α-D-glucuronate residue	Antithrombotic prophylactic in Europe, for interstitial cystitis in the United States	Animal models to treat osteoarthritis, preclinical studies as anticancer agent, inhibits metastasis and angiogenesis	1, 32–37
Phosphomannopentaose sulfate (PI-88)	persulfated α-6-phospho mannose (1 → 3) [α-mannose (1 → 3)]$_3$ (1 → 6)-α-mannose	Antiangiogenic activity as a heparanase inhibitor, HCII-mediated anticoagulant	Preclinical studies inhibitor of tumor metastasis, tumor growth, and angiogenesis	38, 39
Suramin	polysulfonated naphthylurea	Anthelmintic, antiprotozoal, antineoplastic, and antiviral agent	Binds many proteins, i.e., cytokines, epidermal growth factor, and members of the FGF family; inhibits dengue virus infectivity of host cells; very long in vivo half-life, exhibits a wide range of toxic side effects	40–47

© 2003 by Marcel Dekker, Inc.

Table 2 Potential Therapeutic Applications for Heparin and Heparin Analogues

Application	Status	Ref.
Anticoagulant/antithrombotic	Currently used	1
Antiatherosclerotics	Clinical trials	58
Complement inhibitors	Clinical trials	48
Anti-inflammatory	Animal studies	49
Anticancer agents	Animal studies	53
Antiangiogenic agents	Animal studies	54
Antiviral agents	Animal studies	47
Anti-Alzheimers agents	Animal studies	59
Antiprion agents	In vitro studies	60
Antiparasitic agents	Animal studies	50
New biomaterials	Currently used	61

may affect survival of patients with malignancy (53). The hypothesis that heparins affect cancer progression is reported by many recent experimental studies (54,55). Cancer patients who had been treated with LMW heparin for their thrombosis had a slightly improved 3-month survival as compared to cancer patients receiving unfractionated heparin. Heparin can potentially exert its activity at various stages in cancer progression and malignancy-related processes. It can affect cell proliferation, interfere with the adherence of cancer cells to vascular endothelium, regulate the immune system, and have both inhibitory and stimulatory effects on angiogenesis (54). There is recent evidence showing that heparin treatment reduces tumor metastasis in mice by inhibiting P-selectin-mediated interactions of platelets with carcinoma cell-surface mucin ligands (56). Moreover, the extensive studies aimed at understanding the role of endogeneous heparan sulfate in the regulation of cellular growth has suggested the value of heparin analogues as a potential new class of therapeutic agents. Such agents could be used in wound healing and in promoting angiogenesis in the regeneration of vessels following stroke (57).

The GAGs or their analogues may also be administered to: (1) activate protein-based receptors (agonists); (2) inactivate protein-based receptors (antagonists); (3) compete with endogenous GAGs; and (4) inhibit GAG-synthesizing or -metabolizing enzymes. Thus, studies are ongoing to examine the potential for GAG-binding proteins, peptides, peptidomimetics, and analogues to prevent and treat a wide variety of disease processes.

© 2003 by Marcel Dekker, Inc.

V. INTERACTION OF POLYSACCHARIDES WITH PROTEINS

Heparin has been found to bind a large number of proteins (Table 3). The biological activity of heparin and related polysaccharides is usually ascribed to their interaction with heparin-binding proteins. These proteins can be classified into classes including: (1) enzymes, (2) protease inhibitors, (3) lipoproteins, (4) growth factors, (5) chemokines, (6) selectins, (7) extracellular matrix proteins, (8) receptor proteins, (9) viral coat proteins, (10) nuclear proteins, and (11) other proteins (1). Many heparin-binding proteins are enzymes and enzyme inhibitors. For example, proteases in the coagulation cascade, such as factors IIa, IXa, Xa, XIIa, and VIIIa, are heparin-

Table 3 Heparin-Binding Proteins

I. Enzymes	**VI. Selectins**
Lipolytic enzymes	L-selectin
Kinase	P-selectin
Phosphatases	**VII. Extracellular matrix proteins**
Carbohydrate hydrolases, eliminases, transferases	Collagens I–VI
	Fibronectin
Proteases and esterases	Laminin
Nucleases, polymerases, and topoisomerases	Thrombospondin 1 and 2
	Vitronectin (S-protein)
Other enzymes, oxidases, synthetases, dimutases	**VIII. Receptor proteins**
	Steroid receptors
II. Enzyme inhibitors	Growth factor receptors
Antithrombin III (ATIII)	Channel proteins
C1 Inhibitor proteins	**IX. Viral coat proteins**
Heparin cofactor II (HCII)	gp 120 of HIV-1
III. Lipoproteins	gp 140 and gp 160 of HIV-2
Low- and very low-density lipoproteins	Herpes simplex virus-1 (HSV-1)
Apolipoproteins	Dengue
IV. Growth factors	**X. Nuclear proteins**
Fibroblast growth factors	Histones
Epidermal growth factors	Transcription factors
Hepatocyte growth factors	Others
Platelet-derived growth factors	**XI. Other proteins**
Transforming growth factors	Prion proteins
Vascular endothelial growth factors	Amyloid proteins
V. Chemokines	Fibrin
Interleukin 8 (IL-8)	Immunoglobulin G
Neutrophil-activating peptide 2	Protein C inhibitor
Platelet factor IV	

© 2003 by Marcel Dekker, Inc.

binding proteins. Inhibitors of the coagulation cascade, such as ATIII and HCII, as well as the enzymes and the inhibitors of other biochemical cascades, such as the complement pathway, are also heparin-binding proteins (1,13,14,48,49). Other enzymes, such as lipolytic enzymes, contain allosteric sites that are important for both the localization and the control of their activities. Important research is aimed at understanding GAG interaction with growth factors and their cellular receptors, the tyrosine kinases (62). The fibroblast growth factors (FGFs) are among the most extensively studied of the heparin-binding growth factors. Cell surface heparan sulfate PG serves as a reservoir for these growth factors. The currently held mechanism of action for FGF (Fig. 4) involves binding to a GAG side chain of heparan sulfate PG, followed by FGF dimerization. Presentation of dimerized FGF to its tyrosine kinase receptor (also a heparin-binding protein) results in receptor dimerization and autophosphorylation. This reaction begins an intracellular biochemical cascade resulting in cell replication (or growth). A single heparin chain, an oligosaccharide of sufficient length [i.e., dodeca- or tetradeca (62)], or a heparin analogue can often substitute for the GAG and stimulate growth. A number of nuclear proteins, i.e., histones, transcription factors, topoisomerase, also bind heparin (1).

The interaction of heparin-binding proteins with heparin usually involves both ionic and hydrogen-bonding interactions (4,63). Heparin is the strongest acid present in the body and, thus, is present under physiologic conditions as a highly charged polyanion (1,63). Arginine and lysine are positively charged under physiologic pH and capable of ion pairing with the *O*- and *N*-sulfo groups and carboxyl groups of heparin. Hydrogen-bonding interactions can involve basic and other polar (i.e., Asn, Gln, Ser, etc.) amino acids. Typically, ionic and hydrogen-bonding residues lie in a spatially close array on the surface or in a shallow binding pocket on the surface of the heparin-binding protein (1). While hydrophobic interactions have limited importance in heparin binding, substantial hydrophobic contributions to binding may result in the interaction of GAGs having hydrophobic character (i.e., suramin), making these exquisitely potent agents.

The saccharide backbone present in heparin and many heparin analogues present their anionic substituents (sulfo and carboxyl groups) in a complex spatial array, owing to the high level of chirality, different regioisomers, multiple conformers, and secondary structural features of the carbohydrate backbone. Moreover, the flexibility of the saccharide backbone permits reorientation of these charged groups during binding, facilitating these interactions. Heparin (and to lesser extent heparan and dermatan sulfates) contains a flexible L-iduronic acid that in many cases is essential for binding (4). Occasionally, heparin–protein interactions (i.e., selectin, annexins) even require a divalent metal, such as Ca^{2+}, for binding.

© 2003 by Marcel Dekker, Inc.

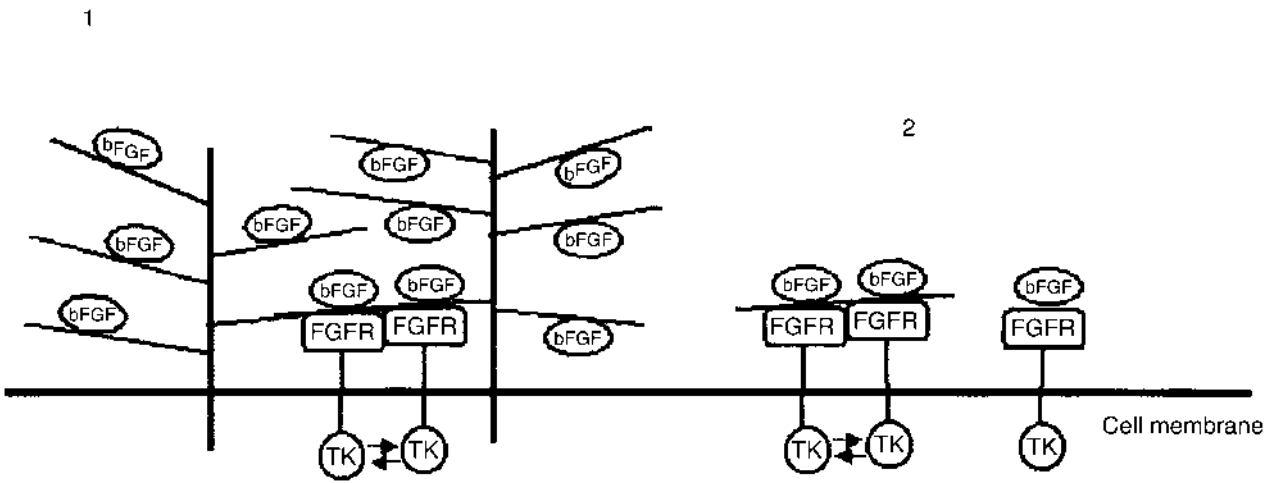

Fig. 4 Interaction of basic FGF on heparan sulfate PG (1) and free GAG (2) induces FGFR dimerization, leading to tyrosine kinase (TK) activation and signal transduction.

© 2003 by Marcel Dekker, Inc.

VI. APPROACHES FOR MEASURING POLYSACCHARIDE–PROTEIN INTERACTIONS

Numerous methods are available for analyzing polysaccharide–protein interactions (63). Many are also applicable to the study of other macromolecular interactions, such as protein–protein (see Chapter 9) and protein–DNA (see Chapter 10) binding. However, because the monovalent binding of polysaccharides to proteins is often relatively low affinity, special considerations apply. For example, many interactions are most easily observed using systems that allow multivalent binding. In addition, because chemical modification of small carbohydrate ligands may significantly alter their binding properties, methods that do not involve traditional labeling techniques are favored. Methods for quantitative analysis of binding interactions can be divided into two groups: those in which one binding partner is immobilized (mixed-phase methods) and those in which both binding partners are in solution (solution-phase methods). Individual methods within these two groups differ in the type of information they afford, as well as in their experimental complexity and the amounts and types of samples needed. No single method is ideal, and a combination of complementary methods often represents the best approach for characterizing polysaccharide–protein interactions. Table 4 presents salient features of the most common methods in use today for the quantitative analysis of polysaccharide–protein binding interactions.

VII. APPLICATIONS OF AFFINITY CAPILLARY ELECTROPHORESIS IN STUDYING POLYSACCHARIDE–PROTEIN INTERACTIONS

Many papers have described methodologies useful for characterizing ligand–protein interactions (63–67). However, among these methods, ACE has been the subject of much attention recently for the evaluation of affinity interactions because of both its high resolution and the extremely small amounts of sample required.

The ACE technique characterizes the interaction between protein and ligand, since under the conditions of electrophoresis the migration of complexed species differs from the migration of free species. The differences in the migration patterns between both species in an electrical field are used to quantify and identify specific binding and to estimate the parameters of the interaction. Since the analyte mobilities are highly dependent on charge, it is evident that interactions with negatively charged ligands, such as sul-

© 2003 by Marcel Dekker, Inc.

Table 4 Quantitative Methods for Characterization of Carbohydrate–Protein Binding Interactions

Method	Type	Principle
Surface plasmon resonance (SPR)	M	Mass-induced refractive index change in real time for direct measurement of association and dissociation rate constants
Affinity chromatography	M	Immobilized ligand on column matrix
Competition ELISA	M	Solution-phase and solid-phase ligands compete for binding to lectin
Scintillation proximity	M	Proximity of radiolabeled ligand to immobilized lectin results in emitted photon from scintillant
Affinity coelectrophoresis (AE)	M/S	Gel retardation: one-dimensional electrophoresis of carbohydrate through protein-impregnated gel
Two-dimensional affinity resolution electrophoresis (2DARE)	M/S	A two-dimensional AE separation
Nuclear magnetic resonance (NMR)	S	Chemical shift, coupling constants, and spectroscopy nuclear Overhauser effect allows calculation of contact points, distances, and conformation
Fluorescence spectroscopy	S	Conformational change with ligand binding induces change in fluorescence properties of intrinsic or extrinsic fluorophore
Circular dichroism (CD)	S	Change in rotation of plane-polarized light upon binding to measure conformational change
Fourier transform infrared spectroscopy (FTIR)	S	Measures protein and carbohydrate vibrational, stretching, and bending energies
Isothermal microtitration calorimetry (ITC)	S	Measures enthalpy of binding directly
Equilibrium dialysis	S	Semipermeable membrane partitions protein but not carbohydrate ligand
Analytical ultracentrifugation	S	Equilibrium sedimentation at different carbohydrate:protein ratios yields stoichiometry of complex
Laser light scattering (LLS)	S	Intrinsic scattering intensities of carbohydrate–protein complex used to calculate stoichiometry

M, mixed phase; S, solution phase (see text).

© 2003 by Marcel Dekker, Inc.

fated oligo- and polysaccharides, are highly suitable for characterization by this method.

The principle and theory of the ACE method is discussed in detail in Part I of this book and were recently reviewed elsewhere (68–70). The remainder of this section is focused on the recent applications of ACE for studying GAG–protein and polysaccharide–protein interactions.

A. Experimental Settings

Based on recent reports on the study of polysaccharide–protein interaction using ACE, two different interaction measurements can be distinguished: the solution-phase method and the mixed-phase method.

The interactions can be studied when both the analyte and the affinity molecule are in free solution. In most polysaccharide–protein interaction studies, the protein is injected as a substrate to the capillary and the polysaccharide is in the running buffer. The change in migration of the protein due to the binding to the polysaccharide is observed, and this allows the affinity of interaction to be determined. However, a mobility change of the polysaccharide might also be observed in cases where little or no change in protein mobility is observed.

The ACE technique has been used to screen heparin-binding sites in serum amyloid P component by observing the migration-shift patterns of this protein in the presence of varying amounts of heparin in buffer (Fig. 5) (71). Following a similar strategy, basic human lactoferin from two different sources, neutrophil granulocytes and milk, were compared on the basis of their affinity for heparin (72). Changes in peak shape and large shifts in migration time were observed, suggesting that the two forms of lactoferin were identical. While several interaction studies have been successfully performed based on this approach, it still has potential drawbacks for the analysis of polysaccharide–protein/peptide interactions: (1) the possibility of varying electroosmotic flow (EOF) at different concentrations of highly charged ligand (i.e., heparin) and (2) the need for a large excess of one of the binding partners.

Interactions can also be studied at the surface of a coated capillary wall. One binding partner is first immobilized on the capillary wall. As a result of the affinity of the second binding partner, the analyte will be delayed, compared with migration times observed in an untreated capillary. Based on this approach, modified capillaries have been prepared and used successfully to study polysaccharide–protein interactions as well as affinity separations. Coating of the capillary wall with heparin and heparan sulfate has been used to determine the affinity of these polysaccharides for synthetic heparin-binding peptides different only in the stereochemistry of a single

© 2003 by Marcel Dekker, Inc.

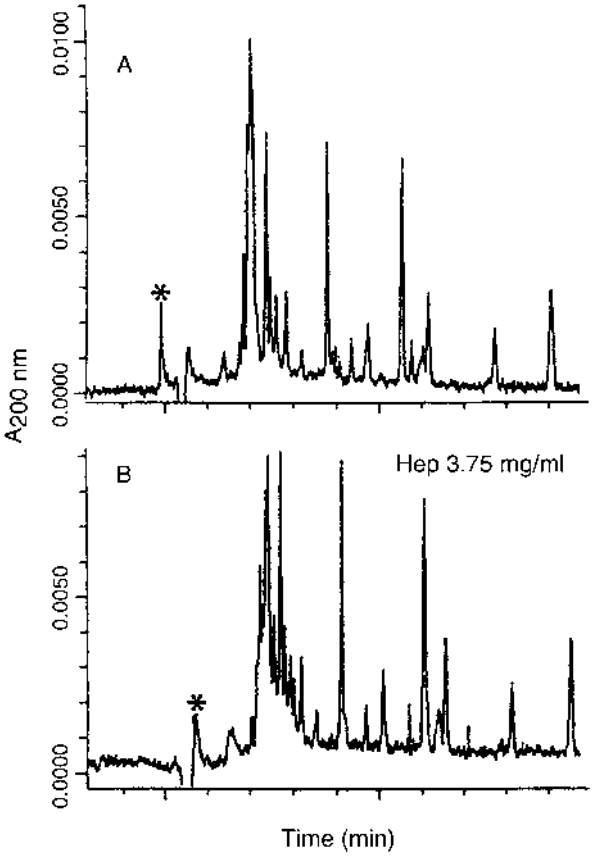

Fig. 5 Screening by affinity CE for interaction of SAP peptides with heparin in solution. An endoproteinase Asp-N-treated Glu-C digest of SAP solubilized in water was injected for 12 s and subjected to CE at 15 kV (detection at 200 nm) in the presence of heparin (Hep) (B) added to the electrophoresis buffer (0.1 M phosphate, pH 7.5) at the concentration indicated. The peptide marked with asterisks was identified by spiking with HPLC-purified fragments and corresponds to the fragment in Figure 6. (From Ref. 71.)

amino acid (upcoming Fig. 8) (73). This approach leads to a fixed concentration of heparin or heparan sulfate ligand and a constant EOF. Moreover, the use of an immobilized ligand offers the advantage of requiring smaller amounts of both ligand and ligate. However, there is still a number of drawbacks to the method. The important potential problems are that it requires additional effort to accurately determine the concentration of the immobi-

© 2003 by Marcel Dekker, Inc.

lized heparin ligand, the immobilized ligand might not be uniformly accessible for all interactions, and there is a risk of altering the ligand characteristics through the derivatization chemistry.

An ultraviolet (UV) monitor is most commonly used in CE experiment. Such interaction studies using the ACE method can also be hampered by the inadequate sensitivity of UV detection. Fluorescence labeling and laser-induced fluorescence (LIF) detection have been employed to enhance the sensitivity of this method, as shown by the mobility-shift assay of fluorescence-labeled sugar caused by the interaction with the lectin, concanavalin A (74). When fluorescent dyes are employed for labeling, LIF detection provides several hundred times more sensitivity than UV detection.

The ACE tecnique has also been used in pharmaceutical and medical research. Affinity interactions of drugs with interfering compounds present in the body are important parameters of the interest for drug discovery, action, and metablism. And ACE has been applied to the analysis of polysaccharide–drug interaction. Amylodextrin oligomers were used as model solutes to investigate certain carbohydrate–drug interactions (75). Fluorescently labeled oligosaccharides, used to observe the interaction of an oligosaccharide with the drug, provided a mobility shift in this ACE experiment. In an analogous procedure, interaction between different starch degradation products and the β-blocker propanolol were studied using gel permeation experiments and ACE (76). The mobility of the drug under electrophoresis is known to be altered by its aggregation with starch. A similar interaction might be responsible for the retarded transport of propanolol over the membranes in the presence of malto-oligosaccharides.

Another interesting and recent application of ACE is the fluorescence-enhanced competition assay for the detection of sugar–lectin interactions (77). Because glucose competes with the fluorescently labeled dextran for the lectin-binding sites, the relative fluorescent intensity due to the displaced dextran is proportional to the concentration of glucose.

The affinity of polysaccharides for drug has also been exploited to assist the separation of enantiomeric drugs (78,79). About 40% of drugs in the marketplace are known to be chiral (79). The pharmacological activity of these drugs is almost entirely restricted to one of the enantiomers. In several cases, unwanted side effects or even toxic effects have been caused by the second, inactive enantiomer. Therefore, the development of methods for enantiomeric separation is of increasing interest. Ionic and neutral polysaccharides have been shown to be useful in such separation of basic drugs. The fundamental aspects and applications of these separations are discussed in detail elsewhere (80,81). Cyclodextrins are the most frequently used chiral selectors (79) (see also Chapter 8). Negatively charged polysaccharides such as heparin, chondroitin sulfate A and C, dextran sulfate, and λ-carrageenan

© 2003 by Marcel Dekker, Inc.

have also been used as chiral selectors for the separation of basic drugs (80,81). Recently, several new GAGs have been investigated as chiral selectors: Dermatan sulfate has been successfully demonstrated to act as an enantiomeric selector for a variety of basic drugs, such as β-sympathomimetics, β-blockers, and antihypertensives (82). More recently, pentosan polysulfate was also investigated as a chiral selector for tryptophan derivatives and several drugs (83).

B. Recent Examples

1. Example 1: Using ACE to Determine the Heparin-Binding Site in Proteins

Based on the solution-phase approach, ACE was used to identify and characterize heparin-binding peptides derived from serum amyloid P (SAP) (71). The protein was digested by proteolytic enzyme, Glu-C endoproteinase. The peptides formed on digestion were examined for binding to heparin by ACE. Heparin was included in the running buffer, and the migration time of peptide was compared with a control (Fig. 5). The binding interactions were characterized by analysis of changes in peak appearance and migration times. Next, the main heparin-interacting peptide was purified from the SAP digest and subjected to analysis and examined for heparin binding by ACE (Fig. 6). By comparing the analysis profile with that of the control experiment, the changes in the migration of complexing peptides were noted. A concentration-dependent decrease in the mobility of the peptide was observed with increasing concentration of heparin in the electrophoresis buffer. No changes in peak shape or size were detected. As expected, the equilibrium shifts toward longer times spent in the complexed form when more heparin is present. Additionally, the heparin-binding sequence in the peptide fragment was characterized and identified by mass spectrometry and amino acid sequencing. This report showed the potential use of the ACE technique for directly mapping binding sites in protein digest.

2. Example 2: Using ACE to Separate Heparin-Binding Peptides

Immobilizing heparin and heparan sulfate onto fused-silica capillaries using biotin–neutravidin conjugation has been applied to ACE analysis (73). These capillaries exhibit markedly reduced electroosmotic flow and were able to distinguish heparin-binding peptides that differed only in the stereochemistry or type of amino acid residue. No resolution of these peptides was observed if heparin or heparan sulfate was included in the buffer phase.

Capillary Modification. The capillary was chemically modified based on the immobilization method used by Cosford and Kuhr (84). The chem-

© 2003 by Marcel Dekker, Inc.

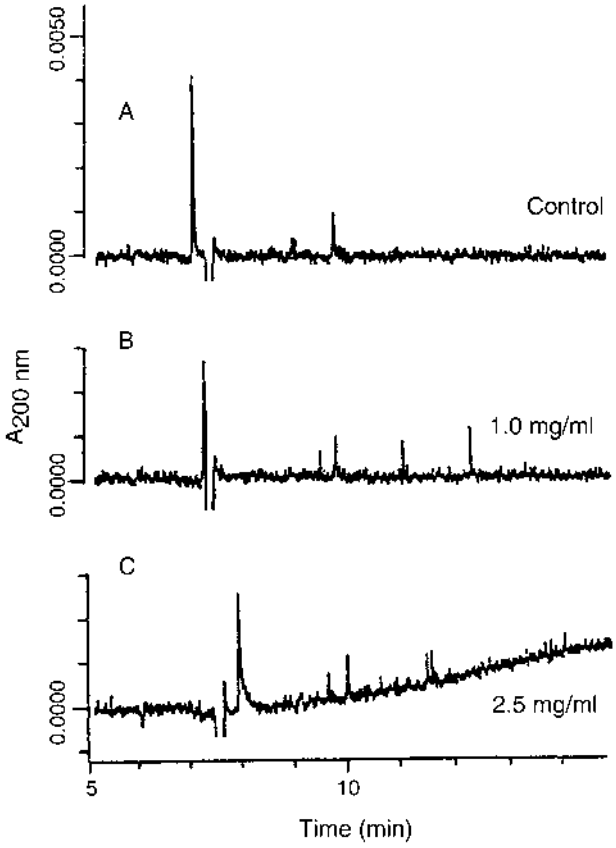

Fig. 6 ACE analysis of a purified heparin-binding peptide fragment of SAP. Demonstration of interaction with heparin. The peptide fragment was analyzed at 20 kV (detection at 200 nm) after a 5-s injection in the presence of the indicated concentrations of heparin in the electrophoresis buffer (0.1 M phosphate, pH 7.5). (From Ref. 71.)

istry of immobilization of the heparin and heparan sulfate onto the surface of the capillary is illustrated in Figure 7. Briefly, the capillary was treated with 3-aminopropyl triethoxysilane (APTES), succinimidyl-6-(biotinamido) hexanoate (NHS-LC-biotin), and neutravidin, respectively. Finally, biotinylated heparin or heparan sulfate was introduced to the capillary wall as an affinity layer. Heparan sulfate was immobilized to the surface through biotin

© 2003 by Marcel Dekker, Inc.

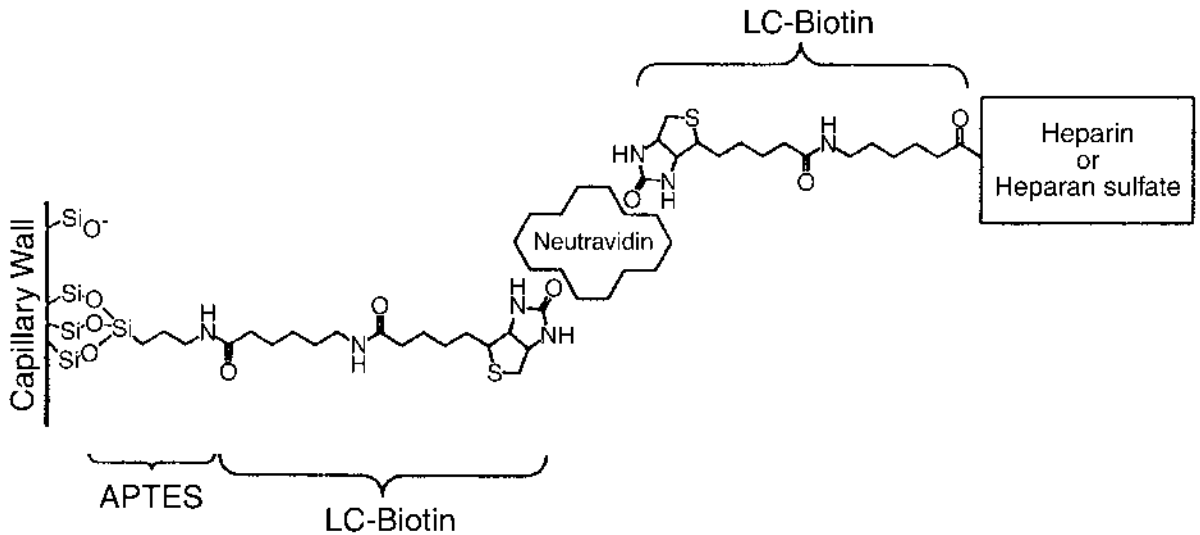

Fig. 7 Schematic diagram showing the immobilization of GAG to the capillary surface. (From Ref. 73.)

© 2003 by Marcel Dekker, Inc.

covalently attached through its primary amino group, whereas heparin was biotinylated through covalent attachment to its carboxyl groups.

Separation of Heparin-Binding Peptides. Two peptides were synthesized based on the heparin-binding domain of acidic fibroblast growth factor (aFGF) having the sequence GLKKNGSCKRGPRTHYGQKA, residues 125–144. These two peptides, which differ only in the stereochemistry of a single amino acid (L-proline to D-proline), showed the interaction to both heparin and heparan sulfate. However, a peptide in which L-proline (the native peptide sequence) showed higher affinity for heparan sulfate. The different dissociation (K_d) constants for the heparan sulfate interaction with these peptides were observed by injecting a racemic mixture of D- and L-proline peptides onto the heparan sulfate–coated capillary, and the mixture was readily separated, as shown in Figure 8. The separation is based on the different affinities of the peptides to heparan sulfate resulting from the different migration times (25.4 and 25.9 minutes for the D- and L-proline-

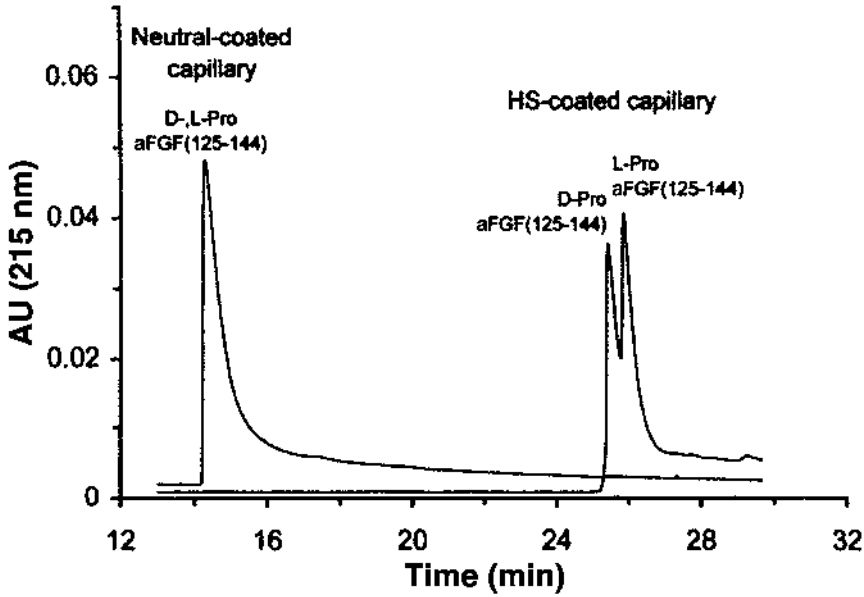

Fig. 8 Separation of D- and L-proline aFGF peptides using neutral and heparan sulfate–coated capillaries. A racemic mixture of D- and L-proline-containing peptides (130 μM) were injected (22 nL) and subjected to electrophoresis using 50 mM sodium phosphate buffer, pH 7.4, 20C, and 20 kV. (From Ref. 73.)

© 2003 by Marcel Dekker, Inc.

containing peptides, respectively). No resolution was observed in control experiments using a normal fused-silica capillary and a neutral hydrophilic polymer–coated capillary.

This report also showed a markedly improved resolution in the separation of arginine (R_5W) and lysine (K_5W) basic polypeptides on a heparan sulfate–coated capillary, compared with a neutral-coated capillary. Arginine (R_5W) and lysine (K_5W) polypeptides, while having an identical charge, differ sufficiently in their properties to be partially separated on the neutral-coated capillary (Fig. 9). A heparan sulfate–coated capillary increases the migration times of both peptides. In addition, the separation of these peptides was significantly enhanced due to the different affinities for heparan sulfate of each peptide (Fig. 9). Arginine-rich peptides are known to bind heparin and heparan sulfate with several-fold higher affinity than do lysine-rich peptides (4).

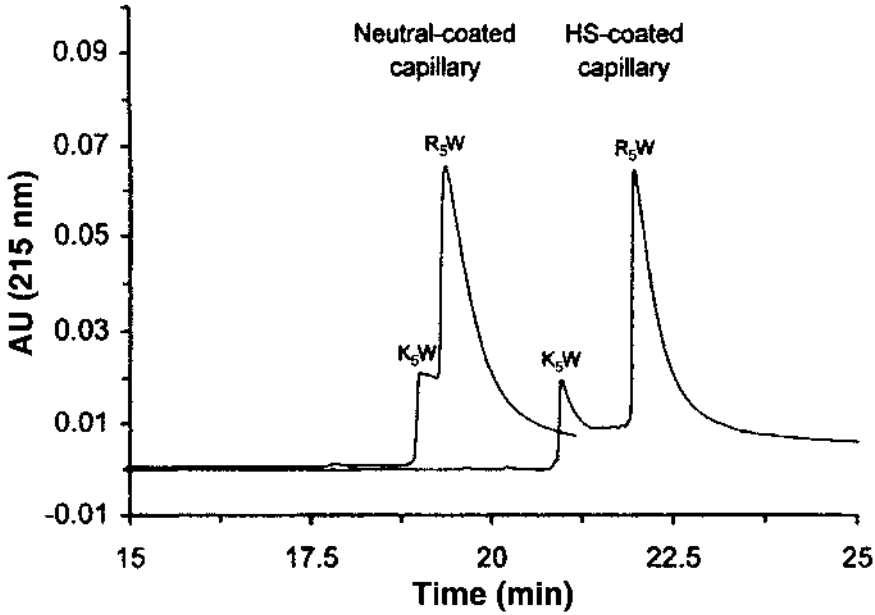

Fig. 9 Separation of K_5W and R_5W peptides using neutral and heparan sulfate–coated capillaries. A mixture of K_5W and R_5W peptides (140 and 400 μM, respectively) were injected (22 nL) onto the capillaries, and electrophoresis was performed as described in Figure 8 legend. (From Ref. 73.)

© 2003 by Marcel Dekker, Inc.

3. Example 3: Using ACE to Study the Affinity Interaction of Heparin with the Serine Protease Inhibitors

Based on the mixed-phase method, ACE is introduced for studying the interaction of heparin with the serine protease inhibitors, antithrombin III (ATIII) and secretory leukocyte proteinase inhibitor (SLPI) (85). An etched capillary, to which heparin has been covalently immobilized, was used in this study. This modified capillary both afforded an improvement in the separation of heparin-binding proteins and required a lower quantity of loaded protein.

Capillary Modification. The capillary was etched with a fluoride compound at high temperature to prepare a whisker column with a 1000-fold increased inner surface area as compared to an unmodified capillary (86). This results in almost the same specific surface area as found in capillary packed with macroporous silica beads. Next, the heparin was covalently immobilized on the surface of an etched capillary through a spacer using silane chemistry.

Separation of Serine Protease Inhibitors. As a control experiment, ATIII was injected into an unmodified capillary in the presence of low-molecular-weight heparin. No change in the migration of ATIII under electrophoresis was observed. The interaction between the proteins with heparin was studied by performing ACE on ATIII, SLPI (heparin-binding proteins), and bovine serum albumin (BSA) (noninteracting protein) using heparinized capillary. The proteins were bound to heparinized capillary, washed with buffer, eluted with sodium chloride, and detected by absorbance. Noninteracting BSA eluted first in buffer, while SLPI and ATIII, having affinity for heparin, were eluted only when the capillary was washed with buffer containing 1 M sodium chloride (Fig. 10). This study demonstrates a new approach to measuring the heparin interaction of both SLPI and ATIII using ACE.

A detailed examination of the affinity of SLPI for the heparinized capillary was next made using a stepwise elution (from 0.1 to 0.9 M NaCl) (Fig. 11). SLPI eluted from the capillary with 0.2 M NaCl. This agreed well with results obtained by traditional affinity chromatography on a heparin-Sepharose matrix. The ACE method has the unique advantages over traditional affinity chromatography in that it requires much smaller quantities of protein and afforded better separation profiles.

4. Example 4: Using ACE to Observe the Complexation Behavior of Amylodextrin Oligomers and Selected Pharmaceuticals

Amylose and amylodextrins have been used in the food and pharmaceutical industries as excipients. Recently, they have been explored as chiral selec-

© 2003 by Marcel Dekker, Inc.

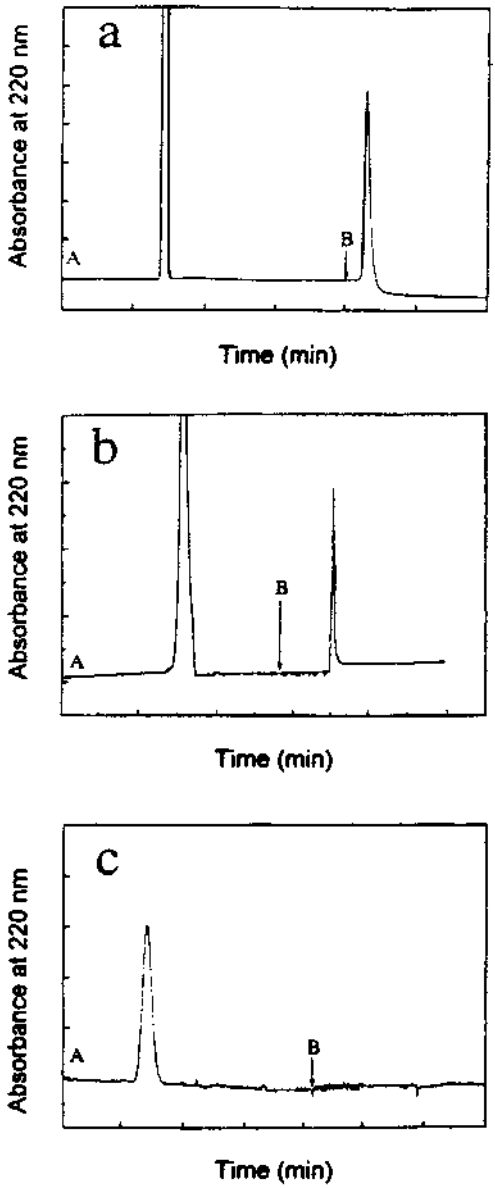

Fig. 10 ACE using an etched capillary with heparin bound. (a) SLPI concentration, 10 mg/mL. ACE condition: etched capillary, 75-μm ID $\times$ 55 cm (47 cm from injection to detection window), heparin bound via silane spacer. Injection mode: gravity, height 55 cm, time 15 s. Washing and elution mode: pressure injection, 2 psi, 300 s. Buffer A, 25 mM sodium phosphate, pH 7.4; buffer B, buffer and 1.0 M NaCl. Detection wavelength, 220 nm. (b) ATIII concentration, 4.5 mg/mL. (c) Bovine serum albumin, 0.3 mg/mL. (From Ref. 85.)

© 2003 by Marcel Dekker, Inc.

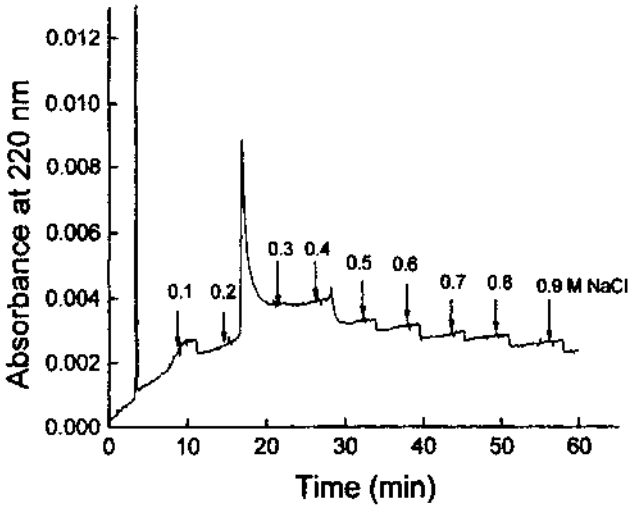

Fig. 11 ACE step elution of SLPI by various concentrations of NaCl containing buffer from heparin-bound etched capillary. NaCl concentration in elution buffer: see Fig. 10 for conditions. (From Ref. 85.)

tors. A fluorescent-labeling approach was applied to this interaction study between amylodextrins and four different pharmaceuticals (ibuprofen, ketoprofen, furosemide, and warfarin) (75). Amylodextrin oligomers were fluorescently derivatized. The complexation behavior was predicted based on observed changes in the migration times and peak shapes of the amylodextrin solutes obtained under electrophoresis in the presence and absence of the binding partner. Further, ^{13}C NMR measurements were performed in support of the ACE complexation studies.

The selectivity of complexation was the subject of this study. The minimum size of sugar oligomer chain able to form the complex was explained. As a model experiment, the interaction study between amylodextrins and (S)-(+)-ibuprofen was performed. The migration profiles of amylodextrins with and without ibuprofen ligands in the buffer clearly showed differences. These results suggested a size selectivity for the formation of oligosaccharide drug complex (Fig. 12). No changes in the retention time and peak shape of dextrin oligomers was observed when the degree of polymerization of this oligosaccharide less than 10, indicative of no interaction taking place between these small amylodextrins and ibuprofen. Interestingly, the decasaccharide (DP = 10) peak was visibly sharpened. This suggested a strong interaction between the decasaccharide and the drug li-

© 2003 by Marcel Dekker, Inc.

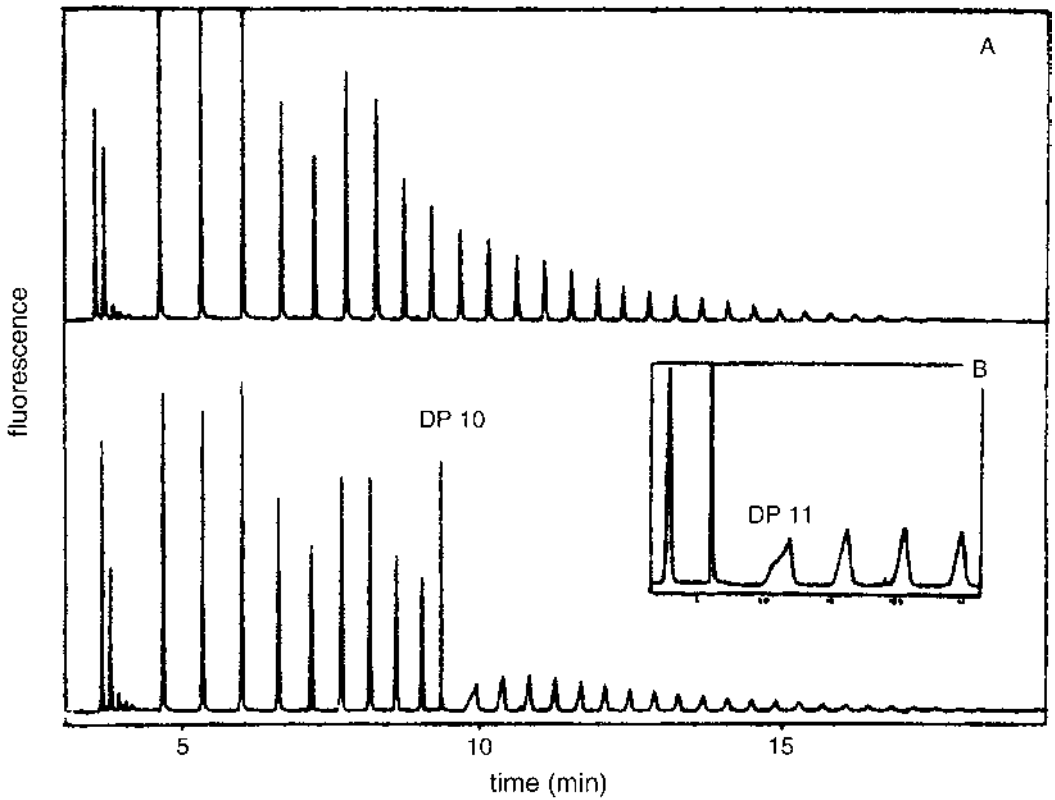

Fig. 12 Electropherograms of amylodextrins with (A) and without (B) (S)-(+)-ibuprofen. Conditions: 46- and 12-cm coated capillaries, 50-μm i.d., 360-μm o.d.; 40 mM acetate-Tris buffer, pH = 5.0, ionic strength 18.3 mM (adjusted by NaCl); LIF detection at 488 nm/514 nm; applied voltage, 25 kV; current: 20 μA. (From Ref. 75.)

© 2003 by Marcel Dekker, Inc.

gand. The sharp peak associated with the decasaccharide drug complex also migrated faster than the decasaccharide in the noncomplexed form, suggesting conformational change due to a tight interaction and an enhanced charge-to-mass ratio of this complex.

This study also suggests that molecular size and structure play a role in this interaction. The binding behaviors of dextrin oligomers for four different pharmaceuticals (ibuprofen, ketoprofen, furosemide, and warfarin) were observed under the same experimental conditions. Ibuprofen and ketoprofen, two compounds that are similar in chemical structure and pharmaceutical use, showed obvious differences in interaction patterns (Fig. 13A and B). Ketoprofen, having an extra aromatic ring, required an octasaccharide (DP = 8) for binding, whereas ibuprofen required a heptasac-

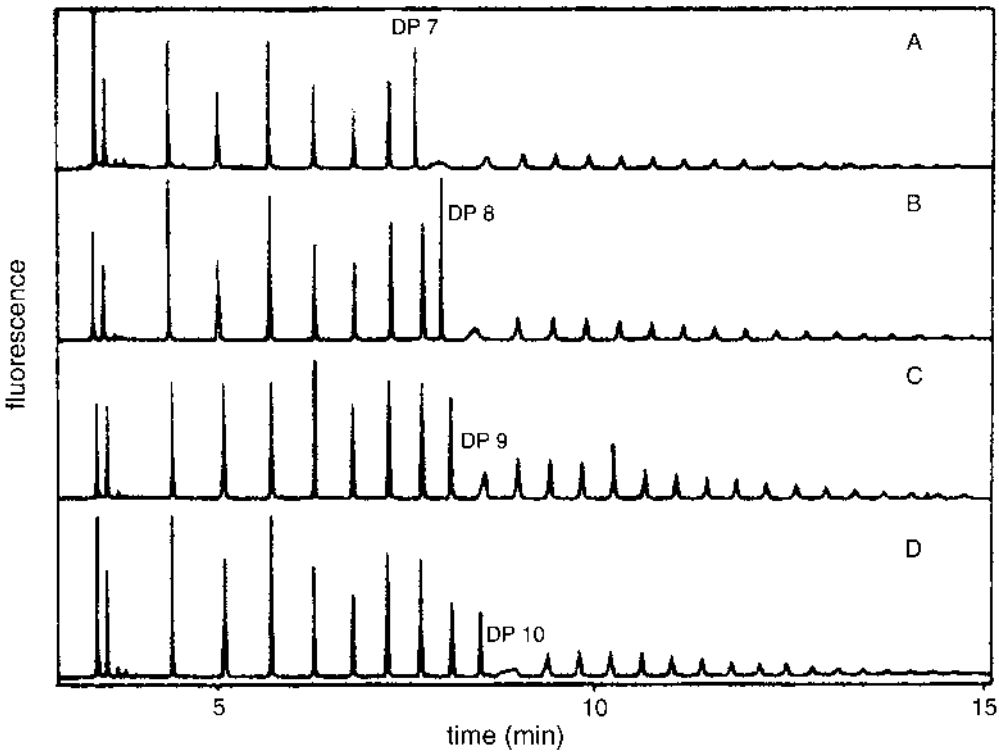

Fig. 13 Electropherograms of amylodextrins with different pharmaceuticals. (A) ibuprofen, (B) ketoprofen, (C) furosemide, (D) warfarin. Electrophoretic conditions: 20 mM phosphate buffer, pH = 7.0, ionic strength 18.3 mM. Other conditions are the same as for Figure 12. (From Ref. 75.)

© 2003 by Marcel Dekker, Inc.

charide (DP = 7) for its interaction. Furosemide and warfarin required longer oligosaccharide chains for complexation, consistent with their larger molecular sizes (Fig. 13C and D).

Several factors that might influence the actual interaction were also examined. Experimental conditions such as pH, ionic strength, and the nature and concentration of organic additives significantly affected the formation of the complex.

VIII. CONCLUSIONS AND FUTURE DIRECTIONS

Heparin is the most commonly used pharmaceutical polysaccharide, having been used for over 60 years as an anticoagulant. Numerous proteins of physiologic and pathologic importance have been found to interact with heparin, offering a large number of potential new therapeutic applications for heparin. A major limitation in utilizing heparin in new ways is that its anticoagulant properties can result in hemorrhagic complications. The introduction of LMW heparins, heparin oligosaccharides, and synthetic analogues of reduced anticoagulant activity has been used to enhance heparin's specificity, required for new applications in the treatment of cancer, viral and bacteria infection, Alzheimer's disease, and transplant rejection. To substitute for heparin in these new applications, an analogue should ideally bind only those proteins that regulate the desired activity. Interaction studies have been performed on heparin and its analogues using a variety of methods. The ACE technique has been the subject of much attention because of its high resolution, high selectivity, and high throughput and the extremely small amounts of sample required. And ACE offers advantages to pharmaceutical and medical researchers in their study of drug interaction with polysaccharides used as excipients (see Chapter 4).

Although the ACE method offers a number of advantages, several important problems still need to be addressed. A major issue is the concentration detection limit. The development of more sensitive detection methods, such as mass detector and LIF detection, should be very helpful in overcoming this marked disadvantage. The combination of CE, fluorescent labeling, and LIF detection might provide an efficient way to quantify the amount of unlabeled molecules in the form of a fluorescent complex. However, a marked disadvantage of LIF is that labeling of the analytes is usually required, which might change the interaction behavior of the solutes under investigation. An alternative detection approach, mass spectrometric (MS) detection, looks very promising. The combination of the high selectivity of ACE and the structural identification of the MS makes ACE-MS a powerful

© 2003 by Marcel Dekker, Inc.

technique (see Chapter 13). Unfortunately, this combination technique is expensive and still not routinely available.

The interaction of the analytes with the capillary wall is another problem that prevents the application of ACE in many cases. Coated capillaries might represent one approach to overcoming this problem. Recent efforts have focused on developing simple, reproducible, and chemically stable coating procedures. There are still many challenges to be solved in developing such coated capillaries.

Important future progress in sensitive detection strategies and the emergence of adequate coating technologies should increase the application of ACE in the study of polysaccharide–protein interaction. This will greatly increase our fundamental understanding of the biology, chemistry, and physics of these interactions. Practical application of ACE is also expected in the fields of high-throughput screening and combinatorial chemistry. Finally, this approach will also be extremely useful for clinical chemistry and diagnostics.

REFERENCES

1. RJ Linhardt, T Toida. Heparin Oligosaccharides: New Analogues Development and Applications. In: ZJ Witczak, KA Nieforth. Carbohydrate as Drugs. New York: Marcel Dekker, 1997, pp 277–341.
2. J Folkman, Y Shing. Control of angiogenesis by heparin and other sulfated polysaccharides. In: DA Lane, I Björk, U Lindahl. Heparin and Related Polysaccharides. New York: Plenum Press, 1992, pp 355–364.
3. AT Riegel, A Wellstein. The potential role of the heparin-binding growth factor pleiotrophin in breast cancer. Breast Cancer Res Treatment 31:309–314, 1994.
4. RE Hileman, JR Fromm, JM Weiler, RJ Linhardt. Glycosaminoglycan–protein interactions: definition of consensus sites in glycosaminoglycan-binding proteins. Bioessays 20:156–167, 1998.
5. U Lindahl, DS Feingold, L Roden. Biosynthesis of heparin. TIBS 11:221–225, 1986.
6. DA Lane, U Lindahl. Heparin, Chemical and Biological Properties, Clinical Applications. Boca Raton, FL: CRC Press, 1989.
7. RJ Linhardt, SA Ampofo, J Fareed, D Hoppensteadt, JB Mulliken, J Folkman. Isolation and characterization of human heparin. Biochemistry 31:12441–12445, 1992.
8. CC Griffin, RJ Linhardt, CL Van Gorp, T Toida, RE Hileman, RL Schubert, SE Brown. Isolation and characterization of heparan sulfate from crude porcine intestinal mucosal peptidoglycan heparin. Carbohydr Res 276:183–197, 1995.
9. D Green, J Hirsh, J Heit, M Prins, B Davidson, AW Lensing. Low-molecular-weight heparin: a critical analysis of clinical trials. Pharmacol Rev 46:89–109, 1994.
10. G Bratt, E Tornebohm, S Granquist, W Aberg, D Lockner. A comparison be-

© 2003 by Marcel Dekker, Inc.

tween low-molecular-weight heparin (KABI2165) and standard heparin in the intravenous treatment of deep venous thrombosis. Thromb Haemostas 54:813–817, 1985.
11. J Biller, EW Massey, JR Marler, HP Adams, JN Davis, A Bruno, RA Henriksen, RJ Linhardt, LB Goldstein, M Alberts, CT Kisker, GJ Toffol, CS Greenberg, KG Banwart, C Bertels, DW Beck, M Walker, HN Maganani. A dose escalation study or org 10172 (low-molecular-weight heparinoid) in stroke. Neurology 39:262–265, 1989.
12. KA Jandik, D Kruep, M Cartier, RJ Linhardt. Accelerated heparin stability studies. J Pharm Sci 85:45–51, 1996.
13. PC Liaw, RC Austin, JC Fredenburgh, AR Stafford, JI Weitz. Comparison of heparin- and dermatan sulfate–mediated catalysis of thrombin inactivation by heparin cofactor II. J Biol Chem 274:27597–27604, 1999.
14. MS Pavao, KR Aiello, CC Werneck, LC Silva, AP Valente, B Mulloy, NS Colwell, DM Tollefsen, PA Mourao. Highly sulfated dermatan sulfates from ascidians. J Biol Chem 273:27848–27857, 1998.
15. I Capila, MJ Hernaiz, YD Mo, TR Mealy, B Campos, RJ Linhardt, BA Seaton. Annexin V–heparin oligosaccharide complex suggests heparan sulfate–mediated assembly on cell surface. Structure 9:57–64, 2001.
16. M Lyon, JA Deakin, H Rahmoune, DG Fernig, T Nakamura, JT Gallagher. Hepatocyte growth factor/scatter factor binds with high affinity to dermatan sulfate. J Biol Chem 273:271–278, 1998.
17. F Peterson, E Brandt, U Lindahl, D Spillmann. Characterization of a neutrophil cell surface glycosaminoglycan that mediates binding of platelet factor 4. J Biol Chem 274:12376–12382, 1999.
18. T Ehnis, W Dieterich, M Bauer, B Lampe, D Schuppan. A chondroitin/dermatan sulfate form of CD44 is a receptor for collagen XIV (undulin). Exp Cell Res 229:388–397, 1996.
19. T Maruyama, T Toida, T Imanari, G Yu, RJ Linhardt. Conformational changes and anticoagulant activity of chondroitin sulfate following its O-sulfonation. Carbohydr Res 306:35–43, 1998.
20. RJ Linhardt, RE Hileman. Dermatan sulfate: a powerful therapeutic agent. Gen Pharmacol 26:443–451, 1995.
21. VD Nadkarni, T Toida, CL Van Gorp, TL Schubert, JM Weiler, KP Hanse, EEO Caldwell, RJ Linhardt. Preparation and biological activity of N-sulfated chondroitin sulfate derivatives. Carbohydr Res 290:87–96, 1996.
22. AJ Day. The structure and regulation of hyaluronan-binding proteins. Biochem Soc Trans 27:115–121, 1999.
23. ML Weiner. Toxicological properties of carrageenan. Agents Actions 32:46–51, 1991.
24. H Greiling, J Scott. Keratan Sulfate Chemistry, Biology, Chemical Pathology. London: T.J. Press, 1989.
25. YS Kim, YT Jo, IM Chang, TE Toida, Y Park, RJ Linhardt. A new glycasaminoglycan from the giant African snail *Achatina fulica*. J Biol Chem 271: 11750–11755, 1996.
26. H Wang, T Toida, YS Kim, I Capila, RE Hileman, M Bernfield, RJ Linhardt.

© 2003 by Marcel Dekker, Inc.

Glycosaminoglycans can influence fibroblast growth factor-2 mitogenicity without significant growth factor binding. Biochem Biophys Res Commun 235: 369–373, 1997.
27. TR Bhardwaj, M Kanwar, R Lal, A Gupta. Natural gums and modified natural gums as sustained-release carriers. Drug Develop Indust Pharm 26:1025–1038, 2000.
28. M Nagaoka, H Shibata, I Kimura-Takagi, S Hashimoto, R Aiyama, S Ueyama, T Yokokura. Anti-ulcer effects and biological activities of polysaccharides from marine algae. Biofactors 12:264–274, 2000.
29. HH Vitalone, GN Torres Nieto de Mercau, JC Valdez, S Davolio, G Mercau. Effect of carrageenan and indomethacin on the growth of a murine fibrosarcoma. Medicina 60:225–228, 2000.
30. G Oshima. Trigger action of dextran sulfate on inactivation of thrombin. Thromb Res 49:353–361, 1998.
31. T Kobayashi, K Tashiro, X Cui, T Konzaki, Y Xu, C Kabata, K Yamamoto. Experimental models of acute respiratory distress syndrome: clinical relevance and response to surfactant therapy. Biology Neonate 80 Suppl 1:26–28, 2001.
32. SM Swain, B Parker, A Wellstein, ME Lippman, C Steakley, R Delap. Phase I trial of pentosan polysulfate. Invest New Drugs 13:55–62, 1995.
33. M Degenhardt, P Ghosh, H Watzig. Studies on the structural variation of pentosan polysulfate sodium (NaPPS) from different sources by capillary electrophoresis. Archiv der Pharmazie 334:27–29, 2001.
34. MG Waters, JF Suleskey, LJ Finkelstein, ME Van Overbeke, VJ Zizza, M Stommel. Interstitial cystitis: a retrospective analysis of treatment with pentosan polysulfate and follow-up patient survey. J Am Osteo Assoc 100:S13–S18, 2000.
35. JF Innes, AR Barr, M Sharif. Efficacy of oral calcium pentosan polysulphate for the treatment of osteoarthritis of the canine stifle joint secondary to cranial cruciate ligament deficiency. Veterinary Rec 146:433–437, 2000.
36. P Ghosh. The pathobiology of osteoarthritis and the rationale for the use of pentosan polysulfate for its treatment. Sem Arthri Rheum 28:211–267, 1999.
37. SW McLeskey, L Zhang, BJ Trock. Effects of AGM-1470 and pentosan polysulphate on tumorigenicity and metastasis of FGF-transfected MCF-7 cells. Br J Cancer 73:1053–1062, 1996.
38. CR Parish, C Freeman, KJ Brown, DJ Francis, WB Cowden. Identification of sulfated oligosaccharide-based inhibitors of tumor growth and metastasis using novel in vitro assays for angiogenesis and heparanase activity. Cancer Res 59: 3433–3441, 1999.
39. CR Parish, C Freeman, MD Hulett. Heparanase: a key enzyme involved in cell invasion. Biochim Biophys Acta 1471:M99–M108, 2001.
40. DJ Cole, SE Ettinghausen, HI Pass, DN Danforth, MW Linhan, CW Myers, MR Cooper, WF Sindelar. Postoperative complications in patients receiving suramin therapy. Surgery 116:90–95, 1994.
41. MA Mitchell, JW Wilks. Inhibitors of angiogenesis. Eds Ann Reports Medicinal Chemistry 27. San Diego: Academic Press, 1992.
42. H Mitsuya, M Popovic, R Yarchoan, S Matsushita, RC Gallo, S Broder.

© 2003 by Marcel Dekker, Inc.

Suramin protection of T cells in vitro against infectivity and cytopathic effect of HTLV-III. Science 226:172–174, 1984.
43. M Botta, F Manetti, F Corelli. Fibroblast growth factors and their inhibitors. Curr Pharm Design 6:1897–1924, 2000.
44. CE Myers. Differentiating agents and nontoxic therapies. Urol Clin North Am 26:341–351, 1999.
45. A Heidenreich, R von Knobloch, R Hofmann. Current status of cytotoxic chemotherapy in hormone refractory prostate cancer. Eur Urol 39:121–130, 2001.
46. A Beedassy, G Cardi. Chemotherapy in advanced prostate cancer. Sem Oncol 26:428–438, 1999.
47. Y Chen, T Maguire, RE Hileman, JR Fromm, JD Esko, RJ Linhardt, RM Marks. Dengue virus infectivity depends on envelope protein binding to target cell heparan sulfate. Nature Med 3:866–871, 1997.
48. RE Edens, RJ Linhardt, JM Weiler. Heparin, not just an anticoagulant anymore: six and one-half decades of studies on the ability of heparin to regulate complement activation. Compl Prof 1:96–120, 1993.
49. MA Fath, X Wu, RE Hileman, RJ Linhardt, MA Kashem, RM Nelson, CD Wright, WM Abraham. Interaction of secretary leukocyte protease inhibitor with heparin inhibits protease involved in asthma. J Biol Chem 273:13563–13569, 1998.
50. D Sawitzky. Protein glycosaminoglycan interactions: infectiological aspects. Med Microbiol Immunol 184:155–161, 1996.
51. SlL Hung, PL Lee, HW Chen, LK Chen, CL Kao, CC King. Analysis of the steps involved in dengue virus entry into host cells. Virology 257:156–167, 1999.
52. RM Marks, H Lu, R Sundaresan, T Toida, A Suzuki, T Imanari, MJ Hernaiz, RJ Linhardt. Probing the interaction of dengue virus envelope protein with heparin: assessment of glycosaminoglycan-derived inhibitors. J Med Chem 44: 2178–2187, 2001.
53. RJ Hettiarachchi, SM Smorenburg, J Ginsberg, M Levine, MH Prins, HR Buller. Do heparins do more than just treat thrombosis? The influence of heparins on cancer spread. Thromb Haemost 82:947–952, 1999.
54. SM Smorenburg, CJ Van Noorden. The complex effects of heparins on cancer progression and metastasis in experimental studies. Pharmacol Rev 53:93–105, 2001.
55. LR Zacharski, DL Ornstein, AC Mamourian. Low-molecular-weight heparin and cancer. Sem Thromb Hemostas 26:69–77, 2000.
56. L Borsig, R Wong, J Feramisco, DR Nadeau, NM Varki, A Varki. Heparin and cancer revisited: mechanistic connections involving platelets, P-selectin, carcinoma mucins, and tumor metastasis. Proc Natl Acad Sci USA 98:3352–3357, 2001.
57. DL Gordan, RJ Linhardt, HP Adams. Low-molecular-weight heparin and heparinoids in cerebrovascular disease. Clin Neuropharmacol 13:522–543, 1990.
58. H Engelberg. Actions of heparin in the atherosclerotic process. Pharmacol Rev 48:327–352, 1996.

© 2003 by Marcel Dekker, Inc.

59. R Kisilevsky, LJ Lemieux, PE Fraser, X Kang, PG Hultin, WA Szarek. Arresting amyloidosis in vivo using small-molecule anionic sulfonates or sulfates —implications for Alzheimers disease. Nature Med 1:143–148, 1995.
60. SL Shyng, S Lehmann, KL Moulder, DA Harris. Sulfated glycans stimulate endocytosis of the cellular isoform of the prion protein, PrP, in cultured cells. J Biol Chem 270:30221–30229, 1995.
61. J Fareed. Current trends in antithrombotic drug and device development. Sem Thromb Hemostas 22:3–8, 1996.
62. S Faham, RJ Linhardt, DC Rees. Diversity does make a difference: fibroblast growth factor–heparin interactions. Curr Opin Struct Biol 8:578–586, 1998.
63. RM Nelson, A Venot, MP Bevilacqua, RJ Linhardt, I Stamenkovic. Carbohydrate–protein interactions in vascular biology. Annu Rev Cell Dev Biol 11: 601–631, 1995.
64. JR Fromm, RE Hileman, JM Weiler, RJ Linhardt. Interaction of FGF-1 and related peptides with heparan sulfate and its oligosaccharides. Arch Biochem Biophys 346:252–262, 1997.
65. EC Nice, B Catimel. Instrumental biosensors: new perspectives for the analysis of biomolecular interactions. Bioessay 21:339–352, 1999.
66. J Schlessinger, AN Plotnikov, OA Ibrahimi, AV Eliseenkova, BK Yeh, A Yayon, RJ Linhardt, M Mohammadi. Crystal structure of a human FGF–FGFR–heparin complex reveals a dual role for heparin in FGFR binding and dimerization. Molecular Cell 6:743–750, 2000.
67. NHH Heegaard, PMH Heegaard, P Roepstorff, FA Robey. Ligand-binding sites in human serum amyloid P component. Eur J Biochem 239:850–856, 1996.
68. RM Guijt-van Duijn, J Frank, GWK van Dedem, E Baltussen. Recent advances in affinity capillary electrophoresis. Electrophoresis 21:3905–3918, 2000.
69. SN Krylov, NJ Dovichi. Capillary electrophoresis for the analysis of biopolymers. Anal Chem 72:111R–128R, 2000.
70. NHH Heegaard, RT Kennedy. Identification, quantitation, and characterization of biomolecules by capillary electrophoretic analysis of binding interactions. Electrophoresis 20:3122–3133, 1999.
71. NHH Heegaard, HD Mortensen, P Roepstorff. Determination of a heparin-binding site in serum amyloid P component using affinity chromatography electrophoresis as an adjunct technique. J Chromagr A 717:83–90, 1995.
72. NHH Heegaard, J Brimnes. Comparison of heparin binding to lactoferrin from human milk and from human granulocytes by means of affinity capillary electrophoresis. Electrophoresis 17:1916–1920, 1996.
73. VA VanderNoot, RE Hileman, JS Dordick, RJ Linhardt. Affinity capillary electrophoresis employing immobilized glycosaminoglycan to resolve heparin-binding peptides. Electrophoresis 19:437–441, 1998.
74. K Shimura, K Kasai. Determination of the affinity constants of concanavalin A for monosaccharides by fluorescence affinity probe capillary electrophoresis. Anal Biochem 227:186–194, 1995.
75. M Hong, H Soini, A Baker, MV Nothy. Complexation between amylodextrin oligomers and selected pharmaceuticals measured through capillary electrophoresis. Anal Chem 70:7590–7597, 1998.

© 2003 by Marcel Dekker, Inc.

76. G Dongowski, RHH Neubert, M Platzer, MA Schwarz, B Schnorrenberger, H Anger. Interaction between food components and drugs. Part 6: Influence of starch degradation products on propanolol transport. Pharmazie 53:871–875, 1998.
77. M Hong, A Cassely, Y Mechref, MV Novothy. Sugar–lectin interactions investigated through affinity capillary electrophoresis. J Chromatogr B 752:207–216, 2001.
78. H Nishi. Enantiomer separation of basic drugs by capillary electrophoresis using ionic and neutral polysaccharides as chiral selectors. J Chromatogr A 735:345–351, 1996.
79. G Gubitz, MG Schmid. Recent progress in chiral separation principles in capillary electrophoresis. Electrophoresis 21:4112–4135, 2000.
80. H Nishi. Enantioselectivity in chiral capillary electrophoresis with polysaccharides. J Chromatogr A 792:327–347, 1997.
81. RMC Sutton, KL Sutton, AM Stalcup. Chiral capillary electrophoresis with noncyclic oligo- and polysaccharide chiral selectors. Electrophoresis 18:2297–2304, 1997.
82. R Gotti, V Cavrini, V Anchisano, G Mascellani. Dermatan sulfate as useful chiral selector in capillary electrophoresis. J Chromatogr A 814:205–211, 1998.
83. X Wang, JT Lee, DW Armstrong. Separation of enantiomers by capillary electrophoresis using pentosan polysulfate. Electrophoresis 20:162–170, 1999.
84. RJO Cosford, WG Kuhr. Capillary biosensor for glutamate. Anal Chem 68: 2164–2169, 1996.
85. X Wu, RJ Linhardt. Capillary affinity chromatography and affinity capillary electrophoresis of heparin-binding proteins. Electrophoresis 19:2650–2653, 1998.
86. JJ Pesek, MT Matyska. Electrochromatography in chemically modified etched fused-silica capillaries. J Chromatogr A 736:255–264, 1996.

© 2003 by Marcel Dekker, Inc.

12
Characterization of Immunoreactions

Andrea Kühn
Martin-Luther-University Halle-Wittenberg, Halle, Germany

Steffen Kiessig
Solvias AG, Basel, Switzerland

Frank Thunecke
UFZ Center for Environmental Research, Leipzig, Germany

I. SCOPE

This chapter will deal mainly with ACE investigations of antigen–antibody interactions. Following the enzyme-linked immunosorbent assays (ELISAs), most of these experiments are also identified as capillary electrophoresis immunoassays (CEIAs), CE-based immunoassays, or immunocapillary electrophoresis. Because of the expected audience, the focus of the chapter is more on the application aspect than on technical details. There are, for example, several successful attempts reported to use immobilized antibodies within the capillary to enhance the separation efficiency of structurally very similar antigens. Because these antigen–antibody interactions are implemented only for separation reasons, they are not covered in this chapter. Experiments using antibody substitutes with oligonucleotide nature, such as aptamers, will also not be described. On the other hand some special applications that may be directed to the future in this field are exemplified, like microchip-based assays and experiments with whole cells or viruses. Finally, the authors decided to include ACE examples dealing with proteins known to be influencing the immune system, such as human immunodeficiency virus (HIV) proteins and the so-called immunophilins. The authors took care to include all relevant references. Still, some noteworthy investigations may have been overlooked. Therefore, readers more interested in this field are

© 2003 by Marcel Dekker, Inc.

referred to some excellent recent reviews (1–5). Also, it is always a good idea to research the review volumes annually released by *Analytical Chemistry*, *Electrophoresis*, or *Journal of Chromatography*.

II. INTRODUCTION

Immunoreactions are the key reactions for identifying and fighting extraneous substances, known as antigens, that might be harmful to physiological functions. Identification implies binding to the antigen molecules, comparison to specific patterns to recognize them as extraneous, and the production of specific molecules, called *antibodies*, as an immune answer. The antibodies bind tightly and specifically to the antigens, thereby forming antigen–antibody complexes (Ag-Ab complexes), which are transported to specific cells to digest the antigens. This process is widely used to stimulate the production of antibodies against diseases. Furthermore, it is utilized to qualitatively and quantitatively detect biomolecules. Such procedures are known as *immunoassays*. In the common format, one assay constituent, mostly the Ab, is immobilized on a surface. To recognize as few molecules as possible it is most often also necessary to label one of the assay components. Very popular is fluorescence labeling with derivatives of fluorescein, rhodamine, or carbocyanine dyes. Other labeling techniques make use of radioactivity, chemiluminescence, or enzyme amplification. However, the immobilization process as well as the labeling can alter the binding affinity to the antigen. Moreover, the antibody source produces a lot of different antibodies with different binding affinities to the antigen and different cross-reactivities to other antigens. In general a single ELISA is most often time-consuming, because it requires a preconcentration procedure on the surface. Furthermore, it will only work with tight-binding antibodies and involves obstacles for complex matrices. Therefore, the development of additional methods allowing detection of Ag–Ab interactions is desirable.

Affinity capillary electrophoresis can be used for the detection of Ag–Ab interactions, because the complexation is likely to change the migration properties. Therefore, it is possible to separate free and complexed Ag or Ab in the case of a high-affinity interaction and slow dissociation rate constants of the complex. These experiments are executed in the equilibrium–mixture mode and called CEIA. Additionally, ACE investigations covering weak Ag–Ab interactions can be carried out using the migration-shift approach.

The first ACE applications for the investigation of Ag–Ab interactions were reported in 1993. Since then the published examples have grown steadily, though not progressively like other ACE investigations. Most application

© 2003 by Marcel Dekker, Inc.

areas of traditional ELISA have been tested to fit for CEIA. The results achieved so far suggest, however, that the method is promising but still in a rather developmental stage. A broader use is hampered for several reasons. To detect Ag–Ab interactions by ACE separation, conditions are necessary that disturb the interaction as little as possible. This especially restricts the choice of background buffer pH and buffer additives. Unfortunately, these are the most powerful conditions changed to prevent protein adsorption on the capillary wall. Therefore, it is hard to predict if a given Ag–Ab interaction will lead to evaluable and repeatable peaks. Another important point is whether CEIA can compete with the well-established ELISA. Advantages of the CEIA format are its better mass sensitivity, its faster analysis of single runs, as well as its low reagent consumption. The CEIA method can handle crude mixtures by separating the unwanted components during the assay. The direct visualization of the immunocomplex formation and dissociation makes it easier to discriminate between specific and nonspecific binding. Furthermore, CEIA is more compatible with automation and on-line hyphenation to other techniques. A major drawback, however, is that the concentration sensitivity is most often poorer compared to ELISA. Moreover, the longer time needed to execute a single ELISA is well compensated by using 96-well plates, thereby allowing high-throughput analysis. There is no CE instrumentation yet commercially available to achieve parallel operation, except for DNA sequencing.

III. CAPILLARY ELECTROPHORESIS IMMUNOASSAY (CEIA)

Similar to ELISA, CEIA experiments can be divided into noncompetitive and competitive modes. The experimental setup of both procedures is illustrated in Figure 1. In the noncompetitive approach (A), a fluoresceinylated antibody is pre-equilibrated with increasing amounts of nonlabeled antigen. Because of the interaction, a new peak emerges for the Ab–Ag complex, whereas the signal of the unbound antibody decreases. The experiment can also be done in such a way that a labeled antigen is mixed with increasing amounts of an unlabeled antibody. These kinds of experiments are also called ''direct'' CEIA or affinity probe capillary electrophoresis. To facilitate a competitive CEIA (B), the nonlabeled antibody is pre-equilibrated with a labeled antigen and increasing amounts of nonlabeled antigen. The nonlabeled antigen displaces the labeled one from the complex, thereby generating a peak for the labeled but unbound antigen, which is used for quantitation. It should be mentioned again that both approaches utilize the equilibrium–mixture mode in the context of ACE. This requires tight-binding and slow

© 2003 by Marcel Dekker, Inc.

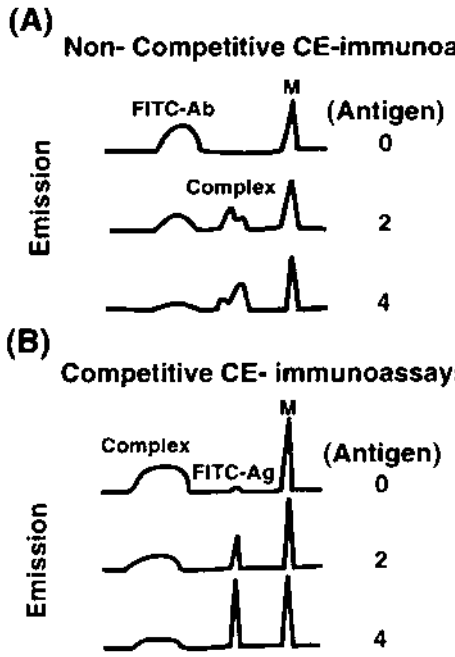

Fig. 1 Principles of noncompetitive (A) and competitive (B) capillary electrophoresis immunoassays (CEIAs) with labeled reagents for the measurement of specific analytes using laser-induced fluorescence detection. (A) Fluoresceinylated antibody (FITC–Ab) and fluorescing marker molecule (M) mixed with increasing amounts of unlabeled antigen (Ag) of low mobility. Complex peaks are double-peaked, corresponding to mono- and bivalent antibody occupancy. (B) Fluoresceinylated antigen (FITC–Ag) and marker (M) are mixed with antibody and with a sample containing increasing amounts of unlabeled antigen that displace FITC–Ag from the antibody–FITC–Ag complex (Complex). Quantitation of unlabeled antigen is based on the area of the resulting FITC–Ag peak. (Reprinted with permission from Ref. 1. Copyright 1998 Elsevier Science.)

off-rates of the complex. Otherwise a significant amount of the complex will dissociate during the experiment and make the results questionable.

To investigate weak Ag–Ab interactions, the mobility-shift mode of ACE is used. In this approach one component is mixed in different concentrations to the background buffer and the change in the migration time of the other assay constituent used for the calculation of the dissociation constant. Because of dissociation constants in the micromolar range or even higher, experiments are executable without reagent labeling using standard UV detection.

© 2003 by Marcel Dekker, Inc.

A. Noncompetitive Capillary Electrophoresis Immunoassays

Shimura and Karger published the first example of a noncompetitive CEIA in 1994 (6). Here a rhodamine-labeled fragment of a mouse monoclonal antibody against human growth hormone (hGH) was used. To separate the free labeled antibody fragment and the fluorescent complex, capillary isoelectric focusing (CIEF) was exemplified. This allowed them to achieve detection limits down to the lower picomolar range, because in CIEF mode the entire capillary is filled with sample prior to the focusing step. It is interesting to note that the complexes of three methionyl rhGH variants could also be easily distinguished from each other.

In one of the earlier applications, Heegaard (7) employed the interaction of phosphotyrosine to monoclonal antiphosphotyrosine antibodies as a model system. He investigated the influence of changed experimental CE conditions, such as pH and field strength, on the calculated dissociation constant. UV detection was used in this study, and the binding constants were in the lower micromolar range.

A method for determination of binding stoichiometries in biochemical systems has been reported by Chu et al. (8). For multivalent, tight-binding systems, these ACE procedures can readily separate stable intermediate species (Fig. 2). The method is generally applicable to both tight- and weak-binding systems and requires only nanograms of proteins and ligands. For high-affinity systems (such as antibody–antigen), samples having a fixed concentration of a receptor protein and various concentrations of the ligand are prepared and injected into a capillary containing the electrophoresis buffer alone. An abrupt change in the slope, in a plot of the integration of free ligand vs. the ratio of $[L]_{total}/[R]$ in samples, corresponds to the binding stoichiometry n of the system studied. The results on binding interactions of a monoclonal antihuman serum albumin (HSA) antibody to its antigen HSA showed that the antibody associates tightly with its antigen to form complexes having different electrophoretic mobilities with a final stoichiometric ratio of 1:2. Stable intermediate species are separated and obtained upon titrating the receptor protein with its ligand for binding systems of $n > 1$.

The dissociation constant (K_d) of a monoclonal antibody with fluorescein isothiocyanate- (FITC)-labeled insulin and unlabeled insulins from several species were measured using CE with laser-induced fluorescence detection (CE-LIF) (9). K_d determinations were made by separating free FITC-labeled insulin and its complex with the antibody in equilibrated solutions in 6 s or less (Fig. 3). Dissociation and association rates for insulin, FITC-insulin, and the antibody are fast enough to reach equilibria in less

© 2003 by Marcel Dekker, Inc.

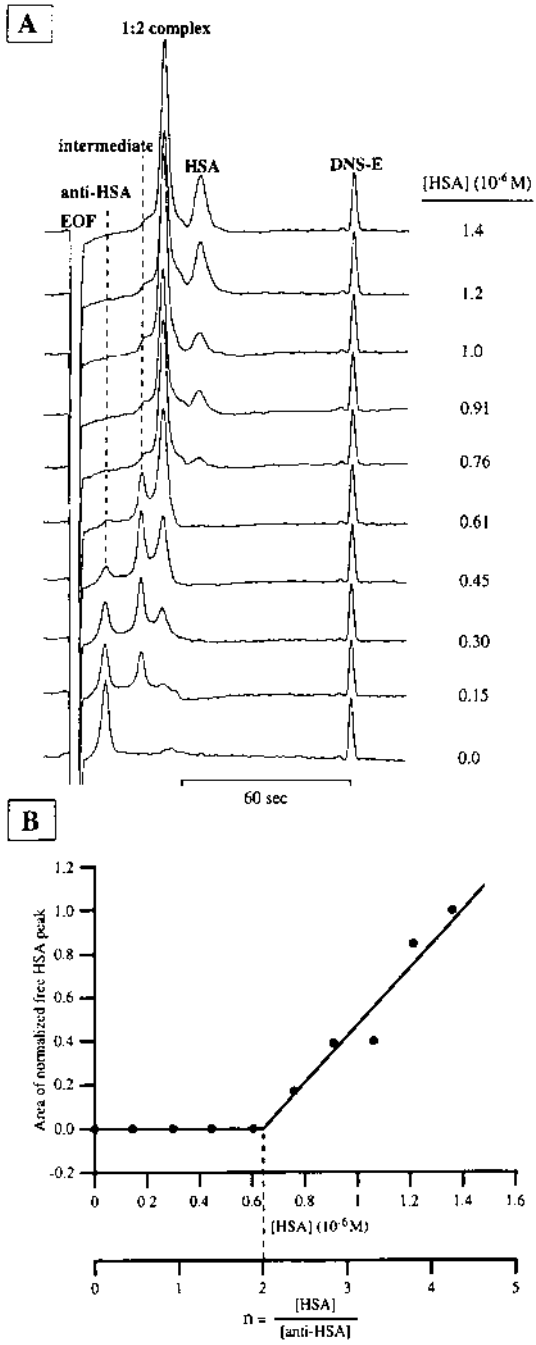

© 2003 by Marcel Dekker, Inc.

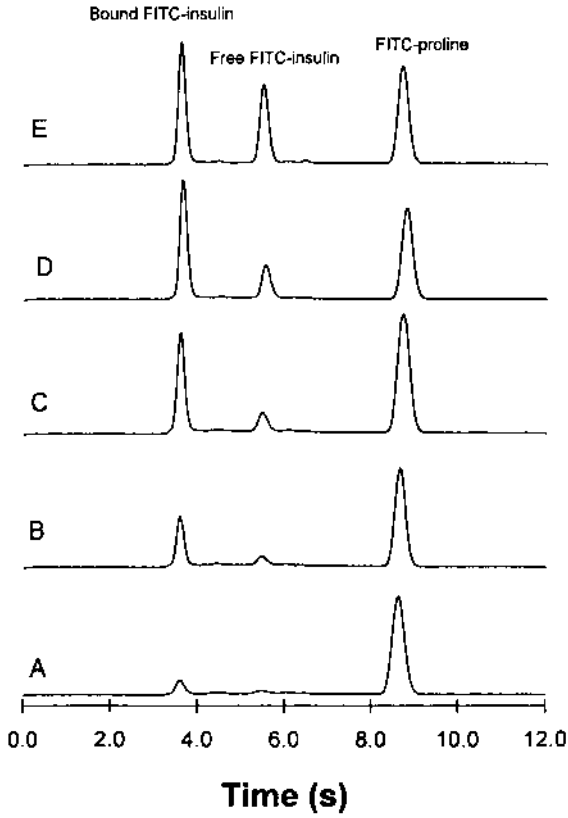

Fig. 3 Electropherograms used for the determination of the dissociation constant between FITC-insulin and the antibody. All samples contained 0.1 nM FITC-proline (internal standard) and 2 nM antibody. Total concentrations of FITC-insulin were: (A) 1 nM, (B) 2 nM, (C) 3 nM, (D) 4 nM, (E) 6 nM. (Reprinted with permission from Ref. 9. Copyright 1997 Wiley-VCH.)

←

Fig. 2 Determination of the binding stoichiometry of human serum albumin (HSA) to its mouse monoclonal IgG antibody (anti-HSA). (A) The concentration of anti-HSA was 0.33 μM. DNS-E was dansylglutamic acid used as internal standard. The intermediate species is considered to be due to the 1:1 complex. (B) A plot of the concentration of free ligand vs. the ratio of [HSA]/[anti-HSA] gives a sharp break at the stoichiometric point. (Reprinted with permission from Ref. 8. Copyright 1994 American Chemical Society.)

© 2003 by Marcel Dekker, Inc.

than 3 min. The use of LIF detection allowed the quantification of free and bound FITC-insulin in the picomolar range. The K_d of FITC-insulin with the antibody was determined to be 0.25 nM by Scatchard analysis. The applicability of the method for competitive and noncompetitive assays was described earlier by Schultz and Kennedy (10). They also observed that high electric field strength is important in obtaining well-shaped complex peaks.

Busch et al. studied the applicability of CZE to the examination of hapten–antibody complex formation (11). The catalytic antibodies examined have been used to accelerate a Diels–Alder reaction. Association constants of two hapten–antibody complexes were investigated and compared to the ELISA method. The samples contained buffer, hapten, and antibody. The constants obtained with CZE are a factor of 3–5 larger than those found with the ELISA method. The free-hapten concentration is measured directly; this allows confirmation of the stoichiometric model. Because of the poor concentration sensitivity of UV detection, the application of an extended optical path length such as a bubble cell is necessary to obtain reliable binding parameters.

Nielsen et al. used this method to separate antigen–antibody complexes of recombinant hGH with monoclonal antibody specific to hGH (12). The complexes were well resolved from the free antibody and antigen in solution. The strong binding affinity of the antibody for hGH results in strong, stable antibody–antigen complexes that form very rapidly in solution; two complexes (IgG-hGH, IgG-$(hGH)_2$) have been observed.

Korf et al. showed the applicability of the green fluorescent protein (GFP) in a CE-based immunoassay (13). Green fluorescent protein and GFP–antibody complex were detected separately at picogram levels using LIF detection, as illustrated in Figure 4. By means of genetic engineering, GFP can be attached to several types of proteins. The GFP fusion method may also be advantageous because it prevents multiple labeling, which often occurs in chemical labeling of proteins. Hence, the use of GFP fusion proteins is a general approach for establishing highly sensitive competitive and noncompetitive immunoassays using CE. Furthermore, specific antibodies raised against GFP can also detect GFP fusion proteins. That means the fluorescent label can also function as antibody target. This provides an effective detection tool for different proteins requiring only a GFP antibody.

An immunoassay using immobilized antibodies was described by Phillips and Chmielinska (14). By means of this approach the determination of the immunosuppressant cyclosporin A (CsA) in tear fluid was obtained using UV detection. Although the detection limit is sufficient using only immunoaffinity capillary electrophoresis, overlapping signals can be avoided. A set of tear samples was quantified. Immunoaffinity CE was able to detect

© 2003 by Marcel Dekker, Inc.

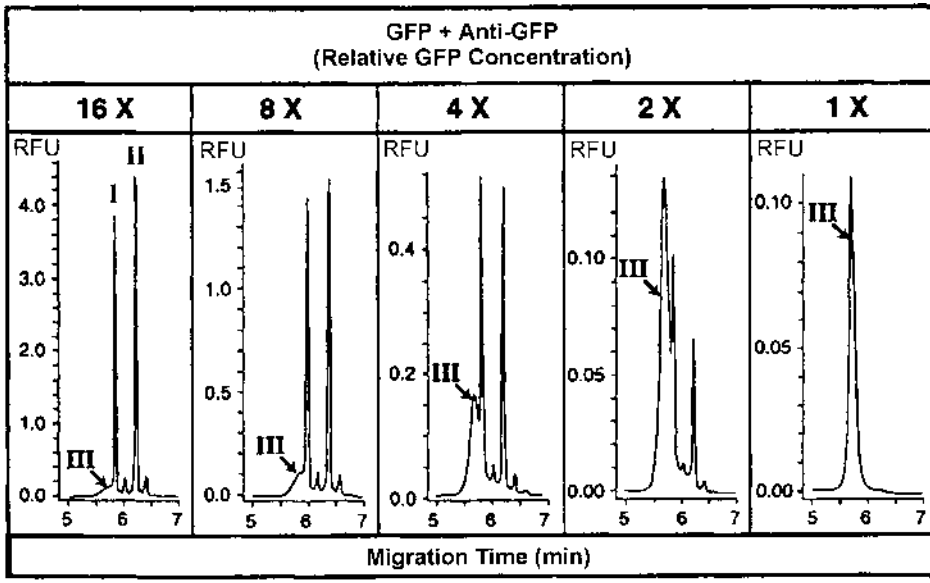

Fig. 4 Separation of free and antibody-bound GFP using CE-LIF. A fixed amount of GFP antisera was added to aliquots of 100 mM borate, pH 8.5, containing relative GFP concentrations of 1, 2, 4, 8, or 16× (corresponding to a final concentration of 1.875, 2.75, 5.5, 11, or 22 ng/mL GFP solution) and then analyzed by CE-LIF. Peaks of the GFP isoforms are marked I and II. The addition of GFP antisera to free GFP results in a distinct complex peak III, as indicated. The RFU scale decreases from 16× to 1×. (Reprinted with permission from Ref. 13. Copyright 1997 Academic Press.)

CsA in the range of clinical interest necessary for the control of patients after CsA treatment because of its narrow therapeutic range.

It has often been realized that the separation efficiency in the competitive CEIA mode is favorable compared to the noncompetitve mode, especially if free and bound antibodies are utilized. Ou and co-workers presented a relatively simple approach to solve this problem (15,16). They used nondenaturing SDS capillary gel electrophoresis (CGE) to analyze anti–bovine serum albumin (BSA) antibodies with UV detection.

An ACE-MS hyphenation was utilized for the linear epitope mapping (17). The tryptic digest of β-endorphin was mixed with an anti-β-endorphin antibody and subsequently analyzed by ACE-ESI-MS. The procedure requires only femtomole amounts of antibody and peptide digest. More technical details of the method are described in Chapter 13 of this book.

© 2003 by Marcel Dekker, Inc.

B. Competitive Capillary Electrophoresis Immunoassays

Steinmann et al. developed a competitive binding immunoassay for the monitoring of theophylline in human serum (18). Separation and analysis of free tracer (fluorescein-labeled theophylline) and the antibody–tracer complex were done using micellar electrokinetic capillary chromatography (MEKC) with LIF detection. Quantitation based upon multilevel calibration using the height of the peak produced by the free tracer (Fig. 5). The SDS present in the MEKC buffer prevents adsorption of proteins to the capillary walls and, thus, permits the performance of hundreds to thousands of runs in a single untreated fused-silica capillary. The calibration range (nonlinear regression) was between 0 and 40 μg/mL. This covers the therapeutic range of theophylline (10–20 μg/mL). The method provides good reproducibility, is simple and reliable in performance, and should lend itself to complete high throughput automation in miniaturized equipment.

In addition Choi et al. utilized FITC-labeled methamphetamine for competitive immunoassay of methamphetamine in urine (19). Instead of purified antibody or antibody fragment, antiserum was used. An aminobutyl derivative of metamphetamine was conjugated with proteins and used as an immunogen to produce antibodies for the assay. The free FITC-labeled tracer was well separated from the antibody-bound fraction, and the detection limit for the CE assay was lower than that for ELISA.

Competitive CEIA was also employed to determine methadone in urine (20) and to screen for urinary amphetamines and analogues (21). The method was extended in subsequent studies to simultaneously analyze four drugs of abuse: methadone, opiates, benzoylecgonine, and amphetamine (22,23). It is important to note that these multiple-analyte investigations exemplify one potential advantage of CEIA over most other immunoassay formats.

Schmerr and Jenny established a CE-based immunoassay for the detection of prion protein (24). In this competitive assay, peptides derived from the prion protein and labeled with fluorescein were used. This allowed them to distinguish scrapie-infected brain preparations from noninfected. For identification, the ratio between the peaks resulting from the free and the complexed peptide with a specific antibody was used. The results were in agreement with other data on the brain preparations achieved by Western blot analysis. The CE-based assay provides the advantage of direct detection of the scrapie protein in blood and tissue preparations with high sensitivity. Furthermore, due to the small sample amount needed for analysis, the CE-based assay is applicable to the putative diagnostics of prion protein in body fluids.

Another approach to detect CsA in body fluids is a CE-based competitive immunoassay using labeled CsA and an anti-CsA antibody (25). In comparison to the direct assay, an immobilization of an antibody is not

© 2003 by Marcel Dekker, Inc.

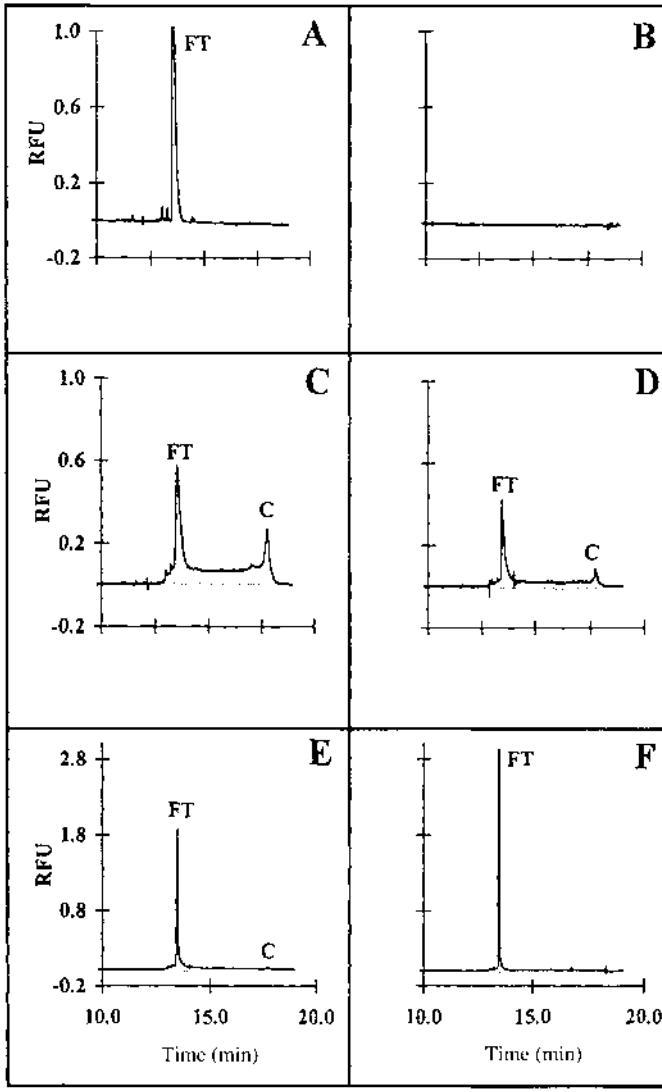

Fig. 5 Competitive CEIA for the monitoring of theophylline in human serum. Solution S: mouse monoclonal theophylline antiserum solution; solution T: theophylline fluorescein tracer solution. Electropherograms of (A) tracer solution T, (B) antiserum solution S, (C) equivolume mixture of solutions T and S, (D) equivolume mixture of blank serum, S, and T, (E) equivolume mixture of a patient serum containing 5.98 μg/mL theophylline, S, and T, and (F) a similar mixture as for (E) but with a patient serum having 15.62 μg/mL theophylline. FT represents the peak of the free tracer, whereas C is assigned to the tracer–antibody complex. (Reprinted with permission from Ref. 18. Copyright 1995 Wiley-VCH.)

© 2003 by Marcel Dekker, Inc.

required. The limiting step is the labeling procedure for either the antigen or the antibody. In the case of CsA, the fluorescein-labeled compound is commercially available. The detection limit achieved for CsA is about 1 nM. This is comparable to other methods, such as fluorescence polarization, used in clinical analytics. The data for the determination of CsA in whole blood samples of treated patients were comparable for the CE- and the fluorescence polarization–based assay. The most important advantage of the CE-based assay is the ability to detect both CsA and metabolites in one run.

Tao and Kennedy (9) also used a competitive approach to determine the dissociation constants of unlabeled insulins from several species to an antibody by fitting bound over free FITC-insulin as a function of unlabeled insulin concentration. The K_d values for the different insulins were between 0.34 and 0.64 nM. In another investigation, the method was further improved to monitor the insulin secretion from single islets of Langerhans (26). To explore the assumed pulsatile fashion of insulin secretion, an instrumental setup was designed that allowed the separation of bound and free FITC-insulin every 3 seconds.

C. Mobility-Shift Assays

The examples mentioned up to now utilized strong Ag–Ab interactions using the equilibrium–mixture mode of ACE. But the quantitation of weak antigen–antibody interaction is also possible by ACE, if the mobility-shift approach, sometimes also called *dynamic equilibrium affinity electrophoresis*, is applied.

Lin et al. used protein additives to the running buffer (27). This is an uncommon technique for proteins due to their tremendous influence on the separation system. Using the mobility-shift assay, the binding of a monoclonal anti-phosphoserine antibody to phosvitin was determined (Fig. 6). The study was later extended to evaluate the binding constant of antiphosphotyrosine Fab fragment to 18-mer diphosphotyrosine peptide (28). Scatchard analysis of the changes obtained in the mobility of the antibody when increasing amounts of the antigen were added to the background buffer yielded a dissociation constant in the range of 10^{-5} M. The results were comparable to classical approaches, such as ELISA. The CE assay is, however, advantageous because it does not require the immobilization of antigen or antibody. Lin et al. also used the method for detecting anti-dinitrophenol antibody (pAb) subpopulations by studying the mobility-shift pattern of dinitrophenol–pAb complexes (29). Two subpopulations were observed, one of low- or very low-affinity antibodies and one of higher-affinity antibodies. The changes in the peak that appear in the electropherograms are thus composed of contributions from antibodies with different binding kinetics.

© 2003 by Marcel Dekker, Inc.

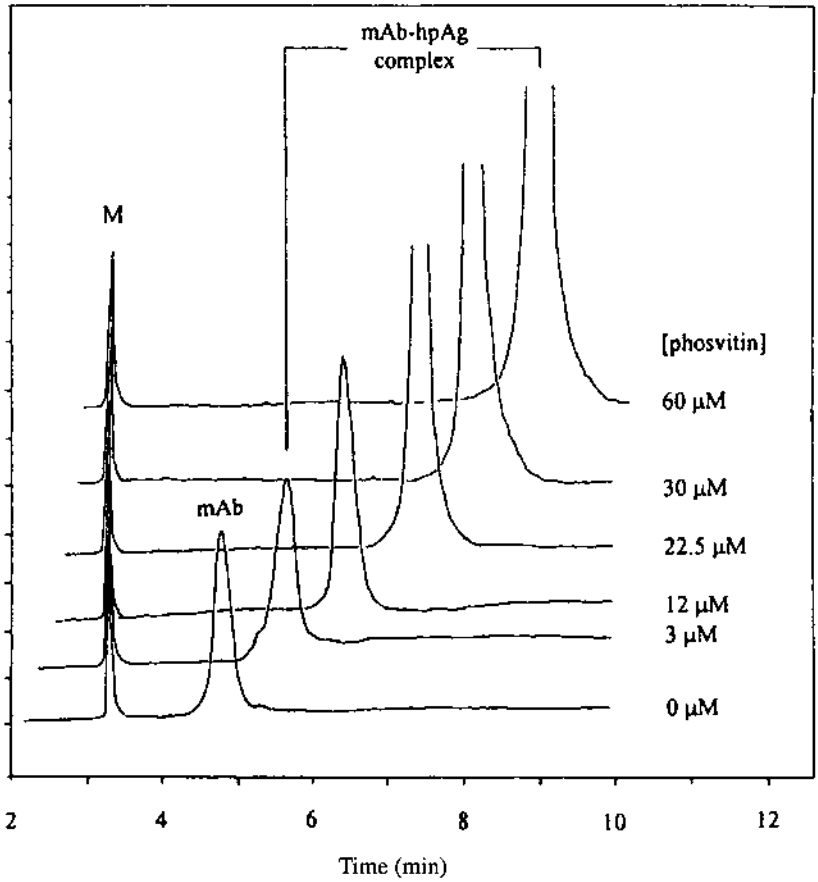

Fig. 6 Evaluation of phosvitin binding to monoclonal anti-phosphoserine antibody by ACE using mobility-shift analysis and UV detection. Peaks: M, internal peptide marker; mAb, free monoclonal anti-phosphoserine antibody; mAb–hpAg complex, monoclonal anti-phosphoserine antibody complexed with homopolyvalent phosvitin antigen. The buffer contained phosvitin within a concentration from 0 to 60 μM. (Reprinted with permission from Ref. 27. Copyright 1997 Academic Press.)

The ACE technique has also been used to determine the two dissociation constants of the complex between anti-*N*-dinitrophenyl (DNP) rat monoclonal IgG_{2b} antibody and charged ligands that contained a DNP group by analyzing the change in the electrophoretic mobility of the antibody (Fig. 7) (30). Singly and multiply charged ligands were used to establish the influence of the charge on the mobility of the complex between IgG and its

© 2003 by Marcel Dekker, Inc.

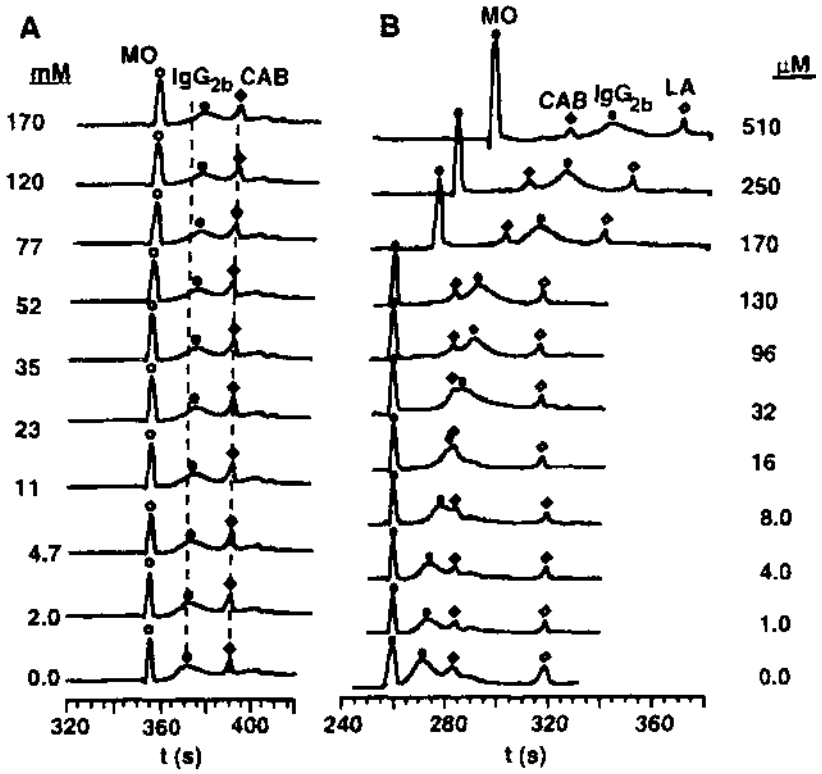

Fig. 7 Mobility-shift assay for the determination of dissociation constant of the complex between anti-DNP rat monoclonal IgG_{2b} antibody and charged ligands that contained the *N*-dinitrophenyl group. Mesityl oxide (MO) served as EOF marker, bovine carbonic anhydrase (CAB) and bovine α-lactalbumin (LA) as internal references. The DNP ligands with a charge of -1 (A) und -9 (B), respectively, were used as additives to the running buffer. (Reprinted with permission from Ref. 30. Copyright 1995 American Chemical Society.)

ligand(s). Zwitterionic buffer additives diminished the adsorption of the protein to the capillary wall. Bovine carbonic anhydrase (CAB) and bovine α-lactalbumin (LA) were used as reference materials. The electropherograms show that the more negatively charged ligand (Fig. 7B) yielded a stronger migration shift of the antibody than the less negatively charged ligand (Fig. 7A). A formula was derived to analyze the binding data for polyvalent systems in which cooperativity between binding events is in question. Five assumptions were used in this analysis: (1) The mobility of the fully com-

© 2003 by Marcel Dekker, Inc.

plexed antibody can be estimated experimentally at high concentrations of the ligand; (2) binding of the ligands to the protein affected the hydrodynamic drag of the protein negligibly; (3) the values of k_{on} and k_{off} are sufficiently large that the observed mobility is a concentration-weighted average of the mobilities of all complexes containing Ig; (4) the proportionality constants that relate electrophoretic mobility to mass and charge are equal in magnitude; (5) the hydrodynamic drag is constant for Ig and its complexes. The analysis indicates that the binding of two ligands to this IgG is noncooperative (independent).

Heegaard et al. used the migration-shift approach to characterize a monoclonal antibody against DNA, which is of interest in the diagnosis of the autoimmune disease systemic lupus erythematosus (31). The minimal DNA size to bind to the antibody was identified as 16 bases. The interaction with a double-stranded 32-mer oligonucleotide was almost an order of magnitude stronger than with a single-stranded oligonucleotide. The dissociation constant for the antibody binding of a single-stranded 32-mer oligonucleotide was estimated as 0.62 μM at pH 7.9, which is in good agreement with published data using biosensor technology.

D. Special Applications

Several successful attempts were done to transfer classical CEIA to a microchip-based format. This kind of miniaturization is a trend that can overcome the limitations of CE in high-throughput systems. On-chip CE offers both parallel analysis of samples and short separation times. Koutny et al. showed the use of an immunoassay on-chip (32). In this competitive approach fluorescein-labeled cortisol was used to detect unlabeled cortisol spiked to serum (Fig. 8). The system showed good reproducibility and robustness even in this problematic kind of sample matrix. Using serum cortisol standards calibration and quantification is possible in a working range of clinical interest. This example demonstrated that microchip electrophoretic systems are analytical devices suitable for immunological assays that can compete with common techniques.

Monoclonal antibody–binding affinity was determined by microchip-based capillary electrophoresis with LIF detection (33). The mixing was carried out off-chip, and the on-chip separations were performed in less than 60 s (Fig. 9). A Scatchard plot analysis resulted in an affinity constant for the monoclonal anti-BSA antibody to fluorescently labeled BSA (BSA*) of $3.5 \pm 0.6 \times 10^7$ $M^{-1}1$ for a 1:1 stoichiometric ratio. Two affinity complexes were separated. One complex was identified by the Scatchard method as having a 1:1 stoichiometric ratio (complex 1). The other complex (complex 2) is proposed to have a stoichiometry with an excess of anti-BSA to BSA*,

© 2003 by Marcel Dekker, Inc.

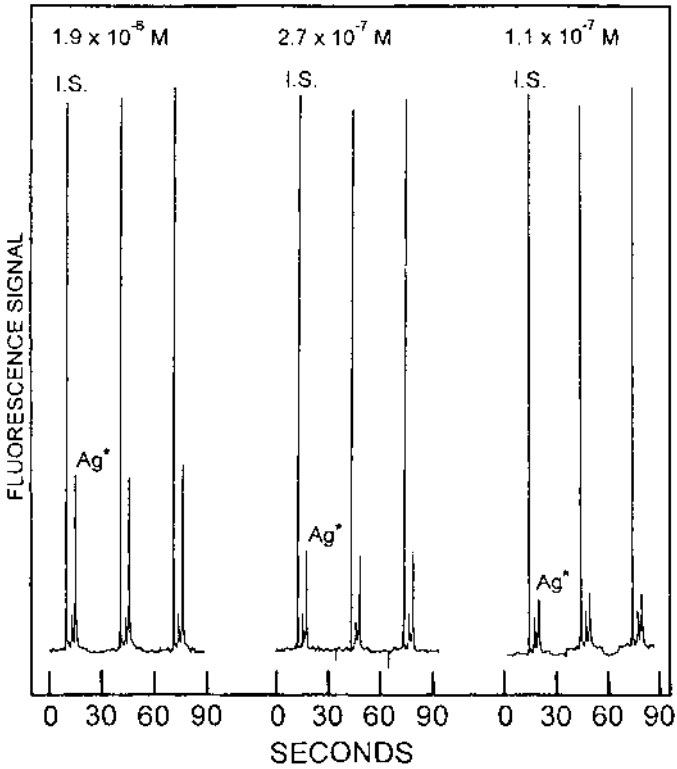

Fig. 8 On-chip immunoassay for the quantification of cortisol in serum samples. Fluorescein-labeled cortisol (Ag*) was used in a competitive assay for the detection of unlabeled analyte cortisol. Three replicate injections for each of three samples with cortisol levels as indicated in the figure. Fluorescein was used as an internal standard (I.S.). (Reprinted with permission from Ref. 32. Copyright 1996 American Chemical Society.)

most likely (anti-BSA)$_2$-BSA*. This was assumed on the basis of a faster migration time than the 1:1 complex, a decrease in the amount of this complex with increasing BSA* concentration, and predictions of theoretical models for multivalent antigens. The more electropositive character of complex 2 indicates it could be formed by two or more antibodies bound to a single BSA*. Affinity constants as well as binding stoichiometries of nonpurified antibody preparations can be rapidly and easily determined, and automation is possible.

In extension to classical immunologic approaches in CE the use for more complex systems than the detection of proteinlike antigens is possible.

© 2003 by Marcel Dekker, Inc.

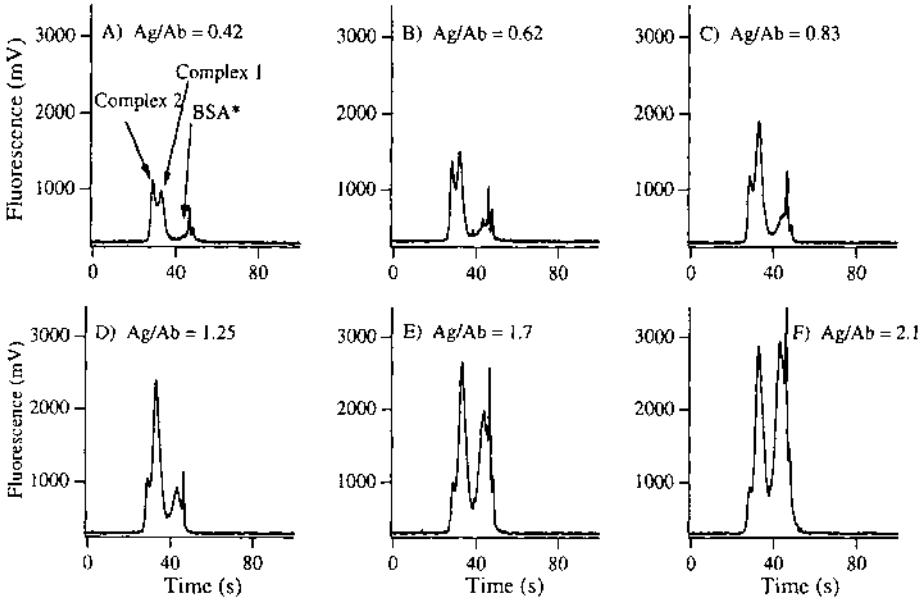

Fig. 9 Series of electropherograms obtained on-chip from mixtures of 361 nM anti-BSA antibody with different concentrations of labeled BSA (BSA*). The ratio of total concentration of BSA* to total concentration of antibody (Ag/Ab) is given at the top of each electropherogram. Two main complex peaks are identified. Essentially no BSA* is seen in A, while BSA* dominates in F. (Reprinted with permission from Ref. 33. Copyright 1998 Wiley-VCH.)

Okun et al. studied the binding of common cold virus to neutralizing antibodies (34). Although viruses are large heterogeneous analytes, a separation of free virus and virus–antibody complex was achieved (Fig. 10). Furthermore, information about the stoichiometry and the stability of the antibody–virus complex for different viruses and antibodies was obtained. The fast and material-saving CE method is a good alternative to other analysis methods, such as size exclusion chromatography and sucrose density gradient sedimentation.

The ACE technique was also used to investigate the binding of viruses to receptor fragments (35). The stoichiometry of virus–receptor binding was determined using the changes of the virus mobility upon incubation with increasing concentrations of receptor fragments. Depending on the different receptor fragments, changes in the stoichiometry were observed. The data on the interaction of viruses demonstrate the ability of ACE for the inves-

© 2003 by Marcel Dekker, Inc.

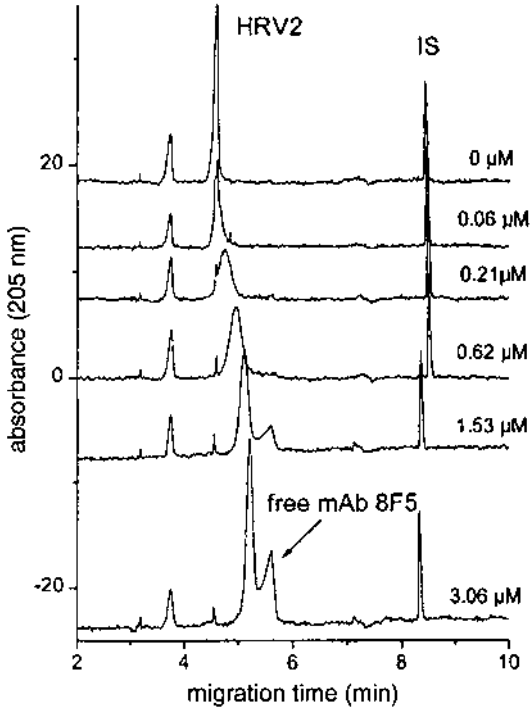

Fig. 10 Formation of complexes between human rhinovirus HRV2 and neutralizing monoclonal antibody mAb 8F5 analyzed by CE. A fixed concentration of HRV2 (15 nM) was incubated with an increasing concentration (indicated in the figure) of mAb 8F5 prior to the CE analysis at room temperature. *O*-phthalic acid was used as internal standard (IS). (Reprinted with permission from Ref. 34. Copyright 2000 American Chemical Society.)

tigation of complex interaction systems without special requirements for separation and detection.

Although CE-based immunoassays are advantageous due to their ability for high throughput combined with minute material consumption, they suffer from higher detection limits than conventional assays. Wang et al. demonstrated the use of sample preconcentration using protein A affinity chromatography (36). The capillary affinity chromatography provided a limit of detection of 80 pM for the detection of anti-BSA. In comparison to the CE-based assay without preconcentration, the limit of detection was improved a hundredfold.

The decision whether mobility-shift or equilibrium–mixture analysis

© 2003 by Marcel Dekker, Inc.

is suitable for binding studies depends on the kinetics of the interaction. For antigen–antibody binding, mostly tight binding equivalent to slow kinetics can be assumed. However, both experimental setups were used to determine the interaction of peptides derived from epitope of the HIV capsid protein p24 and a antibody raised against p24 (37). Interaction of a set of peptides with the commercially available monoclonal antibody were monitored with both setups. The peptides were divided into two groups according to their suitability for mobility-shift or equilibrium–mixture analysis. Using this approach, the peptides were grouped as weak or tight binders, respectively. The correlation of the binding data with the peptide sequence yielded information about the minimal requirements for peptide binding to the antibody.

IV. AFFINITY CAPILLARY ELECTROPHORESIS INVESTIGATIONS OF PROTEINS INVOLVED IN IMMUNOREACTIONS

In HIV research, ACE was used to detect interactions of HIV proteins with possible target proteins of cells. Cellular proteins of T cells were identified as being involved in the incorporation of HIV. The proteins mediated the virus incorporation by binding the viral proteins. In combination with surface plasmon resonance, ACE using equilibrium–mixture analysis was able to detect the protein–protein interaction by changes in the mobility (38,39). In further studies, some viral proteins share the same binding motif with interferon type I. This was used to explain the regulatory effect on the proliferation of lymphocytes. The ACE method was used to demonstrate the binding of interferon type I to the cellular receptor protein of the viral protein (40).

The HIV capsid protein p24 plays an important role in virus infectivity. Its interaction with cyclophilins from host cells is a crucial event in viral replication. For the determination of binding data of p24 to cyclophilins, several methods, such as enzymatic assays, surface plasmon resonance, and isothermal titration calorimetry, were used. Furthermore, ACE was applied to this protein–protein interaction related to the immune system. In ACE, protein–protein interactions are often difficult to detect because of the influence on the separation system. Hence, ACE is limited mostly to equilibrium–mixture analysis and tight-binding systems, e.g., antigen–antibody interactions. Interestingly, in the case of p24, equilibrium–mixture analysis was successfully applied to determine binding data on the interaction with a cyclophilin fusion protein, although the dissociation constant was in the range of 10^{-5} M (41). A dissociation constant of $(20 \pm 1.5) \times 10^{-6}$ M was determined using the observed shift in the mobility of the cyclophilin fusion protein.

© 2003 by Marcel Dekker, Inc.

Different methods were mentioned earlier that detect the immunosuppressant CsA in body fluids. Another investigation explored the interaction of CsA with its cellular receptor protein cyclophilin using ACE (42). Cyclophilin in complex with CsA mediates the immunosuppressive action of CsA by inhibition of the phosphatase calcineurin. Therefore, the cyclophilin–CsA interaction is of special interest. Using equilibrium–mixture analysis, ACE was applied to the investigation of cyclophilin interactions with CsA and derivatives. A separation of free cyclophilin and the cyclophilin complexed with CsA was achieved (Fig. 11). This approach yielded only relative comparison of the binding of the CsA derivatives because of the discrepancy of the used concentration (10^{-6} M) and the dissociation constant (10^{-9} M) known from other methods. However, the application of electrophoretically mediated microanalysis to the investigation of binding constants quantitative data on the cyclophilin-CsA binding was achieved.

Another drug whose immunosuppressive action is mediated by the complexation with a cellular protein of the immunophilins is FK506. FK506 binds to proteins of the FKBP family. The complex formed is involved in the inhibition of the phosphatase calcineurin, similar to the mode of action of CsA after binding to cyclophilin. The ACE method was used to detect

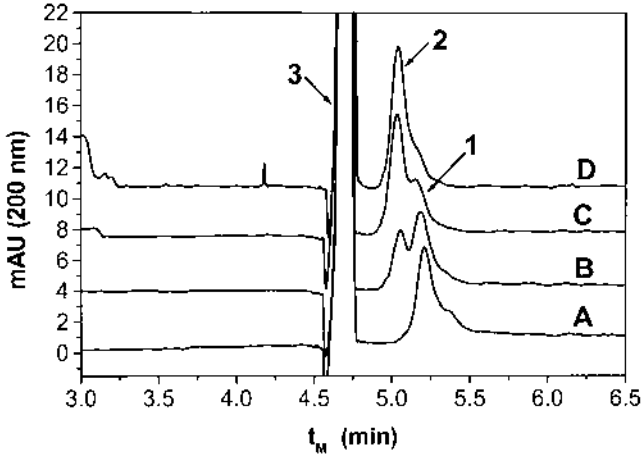

Fig. 11 Separation of human cyclophilin 18 (1) and the corresponding complex with the immunosuppressant cyclosporin A (2) by CE. A fixed concentration of cyclophilin (6.1 μM) and increasing concentrations of cyclosporin (0 μM, A, 2 μM, B, 4 μM, C, 7 μM CsA, D) dissolved in DMSO (3) were incubated prior to the CE separation. (Reprinted with permission from Ref. 42. Copyright 1999 of Elsevier Science.)

© 2003 by Marcel Dekker, Inc.

the interaction of FK506 with human FKBP12 (43). For detection, hyphenation to mass spectrometry provided information on the molecular mass of the detected peaks. A separation of FKBP and FKBP–FK506 complex was achieved. The peaks were easily identified by the molecular masses detected by MS.

V. CONCLUSIONS

The ACE investigations of Ag–Ab interactions focus on the measurement of analyte concentrations rather than on the estimation of binding constants. Although there are numerous impressive applications in very different areas, the method is still in a developmental stage. A broader use of the technique will depend how it compares to traditional ELISA, which is hampered mainly by higher concentration detection limits and a lack of parallel operation in commercial instruments. After realizing multicapillary operation for capillary DNA sequencing in commercial equipment, a transfer of the technology to CE instruments may be on the way. To overcome the problem of the higher detection limits, preconcentration methods such as coupling to affinity chromatography and working in CIEF mode were explored. Other options are technical improvements such as light path extension by detection cells in the bubble or Z-format and the use of labels excitable by diode lasers, which prevent excitation background in biological fluids. One of the main problems that especially hampers noncompetitive CEIA is the tendency of proteins to seriously change the migration behavior of all sample analytes. Besides the use of coated capillaries to diminish adsorption to the capillary wall, the new approach employing nondenaturing SDS CGE may be helpful. Furthermore, it should pointed out again here that because CEIA is based on a high-performance separation method, it is advantageous for applications using multiple analytes.

A further promising development is the implementation of CEIA on microchip devices. In this case the excellent mass detection limit makes it favorable, in contrast to classic ELISA. The use of whole cells and viruses for CEIA applications is also an emerging field.

ABBREVIATIONS

Ab	antibody
ACE	affinity capillary electrophoresis
Ag	antigen
BSA	bovine serum albumin

© 2003 by Marcel Dekker, Inc.

CAB	bovine carbonic anhydrase
CE	capillary electrophoresis
CEIA	capillary electrophoresis-based immunoassay
CGE	capillary gel electrophoresis
CIEF	capillary isoelectric focusing
CsA	cyclosporin A
DNP	2,4-dinitro-phenol
ELISA	enzyme-linked immunosorbent assays
FITC	fluorescein isothiocyanate
GFP	green fluorescent protein
hGH	human growth hormone
HIV	human immunodeficiency virus
HSA	human serum albumin
K_d	dissociation constants
LA	α-lactalbumin
LIF	laser-induced fluorescence (detection)
MO	mesityl oxide
UV	ultraviolet

REFERENCES

1. NHH Heegaard, S Nilsson, NA Guzman. Affinity capillary electrophoresis: important application areas and some recent developments. J Chromatogr B 715:29–54, 1998.
2. NHH Heegaard, RT Kennedy. Identification, quantitation, and characterization of biomolecules by capillary electrophoretic analysis of binding interactions. Electrophoresis 20:3122–3133, 1999.
3. D Schmalzing, W Nashabeh. Capillary electrophoresis based immunoassays: a critical review. Electrophoresis 18:2184–2193, 1997.
4. D Schmalzing, S Buonocore, C Piggee. Capillary electrophoresis-based immunoassays. Electrophoresis 21:3919–3930, 2000.
5. JJ Bao. Capillary electrophoretic immunoassays. J Chromatogr B 699:463–480, 1997.
6. K Shimura, BL Karger. Affinity probe capillary electrophoresis: analysis of recombinant human growth hormone with a fluorescent-labeled antibody fragment. Anal Chem 66:9–15, 1994.
7. NHH Heegaard. Determination of antigen–antibody affinity by immuno-capillary electrophoresis. J Chromatogr A 680:405–412, 1994.
8. YH Chu, WJ Lees, A Stassinopoulos, CT Walsh. Using affinity capillary electrophoresis to determine binding stoichiometries of protein–ligand interactions. Biochemistry 33:10616–10621, 1994.
9. L Tao, RT Kennedy. Measurement of antibody–antigen dissociation constants

© 2003 by Marcel Dekker, Inc.

using fast capillary electrophoresis with laser-induced fluorescence detection. Electrophoresis 18:112–117, 1997.
10. NM Schultz, RT Kennedy. Rapid immunoassays using capillary electrophoresis with fluorescence detection. Anal Chem 65:3161–3165, 1993.
11. MHA Busch, HFM Boelens, JC Kraak, H Poppe, AAP Meekel, M Resmini. Critical evaluation of the applicability of capillary zone electrophoresis for the study of hapten–antibody complex formation. J Chromatogr A 744:195–203, 1996.
12. RG Nielsen, EC Rickard, PF Santa, DA Shakarnas, GS Sittampalam. Separation of antibody–antigen complexes by capillary zone electrophoresis, isoelectric focusing and high-performance size-exclusion chromatography. J Chromatogr 539:177–185, 1991.
13. GM Korf, JP Landers, DJ O'Kane. Capillary electrophoresis with laser-induced fluorescence detection for the analysis of free and immune-complexed green fluorescent protein. Anal Biochem 251:210–218, 1997.
14. TM Phillips, JJ Chmielinska. Immunoaffinity capillary electrophoretic analysis of cyclosporin in tears. Biomed Chromatogr 8:242–246, 1994.
15. JP Ou, QG Wang, TM Cheung, STH Chan, WSB Yeung. Use of capillary electrophoresis–based competitive immunoassay for a large molecule. J Chromatogr B 727:63–71, 1999.
16. JP Ou, STH Chang, WSB Yeung. Separation of bovine serum albumin and its monoclonal antibody from their immunocomplexes by sodium dodecyl sulfate–capillary gel electrophoresis and its application in capillary electrophoresis–based immunoassay. J Chromatogr B 731:389–394, 1999.
17. YV Lyubarskaya, YM Dunayevskiy, P Vouros, BL Karger. Microscale epitope mapping by affinity capillary electrophoresis–mass spectrometry. Anal Chem 69:3008–3014, 1997.
18. L Steinmann, J Caslavska, W Thormann. Feasibility study of a drug immunoassay based on micellar electrokinetic capillary chromatography with laser-induced fluorescence detection—determination of theophyllin in serum. Electrophoresis 16:1912–1916, 1995.
19. J Choi, C Kim, MJ Choi. Immunological analysis of metamphetamine antibody and its use for the detection of metamphetamine by capillary electrophoresis with laser-induced fluorescence. J Chromatogr 705:277–282, 1998.
20. W Thormann, M Lanz, J Caslavska, P Siegenthaler, R Portmann. Screening for urinary methadone by capillary electrophoretic immunoassays and confirmation by capillary electrophoresis mass spectrometry. Electrophoresis 19:57–65, 1998.
21. A Ramseier, J Caslavska, W Thormann. Screening for urinary amphetamine and analogs by capillary electrophoretic immunoassays and confirmation by capillary electrophoresis with on-column multiwavelength absorbance detection. Electrophoresis 19:2956–2966, 1998.
22. J Caslavska, D Allemann, W Thormann. Analysis of urinary drugs of abuse by a multianalyte capillary electrophoretic immunoassay. J Chromatogr A 838: 197–211, 1999.
23. W Thormann, J Caslavska, A Ramseier, C Siethoff. Multianalyte capillary elec-

© 2003 by Marcel Dekker, Inc.

trophoresis assays for screening and confirmation of urinary drugs of abuse. J Microcol Sep 12:13–24, 2000.
24. MJ Schmerr, A Jenny. A diagnostic test for scrapie-infected sheep using capillary electrophoresis immunoassays with fluorescent-labeled peptides. Electrophoresis 19:409–414, 1998.
25. L Ye, C Le, JZ Xing, M Ma, R Yatscoff. Competitive immunoassay for cyclosporine using capillary electrophoresis with laser induced fluorescence polarization detection. J Chromatogr B 714:59–67, 1998.
26. L Tao, CA Aspinwell, RT Kennedy. On-line competitive immunoassay based on capillary electrophoresis applied to monitoring insulin secretion from single islets of Langerhans. Electrophoresis 19:403–408, 1998.
27. S Lin, I Hsiao, SM Hsu. Determination of the dissociation constant of phosvitin-anti-phosphoserine interaction by affinity capillary electrophoresis. Anal Biochem 254:9–17, 1997.
28. S Lin, P Tang, SM Hsu. Using affinity capillary electrophoresis to evaluate average binding constant of 18-mer diphosphotyrosine peptide to antiphosphotyrosine Fab. Electrophoresis 20:3388–3395, 1999.
29. S Lin, JC Tsai, SM Hsu. Characterization of a polyclonal antihapten antibody by affinity capillary electrophoresis. Anal Biochem 284:422–426, 2000.
30. M Mammen, FA Gomez, GM Whitesides. Determination of the binding of ligands containing the *N*-2,4-dinitrophenyl group to bivalent monoclonal rat antibody using affinity capillary electrophoresis. Anal Chem 67:3526–3535, 1995.
31. NHH Heegaard, DT Olsen, KLP Larsen. Immuno-capillary electrophoresis for the characterization of a monoclonal antibody against DNA. J Chromatogr A 744:285–294, 1996.
32. LB Koutny, D Schmalzing, TA Taylor, M Fuchs. Microchip electrophoretic immunoassay for serum cortisol. Anal Chem 68:18–22, 1996.
33. NH Chiem, DJ Harrison. Monoclonal antibody binding affinity determined by microchip-based capillary electrophoresis. Electrophoresis 19:3040–3044, 1998.
34. VM Okun, B Ronacher, D Blaas, E Kenndler. Affinity capillary electrophoresis for the assessment of complex formation between viruses and monoclonal antibodies. Anal Chem 72:4634–4639, 2000.
35. VM Okun, R Moser, B Ronacher, E Kenndler, D Blaas. VLDL receptor fragments of different lengths bind to human rhinovirus HRV2 with different stoichiometry—an analysis of virus-receptor complexes by capillary electrophoresis. J Biol Chem 276:1057–1062, 2001.
36. Q Wang, G Luon, J Ou, WSB Yeung. Noncompetitive immunoassays using protein G affinity capillary chromatography and capillary electrophoresis with laser-induced fluorescence detection. J Chromatogr A 848:139–148, 1999.
37. XH Qian, KB Tomer. Affinity capillary electrophoresis investigation of an epitope on human immunodeficiency virus recognized by a monoclonal antibody. Electrophoresis 19:414–419, 1998.
38. Y Xiao, W Wu, MP Dierich, YH Chen. HIV-1 gp41 by N-domain binds the potential receptor protein P45. Int Arch Allergy Immunol 121:253–257, 2000.

© 2003 by Marcel Dekker, Inc.

39. YH Chen, Y Xiao, W Wu, Q Wang, G Luon, MP Dierich. HIV-2 transmembrane protein gp36 binds to the putative cellular receptor proteins P45 and P62. Immunobiology 201:317–322, 2000.
40. T Yu, Y Xiao, Y Bai, Q Ru, G Luo, MP Dierich, YH Chen. Human interferon-beta inhibits binding of HIV-1 gp41 to lymphocyte and monocyte cells and binds the potential receptor protein P50 for HIV-1 gp41. Immunol Lett 73:19–22, 2000.
41. S Kiessig, J Reissmann, C Rascher, G Küllertz, A Fischer, F Thunecke. Application of a green fluorescent fusion protein to study protein–protein interactions by electrophoretic methods. Electrophoresis 22:1428–1435, 2001.
42. S Kiessig, H Bang, F Thunecke. Interaction of cyclophilin and cyclosporins monitored by affinity capillary electrophoresis. J Chromatogr A 583:469–477, 1999.
43. YL Hsieh, J Cai, YT Li, JD Henion, B Ganem. Detection of noncovalent FKBP-FK506 and FKBP-Rapamycin complexes by capillary electrophoresis–mass spectrometry and capillary electrophoresis–tandem mass spectrometry. J Am Soc Mass Spectrom 6:85–90, 1995.

© 2003 by Marcel Dekker, Inc.

13

Hyphenation of Affinity Capillary Electrophoresis with Mass Spectrometry

Klaus Raith
Martin-Luther-University Halle-Wittenberg, Halle, Germany

I. HYPHENATION WITH MASS SPECTROMETRY: LIQUID CHROMATOGRAPHY/MASS SPECTROMETRY

Interfacing of solution-based separation techniques with mass spectrometry has historically been a challenge because of the incompatibility of the used solvent with the vacuum system. Standard electron impact (EI) ionization with techniques such as particle beam require samples to be vaporized under high vacuum for ion formation to occur.

The first approaches to the coupling of liquid-phase separation techniques with mass spectrometry were designed for HPLC needs, starting in the 1970s with since-forgotten techniques such as direct liquid introduction (DLI) and moving belt. In the 1980s, techniques such as thermospray, continuous-flow–fast atom bombardment (CF-FAB), and particle beam arose.

The real breakthrough in LC/MS development was achieved with the broad introduction in the 1990s of atmospheric pressure ionization (API) techniques, such as electrospray ionization (ESI) and atmospheric pressure chemical ionization (APCI), which enable the analysis of a wide variety of molecular species. The spectrum of available API techniques has been amended meanwhile by the introduction of sonic spray ionization (SSI) and atmospheric pressure photoionization (APPI).

While electron impact ionization is useful only with samples that can be volatilized, large molecules such as proteins, which do not volatilize, can be successfully analyzed by API techniques. Moreover, polar compounds can be transferred to the MS without derivatization.

© 2003 by Marcel Dekker, Inc.

Clearly the most important of these technologies is *electrospray ionization* (ESI; see Fig. 1). Although the pioneering work dates back to the late 1960s (1), the breakthrough was achieved after Fenn and coworkers (2,3) demonstrated the potential of this new method for mass spectrometry. Independently and at approximately the same time, a Russian group had similar results (4). In this technique, the liquid from LC (or CE) flows through a fused-silica capillary surrounded by a stainless steel capillary, the ESI needle. (In other constructions, the fused-silica capillary is connected via fittings to a stainless steel capillary serving as the ESI needle.) The phenom-

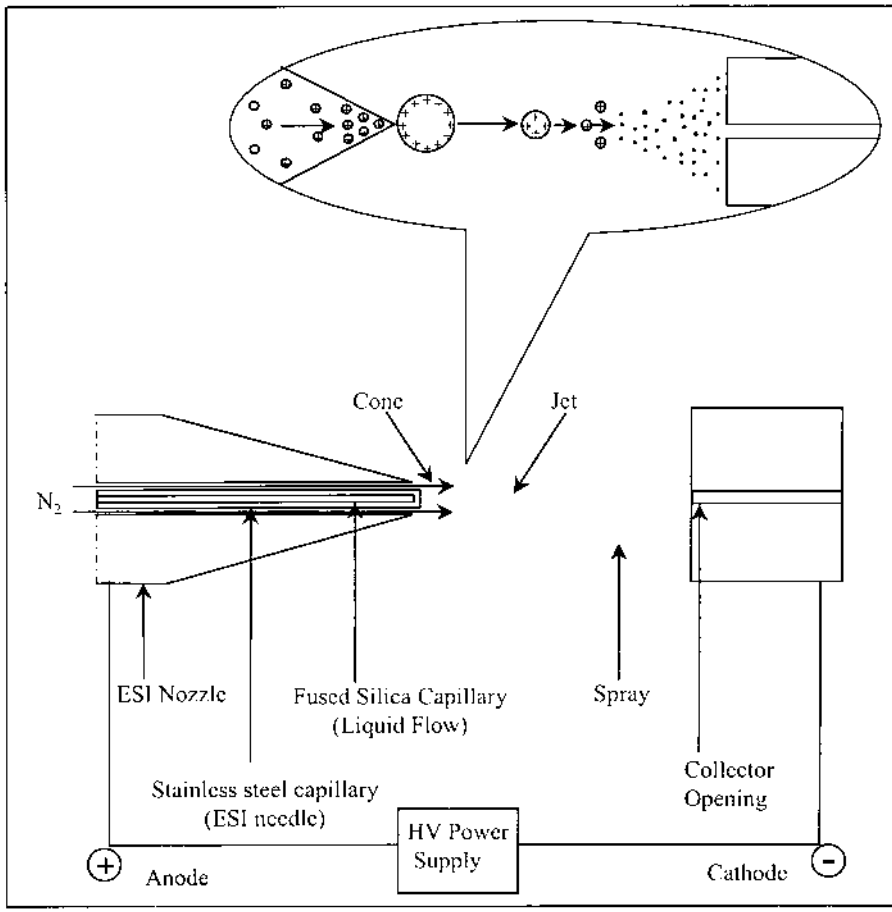

Fig. 1 The macroscopic and microscopic ESI process. The enlarged inset shows the droplet formation and subsequent Coulomb explosions.

© 2003 by Marcel Dekker, Inc.

enon can be likened to an electrical circuit in which the needle is one electrode and the collector opening of the mass spectrometer is the other. The ESI needle and the collector opening (orifice, heated capillary, sampling cone, or similar constructions) are connected via a high-voltage power supply, and the liquid flow as well as the electrospray itself are integral parts of the circuit. Ions in solution migrate from the bulk to the surface of the liquid under the influence of the high field strength near the tip of the needle. Counterions are depleted from the surface of the liquid, leaving a net charge.

Nebulizing gas (usually nitrogen) flows concentrically around the capillary, which shears droplets off as the liquid flows out of the end of the capillary. In the older literature, authors distinguish between ''pure'' electrospray without nebulizing gas and pneumatically assisted electrospray or ionspray. This is because of the mechanistic difference between the way the primary droplets form. Since all commercially available instruments allow the use of nebulizing gas, it is just a question of flow rate as to whether it makes sense or not.

A high-voltage, typically between $\pm 3-5$ kV, is applied to the ESI needle. The strong electric field generated by this potential, combined with the nebulizing gas, produces a fine spray of charged droplets exiting from the end of the capillary. A typical spray geometry results, consisting of a cone (the so-called Taylor cone) that ends in a jet region. Ions are separated from the solvent by evaporation. As each droplet evaporates, the charges within get closer and closer together until the droplet becomes unstable (by reaching the Rayleigh limit). Eventually, the droplet explodes into ever-smaller droplets (so-called Coulomb fissions). For the last step, the formation of free gas-phase ions, two theories are currently discussed. The charged-residue model, originally from Dole and later improved by Röllgen (5), is based on the assumption, that very small droplets (diameter about 1 nm) with only one ionized molecule finally result, which are evaporated. The ion evaporation model (6) states that as the droplet size is reduced, sample ions are emitted from the surface of the charged droplets. It seems that both phenomena may occur, while the importance of each depends on the nature of the sample ions and other circumstances. A detailed consideration on the electrospray mechanism is given in Ref. 7.

Sample ions are generally formed by the gain or loss of a proton, resulting in the pseudo-molecular ions $[M + H]^+$ and $[M - H]^-$, respectively. In some cases, however, sample molecules can interact with ions in solution to create adduct ions. Therefore, the solution chemistry of the mobile phase is very important. Most commonly seen are $[M + Na]^+$ in the positive mode and, much less frequently, $[M + Cl]^-$ in the negative mode.

Solvents suitable for electrospray have to meet two important require-

© 2003 by Marcel Dekker, Inc.

ments. On the one hand, they have to permit the formation of ions in solution; on the other hand, they have to be easily nebulized and desolvated, and the solvation energy should be minimal. Therefore, mixtures of alcohols (methanol, ethanol, isopropanol) or acetonitrile with water have proved best. Other solvents, such as THF, DMF, acetone, and chloroform, are tolerable in smaller quantities.

Polar compounds of low molecular weight will generally form singly charged ions by the loss or gain of a proton or by adduct formation. High-mass biopolymers such as proteins and peptides pick up more than one proton and become multiply charged ions. Since every mass spectrometer analyzes ions according to their mass-to-charge ratio (m/z), each charge that a high-molecular-mass compound picks up will decrease the apparent mass at which that ion would appear.

Nanospray is a miniaturized version of electrospray. In the original setup of Wilm and Mann (8) it is utilized as an off-line technique using disposable, finely drawn (1-μm tip), metallized glass capillaries to infuse samples at 10–30 nL/min flow rates. This allows more than 50 min analysis time with just a 1-μL sample. Due to the formation of much smaller droplets and the more effective ionization, there is often no need for LC separation, since the ''separation'' is accomplished in m/z or by MS/MS. However, limited reproducibility with respect to quantification and a more complex sample preparation can be seen as drawbacks. An on-line version for hyphenation with capillary and nano-LC as well as CE (slightly modified) is now commercially available.

The ESI technique can considered a soft ionization technique, applicable to heat-labile compounds, too. Normally, no fragmentation occurs, and even noncovalent complexes can be evaporated without destruction. On the other hand, this implies that the only structural information available is about molecular weight. Therefore, the artificial fragmentation of molecules by means of *collision-induced decomposition* or *dissociation* (CID) has grown more and more important. All commercially available mass spectrometers allow the application of an acceleration voltage in the source or transport region (also referred to as octopole-region CID, cone voltage fragmentation a.s.o.). Ions traveling through the transport region bump into other molecules, mostly nitrogen. Increasing the CID voltage increases the speed at which ions move. The faster the ions travel, the greater the energy transfer upon impact with other molecules and the more fragment ions are produced. The drawback of source CID is that it is not possible to judge from which precursor (or parent) ion a certain product (or daughter) ion is produced. Therefore it is more valuable to perform CID fragmentation after mass analysis and isolation of a certain precursor ion. Since in this case mass analysis is carried out twice (before and after CID), this approach is referred to as

© 2003 by Marcel Dekker, Inc.

tandem MS or *MS/MS*. To perform MS/MS experiments, two different mass analyzer setups are possible. *Tandem-in-space* means that two separate mass analyzers are set up in sequence, with a collision cell in between. This principle is realized in triple quadrupole mass spectrometers as well as in quadrupole time-of-flight hybrids (and in double-focusing magnetic-sector instruments). *Tandem-in-time* means that all steps occur in the same space, the ion trap, one after the other. This principle is realized in the very common quadrupole ion traps as well as in the more sophisticated Fourier transform–ion cyclotron resonance (FT-ICR) instruments, which can be considered magnetic ion traps. Furthermore, ion traps allow multiple-stage MS experiments (MS^n), which may be useful for structural elucidation.

Atmospheric pressure chemical ionization (APCI) is the most common alternative to ESI in LC/MS. Whereas the application of ESI is generally recommended in the case of polar compounds, which may have a high molecular weight (up to 1 million Da), the problem-solving domain of APCI is limited to compounds with an MW smaller than 1000 Da. However, less polar compounds are accessible than with ESI.

The solution from LC (or CE, very rarely) is introduced via a deactivated fused-silica capillary with nitrogen flowing concentrically around. As in ESI, the gas literally shears droplets off as the liquid flows out of the end of the capillary, creating a fine spray. In contrast to ESI, the capillary end and the spray region are surrounded by a heater, which aids in desolvation, resulting in a hot vapor. Ionization is achieved by the application of a high voltage (again $\pm 3-5$ kV) to a metal discharge needle, which lies close to the end of the probe tip. The vaporized discharge produced by this high voltage causes solvent molecules to elute into the source to be ionized into a reactive gas plasma. A combination of collisions and charge transfer reactions within this reactive plasma results in the ionization of sample molecules. Therefore, the term ''indirect'' ionization would be more appropriate. Although the conditions in APCI are somewhat harsher than in ESI, the fragmentation is limited, making CID techniques necessary as well.

After 20 years of continuous and rapid development of LC/MS technology and applications, LC/MS has become a routine tool for industry, government, and academic analysts to solve challenging problems. The key to the growth and success of LC/MS is in the informing power, reliability, affordability, and availability of commercial systems (9). The current development in LC/MS is influenced by the input of numerous new users, new fields of research, such as proteomics and combinatorial chemistry, and of course the requirements of pharmaceutical and GLP regulations. In this light, four major trends can be observed: firstly, a rapid growth of the whole field; secondly, a diversification of techniques, especially designed for certain needs; thirdly, improved quality of LC/MS information (better separation,

© 2003 by Marcel Dekker, Inc.

new mass analyzers offering improved sensitivity, mass accuracy, and resolution); and fourthly, improved quantity (automated sample preparation, faster separation, fast scanning mass analyzers, more than one LC coupled to one MS).

II. GENERAL CONSIDERATIONS FOR CAPILLARY ELECTROPHORESIS/MASS SPECTROMETRY

The CE/MS coupling was first reported by Smith and coworkers (10). In principle, the problem of CE/MS coupling is similar to that of LC/MS. The analyte is dissolved in a liquid mobile phase that is removed in the course of the ionization process. Therefore, the same types of interfaces as known from the historically older LC/MS should be available for CE/MS. The smaller flow rates should be an advantage with respect to the vacuum system of the MS. Unfortunately, it is not that simple.

The reason CE/MS is such a promising approach is that it represents a combination of the high separation efficiency of CE with the sensitive, highly specific, and principally universal MS detector.

The *advantages* of the CE/MS approach can be summarized as follows:

- High separation efficiency, significantly better than with LC
- High separation speed
- Flat and piston-like flow profile due to the EOF, causing only minimal zone broadening
- Low solvent consumption
- Minimal sample volume
- High mass sensitivity, significantly better than with LC
- Versatility of CE separation modes: zone electrophoresis (CZE), micellar electrokinetic chromatography (MEKC), gel electrophoresis (CGE), isotachophoresis (CITP), isoelectric focusing (CIEF), capillary electrochromatography (CEC, a hybrid with HPLC), and last but not least Affinity CE (ACE)
- Applicability to large biopolymer separations
- MS a more informative detector than conventional techniques such as UV absorbance, electrochemical or laser-induced fluorescence detection
- MS more universal than the techniques just mentioned
- Possible combination with MS/MS and/or MS^n for structural elucidation purposes

© 2003 by Marcel Dekker, Inc.

The *problems* and challenging aspects of CE/MS can be summarized as follows:

- Absence of a CE column exit buffer reservoir
- Need to achieve electrical continuity for both the CE and MS systems
- Low liquid flows from CE (typically in the nL/min range)
- Low sample capacity of CE (typically in the low nL range) to avoid overload
- High analyte concentration detection limits (typically 5–50 μM for both UV and MS detection systems due to the low sample capacity
- Common CE buffers (e.g., phosphate, sulfate, borate, and other inorganic, nonvolatile salts) not compatible with ESI
- MS-compatible, volatile buffers often resulting in a poor separation
- Different, often contradictory requirements of CE and ESI-MS for solution composition:
  Water, high ionic strength, and often detergents for CE
  Alcohols, low conductivity, and low surface tension to enable ESI
- Need to use longer CE capillaries without cooling at the end part

A number of considerations concerning the *instrumental setup* of CE/MS have to be addressed. In principle, any type of mass spectrometer can be coupled with CE. However, some preferences are evident. Due to their affordability and wide application, single-quadrupole mass spectrometers have been used predominantly. Ion traps and triple quadrupoles have been used successfully as well, offering more information because of their MS/MS capability. Time-of-flight mass spectrometers are probably best suited for CE/MS purposes. One of the advantages of these analyzers is their much higher duty cycle compared to quads and traps. Since the high separation efficiency and speed of CE lead to very narrow peaks, a fast-scanning MS is required. The slogan ''fast scanning for fast chromatography'' applies to GC-TOFs as well as to ESI-TOFs. (In the physical sense of the word, a TOF is not scanning but integrating several masses at a certain time.) Of course, Q-TOF hybrids and FT-ICRs are suitable as well.

Without doubt, electrospray is the method of choice in the case of CE/MS hyphenation. The domain of ESI is polar compounds of a wide molecular-weight range, such as the typical CE analytes. Molecules can be transferred directly from the separation capillary to the mass spectrometer via an interface. This allows the detection of multiply chargeable species of high molecular mass.

The APCI method has the potential drawback that it is designed for higher flow rates (optimum between 0.2 and 1 mL/min). Micro-APCI approaches may reduce this problem (one so-called semimicro-APCI interface

© 2003 by Marcel Dekker, Inc.

is currently commercially available that is specified to work with flow rates between 0.05 and 0.3 mL/min). Incompatibilities with CE buffers are detrimental, too. Other API techniques, such as sonic spray and APPI, are potentially useful for CE/MS but have not yet found wide acceptance. Therefore, CE/MS approaches relying on these novel techniques have not or very rarely been reported. Particle beam EI is designed to ionize less polar, volatile compounds. Therefore, and because it lacks sensitivity, it is not recommended for use in CE/MS.

Continuous-flow FAB was reported earlier but is of no practical importance nowadays. Only few reports have been published dealing with (off-line) coupling of CE to MALDI-MS. Recently, a new ionization approach, coordination ion spray (CIS) MS, has been presented (11); in it, charged coordination compounds are formed on-line.

A literature review for the last eight years reveals that the three to four main principles of hyphenating CE with MS have remained the same, although all of them show remarkable drawbacks (12–15). Still, the most popular CE/MS approach by far is the *coaxial sheath flow interface* (see Fig. 2a) as introduced by Smith and co-workers (16). Its simple construction has helped to make CE/MS accessible to a broader analytical community. Working with the standard equipment, it is obvious that the flow rates from CE are mostly insufficient to provide stable electrospray conditions. For this reason (and others explained in more detail in the following text), a makeup liquid is added. The sheath liquid (or layered flow) is added via a concentric stainless steel capillary surrounding the CE separation capillary. The sheath liquid is mixed with the CE buffer at the tip of the capillary tubing, thus providing electrical contact. Many problems arising from the incompatibility of CE and MS requirements can be solved by the choice of an optimized sheath liquid. In principle, the sheath flow should:

- Aid in nebulization and ion evaporation (by adding organics, such as isopropanol)
- Adjust pH to form ions in solution (e.g., acetic acid for positive ionization, triethylamine for negative ionization)
- Provide makeup flow to get stable electrospray conditions (2–5 μL/min)

Several considerations for this layered flow approach have to be taken into account. Concerning CE, the column diameter should not be too large.

Fig. 2 CE/MS interfaces. (a) coaxial sheath liquid, (b) liquid junction, (c) sheathless, and (d) direct electrode. See text for further explanation. (Adapted from Ref. 14.)

© 2003 by Marcel Dekker, Inc.

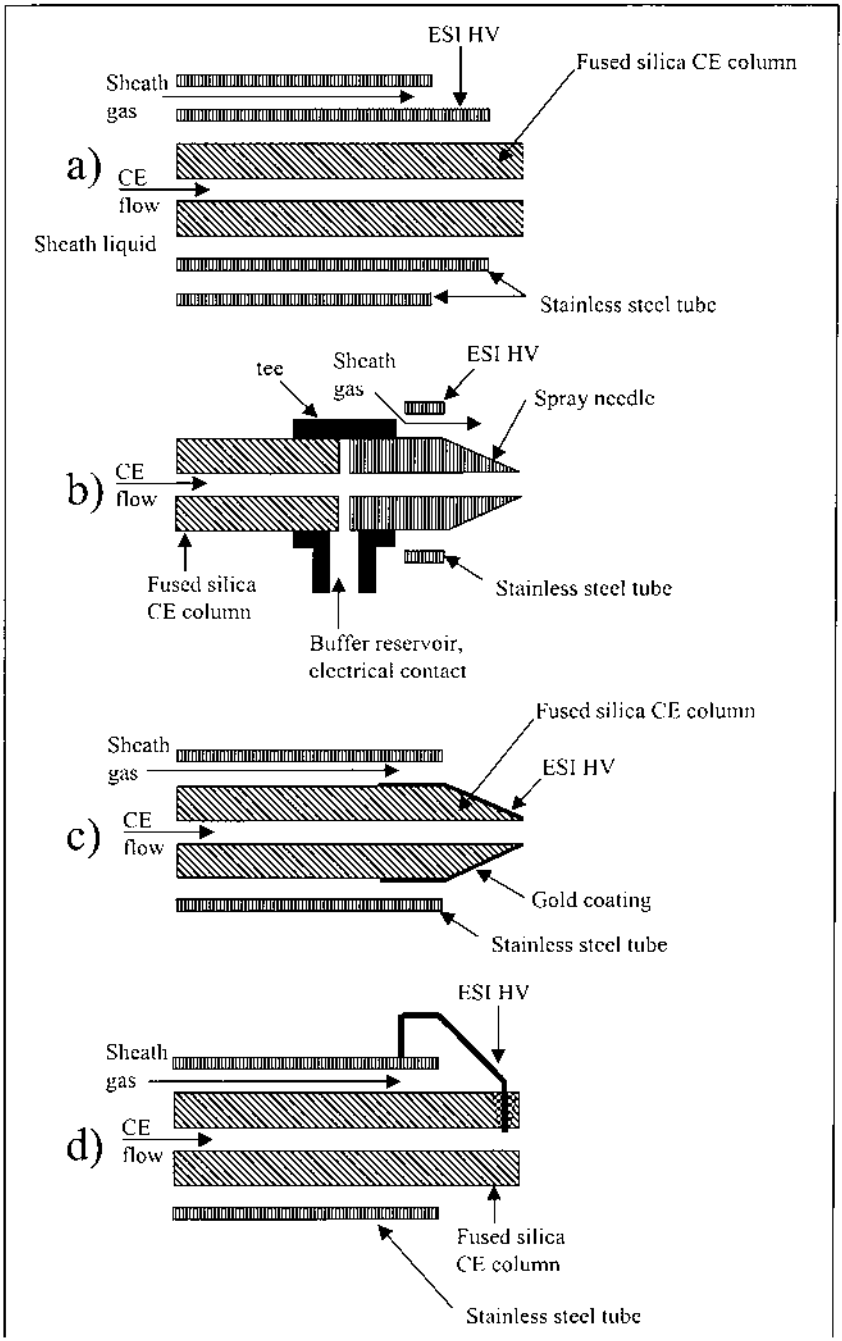

© 2003 by Marcel Dekker, Inc.

An interesting study by Tetler et al. indicates that reducing the dimensions of the capillary results in better operation and sensitivity (17). Another paper describes protein analysis at the attomole level using 5-μm-ID capillaries (18). The electrolyte composition and pH should not be too detrimental. Aspects such as pressure, temperature, and injection technique may have an influence. Concerning the interface, the sheath flow should be optimized with respect to composition, pH, and flow rate. Furthermore, the positions of the fused-silica capillary as well as the API probe need to be carefully optimized. The mixing volume at the tip of the capillary must be kept at a minimum to avoid postcolumn band broadening caused by diffusion.

The unintended negative effects of high buffer-salt concentrations on the efficiency of the electrospray can be significantly reduced by adding an appropriate sheath liquid, thus usually improving the spray stability. However, since the sheath liquid acts as the terminal buffer reservoir, it must contain an electrolyte in order to maintain an efficient electrophoretic separation. Therefore, any choice of sheath flow composition represents a compromise between separation efficiency and spray stability.

Another problem, the potential increase in background noise due to the addition of solvents and modifiers from the sheath liquid (e.g., volatile salts, acids, and bases), has been studied (19). Moreover, because of the different composition of the initial CE buffer reservoir and the sheath liquid, discontinuous and irreproducible conditions may result. These effects can potentially change migration times or even the migration order of the analytes (20).

Many authors claim that the dilution by the sheath flow would not significantly affect the detection sensitivity, because it is completely evaporated in the spray process. Moreover, it has been discussed that in this layered-flow approach, preferably the ''inner layer'' of the spray enters the collector opening. If this were true, the composition of sheath liquid would be less important. Anyhow, it has to be stated that there is a dilution problem in the sheath-flow approach. In addition, it has been proven many times that ESI is a concentration-sensitive, not mass-sensitive, process. Knowing this, it makes sense to reduce the sheath liquid flow rate to the minimum required for stable spray conditions.

This technique has the advantage of allowing the use of common CE capillaries without modification, which is of high practical importance. (The CE column exit may be tapered or pulled out to a fine tip in order to increase the local field strength.)

Although the limitations to CE buffer composition may be relaxed due to the possibility of postcolumn solution chemistry changes, a substitution of nonvolatile buffers is still recommended to avoid decreasing the sensitivity and finally blocking of the MS collector opening. In an instructive study

© 2003 by Marcel Dekker, Inc.

by Moseley et al. (21), several MS-compatible buffer systems were described. The most useful buffer in peptide analysis was 0.01 M, pH 3.4 acetic acid, facilitating positive ionization. Other common buffer systems that have proven useful are ammonium acetate, ammonium formiate, and citric acid.

If nonvolatile buffers cannot be completely avoided, their concentration should be kept at a minimum. High flow rates (due to a strong EOF) prevent rapid crystallization at the tip. Modern off-axis electrospray arrangements (orthogonal or Z-spray) tend to be more tolerant to nonvolatiles than classical on-axis interfaces.

The sheath-flow interface can meanwhile be considered a routine tool, at least for qualitative determinations. Quantification is possible, with relative standard deviations between 5 and 10% typically achieved. Quantification problems may result from the limited lifetime of the capillaries. Due to high local field strengths near the tip, the so-called electrodrilling effect commonly occurs. Modifications of the tip can improve the lifetime (22).

The *liquid-junction interface* (Fig. 2b) was developed by Henion and co-workers (23). The idea is that a small gap of 10–20 μm filled with CE buffer connects the end of the CE capillary with a specially designed ESI needle emitter. The advantage that can be expected from this setup is that the CE separation and the electrospray process are decoupled, at least partially. This electrical and physical disconnection allows choosing of the sheath liquid more freely. A disadvantage lies in the peak broadening effects and thereby a loss of separation efficiency. Probably the greatest problem is the difficult construction of the junction. Furthermore, gas bubbles may occur due to oxygen formation (water oxidation). Therefore, its use was reported very rarely later on. Recently, Waterval et al. (24) have examined several sheathless liquid-junction interfaces in depth. They compared different tapered and pulled tip designs. The one they found most promising consisted of a CE capillary coupled to the spray tip inside a silicon rubber, with a gold wire enabling electrical contact directly into the gap.

The *sheathless interface* (Fig. 2c) is known since the first CE/MS attempt by Olivares et al. (10). In this system the CE capillary was sleeved in a metal tube, whereas in modern sheathless interfaces the capillary exit is carefully sharpened or pulled to a fine point (14). The outer surface of the capillary tip is coated with metal, usually gold, which is readily accessible for electrical contact. This setup enables the maintenance of both electrical circuits from CE and ESI as well. The advantage of the sheathless approach over the coaxial sheath flow interface is that the eluting CE zone is not diluted by makeup flow and therefore the obtainable sensitivity can be quite high, especially when small-ID capillaries (e.g., 10 μm) are used. Detection limits in the low fmol range have been demonstrated (13). A

© 2003 by Marcel Dekker, Inc.

sheath gas such as SF_6 is often used to prevent a corona discharge due to the high local field strength at the tip. This gas serves only as a free-electron scavenger and does not affect the electrospray process.

One technical problem is the instability of the gold coating, causing short lifetimes of the capillaries. Gold is continuously removed from the surface both physically and electrically. To improve the stability, several efforts have been undertaken. First plating the tip with Ni or Ni/Cr alloy before gold coating is helpful. With Cr/Au-coated fused-silica emitters, lifetimes longer than 100 h have been reported (25). Marking the tip with a soft pencil in order to deposit graphite may also help (26).

The sensitivity of CE/ESI-MS has proven significantly better if the sheathless interface is coupled to a micro- or nanoelectrospray source designed for low flow rates.

Another sheathless approach is the *direct electrode interface* (Fig. 2d) presented by Fang et al. (27) and Cao and Moini (28), respectively. In this elegant solution, a gold (or platinum) wire is carefully placed just inside the capillary exit or directly inserted through the capillary side wall and secured with epoxy.

All sheathless approaches have the drawback that the CE buffer has to be compatible with ESI, which means that volatile buffers with low surface tension and low conductivity have to be used.

Comparative studies indicate that a sheathless configuration offers improved sensitivity over sheath flow interfaces. However, this implies the need to use specialized, home-built CE capillaries and electrospray hardware. Therefore, it has not yet been as popular as the easily accessible sheath liquid system.

Several general implications of CE/MS hyphenation have to be taken into consideration. As discussed, both electrical circuits of CE and ESI have to be maintained. This goal is best accomplished if the CE capillary exit is kept at ground potential, as normally done in CE. This is nontrivial and places severe demands on the MS entrance configuration. These aspects are discussed in more detail in Ref. 14.

Microfabricated devices have been introduced that are capable of performing CE on a chip. This development is stimulated by the need for high-throughput analysis with extremely small sample amounts. In Ref. 29 a microdevice is described that is constructed by wet chemical etching of a glass plate. It contains a centrally placed separation channel of length 4.5–11 cm. The microdevice is coupled to an electrospray tip via a liquid junction. The connection of the exit port of the chip to the electrospray is crucial and needs further improvement. Subatmospheric pressure at the ESI interface seems to be useful. More references and details regarding this exciting new field can be found in Ref. 15.

© 2003 by Marcel Dekker, Inc.

III. SPECIAL CONSIDERATIONS FOR AFFINITY CAPILLARY ELECTROPHORESIS/ELECTROSPRAY IONIZATION–MASS SPECTROMETRY

The ACE/ESI-MS technique is certainly the most promising approach to overcoming the limitations of ACE concerning structural identification and characterization as well as detector sensitivity. Of course, the problems discussed for CE/MS hyphenation do apply for ACE/MS in the same way. In principle, there are no special considerations to be made for CE/ESI-MS regarding the separation mode. From this point of view, ACE is only a specialized version of the common CZE approach. The composition of the CE buffer plays a decisive role with respect to solution chemistry, which is crucial for electrospray and, therefore, for sensitivity. The more detrimental the additives that are required for separation, the more challenging the MS coupling will be. A technique such as MEKC, which uses large amounts of surfactants, will certainly cause problems in CE/ESI-MS. In fact, to circumvent these problems, the application of the partial-filling technique, as described by Koezuka et al. (30), is strongly recommended. Partial-filling approaches have also been presented for chiral separations using cyclodextrins (31,32) and for ACE (33) (in order to use small ligand amounts or to prevent UV disturbances), as well as for chiral CE/MS (to avoid contamination of the MS) (34,35). The latter article deals with the chiral separation of local anaesthetics. By means of the partial-filling technique it was possible to prevent the introduction of the nonvolatile chiral selector methyl-β-cyclodextrin into the mass spectrometer. Therefore, a polyacrylamide-coated capillary was partially filled with buffer containing cyclodextrin, prior to sample injection. While the positively charged enantiomers migrate through the neutral pseudostationary phase of the chiral selector, separation is achieved.

Most analytes investigated in ACE, such as proteins, peptides, oligonucleotides, and drugs, can be analyzed in ESI-MS with fairly good to pretty good responses. Only surfactants may cause problems, as discussed earlier.

General CE problems (e.g., wall interactions of proteins) have been discussed elsewhere. All ACE techniques working with a ligand added to CE buffer (classical ACE, Hummel–Dreyer principle, vacancy peak analysis) imply the potential problem that any continuously infused matrix can increase background noise and, even worse, deteriorate the ionization of the analyte due to competition.

Since ACE is based mostly on the calculation of migration-time shifts of analytes upon addition of an interaction partner, migration-time reproducibility is extremely important. If the calculation is based on mobilities, this problem is certainly reduced. However, stable buffer electrolyte conditions are mandatory, which may be critical in sheath flow setups.

© 2003 by Marcel Dekker, Inc.

The most important advantage of ACE/MS compared to ACE with UV detection is clearly the more specific mode of detection, thus facilitating peak assignment. Additional structural information is available using MS/MS and MS^n, respectively.

Another promising aspect of on-line ACE/ESI-MS is the finding that binding interactions may survive the ionization process due to its soft nature (36).

IV. APPLICATIONS OF AFFINITY CAPILLARY ELECTROPHORESIS/ELECTROSPRAY IONIZATION–MASS SPECTROMETRY

Although it can be considered one of the most promising future directions in ACE (37), relatively few papers describe the on-line coupling of ACE with MS. The preferred field of application to date is the characterization of peptide libraries in combinatorial chemistry. The pioneering work in this area comes from Chu et al. (38,39), clearly demonstrating the impressive potential of this new technique. In a solution-based approach, combinatorial libraries are screened for drug leads (see Fig. 3). It is possible to do on-line, one-step selection and structural identification of candidate ligands. As pointed out in the full paper (39), ACE was based on the binding of vancomycin to libraries of all-D-tri- and tetrapeptides as a model system. These peptide libraries consisted of different forms of Fmoc-DDXX and Fmoc-EXX, with up to 361 compounds, thus successfully determining the interacting structural motifs. The conditions used in ACE/MS were: buffer 20 mM Tris-acetate, pH 8.0, 70 μM vancomycin, 15-kV separation voltage; the capillary was a 400-mm-long 50-μm-ID PVA-coated capillary. A 5 mM Tris acetate solution, pH 8.1, in MeOH/water 75:25 was used as sheath liquid at 1.5 μL/min. From the MS point of view it is worth noting that under these conditions, $[M + Tris + H]^+$ adduct ions predominantly occurred. Since the authors used a triple-quadrupole MS, they were able to obtain tandem mass spectra. Furthermore, another 1000-peptide library was screened directly by ACE/MS. The authors have also found that incorporating an affinity solid-phase extraction step prior to ACE/MS is an effective sample preparation, which is helpful, particularly in case of large libraries. It was possible both to remove a large number of noninteracting species as well as to preconcentrate sample components, which facilitates a subsequent sequence determination by on-line MS/MS.

In another paper from the same group (40), a new solution-based approach for linear epitope mapping based on ACE/MS is demonstrated using beta-endorphin as a model substance. The procedure can briefly be described

© 2003 by Marcel Dekker, Inc.

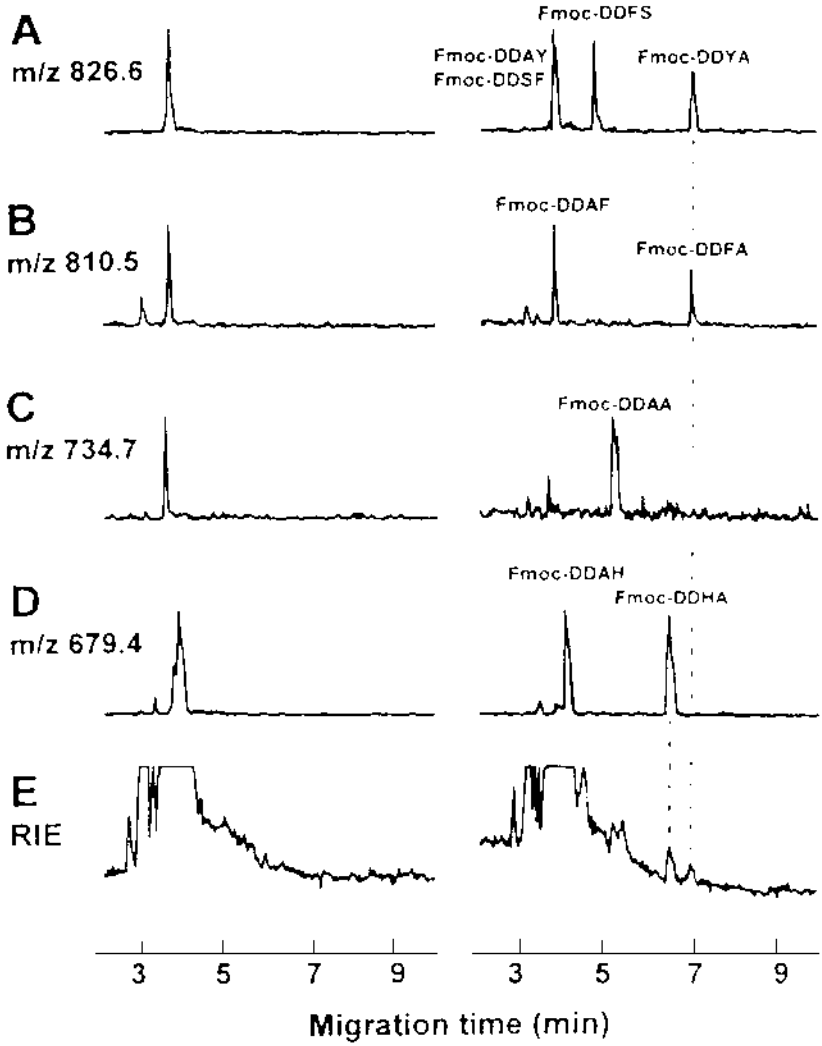

Fig. 3 ACE/MS of a synthetic all-D, Fmoc-DDXX library of 100 tetrapeptides using vancomycin as the receptor. (A–D) Selected ion electropherograms for the masses indicated; (E) reconstructed ion electropherograms for runs without (left) and with (right) vancomycin in the electrophoresis buffer. See text for conditions and further explanations. (Reprinted with permission from Ref. 38. Copyright 1995 American Chemical Society.)

© 2003 by Marcel Dekker, Inc.

as follows: First, tryptic peptides are separated in a neutral coated capillary, as monitored by UV and MS detection. Then the injection of the tryptic digest (4.6 pmol/μL) is followed by the injection of anti-beta-endorphin antibody (4.7 pmol/μL). A peptide that binds to this antibody will disappear, because it is captured (see Fig. 4). This step can be considered subtraction screening. The applied ACE/MS conditions in this study were: buffer 50 mM ε-aminocaproic acid/acetic acid, pH 5.1, 20-kV separation voltage, 350-mm-long 50-μm-ID PVA-coated capillary, negative ESI mode. For measurements in positive ESI mode, the Tris buffer as in Ref. 39 was used. Thereafter, the immunoreactive peptide is individually synthesized or isolated and its binding examined using ACE/MS to confirm that the epitope resides on this peptide. Afterwards, a series of truncated peptides helps to identify the precise necessary structure of the epitope. The authors show that only low femtomole amounts of antibody and peptide digest are consumed per run. Furthermore, it is emphasized that the method is rapid and easily automated.

In a fourth article by this group (41), the binding of a tetrapeptide library to vancomycin was again a matter of investigation. In this work the emphasis was on the simultaneous determination of binding constants for 19 peptides of the type Fmoc-DXYA. It was also shown that the results obtained using ACE/MS are correlate well with data from UV detection experiments. Whereas only one K_d value is accessible in an ACE-UV run, ACE/MS enables multiple K_d determinations. The operating conditions were the same as in Ref. 39, except from the use of uncoated capillaries. (For more experimental details refer to the cited literature.)

In Ref. 42 a similar approach was chosen as in Ref. 39 using stereoisomers of the type Fmoc-L-Asp-L-Asp-D-Xaa-D-Xaa (Xaa = Gly, Ala, Phe, His, Ser, Tyr). Interestingly, in part the findings are different. The ACE/MS hyphenation caused a number of practical problems affecting the reliability of the system. Surprisingly, the authors faced problems with positive ESI and were forced to use negative ionization. Because of the use of the nonvolatile Tris buffer, crystallization problems occurred frequently. Only high-EOF conditions prevented this knockout scenario. However, the description of problems and related solutions is very instructive.

Schwarz et al. used ESI-MS detection to characterize the composition of binary (bile salt/phosphatidylcholine) and ternary (bile salt/phophatidylcholine/fatty acid) mixed micelles that were used in micellar affinity capillary electrophoresis (43,44). The detrimental effects of the surfactants turned out to be tolerable for short-time qualitative determinations.

A number of CE/MS applications have been published in the field of chiral separations, mostly using cyclodextrins as chiral selectors. In some cases the partial-filling technique was used (see earlier). The importance of

© 2003 by Marcel Dekker, Inc.

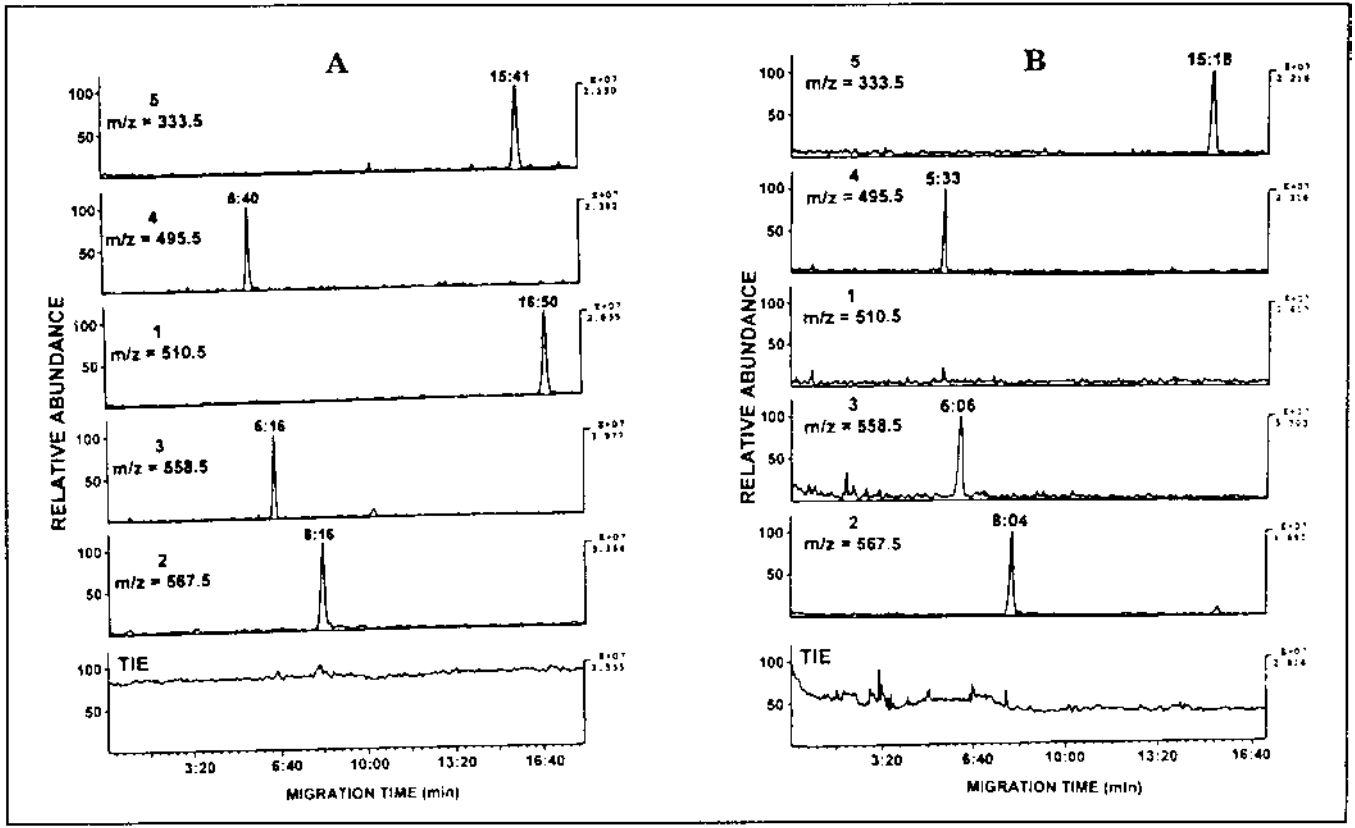

Fig. 4 Epitope mapping by ACE/MS in the positive ESI mode. (A) Tryptic digest, 4.6 pmol/μL, 10-s pressure injection; (B) tryptic digest, 10-s injection followed by 25-s injection of antibody (4.7 pmol/μL). Selected ion electropherograms for the *m/z* indicated and the total ion electropherograms, respectively. It is obvious that peptide 1 (Tyr-Gly-Gly-Phe-Met-Thr-Ser-Glu-Lys) is captured by the antibody. See text for further explanation. (Reprinted with permission from Ref. 40. Copyright 1997 American Chemical Society.)

© 2003 by Marcel Dekker, Inc.

enantiomeric separations is growing, particularly for pharmaceutical purposes. Although this technique is closely related to ACE, it cannot be discussed here in detail.

A technique called *on-line immunoaffinity CE* has been presented (45) that was also coupled to MS. However, in this setup the affinity principle is used to extract the analyte from a complex matrix in a microchamber affinity device prior to CE separation. Therefore, it cannot be considered ACE.

V. CONCLUSIONS

The small number of papers dealing with on-line ACE/MS and the fact that these were all published from 1995 on indicate that this is a newly emerging topic. Probably the main reason is that the problems of interfacing CE itself with MS have prevented the technique from routine use to date. Driven by the need for high-performance analytical methods, however, CE/MS will gain maturity, and new applications can be expected in the near future. We are now in the phase of ''early adoptors,'' right after the innovators of CE/MS and ACE solved the most urgent problems. The field of combinatorial library screening is especially destined for this two-dimensional approach.

Every analyst who has access to CE equipment and ESI-MS may take this new alternative into consideration when appropriate. When is it appropriate? If an analytical problem can be solved using affinity capillary electrophoresis and a more universal and specific detection or structural information is required than is accessible with the help of conventional UV diode array detectors, consider ACE/MS.

REFERENCES

1. M Dole, LL Mack, RL Hines, RC Mobley, LD Ferguson, MB Alice. Molecular beams of macroions. J Chem Phys 49:2240–2249, 1968.
2. CM Whitehouse, RN Dreyer, M Yamashita, JB Fenn. Electrospray interface for liquid chromatographs and mass spectrometers. Anal Chem 53:675–679, 1985.
3. M Yamashita, JB Fenn. Electrospray ion source. Another variation on the free-jet theme. J Phys Chem 88:4451–4459, 1984.
4. ML Alexandrov, LN Gall, VN Krasnov, VI Nikolajew, VA Pawlenko, VA Shkurov. Extrakciya Ionov is Rastvorov pri Atmosferiom Davlenii-Metod Mass-Spectrometricheskovo Analisa Bioorganicheskikh Veshestv. Dokl Akad Nauk SSSR 277:379–383, 1984.
5. G Schmelzeisen-Redeker, L Bütfering, FW Röllgen. Desolvation of ions and molecules in thermospray mass spectrometry. Int J Mass Spectrom Ion Processes 90:139–150, 1989.

© 2003 by Marcel Dekker, Inc.

6. JV Iribarne, BA Thomson. On the evaporation of small ions from charged droplets. J Chem Phys 64:2287–2294, 1976.
7. P Kebarle, Y Ho. On the mechanism of electrospray mass spectrometry. In: RB Cole, ed. Electrospray Ionization Mass Spectrometry. New York: Wiley, 1997, pp 3–63.
8. M Wilm, M Mann. Analytical properties of the nanoelectrospray ion source. Anal Chem 68:1–8, 1996.
9. R Willoughby, E Sheehan, S Mitrovich. A Global View of LC/MS. Pittsburgh, PA: Global View, 1998.
10. JA Olivares, NT Nguyen, CR Yonker, RD Smith. On-line mass spectrometric detection for capillary zone electrophoresis. Anal Chem 59:1230–1232, 1987.
11. C Rentel, P Gfrörer, E Bayer. Coupling of capillary electrochromatography to coordination ion spray mass spectrometry, a novel detection method. Electrophoresis 20:2329–2336, 1999.
12. WMA Niessen, UR Tjaden, J van der Greef. Capillary electrophoresis–mass spectrometry. J Chromatogr A 636:3–19, 1993.
13. J Cai, J Henion. Capillary electrophoresis–mass spectrometry. J Chromatogr A 703:667–692, 1995.
14. JF Banks. Recent advances in capillary electrophoresis/electrospray/mass spectrometry. Electrophoresis 18:2255–2266, 1997.
15. A v. Brocke, G Nicholson, E Bayer. Recent advances in capillary electrophoresis/electrospray–mass spectrometry. Electrophoresis 22:1251–1266, 2001.
16. RD Smith, CJ Barinaga, HR Udseth. Improved electrospray ionization interface for capillary zone electrophoresis–mass spectrometry. Anal Chem 60:1948–1952, 1988.
17. LW Tetler, PA Cooper, B Powell. Influence of capillary dimensions on the performance of a coaxial capillary electrophoresis–electrospray mass spectrometry interface. J Chromatogr A 700:21–26, 1995.
18. JH Wahl, DR Goodlett, HR Udseth, RD Smith. Attomole-level capillary electrophoresis–mass spectrometric protein analysis using 5-μm-i.d. capillaries. Anal Chem 64:3194–3196, 1992.
19. DC Gale, RD Smith. Small-volume and low-flow-rate electrospray ionization–mass spectrometry of aqueous samples. Rapid Commun Mass Spectrom 7: 1017–1021, 1993.
20. F Foret, TJ Thompson, P Vouros, BL Karger, P Gebauer, P Boček. Liquid sheath effects on the separation of proteins in capillary electrophoresis–electrospray mass spectrometry. Anal Chem 66:4450–4458, 1994.
21. MA Moseley, JW Jorgenson, J Shabanowitz, DF Hunt, KB Tomer. Optimization of capillary zone electrophoresis/electrospray ionization parameters for the mass ppectrometry and tandem mass spectrometry analysis of peptides. J Am Soc Mass Spectrom 3:289–300, 1992.
22. C Siethoff, W Nigge, M Linscheid. Characterization of a capillary zone electrophoresis/electrospray–mass spectrometry interface. Anal Chem 70:1357–1361, 1998.
23. ED Lee, W Muck, JD Henion, TR Covey. On-line capillary zone electropho-

© 2003 by Marcel Dekker, Inc.

resis–ion spray tandem mass spectrometry for the determination of dynorphins. J Chromatogr A 458:313–321, 1988.
24. JCM Waterval, P Bestebreurtje, H Lingeman, C Versluis, AJR Heck, A. Bult, WJM Underberg. Robust and cost-effective capillary electrophoresis–mass spectrometry interfaces suitable for combination with on-line analyte preconcentration. Electrophoresis 22:2701–2708, 2001.
25. DR Barnidge, S Nilsson, KE Markides, H Rapp, K Hjort. Metallized sheathless electrospray emitters for use in capillary electrophoresis orthogonal time-of-flight mass spectrometry. Rapid Commun Mass Spectrom 13:994–1002, 1999.
26. YZ Chang, GR Her. Sheathless capillary electrophoresis–electrospray mass spectrometry using a carbon-coated fused-silica capillary. Anal Chem 72:626–630, 2000.
27. L Fang, R Zhang, ER Williams, RN Zare. On-line time-of-flight mass spectrometric analysis of peptides separated by capillary electrophoresis. Anal Chem 66:3696–3701, 1994.
28. P Cao, M Moini. A novel sheathless interface for capillary electrophoresis–electrospray ionization mass spectrometry using an in-capillary electrode. J Am Soc Mass Spectrom 8:561–564, 1997.
29. B Zhang, F Foret, BL Karger. A Microdevice with integrated liquid junction for facile peptide and protein analysis by capillary electrophoresis–electrospray mass spectrometry. Anal Chem 72:1015–1022, 2000.
30. K Koezuka, H Ozaki, N Matsubara, S Terabe. Separation and detection of closely related peptides by micellar electrokinetic chromatography coupled with electrospray ionization mass spectrometry using the partial-filling technique. J Chromatogr B 689:3–11, 1997.
31. A Amini, C Pettersson, D Westerlund. Enantioresolution of disopyramide by capillary affinity electrokinetic chromatography with human α_1-acid glycoprotein (AGP) as chiral selector applying a partial-filling technique. Electrophoresis 18:950–957, 1997.
32. A Amini, U Paulsen-Sörman. Enantioseparation of local anaesthetic drugs by capillary zone electrophoresis with cyclodextrins as chiral selectors using a partial-filling technique. Electrophoresis 18:1019–1025, 1997.
33. J Heintz, M Hernandez, FA Gomez. Use of a partial-filling technique in affinity capillary electrophoresis for determining binding constants of ligands to receptors. J Chromatogr A 840:261–268, 1999.
34. EM Jäverfalk, A Amini, D Westerlund, PE Andrén. Chiral separation of local anaesthetics by a capillary electrophoresis/partial-filling technique coupled on-line to micro-electrospray mass spectrometry. J Mass Spectrom 33:183–186, 1998.
35. S Rudaz, S Cherkaoui, P Dayer, S Fanali, J-L Veuthey. Simultaneous stereoselective analysis of tramadol and its main metabolites by on-line capillary zone electrophoresis–electrospray ionization mass spectrometry. J Chromatogr A 868:295–303, 2000.
36. X Cheng, R Chen, JE Bruce, BL Schwartz, GA Anderson, SA Hofstadler, DC Gale, RD Smith, J Gao, GB Sigal, M Mammen, GM Whitesides. Using elec-

© 2003 by Marcel Dekker, Inc.

trospray ionization FTICR mass spectrometry to study competitive binding of inhibitors to carbonic anhydrase. J Am Chem Soc 117:8859–8860, 1995.
37. NHH Heegard, RT Kennedy. Identification, quantitation, and characterization of biomolecules by capillary electrophoretic analysis of binding interactions. Electrophoresis 20:3122–3133, 1999.
38. YH Chu, DP Kirby, BL Karger. Free-solution identification of candidate peptides from combinatorial libraries by affinity capillary electrophoresis/mass spectrometry. J Am Chem Soc 117:5419–5420, 1995.
39. YH Chu, YM Dunayewski, DP Kirby, P Vouros, BL Karger. Affinity capillary electrophoresis–mass spectrometry for screening combinatorial libraries. J Am Chem Soc 118:7827–7835, 1996.
40. YV Lyubarskaya, YM Dunayewski, P Vouros, BL Karger. Microscale epitope mapping by affinity capillary electrophoresis–mass spectrometry. Anal Chem 69:3008–3014, 1997.
41. YM Dunayewski, YV Lyubarskaya, YH Chu, P Vouros, BL Karger. Simultaneous measurement of nineteen binding constants of peptides to vancomycin using affinity capillary electrophoresis–mass spectrometry. J Med Chem 41: 1201–1204, 1998.
42. F Lynen, Y Zhao, C Becu, F Borremans, P Sandra. Considerations concerning interaction characterization of oligopeptide mixtures with vancomycin using affinity capillary electrophoresis–electrospray mass spectrometry. Electrophoresis 20:2462–2474, 1999.
43. MA Schwarz, K Raith, H-H Rüttinger, G Dongowski, R. Neubert. Investigation of the interactions between drugs and mixed bile salt/lecithin micelles. A characterization by micellar affinity capillary electrophoresis (MACE). Part III. J Chromatogr A 781:377–389, 1997.
44. MA Schwarz, K Raith, G Dongowski, R. Neubert. Effect on the partition equilibrium of various drugs by the formation of mixed bile salt/phosphatidylcholine/fatty acid micelles. A characterization by micellar affinity capillary electrophoresis (MACE). Part IV. J Chromatogr A 809:219–229, 1998.
45. NA Guzman. Determination of immunoreactive gonadotropin-releasing hormone in serum and urine by on-line immunoaffinity capillary electrophoresis coupled to mass spectrometry. J Chromatogr B 749:197–213, 2000.

© 2003 by Marcel Dekker, Inc.

14
Conclusions

Reinhard H. H. Neubert and Hans-Hermann Rüttinger
Martin-Luther-University Halle-Wittenberg, Halle, Germany

The introduction of narrow-bore capillaries into electrophoresis started a tremendous evolution of analytical power as well as speed and reliability of electrophoretic methods. Besides an impressive diversification of analytical procedures, it became evident in recent years that capillary electrophoresis provides very suitable methods for the characterization and quantification of molecular interactions.

We have shown in this book a wide field of interactions, ranging from the molecular level of small drug molecules, biological macromolecules such as polysaccharides, proteins, and DNA to supermolecular aggregates such as micelles, microemulsion droplets, organelles, viruses and cells. All these interactions change the electrophoretic mobility of one or more components of the equilibrium mixture, and thus the migration data contain information on the affinity of drugs to their target or transporters only to give a pharmaceutically relevant example.

The theoretical basis of electrophoresis and the physicochemical background of interaction phenomena are well established and provide the mathematical methods to calculate affinity constants and to relate them to the results of the alternative methods in affinity chemistry.

The advantages of ACE over other relevant methods are:

ACE is extremely time and substance saving.
The method is highly repeatable.
The equipment is easy to handle.
Based on an extended theory, there are effective methods described for explaining and quantifying the results.
Equipment is commercially available.
Convenient software is readily available.

© 2003 by Marcel Dekker, Inc.

It must be kept in mind, however, that CE data resemble a macroscopic effect of complexation and, like ultrafiltration or size exclusion chromatography CE, do not give information on specific binding sites. Despite the existence of a well-established theoretical basis, it is not possible to get reliable complexation constants, for practical reasons, if too many complexation processes are involved at the same time. Often the combination with spectroscopic investigations, especially with NMR and fluorimetry, may provide more details.

Fascinating possibilities are opened by combining ACE with different mass spectrometry (MS) methods in order to overcome the main disadvantage of classical CE and UV detection: the lack of sensitivity. The hyphenated methods are very sensitive and allow us to characterize interactions of very small quantities of molecular entities.

One drawback of capillary electrophoresis is the state of the capillary wall. Often, constituents of the buffer or analyte are absorbed on the surface, causing not only an irreproducible shift of EOF, but even the possibility of questionable binding isotherms. A lot of effort has gone into overcoming this problem. Capillaries with coated inner walls are now commercially available; and capillary electrophoresis on chips of different materials is also under development now. Not only do these chips represent a miniaturized form of capillary electrophoresis, but this technique also enables the incorporation of such sample preparation steps as preconcentration and even PCR and immobilization of immunoreagents. It is not difficult to anticipate a very exciting development in this field, one with a high commercial impact.

We hope that the applications in Parts II and III give a clear idea of the implications that CE methods have already had on progress in the pharmaceutical and life sciences.

The following can be concluded:

- The application of electrophoretic methods such as affinity capillary electrophoresis in pharmaceutics and biopharmaceutics is not only focused on the use of analytical assays but also on the very interesting fields covered in this book.
- Affinity capillary electrophoresis can be a very helpful tool in two of the most fascinating fields of pharmaceutics and biopharmaceutics: controlled drug delivery and drug targeting.
- The combination of ACE with mass spectrometry (hyphenation methods) will increase significantly its applicability in pharmaceutics and biopharmaceutics.
- Due to its advantages, therefore, the use of ACE in pharmaceutics and biopharmaceutics will be substantially extended in the future.

© 2003 by Marcel Dekker, Inc.

The book shows clearly that ACE is a very powerful tool for the:

Characterization of physicochemical and thermodynamic properties of drugs and pharmaceutical vehicle systems.

Characterization and optimization of the affinity of drugs to pharmaceutical vehicle systems.

Studies of interactions of drugs and pharmaceutical vehicle systems with biological structures and biomolecules such as proteins and nucleic acids. Furthermore, it is possible to evaluate interaction between biomolecules, e.g., interactions between protein or between proteins and nucleic acids.

© 2003 by Marcel Dekker, Inc.

about the book . . .

The first of its kind, this reference presents the most recent breakthroughs and techniques in affinity capillary electrophoresis (ACE) to measure and determine the physicochemical and thermodynamic parameters of drug compounds—offering strategies to explore and characterize interactions between drugs, drug vehicles, and biological membranes to facilitate developments in controlled drug delivery and targeting.

Affinity Capillary Electrophoresis in Pharmaceutics and Biopharmaceutics contains current applications and procedures to identify binding constants between drugs, biological structures, proteins, nucleic acids, and plasmids...increase drug bioavailability...enhance the permeability, solubility, strength, and function of drug formulations...examine protein–protein exchanges and reactions...and calculate pK_a values.

about the editors . . .

REINHARD H. H. NEUBERT is Professor in the College of Pharmacy, Martin-Luther-University Halle-Wittenberg, Germany. The author or coauthor of more than 200 journal articles, book chapters, and books, he holds 25 patents and is a member of the German Pharmaceutical Society, the International Association for Pharmaceutical Technology, the American Association of Pharmaceutical Scientists, and the Controlled Release Society. Professor Neubert has given numerous lectures at international conferences and received the Diplompharmazeut (1974), the Ph.D. degree (1978), and the Habilitation (1987) from Martin-Luther-University Halle-Wittenberg, Germany.

HANS-HERMANN RÜTTINGER is Lecturer, Martin-Luther-University Halle-Wittenberg, Germany. The author or coauthor of many journal articles, he holds 25 patents and is a member of the German Chemical Society. He received the Diplomchemiker (1970), the Ph.D. degree (1973), and the Habilitation (1988) from Martin-Luther-University Halle-Wittenberg, Germany.

Printed in the United States of America

MARCEL DEKKER, INC.
NEW YORK • BASEL

ISBN 0-8247-0951-9